MISSILE AND SPACE DIVISION

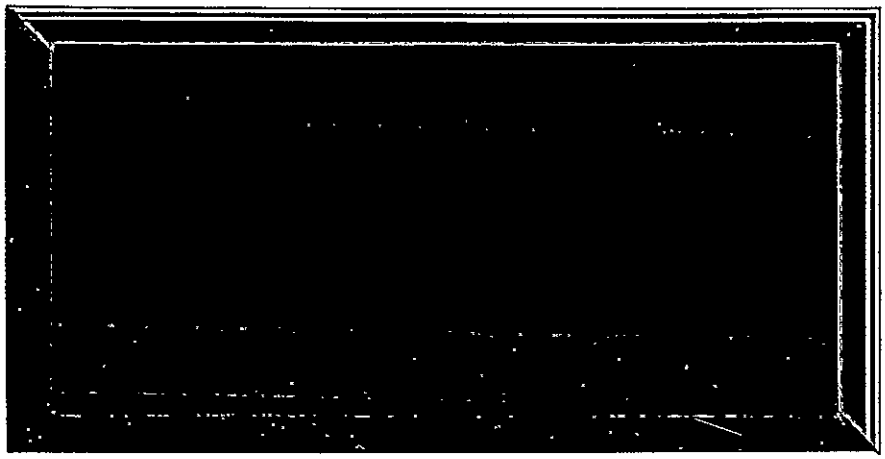

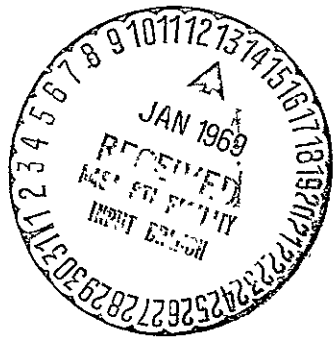

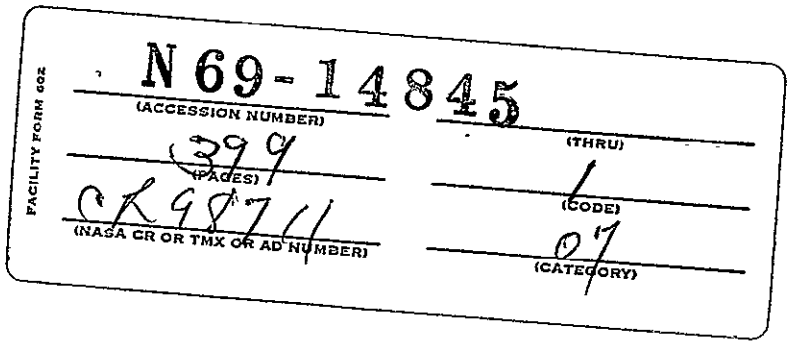

GENERAL ELECTRIC

VOICE BROADCAST MISSION STUDY - VOLUME II: STUDY REPORT

General Electric
Missile and Space Division
Philadelphia, Pennsylvania

14 July 1967

DOCUMENT NO. 67SD4330
JULY 14, 1967

FINAL REPORT
VOICE BROADCAST MISSION STUDY
VOLUME II - STUDY REPORT

NASA CONTRACT NO. NASw-1475

GENERAL ELECTRIC
MISSILE AND SPACE DIVISION
Valley Forge Space Technology Center
P.O. Box 8555 • Philadelphia 1, Penna.

TABLE OF CONTENTS

TABLE OF CONTENTS (Cont'd)

TABLE OF CONTENTS (Cont'd)

TABLE OF CONTENTS (Cont'd)

LIST OF ILLUSTRATIONS

LIST OF ILLUSTRATIONS (Cont'd)

LIST OF ILLUSTRATIONS (Cont'd)

LIST OF ILLUSTRATIONS (Cont'd)

LIST OF ILLUSTRATIONS (Cont'd)

VBMS
FINAL REPORT

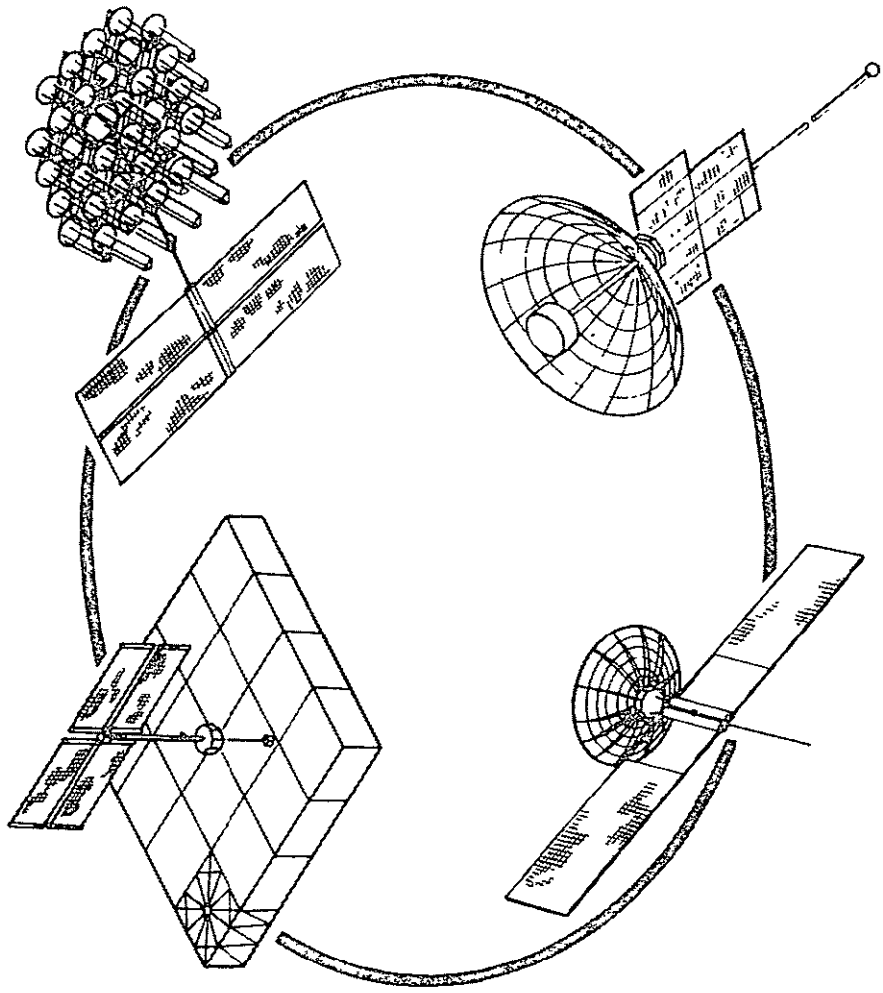

VOICE BROADCAST MISSION STUDY
NASW 1475

GENERAL ELECTRIC
MISSILE AND SPACE DIVISION

SECTION 1

INTRODUCTION

The purpose of the Voice Broadcast Mission Study (VBMS) was to investigate the technological and cost factors associated with satellite designs for direct broadcast of voice programs to home receivers. The investigation included development of satellite conceptual designs for three frequency bands. These were the HF short wave band (15 to 26 MHz), the standard VHF-FM band (88 to 108 MHz), and the UHF-TV band (470 to 890 MHz) for voice-only transmissions. A prime consideration in the conceptual designs was to minimize the need for modifications or expenditures to the home receiving system.

An added purpose of the study was to evaluate man-made noise in the short wave and FM bands by conducting a noise measurement program. The program consisted of measurements of absolute and relative levels of man-made noise at three types of locations; i.e., urban, suburban, and rural. It also included an evaluation of the noise discrimination provided by home antennas.

1.1 SUMMARY

The Voice Broadcast Mission Study resulted in the definition of four conceptual satellite systems, one for the HF band, two for the VHF band, and one for the UHF band. The details of these configurations are summarized in Table 1.1-1. As shown in the table, the resulting configurations encompass a large range of satellite parameters. For example, the range of effective radiated power included is a factor of fifty, the resulting weight has an eight to one range, and the total program costs cover more than a two to one range.

The major conclusions resulting from the study are (1) direct broadcasting from satellites is technically feasible by the early 1970's, and (2) for selected combinations of mission parameters (duty cycle, coverage area, system life), space broadcasting can be comparable or lower in cost than equivalent terrestrial systems. In addition, the following significant technical results were derived:

a. Only circular, equatorial orbits (either synchronous or subsynchronous) are practical for broadcasting at the same time on a daily repeat basis throughout the year.

b. Propagation effects are essentially limited to a factor of two (3 db polarization loss) except at extreme latitudes.

c. Man-made noise is a predominant satellite sizing factor to reach urban audiences in the HF and VHF bands, while building attenuation is an important factor at UHF.

d. Existing satellite attitude control techniques and components appear adequate for the large flexible vehicles but further dynamic analysis and modeling are required.

e. Large, high gain erectable antennas are feasible and will permit low weights and packaging volumes. However, developments to verify deployment techniques by testing in a one g field are required.

f. The high levels of power can be provided by state-of-the-art solar array techniques. Development programs which will support the design of the roll-out arrays are now being conducted.

g. Transmitters for the required high power levels can be designed with existing components (transistors for the HF and VHF frequency bands, and gridded vacuum tubes for the UHF band). However, developments on both device types should be initiated to extend efficiency and operational life.

Table 1.1-1. Configuration Results

Systems Parameter	Configuration			
	HF	VHF No. 1	VHF No. 2	UHF
Frequency, MHz	15.1, 17.7, 21.45, 25.85	100 to 108	100 to 108	870
Effective Radiated Power, dbw	52.1	65.4	48.1	63.6
Orbit Altitude	4356	19323	7556	19323
Antenna Beamwidth, D	20	7.5	18.5	3.75
Antenna Type	Phased Array of Cavity-Backed Spirals	Phased Array of Helix Elements	Parabola	Parabola
Power Supply Level, kw	15.4	11.38	1.36	2.54
Power Supply Type	Oriented Solar Array and Batteries	Oriented Solar Array	Fixed Solar Array	Oriented Solar Array
Transmitter RF Power, kw	8.8 (At 100% modulation)	7.07	0.82	1.15 (575 W per carrier)
Transmitter Type	Transistor	Transistor	Transistor	Tube
Attitude Control Accuracy, Deg.	$\pm$0.2	$\pm$0.1	$\pm$1.0	$\pm$0.1
Attitude Control Type	3 Axis Active	3 Axis Active	Hybrid Gravity Gradient	3 Axis Active
Launch Weight, lb	4870	2649	835	2641
In-Orbit Weight, lb	4741	2560	771	1126
Booster Type	Titan 3F	Titan 3F	Atlas Plus Improved Agena D	Atlas Plus Improved Agena D Plus Apogee Kick Motor
Total System Cost, $\$x10^6$ (includes 2 satellites & boosters)	101.5	99.1	48.2	55.5

1.2 STUDY APPROACH

The study was conducted in three phases as shown in Figure 1.2-1.

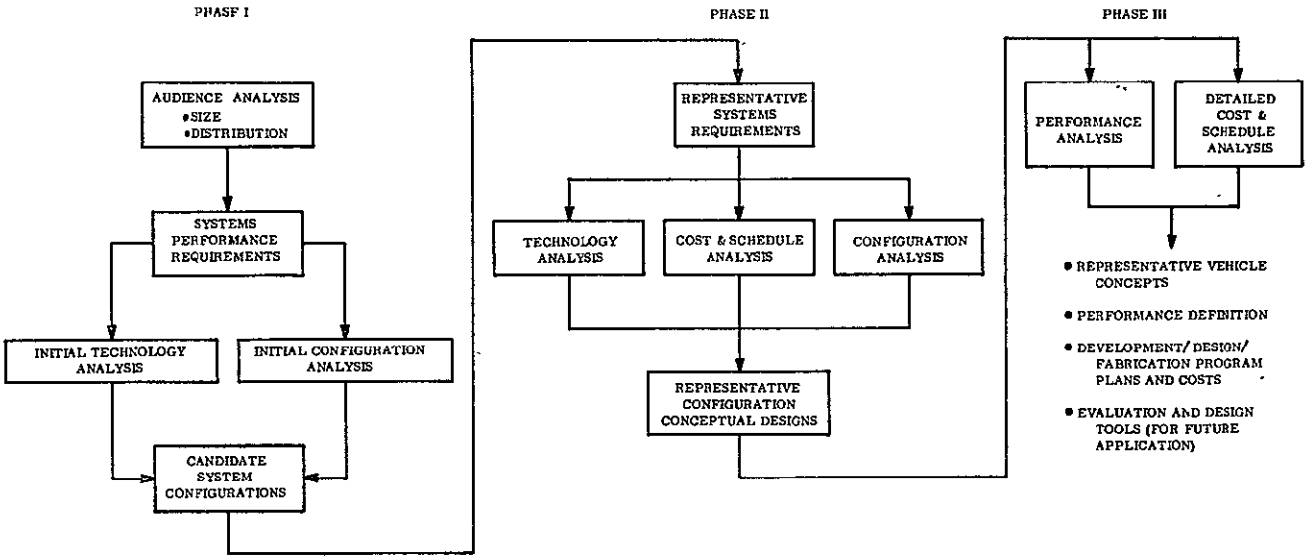

Figure 1.2-1. Study Plan Flow

The first phase (6 weeks) considered the mission requirements in terms of the audience available (receiver distributions) and the signal level requirements for the possible receiving conditions. The mission analysis results were used to define satellite performance requirements from which candidate configurations were developed. In support of the configuration analyses, all of the critical subsystem technologies were evaluated to determine the technical and time limitations on performance. The candidate configurations and analysis results were presented to NASA at a formal briefing at the end of Phase 1.

The second phase effort (6 weeks) was to select satellite system design goals for each of the frequency bands (HF, VHF, and UHF), with the concurrence of NASA, and to develop for each of these sets of goals a representative configuration by conducting the necessary technology, performance, cost, and schedule analyses. The results of the analyses were presented to NASA in a Technical Design Review at the end of Phase 2.

The third phase effort (10 weeks) was to (1) refine the conceptual designs of the preferred configurations, (2) develop detailed performance, cost, and schedule information and (3) to prepare technology recommendations.

Man-made noise measurements were made and evaluated during the study program. Man-made noise data was collected in urban, suburban and rural sites in the Philadelphia area.

1.2.1 PHASE 1 STUDY APPROACH

The Phase 1 tasks included mission, system, technology, and configurations analyses. The key factors considered were:

A. MISSION DEFINITION AND SYSTEMS ANALYSIS

- Audience (Receiver Distribution)
- Frequency Selection
- Coverage Area
- Orbit Mechanics
- Receiver Characteristics
- Signal Quality and Level Requirements
- Effective Radiated Power Requirements

B. COMMUNICATIONS TECHNOLOGY

- Home Antennas
- Propagation Factors
- Satellite Antennas
- Satellite Transmitters
- Uplink Frequency and Equipment

C. SPACECRAFT TECHNOLOGY AND CONFIGURATIONS

- Attitude Control
- Prime Power Sources
- Booster Capabilities

The approach used to interrelate and analyze these factors in illustrated in block diagram form in Figure 1.2-2.

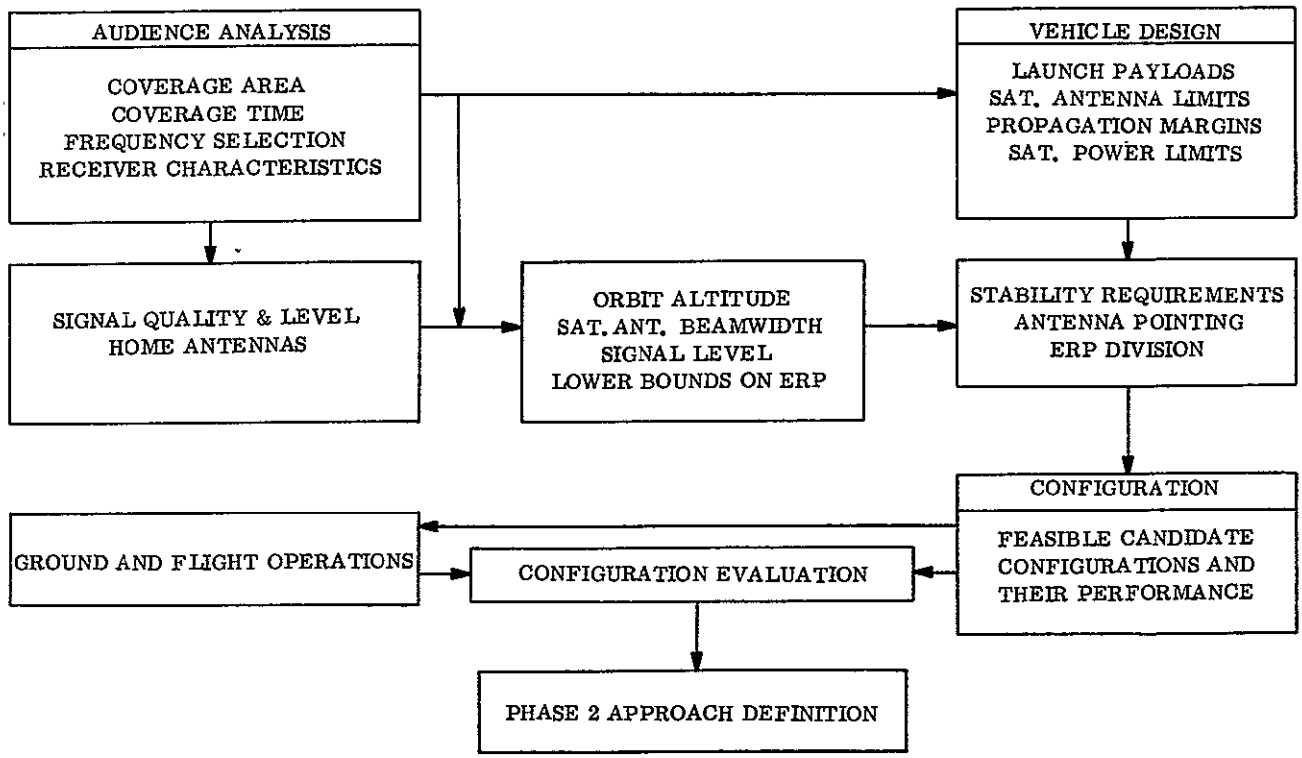

Figure 1.2-2. Phase 1 Study Approach

The mission was defined in terms of the potential audience. The world-wide distribution of various types of radio receivers permitted selection of representative satellite orbits and antenna beamwidths giving appropriate area and time coverages. A study of typical receiving equipment characteristics defined the level of broadcast signals required on the ground to give a specified performance. These factors, taken together, determined the effective radiated power requirements for the satellite.

The vehicle design portion of the diagram shows the studies carried out to place gross bounds on vehicles. These included satellite antenna gain and supply power limitations as well as the constraints due to launch vehicle capabilities and propagation losses. These factors, together with vehicle attitude control and antenna pointing requirements were used to obtain reasonable limits on the division of the Effective Radiated Power (ERP) between antenna gain and satellite power.

The ERP division detemined the satellite requirements to fulfill a particular mission. The mission was specified in terms of the frequency band, the signal level at the ground, and the coverage time and area. These requirements defined feasible configurations, including the ground support.

The evaluation of the resulting candidate configurations relative to the set of mission requirements permitted the selection of specific configuration design goals and optimization criteria for the Phase 2 efforts.

1.2.2 PHASE 1 NASA REVIEW

The candidate configurations synthesized in the Phase 1 effort were presented to NASA in a formal briefing at the end of the phase 1 period. After this review, a set of design goals for the Phase II representative configurations were prepared in conjunction with NASA personnel. The goals defined considered coverage areas and locations, broadcast duty cycles, signal levels, operating life, and launch time for each of the specific frequency ranges. The specific goals selected and the reasons for each are described below.

1.2.2.1 HF Configuration Design Goals

The major advantages of an HF configuration are (1) the large population of receivers and (2) the acceptance by the potential audience of lower quality signals than for the other frequency bands. The major areas of difficulty include the propagation factors, which are not yet adequately defined, and the large antenna aperture sizes necessary to achieve high gain. The design goals, based on these factors, were:

a. Coverage of areas of at least 1.8 million square nautical miles of earth surface (i.e., an area subtended by an earth central angle of 24°) anywhere between North and South latitudes of 45°. Only one such area had to be covered at a particular instant of time. This is consistent with covering all high population density areas of all major languages of the world in temperate zones.

b. This coverage would be for a minimum of 1 hour on a daily repeat. A minimum of three such broadcasts per day to different areas were desired for maximum usage. This is consistent with current broadcast periods in the HF bands, with greatest utilization of the satellite system that can be practically obtained, and with the NASA requirement for at least 1 hour per day coverage to a given area.

c. The system would be designed to deliver between 150 and 400 μv/m to the ground. The maximum upper goal was 400 μv/m 50% of the time. However, at least 150 μv/m (50% of the time) was a lower limit that had to be achieved for the system to be considered practical. These bounds appeared to best fit the goals of currently operational HF broadcast ground stations, would give good coverage to low man-made noise areas, and would allow people in high man-made noise areas to obtain the broadcast with reasonable (i.e., 8 db gain or less) outside antennas.

d. The expected life of the vehicle had to be 2 years.

e. This design had a goal of vehicle launch by mid-1972.

f. This configuration had to have the ability to transmit (one channel at a time) in any one of the four highest HF bands.

1.2.2.2 VHF 1 and VHF 2 Configuration Design Goals

The major advantages of a VHF configuration are : (1) broadcasting in this band is established in most parts of the world, (2) the signal strength requirements are reduced compared to the HF band because of the low man-made noise background at the higher frequency and the improvement factor due to FM modulation, and (3) the reduction of antenna size (both home and satellite) as compared to HF. The only areas of difficulty are (1) getting an accurate definition of the range of receiver characteristics and (2) obtaining coverage over wide areas and simultaneously providing adeuqate quality signals to high-noise urban locations within the coverage area. As a result of these factors, two sets of VHF design goals were established, as follows:

1.2.2.2.1 VHF Configuration 1 Design Goals

a. Broadcast to is the area (USA) with the largest single language potential audience in the VHF band.

b. To give coverage had to be for as long a period throughout the day as possible without requiring broadcasting when the satellite is in the earth shadow. The down time would be less than 2 hours about midnight for a few months of the year.

c. The satellite had to have the ability to transmit to three other locations. The maximum time for these tests, including relocation time, will be 3 months.

These three areas had to be represented by a northern site, a southern site, and an equatorial site. This requirement is consistent with the fact that the potential audience with FM receivers is widely distributed about the world.

d. The system would be designed to deliver between 50 and 180 μv/m signal level to the ground sufficiently large to reach all receivers. The design goal was 180 μv/m 90% of the time. However, at least 50 μv/m (90% of the time) is a lower limit for a practical system. These bounds are consistent with an internationally recognized signal level in a low man-made noise area. The higher goal based on reaching as large an audience as audience as possible in areas of high man-made noise.

e. The expected life of the vehicle had to be 2 years.

f. This design had a goal of vehicle launch by mid-1972.

1.2.2.2.2 VHF Configuration 2 Design Goals

a. Minimum coverage of areas of approximately 1.8 million square nautical miles of earth surface (i.e., an area subtended by an earth central angle of 24°) anywhere between North and South latitudes of 60°. Only one such area had to be covered at a particular instant of time. This size area is consistent with covering all high population density areas of all major languages of the world.

b. The maximum coverage time to a given area had a lower limit of 1 hour per day and an upper limit of 4 hours (on a daily repeat) for a vehicle that did not have to track the sun with solar panels. This permitted coverage of many areas of the earth, which is consistent with the widely distributed FM audience.

c. The signal level design goal of 50 μv/m (90% of the time) was chosen on the basis that this gives good coverage to the areas of low man-made noise with some probability of reaching the audience in a high man-made noise area where outside antennas might be installed.

d. The expected life of the vehicle had to be 2 years.

e. The design had a goal of vehicle launch as early as possible in the early 1970's.

1.2.2.3 UHF Configuration Design Goals

The major advantages of a UHF configuration are (1) smaller coverage areas than in other bands, and (2) ability to use high-gain antennas. The two major areas of difficulty are (1) the requirement for two carriers (picture and aural) to operate the UHF TV receivers, which requires four times more power than an equivalent single channel receiver, and (2) the high-gain antenna advantage can be achieved at the cost of precise pointing. Considering these factors, the design goals selected were:

a. Broadcast to continental U.S. because this is the area in the world with the largest potential audience in the UHF band.

b. Coverage of one time zone at a time to permit utilization of a high-gain antenna.

c. Coverage for as long a period throughout the day as possible without requiring broadcasting when the satellite is in the earth shadow. The down time will be less than 2 hours about midnight for a few months of the year and is not inconsistent with current schedule times of many UHF/TV stations, while giving the longest reasonable demonstration time.

d. The signal level goal was 106 μv/m (99% of the time) for each carrier. This is representative of the required level for an urban located receiver using an outside dipole oriented in azimuth for best signal reception.

e. The expected life of the vehicle had to be 2 years.

f. This configuration was to have a switchover alternate mode of operation capable of broadcasting a wide band signal. This signal was defined as having a baseband of 5 MHz and a deviation of $\pm$15 MHz about the carrier (Note that only one carrier will be transmitted in this mode.) This is compatible with typical data and video distribution system parameters.

g. This design had a goal of vehicle launch as early as possible in the early 1970's.

1.2.3 PHASE 2 STUDY APPROACH

Based on the previously described design goals, the Phase 2 effort was aimed at determining optimum representative configurations, i.e., optimum relative to the criteria defined for each system. The approach used to achieve these goals is illustrated in Figure 1.2-3, which shows the information generation and flow used for synthesizing the configurations.

The first major step was to define the orbital parameters and the ERP. It was then possible to specify a benchmark system. This, by definition, assumed for the convenience of this study, was a limit system utilizing the highest possible antenna gain. That is to say, of all possible ERP divisions, this assumes an antenna whose beamwidth is no larger than that necessary to just cover the specified ground area and the smallest possible power supply. With this as a starting point, these configurations were evaluated with respect to predetermined optimization criteria.

The factors considered for optimizing the systems were cost, interference outside the specified broadcast area, and minimum R&D effort so earliest possible launch may be obtained. The order of priority of these factors was determined for each system based on the considerations peculiar to that system.

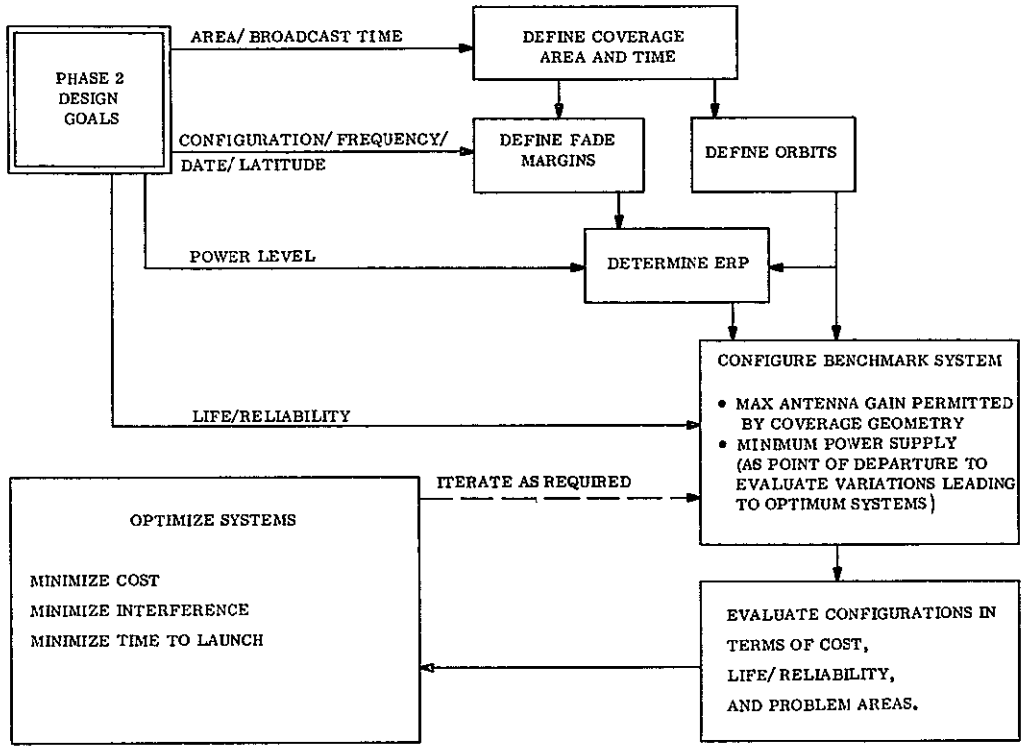

Figure 1.2-3. Ph Tradeoff Analysis Flow

1.2.4 PHASE 2 NASA REVIEW

The representative configurations conceived in Phase 2 were presented to NASA in a formal briefing at the end of the Phase 2 period. NASA concurred with the configurations and the detailed plans for Phase 3.

1.2.5 PHASE 3 STUDY APPROACH

The third and final phase of this study consisted of more detailed analyses of the four representative configurations developed in the second phase. There were three major categories of analysis to be performed. First was an analysis of the performance of each configuration. This included such items as the determination of the signal levels inside and outside the specified coverage area, the system degradation modes, and the reliability performance. Second was an analysis of total program costs for each system. This was determined by analyzing the costs of R&D, initial investment, and operation. Finally, the complete program development schedule was determined for each configuration, including the R&D, manufacturing, and test plans. The items receiving most attention were those having significant effects on performance, costs, and plans.

The approach used to achieve the above goals are diagrammed in Figure 1.2-4. The starting point was the Phase 2 definition of the four configurations. As the long lead

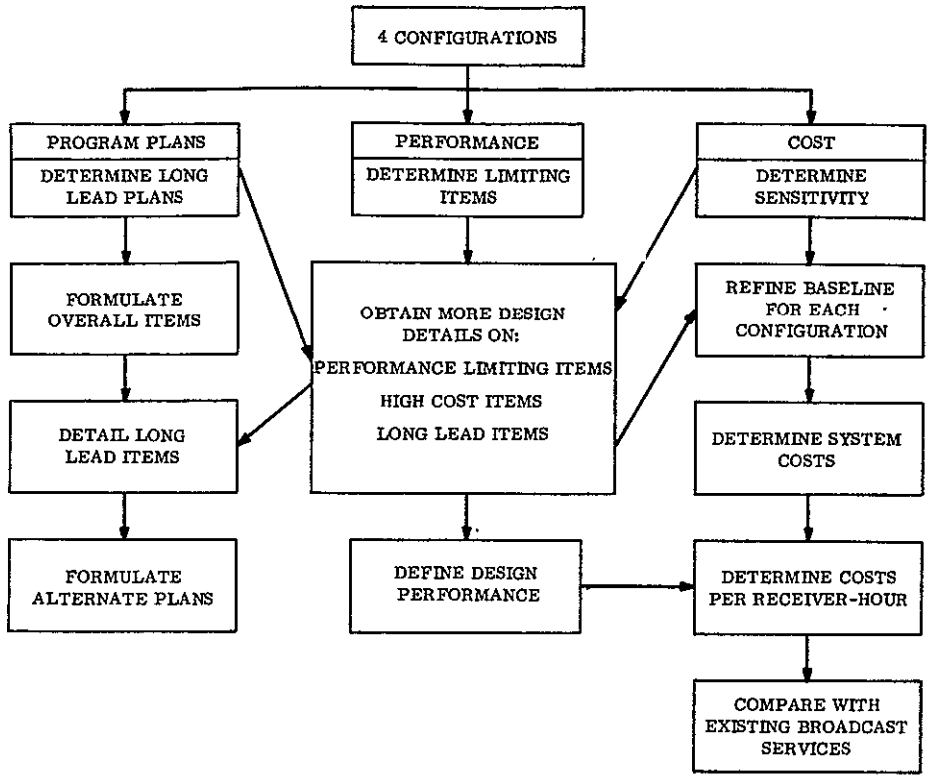

Figure 1.2-4. Phase 3 Study Approach

items were defined, and as the cost sensitive factors were determined, further design details were generated to obtain better information on these items. This permitted an iteration of the plans and costs to refine the results in each area.

Performance and cost were also integrated to define the operating cost per receiver reached per hour of broadcast. These values were compared with the costs per receiver-hour of existing terrestrial services to get an indication of the relative cost-effectiveness of space broadcasting approaches.

1.3 REPORT ORGANIZATION

This VBMS final report has been prepared in two volumes. The first volume, under separate cover, is a brief summary of the study results.

The second, this volume, is a detailed report of the study. The body of this report is organized into six sections as follows:

a. Section 1 - Summary and brief description of the study phases.

b. Section 2 - Mission analysis performed to generate data needed to specify the systems requirements.

c. Section 3 - Systems analysis performed to specify the subsystem requirements for satellites to broadcast in the HF, VHF, and UHF frequency bands.

d. Section 4 - Technology evaluations performed to select and define the necessary subsystems for the four configurations conceived for the three frequency bands.

e. Section 5 - The conceptual drawings of one HF, two VHF, and one UHF broadcast satellites.

f. Section 6 - The evaluation of the four satellite systems in terms of performance, program plans, system costs and cost effectiveness, and recommendations for the technology developments necessary to reduce these concepts to hardware.

SECTION 2

MISSION ANALYSIS

2.1 INTRODUCTION

The principal factors considered in this study for operational broadcast satellites are people, environment, equipment, and time. The variables necessary to define specific missions are shown in Figure 2.1-1.

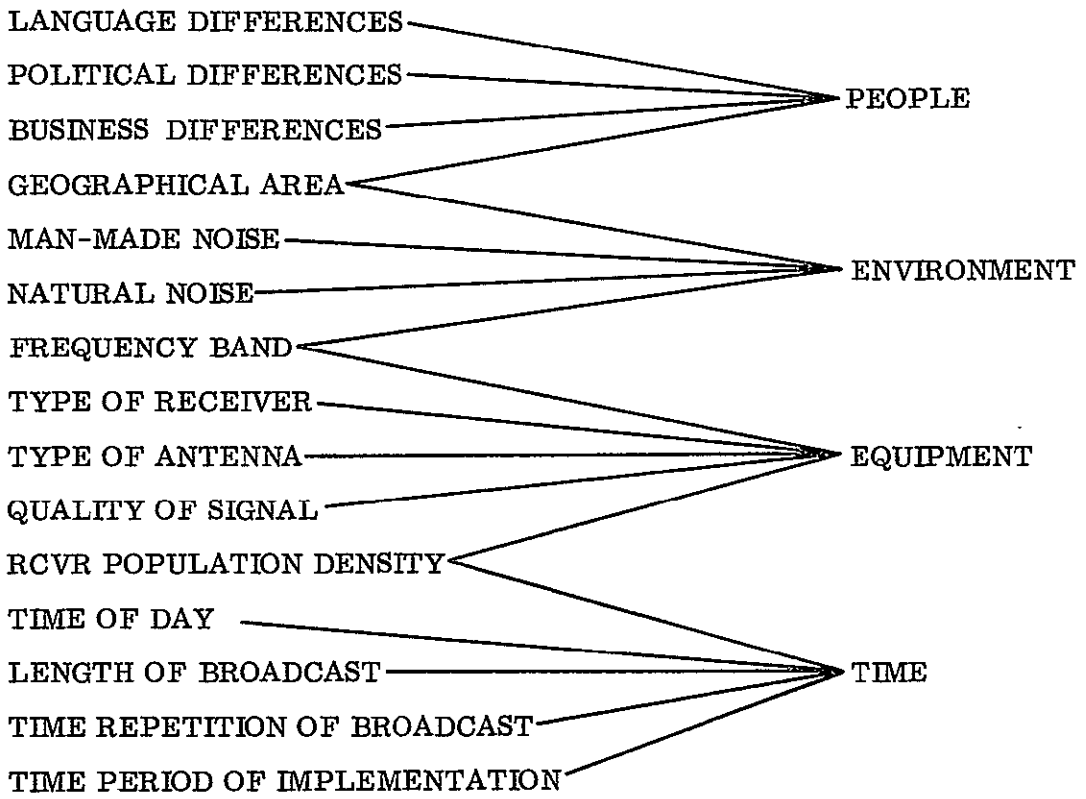

Figure 2.1-1. Variables for System Selection

When considering people, their language differences and geographic location helped to define the necessary area coverage of the satellite. Both political and business considerations may alter these coverage areas, but neither of these factors have been considered in this study.

The receiver environment, in terms of the man-made and atmospheric noise, determined the broadcast signal strengths for a given quality. Noise is a function of location with respect to industrialization, as well as the frequency band of the broadcast. The type of radio receiving equipments (receivers and antennas), their band of operation, and their locations determined the potential audience for a given broadcast signal. The desired quality of signal, in terms of signal-to-noise ratio expected in a given frequency band, affects the signal level required.

Finally, time is important. The various times of interest are the length, or duration, of the broadcast to a given area; the ability to repeat the broadcast on the basis of some given schedule, the time of day, and the calendar year in which the system will be implemented.

The study included an analysis of these factors and the resulting satellite design requirements and implications. The results of the analysis are described in this section of the report.

The orbit analysis evaluated all of the types of orbits potentially useful for space broadcasting and determined that only the synchronous (or subsynchronous), circular, equatorial, posigrade orbits will completely satisfy the requirement of daily repeat broadcasts to a fixed area at the same time of day each day. As a result, the only orbit parameters that had to be specified were altitude (defined by the coverage time), and position for synchronous orbits.

The analysis of environmental factors (noise and propagation effects) determined the following results. The propagation effects (fading, Faraday rotation, absorption, etc.) are significant only at the lower frequencies and at extreme latitudes (greater than 45° from the equator). The noise analysis was conducted as part of a man-made noise measurement program and determined that previous estimates of man-made noise levels were too high, by more than an order of magnitude in urban areas. In addition, the discrimination potential of home antennas to man-made noise was experimentally determined to be one-half the forward gain of the high gain antenna when expressed in db.

Home receiving systems were analyzed from several viewpoints. First, the home antenna characteristics and distribution were evaluated. Second, the characteristics of receivers were evaluated and signal levels necessary to produce satisfactory quality signals determined. Finally, the more significantly, the current and projected distributions of receivers, in each of the frequency bands, throughout the world were determined to allow synthesis of logical voice broadcast missions.

2.2 ORBIT ANALYSIS

2.2.1 INTRODUCTION

This section describes the orbital analysis performed to determine the advantages and disadvantages inherent in various orbits for direct broadcast satellite systems. Posigrade and retrograde orbits with varying altitudes, inclinations, and eccentricities were studied in terms of land area broadcast coverage, and broadcast duty cycles from one hour per day to continuous. This analysis determined that three specific types of orbits were optimum for broadcast demonstration missions. They are:

a The geostationary, circular orbit for continuous broadcasting to specific areas of the world every day of the year at the same local broadcast times.

b. The near-geostationary, circular (walking) orbit for conducting demonstration tests on a world wide basis over a one or two year period. Broadcasts to specific areas could range from one hour per day to continuous at the same local broadcast times each day for intervals from weeks to months.

c. Sun-synchronous, circular, equatorial orbits for one to several hours of broadcasting to specific areas of the world every day of the year at the same local broadcast times.

The specific orbits for each of the four configurations were selected in conjunction with other system trade-off analyses. This information is given in Section 3.

2.2.2 ORBIT TYPES STUDIED AND SELECTED

The requirement to broadcast to the same area each day at the same local time carries two major implications. First, the satellite ground trace must repeat itself on a daily basis. Second, the relative position of the satellite to the earth-sun line must also be the same when passing over the same meridian each day.

2.2.2.1 Geostationary and Near-Geostationary (Walking) Orbits

The geostationary orbit is the only orbit which permits a single satellite to continuously broadcast to a given area on the earth's surface World wide coverage of inhabited land areas would require three satellites in geostationary orbits for continuous broadcasting to any of the areas. Other orbits could also give continuous global coverage if a multiple satellite system were employed. However, the study scope pervented consideration of multiple satellite systems.

A walking, near-geostationary orbit will permit broadcasts on a world wide basis over a one to two year interval by limiting the test to several weeks or months for any one area. The daily broadcasts to several areas within the satellite field-of-view could occur at the

same time of day each day of the test period (weeks or months). The length of the broadcast per day to one area would depend upon the number of areas per day receiving broadcasts. The same performance could be obtained by repositioning the longitudinal location of a geostationary satellite several times during a one to two year demonstration test period.

Analysis of the geostationary orbit is necessary to select the optimum longitudinal satellite location for coverage of a given area on the earth's surface as a function of antenna beamwidth, antenna beam pitch and azimuth pointing angles, maximum slant range and ground antenna elevation angles. Table 2. 2-1 shows the geometry and results of such an analysis for a geostationary satellite which can broadcast to any of the four time zones in the United States. Figure 2. 2-1 is a plot of the antenna beam pitch and azimuth pointing angles as a function of satellite longitudinal location for broadcasting to the entire continental United States. Figure 2. 2-2 is a plot of antenna beamwidth as a function of satellite longitudinal location for broadcasting to the entire continental United States.

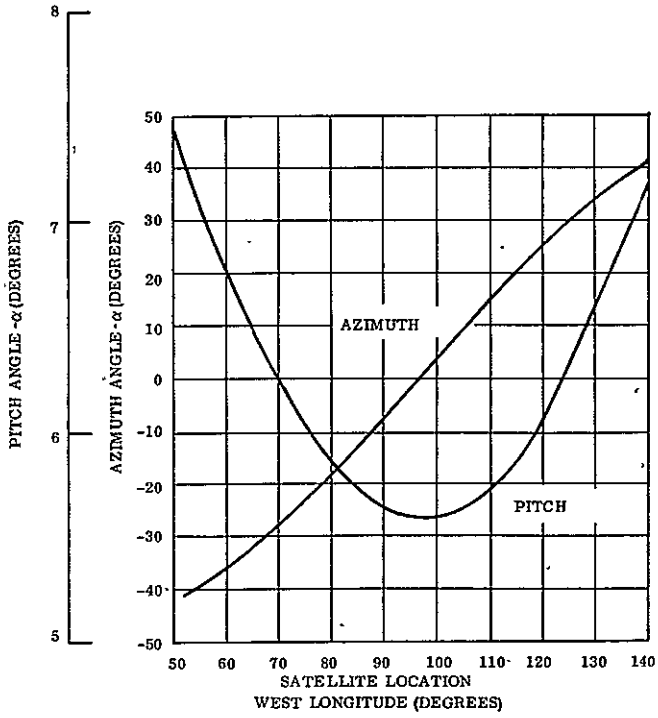

Figure 2. 2-1. Required Beam Pointing Angles of a Synchronous Equatorial Satellite for United State Coverage

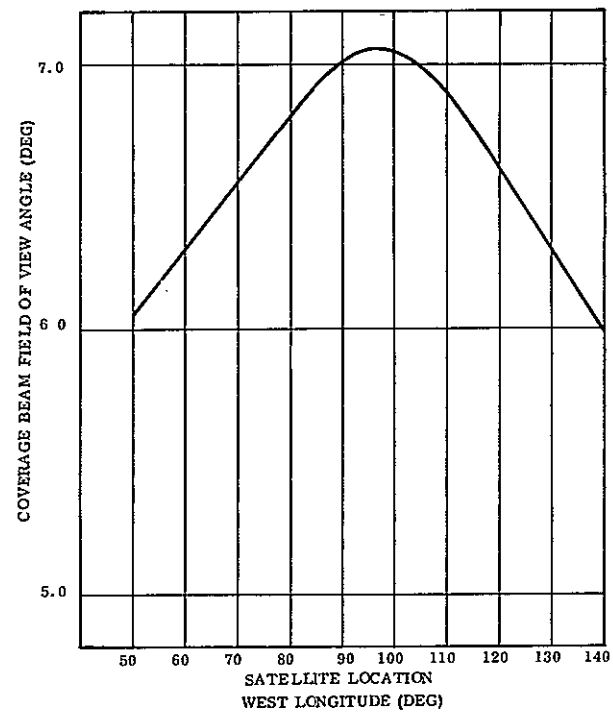

Figure 2. 2-2. Required Coverage Beam Full Angle of a Synchronous Equatorial Satellite for United States Coverage

The results were obtained by positioning the satellite at various station longitudes and then determining both the azimuth and pitch angles necessary to direct the beam to a central position within the United States The satellite beam full angle was then varied and the

Table 2.2-1. Conditions for Transmitting to the United States

TIME ZONE	SATELLITE LOCATION		BEAM $\mathbb{C}_L$ LOCATION		BEAM WIDTH	AZIMUTH	PITCH	SLANT RANGE	GROUND ELEV.
	θ_S	ϕ_S	$\theta_{\mathbb{C}_L}$	$\phi_{\mathbb{C}_L}$	β	$A_{\mathbb{C}_L}$	$\alpha_{\mathbb{C}_L}$	$R_{\mathbb{C}_L}$ (NM)	$\delta_{\mathbb{C}_L}$
EASTERN	0°	-92	37°N	-79°	3.5°	16.12°	6.136°	20200	45°
CENTRAL	0°	-92	37°N	-95°	3.5°	-3.97°	5.915°	20110	47°
MOUNTAIN	0°	-92	37°N	-105°	3.5°	-16.62°	6.136°	20200	45°
PACIFIC	0°	-92	37°N	-112°	3.5°	-24.41°	6.424°	20310	42.3°

θ_S LATITUDE OF SATELLITE LOCATION

ϕ_S LONGITUDE OF SATELLITE LOCATION, POSITIVE EAST

$\theta_{\mathbb{C}_L}$ LATITUDE OF BEAM CENTER LINE ON EARTH

$\phi_{\mathbb{C}_L}$ LONGITUDE OF BEAM CENTER LINE ON EARTH

$A_{\mathbb{C}_L}$ AZIMUTH ANGLE, POSITIVE MEASURED CLOCKWISE FROM NORTH

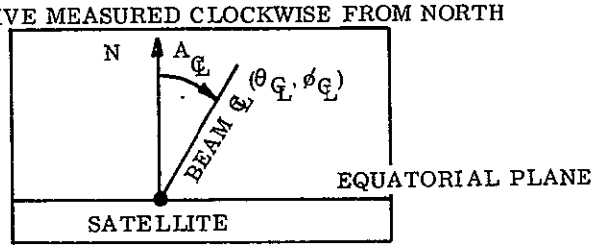

α PITCH ANGLE, POSITIVE MEASURED CLOCKWISE UP FROM THE LOCAL VERTICAL

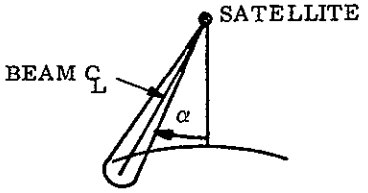

R SLANT RANGE, MEASURED FROM SATELLITE TO BEAM $\mathbb{C}_L$ LOCATION

δ GROUND STATION ELEVATION ANGLE AT $\theta_{\mathbb{C}_L}$, $\phi_{\mathbb{C}_L}$

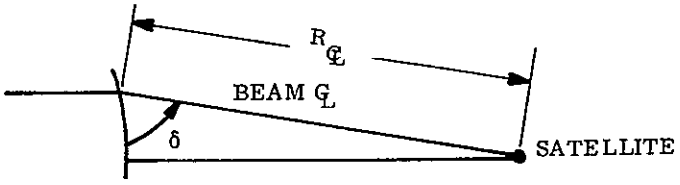

resulting coverage area displayed on a Mercator Map of the world. From these coverage plots a minimum satellite beam angle was then determined. The pitch angle is positive measured up from the local vertical. The azimuth angle is positive measured clockwise from North.

Figure 2. 2. 3 shows the antenna beam-width coverage for each time zone in the United States employing the previously explained analysis technique and the results given in Table 2. 2-1.

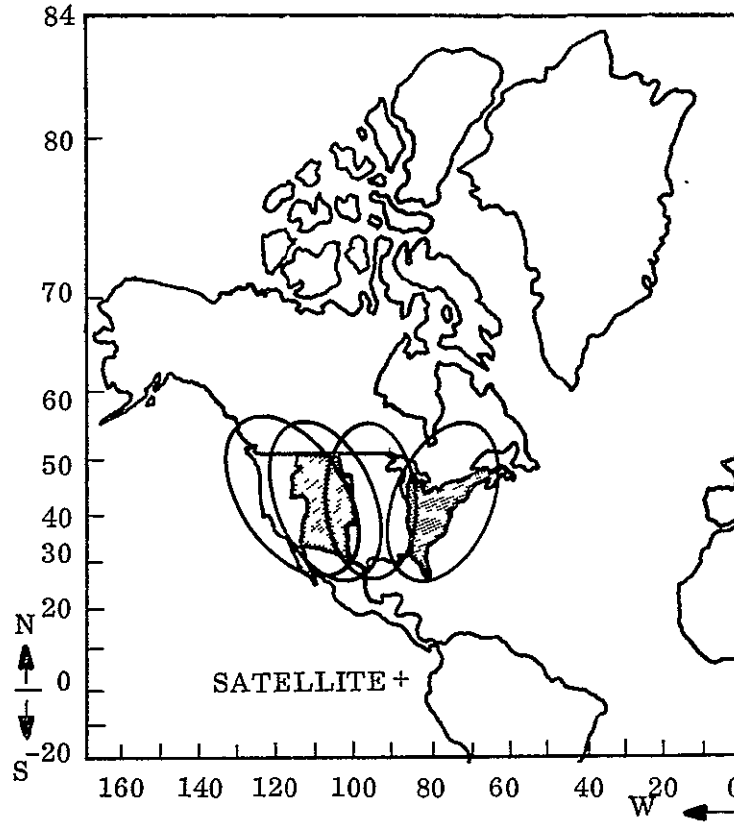

Figure 2. 2-3. U. S. Time Zone Coverage

2. 2. 2. 2 Retrograde Sun-synchronous Orbits

The retrograde sun-synchronous orbits were investigated to determine their capability of permitting a satellite to broadcast to the same area each day at the same local time. By varying altitude, inclination and eccentricity, the forward advance of the orbit plane line of nodes will just equal the inertial rotation of the earth-sun line as the earth revolves around the sun. The average rate of advance is 0. 985 degree/day If a subsynchronous orbit period is found then the satellite will pass over the same time of day each day. A detailed study was made of this type of orbit and the results are plotted in Figure 2. 2-4

Shown on the plot is the class or orbits which:

a. Have periods which are given approximately by the relation

$$T = \frac{24}{\eta} \quad (\eta = 1, 2, 3 \ldots\ldots\ldots\ldots 24)$$

(i. e., the constraints which guarantees daily repeatability) and

b. Have an advance of the line of nodes given approximately by 0. 985 degree/day (i. e., the oblateness-connected constraint which guarantees the sunsynchronism of the orbit).

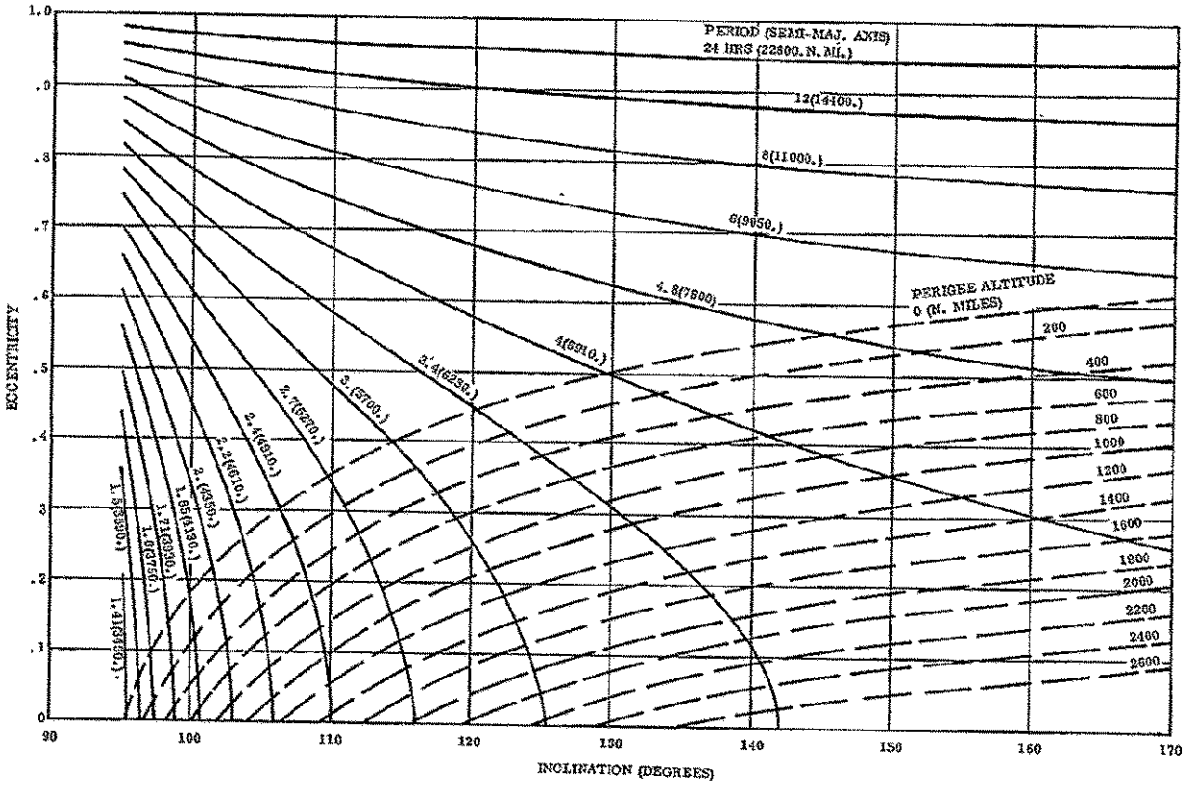

Figure 2.2-4. Retrograde Sunsynchronous Orbits

Eccentricity is plotted as a function of inclination for the family of curves of constant period which meet constraints (a) and (b). The dashed lines represent curves of constant perigee altitude. Note that $95^{o} \leq$ inclination $\leq 170^{o}$; this indicates that all orbits shown are of a retrograde nature. Note also that all points above the zero nm perigee altitude line are to be neglected, as the orbits will intersect the earth. As will be shown later in Figure 2.2-6, this orbit period will not provide the minimum one hour coverage. Eccentric orbits have the additional problem that the line of apsides (major axis direction) gradually rotates within the orbit plane. Thus, the apogee point varies slightly each orbit with the result that the ground trace is not strictly repetitious. The one exception is produced by an orbit whose inclination is 116.6 degrees (-63.4^{o}). For this orbit the line-of-aspides does not rotate and the apogee latitude will remain at its original location. Examination of Figure 2.2-4 shows that only one subsynchronous period has this inclination, 3 hr. The amount of coverage area is no larger than$\approx$ 45 degrees. Figure 2.2-5 shows conditions of 1 hr overlap when the apogee is over the equator. Slightly longer overlap times are attained when apogee is at higher latitudes. These retro-grade orbits barely meet the minimum requirement of time-in-view and coverage area and were rejected for bradcast satellites.

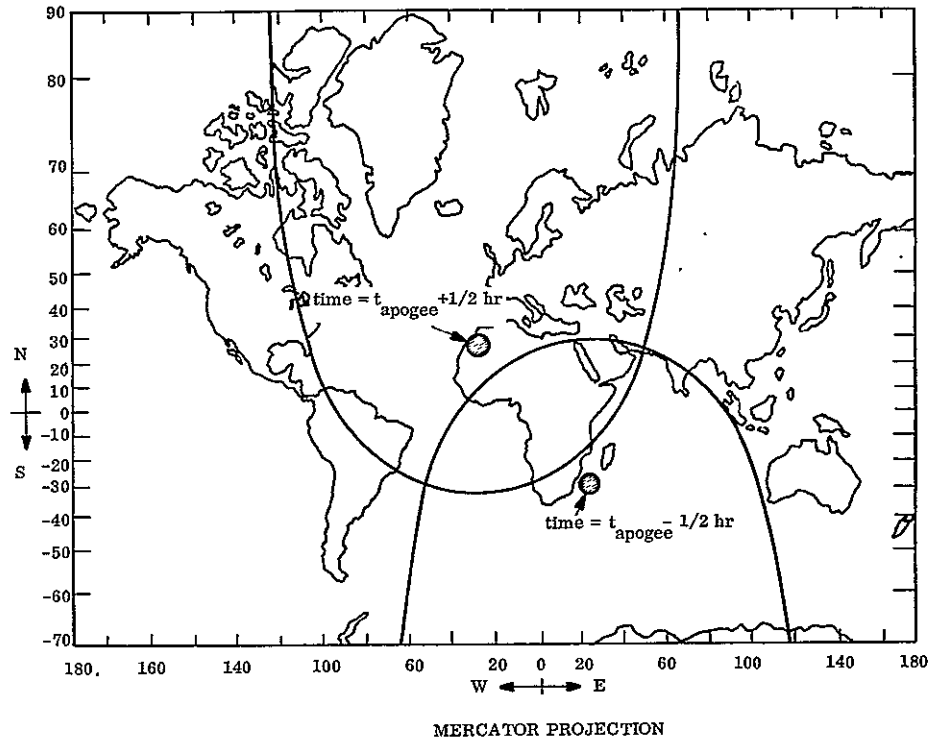

Figure 2.2-5. Retrograde Orbit Coverage Plot, (116.6° Inclined)

2.2.2.3 Posigrade Inclined Orbits

Both circular and eccentric posigrade inclined orbits were considered, but rejected since they would not permit the satellite to broadcast to the same area every day at the same local time. The orbit period could be adjusted to give overfly of the same latitude and longitude but it would not occur at the same time of day each day. Adjustments to the orbit period in order to gain some sort of sun-synchronism, can be made such that the satellite passes over the same meridian at the same local time each day. However, the latitude will change gradually on each orbit and during the course of one year the latitude of overfly would vary over the total range of latitudes defined by the inclination from maximum North latitude to maximum South. Elliptic orbits have the additional problem of line-of-aspides rotation.

2.2.2.4 Posigrade Equatorial Orbits

The only remaining useful orbits for repetitive daily broadcasting are equatorial, both circular and elliptic, whose periods are integers of one siderial day. That is, with periods causing the satellite to make exactly 1, 2, 3, 4.....24 revolutions per day. The orbit period is now adjusted to give rotation of 360.985 degrees per 24 hours, or 720.985 degrees per 24 hours ("12 hour period") or 1080.985 degrees per 24 hour ("8 hour period"), etc. The problem of latitude excursions is nonexistant since the latitude ia always zero.

The elliptical orbits were rejected for three basic reasons:

a. Transmission can take place only in areas near the apogee region. It would be possible to set up specific regions that coincide with apogee, but then there is no flexibility to transmit to other regions.

b. The second disadvantage is the varying altitude (and therefore, beamwidth) during the period of transmission.

c. The third disadvantage is the varying satellite velocity with respect to the broadcast coverage area, requiring more complex attitude control and antenna pointing subsystems.

Medium and low circular, equatorial, sun-synchronous orbits were selected for short broadcast times (one to four hours per orbit) to permit satellites with large antenna beamwidths and high ground signal strength requirements to take advantage of shorter slant ranges to minimize the satellite power required. Figure 2.2-6 shows the coverage time possible (to 24^{o} earth areas) versus the orbit period. Note that only these periods which are subsynchronous will give the required daily repeat. The area of interest is designated to be that area on the surface of the earth generated by a 24 degree Earth-central angle. The plot shows these areas with their respective centers up to 60 degrees latitude. The dotted lines intersecting the abscissa show orbit periods (and radii) for which a spacecraft will go over the same equatorial locations at the same time every day The dotted lines, intersecting the ordinate, indicate coverage times of one hour and four hours.

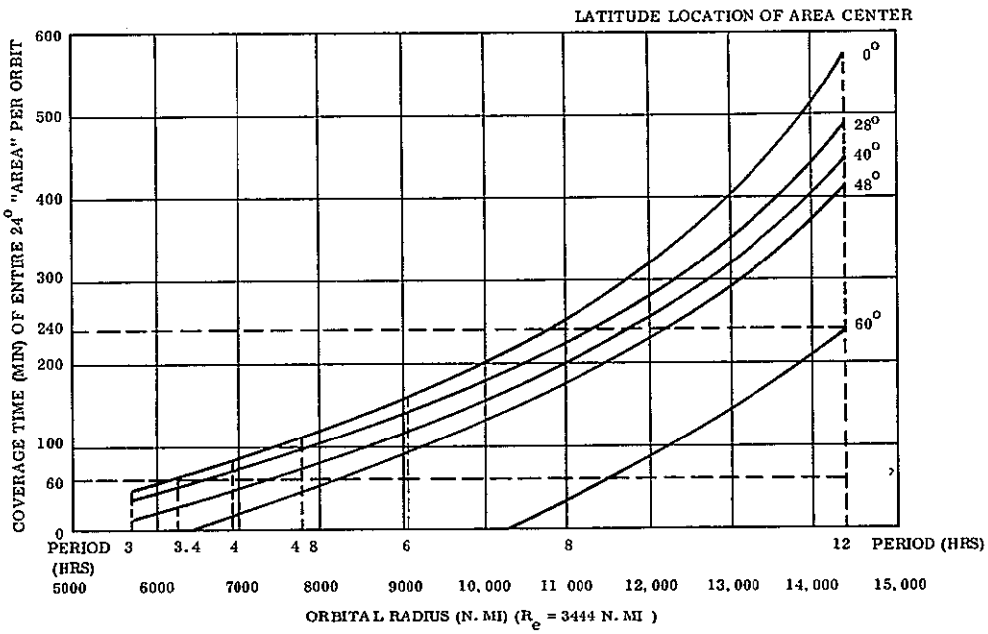

Figure 2.2-6. Coverage Times for 24^{o} Area Located at Various Latitudes as Viewed From a Spacecraft in a Circular Equatorial Orbit

A typical coverage plot of a posigrade equatorial orbit is shown in Figure 2.2-7. The slant lines along the equator show the one-hour durations of transmission that apply to the three overlapping beam projections on the earth at the closest coverage area. One beam represents the area covered at the start of transmission, one at the middle, and one at the end of broadcasting. The area common to all three beams is the ground area usable for broadcasting over the specified period. This type of analysis was repeated for many combinations of beam size, coverage area location, and orbit altitude to evaluate orbits for specific configurations.

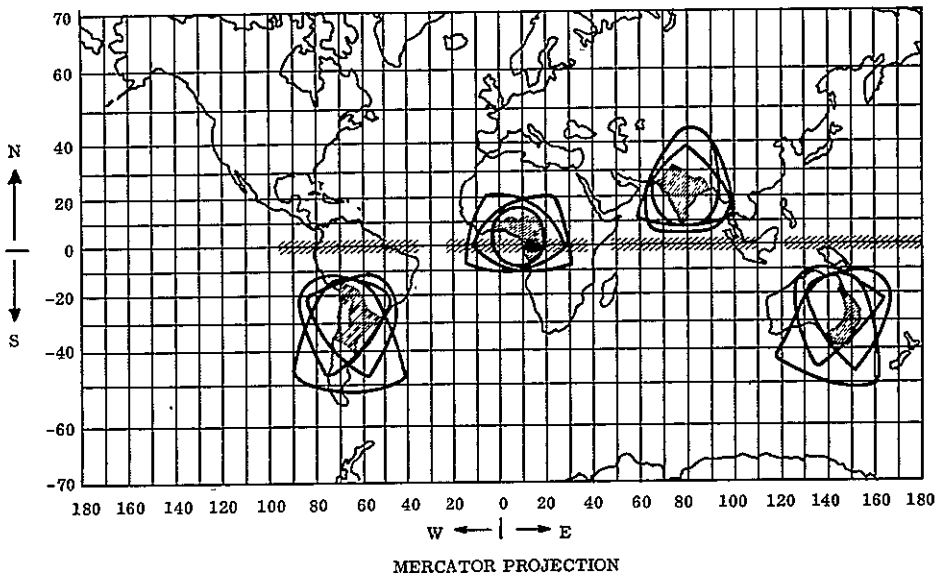

Figure 2.2-7. Example, Coverage Areas for Specified Broadcast Time

2.2.3 SHADOW HISTORIES

Figures 2.2-8 and 2.2-9 show the maximum time per orbit a satellite will spend in umbra and penumbra as a function of semimajor axis for a cirular equatorial orbit.

Figure 2.2-10 shows the time a synchronous satellite spends in the shadow of the earth as a function of date of year. The maximum time in the shadow occurs twice per year: once during the vernal equinox (March 21) and once during the autumnal equinox (September 21). The spacecraft passes into some shadow for about <90 days/year and is completely in the sun for about <270 days per year. This refers to the position of the sun along the ecliptic, where 0^{o} refers to the sun's position at the vernal equinox, 90^{o} to the summer solstice, 180^{o} to the autumnal equinox and 270^{o} to the winter solstice.

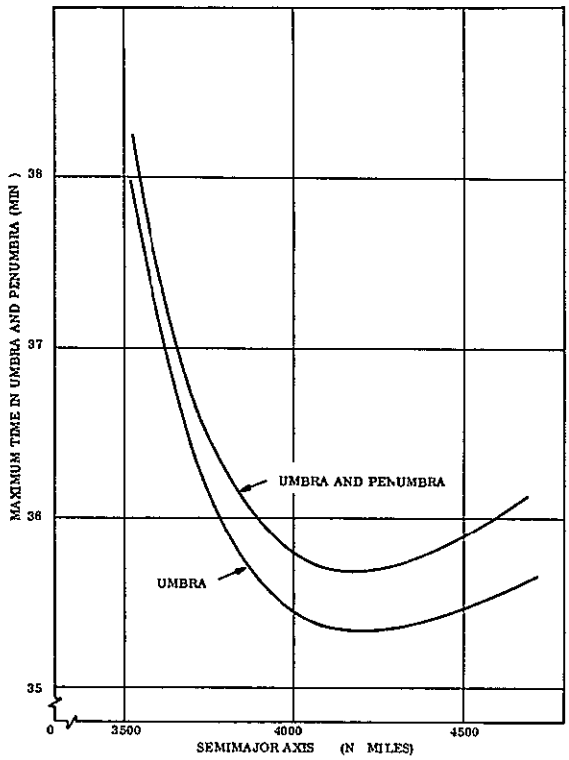

Figure 2.2-8. Shadow History Medium Altitude Orbits

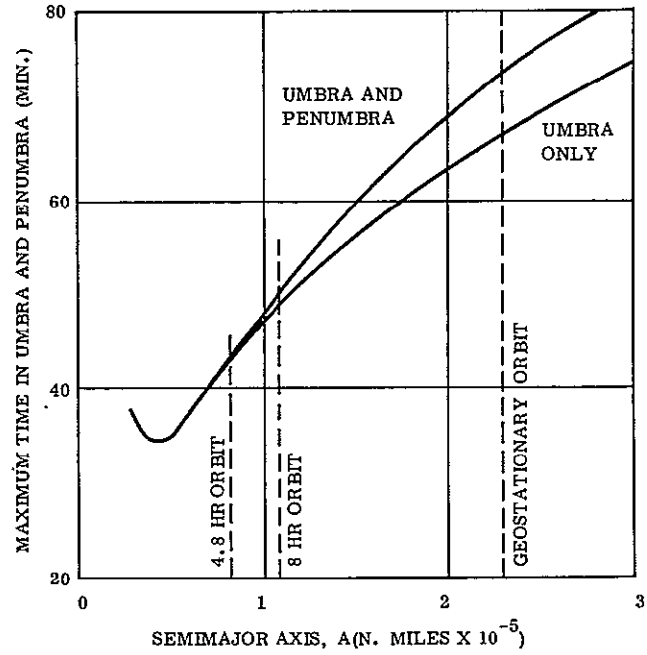

Figure 2.2-9. Shadow History High Altitude Orbits

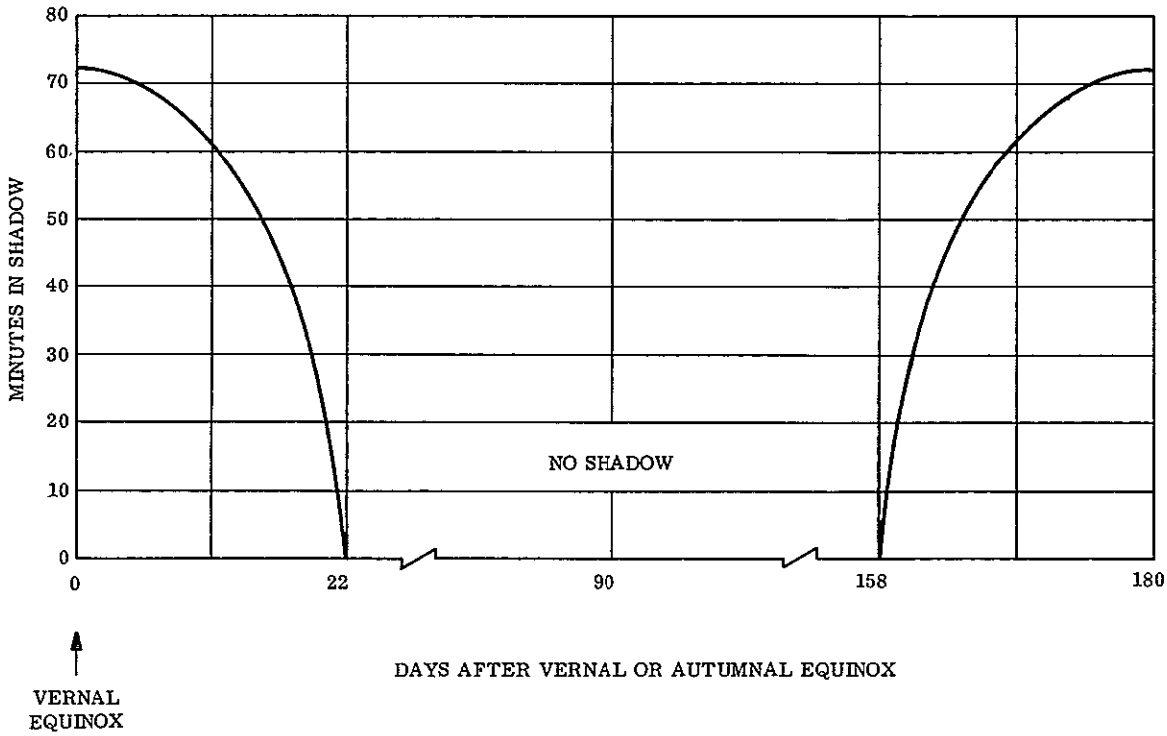

Figure 2.2-10. Daily Satellite Time in Shadow for Synchronous Satellites

Figure 2.2-11 shows a similar shadow history plot for satellites in circular, equatorial orbits with periods of 4.8 and 8 hours.

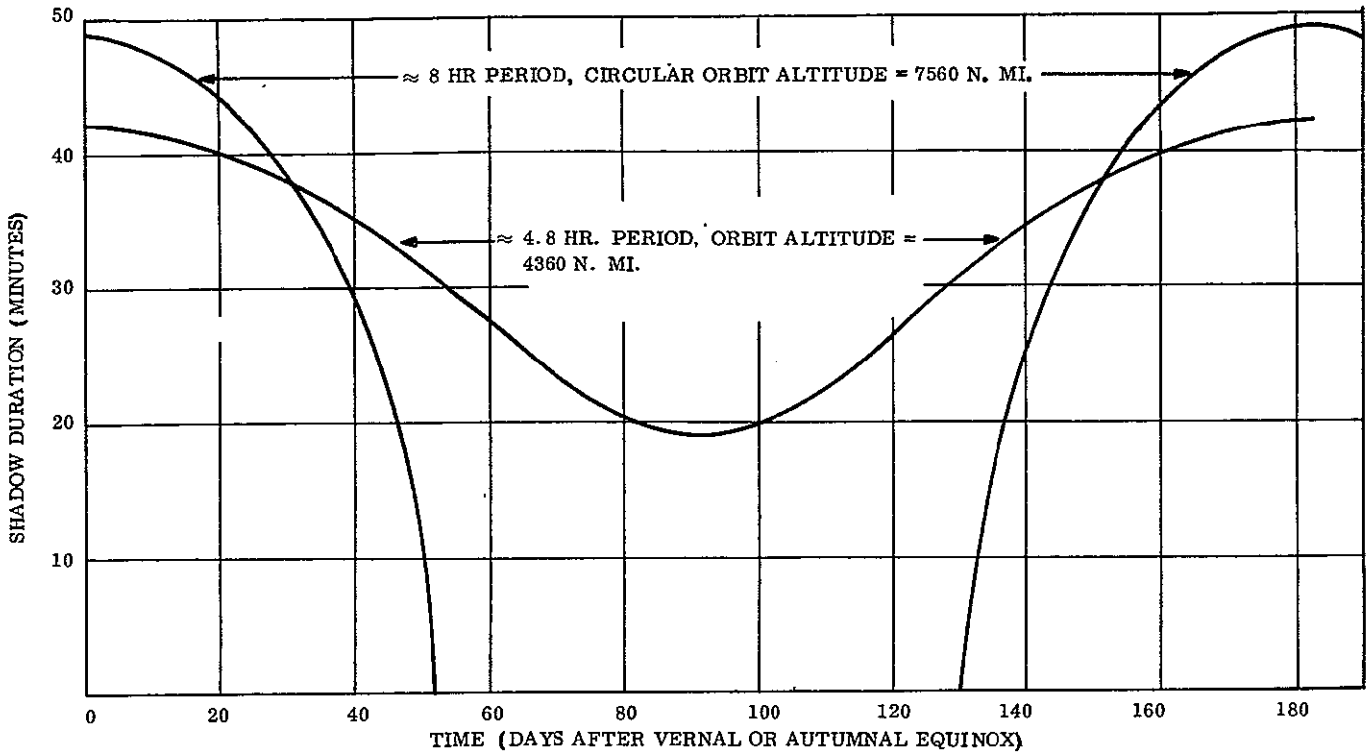

Figure 2.2-11. Shadow Histories, Circular Equatorial Orbits Only

2.3 PROPAGATION ANALYSIS

2.3.1 SUMMARY AND CONCLUSIONS

The selected design parameters of the four configurations are such that most propagation effects are small. The major exceptions, and the effects are listed below:

Effect	Effect on System
Scintillation	Requires selection of HF transmission schedules and areas. Negligible at VHF and UHF.
Absorption	Requires selection of HF transmission schedules and areas negligible at VHF and UHF.
Refraction	Variation of MUF requires scheduling of HF frequencies to compensate. Negligible at VHF and UHF.
Faraday rotation	Requires circular polarization, with consequent 3 db loss in linear receiver antennas, at HF and VHF frequency bands.
Building loss	Severe effects on signal strength. Requires maximum power, restricts audience reached. Effect increases with frequency.

The effects of propagation are summarized more completely in Table 2.3-1 and discussed in the remainder of this section.

2.3.2 IONOSPHERIC SCINTILLATION EFFECTS

Scintillation is a random fluctuation in phase and amplitude of a radio wave, caused by the movement of the satellite past scattering irregularities in the ionosphere. Patches of these irregularities may extend over wide geographic areas. Under normal ionospheric conditions these patches may be regarded as a diffraction screen, which phase-modulates the incidence wave and produces a diffraction pattern on the ground. The movement of the irregularities with ionospheric drift and the orbital motion of the satellite cause this pattern to travel across the ground and produce scintillation.

Scintillations in amplitude cause signal fading, while phase scintillations appear as noise in an FM receiver.

2.3.2.1 Amplitude Scintillation

The magnitude of the amplitude scintillation is described using the concept of a scintillation index or scintillation amplitude. The scintillation index is defined as the ratio of the rms value of the scintillations to the mean value of the signal. The quantitative expression is

Table 2.3-1. Propagation Summary

VBMS Propagation Effects			Effects on VBMS Configurations*			
Effect	Mechanism	Effects on Signals	HF	VHF No. 1	VHF No. 2	UHF
Amplitude Scintillations	Motion of the satellite past ionospheric scattering, irregularities	Causes fading; require provision of additional signal strength, or "fade margin"	Zero; transmission schedules and areas were selected for this purpose	0.3 db	0.7 db	0.1 db
Phase Scintillations	Motion of the satellite past ionospheric scattering, irregularities	No AM effect. Generates noise in FM systems	No effect; amplitude modulation	Negligible; well below KT_oB	Negligible, well below KT_oB	Negligible; well below KT_oB
Transmission Path Loss (Absorption)	Collisions of oscillating electrons with ionospheric constituents	Reduces signal strength	Negligible; schedules and areas were chosen for this purpose	Negligible	Negligible	Negligible
Changes in MUF	Refraction of radio wave back into space by the ionosphere	Reduces signal strength, requiring shifts in frequency	Forces scheduled frequency shifts as MUF changes	Negligible	Negligible	Negligible
Phase Dispersion	Nonlinear phase shift across the band, caused by variation of ionospheric index of refraction with frequency	Little effect in AM audio. Affects timbre to some extent. Creates distortion in FM systems.	Negligible	Small**	Small**	Negligible
Faraday Rotation	Rotation of plane of polarization as the wave travels through the ionosphere	Causes fading, countered by generating circularly polarized waves, accepting 3 db loss at linear receiving antennas	Requires circular polarization	Requires circular polarization	Requires circular polarization	Negligible (yaw rotation of antenna dictated use of circular polarization)
Doppler Shift	Doppler effect-change of frequency with radial velocity between transmitter and receiver	Causes detuning and interference	86 Hz – Negligible	0 Hz – Synchronous Orbit	298 Hz – Negligible	0 Hz – Synchronous Orbit
Building Loss	Attenuation of wave in passing through building walls, etc., to reach receiver antennas	Causes severe reduction in signal strength; limits access in some circumstances to sets having outdoor antennas	Urban 12.4 db Suburban 4.8 db Rural 0	Urban 17.7 db Suburban 9.5 db Rural 0	Urban 17.7 db Suburban 9.5 db Rural 0	Urban 26.9 db Suburban 17.8 db Rural 10.4 db
Atmospheric Turbulence, Scattering and Refraction	Discontinuities in atmospheric densities and moisture content	Causes fading and multipath	Negligible at all frequencies below 1 GHz			
Meteor Scatter	Meteor trails in atmosphere specularly reflect radio waves	Causes multipath when properly oriented	Negligible; too few meteor trails are properly oriented to cause significant effects			
Auroral Effects	Refraction, scatter and scintillation from aurora	Causes severe fading, attenuation and multipath	Negligible; VBMS does not broadcast into auroral latitudes (>60° latitude)			
Aircraft and Structures	Reflection of radio waves	Multipath selective fading, and shadow zones	Small; with satellite altitude, these effects are smaller than for ground transmitters			
Terrain	Reflection of radio waves	Multipath selective fading, and shadow zones	Small; with satellite altitude, these effects are smaller than for ground transmitters			

*Normal ionosphere is assumed. Effects of infrequent severe disturbences are not included.

**On the basis of preliminary investigations.

$$F_{rms} = \left[\frac{\overline{(A-\bar{A})^2}}{(\bar{A})^2} \right]^{1/2} = \sqrt{\frac{\overline{(\Delta A)^2}}{(\bar{A})^2}} = \frac{1}{\bar{A}} \sqrt{\overline{(\Delta A)^2}}$$

where

A = Instantaneous signal amplitude

$\bar{A}$ = Mean value of A (Over period long compared with fluctuation time)

$\Delta A = A - \bar{A}$

F_{rms} = rms value of scintillation index

In computing the values of amplitude scintillation, the factors which determine scintillation (time of day, geomagnetic latitude, zenith angle, satellite altitude and frequency) are used to determine the scintillation index. Then from available curves, the fading statistics are determined from the value of the scintillation index.

The objective in determining the effects of amplitude scintillations is to find the required fade margin.

A procedural block diagram for this computation is shown in Figure 2.3-1.

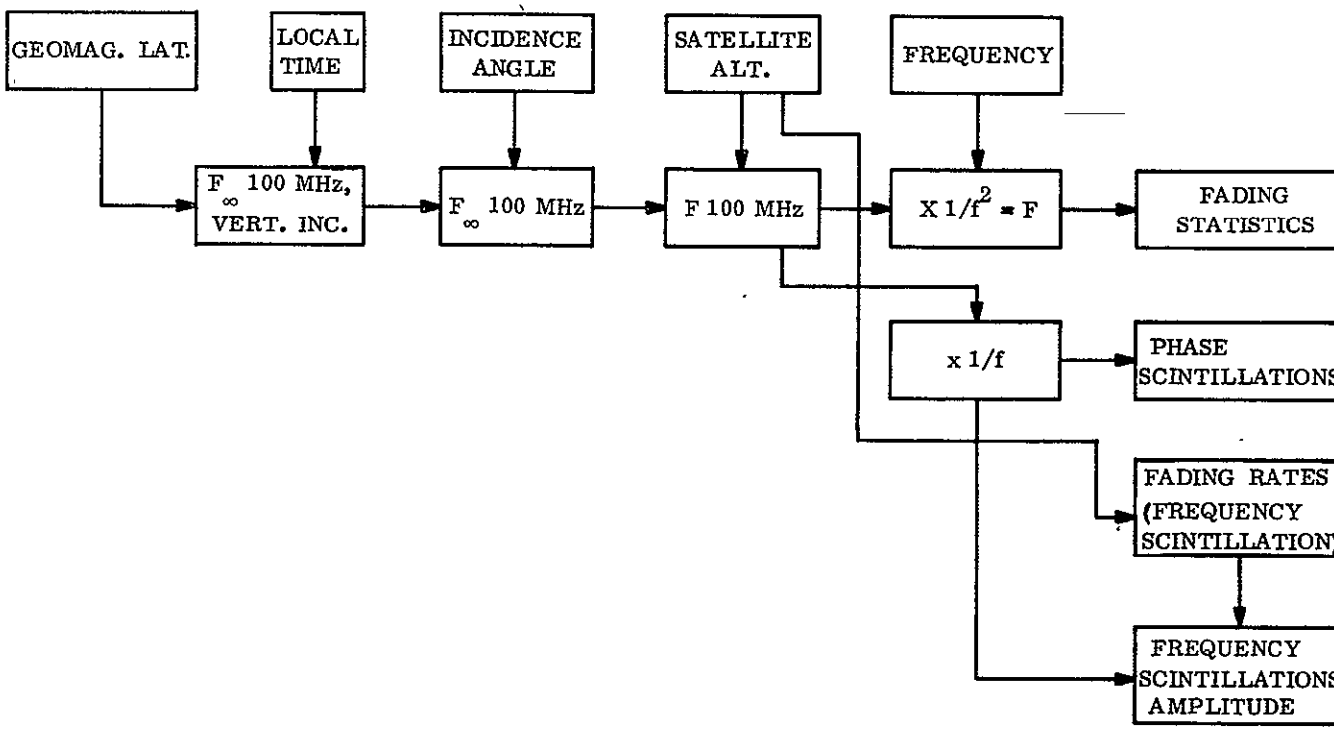

Figure 2.3-1. Procedural Block Diagram for Computation of Ionospheric Scintillations

The procedure described below is followed by example calculations.

The scintillation index F_{rms} is given by:

$$F_{rms} = (F_{\infty, 100}) (\text{Sec } \chi)^{3/2} \left[\frac{Z}{h_1 + Z}\right] \left(\frac{100}{f}\right)^2$$

Where

F_{rms} = Scintillation index

$F_{\infty, 100}$ = Scintillation index reduced to vertical incidence, 100 MHz and infinite height

χ = zenith angle

f = frequency in MHz

Z = height of satellite above irregularity layer

h_i = height of irregularity layer ($\cong$ 300 km)

In Figure 2.3-2, $F_{\infty, 100}$ is plotted as a function of geomagnetic latitude and local time.

The steps in the computation procedure are as follows:

1. Specify:
   - Frequency
   - Geomagnetic latitude
   - Time of Day
   - Zenith angle
   - Satellite Height
2. From Figure 2.3-2, determine, $F_{\infty,100}$ for the given geomagnetic latitude and local time.
3. From Figure 2.3-3, find $(\text{Sec}\chi)^{3/2}$ for the zenith angle given. (Note: the angle desired is actually the angle of incidence at the ionosphere, but this is well approximated by the zenith angle.)
4. From Figure 2.3-4, determine the correction factor for satellite altitude.
5. From the frequency calculate $\left(\frac{100}{f}\right)^2$
6. Using the values from steps 2 to 5 above in Equation 2.3-1, calculate F_{rms}.

7. From Figure 2.3-5, determine the required amplitude factors.

8. Compute the required fade margin in db, using the expression:

$$db = 10 \log_{10} (\text{amplitude factor})^2$$

An example of calculation for the VBMS VHF No. 1 configuration is shown below.

1. Specifications

• Geomagnetic Latitude	48°
• Time of Day	1:00 A.M.
• Zenith Angle	62°
• Satellite Height	19323 nm
• Frequency	100 MHz

2. From Figure 2.3-2, $F_{\infty,100} = 0.03$

3. From Figure 2.3-3: $(\text{Sec } \chi)^{3/2} = 3.0$

4. From Figure 2.3-4: altitude correction factor 0.99

5. $\left(\frac{100}{f}\right)^2 = \left(\frac{100}{100}\right)^2 = 1$

6. $F_{rms} = 0.03 \times 3 \times 0.99 \times 1 = 0.0891 = (8.91\%)$

7 From Figure 2.3-5 for 90%; fade margin = 0.96, or 0.3 db

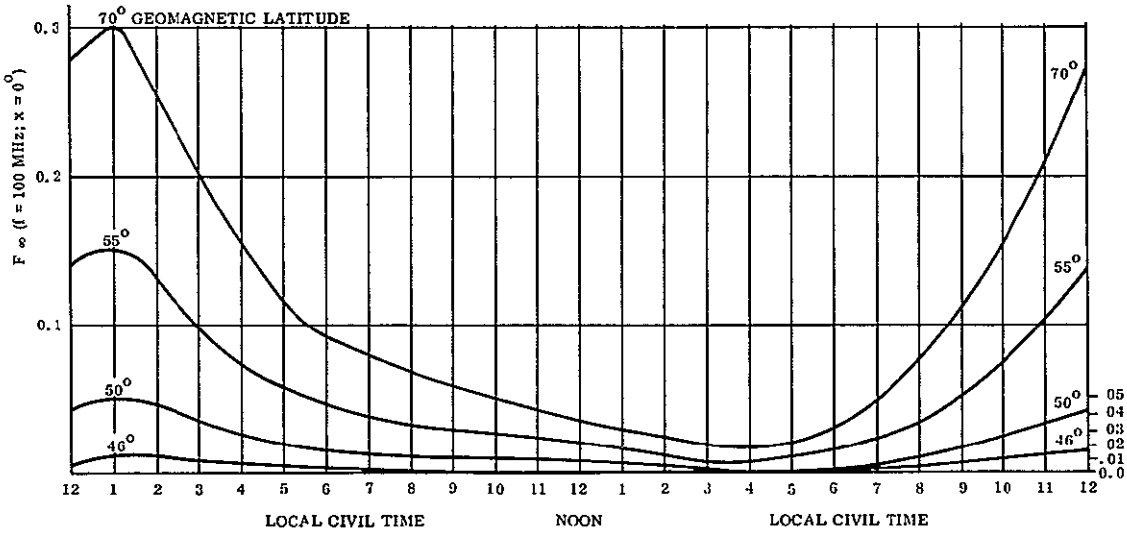

Figure 2.3-2. Scintillation Index ($F_{\infty,100}$) Versus Local Civil Time for Vertical Incidence

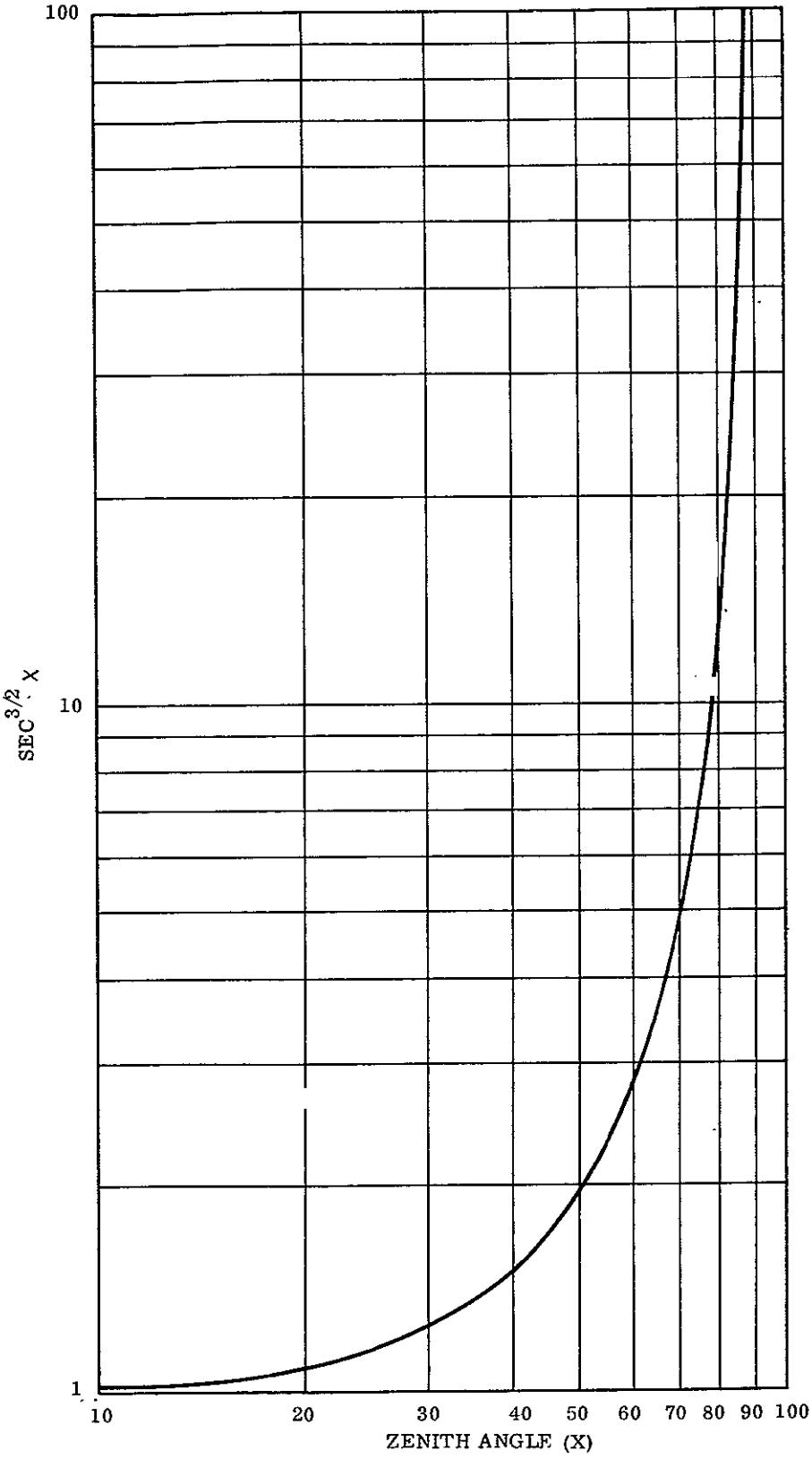

Figure 2.3-3. Scintillation Index Factor Versus Zenith Angle

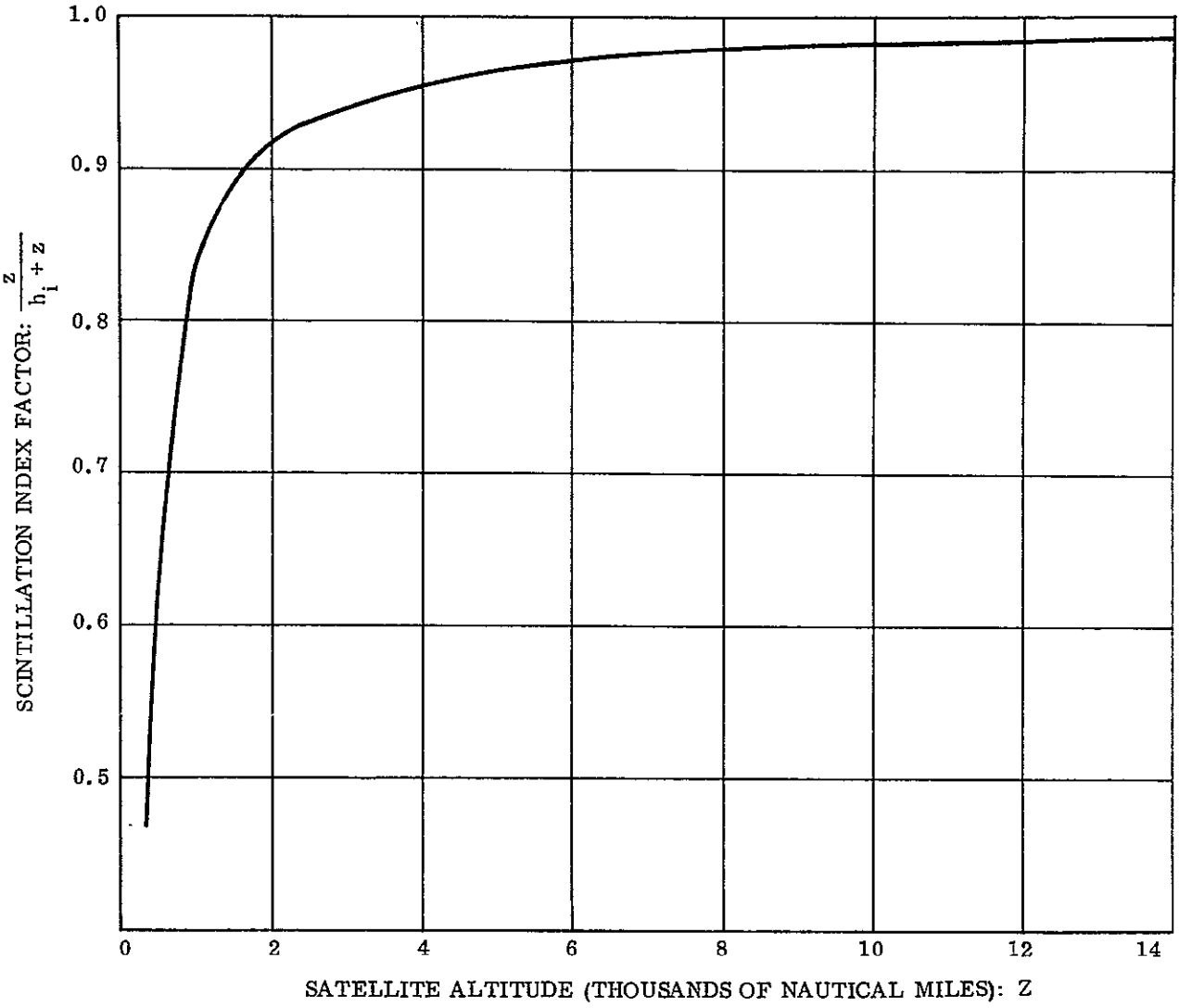

Figure 2.3-4. Scintillation Correction Factor for Satellite Altitude

The fade margin required for the HF, VHF No. 2, and UHF configuration are determined in the same fashion. These margins, together with the intermediate values in the computations, are shown in Table 2.3-2.

2.3.2.2 Phase Scintillations

The rms magnitude of the Phase scintillations is given by

$$\overline{(\Delta\phi)^2} = \frac{Z_f^2}{Z^2} \left(\overline{\frac{\Delta A}{A}} \right)^2$$

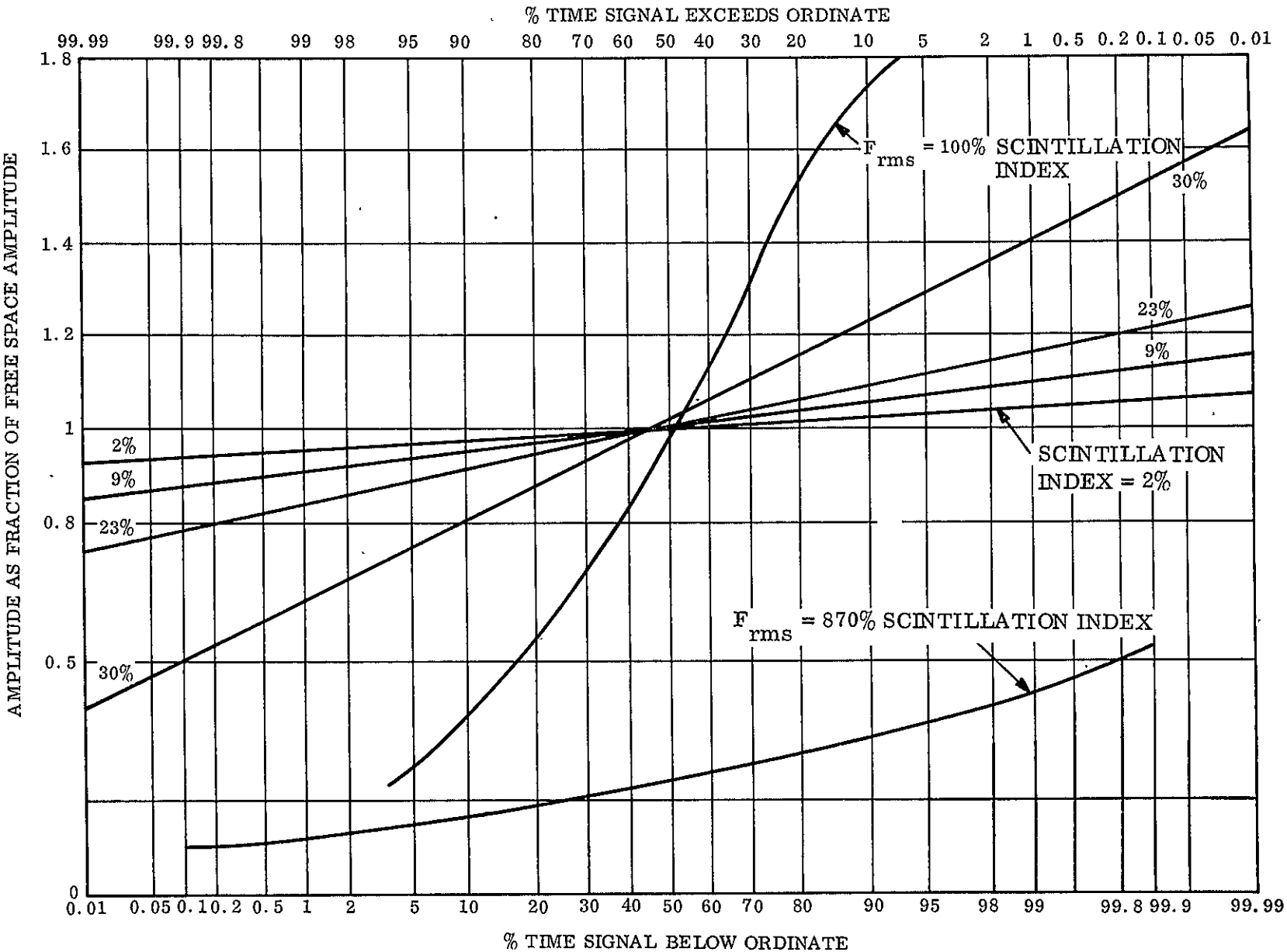

Figure 2.3-5. Amplitude Scintillation Statistics

Table 2.3-2. Fading Calculation Summary

Configuration	$F_{\infty, 100}$ From Figure 2.3-2			$(\sec \chi)^{3/2}$ From Figure 2 3-3		$\frac{z}{h_i + z}$ From Figure 2.3-4		Frequency Correction $\frac{100^2}{f}$		Fade Factor from Figure 2.3-5			Fade Margin from db = 10 $\log_{10}$ x (Amplitude Factor)^2
	Max Cov. Lat.	Local Earth time	Factor	Max. Zenith Angle*	Factor	Sat. Alt. in nm	Factor	Broadcast Frequency	Factor	Product of Factors	% of Time Fade Margin Exceeded	Amplitude Factor	Fade Margin
HF	46°	6 30 PM	0 00	78°	9.5	4356	0.96	15 MHz	44.3	0	50%	0.00	0 db
VHF No. 1	48°	1 00 AM	0 03	62°	3.0	19323	0.99	100 MHz	1	8.9%	10%	0.96	0 3 db
VHF No. 2	55°	6 30 PM	0.02	76°	8.15	7556	0.98	100 MHz	1	16%	10%	0 93	0 7 db
UHF	48°	1-00 AM	0.03	66°	3 9	19323	0 99	870 MHz	0.013	0.1%	1%	0 99	0 1 db

*Maximum zenith angle is 90° (minimum elevation angle).
Minimum elevation angles as derived for the example coverage areas

Where

$\overline{(\Delta \phi)^2}$ = mean square fluctuations in radians^2

$\overline{\left(\frac{\Delta A}{A}\right)^2}$ = mean square amplitude fluctuations

Z = distance to ionosphere form observation point

Z_f = fresnel zone distance = $\frac{L^2}{\lambda}$

L = irregularity size $\approx$ 5 km

The phase scintillations have no significant effects in AM systems, but produce noise in FM systems. The rate of change of phase gives a frequency shift which may be regarded as a frequency scintillation. This is expressed by

$$f_i(t) = \frac{1}{2\pi} \frac{d\phi}{dt}$$

where

$f_i(t)$ = Instantaneous frequency in Hz

$\frac{\lambda \phi}{dt}$ = Rate of change of phase in radians/sec

To determine the value of $\frac{d\phi}{dt}$, it is necessary to describe the behavior of $\Delta\phi$ as a function of time. If phase fluctuations are assumed to be sinusoidal, a conservative value will be obtained for the lowest frequency component of and the resultant changes in frequency, Δf. Because the spectral density of the FM noise caused by the phase fluctuations varying approximately, inversely with frequency, it is then possible to determine the approximate values of Δf in the regions of interest.

With the assumption of sinusoidal fluctuations

$$\Delta\phi = \Delta\phi_m \sin \Omega t$$

where

$\frac{\Omega}{2\pi}$ = fading rates in fades per second

$\Delta\phi_m$ = the maximum value of $\Delta\phi$

and a transmitted carrier $A \cos \omega_c t$ would be received as

$$A \cos \left[\omega_c t + \Delta\phi(t)\right]$$

An ideal AM envelope detector would produce only d.c. at its output; i.e., the phase scintillation has no effect. An ideal FM discriminator would produce at its output:

$$e_o(t) = \frac{d}{dt}\left[\omega_{ct} + \Delta\phi_m \sin \Omega t\right]$$

$$= \omega_c + \Omega\, \Delta\phi_m \cos \Omega t$$

$$\Delta f_m = \frac{\Omega}{2\pi}\, \Delta\phi_m\, H_2$$

The value of $\Delta\phi_{rms}$ is given as a function of satellite senith angle normalized to 100 MHz in Figure 2.3-6. The value of $\frac{\Omega}{2\pi}$ is given as a function of satellite altitude in Figure 2.3-7.

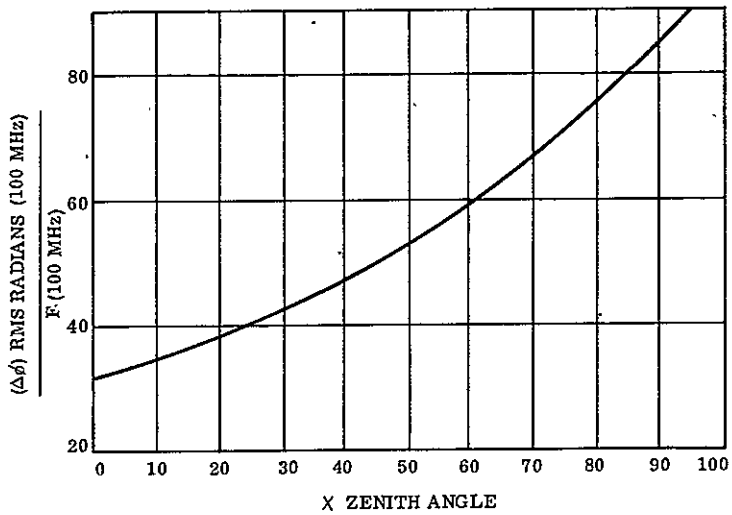

Figure 2.3-6. $\Delta\phi$ Versus Zenith Angle, Normalized to 100 MHz

From the equations and Figures 2.3-6 and 2.3-7, it is possible to compute the values of Δf for the VBMS configurations. An example computation for the VHF No. 1 configuration is shown below.

From Figure 2.3-6, $\Delta\phi_{rms} = 60\, f_{100}$ radians for maximum zenith angle 62^{o}

From Figure 2.3-7, for 22300 miles altitude

$$\frac{\Omega}{2\pi} = 0.5 \text{ Hz}$$

$$\Delta f_m = \frac{\Omega}{2\pi} \Delta\phi_m = 0.5 \quad 2 \times 60 \times 0.089 = 3.77 \text{ Hz at } 0.5 \text{ Hz}$$

At 400 Hz,

$$\Delta f_m = \frac{3.77}{400} \times 0.5 = 0.0047 \text{ Hz}$$

Because a test tone at 400 Hz is normally deviated 22.5 kHz, the FM noise is insignificant. FM noise in the VHF No. 2 and UHF configurations is also negligible, while the HF configuration uses amplitude modulation.

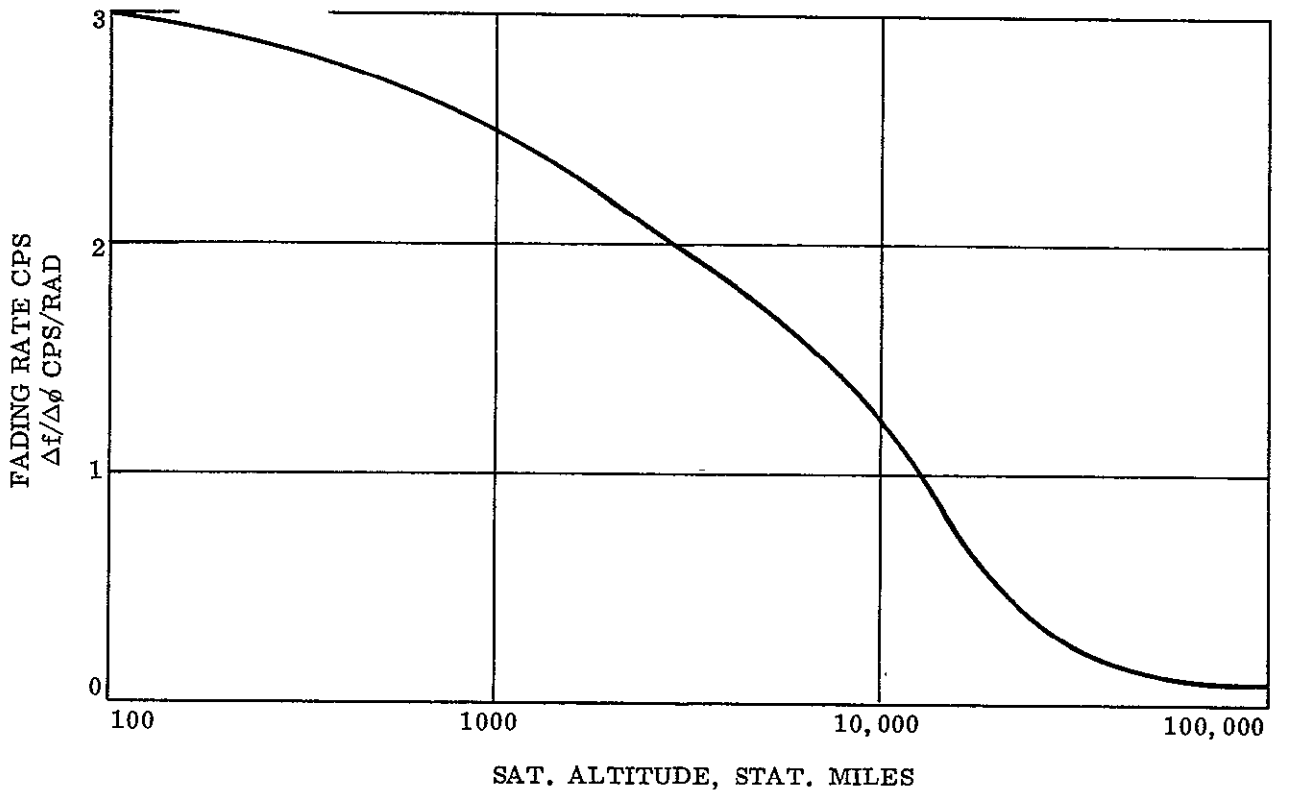

Figure 2.3-7. Fading Rate Versus Satellite Altitude

2.3.3 TRANSMISSION PATH LOSS

At the latitudes of interest to the VBMS (60^{o} or less), the dominant path loss mechanism is normally the absorption caused by the collision of electrons, oscillating under the influence of the incident wave with the other ionospheric constituents.

Absorption is a function of electron density and collision frequency, frequency of the incident radio wave, and incidence angle on the layer.

Electron density and collision frequency are in turn functions of the zenith angle of the sum and the sunspot number.

For convenience in computation, curves of absorption for an operating frequency of 10 MHz, are shown as functions of latitude and local civil time for the through seasons corresponding to December, June, and March-September in Figures 2.3-8, 2.3-9 and 2.3-10, respectively. The multiplying factors for converson to other frequencies and incidence angle are shown in Figure 2.3-11.

Figures 2.3-8 through 2.3-11 show that the absorption for all four configurations is well below 1 db and therefore may be regarded as insignificant.

2.3.4 IONOSPHERIC CONSTRICTION OF COVERAGE (MUF)

At frequencies near the MUF (the HF configuration in the VBMS), ionospheric refraction effects can result in a limited cone angle about the zenith at which the wave can be received; i.e., signals from the satellite may disappear while the satellite is well above the horizon.

The mechanism of this refraction is the absorption and out-of-phase re-radiation of the energy from the radio waves by ionospheric electrons, giving the ionosphere an effective index of refraction of less than unity and causing it to refract the radio wave away from regions of higher electron density. For sufficiently large zenith angles, the incident wave from a satellite will be refracted back into space. If this angle is less than 90^{o}, the cone of radiation is limited.

The chief practical effect of this refraction on the VBMS is to raise the MUF. As 15 MHz, cone angles may be severly limited. At the region of highest electron density near the equator, the critical frequency (f_c) sometimes becomes greater than 15 MHz, causing total reflection from the ionosphere with consequent complete loss of signal. It is then necessary to shift to one of the higher frequencies.

VBMS broadcast schedules will be arranged to conform with the changing values of MUF. This procedure is discussed in Section 2.6.1.1. The objective of such scheduling is to be able to broadcast on the lower frequencies when ionospheric conditions permit because more receivers exist on those frequencies.

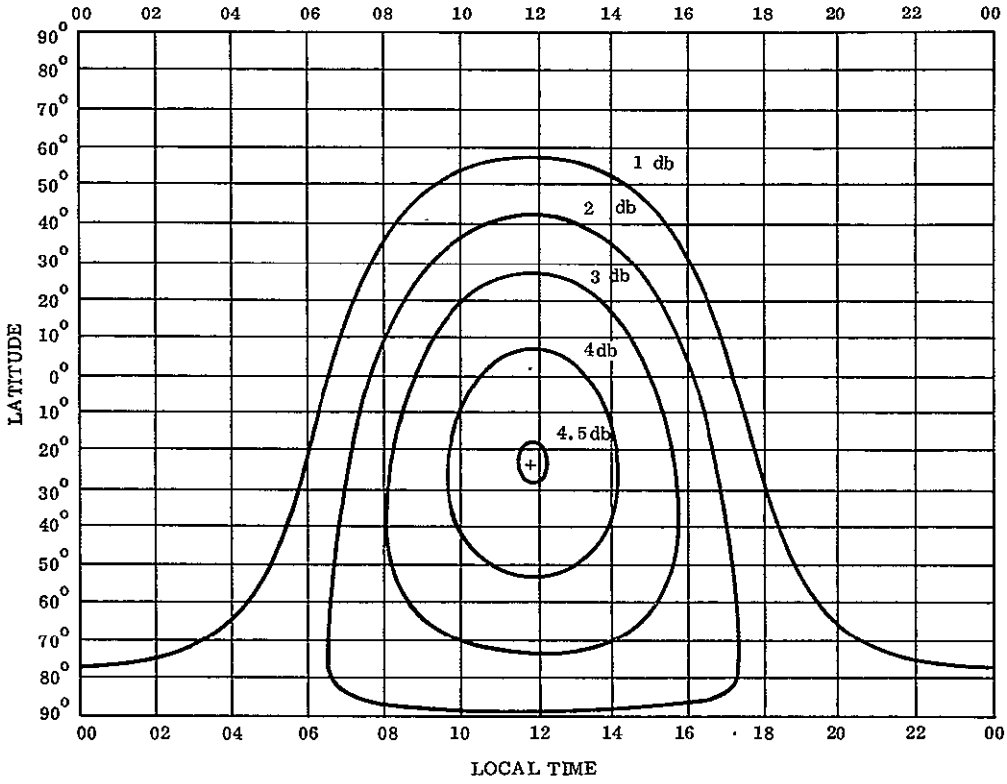

Figure 2.3-8. Vertical Incidence Attenuation (10 MHz, SSN = 200), December

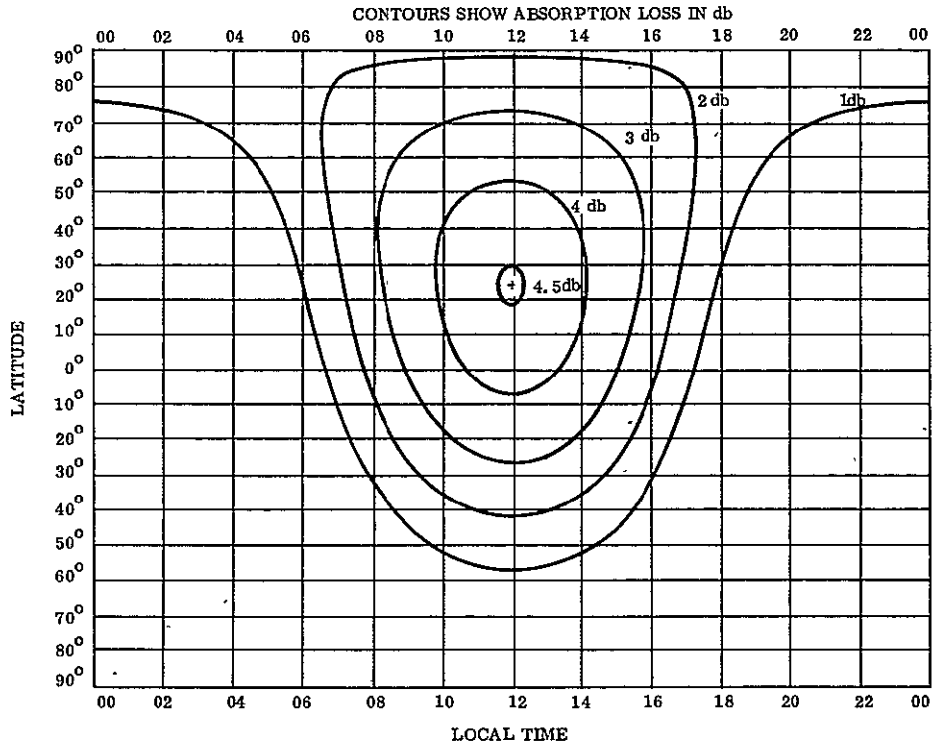

Figure 2.3-9. Vertical Incidence Attenuation (10 MHz, SSN = 200), June

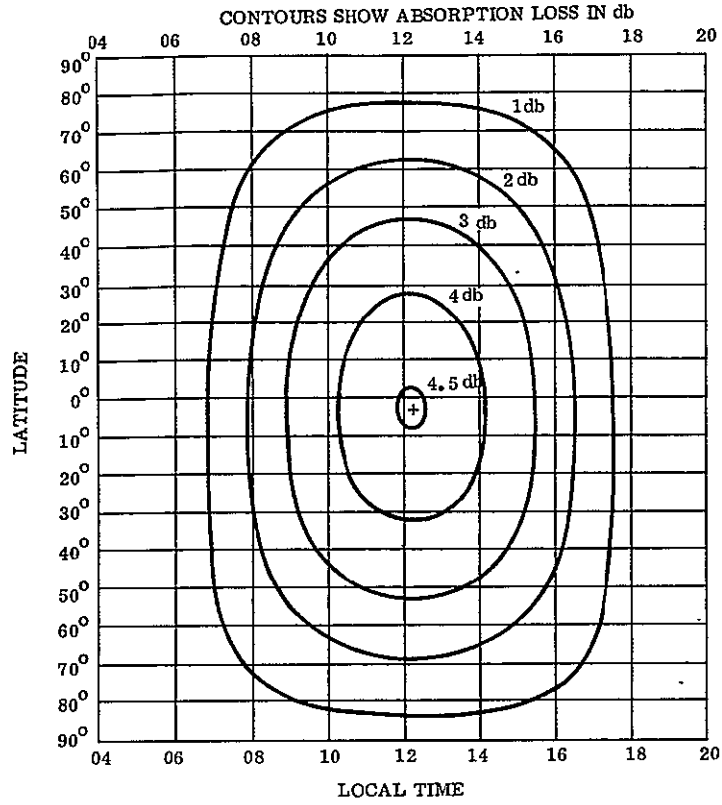

Figure 2.3-10. Vertical Incidence Attenuation (10 MHz, SSN = 200), March-September

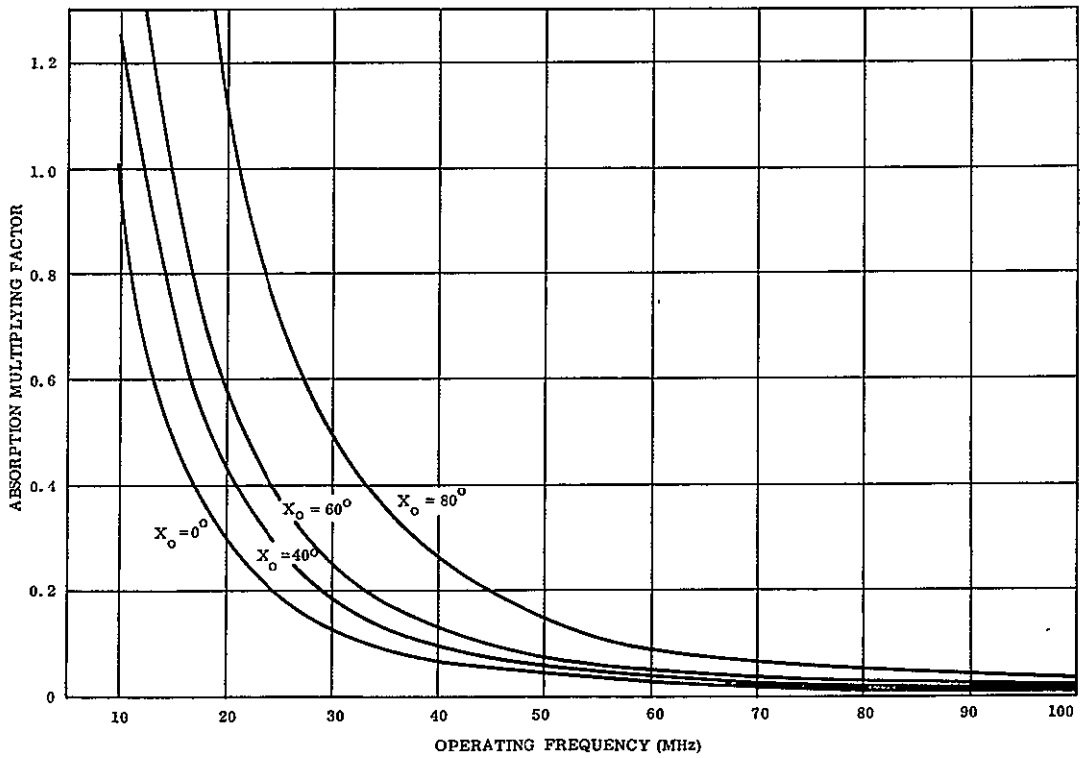

Figure 2.3-11. Vertical Incidence Attenuation-Conversion Factors

2.3.5 BANDWIDTH LIMITATIONS

There are two bandwidth limiting effects associated with space-to-earth propagation through the ionosphere-phase dispersion and selective fading caused by ionospheric multipath.

2.3.5.1 Phase Dispersion

Phase dispersion, or dispersion group delay, is caused by the variation of ionospheric index of refraction with frequency. This causes the group delay imposed by the ionosphere to change also with frequency.

Preliminary investigation indicates that distortion caused by this effect will be small.

2.3.5.2 Selective Fading

Because scattering of the incident wave by ionospheric irregularities will cause multipath transmission, selective fading may result. Selective fading associated with multipath is caused by the path length difference being such that some frequency components are more nearly cancelled than others. If the frequency band is wide enough, it may contain one or more "nulls" (frequencies at which fading is at maximum).

The maximum bandwidth that may be transmitted with negligible selective fading is called the "correlation bandwidth"; so named because it is the widest band over which the correlation of scintillation at the various frequencies is not diminished *.

For the weak-scattering case (i.e., for the normal ionosphere at latitudes of concern to the VBMS) the correlation bandwidth is of the order of half the center frequency, and separation between nulls, which is twice the correlation frequency, is of the order of the center frequency. Therefore, for a normal ionosphere outside the high latitudes ($> 60^{o}$) selective fading may be disregarded.

2.3.6 POLARIZATION EFFECTS AND FARADAY ROTATION

The only polarization effect of interest to the VBMS is Faraday rotation; i.e., the rotation of the plane of polarization of a linearly polarized wave as the wave propagates through the ionosphere in the presence of the geomagnetic field. The magnitude of Faraday rotation varies widely with time, zenith angle and frequency. The maximum values to be expected for the VBMS configurations are greater than 2π radians for all but the UHF configurations. Therefore, for all but the UHF configuration, circular polarization is required to prevent severe polarization fading. This will result in a 3 db loss for conventional linearly polarized receiving antennas.

*Foryth, Vagan, Hansen and Hines, "The Principles of JAWET - A Meteor Burst Communication System" Proceedings IRE 45, 1642, December 1957.

The computations were made using the usual method of computing Faraday rotation effects of frequencies of 30 MHz or greater, which assumes that propagation is Quasi Longitudinal (QL)*. The value of the rotation is then given by:

$$\Omega = \frac{Q}{f^2} \int_{ray} NH \cos\theta \, d\ell$$

where

Ω = angle of polarization rotation, radians

Q = 2.97×10^{-2} (in mks units)

f = frequency in Hz

N = Electron density, electrons/m^3

H = Magnetic field intensity, ampere turns/meter

θ = angle between wave normal and geomagnetic field

L = path length, meters

2.3.7 SCATTERING PHENOMENA AND MULTIPATH

In addition to the multipath effects of ionospheric scattering discussed in Section 2.3.5, there are numerous other sources of scattering and multipath. Effects from these sources are negligible for the VBMS. These sources, together with the justification for disregarding them, are listed below:

Source	Reasons for Disregarding
Atmospheric turbulence	Small at frequencies below 10 GHz
Meteor scatter	Percentage of correctly oriented trails too small to be significant
Auroral effects	Contined to high latitudes, beyond areas of interest to VBMS.
Aircraft structures	Limited scattering cross sections confine effects to immediate vicinity of scatter: overall effects negligible
Terrain	Satellite elevation angle reduces effects to much below those for ground transmitter.

*Foryth, Vagan, Hansen and Hines, "Principles of JAWET - A Meteor Burst Communication System" Proceedings IRE 45, 1642, December 1957.

There will be some local exceptions to the above, as in shadowing by mountains or large buildings, but the overall effect will be small.

2.3.8 DOPPLER SHIFT

For satellites above 1000 miles altitude, it can be shown that the effect of the ionosphere upon the Doppler shift is negligible. Therefore, the Doppler shift is given by the standard expression

$$\Delta f = f_o \frac{V}{c}$$

where

Δf = frequency shift

f_o = frequency of radio wave of the transmitter

V = closing velocity between the satellite and the receiver

C = speed of light in free space

The maximum Doppler shift is of interest to the VBMS because of possible detuning and interference.

The closing velocity is the sum of the component of satellite velocity in the direction of the receiver, and the receiver velocity in the direction of the satellite. The worst case discussed herein occurs when the satellite orbits cross over the receiver. Because all orbits cross the equator, the worst case point will always be on the equator. The applicable parameters are the satellite altitude, h, and the inclination of the orbit with respect to the earth equator, β. Figure 2.3-12 shows the case of maximum closing velocity.

The rate of change of the slant ranges is given by

$$ds/dt = v = v_{sr} + v_{rs}$$

where

v_{sr} is the component of orbital velocity of the satellite towards the receiver

$v_{rs} = V_c \cos \beta$ = component velocity of receiver towards the satellite

v_e = earth's velocity at equator = 900 nm/hr = 465 meters/sec

β = inclination of the satellite orbit with respect to the earth's equator.

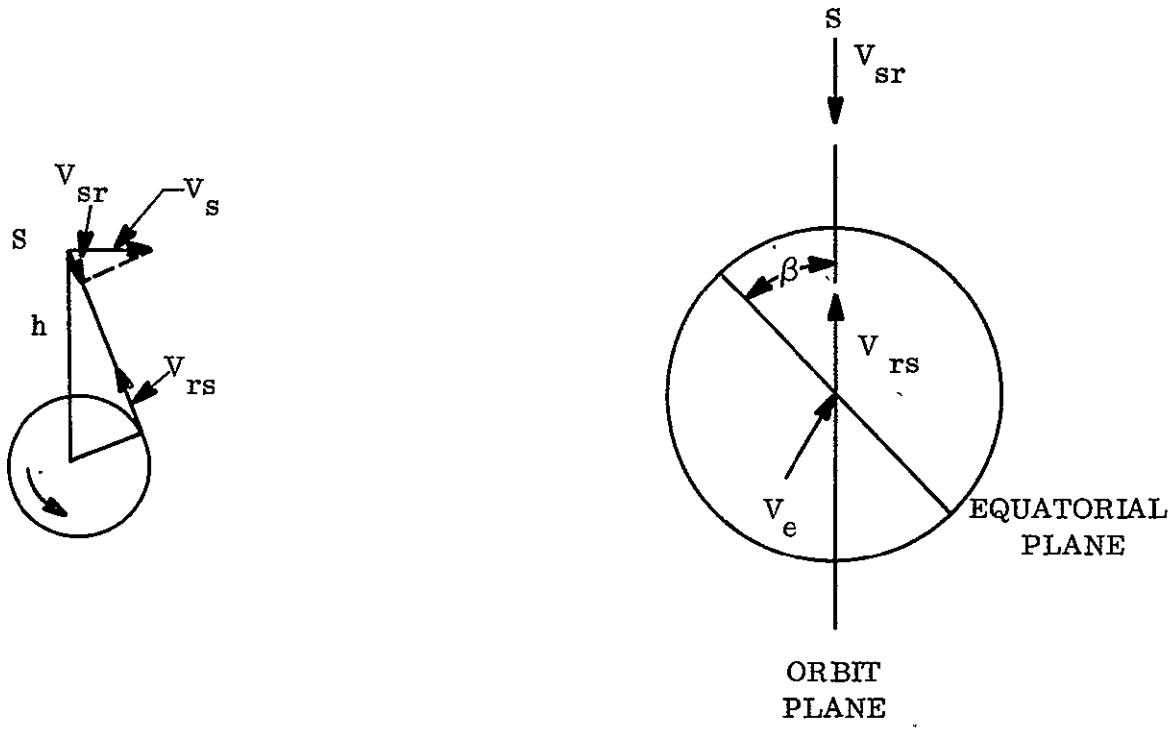

Figure 2.3-12. Closing Velocity on Horizon

Also by geometry we see that

$$v_{sr} = v_s \frac{a}{h + a}$$

where

v_s = satellite velocity in orbit

a = earth's radius = 3,437 nm

h = satellite altitude.

By Newton's laws we know v_s is proportional to $1/(h + a)^{1/2}$

Combining all the above factors gives

$$v = \frac{ka}{(h + a)}^{3/2} - v_e \cos \beta$$

In this equation, K is constant which may be conveniently evaluated at synchronous altitude (h = 19, 300 nm) where v = 0 when $\beta = 0$. Substituting appropriate values of a, h and v_e gives

$$\frac{ka}{(h+a)^{3/2}} = 900/3600 = 1/4 \text{ nm (sec)}$$

$$k = \frac{ka}{(h+a)\frac{3}{2}} = \frac{900}{3000} = 1/4 \text{ nm/sec} = 4.42 \times 10^6/4 \times 3437 = 248$$

substituting the value obtained for z:

$$V = 248 \frac{a}{(h+a)\frac{3}{2}} - v_e \cos\beta$$

since all VBMS orbits have zero inclination ($\beta = 0$)

$$V = 248 \frac{a}{(h+a)\frac{3}{2}} - V_e$$

By this expression, the Doppler shifts for the VBMS can be calculated, and results are shown below.

Configuration	Maximum Radial Velocity	Doppler Shift, Hz
HF	1720 meters/sec	86
VHF No. 1	0	0
VHF No. 2	895 meters/sec	298
UHF	0	0

These amounts of frequency shift have negligible effects, being less than 0. 0006% of the frequency in each case when compared with established tolerances at 0. 02% for HF and about 0. 002% for VHF FM broadcasting.

2. 3. 9 BUILDING LOSSES

A special problem occurs in broadcasting because most receivers are inside buildings. Many do not have outside antennas. To reach these latter receivers, the radio wave must penetrate the buildings; therefore, the question of losses in such penetration becomes important.

A limited program was conducted by the FCC for 1 year, in measurements of television signals in the New York City area. Included in these measurements were the received signal levels, both inside the house and on the roof-top, at each of the test sites which ranged from central Manhattan to 25 miles from the Empire State Building. These data were reported in the FCC Research Division Report No. R-6303, March 1963, by George V. Waldo. Analysis of these data have shown that the building loss is proportional to the distance from the center of the urban area and can be generally approximated by the following equation:

$$L_B = K - ad, \text{ in db}$$

where K and a are constants for a given frequency, and d is the distance from the urban center in miles.

The measurement program used television Channels 2, 7 and 31 for their test signals. The values of the above constants for these channels are:

	K	a
Channel 2	24	2/3
Channel 7	25	2/3
Channel 31	34	3/4

The distance from the urban center has been divided into the following categories:

Area	Distance from Urban Center (Miles)
Canyon	0 to 4
Urban	4 to 12
Residential	12 to 36
Suburban	24 to 36
Rural	> 36

For these defined areas, the building losses have been plotted in Figure 2.3-10 versus frequency using as an additional point a building loss of 0 db at 0 frequency. From this graph the values are taken for the HF, and UHF signals of the direct broadcast configurations. The values are shown below ("urban" has been redefined to be an average of the urban and residential areas):

	Building Losses		
	HF	VHF	UHF
Urban Suburban	12.4 db	17.7 db	26.9 db
Suburban	4.8 db	9.5 db	17.8 db
Rural	0 db	0 db	10.4 db

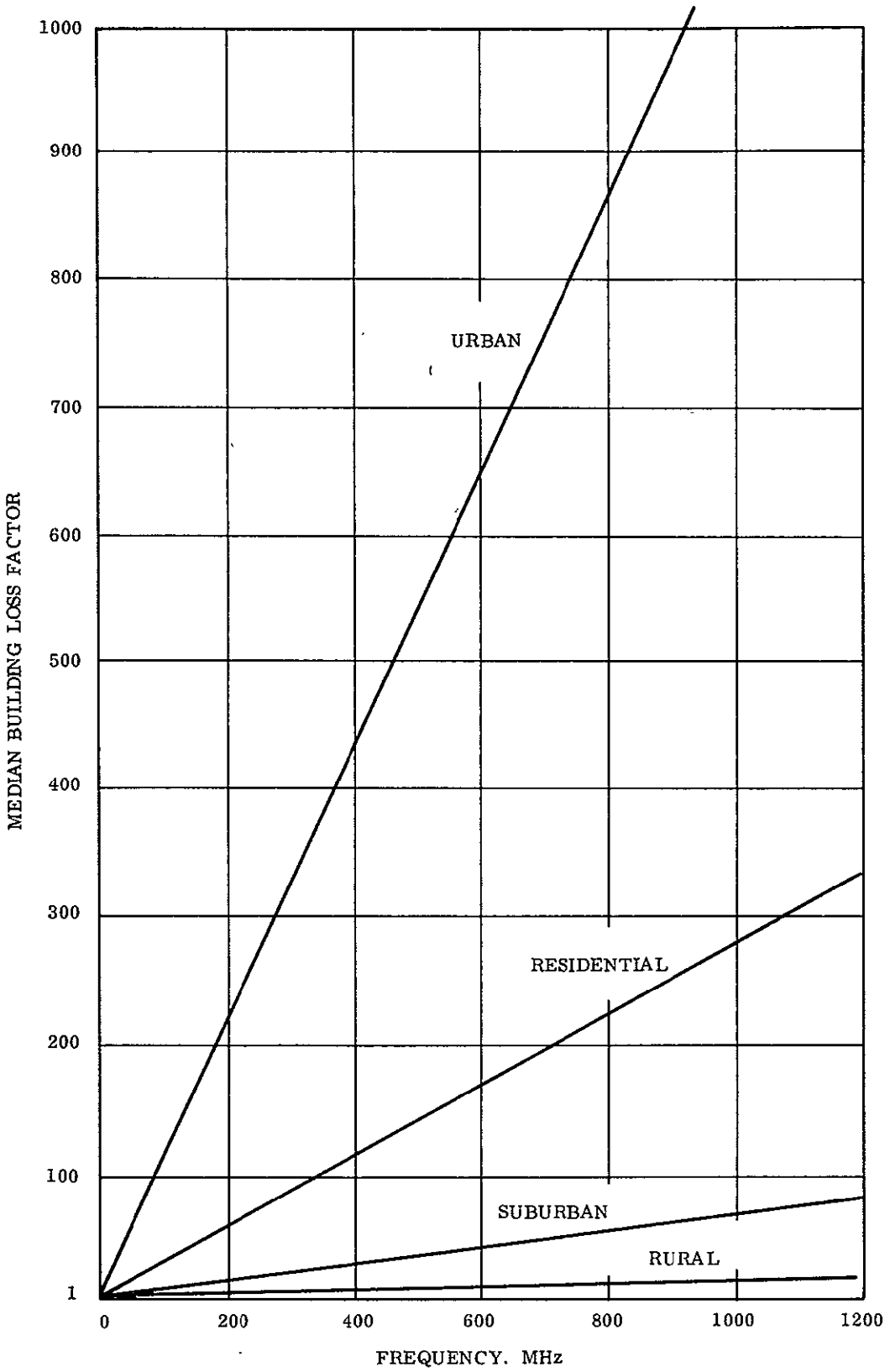

Figure 2.3-13. Building Losses Versus Frequency Versus Environment

2.4 HOME ANTENNA ANALYSIS

2.4.1 INTRODUCTION

Because the home receiver antenna performance affects the required field strength and hence the required satellite ERP, it was necessary to examine the home antenna problem in sufficient detail to determine what performance is likely to be available. In the examination, the antennas were divided into two classes: (1) HF and VHF antennas and (2) UHF antennas.

2.4.2 HF AND VHF ANTENNAS

The investigation of the home antenna problem was begun with a survey of various catalogs to obtain a list of typical antennas available. Table 2.4-1 shows survey results as applied to HF and VHF antennas. All antennas are linearly polarized, and almost all are of the Yagi type. The antennas used to receive satellite broadcasts will be similar to these, but not necessarily modified for circular polarization.

Because the HF and VHF bands are associated with considerably different wavelengths and therefore different dimensions, the choice of antennas and parameters will vary considerably. Therefore, the following discussion of characteristics will treat the two bands separately.

In the VHF band (88 to 108 MHz) the wavelength is approximately 10 feet. The maximum gain expected from an endfire antenna one wavelength long is on the order of 13 db. Because antennas with booms longer than 10 feet are not expected to be practical for the VHF band, 13 db may be considered as the upper bound for gain.

The percentage bandwidth required of a single antenna to cover the entire VHF band is slightly more than 20%. The VHF antennas listed in Table 2.4-1 are such broadband antennas. Therefore, they do not have the maximum gains achievable by a Yagi. (For example, a 6-element Yagi can be designed to yield 12 db of gain over a 4.5% band, but with a 20% band only about 6 db can be achieved.) In designs for the entire VHF band, therefore, gain is sacrificed for bandwidth.

Other antenna designs which may be worth consideration are helix, equiangular spiral, and log periodic antennas. The maximum gains of the equiangular spiral and the log periodic antennas will not exceed 10 db. The helix which can easily cover the entire FM band is perhaps the most reasonable. A 12-db helix at 100 MHz would have a diameter of $\approx$3.3 feet and a length of $\approx$9 feet, (depending on mid-band frequency choice).

For HF, some of the antennas listed in Table 2.4-1 are single band, i.e., CB, 10, 15, or 20 meter, others are multiband, 10, 15 or 20 meters being typical. The major differences between the HF and VHF antennas are physical dimensions and number of elements. Because of the longer wavelengths associated with HF, the antennas are considerably larger than for VHF: a half-wave dipole is 33 feet long at 15 MHz and 16.5 feet long at 30 MHz.

Table 2.4-1. Typical Antennas for HF and VHF Bands

VHF Band (87 to 108 mc)
Linear Polarization

Manufacturer	Type of Antenna	Gains	Cost
Jerrold FM-5	Yagi	6 db	$ 6.90
Jerrold FM-10	9-element Yagi	9 db	11.97
Blonder Tongue	5-element Yagi	5 db	9.20
Blonder Tongue	8-element Yagi	8 db	10.40

HF Band (15 to 30 mc)
Linear Polarization

Manufacturer	Type of Antenna	Band	Major Element Sizes	Gain	Cost
Master Mobile	3-element Yagi	10 meter	Boom 10 ft, maximum elevation 18 ft	8.0 db	$24.95
Mosley.	3-element Yagi	10, 15, 20 meter	Boom 12 ft, maximum elevation 19 ft	8.9 db	41.36
Mosley	3-element Yagi	CB	Boom 12 ft, maximum elevation 18 ft	8.0 db	35.00
Mosley	3-element Yagi	CB	Boom 24 ft, maximum elevation 18 ft	9.5 db	55.00
Master Mobile	Cubical Quad	CB	Boom 5.5 ft, longest elevation 9 ft	8.0 db	40.00
New Tronics	3-element Yagi	CB	Boom 9 ft, maximum elevation 18 ft	8.0 db	29.95
New Tronics	4-element Yagi	CB	Boom 14 ft, maximum elevation 18 ft	9.0 db	39.95
New Tronics	5-element Yagi	CB	Boom 19 ft, maximum elevation 18 ft	10.0 db	49.95
Mosley	1-element (Dipole)	10, 15, or 20 meter	Maximum element 27 ft.	2.0 db	23.85
Mosley	2-element Yagi	10, 15, or 20 meter	Boom 6 ft, maximum elevation 27 ft	5.0 db	51.98
Mosley	3-element Yagi	10, 15, or 20 meter	Boom 12 ft, maximum elevation 27 ft	8.0 db	72.98

Because the percentage bandwidth required to cover a particular band (10, 15, or 20 meter) in the HF band is less than 10%, the Yagi antennas may be operated near peak gain, which explains why considerably fewer elements are required to yield gains comparable with the VHF band antennas listed.

2.4.3 UHF ANTENNAS

2.4.3.1 UHF Antenna Types

Receiver antennas at UHF cover a wide range of individual designs, depending upon the antenna manufacturer. Insofar as the antennas furnished with the receiver are concerned, the most popular one consists of a simple single-turn wire loop attached to terminals on the back of the receiver. The loop may have a diameter of about 6 or 7 inches. The plane of the loop is made adjustable from the horizontal plane because the transmitted wave is horizontally polarized. When the receiver is operated inside buildings, however, the plane of the wave may be changed by reflection and reradiation from metal objects such as plumbing and house wiring, since the best reception sometimes occurs in other planes the loop antenna is made adjustable from the horizontal plane. The antenna is surprisingly effective when the field strength is sufficient.

When the signal delivered to the receiver terminals falls to low marginal levels, however, some kind of outdoor antenna may be needed. The type of outdoor antenna employed depends upon the gain required to render satisfactory service. The antennas commercially available range from a simple dipole to directional antennas of all descriptions such as broadside arrays, corner reflector types, and stacked "V" arrays. The gains vary from 2 db for the half-wave dipole to figures given by the manufacturers of up to 14 db, although with these higher figures there is usually no accompanying statement as to whether the gain is referred to a half-wave dipole or to an isotropic antenna.

2.4.3.2 Physical Construction of Antennas

Many high-gain antenna system designs may be found in the literature. Some of them are listed below:

a. Yagi
b. End-fire arrays of dipoles
c. Broadside arrays of dipoles
d. Rhombic
e. V-long wires
f. Corner reflector
g. Cylindrical parabolic reflector
h. Parabolic reflector
i. Log periodic
j. Open-sided horn
k. Pyramidal horn
l. Sectoral horn
m. Conical horn
n. Helix

Yagi and reflector types, if the gain has to be very high, are the most applicable for home use because of their reasonable dimensions and independence of critically tuned elements. When the gain required is relatively low or moderate, simple antennas systems consisting of a dipole with one parasitic reflector or one reflector and one director may be used.

2.4.3.3 Survey of Current UHF Antenna Installations

A survey of current practices in receiver UHF antenna installations was conducted. The latest available figures regarding TV receiver count is dated August 1965. At that time there were 53,675,000 in the United States. The number of homes having one or more receivers actually used to receive UHF television was 12,225,000 or 22.8%.

Thus, approximately 75% of all TV receivers do not employ any UHF antenna. Of the 25% that do employ some kind of UHF antenna, it is estimated that 25% use the simple 7-inch-diameter loop or "ring" fastened to the terminals on the back of the receiver; that 65% of the 25% use a dipole, usually of the "bow-tie" shape with or without a reflector; and that 10% of the 25% are more directional, usually of the corner reflector or of the Yagi types.

These percentages when converted into the number of homes employing the various types of antennas are shown in Table 2.4-2.

Table 2.4-2. UHF Antennas in Use in United States

UHF Antenna Type	Percent U.S. Homes with this antenna	Number of U.S. Homes with this antenna
Ring or loop on receiver back	6.25	3,360,000
Outside dipole with or without a reflector	16.25	8,740,000
Corner reflector or Yagi beam	2.50	1,340,000

If the UHF signal is of low field strength, the use of a high-gain beam receiving antenna may often lead to rather disappointing results. The principal reason for this is that propagation conditions have been found to be quite variable at UHF at distances beyond the optical horizon so that at one hour a fairly good picture may be received but a couple of hours or a day later practically no picture may be received. This experience accounts for the relatively few beam antennas in use.

2.4.4 HOME ANTENNA PERFORMANCE LIMITATIONS

Table 2.4-3 summarizes the study results obtained for manufactured home antennas.

Table 2.4-3. Home Antenna Performance Limitations

Band	Antenna Type	Antenna Gain	Mismatch Loses*	Polarization Loses	Notes
HF	Whip	5 db	3 db	3 db	Built-in unit
HF	Loop	1.76 db	10 db	3 db	Built-in unit
HF	3-element Yagi	8 db	0.2 db	3 db	External unit
HF	3-element Yagi				
HF	Cubical Quad	8 db	0.2 db	0 db	Home made
HF	2-turn helix				
FM	Whip antenna	5 db	0.2 db	3 db	Built-in unit
FM	Half-wave dipole	2.17 db	0.2 db	3 db	Built-in unit
FM	3-element Yagi	8 db	0.2 db	3 db	External unit
FM	6-element Yagi	12 db	0.2 db	3 db	External unit
FM	5-turn helix	12 db	0.2 db	0 db	Special design
FM	3-element Yagi				
FM	Cubical Quad	7 db	0.2 db	0 db	Home made
FM	3-turn helix				
UHF	Rabbit ears	2 db	0.2 db	3 db	Built-in unit
UHF	Half-wave dipole	2.17 db	0.2 db	3 db	External unit
UHF	3-element Yagi	8 db	0.2 db	3 db	External unit
UHF	6-element Yagi	12 db	0.2 db	3 db	External unit
UHF	15 element Crossed Yagi				
UHF	5-foot dish	18 db	0.2 db	3 db	Special Design

*Matching Transformers (e.g., baluns) are assumed where required. Such transformers will reduce VSWR to the order of 15:1, with corresponding losses less than 0.2 db.

Figure 2.4-1 shows the way in which these antennas are distributed. The distribution shows approximately 50% are indoor and 50% outdoor. These values are based on data gathered from GE Television Service Department for UHF in the United States. Estimates from world wide users indicates that this distribution applies to all bands.

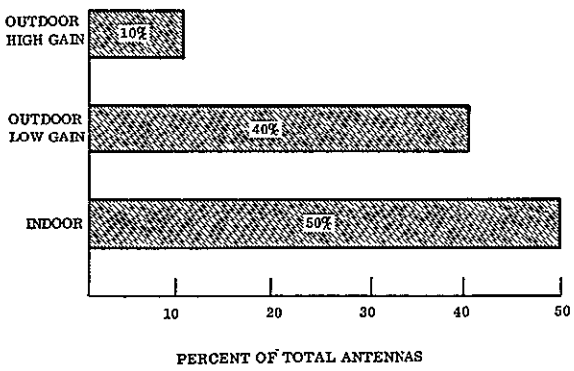

Figure 2.4-1. Antenna Distribution

2.5 NOISE MEASUREMENT PROGRAM

2.5.1 INTRODUCTION

2.5.1.1 Summary

As an integral part of the Voice Broadcast Mission Study (VBMS) General Electric has conducted a limited program for measurement of man-made noise. This program was necessary to gain a better understanding of the distribution of man-made noise for frequencies and conditions of interest in the VBMS. In addition, the information derived from these measurements can be extrapolated to further define the man-made noise environment at UHF and to compare with other measurements.

A major factor in the analysis of signal quality at the receiver is the external noise. This includes both man-made and natural (galactic and atmospheric) noise sources. The natural sources are fairly well understood because of the extensive measurements taken over many decades. The man-made noise is less well described but, at low frequencies, is the most important source because of its high levels.

It was also believed desirable to measure the amount of discrimination to man-made noise afforded by a high gain antenna that is elevated from the horizon. This would be the situation that would exist in the case of a high gain receiving antenna looking at a broadcast satellite in orbit.

2.5.1.2 Conclusions

The noise data derived from this program can be used directly in studies such as the Voice Broadcast Mission Study (VBMS) or extrapolated to higher frequencies to define the required vehicle/satellite effective radiated power to meet a desired signal-noise ratio in the various noise environments. To specify the required satellite effective radiated power and required ground-receiving antenna gains, the total receiving system effective temperature must be known. This effective temperature must include the effects of receiver noise, atmospheric noise, galactic noise, and man-made noise for typical urban, suburban, and rural receiving sites. It is believed that the noise data derived from this program is fairly representative of typical urban, suburban, and rural environments. In particular, the suburban data obtained is significant as very little, if any, meaningful data has been obtained for a typical suburban environment at these frequencies.

In Table 2.5-1 the results of the GE noise measurements are compared to values from other surveys that have been made and for which the method of measurement is known. All data have been converted to average noise power in db above KT_0B.

where

KT_0B = Effective receiver noise power

K = Boltzmann's constant = 1.38×10^{-23} joule/degree Kelvin

T_0 = Absolute temperature in degrees Kelvin

B = Receiver bandwith

Table 2.5-1. Comparison with Other Surveys

Location	Frequency (MHz)	GE	Average Noise Power in db Above KT_0B			
			Beverage	Hammer	ESSA	ITT
Urban	25.8	42	44	66	50	60.5
Suburban	25.8	24	27	-	-	53
Urban	90.4	32	31	45	35.5	45.5
Suburban	90.4	16.5	17	-	-	40
Rural	25.8	18	-	-	17.5	-

The GE data is in very close agreement with that of Beverage for the locations considered and is also in close agreement with ESSA, except for the urban site. This amount of difference can certainly be expected for different urban areas or, for that matter, different locations in a particular urban area. It can be seen that the ITT and Hammer data is considerably higher than any of the others.

The results of the antenna discrimination measurements indicate that a high gain antenna elevated 45 degrees from the horizon provides a reduction in the man-made noise of approximately half the antenna forward gain. The noise is approximately at the galactic level at both 25.8 MHz and 90.4 MHz. The 45-degree inclination would be representative of a ground receiving antenna elevated to receive a signal from a satellite in synchronous orbit, and this amount of discrimination to the man-made noise environment should be taken into consideration in systems performance analysis for this case.

The effect of antenna height on the reception of man-made noise was measured at the urban site. Three heights were utilized: the roof top of an eight story building, 20 feet above ground level, and 10 feet above ground level. The highest noise level was from the roof top level. At this height, a much larger field of view of the noise sources was available, since the near ground levels were masked to a large extent by large surrounding buildings. It would be expected that for a homogeneous distribution of noise sources, such as exists in an urban site, the noise would not vary with antenna height to any degree. The decrease in noise at the lower heights can be attributed to the attenuation afforded by the large building structures. The noise at 25.8 MHz at the 10-foot level was actually higher than at 20 feet. This could have been due to power line noise from the buildings or increase in reception of automobile ignition noise at the lower height. For an extremely quiet location, the reception of man-made noise would tend to increase with antenna height as more distant noise sources come into view.

2.5.2 TEST PROCEDURE

The program consisted of measurements of man-made noise using the GE Noise Amplitude Distribution Measurement equipment (NADME) at two frequencies, HF and VHF, over a two-week period at each of three sites, urban, suburban,and rural. Measurements were made during both daytime and nighttime hours. The site selections are shown in Figure 2.5-1. The urban site is the GE installation in downtown Philadelphia; the Suburban, the GE complex at Valley Forge; and the rural in farmlands near Bucktown, Pa. The urban, suburban, and rural site installations are shown in Figures 2.5-2 through 2.5-4. At the urban site, the antennas were installed on a 20-foot tower on the roof of an eight-story building. At the suburban and rural sites, the antennas were installed on a 40-foot tower. An automatic rotator was used to select different azimuth positions,and the elevation positions of the high gain antennas were varied by means of cables and pulleys.

The frequencies used for measurement were 25.8 MHz and 90.4 MHz. These were selected on the basis of minimum interference from broadcast signals in this area.

The equipment used for the measurements was the General Electric-designed NADME which consists of eight solid-state amplitude detectors and counters. Each amplitude detector is adjusted to respond to a preset amplitude,and the counters are used to count the number of pulses exceeding each preset amplitude over an interval of time. The average of noise pulses per second is then calculated. Two sets of NADME (Figure 2.5-5) were utilized for each frequency and were connected to the IF outputs of crystal-controlled solid-state receivers tuned to the frequency of operation. One set of NADME was utilized to provide a baseline measurement of the noise with a horizontal dipole antenna, and this information was used in converting to the average noise power in db above KT_0B. The other set of NADME was used in conjunction with the high gain antennas for noise discrimination tests. The high gain antennas used for the discrimination tests were an 8 db linear yagi, an 11 db circular helix at 90.4 MHz and a 6 db linear yagi at 25.8 MHz. Discrimination measurements were made at elevation angles of 0, 45 and 90 degrees for each of three azimuth positions (0, 110 and 200 degrees). The antennas are shown in Figure 2.5-6.

A gross measurement of the noise was also made at all three sites by continuously recording the outputs of receivers for each frequency over the entire six-week measurement period. This measurement was intended to show any major changes in the noise environment at each site over a long term period before, during, and after the interval when NAD measurements were being made.

Figure 2.5-1. Map of Sites

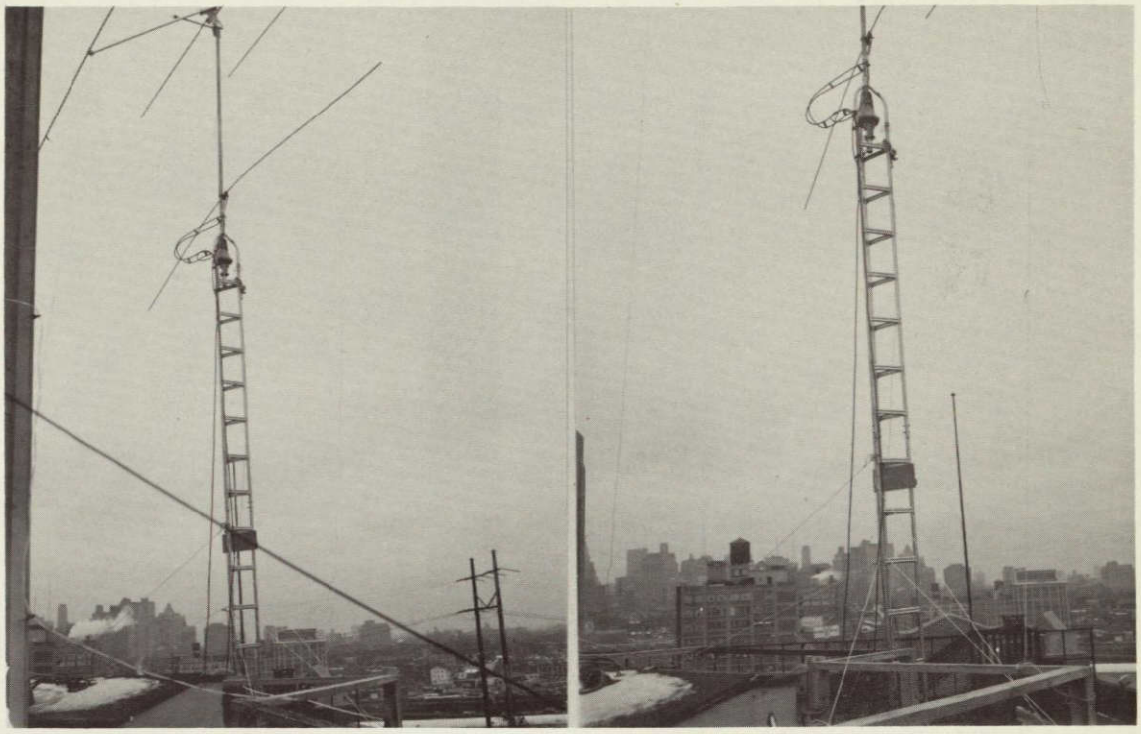

Figure 2.5-2. Urban Site

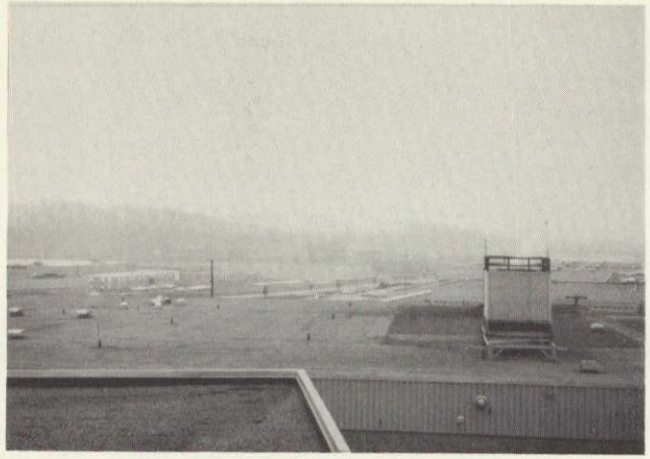

(a) Direction of Allendale Road and CC&F1

(b) Road Adjacent to CC&F1

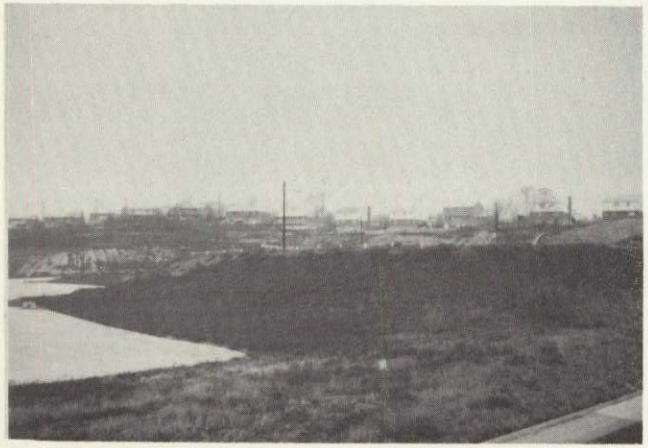

(c) Azimuth Angle = 0 Degrees (Approx.)

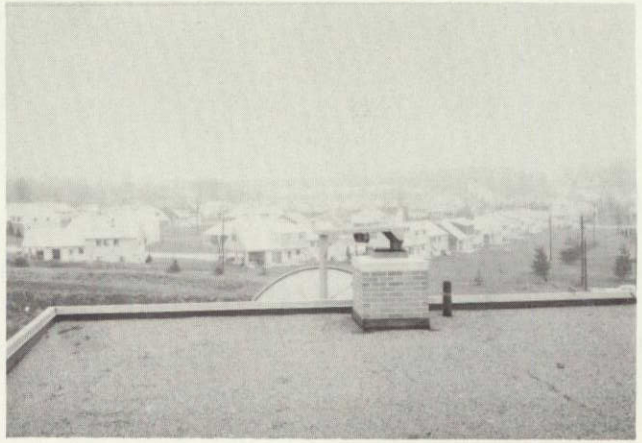

(d) Azimuth Angle = 120 Degrees (Approx.)

Figure 2.5-3. Suburban Site

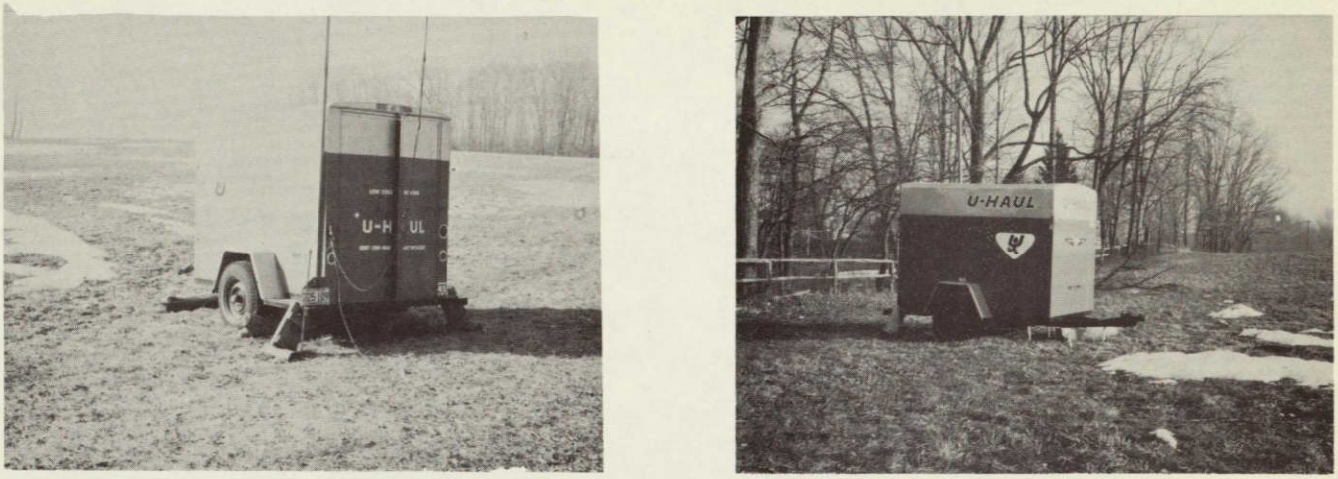

Figure 2.5-4. Rural Site

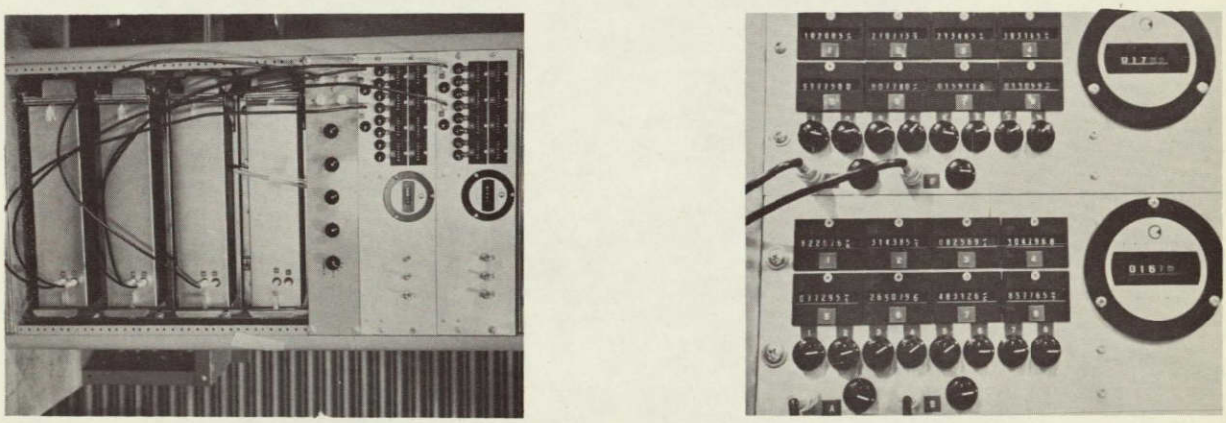

NADME Unit

Closeup of NADME Counters

Figure 2.5-5. Measurement Equipment

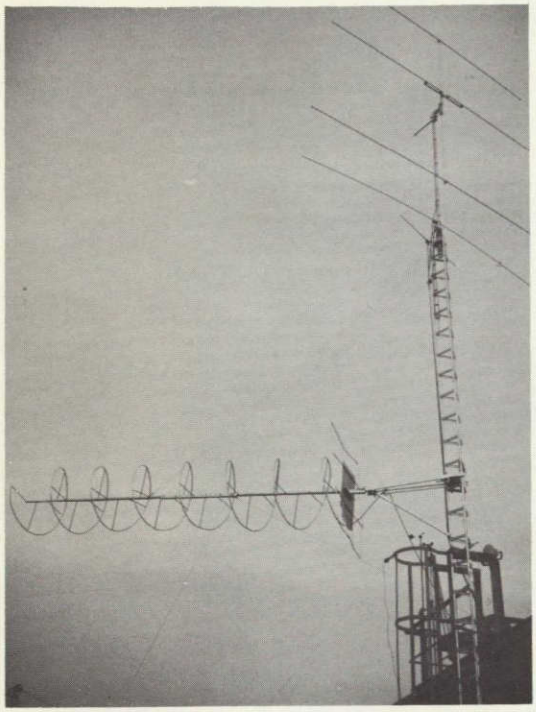

(a) Helix at 0 Degrees Elevation, 0 Degrees Azimuth

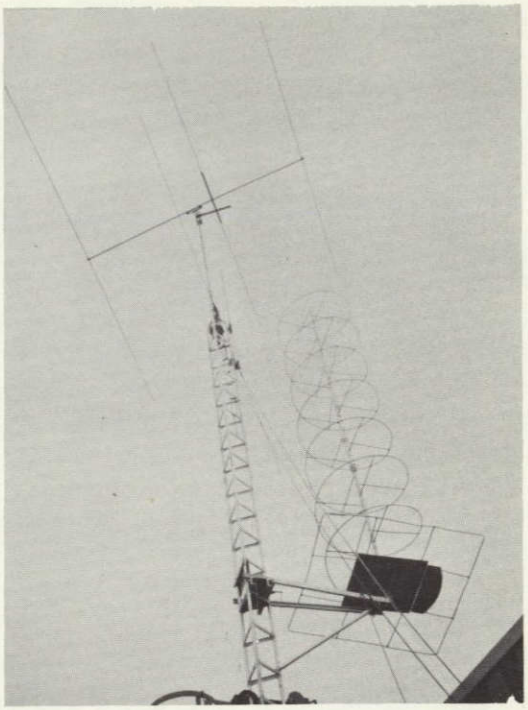

(b) 90 mc Helix and 10 Meter Beam

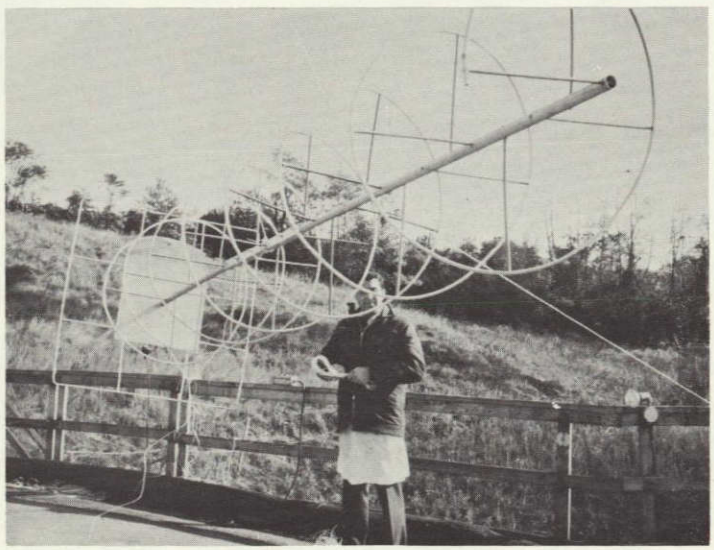

(c) Checking Helix Pattern on RCS Range

Figure 2.5-6. Antennas

2.5.3 RESULTS OF NOISE MEASUREMENTS

The results of the noise measurements are shown in Tables 2.5-2 through 2.5-5.

Table 2.5-2. Urban Site-Average Noise Power

25.8 MHz	
Daytime	44 db above KT_oB - 7.27 x 10^6 °K
Nighttime	41 db above KT_oB - 3.74 x 10^6 °K
Average Day and Night	42 db above KT_oB - 4.6 x 10^6 °K
90.4 MHz	
Daytime	32 db above KT_oB - 4.6 x 10^5 °K
Nighttime	32 db above KT_oB
Average Day and Night	32 db above KT_oB

Table 2.5-3. Urban Site - Effect of Antenna Height on Received Noise (Noise Power in db Above KT_oB)

Frequency	10 Feet Above Ground	20 Feet Above Ground
25.8	38.5	31.5
90.4	26.5	25.5

Table 2.5-4. Suburban Site - Average Noise Power

25.8 MHz	
Daytime	29.4 db above KT_oB - 2.53 x 10^5 °K
Nighttime	18 db above KT_oB - 1.83 x 10^4 °K
Average Day and Night	24 db above KT_oB - 7.25 x 10^4 °K
90.4 MHz	
Daytime	17 db above KT_oB - 1.45 x 10^4 °K
Nighttime	16 db above KT_oB - 1.16 x 10^4 °K
Average Day and Night	16.5 db above KT_oB - 1.295 x 10^4 °K

Table 2.5-5. Rural Site-Average Noise Power

25.8 MHz	
Daytime	18 db above KT_oB - 1.83 x 10^4 °K
Nighttime	18 db above KT_oB
Average Day and Night	18 db above KT_oB
90.4 MHz	
Daytime	4 db above KT_oB - 725 °K
Nighttime	4 db above KT_oB
Average Day and Night	4 db above KT_oB

The results of these measurements are shown in Figure 2.5-7 along with the ESSA data for urban and rural sites. This data is the average of the day and night measurements, except for the 25.8 MHz suburban data where the nighttime data is actually at the galactic noise value and should not be classified as man-made noise.

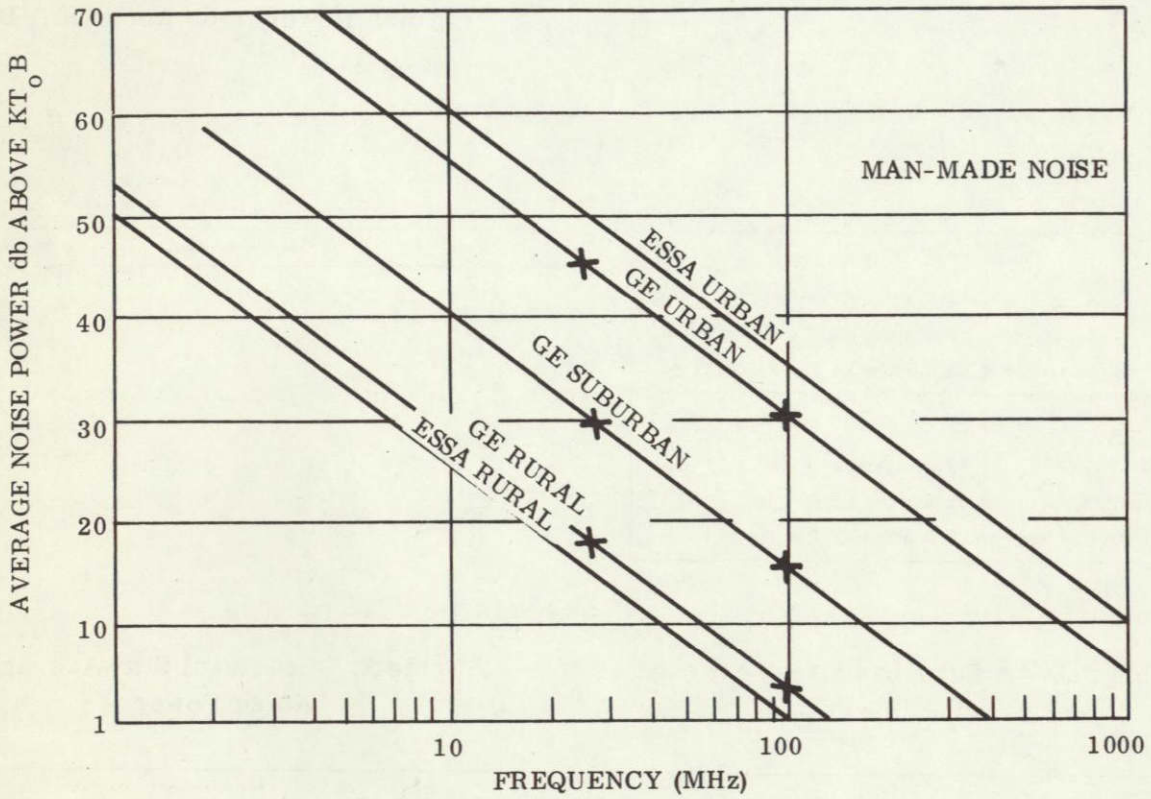

Figure 2.5-7. Man-Made Noise

It can be seen that for the urban environment, the man-made noise is very high for both frequencies, day and night. A low noise receiver or preamplifier would therefore be of little value in this situation.

For the suburban location, the man-made noise at 25.8 MHz is moderately high during the daytime, but is approximately at the galactic noise level at night. At 90.4 MHz, the noise is moderately low during both day and night. At the rural site, the noise level is very low, being approximately at galactic level at both 25.8 and 90.4 MHz.

2.5.4 RESULTS OF ANTENNA DISCRIMINATION MEASUREMENTS

The results of the antenna discrimination measurements are shown in Table 2.5-6.

Table 2.5-6. Antenna Discrimination Measurements

Frequency (MHz)	Antenna	Discrimination at 45° Elevation (db)	Discrimination at 90° Elevation (db)
Urban Site			
25.8	6 db Linear Yagi	3.5	5.8
90.4	8 db Linear Yagi	5.5	8.8
90.4	11 db Circular Helix	7.0	6.0
Suburban			
25.8	6 db Linear Yagi	3	2
90.4	8 db Linear Yagi	5	4.5
90.4	11 db Circular Helix	6	9
Rural			
25.8	6 db Linear Yagi	1.65	3.45
90.4	8 db Linear Yagi	*	*
90.4	11 db Circular Helix	*	*

*Impossible to perform discrimination measurements at this frequency as the ambient noise level approaches the receiver noise level.

2.5.5 GROSS NOISE MEASUREMENTS

The gross noise measurements were not meant to produce a quantitative measurement of average noise power, but to serve as an indication of any major changes in the noise environment during the measurement program. These measurements were made at all three sites by continuously recording the outputs of receivers for each frequency over the six-weeks measurement period.

Examination of the strip-chart recordings shows that no major continuing changes occurred at any of the sites during this period. There were, however, normal variations during peak traffic hours and during working hours of local industry.

The recordings for the urban site of 25.8 MHz show the noise to be moderately high, both day and night, with the night reading being somewhat lower. At 90.4 MHz the noise is considerably less than at 25.8 MHz and is approximately the same both day and night with some periodic bursts occurring.

For the suburban site, the noise is moderate during the daytime hours at 25.8 MHz and is relatively low at nighttime. At 90.4 MHz the noise is moderately low both day and night.

At the rural site, the noise is moderately low at 25.8 MHz, both day and night, and is extremely low both day and night at 90.4 MHz.

Qualitatively, these recordings are in reasonably close agreement with the much more accurate NAD measurements. A representative strip-chart recording for a-24 hour period at each site is shown in Figure 2.5-8.

2.5.6 MEASUREMENT TECHNIQUES

The Noise-Amplitude Distribution (NAD) is a description of various types of noise presented in curve form on semi-logarithmic paper. The amplitude scale of the NAD is in peak voltage across 50 ohms with units of db above 1 μv/MHz. The abscissa scale is in average pulses per second exceeding each amplitude. The advantages of using the NAD over other methods of displaying noise data are:

a. The data presentation is of the form of an interface specification at the receiver input terminals; thus no conversion is required.

b. No conversion curves are required to convert from one bandwidth to another since the amplitude is on a per-MHz basis.

c. The amplitude scale is in units normally found on impulse noise generators.

d. The NAD can be converted to the portion of an Amplitude Probability Distribution (APD) which represents nonoverlap on filter response and for a given filter with known impulse response.

e. The equipment used to measure the NAD can be used to obtain statistics other than the average number of pulses (such as time spacings between noise bursts) by adjusting the measurement times.

f. The NAD includes important properties of the noise such as its slope, saturation knee, and node.

g. The NAD can be converted to quasi-peak readings for any well-defined metering circuits.

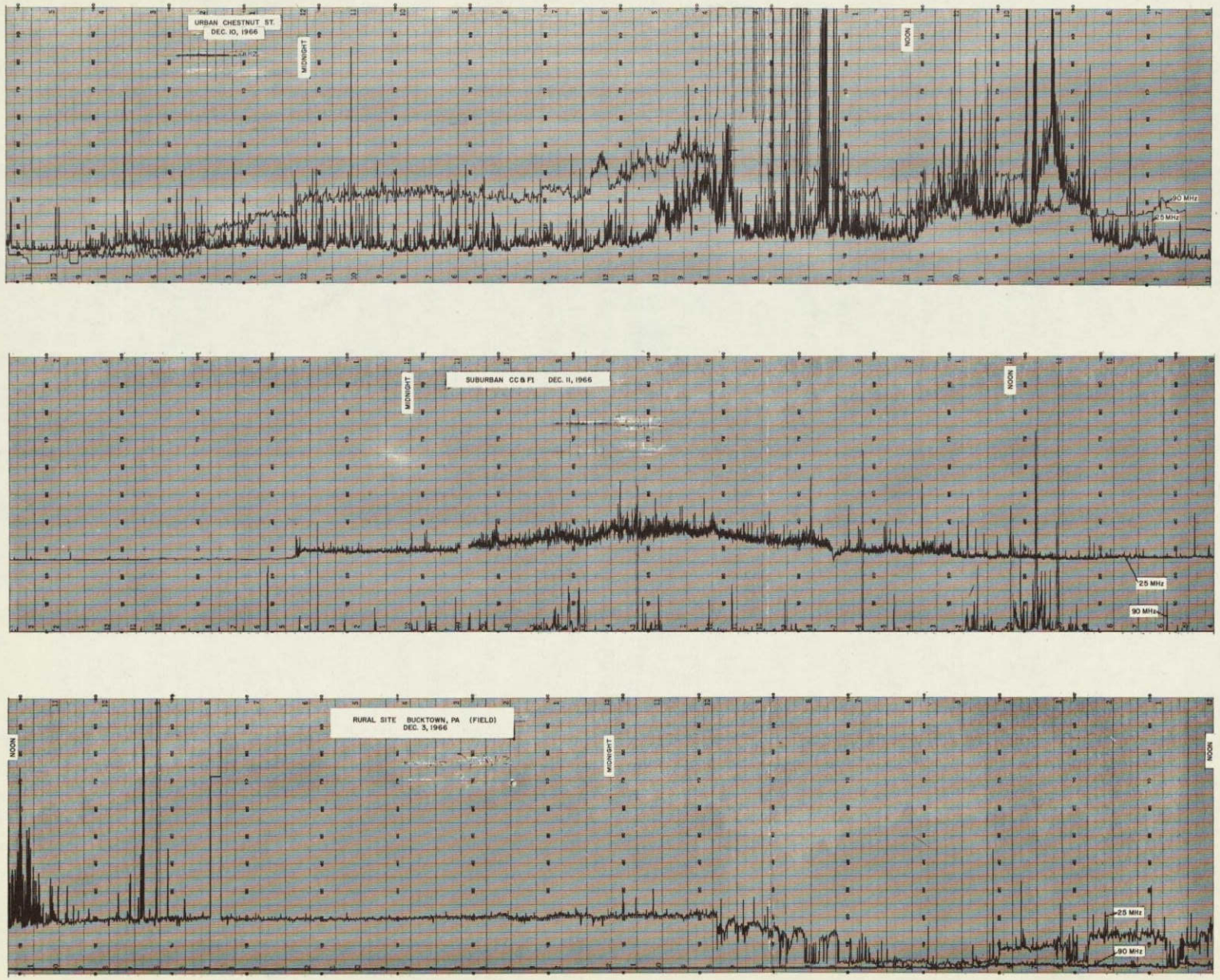

Figure 2.5-8. Urban, Suburban, and Rural Gross Measurements

The noise properties are defined as follows:

a. Noise Slope - Noise slope is defined as the rate of change of the impulse amplitude versus pulse rate and is expressed in db per decade change in pulse rate.

b. Noise Saturation - Noise saturation is defined as the impulse amplitude above which the noise slope is less than 3 db/decade.

c. Noise Knee - Noise knee is defined as the impulse amplitude below which the noise slope increases due to increase in propagation attenuation. The noise knee is frequently obscured by the noise figure of the measurement equipment.

d. Noise Node - Noise node is defined as the impulse amplitude where the noise slope increases or decreases as a result of non-homogeneous noise sources.

2.5.6.1 Measurement of the NAD

The Noise Amplitude Distribution is measured by recording the reading of each counter prior to turning on the NAD equipment, with each of the eight amplitude detectors adjusted to respond to a certain pulse amplitude. (This amplitude is generally 40 to 80 db, but it depends on the noise environment at the site.) The equipment is then turned on and allowed to count for a specified period (5 minutes, 15 minutes, 24 hours, etc.) When the counters are turned off, a reading is made of each counter and the reading prior to starting is subtracted to give the number of counts during the run. The average number of pulses per second for each amplitude is then calculated by multiplying the number of counts by the division factor and dividing by the time in seconds. From this data, the NAD is plotted.

2.5.6.2 Conversion of NAD to Average Power Above KT_oB

A portion of all of the NAD can be converted to a single quantity of noise power by the use of Figures 2.5-9 and 2.5-10, provided the noise slope is relatively constant for that portion of the NAD for which the conversion is desired.

Figure 2.5-9 is first used to convert the saturation point and its corresponding pulse rate to db above KT_oB. Figure 2.5-10 is then used to increase the quantity obtained from Figure 2.5-9 by a number of db corresponding to the noise slope and the number of decades for which conversion is desired.

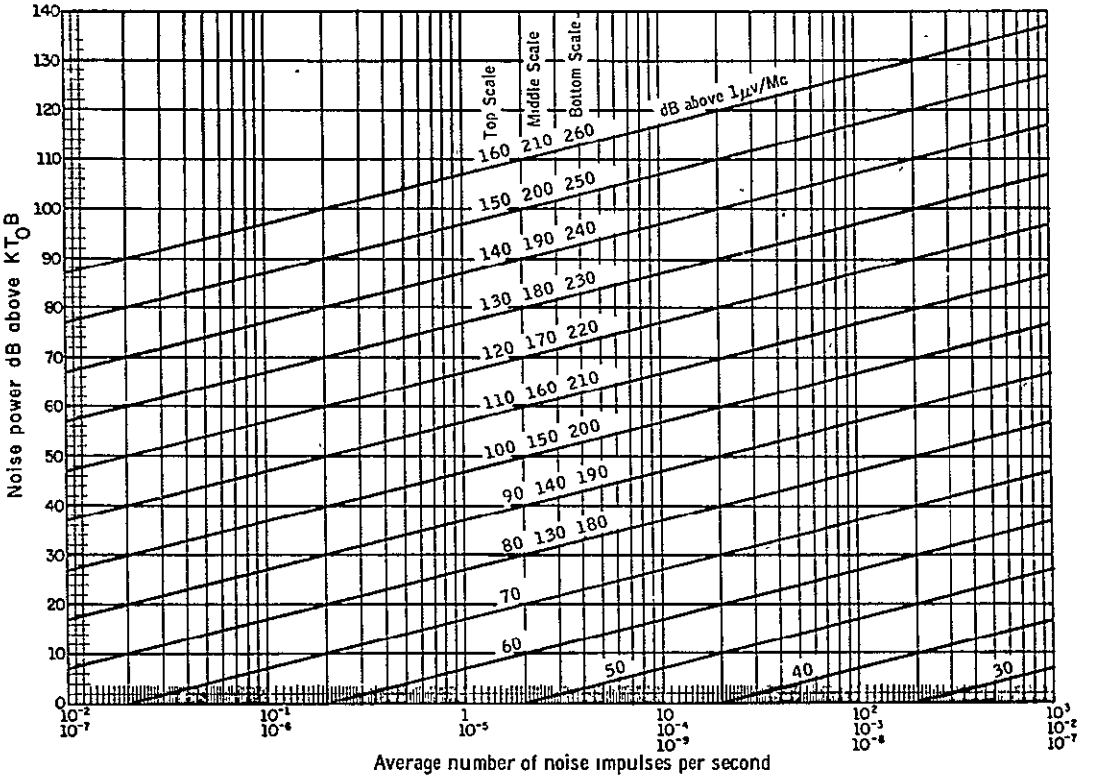

Figure 2.5-9. Conversion of NAD to Power

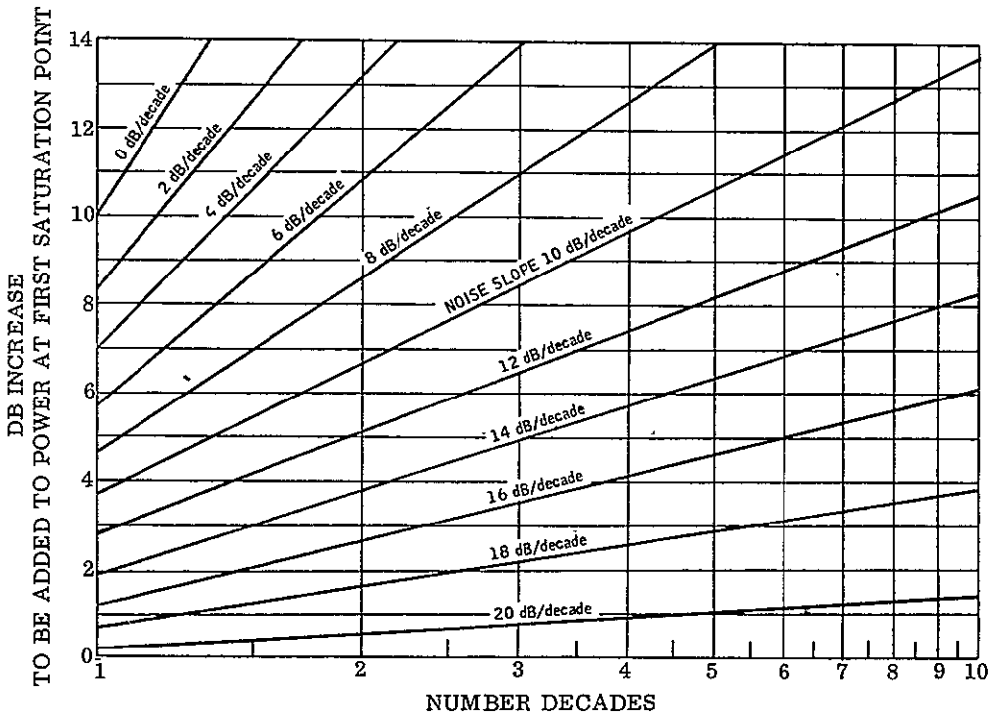

Figure 2.5-10. Conversion of NAD to Power

As an example of conversion from the noise curve to noise power, the estimated atmospheric curve in Figure 2.5-11 is used. The saturation point is 191 db above 1 μv/MHz at a pulse rate of 1.64×10^{-8} pulse per second which gives a noise power of 60 db above KT_0B from Figure 2.5-9. The NAD slope is constant at 10 db/decade for about 10.5 decades. The conversion curve, Figure 2.5-10 shows that about 14 db should be added to the 60 db to make a total noise power of 74 db above KT_0B.

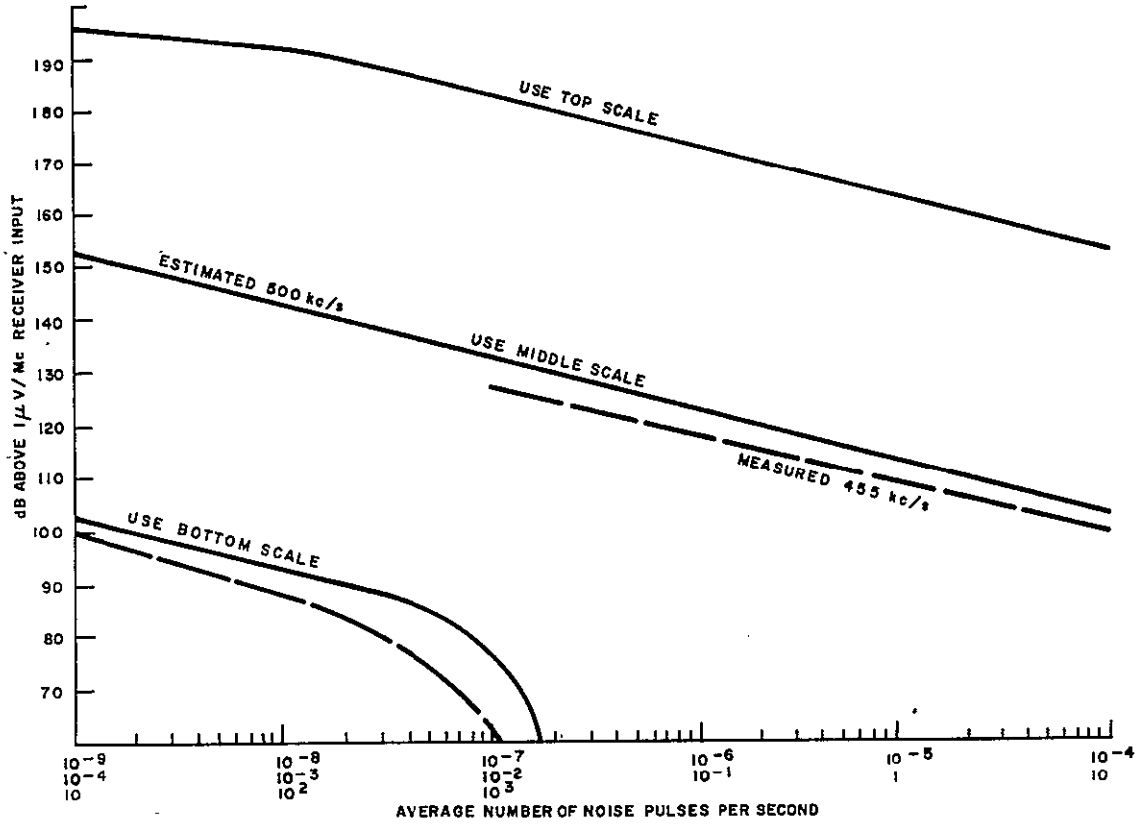

Figure 2.5-11. Typical Atmospheric Noise, Measured and Estimated for Winter Nighttime

2.5.7 NAD EXPERIMENTAL DATA

The results of the noise measurement program are represented as Noise Amplitude Distribution (NAD) plots, and examples are presented for the urban, suburban, and rural site locations. These plots are presented under the following headings:

a. NAD Urban plots

b. NAD Suburban plots

c. NAD Rural plots

2.5.7.1 NAD Urban Plots

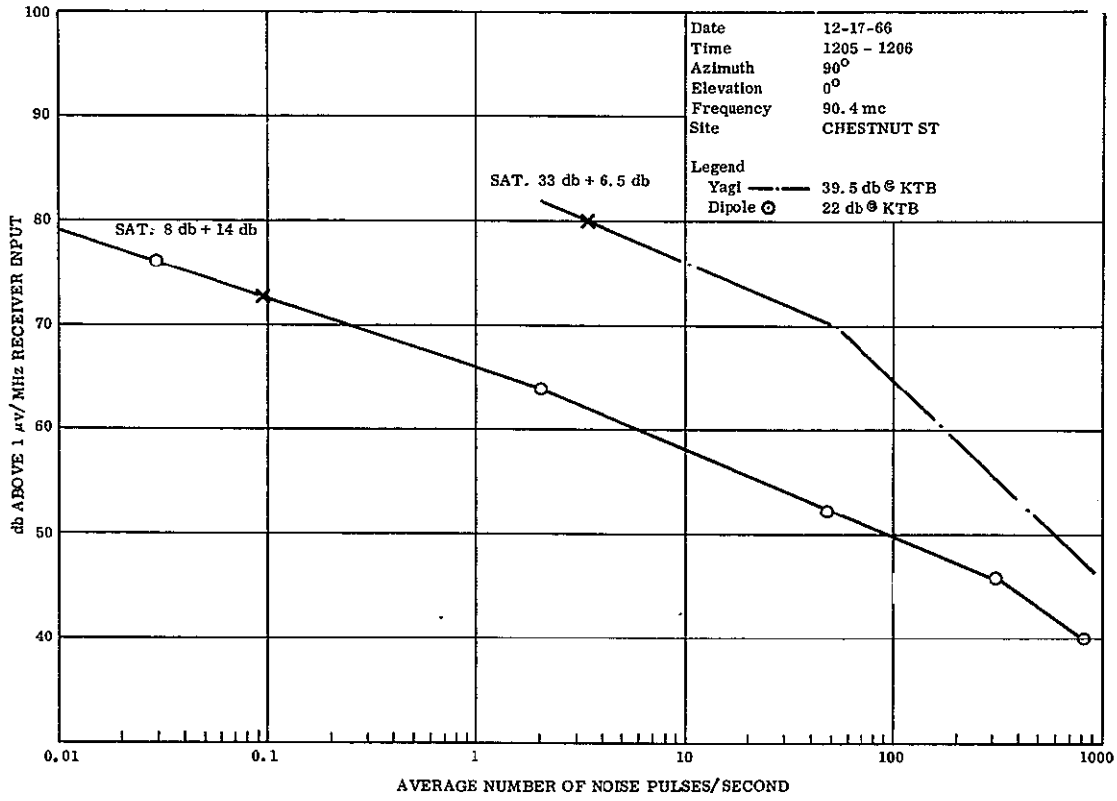

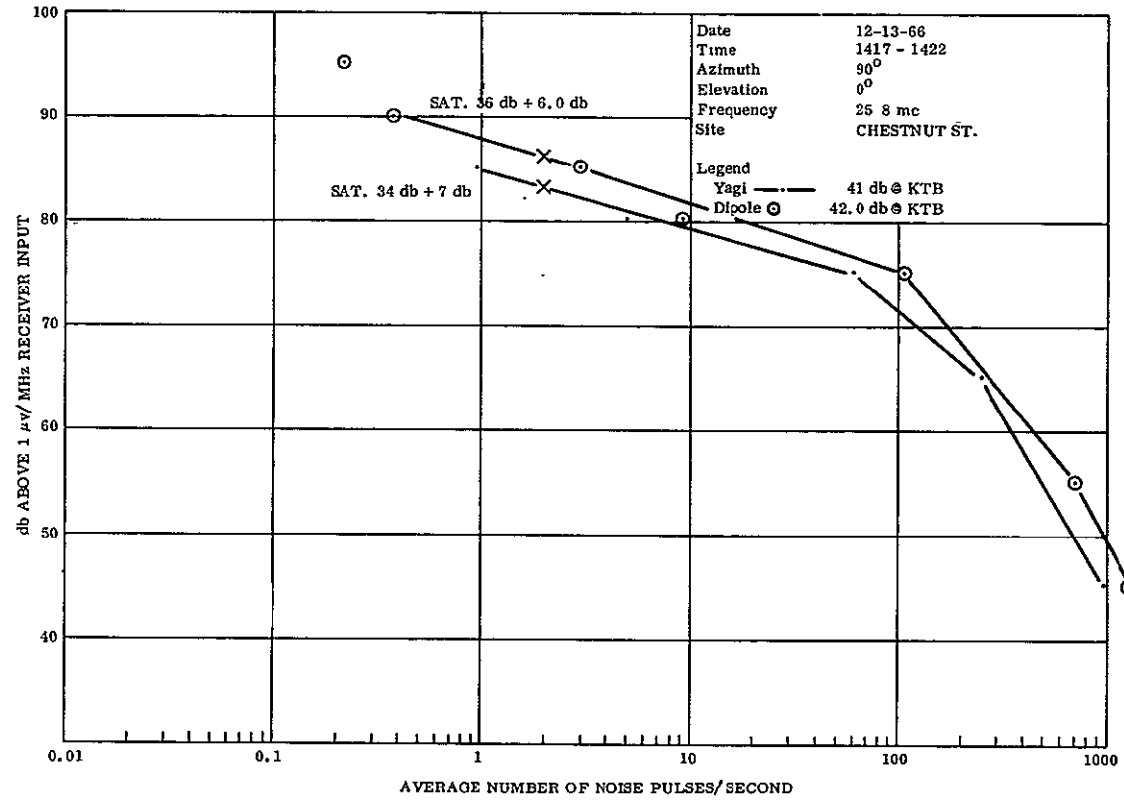

2.5.7.2 NAD Suburban Plots

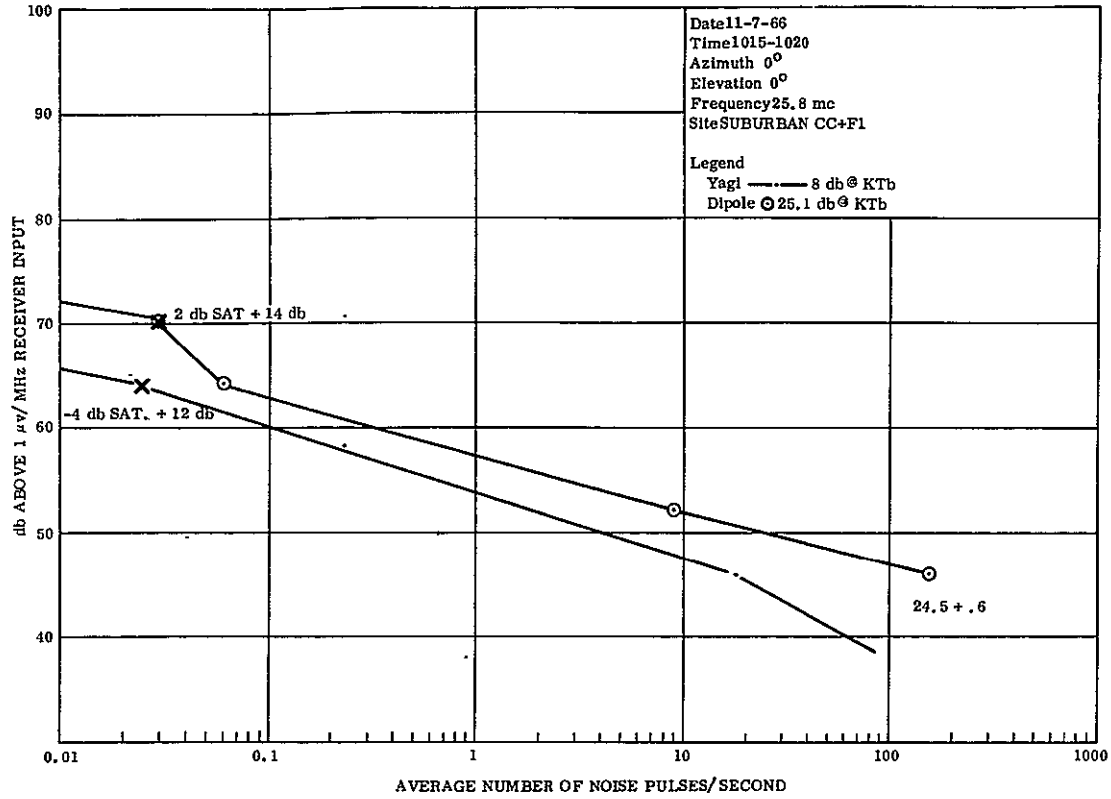

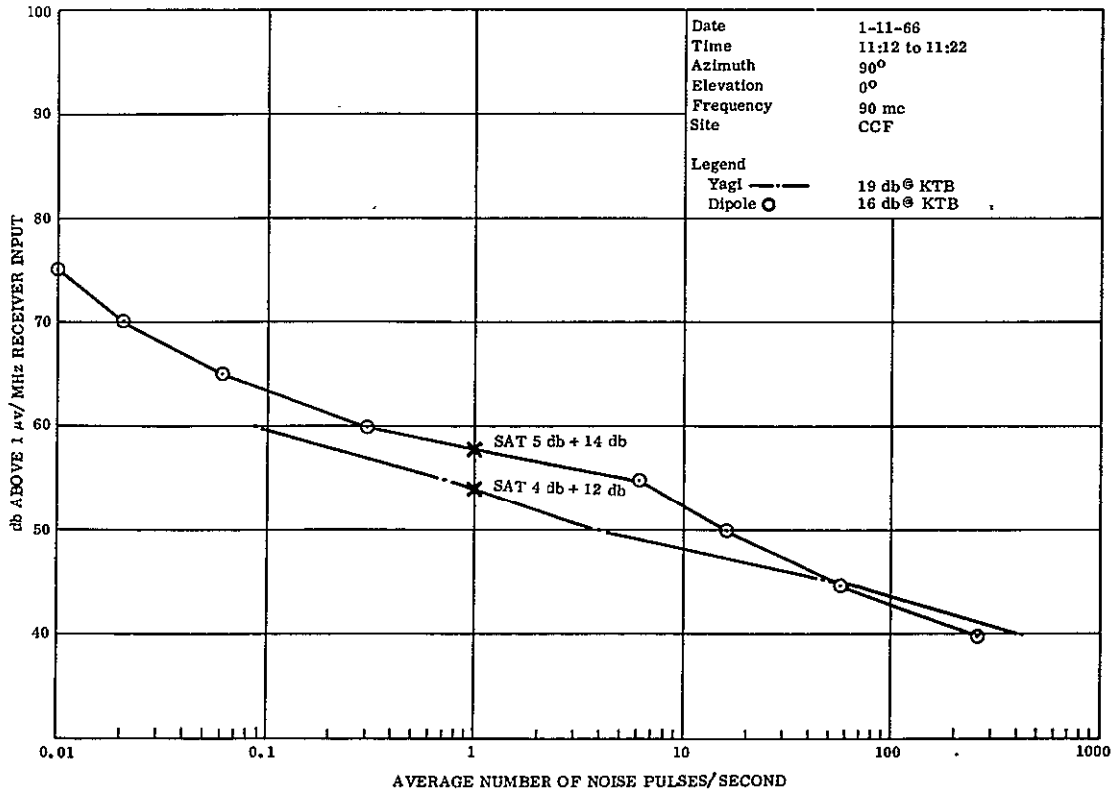

2.5.7.3 NAD Rural Plots

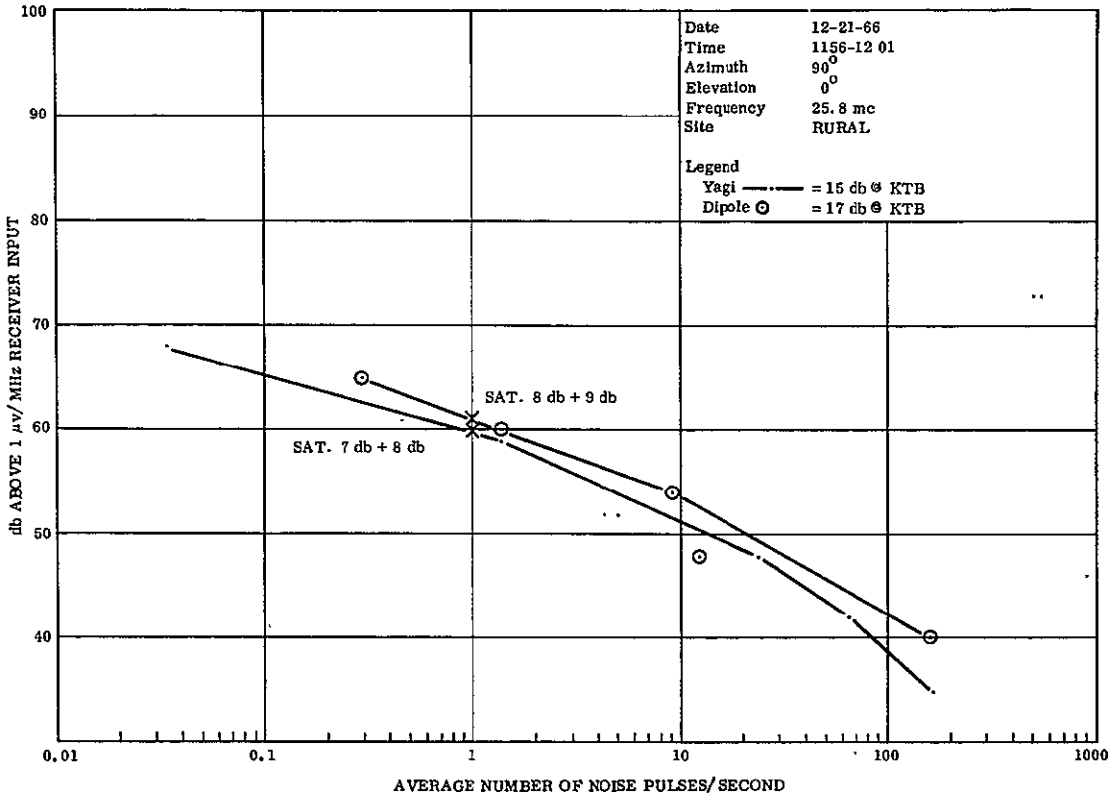

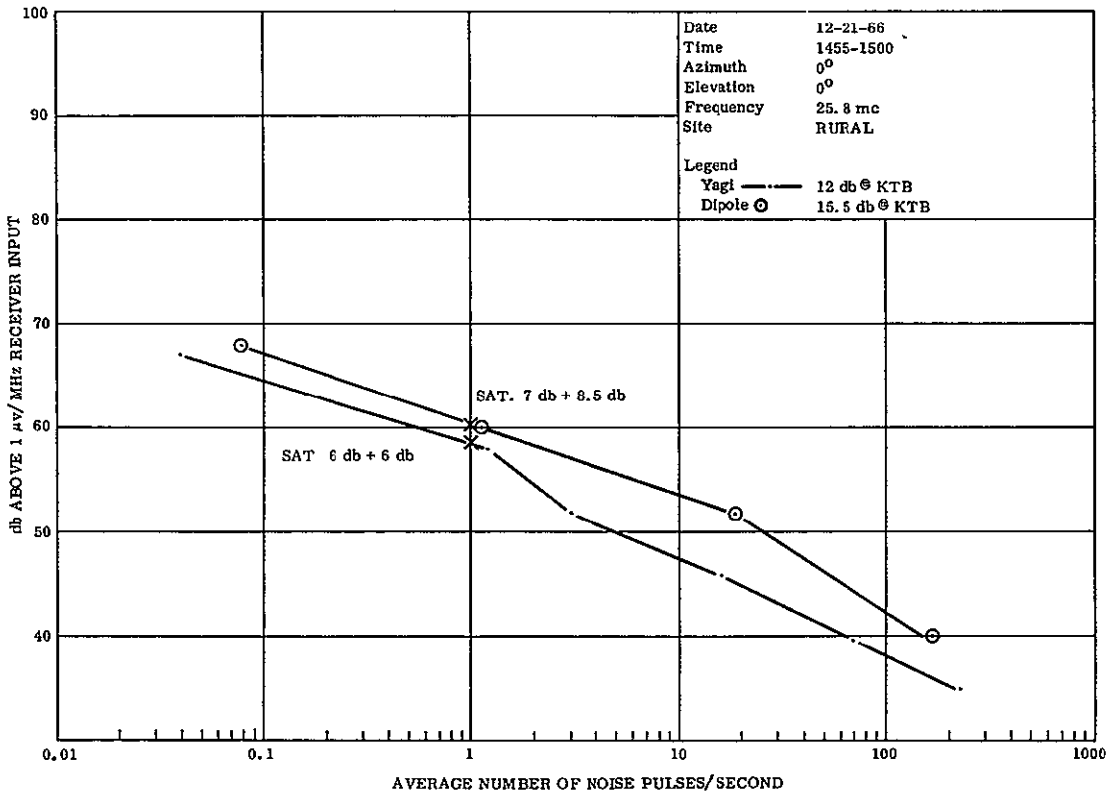

2.6 AUDIENCE ANALYSIS

The audience analysis was composed of two parts, distribution of receivers and signal level requirements. These topics are discussed below in detail for each of the three frequency bands (HF, VHF, and UHF).

The selection of broadcast frequency is directly affected by the potential audience. The study has attempted to define the potential audience available for broadcast missions in terms of the current and projected distribution of receivers. A summary of the receiver distribution projected to 1970 for the seven major world areas is shown in Figure 2.6-1.

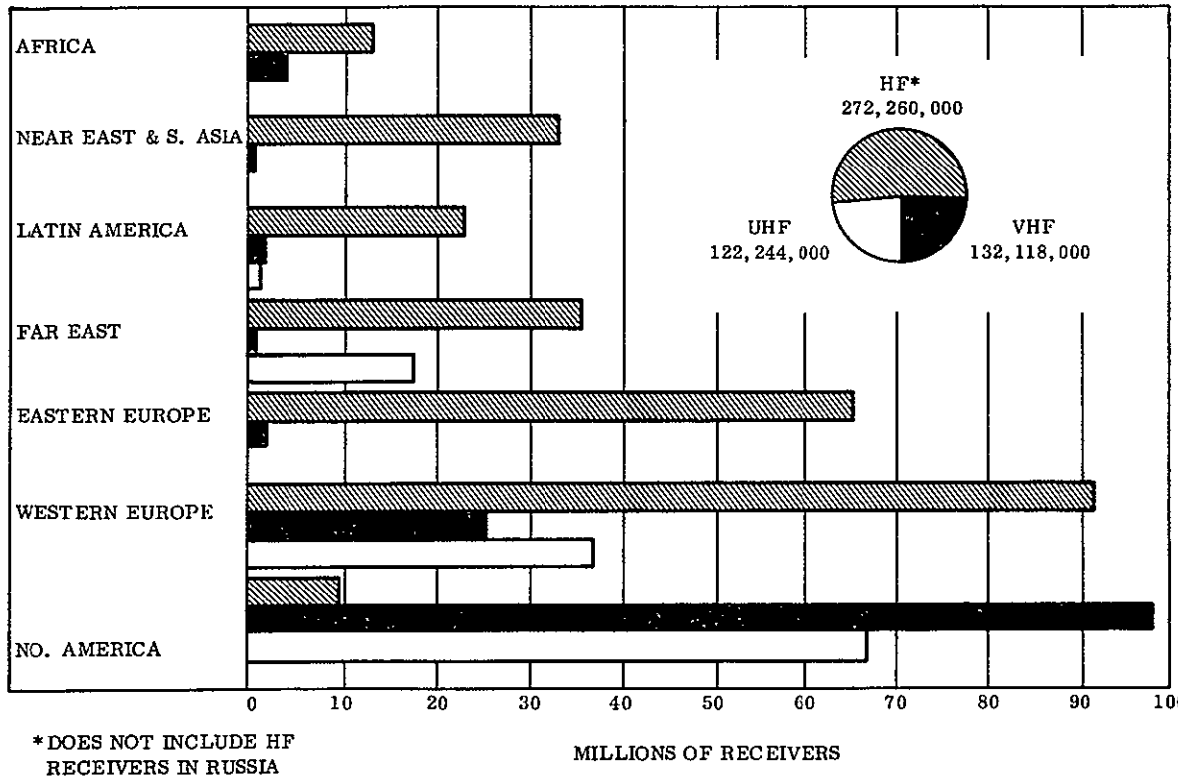

Figure 2.6-1. 1970 Distribution of Receivers

The top bar for each area represents the number of AM shortwave (SW) receivers. As can be seen, there will be more receivers in the HF band (over 270 million) than in the VHF and UHF bands combined. The second bar represents the number of FM sets in the VHF band. Only western Europe and North America will have any appreciable quantity of sets. Finally, the third band which is nonexistent in Africa, the Near East, South

Asia, and the Eastern European areas, shows the number of UHF/TV sets expected by 1970. Western Europe and North America are the major areas with the largest potential audiences.

2.6.1 HF RECEIVER DISTRIBUTION

The first factor considered in defining receiver distribution was the determination of the world areas which are uninhabited, defined for the study as areas where the population density is less than one person per square mile. This is illustrated in Figure 2.6-2, the black land mass areas being those considered uninhabited. This map shows that space broadcasting missions could be limited to areas between 70°N and 50°S latitude without significantly reducing the potential audience.

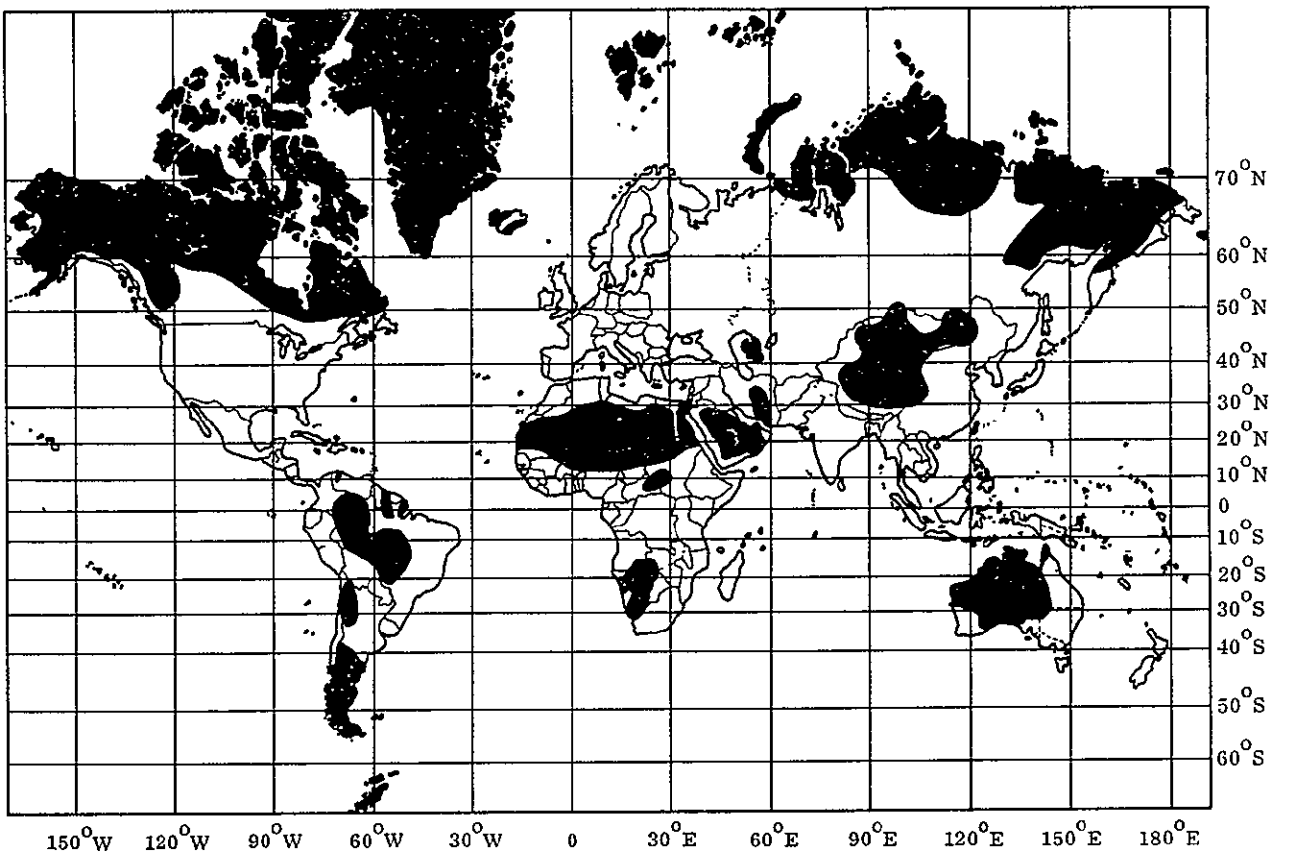

Figure 2.6-2. Uninhabited Areas of the World (< 1 person/mi^2)

The inhabit areas where HF broadcasting is in operation are shown in the unshaded land areas Figure 2.6-3. The map does not show operations in the USSR because of limited information available to define the HF broadcasting in that country.

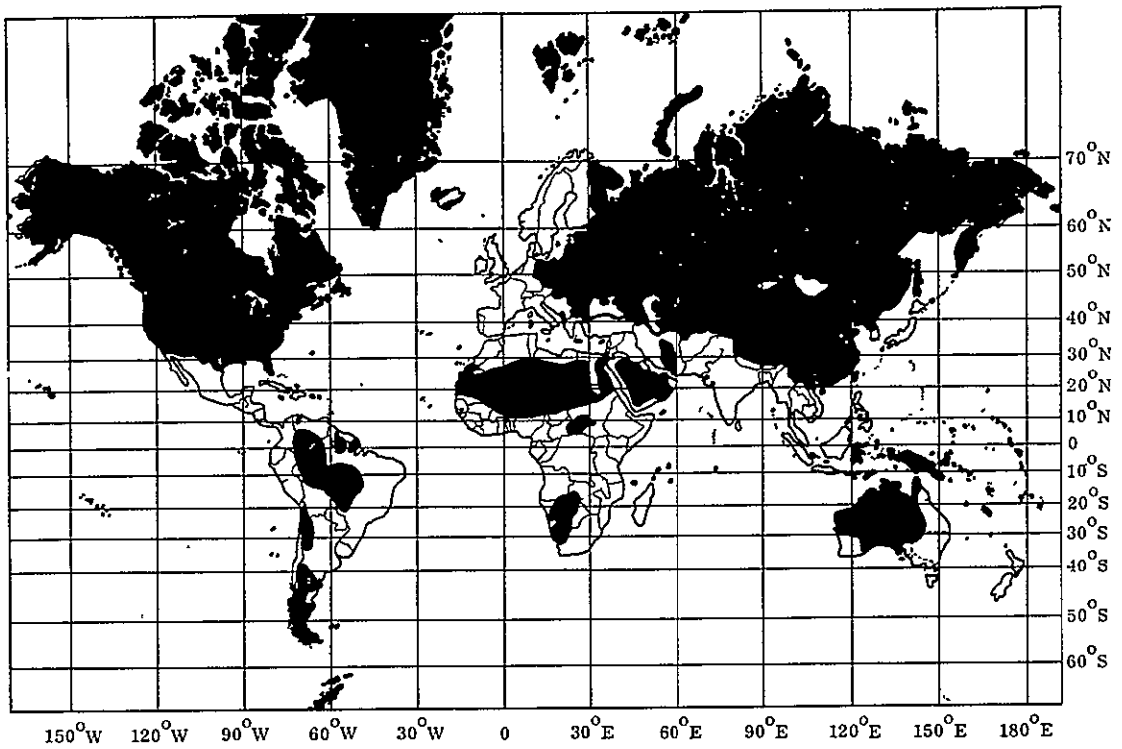

NOTE: BLACK LAND AREAS NOT INHABITED (USSR INCLUDED SINCE DATA WAS NOT AVAILABLE)

Figure 2.6-3. World Areas Using HF Broadcasting

These areas have been grouped by primary language(s) to define the potential mission coverage areas in terms of the area spanned in earth-central-angle (ECA) and in time zones. These results are summarized in Table 2.6-1 below.

Table 2.6-1

Language	Geographical Areas	ECA Area Span/ Time Zones
English	England/West Africa	58°/2
English	South East Africa	54°/3
English	India/Indonesia/Phillippines	58°/4
English	Australia/New Zealand	50°/4
Russian	USSR	71°/10
Russian	Urban Russia	24°/2
Spanish	Spain/Morocco	19°/2
Spanish	South America	57°/3
Spanish	Central America	45°/2
Arabic	North Africa	33°/3
Arabic	Ethiopian Area	37°/2
Arabic	Arabian Area	25°/3
German	Germany	7°/1
Hindu/Urdu/ Hindustani and Bengali	India/Pakistan/Nepal	32°/1

This grouping of areas shows that a satellite coverage capability of 58 degrees in earth central angle could broadcast to each geographical area with a common language, except for the USSR. A 24 degree earth central angle coverage capability could cover all the high population density areas for the major languages.

The above information was not sufficient to define specific missions. The next step was to collect and analyze detailed receiver distribution data for each of the world countries.

2.6.1.1 HF Distribution Data

The first factor considered was the distribution of receivers with different HF band capabilities. This distribution is illustrated in Figure 2.6-4. This shows that the largest potential audience is between 6 and 17 MHz (49 to 16 meter bands). The four shaded bands are those selected for the HF configuration.

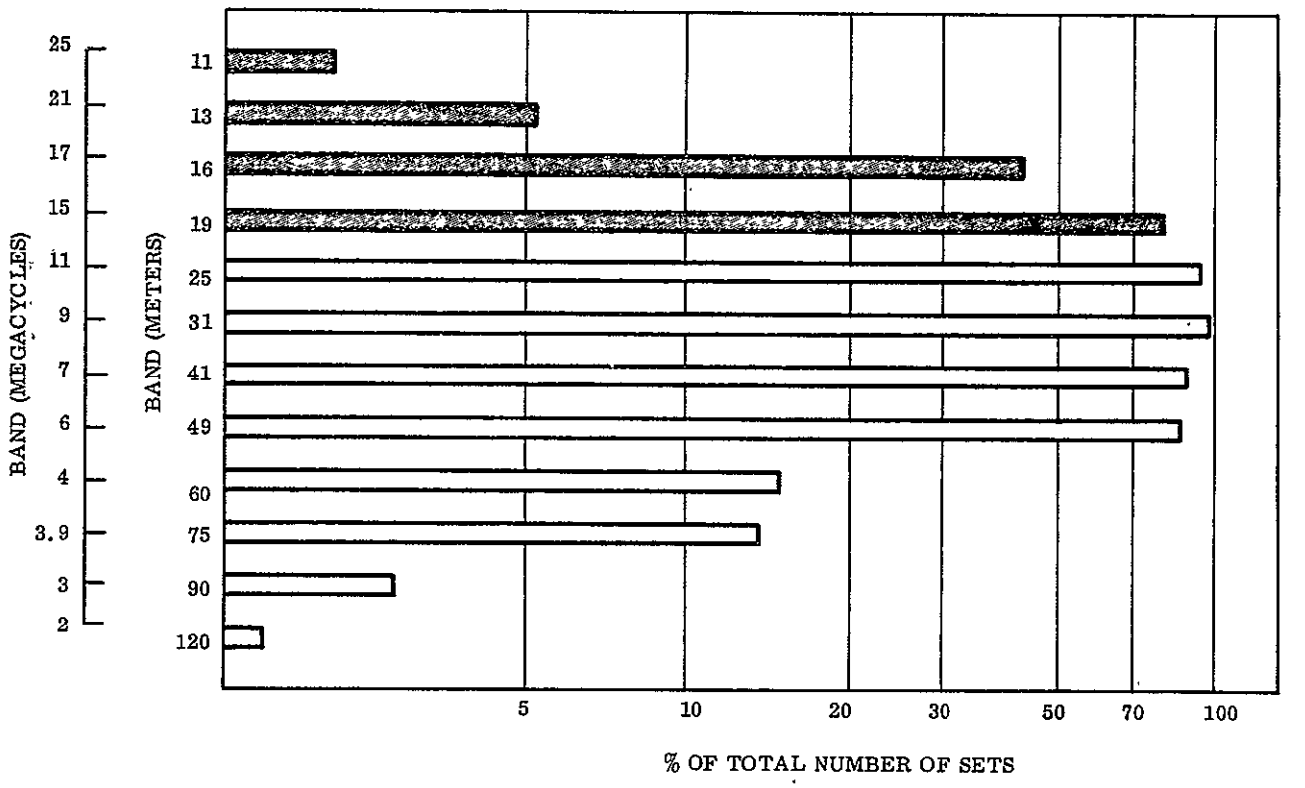

Figure 2.6-4. Receiver Distribution by Band

The total number of HF receivers, projected to 1970 by the technique described in Section 2.6.1.2, is shown in Table 2.6-2.

Table 2.6-2. Total SW Receivers Projected to 1970

Area	SW Receivers
Africa	13,230,000
Near East and South Asia	33,600,000
Latin America	23,100,000
Eastern Europe	65,700,000
Far East	35,500,000
Western Europe	91,200,000
North America	9,930,000
Total	272,260,000

The details of the distribution of short wave (HF) receivers are listed by country in Table 2.6-3.

Table 2.6-3. HF Radio Distribution as of December, 1965

Area	Country	Total Sets in Use	Estimated Total Audience	Estimate of Sets Equipped to Receive (%)		Estimate of Radios Actually Used For SW Listening (%)	Radios Currently Sold			Comments
				SW	MW		Estimated Equipped to Receive SW (%)	Usual Frequency Range of SW (Meters) From	To	
Latin America	Argentina	7,250,000	16,500,000	80*	100 -	0-9	80*	16	31	*Only 20% in operating condition, i e., only 20% install aerial, etc
	Bolivia	1,300,000	2,600,000	70	100	30	80	19	49	Urban predominantly MW Rural predominantly SW
	Brazil	10,000,000	50,000,000	45	100	15	70	16	49	Urban predominantly MW Rural MW and SW
	Chile	2,500,000	5,000,000	20	100	15	20	31	49	Predominantly MW
	Costa Rica	300,000	800,000	75	100	25	80	13	40	Predominantly MW
	Dominican Republic	797,000	2,000,000	90	100	90	90	19	31	Predominantly MW
	Ecuador	700,000	3,200,000	65	90	30	25	6	17	Rural predominantly MW Urban 60% MW, 40% SW
	British Guiana	75,600	375,000	80	100	0-9	80	11	49	Predominantly MW
	Surinam	60,110	250,000	30	100	1	35	12	25	Predominantly MW
	Guatemala	282,000	1,198,000	60	40	30	45	25	49	Urban. 60% MW, 40% SW Rural 65% MW, 35% SW
	Haiti	280,010	3,000,000	30	95	15	25	19	49	Predominantly MW
	Jamaica	250,440	1,000,000	70	100	10	75	16	31	Predominantly MW
	French West Indies	96,700	504,350	80	100	10	80	16	49	Predominantly MW
	Mexico	4,200,000	14,000,000	5	100	2 5	5	18	49	Predominantly MW
	Nicaragua	500,000	1,000,000	80	100	20-39	80	19	49	Predominantly MW
	Panama	480,000	960,000	70	100	20-39	60	16	49	Urban: 80% MW, 20% SW Rural 60% MW, 40% SW
	Paraguay	700,000	1,600,000	50	100	40-50	60	19	49	Higher percentage of sets now being sold with SW
	Peru	1,700,000	8,500,000	95	5	2	95	31	49	SW on large scale due to Geographical conditions Rural. Predominantly SW, Urban Predominantly LW
								11	93 8	
	Trinidad	49,000	700,000	55	100	65	97	185	600	Predominantly MW
	Venezuela	2,680,000	7,100,000	50	100	30	50	16	120	Predominantly MW
Europe	Austria	2,243,321	6,500,000	70	100		50	19	49	Predominantly MW
	Belgium	4,033,387	12,000,000	100	100	30	100	15	49	Predominantly MW
	Denmark	1,750,000	1,159,635	70	90	20	85	16	49	Predominantly MW
	France	12,500,000	28,000,000	75	100	20-39	80	25	49	Predominantly MW and LW
	Iceland	116,120	160,000	85	100	5	65	19	49	Predominantly LW
	Italy	11,049,009	44,196,036	60	100	0-9	75	19	49	Predominantly MW
	Netherlands	3,600,279	12,000,000	60-79		25	90	19	41	Predominantly MW
	Portugal	1,326,000	4,400,000	85	100	10-20	95	19	49	
	Spain	8,000,000	24,000,000	95	100	8-10	95	19	50	Predominantly MW
	Yugoslavia	2,085,039	15,000,000	90	100	60	100	17	50	Predominantly MW
Far East	Australia	7,613,075	26,600,000	20		15	15			Predominantly MW
	Burma	335,249	2,400,000	90	10	90	90	13	49	Urban Predominantly MW Rural Predominantly SW
	Hong Kong	700,000	2,200,000	30-40	100	10-20	30-40	16	90	Predominantly MW Many sets equipped to receive SW but no antennas
	Korea	1,066,961	5,300,000	5	95	0.1	50	20	65	Predominantly MW
	Malaysia	399,162	2,000,000	80	65	40	80	11	62	Urban Predominantly MW Rural Predominantly SW
	New Zealand	1,390,000	2,250,000	15	100	12	60	11	50	Predominantly MW
	Philippines	2,000,000	10,000,000	10	100	5	10	88	102	Predominantly MW
	Singapore	225,000	1,559,000	80	100	25	80	13	62	Predominantly MW
	Taiwan	1,436,855	7,200,000	90	100	15	90	16	49	Predominantly MW
	Thailand	2,500,000	13,650,000	35	100	30	50	16	49	Predominantly MW
Near East and South Asia	Afghanistan	510,000	4,000,000	95	90	65	95	41	75	Urban Predominantly SW Rural Predominantly MW
	Ceylon	421,215	2,210,000	98	95	70	95	49	61	Rural Predominantly SW Urban Predominantly MW
	Cyprus	135,000	600,000	50	100	5-10	90	25	31	Predominantly MW
	Greece	1,370,000	5,837,000	70	100	0-9	75	13	49	Predominantly MW, transistor radios, totaling 30%, not usually equipped for SW
	India	4,980,000	17,100,000	95	100	95	95	16	80	Predominantly MW with some SW in urban centers
	Iraq	1,030,000	5,600,000	95		80	95	16	49	Predominantly MW
	Kuwait	152,000	300,000	65	100	10-15	50	16	49	Predominantly MW
	Lebanon	327,000	1 500 000	90	100	20	85	16	50	Predominantly MW

Table 2.6-3. HF Radio Distribution as of December, 1965 (Cont'd)

Area	Country	Total Sets in Use	Estimated Total Audience	Estimate of Sets Equipped to Receive (%)		Estimate of Radios Actually Used For SW Listening (%)	Radios Currently Sold			Comments
				SW	MW		Estimated Equipped to Receive SW (%)	Usual Frequency Range of SW (Meters) From	To	
Near East and South Asia (Cont'd)	Nepal	50,000	155,000	100	100	100	100	16	60	Predominantly SW
	Syrian Arab Republic	1,000,000	4,170,000	60	100	15	50	19	49	
	Turkey	2,540,000	13,600,000	60	100	25	90	19	50	Predominantly MW Large number of community receivers
	United Arab Republic	5,000,000	15,000,000	50	100	10	50	19	49	All locally assembled sets equipped for SW and MW Country flooded with smuggled pocket transistors. MW only, remote areas SW
	Yemen	100,000		95	100	30				
Africa	Algeria	1,925,000	7,600,000	70	30	25		16	49	
	Cameron	200,000	1,000,000	90	90	65	95	19	41	Urban Predominantly MW Rural- Predominantly SW
	Ghana	292,000*	4,051,000	100	100	100	100	11	90	*Includes wired loudspeakers Predominantly SW
	Kenya	490,000	3,000,000	75	100	50	100	13	75	Urban Predominantly MW Rural: Predominantly SW
	Morocco	577,500	3,000,000	75	100	35	80	10	60	Predominantly MW
	Mali	50,000	300,600	90	100	90	95	16	49	Predominantly MW
	Niger	40-70,000								SW 95% LW 5%
	Senegal	250,000	1,600,000	70	90	40	80			Urban Predominantly MW Rural 50% MW 50% SW
	Somali Republic	113,000	1,500,000	100	0	100	100	25	60.36	Entirely SW
	Republic of South Africa	3,100,000	10,000,000	90	100	60	90	11 25	120 75	Urban Predominantly MW Rural 50% MW, 50% SW
	Togo	23,000		90-100		90-100				SW 75%, MW 20%, LW 5%
	Tunisia	400,000	2,275,000	50	100	35-40	50	16	49	25 percent of sets equipped for 11 to 49 meters Predominantly MW
	Upper Volta	50,000	4,000,000	90	100	65	90	13 5	90	

The above data describes the distribution for all of the HF bands. However, ionospheric propagation factors limit the minimum frequence consistently usable to about 15 MHz (19 meter band). To reach the largest audience it is desirable to have a broadcast frequency capability as low as 15 MHz. Thus, it seems necessary to be able to operate in any one of the top 4 channels. The chosen channel at any particular time would depend on ionospheric conditions. As with current ground station practice in the HF band, the operating frequency would be scheduled in advance and these schedules posted with the International Frequency Registration Board. In this manner, interference may be minimized by the posted schedules of all the HF stations around the world. The ability of these stations to shift channels when interference occurs should be carried over into the satellite design.

In addition to the lower bound on frequencies usable by the satellite, there is another range of frequencies between this lower bound and the Maximum Usable Frequency (MUF) that must be considered separately because within this range both satellite and international terrestrial transmitters can operate. This frequency range represents a region of potential mutual interference between the satellite and terrestrial transmissions. The MUF is a variable depending upon the time of day, latitude, and the time in the sun spot cycle. This is illustrated in Figure 2.6-5 for very low and very high sun spot conditions. The variation of the MUF with sun spot conditions is shown in Figure 2.6-6. The time period between successive sun spot maximums is approximately eleven years and the variation of the average sun spot number within the eleven-year cycle is approximately sinusoidinal. The last peak in the cycle occurred in 1958.

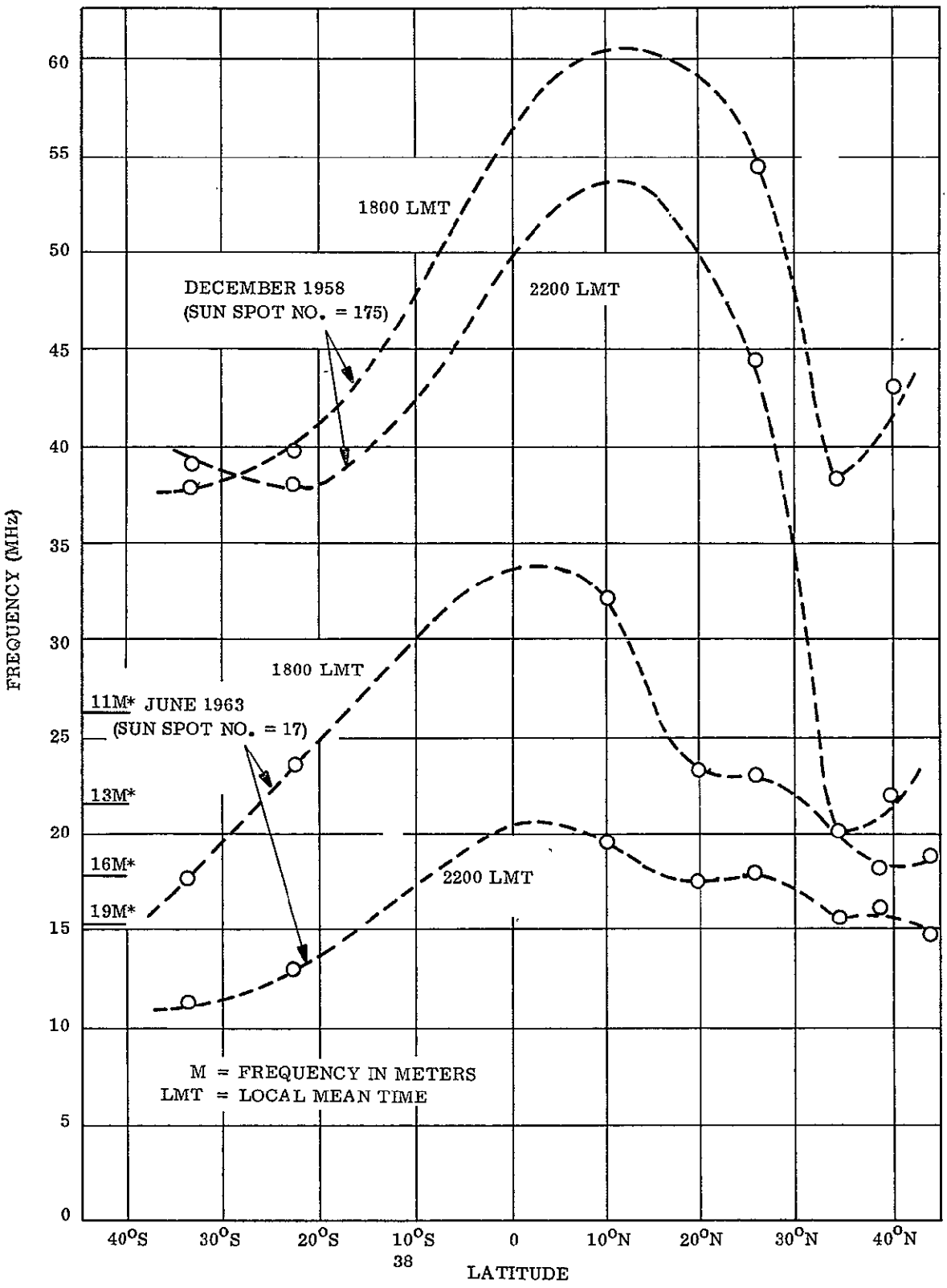

Figure 2.6-5. Maximum Usable Frequency versus Latitude

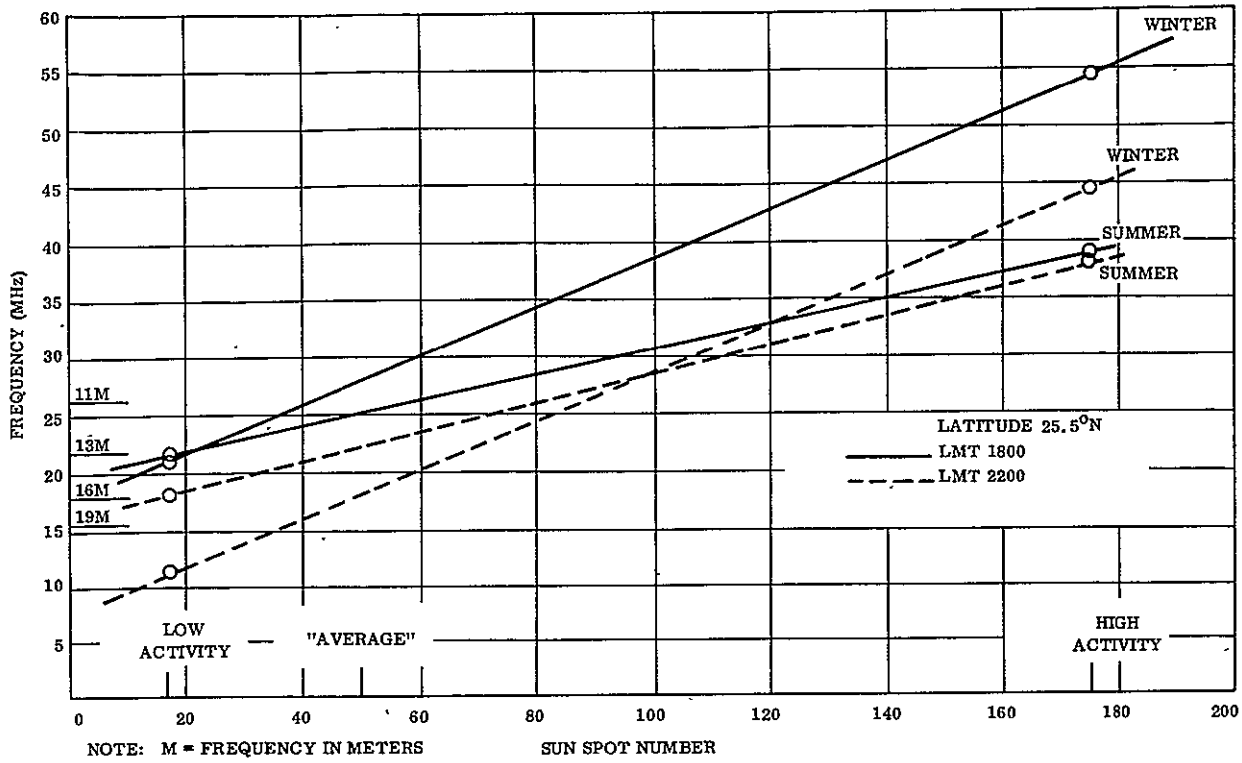

Figure 2.6-6. Minimum Usable Frequency versus Sun Spot Number

The resulting interference potential (between satellite and ground broadcast systems) was calculated, for any location at 25°N latitude, as a percentage of the time each of the top four HF bands are available without interference. These results are summarized in Table 2.6-4.

Table 2.6-4. Estimated Band Availability (25° Latitude)

Frequency Band	Sun Spot Number	Percent of Time Band is Available Without Interference	
		1800 LMT to 2200 LMT	
11 Meter	17	100%	100%
	50	22%	100%
	100	0	10%
13 Meter	17	50%	100%
	50	1%	46%
	100	0	0
16 Meter	17	3%	50%
	50	0	3%
	100	0	0
19 Meter	17	0	15%
	50	0	0
	100	0	0

For each of these top four HF bands, the distribution of receivers in the International Telecommunication Union (ITU) member countries was tabulated and is shown in Table 2.6-5.

Table 2.6-5. Distribution of HF Receivers-December 1965

Area	Country	Area (Sq. miles)	Prin. Languages	Local Time		# SW receivers				average receiver sensitivity uv
				Normal Clock Time	Summer Time	11 m	13 m	16 m	19 m	
Western Europe	Austria	32,374	German	+1	+1	0	0	0	1,570,000	20
	Belgium	11,781	French, Dutch, German	+1	+1	0	0	4,033,000	4,033,000	20
	Denmark	16,619	Danish	+1	+1	0	0	1,230,000	1,230,000	20
	Finland	130,120	Finnish, Swedish	+2	+2	0	0	192,000	922,000	20
	France	211,207	French	+1	+1	0	0	0	0	20
	W. Germany	95,743	German	+1	+1	0	0	2,190,000	10,500,000	20
	Gibraltar	2.25	English, Spanish	+1	+1	0	0	548	2,630	20
	Iceland	39,768	Icelandic	-1	GMT	0	0	0	98,600	20
	Ireland	27,135	Irish, English	GMT	+1	0	0	65,700	316,000	20
	Italy	116,303	Italian	+1	+2	0	0	0	6,600,000	20
	Liechtenstein	61.4	German	N.A.	N.A.	0	0	328	1,580	20
	Luxembourg	998	Luxembourgian, French	+1	+1	0	0	12,000	57,800	20
	Malta	122	English, Maltese	+1	+1	0	0	3,840	18,400	20
	Monaco	.606	French	+1	+1	0	0	680	3,260	20
	Netherlands	12,978	Dutch	+1	+1	0	0	0	2,500,000	20
	Norway	125,181	Norwegian	+1	+1	0	0	198,000	950,000	20
	Portugal	35,510	Portugese	GMT	+1	0	0	0	1,120,000	20
	Spain	194,884	Spanish	+1	+1	0	0	0	7,600,000	20
	Sweden	173,666	Swedish	+1	+1	0	0	339,000	1,630,000	20
	Switzerland	15,941	German, French Italian, Romanch	+1	+1	0	0	240,000	1,150,000	20
	United Kingdom	94,220	English	GMT	+1	0	0	2,750,000	13,200,000	20
Eastern Europe	Albania	11,000	Albanian	+1	+1	N.A.	N.A.	N.A.	N.A.	N.A.
	Bulgaria	42,729	Bulgarian	+2	+2	N.A.	N.A.	N A.	N.A	N A.
	Czechoslovakia	49,370	Czech., Slovak	+1	+1	N.A.	N.A.	N A.	N.A.	N.A.
	Hungary	35,919	Hungarian	+1	+1	N.A.	N A.	N.A.	N.A.	N.A
	Poland	120,664	Polish	+1	+1	N.A.	N.A.	N.A.	N.A.	N.A
	Rumania	91,699	Rumanian	+2	+2	N.A.	N.A.	N.A.	N.A.	N.A
	USSR	8,649,512	See Note 1	Note 5	Note 5	Note 3	Note 3	Note 3	Note 3	N.A
	Yugoslavia	98,766	Serbo-Croat, Slovenian, Macedonian	+1	+1	0	0	1,880,000	1,880,000	N.A.
Near East and South Asia	Afghanistan	253,861	Pushtu, Dari, Persian	+4-1/2	+4-1/2	0	0	0	0	N.A.
	Ceylon	25,332	English, Sinhalese, Tamil	+5-1/2	+5-1/2	0	0	0	0	N.A.
	Cyprus	3,572	Greek, English, Turkish	+2	+2	0	0	0	0	N.A.
	Greece	50,944	Greek	+2	+2	0	960,000	960,000	960,000	N.A.
	India	1,176,153	See Note 2	+5-1/2	+5-1/2	0	0	4,730,000	4,730,000	N.A.
	Iran	636,294	Persian	+3-1/2	+3-1/2	0	121,000	886,000	1,470,000	N.A.
	Iraq	173,260	Arabic, Kurdish, Turkuma	+3	+3	0	0	980,000	980,000	N.A.
	Israel	7,992	Hebrew, Arabic	+2	+2	0	33,600	246,000	410,000	N.A.
	Jordan	37,738	Arabic, English	+2	+2	0	10,900	80,300	134,000	N.A.
	Kuwait	6,178	Arabic	+3	+3	0	0	98,900	98,900	N.A.
	Lebanon	4,015	Arabic, French, English	+2	+3	0	0	294,000	294,000	N.A.
	Nepal	54,362	Nepali, Newari, Hindu, English	+5.40	+5.40	0	0	50,000	50,000	N.A.
	Pakistan	365,529	Urdu, Bengali	West +5 East +6	+5 +6	0	57,700	423,000	705,000	N.A.
	Saudi Arabia	870,001	Arabic	+3	+3	0	16,400	120,000	200,000	N.A
	Syrian Arabic Republic	71,498	French, Arabic	+2	+2	0	0	0	600,000	N.A
	Turkey	301,381	Turkish	+2	+2	0	0	0	1,520,000	N.A.
	United Arab Republic	386,101	Arabic	+2	+3	0	0	0	2,500,000	N.A.
	Yemen	75,290	Arabic	+3	+3	0	600	4,400	7,320	N.A.
Africa	Algeria	919,593	French, Arabic, Kahyl	GMT	GMT	0	0	1,350,000	1,350,000	N.A.
	Angola	481,351	Portugese	+1	+1	18,800	30,200	75,000	80,300	N.A.
	Basutoland, Bechuanaland, Swaziland	293,420	Sesotho, English Vernaculars	+2	+2	1,410	2,270	5,620	6,020	N.A
	Burundi	10,747	Kirundi, Kiswahili, French	+2	+2	5,650	9,070	22,500	24,100	N.A.
	Cameroon	183,569	French, English, Vernaculars	+1	+1	0	0	0	180,000	N.A.
	Cape Verde Island	N.A.	Portugese, English	-2	-2	940	1,510	3,740	4,010	N.A.
	Central African Republic	238,224	French, Sango	+1	+1	5,080	8,150	20,300	21,700	N.A.
	Chad	495,754	French, Arabic, Sara	+1	+1	3,390	5,450	13,500	14,400	N.A.

Table 2.6-5. Distribution of HF Receivers-December 1965 (Cont'd)

Area	Country	Area (Sq. miles)	Prin. Languages	Local Time		# SW receivers				average receiver sensitivity uv
				Normal Clock Time	Summer Time	11 m	13 m	16 m	19 m	
Africa (Cont'd)	Comoro Island	850	French Vernaculars	+3	+3	565	908	2,250	2,410	N.A.
	Congo Republic (Brazzaville)	132,047	French, English Portugese	+1	+1	9,400	15,100	37,400	40,100	N.A.
	Congo Republic (Leopoldville)	905,565	French, Lingala Kikongo, Tshiluba Swahili	Leopold-ville +1 Elisabeth-ville +2	+1 +2	33,000	53,000	131,000	141,000	N.A.
	Dahomey	43,483	French, Vernaculars	+1	+1	6,030	9,690	24,000	25,700	N.A.
	Ethiopia	457,267	Amharic, Arabic English, Somali	+3	+3	37,800	60,600	150,000	161,000	N.A.
	Gabon	103,089	French	+1	+1	8,530	10,600	26,000	28,100	N.A.
	Gambia	4,003	English, Mandinka, Wolloff, Vernaculars,	GMT	GMT	1,880	3,030	7,500	8,030	N.A.
	Ghana	92,099	Akan, Ewe, Ga, Dagbani, Hausa, Nzerna	GMT	GMT	240,000	240,000	240,000	240,000	N.A.
	Guinea	94,926	French, Vernaculars	GMT	GMT	14,100	22,700	56,200	60,200	N.A.
	Guinea (Portugese)	13,948	Portugese	-1	-1	377	606	1,500	1,610	N.A.
	Guinea (Spanish)	N.A.	Spanish	+1	+1	377	606	1,500	1,610	N.A.
	Ivory Coast	124,503	French, Vernaculars	GMT	GMT	14,100	22,700	56,200	60,200	N.A.
	Kenya	224,960	English, Swahili, Hindustani	+3	+3	0	368,000	368,000	368,000	N.A.
	Liberia	43,000	English, Liberian-Vernaculars	-3/4	-3/4	23,500	37,800	93,600	100,000	N.A.
	Libya	679,360	Arabic	+2	+2	35,200	56,600	140,000	150,000	N.A.
	Malagasy Republic	N.A.	Malgache, French	+2	+2	47,200	75,800	188,000	201,000	N.A.
	Nalawi	46,066	English, Nyanja, Tumbuka	+2	+2	1,880	3,020	7,500	8,030	N.A.
	Mali	463,949	French, English, Vernaculars	GMT	GMT	0	0	45,000	45,000	N.A.
	Mauritania	419,230	French, Arabic, Vernaculars	GMT	GMT	2,820	4,530	11,200	12,000	N.A.
	Mauritius	720	English, French Hindustani, Chinese	+4	+4	11,300	18,100	45,000	48,200	N.A.
	Morocco	171,834	Arabic, French, Spanish, English, Benber	GMT	GMT	434,000	434,000	434,000	434,000	N.A.
	Mozambique	N.A.	Portugese, English, Afrikaans, Vernaculars	+2	+2	18,800	30,200	75,000	80,300	N.A.
	Niger	489,190	French, Hausa, Djerma, Tamachek, Peulh, Beriberi	+1	+1	2,820	4,540	11,200	12,000	N.A.
	Nigeria	356,669	English, Yoruba, Hausa, Ibo	+1	+1	188,000	302,000	750,000	803,000	N.A.
	Reunion	970	French	+4	+4	4,710	7,580	18,800	20,100	N.A.
	Rhodesia	152,804	English, Shona Sindebele	+2	+2	26,400	42,500	105,000	113,000	N.A.
	Rwanda	10,169	Kinyarwanda, Swahili, French	+2	+2	3,780	6,060	15,000	16,100	N.A.
	Senegal	75,750	French, Ouolof, Toucoulour, Serere Portugese	GMT	GMT	39,600	63,500	157,000	169,000	N.A
	Seychelles	156	English, French Creole	+4	+4	745	1,200	2,970	3,180	N.A.
	Sierra Leone	27,699	English, Mende Temne, Krio	GMT	GMT	11,700	18,700	46,500	49,800	N.A.
	Somali Republic	246,202	Somali, Arabic, Italian, Swahili, English	+3	+3	0	0	0	0	N.A.
	Sonalliland (French)	N.A.	French, Somali, Afar, Arabic	+2	+2	1,510	2,420	6,000	6,420	N.A.
	South Africa	471,446	English, Bantu, Afrikaans	+2	+2	0	0	0	0	5
	Sudan	967,501	Arabic, English	+2	+2	37,700	60,600	150,000	161,000	N.A.
	Tanzania	361,800	Swahili, English	+3	+3	28,200	45,400	112,000	120,000	N.A.
	Togo	21,853	Ewe, Cotocolia, Cabrais, Hausa, Moba, Bassari	GMT	GMT	4,930	7,920	19,600	21,000	N.A.

Table 2.6-5. Distribution of HF Receivers-December 1965 (Cont'd)

Area	Country	(Sq. miles)	Prin. Languages	Local Time		# SW receivers				average receiver sensitivity, uv
				Normal Clock Time	Summer Time	11 m	13 m	16 m	19 m	
Africa (Cont'd)	Tunisia	48,332	Arabic	+1	+1	0	0	200,000	200,000	N A.
	Uganda	91,134	Note 4	+3	+3	32,100	51,500	128,000	137,000	N.A.
	Upper Volta	105,869	French, More	GMT	GMT	0	45,000	45,000	45,000	N.A.
	Zambia	288,130	English, 7 African Vernaculars	+2	+2	18,800	30,200	75,000	80,300	N A.
Far East	Australia	2,971,083	English	Note 6	Note 6	155,000	292,000	1,000,000	1,460,000	N.A.
	Brunei	2,226	Malay, English, Chinese	+8	+8	421	793	2,710	3,970	N.A.
	Burma	261,789	Burmese, English	+6-1/2	+6-1/2	0	301,000	301,000	301,000	N.A.
	Cambodia	69,898	Cambodian, French English	+7	+7	21,000	39,500	135,000	198,000	N.A
	Fiji Islands	7,083	English, Fijian, Hindustani	+12	+12	1,840	3,460	11,800	17,300	N.A.
	Guam	225	English, Chamono Philippine dialects	+10	+10	421	794	2,710	3,970	N.A.
	Hong Kong	391	Chinese	+8	+9	0	0	245,000	245,000	N A.
	Indonesia	575,894	Indonesian	Note 7	Note 7	143,000	269,000	919,000	1,350,000	N.A.
	Japan	142,726	Japanese	+9	+9	1,740,000	3,280,000	11,200,000	10,400,000	N.A
	Korea (South)	38,004	Korean	+9	+9	0	0	0	53,000	N.A.
	Laos	91,429	Kuotian, French	+7	+7	3,700	6,950	23,700	34,800	N.A
	Macao	N.A.	Portugese, Chinese English	+8	+8	525	990	3,389	4,970	N.A
	Malaysia	50,700	Malay, English Chinese	+8	+8	319,000	319,000	319,000	319,000	N.A.
	Mongolia	592,665	Mongolian	+8	+8	0	0	75,000	75,000	N.A.
	New Calendonia	N.A.	French	+11	+11	316	595	2,030	2,980	N.A.
	New Zealand	103,736	English, Maori	+12	+12	209,000	209,000	209,000	209,000	N.A
	Philippines	115,830	English, Tagalog Ilocano, Visayan	+8	+8	0	0	0	0	N.A
	Taiwan	13,885	Chinese	+8	+8	0	0	1,290,000	1,290,000	N.A.
	Thailand	198,456	Thai	+7	+7	0	0	875,000	875,000	N.A
	Vietnam (South)	65,800	Vietnamese	+8	+8	26,700	50,300	172,000	252,000	N.A.
Latin America	Argentina	1,072,070	Spanish	-4	-3	0	0	5,800,000	5,800,000	20
	Bolivia	424,163	Spanish	-4	-4	0	0	0	910,000	20
	Brazil	3,286,478	Portugese	Note 8	Note 8	0	0	4,5000,000	4,500,000	20
	Chile	286,397	Spanish	-4	-4	0	0	0	0	20
	Colombia	439,513	Spanish	-5	-5	65,300	93,500	1,510,000	1,510,000	20
	Costa Rica	19,575	Spanish	-6	-6	0	225,000	225,000	225,000	20
	Cuba	44,218	Spanish	-5	-4	40,400	57,800	935,000	1,050,000	20
	Dominican Republic	18,816	Spanish	-5	-4	0	0	0	718,000	20
	Ecuador	104,506	Spanish, Quechua	-5	-5	455,000	455,000	455,000	0	20
	El Salvador	8,260	Spanish	-6	-6	6,480	9,260	150,000	174,000	20
	Guatemala	42,042	Spanish	-6	-6	0	0	0	0	20
	Haiti	10,714	French, Creole	-5	-5	0	0	0	84,000	20
	Honduras	43,277	English, Spanish	-5	-6	3,860	5,500	89,500	105,000	20
	Jamaica	4,232	English	-5	-5	0	0	175,000	175,000	20
	Mexico	761,602	Spanish	-6	-6	0	0	0	210,000	20
	Nicaragua	53,938	Spanish	-6	-6	0	0	0	400,000	20
	Panama	29,209	Spanish	-5	-5	0	0	336,000	336,000	20
	Paraguay	157,047	Spanish	-4	-4	0	0	0	350,000	20
	Peru	496,223	Spanish	-5	-5	0	0	0	0	20
	Trinidad & Tobago	1,980	English	-4	-4	32,000	32,000	32,000	32,000	20
	Uruguay	72,172	Spanish	-3	-3	10,800	15,500	251,000	294,000	20
	Venezuela	352,143	Spanish	-4	-4	0	0	1,340,000	1,340,000	20
North America	Canada	3,851,812	English, French	Note 9	Note 9	2,670,000	2,670,000	2,670,000	2,670,000	N A.
	U.S.A.	3,615,211	English	Note 10	Note 10					N.A.

NOTES:

The differences marked + indicate the number of hours ahead of GMT. Differences marked - indicate number of hours behind GMT.

1. Russian, Ukrainian, Byelorussian, Uzbek, Tatar, Kazakh, Azerbaidjanian, Armenian, Georgian, Lithuanian, Moldavian, German, Estonian, Latvian, Chuvash, Tadjik.
2. Hindi, Marathi, Gujarati, Oriya, Benegali, Assamese, Tamil, Telegu, Urdu, Kannada, Kashmiri, Sanskrit, Dogri, Sindhi, Punjabi, Malayalam, English.
3. Since 1958, no sets have been manufactured for internal distribution having SW bands of less than 25 meters.
4. English, Lugando, Lwo, Ateso, Runyoro, Rutooro, Runyankore/Rukiga.

5.

	Normal Clock Time	Summer Time
Moscow, Leningrad	+3	+3
Baku	+4	+4
Sverdlovsk	+5	+5
Tsskkent	+6	+6
Novosibirsk	+7	+7
Irkutsk	+8	+8
Yakutsk	+9	+9
Khabarovsk	+10	+10
Magadan	+11	+11
Petropavlovsk	+12	+12
Anadyr	+13	+13

6.

	Normal Clock Time	Summer Time
a) Victoria, New South Queensland, Tasmania	+10	+10
b) N. Territory, S. Australia	+9-1/2	+9-1/2
c) W. Australia	+8	+8

7.

	Normal Clock Time	Summer Time
a) North Sumatra	+6-1/2	+6-1/2
b) South Sumatra	+7	+7
c) Java, Borneo, Bali	+7-1/2	+7-1/2
d) Celebes	+8	+8
e) West Irian	+9	+9

8.

	Normal Clock Time	Summer Time
a) Eastern and Coastal	-3	-2
b) Manaos	-4	-3
c) Acre	-5	-4

9.

	Normal Clock Time	Summer Time
a) New Foundland	-3-1/2	-2-1/2
b) Atlantic (Labrador, Nova Scotia)	-4	-3
c) Eastern (Ontario, Quebec)	-5	-4
d) Central (Manitoba)	-6	-5
e) Mountain (Aberta)	-7	-6
f) Pacific (Br. Columbia)	-9	-8
g) Yukon	-9	-8

10

	Normal Clock Time	Summer Time
a) Eastern Zone	-5	-4
b) Central Zone	-6	-5
c) Mountain Zone	-7	-6
d) Pacific Zone	-8	-7

2.6.1.2 Projection of Number of HF Receivers, 1970

In order to demonstrate the feasibility of a direct broadcast satellite, it is important to obtain reasonable estimates for the 1970 era and beyond.

Most countries of the world (approximately 70 percent) require licensing. Some idea of the overall growth in use of radios can be gained, therefore, by considering the curve of total number of licenses in force as a function of time. Figure 2.6-7 is a graph reproduced from a report on the radio industry in Pakistan as an example of the projection procedure used (Reference 1). The projected trend indicated on this graph is based on the assumption that the total number of sets in use continued to grow at least to 1958 at a rate comparable to that indicated on the chart from 1948 to 1955. Also, from 1958 to 1970, the rate of growth in total sets may safely be predicted to be about 15 percent a year. The further assumption is made that radios will be replaced on the average every 7 years (i.e., replacement rates in any year will equal the number of sets sold in the seventh preceding year).

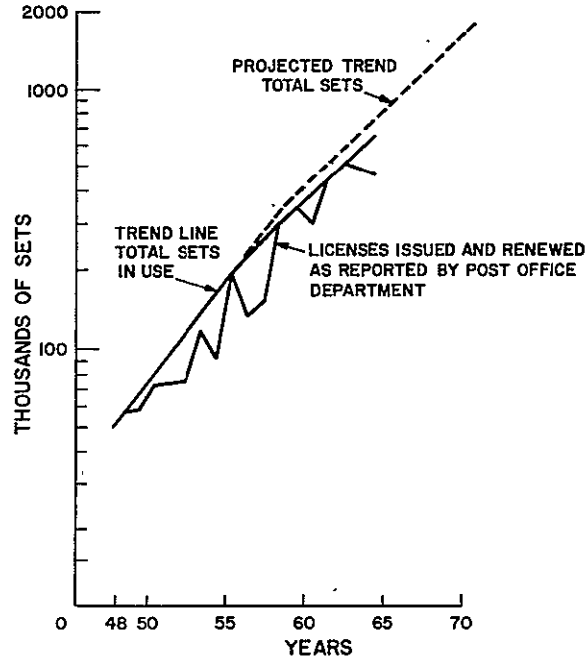

Figure 2.6-7. Projection of Radio Sets in Use in West Pakistan, 1948 to 1970

Applying this projection procedure to selected world areas resulted in the totals shown in Table 2.6-6. The estimate only includes HF receivers capable of receiving the upper four bands (11 to 19 meters). The world areas selected for this table are consistant with the coverage of the HF configuration as discussed in Section 6.4.

Table 2.6-6. Estimated HF Receivers in Upper Four Bands, 1970

United States	2,670,000
South America	18,700,000
Africa	8,760,000
India	7,220,000

A further analysis of these results was performed to show the breakdown by urban, suburban, and rural areas. This breakdown varied from one country to another depending on the degree of industrial development of that country. However, for the sake of reasonable simplification, average values were used. The values assumed for the three cases are listed in Table 2.6-7.

Table 2.6-7. % Population Distribution

Urban	20%
Suburban	40%
Rural	40%

2.6.1.3 HF Signal Level Requirements

The signal level necessary to provide satisfactory operation of HF receiving systems is a function of the receiver sensitivity, the local noise environment, and the antenna gain. The effects of building attenuation can be neglected in this band because they are small compared to the effects of noise.

The receiver sensitivity was evaluated by examining test measurements made on "comparison shopping" receivers by the GE Radio Receiver Department. In all cases, the receiver sensitivities were greater than the signals required for reasonable quality reception (at least 20 db S/N of audio output) so the distribution of receiver sensitivities could be neglected.

The range of values of antenna gain assumed for HF home antennas was described in Section 2.4. The noise environment was described in Section 2.5. Combining these results with the distribution of receivers in the urban, suburban and rural areas, with an assumed antenna distributions 10% high antenna gain outdoor antenna, 40% low gain outdoor antenna, and 50% low gain gain indoor antenna permits a determination of the signal strength, in μ v/m, required for each combination of the above factors.

The resulting signal strength requirements are illustrated in Figure 2.6-8.

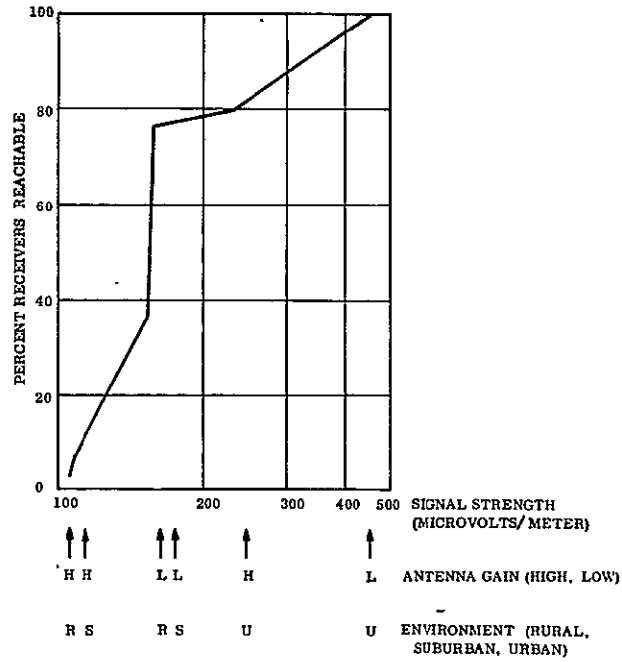

Figure 2.6-8. Potential Audience Vs. Signal Strength

The assumptions and data used to determine signal strength are shown below.

Minimum Output S/N = 20 db
Modulation Index = 0.8
RF Bandwidth = 10 kHz
Receiver Input Impedance = 400 ohms
Receiver Noise Figure = 10 db

Noise (^{o}K)

	Man-Made	Atmospheric	Galactic
Urban	9.15×10^{7}	9.1×10^{6}	8.5×10^{4}
Suburban	9.15×10^{5}	9.1×10^{6}	8.5×10^{4}
Rural	2.9×10^{4}	9.1×10^{6}	8.5×10^{4}

Noise Data Sources

Urban and Rural Man-Made:	ESSA
Suburban Man-Made:	GE Measurements
Atmospheric:	CCIR Maximum at equator
Galactic:	Average from number of sources including ESSA.

Antenna

	Maximum Gain	Effective Antenna Gain	Line Loss
Low Gain (10 db mismatch)	1.76 db	-1.24 db (3db polarization loss)	0 db Polarization
High Gain	8 db	2 db (3 db polarization loss; 3 db pointing loss)	2 db Polarization

The equations used to derive these results are shown below.

The relationship between the output signal-to-noise ratio and the IF power (S_i) to an AM receiving system is:

$$\frac{So}{No} = \frac{\frac{m^2}{1 + \frac{m^2}{2}}}{KB_{if}\left\{T_a + T_o\left[(L-1) + L(F-1)\right]\right\}}$$

where

- m = modulation index
- K = Boltzmann's constant = 1.38×10^{-23}
- T_a = input noise temperature from external sources
- F = receiver noise factor
- L = line loss, if any
- T_o = 290^{o}K
- B_{i_f} = IF bandwidth

The relationship between the input power (Si) and the input voltages is simply:

$$\frac{e_S^2}{4R} = \frac{Si}{L}$$

where e_S = voltage at receiver terminals

R = receiver input impedance

Finally, the conversion to field strength (E) may be made by the equation:

$$E = \frac{480\pi^2 S_i}{G_r \lambda^2}^{1/2}, \text{ V/m}$$

2.6.2 VHF AUDIENCE ANALYSIS

VHF broadcasting is practiced in most countries of the world, as is illustrated in Figure 2.6-9. The white land areas denote where VHF broadcasting is practiced. Excluded are the areas defined for the study as uninhabited (less than one person per square mile).

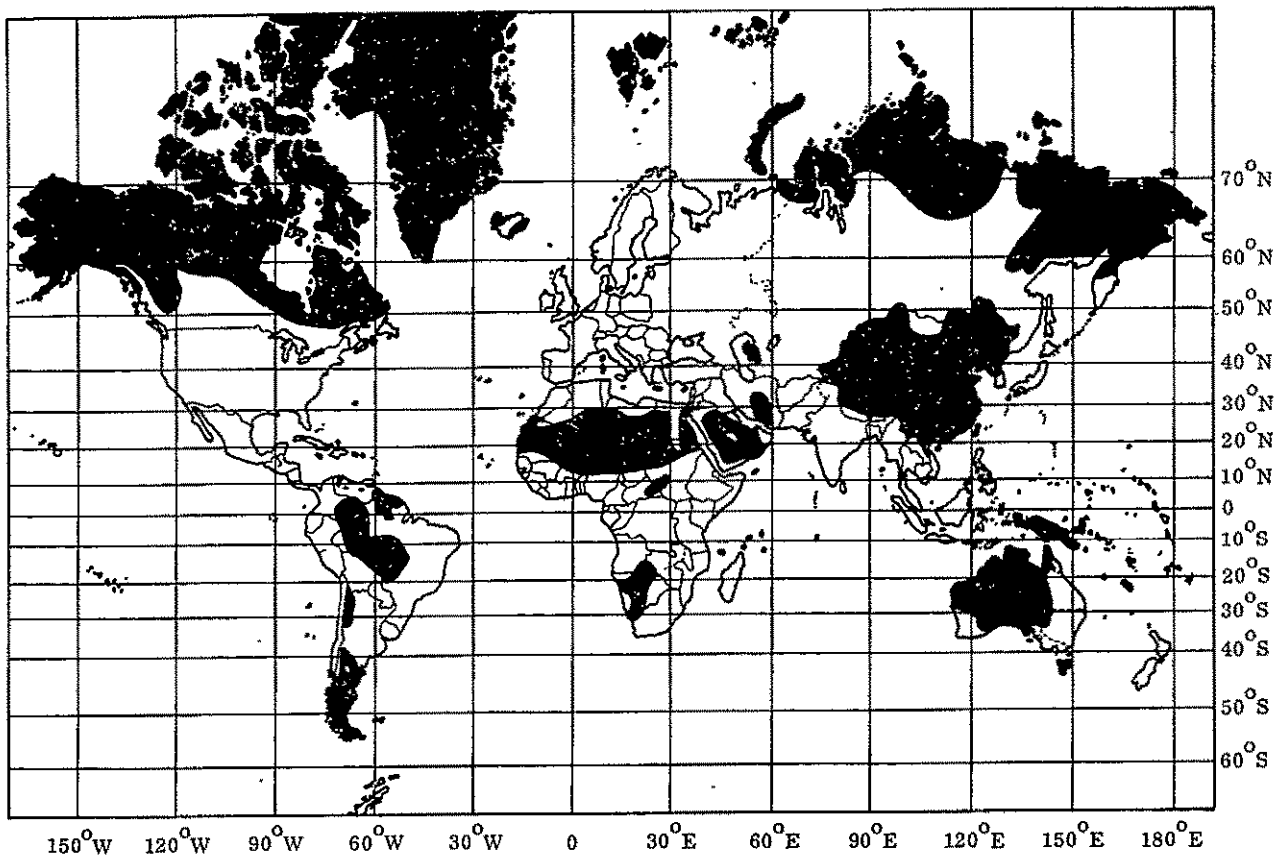

Figure 2.6-9. Inhabited Areas Where FM Broadcasting is Practiced

Because of the wide usage of VHF (FM) broadcasting, grouping areas by language was considered. The major languages and their geographical areas are listed in Table 2.6-7 in the terms of their surface span in degrees of earth central angle (ECA) and the number of time zones included in each area. As an upper bound, a span of 58 degrees would be great enough to cover any of the single-language geographical areas with the single exception of the USSR. The USSR, however, covers 10 time zones which is not very compatible with broadcast practices. The more densely populated portion of Russia would be a more manageable area. A 24 degree span represents a reasonable lower bound based on the high population density areas of a single language.

Table 2.6-7. VHF Coverage Possibilities

Language	Geographical Areas	ECA Area Span/Time Zones
English	US/Canada	58°/5
English	England/West Africa	58°/2
English	South East Africa	54°/3
English	India/Indonesia/Philippines	58°/4
English	Australia/New Zealand	50°/4
Russian	USSR	71°/10
Russian	Urban Russia	24°/12
Spanish	Spain/Morocco	19°/2
Spanish	Central America	45°/2
Spanish	South America	57°/3
Arabic	North America	33°/3
Arabic	Ethopian Area	37°/2
Arabic	Arabian Area	25°/3
German	Germany	7°/1
Hindu/Urdu/ Hindustani and Bengali	India/Pakistan/Nepal	32°/1

It was assumed that FM broadcasting is strictly domestic and, by estimating the number of receivers per transmitter for each country, it was possible to estimate receivers in use. Figure 2.6-10 shows the countries (or island areas) maintaining FM broadcasting facilities as of 1 March 1965. Figure 2.6-11 shows the estimated density distribution of FM Receivers.

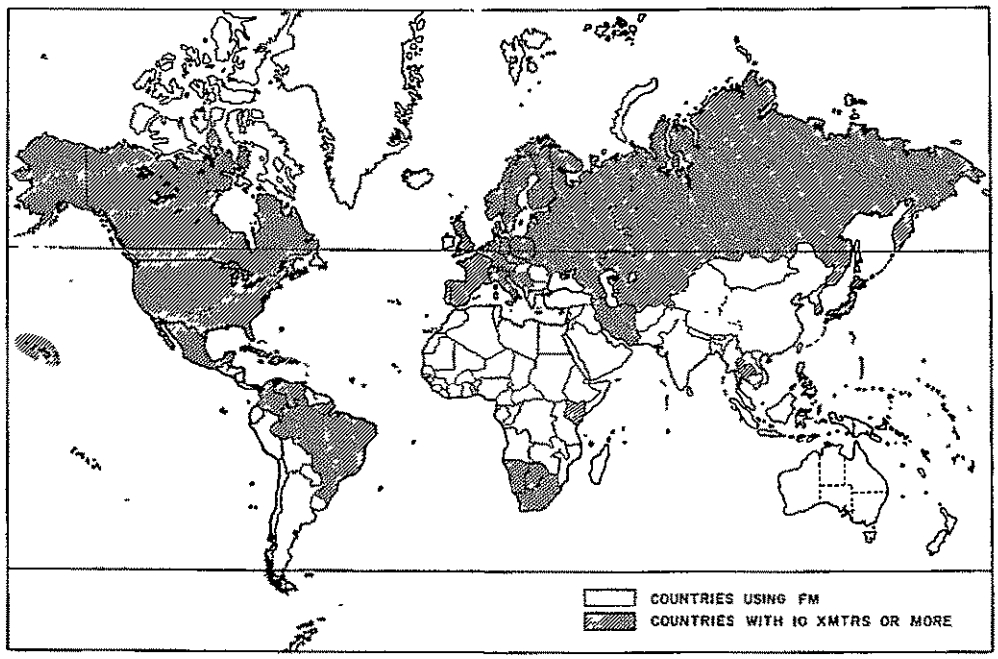

Figure 2.6-10. World Use of FM Radio

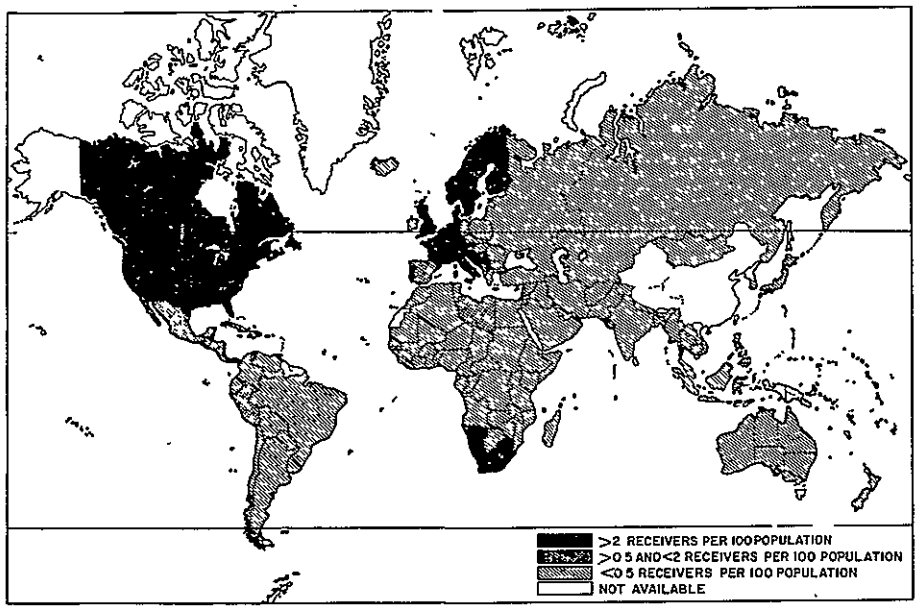

Figure 2.6-11. Density Distribution of FM Radio Receivers (87.5 to 108 MHz)

The detailed distribution data of VHF receivers was collected for the ITU member countries and is summarized in Table 2.6-8 below. The data was derived from sources current to December 1965.

Table 2.6-8. Distribution of UHF Receivers - December 1965

				Local Time*		FM, 87.5 - 108 mc								
Area	Country	Area (Sq miles)	Prin. Languages	Normal Clock Time	Summer Time	# of receivers 87.5 - 108 mc	Est. max. freq. covered by sets, mc	Authorized** maximum freq., mc	Total # broadcast stations	# stations ≥ 1000 watts	# stations 100-108 mc	# stations 100-108 mc ≥ 1000 watts	frequency of used channels 100-108 mc	average receiver sensitivity uv
Western Europe	Austria	32,374	German	+1	+1	775,000	104	104*	50	31	1	0	100 3	10
	Belgium	11,781	French, Dutch German	+1	+1	400,000	104	104*	18	18	0	0	0	10
	Denmark	16,619	Danish	+1	+1	600,000	104	104*	24	24	0	0	0	10
	Finland	130,120	Finish, Swedish	+2	+2	1,350,000	104	100	68	54	0	0	0	10
	France	211,207	French	+1	+1	2,400,000	104	100	131	96	0	0	0	10
	W Germany	95,743	German	+1	+1	4,175,000	104	104*	215	167	1	1	102.4	10
	Gibraltar	2.25	English, Spanish	+1	+1	0	104	100	0	0	0	0	0	10
	Iceland	39,768	Icelandic	-1	GMT	0	104	100	3	0	0	0	0	10
	Ireland	27,135	Irish, English	GMT	+1	0	104	100	0	0	0	0	0	10
	Italy	116,303	Italian	+1	+2	3,525,000	104	104*	1338	141	0	0	0	10
	Liechtenstein	61.4	German	N A	N A	0	104	100	0	0	0	0	0	10
	Luxembourg	998	Luxembourgian French	+1	+1	100,000	104	100	4	4	0	0	0	10
	Malta	122	English, Maltese	+1	+1	0	104	100	0	0	0	0	0	10
	Monaco	.606	French	+1	+1	25,000	104	100	2	1	0	0	0	10
	Netherlands	12,978	Dutch	+1	+1	350,000	104	104*	15	14	0	0	0	10
	Norway	125,181	Norwegian	+1	+1	850,000	104	100	68	34	0	0	0	10
	Portugal	35,510	Portugese	GMT	+1	300,000	104	100	14	12	0	0	4	10
	Spain	194,884	Spanish	+1	+1	500,000	104	104*	27	20	0	0	0	10
	Sweden	173,666	Swedish	+1	+2	2,325,000	104	100	103	80	0	0	0	10
	Switzerland	15,941	German, French Italian, Romansh	+1	+1	675,000	104	104*	60	27	0	0	0	10
	United Kingdom	94,220	English	GMT	+1	2,550,000	104	100	108	102	0	0	0	10
Eastern Europe	Albania	11,100	Albanian	+1	+1	0	N A.	100	0	0	0	0	0	N A.
	Bulgaria	42,729	Bulgarian	+2	+2	0	N A.	100	0	0	0	0	0	N A
	Czechoslovakia	49,370	Czech , Slovak	+1	+1	0	N A.	100	0	0	0	0	0	N A
	Hungary	35,919	Hungarian	+1	+1	0	N A.	100	0	0	0	0	0	N A
	Poland	120,664	Polish	+1	+1	30,000	N A	100	3	3	0	0	0	N A
	Rumania	91,699	Rumanian	+2	+2	0	N A.	100	0	0	0	0	0	N A.
	USSR	8,649,512	See note 2	Note 14	Note 14	0	N A	100	0	0	0	0	0	N A
	Yugoslavia	98,766	Serbo-Croat, Slovenian, Macedonian	+1	+1	430,000	N A.	104*	58	43	0	0	0	N A
Near East and South Asia	Afghanistan	253,861	Pushtu, Dari, Persian	+4 1/2	+4 1/2	0	N A.	108	0	0	0	0	0	N A.
	Ceylon	25,332	English, Sinhalese, Tamil	+5 1/2	+5 1/2	0	N A	108	3	0	2	0	100 1, 100 6 101.1	N A
	Cyprus	3,572	Greek, English Turkish	+2	+2	20,000	N A	100	2	2	0	0	0	N A
	Greece	50,944	Greek	+2	+2	0	N.A	100	0	0	0	0	0	N.A.
	India	1,176,153	See note 3	+5 1/2	+5 1/2	0	N A.	108	0	0	0	0	0	N A
	Iran	636,294	Persian	+3 1/2	+3 1/2	0	N A	108	1	0	0	0	0	N.A.
	Iraq	173,260	Arabic, Kurdish, Turkuma	+3	+3	0	N A.	100	0	0	0	0	0	N A.
	Israel	7,992	Hebrew, Arabic	+2	+2	0	N A.	104*	0	0	0	0	0	N A
	Jordan	37,738	Arabic, English	+2	+2	0	N A.	100	0	0	0	0	0	N A
	Kuwait	6,178	Arabic	+3	+3	0	N A	100	0	0	0	0	0	N A
	Lebanon	4,015	Arabic, French English	+2	+3	0	N A.	100	0	0	0	0	0	N A
	Nepal	54,362	Nepali, Newari, Hindi, English	+5 40	+5 40	0	N A.	108	0	0	0	0	0	N A
	Pakistan	365,529	Urdu, Bengali	West +5 East +6	+5	0	N A.	108	0	0	0	0	0	N A

Table 2.6-8. Distribution of UHF Receivers - December 1965 (Cont'd)

Area	Country	Area (Sq miles)	Prin. Languages	Local Time* Normal Clock Time	Local Time* Summer Time	FM, 87.5 - 106 mc: # of receivers 87.5 - 106 mc	Est. max. freq covered by sets, mc	Authorized** maximum freq., mc	Total # broadcast stations	# stations ≥ 1000 watts	# stations 100 - 105 mc	# stations 100-108 mc ≥ 1000 watts	Frequency of used channels 100-108 mc	average receiver sensitivity uv
Near East and South Asia (Cont'd)	Saudi Arabia	870,001	Arabic	+3	+3	0	N.A.	100	0	0	0	0	0	N.A.
	Syrian Arabic Republic	71,498	French, Arabic	+2	+2	0	N.A.	100	0	0	0	0	0	N.A.
	Turkey	301,381	Turkish	+2	+2	0	N.A.	100	2	0	0	0	0	N.A.
	United Arab Republic	386,101	Arabic	+2	+3	70,000	N.A.	100	7	0	0	0	0	N.A.
	Yemen	75,290	Arabic	+3	+3	0	N.A.	100	0	0	0	0	0	N.A.
Africa	Algeria	919,593	French, Arabic, Kabyl	GMT	GMT	0	N.A.	100	0	0	0	0	0	N.A.
	Angola	481,351	Portugese	+1	+1	0	N.A.	108	1	0	0	0	0	N.A.
	Basutoland Bechuanaland Swaziland	293,420	Sesotho, English Vernaculars	+2	+2	0	N.A.	100	0	0	0	0	0	N.A.
	Burundi	10,747	Kirundi, Kiswahili, French	+2	+2	0	N.A.	100	0	0	0	0	0	N.A.
	Cameron	183,569	French, English, Vernaculars	+1	+1	0	N.A.	100	0	0	0	0	0	N.A.
	Cape Verde Island	N.A.	Portugese, English	-2	-2	0	N.A.	100	0	0	0	0	0	N.A.
	Central African Republic	238,224	French, Sango	+1	+1	0	N.A.	100	0	0	0	0	0	N.A.
	Chad	495,754	French, Arabic Sara	+1	+1	0	N.A.	100	0	0	0	0	0	N.A.
	Comoro Island	850	French, Vernaculars	+3	+3	0	N.A.	100	0	0	0	0	0	N.A.
	Congo Republic (Brazzaville)	132,047	French, English Portugese	+1	+1	10,000	N.A.	100	0	0	0	0	0	N.A.
	Congo Republic (Leopoldville)	905,565	French, Lingala Mikongo Tshiluba Swahili	Leopoldville +1 Elizabethville +2	+1 +2		N.A.	100	2	1	0	0	0	N.A.
	Dahomey	43,483	French Vernaculars	+1	+1	0	N.A.	100	0	0	0	0	0	N.A.
	Ethiopia	457,267	Amharic, Arabic English, Somali	+3	+3	0	N.A.	100	0	0	0	0	0	N.A.
	Gabon	103,089	French	+1	+1	0	N.A.	100	0	0	0	0	0	N.A.
	Gambia	4,003	English, Mandinka, Wolloff, Vernaculars,	GMT	GMT	0	N.A.	100	0	0	0	0	0	N.A.
	Ghana	92,099	Akan, Ewe, Ga, Dagbani, Hausa, Nzema	GMT	GMT	0	N.A.	100	0	0	0	0	0	N.A.
	Guinea	94,926	French, Vernaculars	GMT	GMT	0	N.A.	100	0	0	0	0	0	N.A.
	Guinea (Portugese)	13,948	Portugese	-1	-1	0	N.A.	100	0	0	0	0	0	N.A.
	Guinea (Spanish)	N.A.	Spanish	+1	+1	0	N.A.	100	0	0	0	0	0	N.A.
	Ivory Coast	124,503	French, Vernaculars	GMT	GMT	0	N.A.	100	0	0	0	0	0	N.A.
	Kenya	224,960	English, Swahili, Hindustani	+3	+3	30,000	N.A.	100	3	3	0	0	0	N.A.
	Liberia	43,000	English, Liberian-Vernaculars	-3/4	-3/4	0	N.A.	100	0	0	0	0	0	N.A.
	Libya	679,360	Arabic	+2	+2	20,000	N.A.	100	2	2	0	0	0	N.A.
	Malagasy Republic	N.A.	Malgache, French	+3	+3	0	N.A.	100	0	0	0	0	0	N.A.
	Malawi	46,066	English, Nyanja, Tumbuka	+2	+2	0	N.A.	100	0	0	0	0	0	N.A.
	Mali	463,949	French, English Vernaculars	GMT	GMT	0	N.A.	100	0	0	0	0	0	N.A.
	Mauritania	419,230	French, Arabic, Vernaculars	GMT	GMT	0	N.A.	100	0	0	0	0	0	N.A.
	Mauritius	720	English, French, Hindustani, Chinese	+4	+4	0	N.A.	100	0	0	0	0	0	N.A.
	Morocco	171,834	Arabic, French, Spanish, English, Berber	GMT	GMT	26,000	N.A.	100	7	2	0	0	0	N.A.
	Mozambique	N.A.	Portugese, English, Afrikans, Vernaculars	+2	+2	0	N.A.	100	1	0	0	0	0	N.A.
	Niger	459,190	French, Hausa, Djerma, Tamachek, Peuh, Beriberi	+1	+1	0	N.A.	100	0	0	0	0	0	N.A.
	Nigeria	356,669	English, Yoruba, Hausa, Ibo	+1	+1	0	N.A.	100	1	0	0	0	0	N.A.
	Reunion	970	French	+4	+4	0	N.A.	100	0	0	0	0	0	N.A.
	Rhodesia	152,804	English, Shona Sindebele	+2	+2	0'	N.A.	100	0	0	0	0	0	N.A.
	Rwanda	10,169	Kinyarwanda, Swahili, French	+2	+2	0	N.A.	100	0	0	0	0	0	N.A.
	Senegal	75,750	French, Ouolof, Toucoulour, Serere Portugese	GMT	GMT	0	N.A.	100	0	0	0	0	0	N.A.
	Seychelles	156	English, French Creole	+4	+4	0	N.A.	100	0	0	0	0	0	N.A.
	Sierra	27,699	English, Mende Temne, Krio	GMT	GMT	0	N.A.	100	0	0	0	0	0	N.A.
	Somali Republic	246,202	Somali, Arabic, Italian, Swahili, English	+3	+3	0	N.A.	100	0	0	0	0	0	N.A.
	Somaliland (French)	N.A.	French, Somali, Afar, Arabic	+3	+3	0	N.A.	100	0	0	0	0	0	N.A.
	South Africa	471,446	English, Bantu Afrikaans	+2	+2	1,675,000	108	108	75	67	31	27	Note 5	30
	Sudan	967,501	Arabic, English	+2	+2	0	N.A.	100	0	0	0	0	0	N.A.
	Tanzania	361,800	Swahili, English	+3	+3	0	N.A.	100	0	0	0	0	0	N.A.
	Togo	21,853	Ewe, Cotocolla, Cabrais, Hausa, Moba, Bassari	GMT	GMT	0	N.A.	100	0	0	0	0	0	N.A.
	Tunisia	48,332	Arabic	+1	+1	10,000	N.A.	100	3	1	0	0	0	N.A.
	Uganda	91,134	Note 4	+3	+3	0	N.A.	100	0	0	0	0	0	N.A.
	Upper Vota	105,869	French, More	GMT	GMT	0	N.A.	100	0	0	0	0	0	N.A.
	Zambia	288,130	English, 7 African Vernaculars	+2	+2	0	N.A.	100	0	0	0	0	0	N.A.
Far East	Australia	2,971,063	English	Note 15	Note 15	0	N.A.	108	0	0	0	0	0	N.A.
	Brunei	2,226	Miay, English Chinese	+8	+8	0	N.A.	108	1	0	0	0	0	N.A.
	Burma	261,789	Burmese, English	+6 1/2	+6 1/2	0	N.A.	108	1	0	1	0	100 0	N.A.
	Cambodia	69,898	Cambodian, French English	+7	+7	0	N.A.	108	0	0	0	0	0	N.A.
	Fiji Islands	7,083	English, Fijian, Hindustani	+12	+12	0	N.A.	108	0	0	0	0	0	N.A.
	Guam	225	English, Chamcoo Philippine dialects	+10	+10	0	N.A.	108	0	0	0	0	0	N.A.
	Hong Kong	391	Chinese	+8	+9	20,000	N.A.	108	2	2	0	0	0	N.A.
	Indonesia	575,894	Indonesian	Note 16	Note 16	0	N.A.	108	0	0	0	0	0	N.A.
	Japan	142,726	Japanese	+9	+9	50,000	80-99	108	10	5	0	0	0	N.A.
	Korea (South)	38,004	Korean	+9	+9	0	N.A.	108	3	0	2	0	102.6 104 0 106 2	N.A.

Table 2.6-8. Distribution of UHF Receivers - December 1965 (Cont'd)

Area	Country	Area (Sq miles)	Prin. Languages	Local Time* Normal Clock Time	Local Time* Summer Time	FM, 87.5 – 108 mc: # of receivers 87.5 – 108 mc	Est. max. freq covered by sets, mc	Authorized** maximum freq., mc	Total # broadcast stations	# stations ≥ 1000 watts	# stations 100 – 108 mc	# stations 100-108 mc ≥ 1000 watts	frequency of used channels 100-108 mc	average receiver sensitivity uv
Far East (Cont'd)	Laos	91,429	Laotian, French	+7	+7	0	N.A.	108	0		0	0	0	N.A.
	Macao	N.A.	Portugese, Chinese	+8	+8	10,000	N.A.	108	1	1	0	0	0	N.A.
	Malaysia	50,700	English Malay, English Chinese	+8	+8	0	N.A.	108	0	0	0	0	0	N.A.
	Mongolia	592,665	Mongolian	+8	+8	0	N.A.	108	0	0	0	0	0	N.A.
	New Caledonia	N.A.	French	+11	+11	0	N.A.	108	0	0	0	0	0	N.A.
	New Zealand	103,736	English, Maori	+12	+12	0	N.A.	108	0	0	0	0	0	N.A.
	Philippines	115,830	English, Tagalog Ilocano, Visayan	+8	+8	10,000	N.A.	108	9	1	5	0	Note 9	N.A.
	Taiwan	13,885	Chinese	+8	+8	0	N.A.	108	1	0	1	0	100.1	N.A.
	Thailand	198,456	Thai	+7	+7	10,000	N.A.	108	13	1	3	0	100.0 100.5 105.0	N.A. N.A.
	Vietnam (South)	65,800	Vietnamese	+8	+8	0	N.A.	108	4	0	3	0	103.3 105.1 107.0	N.A.
Latin America	Argentina	1,072,070	Spanish	-4	-3	25,000	N.A.	108	2	1	0	0	0	N.A.
	Bolivia	424,163	Spanish	-4	-4	0	N.A.	108	1	0	0	0	0	N.A.
	Brazil	3,286,478	Portugese	Note 17	Note 17	150,000	N.A.	108	119	6	51	2	Note 12	N.A.
	Chile	285,397	Spanish	-4	-4	25,000	N.A.	108	20	1	3	0	100.1 100.3 104.3	N.A.
	Colombia	439,513	Spanish	-5	-5	25,000	N.A.	108	104	1	8	0	Note 10	N.A.
	Costa Rica	19,575	Spanish	-6	-6	0	N.A.	108	3	0	0	0	0	N.A.
	Cuba	44,218	Spanish	-5	-4	25,000	N.A.	108	10	1	6	0	Note 11	N.A.
	Dominican Republic	18,816	Spanish	-5	-4	25,000	N.A.	108	14	1	2	0	100.0 105.0	N.A.
	Ecuador	104,506	Spanish, Quechua	-5	-5	0	N.A.	108	2	0	1	0	105.9	N.A.
	El Salvador	8,260	Spanish	-6	-6	75,000	N.A.	108	7	3	3	1	101.0 102.0 101.7	N.A.
	Guatemala	42,042	Spanish	-6	-6	0	108	108	6	0	1	0	101.75	N.A.
	Haiti	10,714	French, Creole	-5	-5	0	108	108	0	0	0	0	0	N.A.
	Honduras	43,277	English, Spanish	-5	-6	25,000	108	108	6	1	2	0	100.0 105.0	N.A.
	Jamaica	4,232	English	-5	-5	75,000	108	108	4	3	0	0	0	N.A.
	Mexico	761,602	Spanish	-6	-6	650,000	108	108	78	26	12	9	Note 6	N.A.
	Nicaragua	53,938	Spanish	-6	-6	25,000	108	108	7	1	0	0	100.0	N.A.
	Panama	29,209	Spanish	-5	-5	150,000	108	108	17	6	3	0	102.0 103.0 105.0	N.A.
	Paraguay	157,047	Spanish	-4	-4	0	108	108	2	0	2	0	105.0 105.1	N.A.
	Peru	496,223	Spanish	-5	-5	125,000	108	108	8	5	4	4	100.0 101.0 102.8 103.5	N.A.
	Trinidad & Tobago	1,980	English	-4	-4	25,000	108	108	2	1	0	0	0	N.A.
	Uruguay	72,172	Spanish	-3	-3	0	108	108	1	0	1	0	101.9	N.A.
	Venezuela	352,143	Spanish	-4	-4	0	108	108	32	0	6	0	Note 7	N.A.
North America	Canada	3,851,812	English, French	Note 18	Note 18	925,000	108	108	80	37	12	8	Note 8	N.A.
	U.S.A.	3,615,211	English	Note 19	Note 19	39,500,000	108	108	1515	1247	552	508	Note 13	N.A.

NOTES

Note +- The differences marked + indicate the number of hours ahead of GMT. Differences marked – indicate number of hours behind GMT.

Note *- In Austria, Belgium, Spain, Israel, Italy, Yugoslavia, Switzerland and, if necessary, Denmark, the Netherlands, and the F. R. of Germany, the band 100 to 104 mc/s is allocated on a permitted basis to the broadcasting service. The introduction of the broadcasting service for these countries is subject to special arrangements between the interested and affected administrations to ensure that harmful interference is not caused to the services of the other countries operating in accordance with the Radio Regulations.

**Note 1- These authorizations from the Radio Regulations were adopted by The Administrative Radio Conference, Geneva, 1959.

Note 2 Russian, Ukrainian, Byelorussian, Uzbek, Tatar, Kazakh, Azerbaidjanian, Armenian, Georgian, Lithuanian, Moldavian, German, Estonian, Latvian, Chuvash, Tadjik.

Note 3 Hindi, Marathi, Gujarati Oriya, Bengali, Assamese, Tamil, Telugu, Urdu, Kannada, Kashmiri, Sanskrit, Dogri, Sindhi, Punjabi, Malayalam, English.

Note 4 English, Luganda, Lwo, Ateso, Runyoro, Rutooro, Runyankore/Rukiga.

Note 5 100.590 100.848, 101.364, 101.622 102.396 102.654 102.740, 102.998, 103.170, 103.428, 103.514 103.944, 104.546, 104.804 105.320, 105.578, 105.836, 106.352 106.610, 106.696, 106.954, 107.126 107.384 107.728

Note 6 100.1; 100.3; 100.9, 101.7 102.5, 103.3, 104.1, 106.0, 106.5, 106.8; 107.2 107.3

Note 7 100.0, 101.1, 102.8, 103.5 103.9

Note 8 100.3 100.5, 100.7, 102.9; 101.5 102.1 102.7, 103.3, 103.5, 104.3, 104.5, 105.7

Note 9- 101.3 102.1, 103.1, 103.5, 107.0

Note 10 102.1, 102.4, 103.1, 104.2, 105.0, 107.1, 107.5

Note 11 100.1; 102.7, 105.6, 106.1 106.9 107.7

Note 12 100.1; 100.5 101.1, 101.3, 101.5, 102.1, 102.5 102.9, 103.1, 104.5 105.1; 105.3, 106.1; 106.3, 106.5 106.7, 106.9, 107.1, 107.3, 107.7, 107.9

Note 13 100.1, 100.3, 100.5, 100.7 100.9 101.1, 101.3, 101.5, 101.7, 101.9, 102.1, 102.3 102.5 102.7, 102.9; 103.1, 103.5 103.7 103.9 104.1 104.3 104.5 104.7, 104.9, 105.1, 105.3, 105.5 105.7 105.9, 106.1; 106.3, 106.5, 106.7 106.9, 107.1, 107.3, 107.5 107.7; 107.9

Table 2.6-8. Distribution of VHF Receivers - December 1965 (Continued)

NOTES CONTINUED

Note 14

	Normal Clock Time	Summer Time
Moscow, Leningrad	+ 3	+ 3
Baku	+ 4	+ 4
Sverdlovsk	+ 5	+ 5
Tashkent	+ 6	+ 6
Novosibirsk	+ 7	+ 7
Irkutsk	+ 8	+ 8
Yakutsk	+ 9	+ 9
Khabarovsk	+10	+10
Magadan	+11	+11
Petropavlovsk	+12	+12
Anadyr	+13	+13

Note 15

	Normal Clock Time	Summer Time
a) Victoria, New South Wales, Queensland, Tasmania	+10	+10
b) N Territory, S Australia	+9-1/2	+9-1/2
c) W Australia	+8	+8

Note 16

	Normal Clock Time	Summer Time
a) North Sumatra	+6-1/2	+6-1/2
b) South Sumatra	+7	+7
c) Java, Borneo, Bali	+7-1/2	+7-1/2
d) Celebes	+8	+8
e) West Irian	+9	+9

Note 17

	Normal Clock Time	Summer Time
a) Eastern and Coastal	-2	-2
b) Manaus	-4	-3
c) Acre	-5	-4

Note 18

	Normal Clock Time	Summer Time
a) New Foundland	-3-1/2	-2-1/2
b) Atlantic (Labrador, Nova Scotia)	-4	-3
c) Eastern (Ontario, Quebec)	-5	-4
d) Central (Manitoba)	-6	-5
e) Mountain (Alberta)	-7	-6
f) Pacific (British Columbia)	-8	-8
g) Yukon	-9	-8

Note 19

	Normal Clock Time	Summer Time
a) Eastern Zone	-5	-4
b) Central Zone	-6	-5
c) Mountain Zone	-7	-6
d) Pacific Zone	-8	-7

2.6.2.1 Projection of Number of Receivers, 1970

The projection of the distribution of VHF receivers to 1970 (using the procedure described in Section 2.6.1.2) was estimated for major world areas. The results are tabulated in Table 2.6-9 for major areas.

Table 2.6-9. Estimated Receivers (1970)

Area	VHF-FM
Africa	4,036,000
Near East and South Asia	230,000
Latin America	1,760,000
Far East	172,000
Eastern Europe	1,820,000
Western Europe	25,600,000
North America	98,500,000
Total	132,118,000

Further analysis of the audience potential must take into account the receiver noise environments. The assumptions used as world averages are shown in Table 2.6-10.

Table 2.6-10. % Population Distribution

Urban	25%
Suburban	45%
Rural	30%

Since the majority of VHF sets in the world exist in the United States, their distribution will closely follow the population distribution in the United States, as shown here. This is different than the HF case described in Section 2.6.1.2 where the majority of sets existed outside the United States.

2.6.2.2 VHF Signal Level Requirements

As previously discussed in the HF Section, the signal levels required were based on the set sensitivity, noise environment, and the gain of the home antenna.

A receiver sensitivity curve was derived from test measurement data taken by the GE Radio Receiver Department on "Comparison Shopping" receivers. The curve, shown in Figure 2.6-12, includes low cost portable receivers. Also shown on Figure 2.6-12 are the measurement conditions, CCIR recommended values and the South Africa minimum sensitivity specified by law.

The sensitivity, noise and home antenna factors, discussed in previous sections, were combined with the assumed home antenna distributions (10% high gain outdoor antennas, 40% low gain outdoor antennas, and 50% low gain indoor antennas). The field strengths required for these combinations are shown in Figure 2.6-13, which is a plot of the number of receivers reachable versus the signal strength provided.

This curve shows, for example, that 50% of the receivers can be reached with a signal level of 30 μv/m. The curve shows that reception in general is receiver-limited. That is, as signal level is increased, there is a gradual increase in the number of receivers which are reachable in a given environment. The noise environment in the urban area is such that no significant reception appears possible below 77 μv/m.

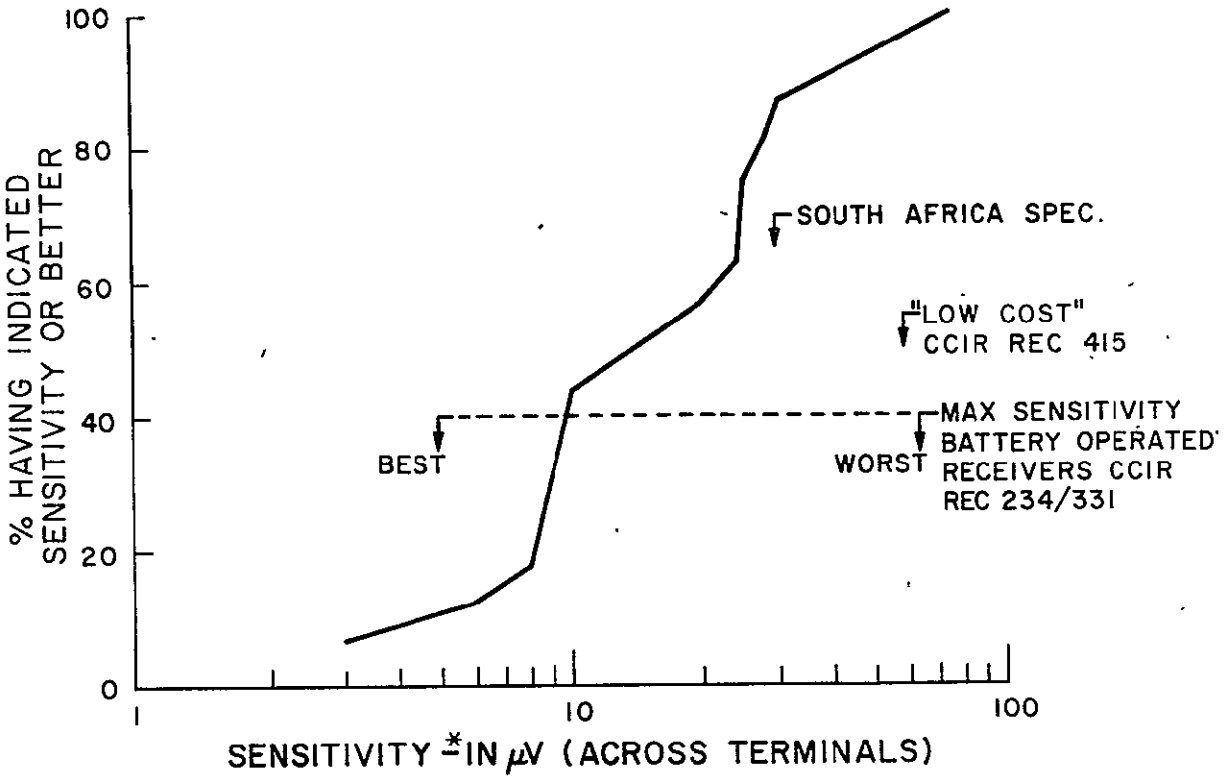

Figure 2.6-12. VHF Receiver Sensitivity Distribution

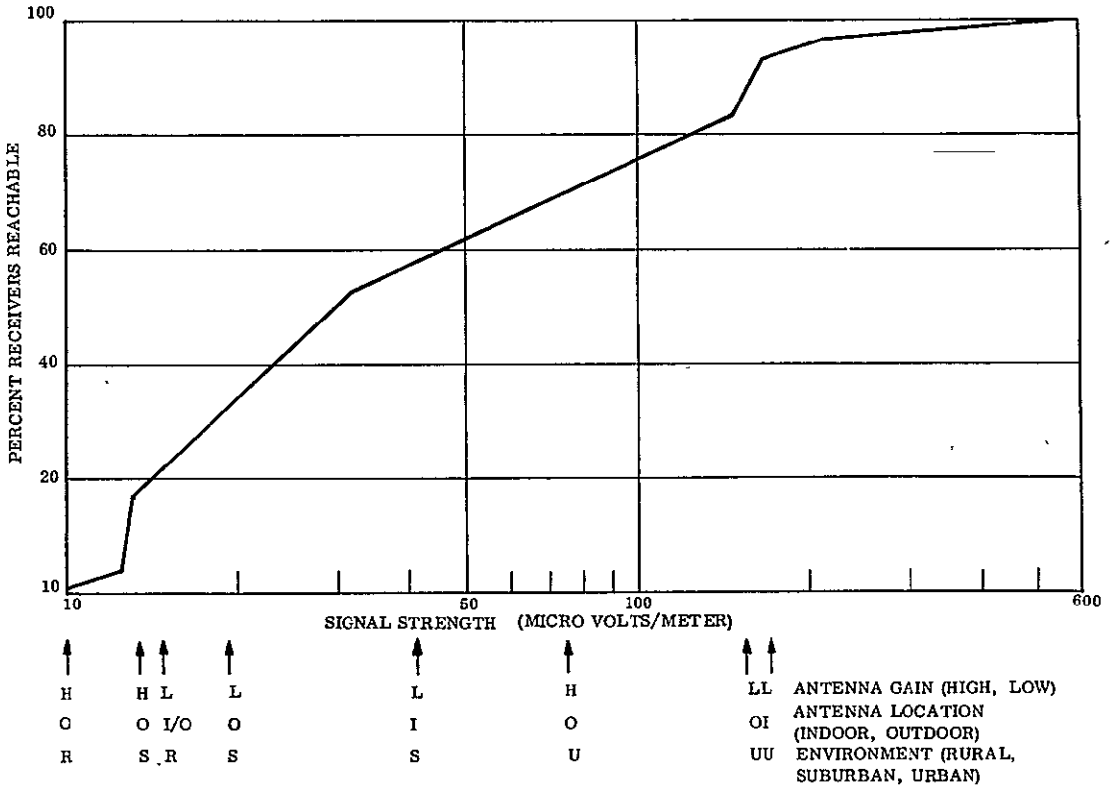

Figure 2.6-13. Number of VHF Receivers Versus Signal Strength

The assumptions and data used in the VHF signal strength calculation are as follows:

Modulation: FM

Frequency: 100 MHz

Required IF C/N = 10 db
IF Bandwidth = 175 kHz
Audio bandwidth = 15 kHz
100% modulation
9 db deemphasis
Receiver Input Impedance = 300 ohms
Receiver Noise Figure = 10 db
Peak Frequency Deviation ± 75 kHz
Note that these assumptions will produce a minimum output S/N = 45.5 db.

Noise (^{o}K)

	Man-Made	Galactic
Urban	9.15×10^5	3×10^3
Suburban	9.15×10^3	3×10^3
Rural	2.9×10^2	3×10^3

Noise Data Sources

Urban and Rural Man-made: ESSA
Suburban man-made: GE Measurements
Atmospheric: CCIR(± 40° Latitude: average of median; all seasons; 1600 to 2000 hrs.)
Galactic: average from number of sources, including ESSA

Antennas:

	Max. Gain	Effective Gain	Line Loss
Low Gain	2.2 db	-0.8 db (3 db polarization loss)	0.5 db
High Gain	8 db	2 db (3 db polarization loss; 3 db pointing loss)	0.5 db

Building Losses:

Urban	Suburban	Rural
17.7 db	9.5 db	0 db

The carrier-to-noise ratio in the IF is given by:

$$\frac{C}{N} = \frac{S_i}{\eta B_{if}}$$

where:

$$\eta = K \left\{ T_a + T_o \left[(L - 1) + (F - 1) L \right] \right\}$$

$$Si = \text{carrier power delivered by antenna} = \frac{E^2 G_r \lambda^2}{480 \pi^2}$$

B_{if} = IF bandwidth

where

K = Boltzmann's constant = 1.38×10^{-23}

T_a = input noise temperature from external sources

L = Line loss, if any

F = receiver noise factor

T_o = $290^{o}K$

E = Field strength

G_r = Receiving antenna gain

λ = Wavelength

2.6.3 UHF RECEIVER DISTRIBUTION

The distribution of UHF television receivers has been investigated. The results, illustrated in Figure 2.6-14 show that there are only three major areas (North America, Europe, and the Far East) with receivers in existance. Note that they are all north of the equator. The distribution of receivers in place as of December 1965 is shown on the map.

The investigation of UHF receiver distribution also considered grouping areas by location and language, time zone span, and the size of coverage area as measured in degrees of earth central angle (ECA). The results are listed in Table 2.6-11.

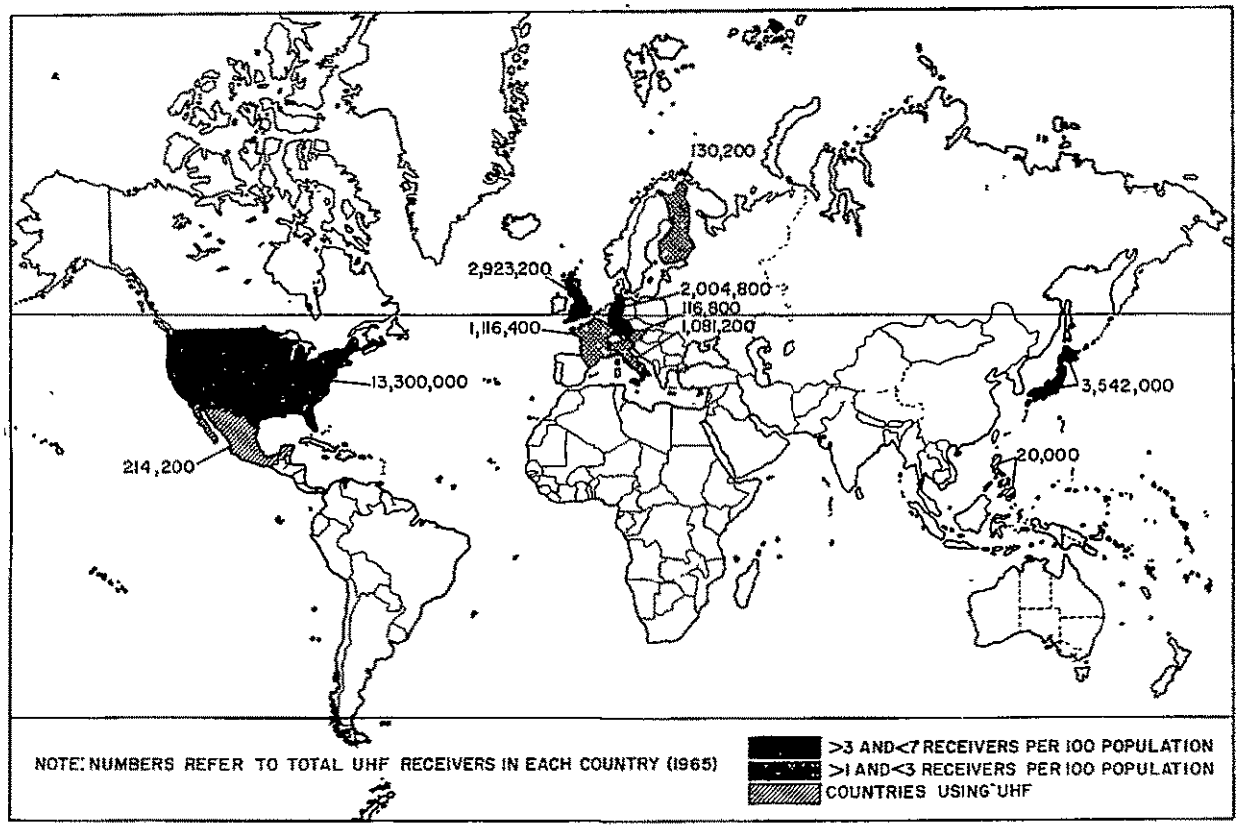

Figure 2.6-14. Distribution of UHF Television Receivers

Table 2.6-11 shows a 42° span will cover any one of these major areas. The 42° earth central angle is sufficient to also tie together the eastern coast of the United States with the western edge of Europe. This is of interest due to the fact that this represents the greatest flow of communication and commerce between any two of the major areas shown. Thus, a 42° span represents a good upper bound for a desirable coverage area for a UHF broadcast satellite. The column on the left shows the earth central angle spans for the individual countries. This also generally coincides with areas of common language. Thus, a 20° span appears to be a reasonable lowerbound of practical interest for a UHF satellite.

Table 2.6-11. UHF Coverage Possibilities

MINOR AREA SPAN/TIME ZONES	GEOGRAPHICAL AREAS	MAJOR AREA ECA-SPAN/TIME ZONES		INTRA-AREA ECA-SPAN/TIME ZONES
$20^{\circ}/2$ (URBAN)	UNITED STATES (ENGLISH)	$42^{\circ}/4$	$58^{\circ}/7$	$42^{\circ}/5$
$27^{\circ}/2$	MEXICO (SPANISH)			
$17^{\circ}/1$	JAPAN (JAPANESE)	$42^{\circ}/2$	$82^{\circ}/9$	
$14^{\circ}/1$	PHILIPPINES (ENGLISH)			
$10^{\circ}/1$	FINLAND (FINNISH)	$31^{\circ}/3$		
$15^{\circ}/2$	WESTERN EUROPE (ENGLISH, FRENCH, GERMAN, ITALIAN)			

Each of the UHF areas in the world can individually be covered by a 6.8° antenna beam width from a satellite in a synchronous equatorial orbit shown in Figure 2.6-15. A satellite positioned at 95° west longitude with its antenna pointed at 35° north latitude will give complete coverage of the United States and Mexico. Similarly, a vehicle stationed at 14° east longitude above the equator and pointed to 45° north latitude will cover the entire European area. The area comprised of Japan and the Phillipines can be reached by a satellite at 140° east longitude pointing at 20° north latitude. It should also be pointed out that the horizon of a satellite located at 45° west longitude will include an area of the world containing both the North American and the European UHF/TV audience. Such wide coverage would require broadening the antenna beamwidth to 17.3° and making up for the subsequent reduction of antenna gain by broadcasting at a higher power level.

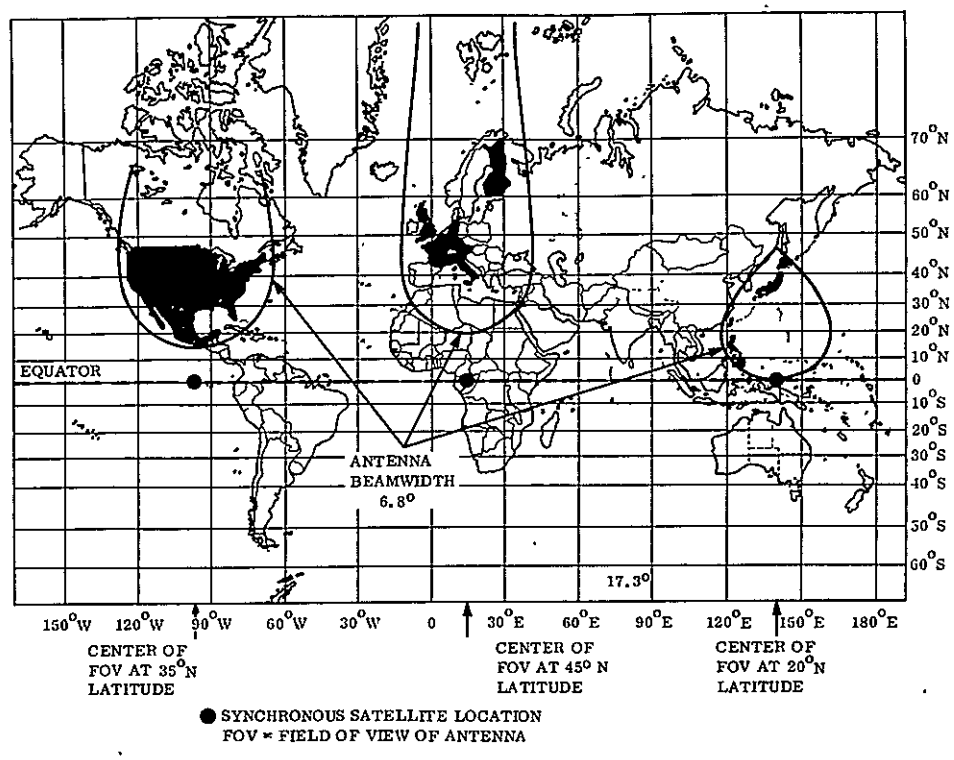

Figure 2.6-15. 24 Hour Continuous Coverage of Countries with UHF

2.6.3.1 UHF Projection of Number of Receivers, 1970

Of the geographical areas previously mentioned, only the United States and Western Europe currently have a significant number of UHF receivers. Table 2.6-12 gives estimates of the number of UHF receivers projected to 1970 using the projection technique described in Section 2.6.1.2.

Table 2.6-12. Projected Number of UHF Receivers - 1970

Area	UHF/FM
North America	66, 500, 000
Latin America	1, 071, 000
Western Europe	36, 863, 000
Far East	17, 810, 000
Total	122, 244, 000

The distribution of these receivers with respect to their noise environment is assumed to be the same as for the VHF sets as shown in Table 2.6-10.

2.6.3.2 UHF Receiver Characteristics

In the UHF case, a study was made to determine the feasibility and constraints of using conventional home television receivers to provide service making use of FM modulation of an aural carrier.

General Requirements for the Radiated Signal

In the early days of television broadcasting, before 1950, receivers were constructed so that independent use was made of the picture and aural signals. In such receivers, separate intermediate frequency channels and second detectors were provided. Since those days, however, industry has universally adopted the intercarrier method of sound reception. Very few, if any, of the separate channel receivers are still in use, so that probably 99.9% of the receivers used today are of the intercarrier sound type. These receivers have but one intermediate frequency channel; this channel passes both picture IF and sound IF. The second detector is an envelope detector producing output signals for the video pattern of the receiver as well as an FM aural output of 4.5 MHz. The picture portion, usually extending not beyond 4.2 MHz, is filtered out of the detector composite signal and is portrayed on the picture tube. The sound portion, a narrow band some 120 kHz wide, is filtered out, amplified, and applied to a suitable discriminator-detector to obtain audio frequency, which, after amplification, is applied to a loud-speaker.

Thus, although it is theoretically possible to transmit only the FM aural carrier to provide sound, actually, in practice, receivers rely on both carriers being present; it is therefore necessary to supply both a picture carrier and the aural carrier. The picture carrier may come from the satellite radiating the FM aural wave or, the picture carrier could be generated by receiver modification and injected into the receiver along with the incoming FM aural signal.

There are several reasons for preferring that the picture carrier be supplied from the satellite rather than from modifying the receiver. One most compelling reason is the simple economic fact that this modification to the receiver is expensive, because the oscillator would have to be quartz crystal and temperature controlled and would have to include frequency multipliers to obtain the final picture carrier frequency. A list price of from $40 to $50 seems reasonable.

Another reason for the undesirability of providing the picture carrier locally is that receivers are designed to operate with a specific ratio of picture to aural carrier powers. If the picture carrier to aural carrier power is too great, automatic gain control would reduce the receiver gain to such a low level that the 4.5 MHz signal would be too feeble to provide good limiting and sufficient sound output. If on the other hand, the ratio of picture to aural power were too low, the resultant 4.5 MHz signal would not only be low in amplitude, but would be very noisy; in this case, the noise would come from the 120 KHz noise band surrounding the picture carrier frequency. One could give the user a control knob to adjust the amplitude of the locally injected picture carrier, but it has been found in practice that the proper use of the control is both difficult to teach the average customer and difficult to make the customer use it.

It is therefore, concluded that the general requirements for the radiated signal are (1) that an FM aural carrier, modulated according to TV standards be radiated, and (2) that an unmodulated picture carrier wave be radiated. Both signals, would of course, be radiated from the satellite.

Specific Technical Requirements of the Radiated Waves

The question arises as to specifications for the two radiated carrier. It would be most sirable to modulate only the aural carrier and to provide no modulation whatsoever on the picture carrier so as to simplify the satellite equipment and to reduce its power consumption to a minimum. This appears to be entirely feasible.

The present TV aural carrier is frequency-modulated with the audio information in accordance with FCC television broadcast standards of:

Maximum deviation: $\pm$ 25 kHz
Pre-emphasis time constant: 75 microseconds
Audio band: 50 to 15, 000 Hz

Normally the picture carrier is, of course, amplitude-modulated with synchronizing pulses, blanking pulses, and picture signals. These are required if a picture is to be transmitted and received; however, because the service to be rendered in the present instance does not involve picture reception, it is clear that at least no picture or blanking signals need be transmitted. The only question to be resolved, then, is that of any necessity of transmitting synchronizing signals.

Synchronizing signals are used, of course, to synchronize the receiver horizontal (line) and vertical (field) scanning oscillators. Additionally, horizontal scanning pulses are employed in many television receiver automatic gain control (AGC) systems. Fortunately, the modern television receiver employs fairly precise horizontal oscillators, of which the self oscillation frequencies differs from the 15, 750 Hz horizontal sweep frequency by less than $\pm$2%. Consequently, the absence of horizontal synchronizing pulses will cause no appreciable frequency change in the horizontal oscillator frequency. As a result of the relative constancy in frequency, the amplitude of the scanning pulses fed to the keyed AGC system is also relatively constant. Thus, the AGC voltage will be a function of the noise plus signal voltage appearing at the second detector during the period of the horizontal pulse.

As far as the vertical scanning frequency is concerned, the free running oscillator frequency may run some 5% to 20% below the synchronized frequency of 60 Hz and will in most cases cause no audible bad effects. The reason for this is that in most receivers the designers have been careful to keep vertical signals out of the audio channel through isolation in order to avoid the staccato audible type of vertical interference caused, not so much by the fundamental, as by the rich harmonic content of the sawtooth waves.

A small percentage of television receivers do not employ keyed AGC. Instead, these receivers derive their AGC bias voltages from a combination of the dc component present at the second detector and the dc component present at the grid of the sync separator. The absence of sync pulses will cause the sync separator dc component to virtually disappear, but compensating for this is the fact that the dc component at the second detector will be greater in the absence of sync pulses. The end result is a tradeoff that scarcely affects the AGC so that sync pulses are not at all necessary for AGC operation.

It may be concluded, therefore, that the picture carrier need not be modulated at all. Indeed, it is preferable that it not be modulated, because the absence of modulation reduces the possibility of "buzz" originating from the variable level picture carrier having some of its amplitude modulation transferred to the 4.5 MHz intercarrier sound frequency. While the limiter and discriminator ordinarily tend to remove amplitude modulation effects, some buzz could still show up, particularly when signals approached or fell below a certain amplitude. The picture carrier, then, wave should be free of any modulation, while the aural carrier should be frequency-modulated with the desired audio in accordance with FCC standards. The two carrier waves should differ in their nominal carrier frequencies by 4.5 MHz $\pm$ 4 kHz to be in accordance with the FCC Standards used in the United States.

Standards Other Than the FCC Standards of the United States of America

The transmission, in accordance with the FCC standards, is receivable only where receivers have corresponding characteristics (North America, Japan and parts of South America).

In Western Europe and India, where the so-called CCIR standards are employed, receivers are designed for a 5.5 MHz spacing between the picture and aural carrier frequencies, for a frequency deviation of $\pm$ 50 kHz, and a pre-emphasis time constant of 50 microseconds.

There are two available means for handling these differences in receiver characteristics. One is to provide as many separate satellites as there are different standards. Another is to provide means for switching the picture carrier and/or the sound carrier frequencies to the required frequency spacing. Because at most a change of only 2 MHz is required, the transmitters and antennas can be made to be broad enough in frequency response to handle the frequency change without retuning. Only the low power exciter frequencies, therefore, need to be switched.

Relative Power Levels of Picture and Aural Waves

The major difference from the VHF FM transmission in using UHF TV receivers for voice-only reception is the requirement for 2 carriers. The effect on satellite designs is to require four times the power that would be necessary for a single channel receiver, such as the VHF receivers previously described. The factor of four increase is due to a factor of two increase for the second carrier and another factor of two to overcome the noise contribution from the picture carrier. The details of these factors are described in the following summary of the UHF receiver analysis.

The following presents an analysis of this problem in which the input to the nonlinear detector is assumed to consist of white noise, in addition to the picture and sound carriers, over a 6 MHz bandwidth. A refinement of this analysis is presented, later in this section, to evaluate the effect of a more limited bandwidth.

The IF input to the diode detector is assumed to have the spectrum as follows.

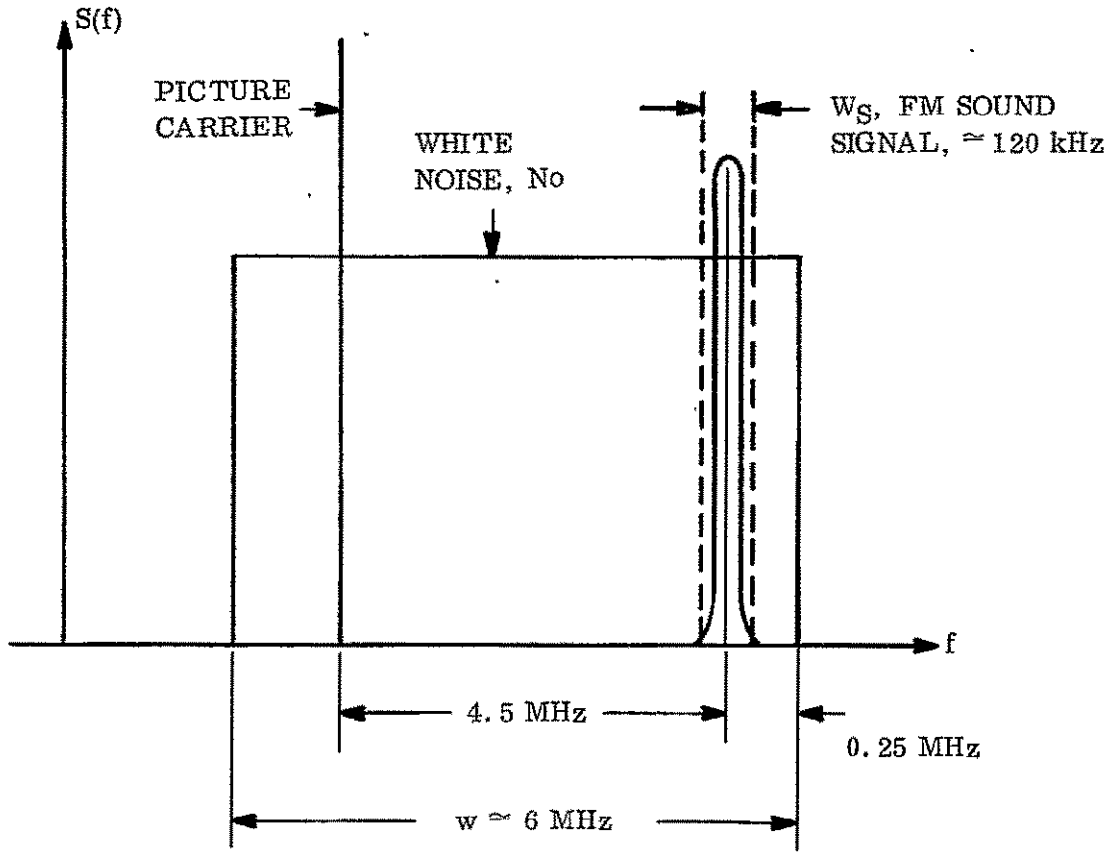

The picture carrier is represented as B cos $\omega_c t$.

The sound signal is represented as A cos $\left[\omega_s t + \theta(t)\right]$

where $f_s - f_c = 4.5$ MHz, and $\frac{d}{dt}\theta(t)$ is the audio signal.

The white noise is given by the well-known representation $n(t) = \sum_{n=n_o}^{n_f} a_n \cos(\omega_n t + \theta_n)$;

$\omega_{n+1} - \omega_n = \Delta W$; $\omega_{nf} - \omega_{n_o} \cong 2\pi \times 6 \times 10^6$

Where the a independent Gaussian distributed variables and θ_n are independent and uniformly distributed. The noise power is given by

$$\overline{n^2(t)} = \Sigma a_n^2/2 = N_o W$$

where N_o is the noise spectral density.

The signal input to the detector is then

$$e_i(t) = B \cos \omega_c t + A \cos \left\{\omega_s t + \theta(t)\right\} + \Sigma a_n \cos(\omega_n t + \theta_n)$$

The question as to what representation to use for the detector is somewhat debatable. However, nonlinear devices in general have similar behavior and tend to give close results insofar as the output SNR is concerned. Therefore, in the interests of tractability, a square-law device is assumed. The output is therefore,

$$e_o(t) = \left\{ B \cos \omega_c t + A \cos \left\{ \omega_s t + \theta(t) \right\} + \Sigma a_n \cos (\omega_n t + \theta_n) \right\}^2$$

$$= B^2 \cos^2 \omega_c t + A^2 \cos^2 \left\{ \omega_s t + \theta(t) \right\} + \left\{ \Sigma a_n \cos (\omega_n t + \theta_n) \right\}^2$$

$$+ 2AB \cos \omega_c t \cos \left\{ \omega_s t + \theta(t) \right\} + 2B \cos \omega_c t \cdot \Sigma a_n \cos (\omega_n t + \theta_n)$$

$$+ 2A \cos \left\{ \omega_s t + \theta(t) \right\} \cdot \Sigma a_n \cos (\omega_n t + \theta_n).$$

$$= \left\{ \Sigma a_n \cos (\omega_n t + \theta_n) \right\}^2$$

$$+ AB \cos \left\{ (\omega_s - \omega_c) t + \theta(t) \right\}$$

$$+ B \Sigma a_n \cos \left\{ (\omega_n - \omega_c) t + \theta_n \right\}$$

$$+ A \Sigma a_n \cos \left\{ (\omega_n - \omega_s) t - \theta(t) + \theta_n \right\}$$

The terms which disappeared in the above expression are either at d. c. or in the vicinity of twice the carrier (video or sound) frequency and are assumed filtered out. The remaining terms have the following meaning: (1) The term $AB \cos \left\{ (\omega_s - \omega_c) t + \theta(t) \right\}$ is clearly the desired FM sound signal centered on 4. 5 MHz and results from the "beating" of the sine-wave picture carrier and the FM sound carrier, (2) the term $B \Sigma a_n \cos \left\{ (\omega_n - \omega_c) t + \theta_n \right\}$ results from the beating of the picture carrier and the noise.

Its single-sided power spectrum is as follows in the illustration:

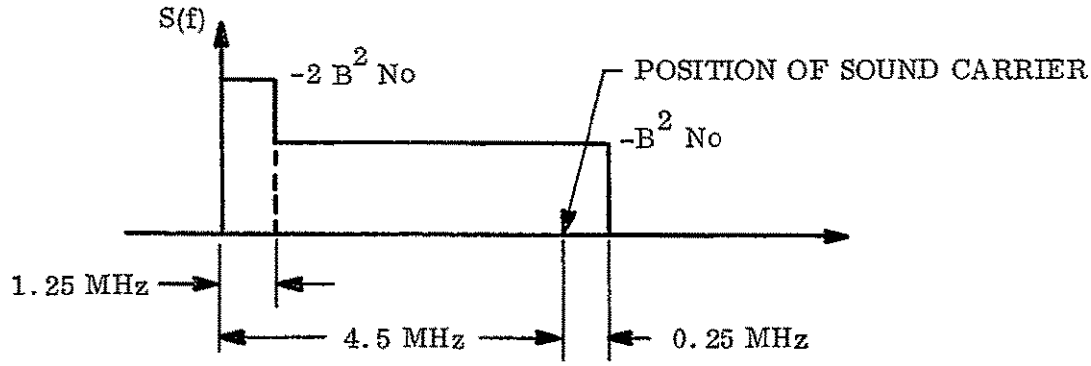

(3) The term $A \Sigma a_n \cos \left\{ (\omega_n - \omega_s) t - \theta(t) + \theta_n \right\}$ results from the beating of the FM sound carrier and the noise. It is very difficult to analyze for arbitrary $\theta(t)$. However, in the analysis of this term a very good approximation results if $\theta(t) = 0$, i. e., if the sound carrier is assumed unmodulated.

This assumption is justified by the fact that the FM modulation is narrowband and will spread the spectrum very little compared to the wideband noise present. Under this assumption the power spectrum of this noise term is then as shown below:

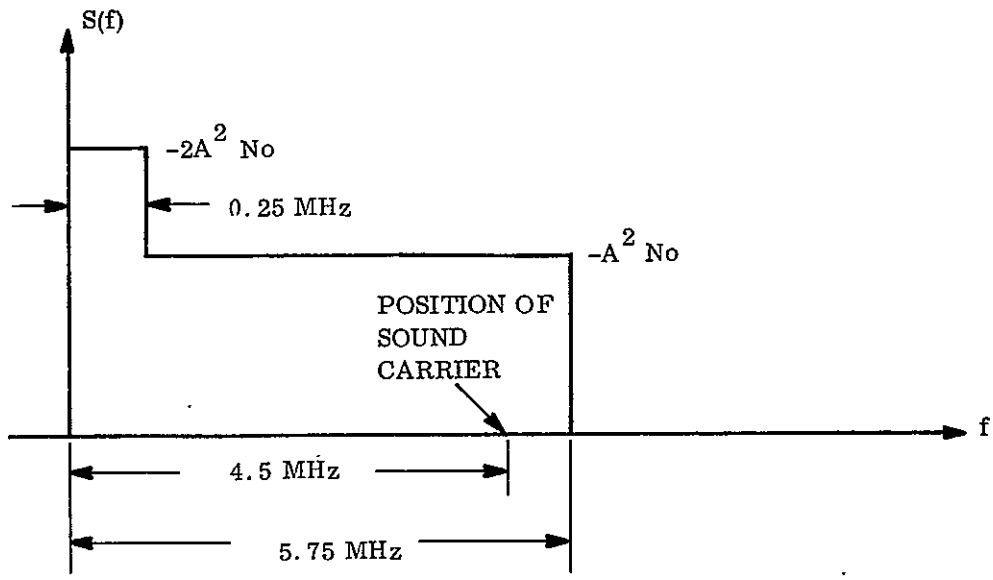

(4) The term $\left\{\Sigma a_n \cos(\omega_n t + \omega_n)\right\}^2$ represents the noise beating with itself.

The low-pass power spectrum (excluding the d. c. term) arises from the convolution of the original noise spectrum with itself and looks as in the following illustration:

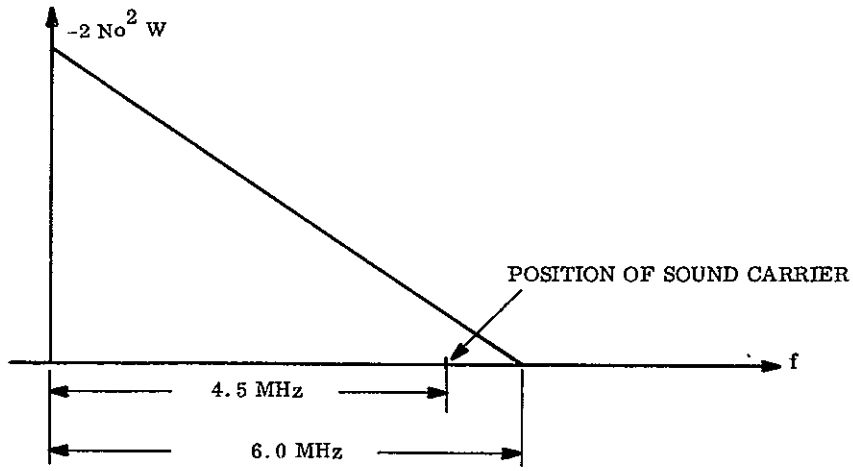

Now, the second signal to noise ratio at the detector input is

$$\left(\frac{S}{N}\right)_{in} = \frac{A^2}{2N_o W_s} \; ; \quad W_s \cong \text{FM sound signal bandwidth}$$

At the detector output, the corresponding SNR, is, from the three preceding sketches,

$$\left(\frac{S}{N}\right)_o = \frac{(AB)^2/2}{(B^2N_o + A^2N_o + N_o^2W/2)\,W_s} \; ;$$

this is of course, the "carrier-to-noise" ratio at the input to the discriminator and must exceed the FM threshold for good operation.

To see the effect of the (square-law) detector, write the last equation as

$$\left(\frac{S}{N}\right)_o = \frac{A^2}{2N_o W_s} \cdot \frac{B^2}{(B^2 + A^2 + N_o W/2)}$$

$$\left(\frac{S}{N}\right)_o = \left(\frac{A^2}{2 N_o W_s}\right) \frac{(B/A)^2}{\left(1 + \left[\frac{B}{A}\right]^2 + \frac{N_o W}{2A^2}\right)}$$

This last equation simplifies to:

$$\left(\frac{S}{N}\right)_o = \left(\frac{S}{N}\right)_{in} \left[\frac{(B/A)^2}{1 + (B/A)^2 + \frac{1}{4\left(\frac{S}{N}\right)_{IF}}}\right]$$

where $\left(\frac{S}{N}\right)_{IF} = \frac{W_s}{W}\left(\frac{S}{N}\right)_{in}$. Thus the S/N is reduced by both the presence of the picture carrier and a degradation in the video detector.

A refinement of this approach, allowing for the effects of the IF passband, was completed to determine the validity of using the above result. This analysis, described below, shows the above result (which was used for system calculations) to be conservative by approximately 0.3 db.

TV Sound Reception

Let the signal at the RF input be

$$e_i(t) = A \cos \left[w_s t + \theta(t) \right] + B \cos w_c t + n(t)$$

where the first term is the FM sound carrier; the second term is the picture carrier; n(t) is the noise referred to RF input with spectral density N_0 watts/Hz (single-sided) so that noise power in bandwidth B is $N_0 B$; further, the input bandwidth at this point is assumed flat.

After amplification signal and noise are passed through an IF filter with the following assumed voltage transfer characteristic, H (jw):

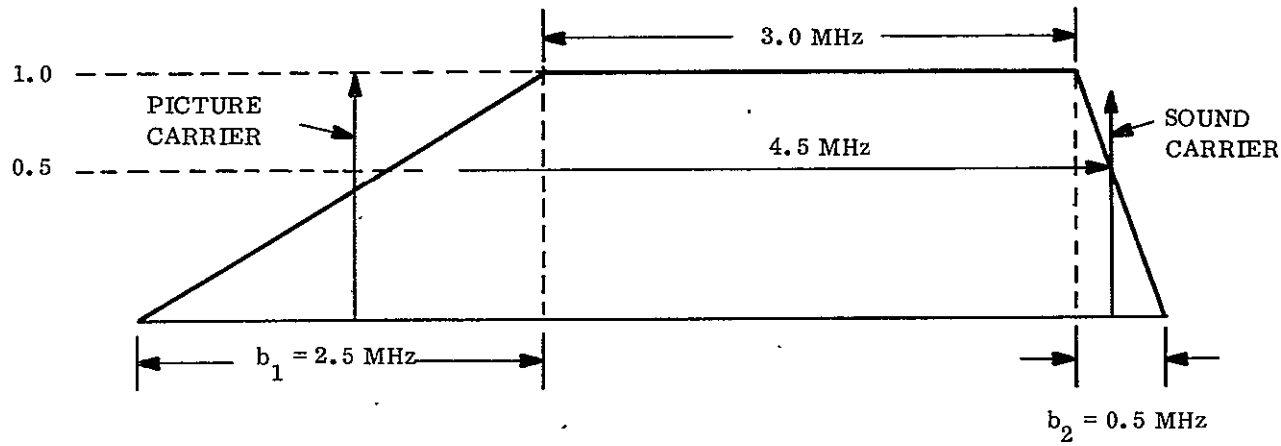

Figure 2.6-16. Voltage Transfer Characteristic

The output of this filter is the input, $e_s(t)$, to the square-law detector:

$$e_s(t) = \frac{A}{2} \cos \left[w_s t + \theta(t) \right] + \frac{B}{2} \cos w_c t + n'(t)$$

Note that the form of the first term has assumed the FM modulation to be narrowband with respect to the transfer characteristic for its has implicitly assumed a sine-wave. The noise, N'(t), is now such that its power spectrum at the detector input, $N_0 \left| H(jw) \right|^2$ is as follows:

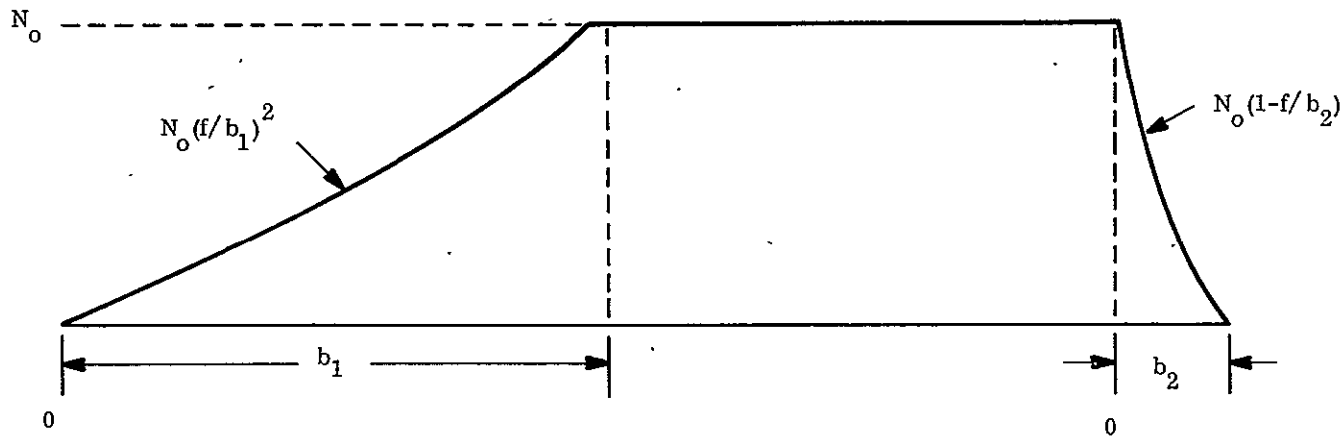

(NOTE THAT THE TWO PARABOLIC EQUATIONS HAVE DIFFERENT ORIGINS).

Figure 2.6-17. Power Spectrum at the Detector Input

The detector output is

$$e_{s,o}(t) = e_s^2(t).$$

$$= \frac{A^2}{4}\cos^2\left[w_s t + \theta(t)\right] + \frac{B^2}{4}\cos^2 w_c t + n'^2(t)$$

$$+ \frac{AB}{2}\cos w_c t \cos\left[w_s t + (t)\right] + B\cos w_c t \cdot n'(t)$$

$$+ A\cos\left[w_s t + \theta(t)\right] \cdot n'(t)$$

The low-pass signal output is

$$e_{sig}(t) = \frac{AB}{4}\cos\left[(w_s - w_c)\,t + \theta(t)\right]$$

The low-pass signal x noise terms are

(1) $\frac{B}{2}\Sigma a_n H(jw_n)\cos\left[(w_n - w_c)\,t + \theta n\right]$ (picture carrier x noise)

and

(2) $\frac{A}{2}\Sigma a_n H(jw_n)\cos\left[(w_n - w_s)\,t + \theta_n - \theta(t)\right]$ (sound carrier x noise)

The output power spectrum due to term (1) is

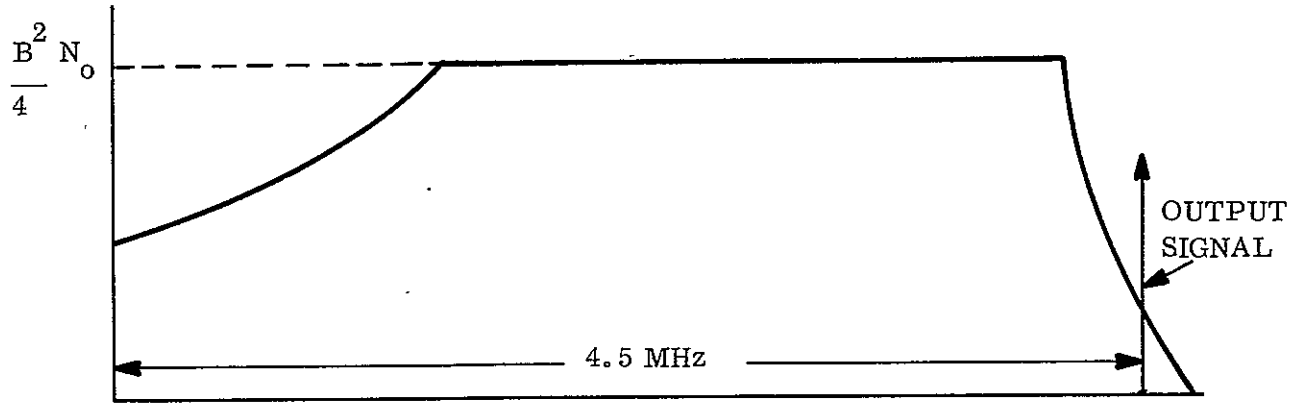

Figure 2.6-18. Output Power Spectrum Due to Term (1)

The output power spectrum due to term (2) is (assuming narrowband $\theta(t)$)

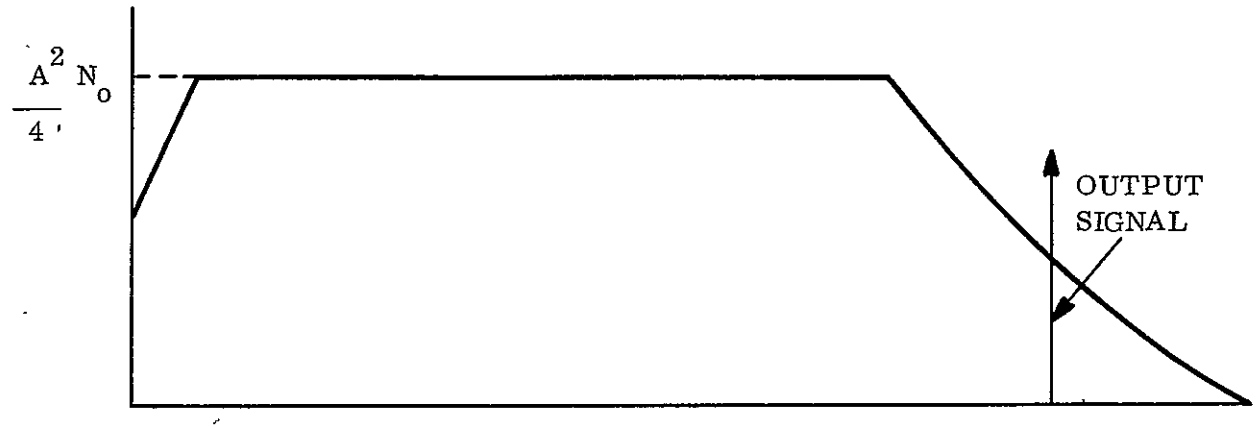

Figure 2.6-19. Output Power Spectrum Due to Term (2)

The signal x noise term has a power spectrum (excluding d.c.)

$$S_{nxn}(f) = 2\int_{-\infty}^{\infty} S_n(\Omega)\, S_n(f-\Omega)\, d\Omega;$$

$S_n(f)$ is the (double-sided) noise power spectrum at the detector input. (See, e.g., Davenport and Ruet, "An Introduction to the Theory of Random Signals and Noise," McGraw-Hill, 1958, P. 255). In our case, $S_n(f)$ is shown in Figure 2.6-17 for positive frequencies with $N_o \rightarrow N_o/2$. The convolution is quite tedious and so has been done only for the low-pass output between 3.5 and 5.5 MHz (which includes the region of interest).

The result is (for single-sided spectrum)

$$S'_{nxn}(f) = \frac{2N_o^2 \times 10^6 (2-\Delta)^3}{3b_1^2} + \frac{2N_o^2 \times 10^6}{b_1^2 b_2^2}\left\{\frac{b_2^5}{30} + \frac{(2-\Delta)^2 b_2^3}{3} + \frac{(2-\Delta) b_2^4}{6}\right\}$$

where b_1 and b_2 are measured in MHz and Δ is measured in MHz from 3.5 MHz; i.e., at 3.5 MHz, $\Delta = o$; $o \le \Delta \le 2$.

The output noise due to this term is bandwidth W centered on f_o is

$$N_{out} = S'_{nxn}(f_o)\, W,$$

assuming W relatively small.

For W about 0.1 MHz, this last assumption is good; we are interest in $f_o = 4.5$ MHz, or $\Delta = 1.0$. Hence,

$$S'_{nxn}(f)\Big|_{4.5\ MHz} = \frac{2N_o^2 \times 10^6}{3b_1^2} + \frac{2N_o^2 \times 10^6}{b_1^2 b_2^2}\left\{\frac{b_2^5}{30} + \frac{b_2^3}{3} + \frac{b_2^4}{6}\right\}$$

The noise output due to Figures 2.6-18 and -19 is the integral of these curves from (4.5-w/2) MHz to (4.5 + w/2) MHz.
From Figure 2.6-18

$$N_{out(1)} = \frac{B^2}{4}\frac{N_o}{b_2^2}\int_{\frac{b_2}{2}-\frac{W}{2}}^{\frac{b_2}{2}+\frac{W}{2}} f^2\, df$$

$$= \frac{B^2}{12}\frac{N_o}{b_2^2}\left(\frac{W^3}{4} + \frac{3 b_2^2 W}{4}\right)$$

and from Figure 2.6-19

$$N_{out(2)} = \frac{A^2}{4} \frac{N_o}{b_1^2} \int_{\frac{b_1}{2} - \frac{W}{2}}^{\frac{b_1}{2} + \frac{W}{2}} f^2 \, df$$

$$= \frac{A^2}{12} \frac{N_o}{b_1^2} \left(\frac{W^3}{4} + \frac{3 b_1^2 W}{4} \right)$$

Now, the total noise power out is

$$N_{out} = N_{out(1)} + N_{out(2)} + S'_{nxn} (4.5) \cdot W$$

The signal power out is

$$S_o = 1/2 \, (AB/4)^2 = (AB)^2/32$$

Assuming A = B and combining the previous expressions,

$$(C/N)disc. \frac{(A^2/2) \cdot 1/16}{N_o W \times 10^6 \left\{ 1/48 \left[(W/b_1)^2 + (W/b_2)^2 \right] + 1/8 + \frac{2N_o \times 10^6}{A^2 b_1^2} \left[\frac{1}{3} + \frac{b_2}{3} + \frac{b_2^2}{6} + \frac{b_2^3}{30} \right] \right\}}$$

Putting in $b_1 = 2.5$, $b_2 = 0.5$, W - 0.12, and taking into account input (RF) resistance R,

$$(C/N)disc. = \frac{(A^2/2R) \cdot 1/16}{(0.12) (10^6) N_o \left\{ 1/8 + \frac{N_o R \times 10^6}{(5.72) A^2} \right\}}$$

Putting this equation into the form equivalent to the expression for C/N determined by the rough analysis (6 MHz IF flat noise) yields:

$$(C/N)_{disc.} = \frac{S}{N} = \left(\frac{S}{N} \right)_{IN} \cdot \frac{1}{2 + \frac{1}{5.72 \left(\frac{S}{N} \right)_{IF}}}$$

The previously calculated expression was (assuming B = A):

$$\left(\frac{C}{N}\right) = \frac{S}{N} = \left(\frac{S}{N}\right)_{IN} \left[\frac{1}{2 + \frac{1}{4\left(\frac{S}{N}\right)_{IF}}}\right]$$

With an input S/N on the order of -4 db, the initial C/N expression differs from the refined version by only 0.3 db. Thus, the initial expression was used for system calculations.

The following simplified equation,

$$\left(\frac{S}{N}\right)_o = \left(\frac{S}{N}\right)_{in} \frac{\rho}{1+\rho} \; ; \; \rho \cong (B/A)^2$$

allows one to determine the tradeoff between S/N and power and thus to choose an "optimum" operating point. This point can be determined by examining the expression. $\rho/(1+\rho)$ which is tabulated below:

$\frac{\rho}{1+\rho}$	ρ	$\Delta\rho$
0.0099 (-20.04db)	0.01	
0.091 (-10.4db)	0.1	0.09
1/3 (-5db)	0.5	0.4
1/2 (-3db)	1.0	0.5
3/5 (-2.2db)	1.5	0.5
2/3 (-1.8db)	2.0	0.5
0.91 (-0.4db)	10.0	8.0

The tradeoff in power (ρ) against S/N ($\rho/(1+\rho)$) is fairly clear from the table. It can be seen that at very low values of ρ, the improvement in S/N is most efficient per unit increment in ρ while for very large values of ρ, the S/N increase per increase in ρ rises very slowly. On the other hand, even though the tradeoff efficiency is best at low values of ρ, the S/N loss is so severe there that the signal would become unusable. The "optimum" point, therefore, appears to lie approximately at $\rho = 1$, i.e., equal picture and sound carrier powers.

The above conclusion is corroborated by a somewhat different approach. The total (picture and sound) power delivered to the detector is

$$P_{in} = 1/2\,(A^2 + B^2) = 1/2\,A^2\,(1+\rho)$$

Suppose we normalize the input noise to unity, i.e., $N_o W_s = 1$, and that we require $(S/N)_o$ to be kept constant, say also at unity. We then have

$$\frac{S}{N}_{o} = 1 = (A^2/2) \cdot \frac{\rho}{1+\rho}$$

For different values of ρ, keeping $(S/N)_o = 1$, we then have the following table (Table 2.6-13).

Table 2.6-13. Different Valves of ρ

ρ	$\frac{\rho}{1+\rho}$	A^2	$P_{in}=A^2(1+\rho)$
0	0	∞	∞
0.1	0.091	11	12.1
0.5	1/3	3	4.5
1.0	1/2	2	4.0
1.5	3/5	5/3	4.16
2.0	2/3	3/2	4.5
10	10/11	11/10	12.1

Therefore, when the criterion is to keep the output S/N constant, the total input power is minimized for equal picture and sound carriers.

As to the preferred tuning condition, there is none based on S/N, but from a gain standpoint, it is preferable to tune so as to make either the aural or the visual frequency lie reasonably close to the frequency of maximum gain for the receiver. The reason for this is that the second detector is linear only for signals greater than about 0.2 volt rms; otherwise, the detector becomes square law with a corresponding decrease in the desired 4.5 MHz signal amplitude.

Further Analysis Required

The previous analyses of necessity had to depend upon many assumptions on the characteristics of UHF TV receivers. While these were reasonable assumptions for the purpose of a conceptual study, more precise values would be required to implement a hardware design of a UHF voice satellite. The values needed (such as noise figure, threshold, and bandwidths at several places in the receiver) are not available. It is recommended that an extensive receiver test program be initiated to determine the current nominal value and range of values for thse parameters and that an analysis be conducted to determine the changes in these values that could be expected for the receiver technology in the time period of interest.

Input Signal Levels Required at Receiver Terminals for Capture to Take Place

The noise to the receiver comes from the antenna resistance and is transmitted to the receiver by the interconnecting transmission line. Typical receivers have a 300-ohm input impedance; thus, assuming the transmission line surge impedance and the antenna radiation resistance to be 300 ohms also, as in the matched condition, at 25°C the thermal noise voltage generated in the antenna resistance is

$$e_1 = 1.28\,(RF)^{1/2}\,10^{-10} \text{ volts rms} \qquad (1)$$

where R = noise resistance in ohms
F = noise bandwidth in Hz.

Thus, because R = 300 and F = 240,000

$$e_1 = 1.28\,(300 \times 240,000)^{1/2}\,10^{-10} = 1.09 \times 10^{-6} \text{ volts} \quad (2)$$

Most of the television receivers equipped for UHF reception have been built in the past 2-1/2 years because of the FCC action stipulating that provision be made for UHF reception. These more modern receivers use fairly efficient diode converters so that noise figures of 12 to 14 db are obtained. (Older receivers had noise figures in the range from 14 to 17 db). Some of the 'hotter" crystal diodes provide noise figures ranging down to 10 db. For the purposes of the present analysis, a conservative noise figure of 14 db will be used.

When the effect of this noise figure is applied to the antenna noise of Equation (2), the apparent noise voltage at the antenna source is thus:

$$e_{n1} = 5 \times 1.09 \times 10^{-6} = 5.45 \times 10^{-6} \text{ volts} \quad (3)$$

Because the input system is matched, half of this voltage would appear across the receiver terminals, or

$$e_{n2} = \frac{5.45 \times 10^{-6}}{2} = 2.72 \times 10^{-6} \text{ volts} \quad (4)$$

The amplitude of the aural and picture carrier waves at the receiver terminals should be twice this figure for good capture, or

$$e_{S2} = 2.72 \times 10^{-6} \times 2 = 5.45 \times 10^{-6} \text{ volts} \quad (5)$$

Verification of Input Levels Required at Receiver Terminals for Capture to Take Place

A General Electric television receiver employing a monochrome chassis, (type DB, which is used in more receivers built by GE than any other single chassis), was measured for FM capture. This chassis is representative of many chassis employed by most manufacturers for the backbone of their lines. Such a chassis employs only a 2-stage IF amplifier instead of a 3-stage IF as found in color and in deluxe monochrome receivers so that the resultant figures could be construed to be on the conservative side.

The receiver performance was measured at Channel 4 on the VHF band where the noise figure is approximately 4 db. The video sensitivity on Channel 4 was found to be 12 microvolts. Due to the availability of equipment, measurements were made at VHF and extrapolated to UHF.

Measurements on the receiver for sound only yielded results shown in Table 2.6-14.

Table 2.6-14. Sound-Receiver Measurements

S/N Ratio Qualitative	Input Signal Microvolts (VHF; NF = 4 db)
Sound just detectable in noise	0.8
Usuable sound but somewhat noisy	1.0
Solid capture with little noise	1.25

It is seen that good sound performance was obtained at only 10% of the input for video sensitivity.

Table 2.6-14 may be converted to UHF by adding 10 db to the signal levels with the resulting Table 2.6-15.

Table 2.6-15. UHF Sound Receiver Measurements

S/N Ratio Qualitative	Input Signal Microvolts (UHF; NF - 14 db)
Sound just detectable in noise	2.52
Usable sound but somewhat noisy	3.16
Solid capture with little noise	3.95

The 3.95 microvolt figure of Table 2.6-15 is in quite close agreement with the calculated figure for solid capture of 5.45 microvolts found by the theoretical analysis in Equation (4).

It should be noted that the particular receiver tested appeared to be somewhat "hotter" than the average receiver, so the 5.45 microvolt figure might very well represent average performance. This figure was used in defining the UHF TV receiver sensitivity for the UHF satellite system.

2.6.3.3 UHF Signal Level Requirements

To determine how many of the above receivers can be reached, as a function of the signal strength provided, the analysis considered the receiver sensitivity, antenna-type distribution and receiver distribution (by noise environment).

The results of this analysis are shown in Figure 2.6-20. The signal level at which 50% of the receivers are reachable occurs at about 100 μv/m. The curve shows the strong effect of building loss on the potential audience as practically no receivers with indoor antennas are reached below a signal level of 150 μv/m.

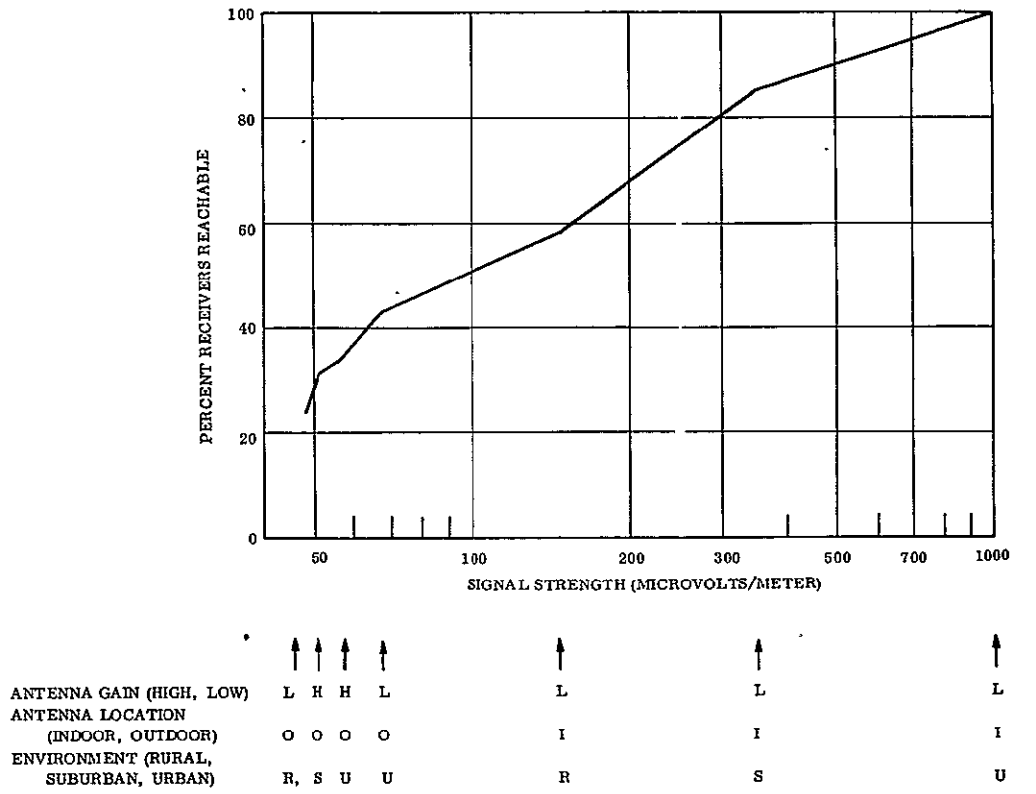

Figure 2.6-20. UHF Potential Audience vs Signal Strength

The assumptions used in the UHF signal strength calculations are as follows:

Required sound IF C/N = 6 db
IF bandwidth = 120 kHz
Audio bandwidth = 15 kHz
Peak Frequency Deviation = 25 kHz
% Modulation = 100%
De-emphasis 9 db
Receiver Input impedance = 300 ohms
Receiver Noise Figure = 10 db
Note that these assumptions will produce a minimum output S/N = 31.6 db.

Modulation: FM
Frequency: 890 MHz

Noise (^{o}k)

	Man-Made	Galactic
Urban	2780.0	300
Suburban	51.5	300
Rural	1.3	300

Sources: Same as for VHF calculation

Antennas:

	Max. Gain	Effective Gain	Line Loss
Low Gain	2.2 db	-0.8 db (3 db polarization loss)	3 db
High Gain	8 db	2 db (3 db polarization loss; 3 db pointing loss)	3 db

Building Loss:

Urban	Suburban	Rural
28 db	22 db	16 db

The calculations at UHF are the same as in the VHF case except that the effective noise bandwidth is 240 kHz.

REFERENCES (Section 2.6)

(1) Survey of Radio Industry in Pakistan, Report K-192-P, Prepared by Investment Advistory Centre of Pakistan Karachi-Dacca-Lahore, August 1965.

(2) FM receiver estimates from Radio Advertising Bureau.

(3) Broadcasting Stations of the World, 1953, 1960, 1963, 1965 Foreign Broadcast Information Service, Washington 25, D.C.

(4) United States State Department Foreign Service Dispatch 255, October 20, 1959.

(5) World Wide Distribution of Radio Receiver Sets
United States Information Agency
Research and Reference Service Reports:

1) R-18-62 (C) February 21, 1962
2) R-40-63 (C) March 14, 1963
3) R-99-64 July 1964
4) R-52-65 May 1965

(6) The United States of America data comes from Radio Advertising Bureau.

(7) The productions statistics were compiled by B.F. Osbahr, editor "Electonic Industries" and appeared in the 1966 Yearbook Issue of Broadcasting. The number of radio receivers in use before 1946 was obtained from TV Digest. The more recent statistics are from the Statistical Office of the United Nations: Statistical Yearbook.

(8) 1966 World Radio TV Handbook, Published by World Radio-Television Handbook Company Ltd. Hellerup, Denmark.

(9) Broadcasting Stations of the World, Part III, Frequency Modulation Broadcasting Stations, March 1, 1965, Foreign Broadcast Information Service, Washington 25, D.C.

(10) The Europa Yearbook, Vols. I and II, 1965 Europa Publications Limited.

(11) The Encyclopedia Britannica Geographic Summaries.

(12) The Demographic Yearbook, 1963, United Nations Department of Economic and Social Affairs.

(13) U.S. Army Area Handbook for India, Department of The Army Pamphlet No. 550-21 excerpt adapted from India, Census Commission 1961 Census of India Paper No. 1 of 1962.

(14) U.S. Army Handbook for Germany, Department of the Army Pamphlet No. 550-29, excerpts from Statistical Yearbook for Federal Republic of Germany, 1958, and Statistical Yearbook of the German Democratic Republic, 1957.

(15) The U.S. Book of Facts, Statistics, and Information, 1966, Bureau of the Census, U.S. Department of Commerce.

SECTION 3

SYSTEMS ANALYSIS

3.1 INTRODUCTION

This section describes the system analysis performed in specifying system and subsystem requirements listed in Section 1.2

The steps employed in this analysis were:

a. Select the frequency channel

b. Establish the specific orbit altitude for each configuration from tradeoffs of coverage, broadcast duty cycle, and minimum effective radiation power (ERP).

c. Determine the field of view necessary to illuminate the desired coverage area during the broadcast time. Establish antenna pointing error and boresight goals so that antenna beamwidth can be calculated.

d. Determine radiated power and the antenna beamwidth to arrive at the most cost effective approach. This ERP division substantially synthesized the configuration by determining attitude control pointing accuracy and the size of the solar array and broadcast antenna.

e. Calculate the ERP required for each specific orbit and meet the goals set for ground signal strength (μv/m). Calculate the downlink power budgets.

These nominal system design steps were the starting point for the synthesis of the conceptual configuration designs described in Sections 4 and 5. A summary of these nominal design goals are given in Table 3.1-1.

3.2 FREQUENCY SELECTION

The uplink frequency channel. (The possibilities and the selection recommendation are discussed in the Section 4.4).

The downlink frequency within a band had to be chosen, as well as the band of operation. The bands of operation considered were the UHF/TV band (470 to 890 MHz), the VHF/FM band (88 to 108 MHz), and HF/AM short wave band (approximately 2 to 30 MHz).

The receivers operating at the lowest frequencies (HF bands) are all limited by man-made noise, even in the relatively quiet rural areas. However, at the highest frequencies (UHF band) the effects of man-made noise are of little concern, and the limiting factors are in the receiver design.

Table 3-1.1. Nominal System Design Goals

Satellite Design Parameters	Configurations			
	HF	VHF No. 1	VHF No. 2	UHF
Frequency for Power Budget Calculations	15 MHz	100 MHz	100 MHz	870 MHz
Orbit (circular equatorial) Altitude Period	 4356 nm 4.8 hours	 1932 nm 24 hours	 7556 nm 8 hours	 19323nm 24 hours
Field of View, Coverage and Pointing Errors Field of View (FOV) Required for Coverage Pointing Error for each Axis Antenna Beamwidth	 18.5° ±0.2° 20°	 7° ±0.1° 7-1/2°	 10.8° ±1° yaw & roll, ±2° pitch 18-1/2°	 3.4° ±0.1° 3-3/4°
*Ground Field Strength Design Goal	150 μv/m	180 μv/m	50 μv/m	106 μv/m
Satellite ERP at Antenna Beam Edge	50.1 dbw	62.1 dbw	44.4 dbw	57.5 dbw
Antenna Gain at beam center Loss to edge of beam	 14.4 db 2 db	 26.9 db 3 db	 19.0 db 3 db	 33.0 db 3 db
Propagation Fade Margin	None	0.3 db	0.7 db	0.1 db
Second Carrier Power	None	None	None	3 db
Total Satellite ERP Power	52.1 dbw	65.4 dbw	48.1 dbw	63.6 dbw
Satellite RF Power Required (ERP-Antenna Gain)	 37.7 db 5.91 kw	 38.5 dbw 7.07 kw	 29.1 dbw 0.82 kw	 30.6 dbw 1.15 kw

*Performance exceeded design goals (see Section 6.4.1)

Propagation losses are also less severe at the higher frequencies. Fade margins in the UHF band are measured in terms of tenths of a db, but may become as high as 20 db in the HF band. However, the mission selected for HF (broadcast to the emerging nations between 40°S and 40°N latitude) resulted in a small enough azimuth angle at the time of broadcast so that no propagation fading would occur.

From the standpoint of vehicle configuration, both high and low bands present design problems. For a UHF sound broadcast to be detected by a TV receiver, it is necessary to transmit an unmodulated picture carrier as well as the frequency modulated sound carrier. The HF designs are made difficult by the large size of broadcast antennas due to the long wavelengths.

3.2.1 HF CHANNEL SELECTION

The reasons for selection of the top four HF channels (15.1, 17.7, 21.45 and 28.85 MHz) were described in Sections 2.3 and 2.6.1.

3.2.2 VHF CHANNEL SELECTION

Channel selection for VHF broadcasting was primarily concerned with interference rather than slight technical differences. An investigation of channel occupancy has shown that only five channels have as few as 15 transmitters assigned. These are:

Frequency	No. of Transmitters
100.9 mc	12
105.3 mc	15
105.9 mc	13
106.7 mc	14
107.5 mc	8

At these frequencies there is a better opportunity to negotiate a frequency change with the few stations on a particular channel (most of these stations are in the US), or of not broadcasting to the areas of the world where these stations exist. (In other words, the satellite might switch channels depending upon the world area being covered at a particular time.) Most European countries do not allocate FM broadcast channels above 100 MHz. This is one reason that no stations are currently assigned to these channels in Europe. Figure 3.2-1 illustrates the geographical distribution of FM broadcasting stations at selected frequencies in the 100 to 108 MHz range. These frequencies represent channels of minimum occupancy.

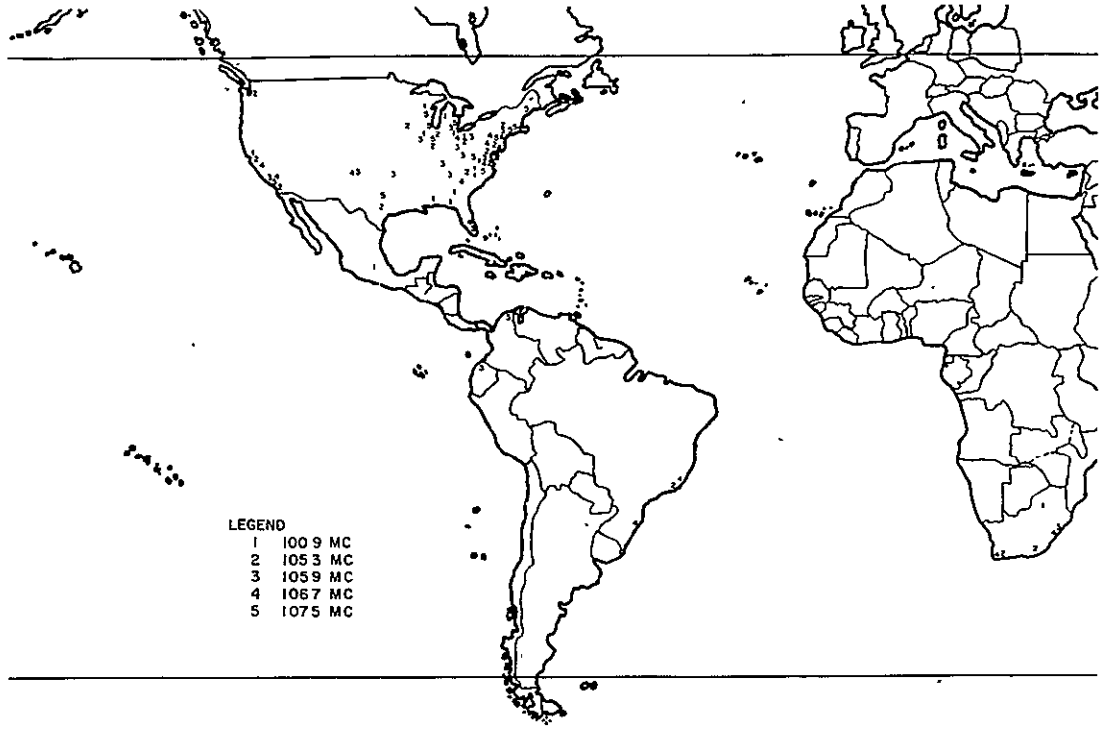

Figure 3.2-1. World Distribution of FM Broadcasting Stations at Selected Frequencies

3.2.3 UHF CHANNEL SELECTION

The selection of specific channels within the UHF band required analysis of two basic factors, technical and interference. As described in Section 2.6.3, the technical evaluation resulted in recommending the top end of the band. The interference evaluation also produced this result for operation in the United States because of the special use of the top 14 channels for translator service. The 14 highest frequency channels have been reserved in the United States by the FCC for very low power use (less than 100 watts). These are called the translator bands and are used for rebroadcasting of prime stations from urban areas to other areas with poor reception, such as those in a valley shadowed by intervening terrain. These channels would appear to be most free of interference and allow satellite operation at the highest possible frequency in the UHF band.

On an international basis, channel selection for interference-free operation would be limited to a small number of channels in the upper portion of the UHF band, as shown in Figure 3.2-2. This illustrates the UHF band occupancy from 600 MHz up (as of 1965) and shows that only three channels have as many as 15 stations worldwide, eight channels are unused, and one is reserved for radio astronomy.

The 870 MHz channel was selected for UHF satellite broadcasting because this channel is not used outside of the United States and is used only as a translator channel in the United States.

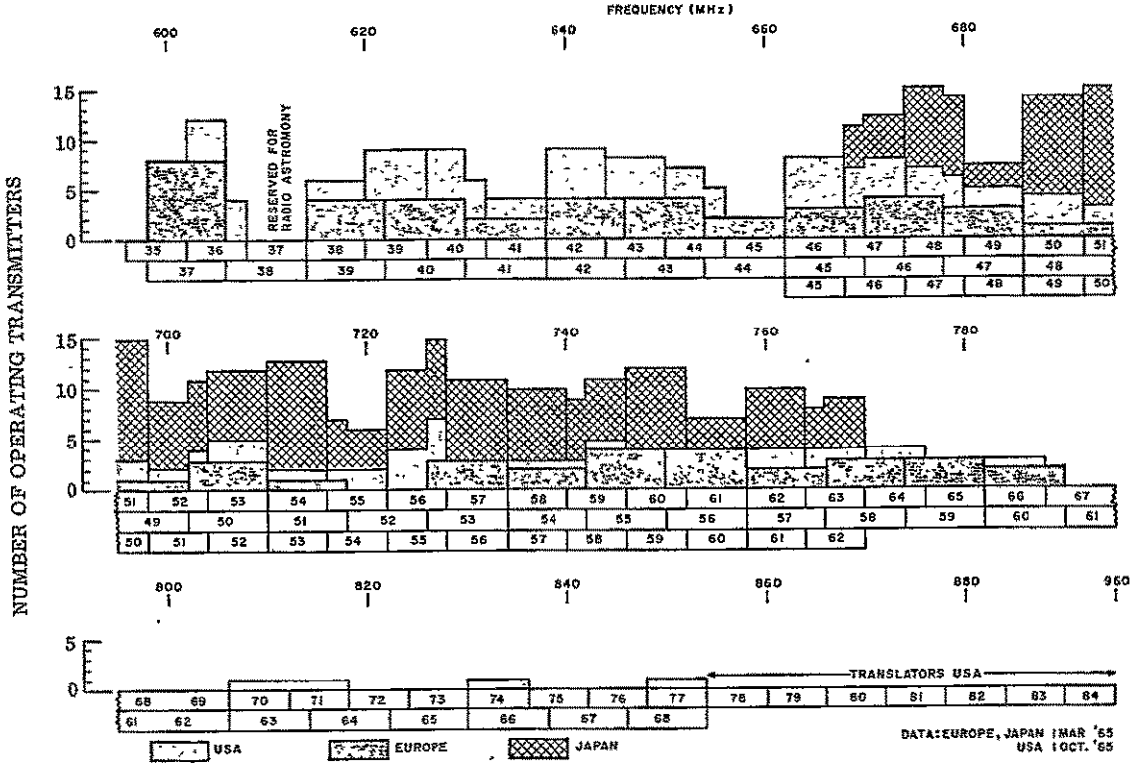

Figure 3.2-2. UHF Band Occupancy

3.3 SELECTION OF ORBITS

The general orbit analysis described in Section 2.2 determined that the optimum orbits were circular, equatorial, and either synchronous or subsynchronous depending on broadcast duty cycle. These orbits permitted broadcasts to the same area on the ground at the same time of day, every day of the year. The details of the selection of orbits for specific configurations are as follows:

3.3.1 ORBIT FOR HF

The HF configuration was selected to cover areas of at least 1.8 million square nautical miles of earth surface (i.e., an area subtended by an earth central angle (ECA) of 24°) anywhere between North and South latitudes of 45°. Only one such area will be covered during one orbital pass. This coverage is to be for a minimum of one hour per area each day. A minimum of three such broadcasts per day will be required.

Figure 3.3-1 shows the results of the analysis to select the optimum orbit for the HF system.

The left graph shows the minimum coverage time per orbit as a function of orbit period for ground areas of 24° earth central angle between 45°N and 45°S latitudes. The one hour lower limit on coverage time per orbit shows that the 4-hour orbit is the lowest one that can be considered.

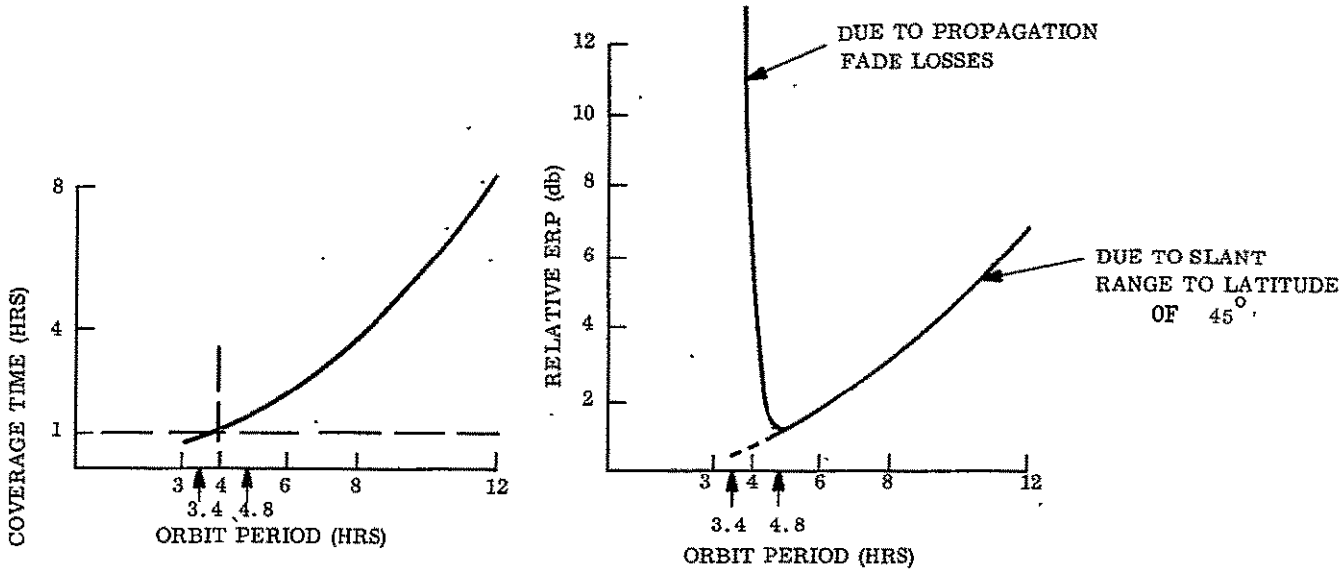

Figure 3.3-1. HF Orbit Altitude Selection

The right graph indicates that the 4-hour orbit, because of fading, causes too great a loss to be a good choice. The minimum ERP occurs with the 4.8-hour orbit. Thus, the 4356 nm altitude orbit was chosen for the HF configuration.

3.3.2 ORBIT FOR VHF NO. 1

For the VHF No. 1 configuration, an almost continuous coverage of the continental U.S. was selected on the basis that this is the single language area in the world with the largest potential audience in this band.

Coverage was for as long a period throughout the day as possible without requiring broadcasting when the satellite is in the earth's shadow. The downtime will be no more than 72 minutes, about midnight for a few months of the year.

The satellite must transmit to three other locations. The maximum time allocated for these tests, including relocation time, will be 3 months. These three areas will be represented by a northern site, a southern site, and an equatorial site. This requirement is consistent with the fact that the potential audience with FM receivers is widely distributed over the world.

The requirement to broadcast continuously to the United States dictates that a geostationary orbit be selected. The initial 3-month demonstration broadcast to other areas can be accomplished by using a walking near-geostationary orbit.

Figure 3.3-2 (left graph) shows the variation of slant range, field of view (FOV) beamwidth of the continental United States as viewed from the satellite, and the elevation angle of the ground antenna as a function of the longitude. Note that the favorable conditions of shortest slant range and highest elevation angle are counteracted by the requirement for the largest antenna beamwidth (i.e., the lowest antenna gain).

Calculating required satellite ERP's for the variables in the left graph leads to the results shown in the right graph. The conclusion of this analysis is that it makes little difference where the satellite is located in longitude between 80°W and 120°W longitude in terms of the ERP requirement.

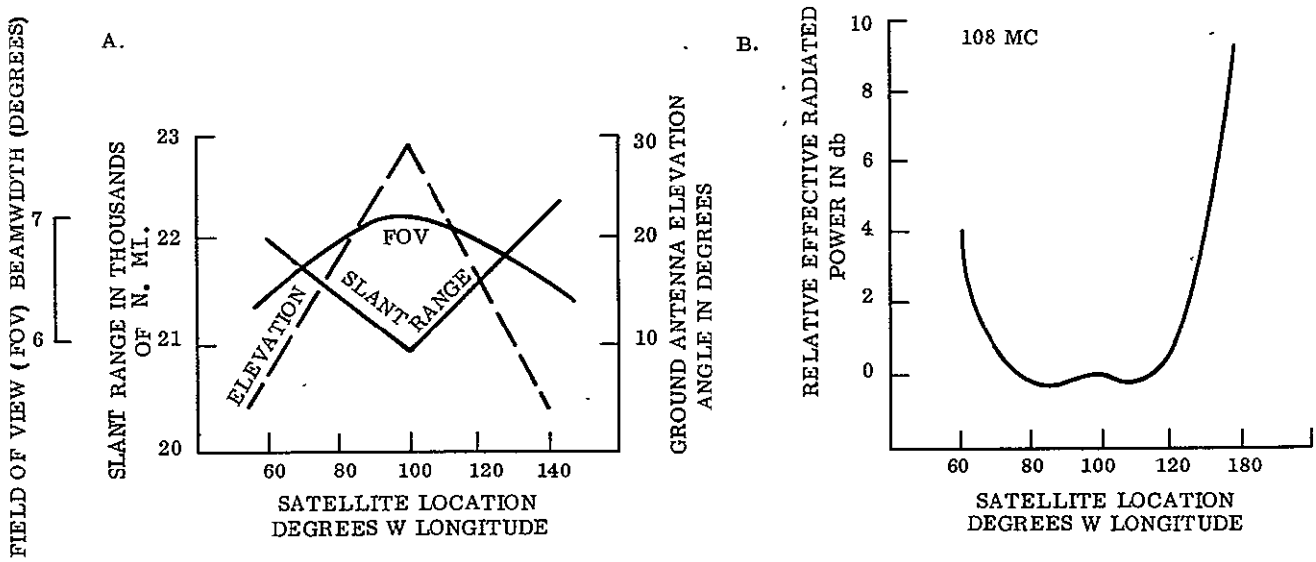

Figure 3.3-2. Satellite Location at Synchronous Orbit for VHF No. 1

3.3.3 ORBIT FOR VHF No. 2

The orbit for the VHF No. 2 configuration was selected for minimum coverage of areas of approximately 1.8 million square nautical miles of earth surface (i.e., an area subtended by an earth central angle (ECA) of 24°) anywhere between North and South latitudes of 60°. Only one such area will be covered at a particular instant of time.

This orbit allows a minimum coverage time of 1 hour per orbit on a daily repeat for a vehicle that does not have to track the sun with solar panels.

Figure 3.3-3 shows the results of the analysis to select the optimum orbit for the VHF No. 2 system.

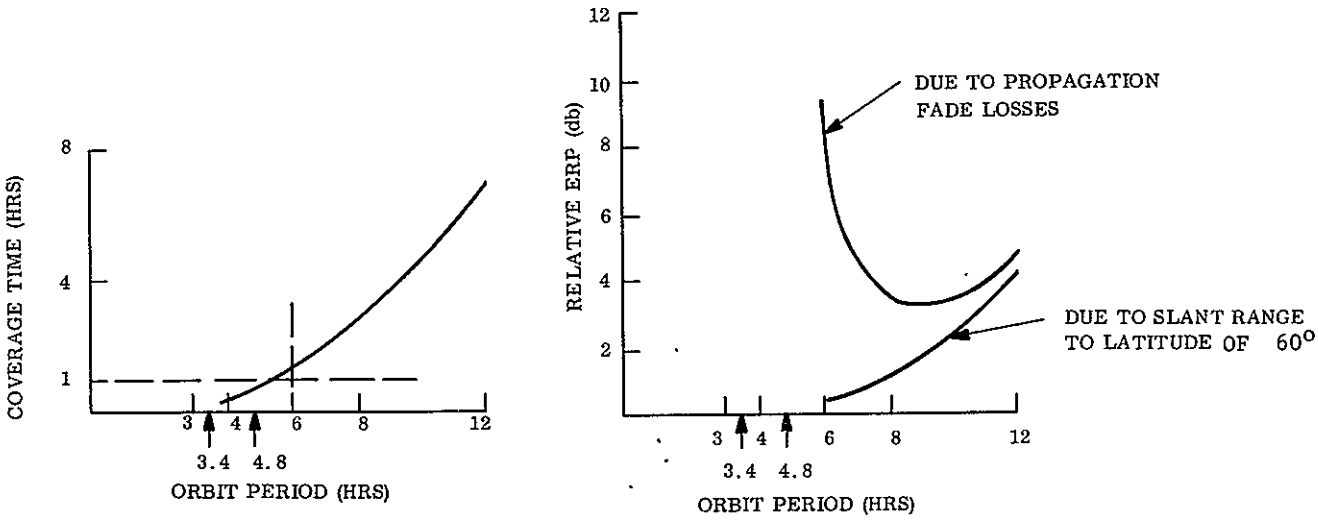

Figure 3.3-3. VHF No. 2 Orbit Altitude Selection

The left graph of Figure 3.3-3 shows the coverage time of the various subsynchronous circular equatorial orbits broadcasting to an area subtended by a 24° earth central angle that is tangent to 60° latitude (i.e., its center is located at 48° latitude). For a coverage time of at least 1 hour per orbit, it may be seen that the orbit must have a 6-hour or longer period.

The right graph shows the relative effective radiated power required of a satellite to produce a given signal strength to the ground area located at 48° latitude for the various orbit periods. The higher the orbit altitude is, the greater the range losses are. However, the elevation angle of the ground receiving antennas, as they view the satellite in these orbits, is increasing for increasing altitudes. This reduces the system fade margin.

The results of this analysis show that the orbit with an 8-hour period offers the lowest possible satellite ERP that will give at least 1-hour coverage time per orbit to the extreme areas of interest. Thus, for the VHF No. 2 configuration the chosen orbital altitude was 7556 nm.

3.3.4 ORBIT FOR UHF

The UHF configuration was selected to provide 5 hours per day coverage of each United States time zone on the basis that this is the area in the world with the largest potential audience in this band. Coverage of one time zone at a time permits utilization of a high

gain antenna possible at these high frequencies, and utilizes the time difference of 4 time zones across the United States.

Coverage must be for as long a period throughout the day as possible without requiring broadcasting when the satellite is in the earth shadow. The downtime will be less than 72 minutes centered about midnight for a few months of the year.

Figure 3.3-4 shows the results of the analysis performed to select the satellite location for the UHF system. The top graph shows the variation of slant range, field of view (FOV) beamwidth of the continental United States as viewed from the satellite, and the elevation angle of the ground antenna as a function of the longitude. Note that the favorable conditions of shortest slant range and highest elevation angle are counteracted by the requirement for the largest antenna beamwidth (i.e., the lowest antenna gain).

Calculating required satellite ERP's for the variables in the top graph leads to the results shown in the bottom graph. The conclusion of this analysis is that it makes little difference where the satellite is located in longitude in terms of the ERP requirement.

The choice of latitude then could be based on other considerations. A latitude of 92° W longitude is the midpoint of the central and largest time zone in the United States. When pointing to the other zones, it is advantageous to use the central zone as a reference and point to either side. The symmetry leads to a simpler system for the interferometer reference as explained in Section 4.5.

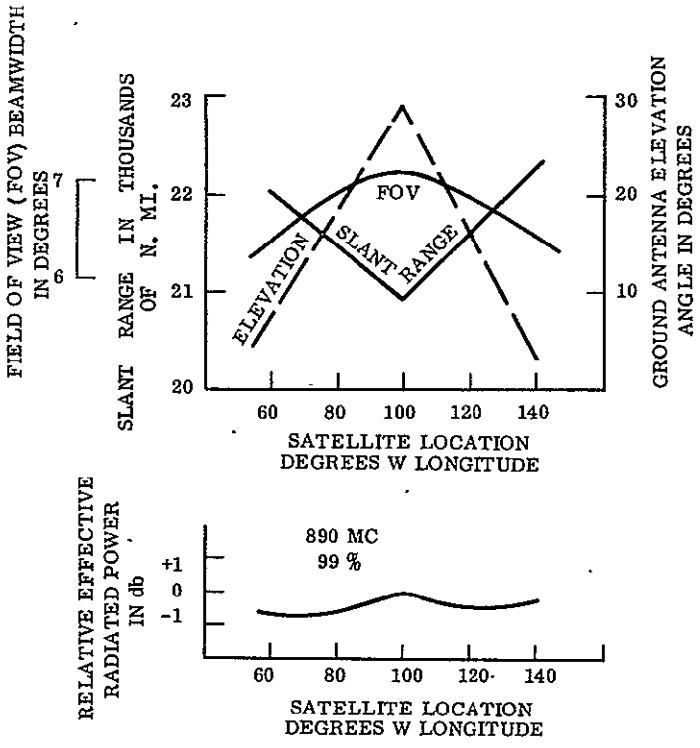

Figure 3.3-4. Satellite Location at Synchronous Orbit for UHF

3.4 DIVISION OF EFFECTIVE RADIATED POWER (ERP)

The division of satellite ERP between the antenna gain and the RF power was selected for each configuration to best satisfy the design goal of lowest satellite cost.

The first step was to estimate the weight of a satellite design consisting of a combination of subsystems based on pointing errors of three representative attitude control types (active, hybrid, and passive). This was accomplished by assuming the broadcast antenna half-power beamwidth to be defined by the sum of the necessary field of view, the pointing errors introduced by the chosen type of attitude control, and the boresight errors. With this antenna defined, the power supply was sized (i.e., the ERP division was determined as a function of each basic type of attitude control subsystem for each configuration).

The second step, given the vehicle weights, was to determine the booster required to place each vehicle in the orbit defined for each configuration, and then to obtain a cost comparison of each resultant system. The cost comparison only took into account the major contributing variables. These turned out to be the cost of the booster, the power supply, and the attitude control. The cost variation of the broadcast antenna was small by comparison and thus was neglected.

The final step was to select the most economical system as defined by the relative cost values.

For the HF, VHF No. 1, and the UHF configurations, the minimum cost system was obtained with an active attitude control subsystem and pointing errors not exceeding 0.2 degrees per axis. For the VHF No. 2 configuration, the minimum cost system was the one using a hybrid attitude control subsystem with a maximum pointing error of 1^{o} in yaw and roll, and 2^{o} in pitch.

3.5 COVERAGE AND ANTENNA BEAMWIDTH

3.5.1 INTRODUCTION

Representative coverage areas were selected for each of the four configurations based upon the audience analysis described in Section 2.6 and each satellite orbit selected in Section 3.3. The field of view (FOV) required for these coverage areas was determined by a map overlay procedure and verified by the computer program described later in Section 6.4.1. (The computer program determined the field of view as a function of the ground signal strength variation from the center to the edge of the field of view for each coverage area.) The pointing error associated with the type of attitude control system selected in Section 3.4 was added to the estimated boresight error to arrive at the required antenna beamwidth. The following sections present the results of the above procedure for each of the four configurations.

3.5.2 HF CONFIGURATION COVERAGE AND ANTENNA BEAMWIDTH

In Figure 3.5-1 the shaded regions show the five coverage areas selected as representative for the HF configuration. These areas require an 18.5 degree field of view as viewed from the satellite to guarantee one hour of coverage per area per orbit. The heavy lines on the equator show the motion of the satellite relative to the earth during the 1 hour per orbit broadcast period to each area. The satellite orbits the earth five times per day, therefore broadcasts can be made to each area each day between 5:30 and 6:30 P.M. local time. Figure 3.5-1 also shows the languages spoken in each region.

The active attitude control subsystem selected for the HF satellite has an error of $\pm 0.2^{\circ}$ per axis. The maximum possible three-axis pointing error is the vector sum of the pitch and roll errors (the yaw error is insignificant for small angles) which equals $\pm 0.28^{\circ}$. The estimated antenna boresight error is $\pm 0.47^{\circ}$. The required antenna full beamwidth is the sum of the field of view plus twice the pointing error plus twice the antenna boresight error which equals 20°.

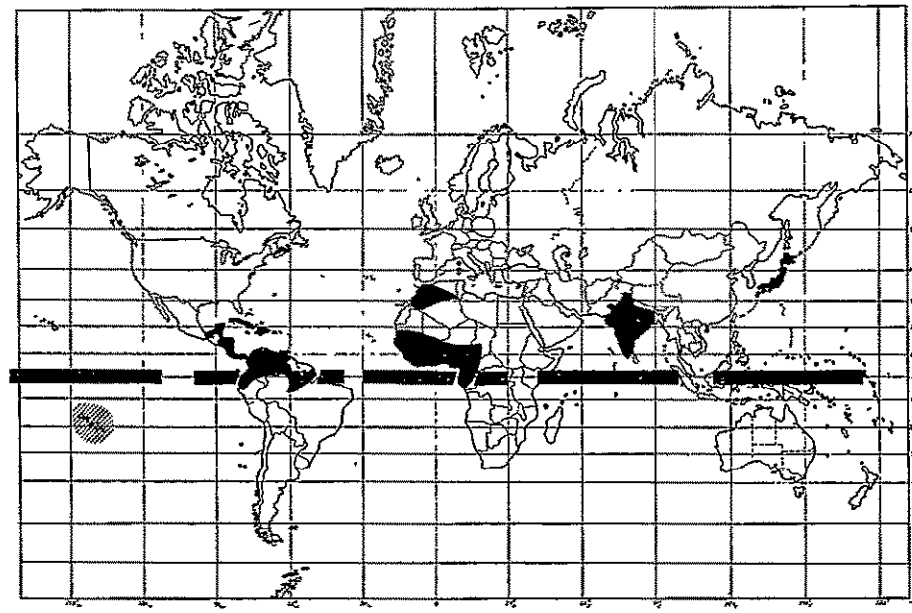

Figure 3.5-1. Coverage for HF Configuration

3.5.3 VHF NO. 1 CONFIGURATION COVERAGE AND ANTENNA BEAMWIDTH

In Figure 3.5-2 the shaded regions show five coverage areas selected as representative for the VHF No. 1 configuration. The satellite is injected into a near-synchronous orbit at 99°E longitude. It is "walked" to 135°E longitude in the launch deployment mode, deployed

and checked out using an Australian ground station. It is then pushed West in a slow walking mode (2.3° per day) to perform demonstrations to any desired world area between 70°N and 50°S latitude. It is then made stationary at 97°W for demonstrations to the United States. The heavy lines on the equator show the motion of the satellite with respect to the earth during the several weeks of broadcasts to each shaded area. The circle on the equation is the longitudinal location of the satellite during the stationary mode for demonstrations to the United States.

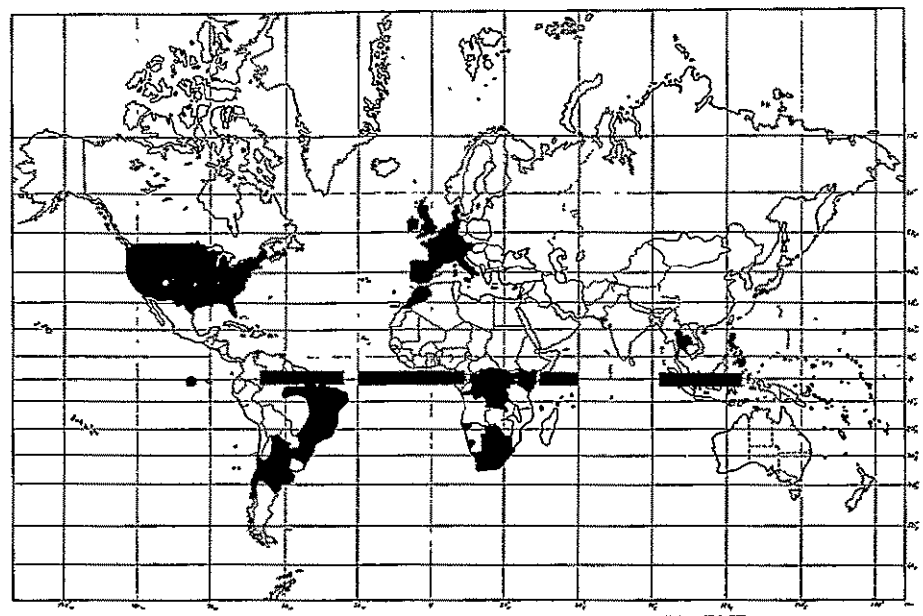

AREAS:	UNITED STATES	LATIN AMERICA	WEST EUROPE	AFRICA	FAR EAST
LANGUAGES	ENGLISH	PORTUGESE SPANISH	ENGLISH GERMAN FRENCH ITALIAN SPANISH	ENGLISH	ENGLISH

ORBIT: WALKING NEAR-GEOSTATIONARY FIRST 3 MONTHS; GEOSTATIONARY REST OF TIME (SATELLITE AT 97°$_W$ LONGITUDE)

BROADCASTING: CONTINUOUS EXCEPT DURING SHADOW; WORLD AREAS FOR SEVERAL WEEKS EACH DURING FIRST 3 MONTHS; UNITED STATES FOR REST OF SATELLITE LIFE.

Figure 3.5-2. Coverage for VHF No. 1 Configuration

During the walking mode, coverage of the largest area requires a 6° field of view. During the stationary mode, coverage of the United States requires a 7° field of view. A 7-1/2° full antenna beamwidth was determined by using attitude control errors of 0.2° per axis during the walking mode and 0.1° per axis during the stationary mode. The same attitude control subsystem is employed for both modes but an interferometer based in the United States is used as an antenna pointing reference to decrease the error for the stationary mode. The following are the calculations for the antenna beamwidth.

Mode	FOV	Maximum 3-Axis Pointing Error	Boresight Error	Antenna Beamwidth
Walking	6.0^{o}	$\pm 0.28^{o}$	$\pm 0.47^{o}$	$7\text{-}1/2^{o}$
Stationary	7.0^{o}	$\pm 0.14^{o}$	$*\pm 0.11^{o}$	$7\text{-}1/2^{o}$

*Requires boresight calibration tests in stationary orbit.

3.5.4 VHF NO. 2 CONFIGURATION AND ANTENNA BEAMWIDTH

In Figure 3.5-3, the shaded regions show the three coverage areas selected as representative for the VHF No. 2 configuration. The western United States requires a 10.8^{o} field of view to guarantee 1 hour of coverage per area per orbit. The heavy lines on the equator show the motion of the satellite relative to the earth during 1 hour per orbit broadcast period to each area. The satellite orbits the earth three times per day, therefore broadcasts can be made to each area each day between 5:30 and 6:30 P.M. local time.

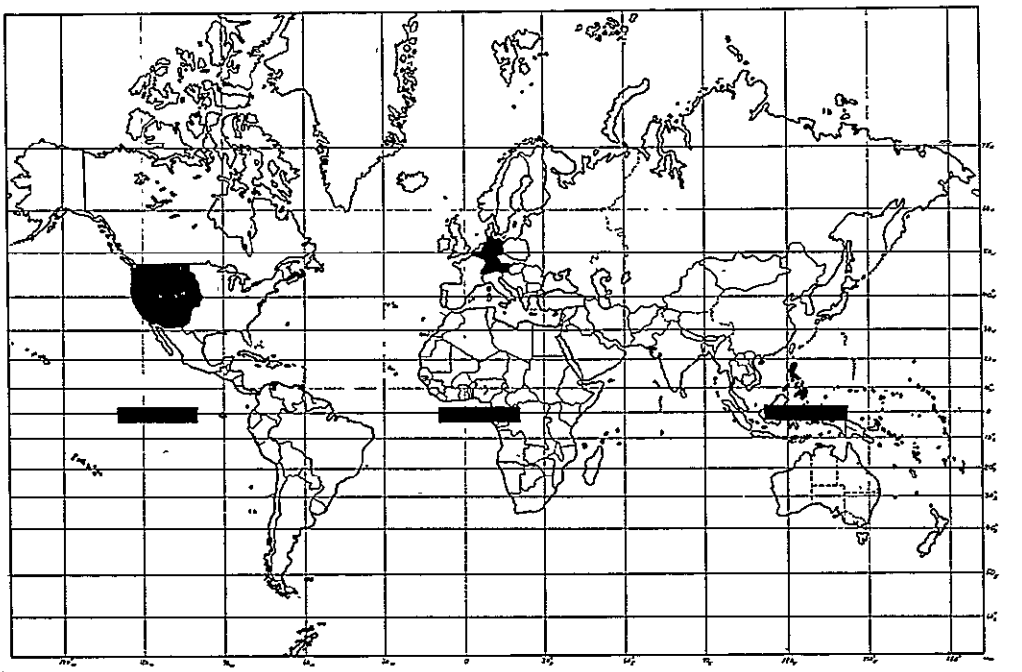

Figure 3.5-3. Coverage for VHF No. 2 Configuration

The hybrid attitude control subsystem selected for the VHF No. 2 satellite has the following errors: 2^{o} pitch error, 1^{o} roll error, 1^{o} yaw error. The maximum possible three-axis pointing error is the vector sum of the pitch and roll errors (the yaw error is insignificant

for small angles) which equals $\pm 2.22^{\circ}$. The estimated antenna boresight error is $\pm 1.63^{\circ}$. The required antenna full beamwidth is the sum of the field of view plus twice the pointing error plus twice the antenna boresight error which equals $18\text{-}1/2^{\circ}$.

3.5.5 UHF CONFIGURATION AND ANTENNA BEAMWIDTH

In Figure 3.5-4, the shaded regions show the four U.S. time zones selected as coverage areas for the UHF configuration. The four ovals are the coverage obtained with a 3.4° field of view from the satellite. The circle on the equator is the longitudinal location of the satellite. Broadcasting is accomplished sequentially from time zone to time zone for a total of 20 hours per day. Broadcasts to each time zone occur in 1 hour schedules from 6 to 7 A.M., 10 to 11 A.M., 2 to 3 P.M., 6 to 7 P.M. and 10 to 11 P.M.

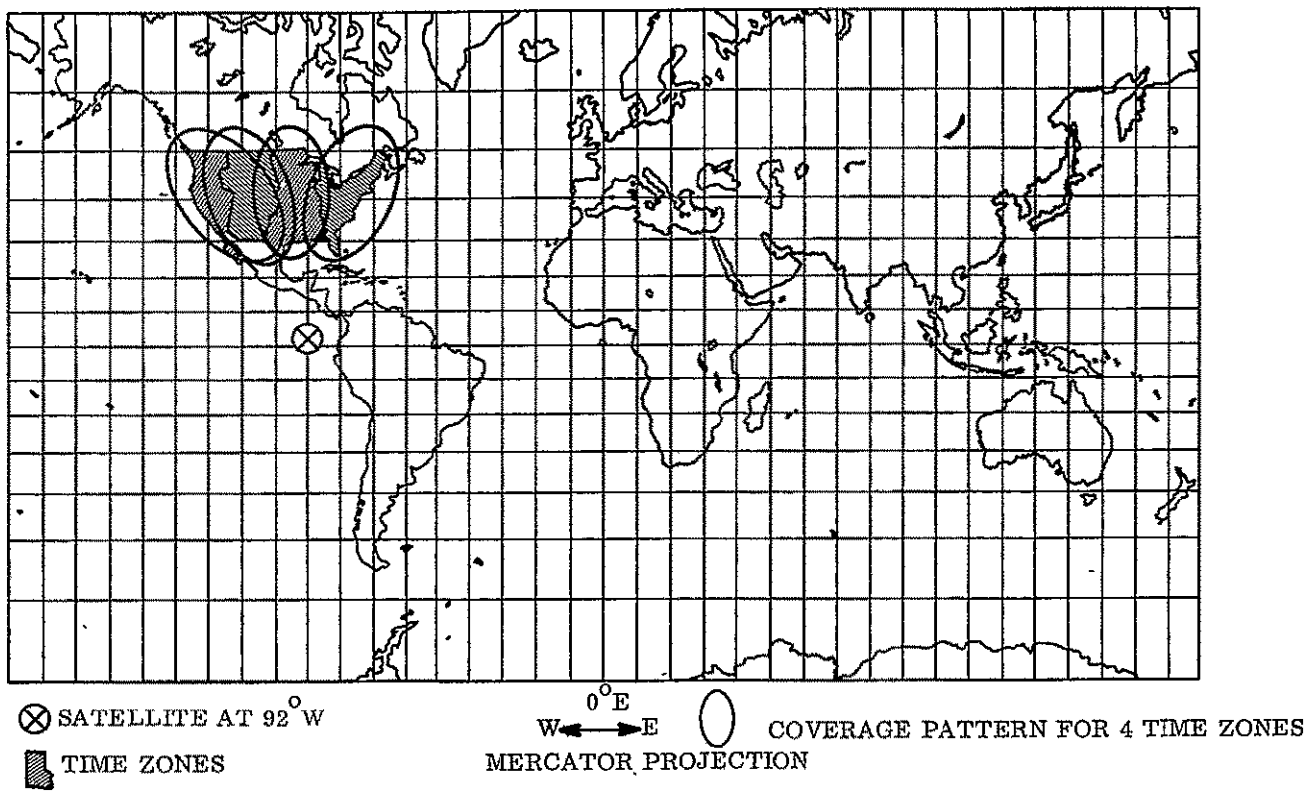

Figure 3.5-4. Coverage for UHF Configuration

The active attitude control subsystem selected for the UHF satellite has an error of ± 0.1 degree per axis. The maximum possible three-axis pointing error is the vector sum of the pitch and roll errors (the yaw error is insignificant for small angles) which equals $\pm 0.14^{\circ}$. The estimated antenna boresight error is $\pm 0.03^{\circ}$. The required antenna full beamwidth is the sum of the field of view plus twice the pointing error plus twice the boresight error which equals $3\text{-}3/4^{\circ}$.

3.6 POWER BUDGET CALCULATIONS

3.6.1 ERP CALCULATIONS

Figure 3.6-1 shows the geometry involving the angles and distances from a satellite in a given orbit to the earth area of interest. This geometry has been put into the form of a simple computer program to calculate ERP as a function of orbit geometry and field strength.

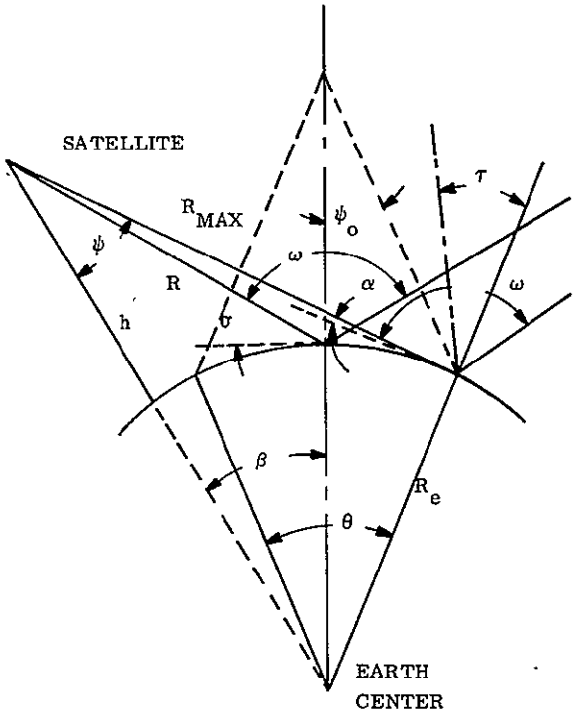

Values to be specified

θ	=	earth central angle subtending coverage area (degrees)
β	=	earth central angle to satellite (degrees)
h	=	satellite altitude (nm)
E	=	field strength at earth surface (in μv/m)

(Assuming Re = 3440 nm).

Parameters to be determined

R	=	slant range (nm)
σ	=	antenna elevation angle (note: $\sigma = 90^o - \frac{\omega}{2}$) (degrees)
R max	=	maximum slant range (nm)
α	=	minimum antenna elevation angle (degrees)
ψ	=	maximum half beamwidth of satellite antenna (degrees)
ψ_o	=	minimum half beamwidth of satellite antenna (degrees)
τ	=	antenna tip angle (degrees)
P erp	=	effective radiated power (db) at antenna beam edge

Figure 3.6-1. Desk Side Computer Geometry and Parameters

Table 3.6-1 presents the results of the computer runs for the four configurations. Cases where the antenna was pointed off the subsatellite ground trace resulted in three dimensional geometry not directly solvable. For these cases, β was calculated using spherical geometry for each orbit and coverage area.

3.6.2 DOWNLINK POWER BUDGETS

The downlink power budgets for each of the four configurations are given in Tables 3.6-2, -3, -4 and -5. For each configuration both the downlink calculations and the input data assumptions are given. These downlink power budgets were calculated for the following reasons:

Table 3.6-1. Desk Side Computer Results

Parameters		Configurations			
		HF	VHF No. 1	VHF No. 2	UHF
Inputs	θ	24	42	24.	25
	β	40.1	32	49.7	42
	h	4356	19323	7556	19323
	E	150	180	50	106
Outputs	R	5619.92	19906.36	9155.0	20314.41
	σ	26.68	52.75	23.65	41.49
	R_{max}	6297.87	20851.54	9842.75	20930.59
	α	12.27	29.43	10.38	27.81
	ψ	25.53	7.57	17.92	7.69
	ψ_o	9.17	3.61	5.35	2.20
	τ	14.31	23.32	13.27	13.68
	P_{erp}	50.07	62.06	44.41	57.49

(1) To document in one section of this report the nominal design assumptions and system parameters which are explained in detail in other sections of this report.

(2) To verify that the selected ERP values will provide adequate signal quality at the ground receiver output.

Note that the values for signal-to-noise ratio and ground signal strength (μv/m) are nominal design values used to size the system. The actual values obtained by the configurations are presented in Section 6.4.

3.7 UHF WIDE BAND LINK

The requirement to include a wideband FM mode in the UHF ground satellite was analyzed to determine the variation of output signal-to-noise ratio of the ground receiver for variations of the ground receiving parameters. The basic assumptions were:

a. Baseband bandwidth = 5 MHz

b. Maximum Frequency Deviation = 15 MHz

c. Carrier Frequency = Same as for voice system (890 MHz assumed)

d. Satellite ERP shall be the value defined for the voice system

e. Satellite position to be at 92°W in a synchronous equatorial orbit

f. Path loss based on slant range to farthest U.S. border (20, 930 nm)

Table 3.6-2. HF Downlink Power Budget Assumptions and Calculations

A. INPUT DATA AND ASSUMPTIONS

ITEM DESCRIPTION		DESIGN VALUE	REMARKS
Transmitting Frequency		15 MHz	
Orbit		4356 nm circular equatorial	
ASSUMED RECEIVING SITUATION USED IN DETERMINING FINAL ERP			
a.	Environment	Rural	
b.	Galactic Noise Temperature	8.5×10^4 °K	(mean value)
c.	Manmade Noise Temperature	2.9×10^4 °K	(ESSA data)
d.	Atmospheric Noise Temperature	9.1×10^6 °K	(max. at equator)
e.	Antenna Type and Location	3 element yagi-outdoor	
f.	Receiving Antenna on-Axis Gain	8 db	
g.	Discrimination Against Manmade Noise	0 db	(horizontal ant.)
h.	Net Antenna Noise Temperature	9.2×10^6 °K	(sum of b, c, & d above)
i.	Cable Loss for Specified Antenna Location	2 db	(typical)
j.	Building Attenuation	0	
k.	Polarization Loss for Revr. Antenna	3 db	(cir. polar. xmtr ant., linear revr. ant.)
l.	Pointing Loss for Revr. Antenna	3 db	
m.	Receiver Noise Figure	10 db	(typical)
n.	IF Noise Bandwidth	10 kHz	(typical)
o.	% Modulation	80%	
p.	Maximum Audio Frequency	5 kHz	(standard practice)
q.	Deemphasis Improvement	0	(N.A.)
r.	Output S/N	30.5 db	(perf. derived)
ASSUMED SPACECRAFT SITUATION			
s.	Transmitting Antenna Type	16 element cavity backed spiral array	
t.	Antenna Gain at Half Power Point	11.4 db	@ 15 MHz (includes cable & feed losses)
u.	Other S/C Losses	0.4 db	(ant. pointing loss)
ASSUMED DOWNLINK LOSSES			
v.	Absorption Losses	0	
w.	Ionospheric Losses (Fading)	0	(50% conf., 45° lat., 6:30 PM tm.)
x.	Free Space Path Loss	137.5	(7240 stat. miles slant range)
y.	Other Transmission Losses	1.6 db	(sat. ant. beam edge)

B. CALCULATIONS

ITEM DESCRIPTION			
1.	Transmitter RF Power Output		37.7 dbw
2.	Spacecraft Losses	0	
3.	Transmitter Antenna Gain	14.4 db	
4.	Net Gain	14.4 db	
5.	Effective Radiated Power		52.1 dbw
6.	Free Space Path Loss	-137.5 db	
7.	Atmospheric Loss	0	
8.	Ionospheric Loss	0	
9.	Other Transmission Losses	-2.0 db	
10.	Building Attenuation	0	
11.	Design Ground Signal Strength		150 μv/m
12.	Pointing Loss (RCVE)	-3 db	
13.	Polarization Loss	-3 db	
14.	Receiving Antenna On-Axis Gain	8 db	
15.	Net Losses	-137.5 db	
16.	Carrier Power at Antenna Terminals		-85.4 dbw
17.	Manmade Noise Temperature	2.9×10^4 °K	
18.	Antenna Discrimination Factor	1	
19.	Antenna Discrimination Factor	2.9×10^4 °K	
20.	Galactic Noise Temperature	8.5×10^4 °K	
21.	Atmospheric Noise Temperature	9.1×10^6 °K	
22.	Building Attenuation	0	
23.	Net Antenna Noise Temperature	9.2×10^6 °K	
24.	Receiver Noise Figure	10 db	
25.	Antenna Cable Loss	2 db	
26.	Receiver Noise Temp. (Ref. to Ant. Terminals)	4.3×10^3 °K	
27.	System Noise Temp. (Ref. to Ant. Terminals)	9.2×10^6 °K	
28.	Receiver IF Noise Bandwidth	10 kHz	
29.	Receiver Noise Power		-119 dbw
30.	Receive Output S/N (at 80% mod.)	30.5 db	

Table 3.6-3. VHF No. 1 Downlink Power Budget Assumptions and Calculations

A. INPUT DATA AND ASSUMPTIONS

ITEM DESCRIPTION	DESIGN VALUE	REMARKS
Transmitting Frequency	100 MHz	
Orbit	circular/synchronous/ equitorial	
ASSUMED RECEIVING SITUATION USED IN DETERMINING FINAL ERP		
a. Environment	Urban	
b. Galactic Noise Temperature	3000 ^{o}K	
c. Man-made Noise Temperature	9.15×10^{5} ^{o}K	(ESSA data)
d. Antenna Type and Location	dipole-outdoors	
e. Receiving antenna on-Axis Gain	2.2 db	
f. Discrimination Against Manmade Noise	0 db	(horizontal ant.)
g. Net Ant. Noise Temperature	9.18×10^{5} ^{o}K	(sum of b & c above)
h. Cable Loss for Ant. Location	1/2 db	(typical)
i. Building Attenuation	0	
j. Polarization Loss for Rcvr. Ant.	3 db	(cir. polar. xmtr. ant., linear rcvr. ant)
k. Pointing Loss for Rcvr. Ant.	0	
l. Receiver Noise Figure	10 db	
m. IF Noise Bandwidth	175 kHz	(typical)
n. Peak Frequency Deviation	75 kHz	
o. % Modulation	100%	
p. Max. Audio Frequency	15 kHz	(standard practice)
q. Deemphasis Improvement	9 db	(75 μ sec)
r. Output S/N	49.0 db	(perf. derived)
ASSUMED SPACECRAFT SITUATION		
s. Transmitting Ant. Type	32 element helix array	
t. Ant. Gain at Half Power Point	23.9 db	(includes cable and feed losses)
ASSUMED DOWNLINK LOSSES		
u. Absorption Losses	0	
v. Ionspheric Losses (Fading)	0.3 db	(90% conf., 60° lat., 1:00 PM time)
w. Free Space Path Loss	164.2 db	(24,000 stat. miles slant range)
x. Other Transmission Losses	3.0 db	(sat. ant. beam edge)

B. CALCULATIONS

ITEM DESCRIPTION		
1. Transmitter RF Power Output		38.5 dbw
2. Spacecraft Losses	0	
3. Transmitter Ant. Gain	26.9 db	
4. Net Gain	26.9 db	
5. Effective Radiated Power		65.4 dbw
6. Free Space Path Loss	-164.2 db	
7. Atmospheric Loss	0	
8. Ionospheric Loss	-0.3 db	
9. Other Transmission Losses	-3.0 db	(trans. ant. beam edge)
10. Building Loss	0	
11. Design Ground Signal Strength		180 μv/m
12. Pointing Loss (Rcvr.)	0	
13. Polarization Loss	-3.0 db	
14. Receiving Ant. on-Axis Gain	2.2 db	
15. Net Losses	-168.3 db	
16. Carrier Power at Ant. Terminals		-102.9 dbw
17. Manmade Noise Temperature	9.15×10^{5} ^{o}K	
18. Ant. Discrimination Factor	1	
19. Effective Manmade Noise Temperature	9.15×10^{5} ^{o}K	
20. Galactic Noise Temperature	3000 ^{o}K	
21. Building Attenuation	0	
22. Net Antenna Noise Temperatue	9.18×10^{5} ^{o}K	
23. Receiver Noise Figure	10 db	
24. Ant. Cable Loss	0	
25. Receiver Noise (Ref. to Ant. Terminals)	2900 ^{o}K	
26. System Noise Temp. (Ref. to Ant. Terminals)	9.21×10^{5} ^{o}K	
27. Receiver IF Noise Bandwidth	175 kHz	
28. Receiver Noise Power		-116.5 dbw
29. IF Carrier noise Ratio		13.6 db
30. Threshold	10 db	
31. Threshold Margin	3.6 db	
32. Deemphasis Improvement	9 db	
33. FM Improve Factor	26.4 db	
34. Receive Output S/N	49.0 db	

Table 3.6-4. VHF No. 2 Downlink Power Budget Assumptions and Calculations

A. INPUT DATA AND ASSUMPTIONS

ITEM DESCRIPTION	DESIGN VALUE	REMARKS
Transmitting Frequency	100 MHz	
Orbit	7556 nm circular equitorial	
ASSUMED RECEIVING SITUATION USED IN DETERMINING FINAL ERP		
a. Environment	Suburban	
b. Galactic Noise Temperature	3000 ^{o}K	
c. Manmade Noise Temperature	9.15×10^{3} ^{o}K	(ESSA)
d. Ant. Type and Location	dipole-outdoors	
e. Receiving Ant. on-Axis Gain	2.2 db	
f. Discrimination Against Manmade Noise	0 db	(horizontal antenna)
g. Net Ant. Noise Temperature	12.15×10^{3} ^{o}K	(sum of b & c above)
h. Cable Loss for Specified Ant. Location	1/2 db	(typical)
i. Building Attenuation	0	
j. Polarization Loss for Rcvr. Ant.	3 db	(cir. polar. xmtr. ant., linear rcvr. ant.)
k. Pointing Loss for Rcvr. Ant.	0	
l. Rcvr. Noise Figure	10 db	
m. IF Noise Bandwidth	175 kHz	
n. Peak Frequency Deviation	75 kHz	
o. % Modulation	100%	
p. Max. Audio Frequency	15 kHz	(standard practice)
q. Deemphasis Improvement	9 db	(75 μ sec)
r. Output S/N	53.4 db	(performance derived)
ASSUMED SPACECRAFT SITUATION		
s. Transmitting Antenna Type	parabola	
t. Antenna Gain at Half Power Point	16 db	(includes feed and cable losses)
ASSUMED DOWNLINK LOSSES		
u. Absorption Losses	0	
v. Ionospheric Losses (Fading)	0.7 db	(90% confidence, 60° lat., 6:30 PM time)
w. Free Space Path Loss	-157.6 db	(11300 stat. miles slant range)
x. Other Transmission Losses	3.0 db	(sat. ant. beam edge)

B. CALCULATIONS

ITEM DESCRIPTION		
1. Transmitter RF Power Output		29.1 dbw
2. Spacecraft Losses	0	
3. Transmitter Antenna Gain	19 db	
4. Net Gain	19 db	
5. Effective Radiated Power		48.1 dbw
6. Free Space Path Loss	-157.6 db	
7. Atmospheric Loss	0	
8. Ionospheric Loss	-0.7 db	
9. Other Transmission Losses	-3.0 db	(trans. ant. beam edge)
10. Building Attenuation	0	
11. Design Ground Signal Strength		50 μv/m
12. Pointing Loss	0	
13. Polarization Loss	-3.0 db	
14. Receiving Antenna on-Axis Gain	2.2 db	
15. Net Losses	-162.1 db	
16. Carrier Power at Antenna Terminals		-114.0 dbw
17. Manmade Noise Temperature	9.15×10^{3} ^{o}K	
1 Antenna Discrimination Factor	1	
18. Effective manmade Noise Temperature	9.15×10^{3} ^{o}K	
20. Galactic Noise Temperature	3000 ^{o}K	
21. Building Attenuation	0	
22. Net Antenna Noise Temperature	12.15×10^{3} ^{o}K	
23. Receiver Noise Figure	10 db	
24. Antenna Cable Loss	1/2 db	
25. Receiver Noise Temp. (ref. to Ant. Term.)	2900 ^{o}K	
26. System Noise Temp. (ref. to Ant. Term.)	15.1×10^{3} ^{o}K	
27. Receiver IF Noise Bandwidth	175 kHz	
28. Receiver Noise Power		-132.0 dbw
29. IF Carrier-to-Noise Ratio		20.4 db
30. Threshold	10 db	
31. Threshold Margin	10.4 db	
32. Deemphasis Improvement	9 db	
33. FM Improve Factor	26.4 db	
34. Receive Output S/N	55.8 db	

Table 3.6-5. UHF Downlink Power Budget Assumptions and Calculations

A. INPUT DATA AND ASSUMPTIONS

ITEM DESCRIPTION	DESIGN VALUE	REMARKS
Transmitting Frequency	870 MHz circular/ synchronous/equitorial	
ASSUMED RECEIVING SITUATION USED IN DETERMINING FINAL ERP		
a. Environment	Urban	
b. Galactic Noise Temperature	300°K	
c. Manmade Noise Temperature	3780 °K	(Extrapolated ESSA data)
d. Antenna Type and Location	dipole-outdoors	
e. Receiving Antenna on-Axis Gain	2.2 db	
f. Discrimination Against Manmade Noise	0	(horizontal ant.)
g. Net Antenna Noise Temp.	4080 °K	(sum of b & c above)
h. Cable Loss for Ant. Location	3 db	(typical)
i. Building Attenuation	0	
j. Polarization Loss for Rcvr. Ant.	3 db	(circ. polar. xmtr. ant. linear rcvr. ant.)
k. Pointing Loss for Rcvr. Ant.	0	
l. Receiver Noise Figure	10 db	
m. IF Noise Bandwidth	120 kHz	
n. Peak Frequency Deviation	25 kHz	
o. % Modulation	100%	
p. Maximum Audio Frequency	15 kHz	(standard practice)
q. Deemphasis Improvement	9 db	(75 μ sec)
r. Output S/N	31.6 db	(performance derived)
ASSUMED SPACECRAFT SITUATION		
s. Transmitting Antenna Type	parabola	
t. Antenna Gain at Half Power Points	30 db	(includes feed and cable losses)
ASSUMED DOWNLINK LOSSES		
u. Atmospheric Losses	0	
v. Ionospheric Losses (Fading)	-01. db	(90% confidence, 60° lat., 1:00 AM time)
w. Free Space Path Loss	-183.1 db	(24050 stat. miles slant range)
x. Other Transmission Losses	3 db	(sat. ant. beam edge)

B. CALCULATIONS

ITEM DESCRIPTION		
1. Transmitter RF Power Output (per transmitter)		27.6 dbw
2. Spacecraft Losses	0	
3. Transmitter Antenna Gain	33 db	
4. Net Gain	33 db	
5. Effective Radiation Power (single carrier)		60.6 dbw
6. Free Space Path Loss	-183.1 db	
7. Atmospheric Loss	0	
8. Ionospheric Loss	-0.1 db	
9. Other Transmission Losses	-3.0 db (trans. ant. beam edge)	
10. Building Attenuation	0	
11. Design Ground Signal Strength		106 μv/m
12. Pointing Loss	0	
13. Polarization Loss	-3.0 db	
14. Receiving Antenna on-Axis Gain	2.2 db	
15. Net Losses	-187.0 db	
16. Carrier Power at Antenna Terminals		- 126.4 dbw
17. Man-made Noise Temperature	3780°K	
18. Antenna Discrimination Factor	1	
19. Effective Manmade Temperature	3780°K	
20. Galactic Noise Temperature	300°K	
21. Building Attenuation	0	
22. Net Antenna Noise Temperature	4080°K	
23. Receiver Noise Figure	10 db	
24. Antenna Cable Loss	3 db	
25. Receiver Noise Temp. (ref. to Ant. Term.)	5500°K	
26. System Noise Temp. (ref. to Ant. Term.)	9580°K	
27. Receiver IF Noise Bandwidth	4.5 MHz	
28. Receiver Noise Power		-122.3 dbw
29. Intercarrier Mixer Degradation (UHF only)	4.2 db (prior to video detector)	
30. Sound IF Carrier to Noise Ratio		7.4 db
31. IF Carrier-to-Noise Ratio		-4.1 db
32. Threshold	6 db	
33. Threshold Margin	1.4 db	
34. Deemphasis Improv.	7.95 (9 db)	
35. FM Improv. Factor	33.4 (15.2 db)	
36. Receive Output S/N	31.6 db	

The basic equation for determining the receiver output signal-to-noise ratio (S/N) is:

$$S/N = C/N + 10 \log 3 M^2 + 10 \log B_{if}/2\,fb + \alpha$$

where

M = Modulation index = f/fb = 15 MHz/5 MHz = 3

Δf = Minimum carrier deviation

fb = Baseband frequency bandwidth

B_{if} = $2(M + 1)fb = 2(3 + 1)\ 5\ MHz = 40\ MHz$ (std. FM)
$2(M/k + 1)fb = 2(3/1.11 + 1)\ 5\ MHz = 37\ MHz$ (FM FB)

α = Improvement factor which includes the noise weighting factor, pre-emphasis factor, and improvements resulting from averaging peak values to rms and from using a positive synchronization signal. The range of values α varies from about 2.5 db, for a color TV signal with no pre-emphasis factor and no peak averaging or sync reversal improvements, to 33.4 db for a black and white signal which includes all of these improvements. The following results consider both limit values:

C/N = P_R/N

N = Received Noise Power = $K\,T_{eff}\,B_{if}$

$K\,T_{eff}$ = Noise Power Density at the receiver

P_R = Received Signal Power

P_R = ERP - Path loss + Receiving Antenna Gain

ERP = Effective Radiated Power from the satellite expressed in dbw. The ERP value for the first calculation of the voice UHF system was 63 dbw. Other values of ERP have been evaluated, as shown in subsequent graphs.

L_P = Path Loss = 183.1 db

G_R = Receiving Antenna Gain - A range of values has been analyzed substituting in Equation (1):

K = $6 \times 10^6/fb + 4.1 \times 10^5$ for $fb \leq 5.59 \times 10^6$

S/N = $ERP - L_p + G_R - K\,T_{eff}\,B_{if} + 10 \log 3 M^2 + 10 \log B_{if}/2\,fb + \alpha$

A separate calculation of the C/N values vs. ERP is shown in Figure 3.7-1.

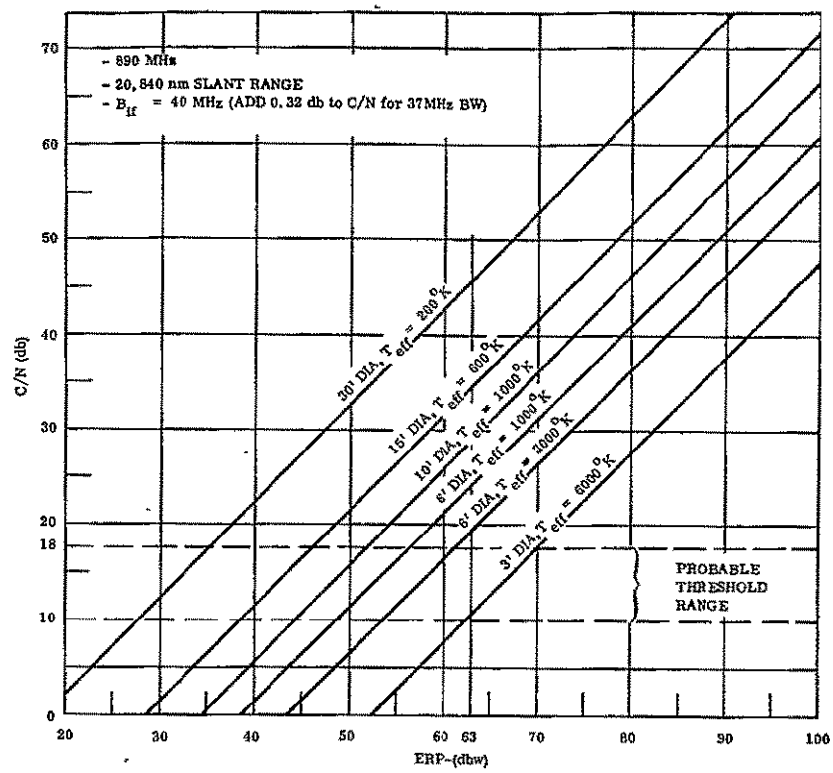

Figure 3.7-1. C/N Versus ERP and Satellite Antenna Diameter

Evaluating the other parameters reduces the S/N equation to:

$$S/N = C/N + 22.8 \text{ db}, \text{ for } \alpha = 2.5 \text{ db}$$

and

$$S/N = C/N + 51.2 \text{ db}, \text{ for } \alpha = 33.4 \text{ db}.$$

These two equations are plotted in Figures 3.7-2 and 3.7-3 with ERP and ground parameters as variables. These equations hold only if the value of C/N is at least threshold. A minimum value of threshold for standard FM is about 10 db.

Each of the equations have been plotted for an 80 db range of ERP and for several specific example antenna sizes and system effective noise temperatures (T_{eff}). The ground system values assumed are:

Antenna Diameter (ft)	Gain at 890 MHz	T_{eff}	G/Te
3	16 db	$6000^{\circ}K$	6.7×10^{-3}
6	22 db	$3000^{\circ}K$	5.3×10^{-2}
6	23 db	$1000^{\circ}K$	1.58×10^{-1}
10	26.5 db	$1000^{\circ}K$	4.47×10^{-1}
15	30 db	$600^{\circ}K$	1.67
30	36 db	$200^{\circ}K$	20

From Figure 3.7-2, the values of ERP to achieve the desired S/N (51 db) have been combined with a satellite antenna gain of 33 db (to cover a single time zone in the U.S.). The resulting satellite prime power requirements, assuming a 50% DC-to-RF efficiency, are listed below for the minimum value of α(2.5 db):

Ground Antenna and Effective Temperature	Satellite Prime Power
3' Dia, $6000^{\circ}K$	76 kw
6' Dia, $3000^{\circ}K$	7.25 kw
6' Dia, $1000^{\circ}K$	2.4 kw
10' Dia, $1000^{\circ}K$	710 watts
15' Dia, $600^{\circ}K$	240 watts
30' Dia, $200^{\circ}K$	21 watts

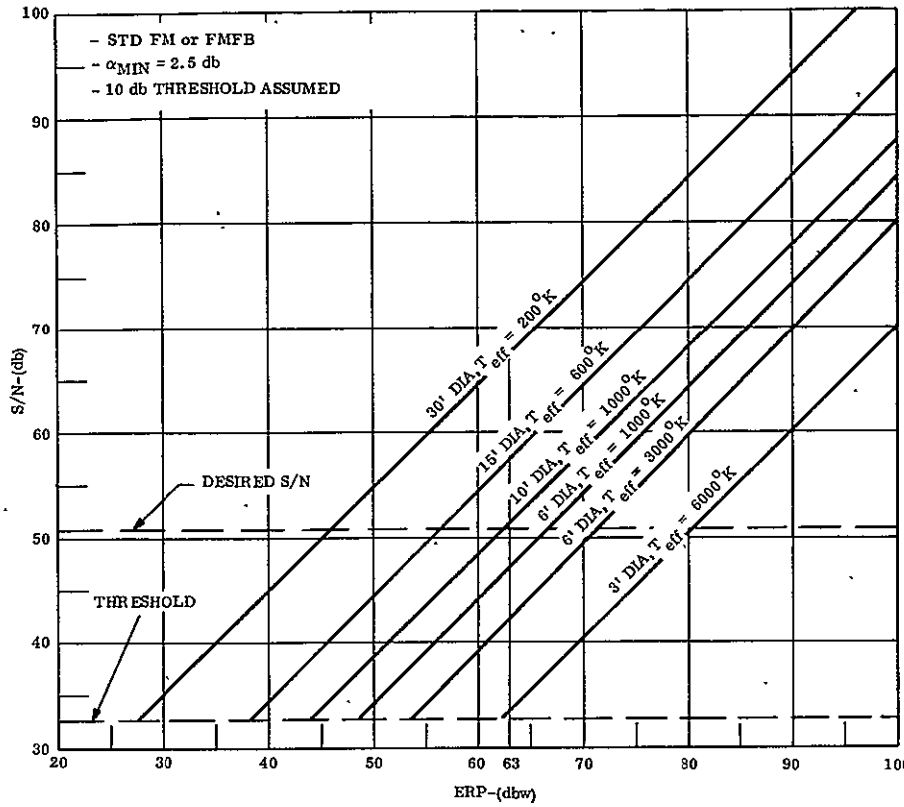

Figure 3.7-2. S/N Versus ERP versus Antenna Diameter

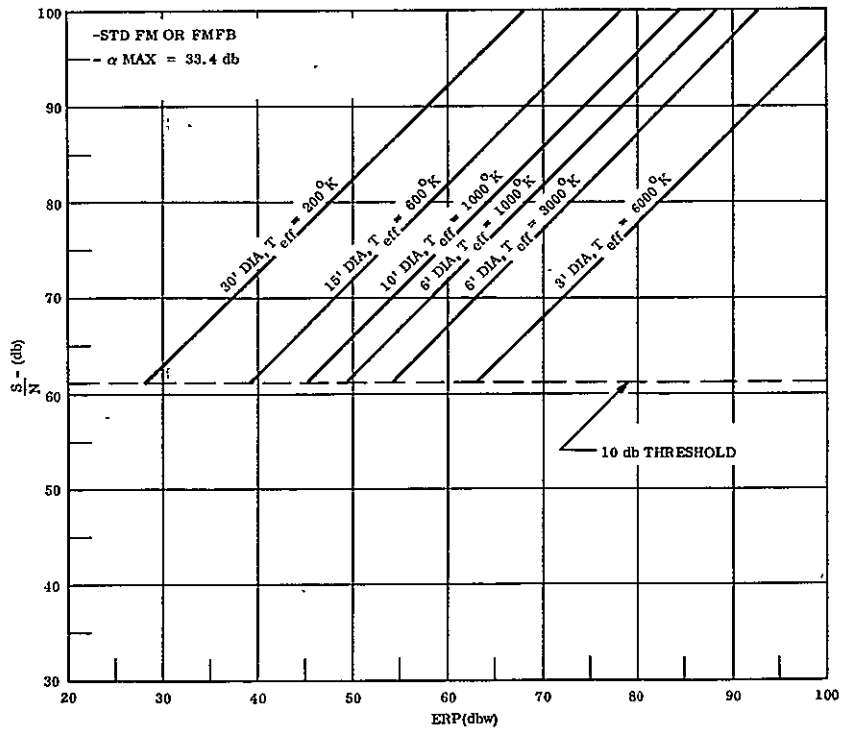

Figure 3.7-3. S/N Versus ERP Versus Antenna Diameter

SECTION 4

TECHNOLOGY AND SUBSYSTEM EVALUATION

4.1 INTRODUCTION

This section describes the subsystems selected for each of the four baseline configurations and the technology evaluations performed to select these subsystems. The following subsystems are covered in this section:

a. Broadcast Antenna Subsystem

b. Broadcast Transmitter Subsystem

c. Ground-to-Satellite Uplink

d. Attitude Control Subsystem

e. Autopilot Subsystem

f. Satellite Power Subsystem

g. Telemetry, Tracking and Command (TT&C) Subsystem

h. Propulsion Subsystem

i. Thermal Control Subsystem

4.2 SATELLITE ANTENNAS

4.2.1 INTRODUCTION

4.2.1.1 Summary

The satellite antenna analyses and design efforts for the Voice Broadcast Mission Study consisted of the following:

a. A large range of possible antenna types were evaluated for suitability on voice broadcast missions. The evaluation considered the electrical and mechanical parameters and the constraints imposed by vehicle interfaces.

b. From this list, a smaller number of candidate types were selected for a more detailed analysis to permit tradeoffs for each of the four selected configurations' design requirements.

c. A final selection was made among the candidates based on the capability of meeting the mission performance requirements and the design priorities imposed (including cost, weight, and development schedule).

d. For the final choices, a detailed conceptual design was completed which included analyses to refine the previous estimates of electrical and mechanical performance. Also included were calculations of the vehicle interface parameters, dynamic properties, and the packaging and deployment factors.

The resulting four antenna designs included two paraboloids (VHF and UHF), a 32 element helix array (VHF), and a 16 element array of cavity-backed spirals (HF). The construction method selected for each of the antennas was the wire-grid-tube. A detailed description of these antennas, the reasons for selection, and the results of the analyses are presented in the following sections.

4.2.1.2 Conclusions

Three significant conclusions resulted from the antenna investigations. First, large, high gain antennas in the 15 to 890 MHz band are technically feasible and can be available for flights in the early 1970's. However, development should be initiated soon to minimize the risk in the critical area of deployment. Second, for satellites with significant levels of ERP, the total satellite cost is minimized by selecting the highest gain antenna consistent with the coverage area and vehicle attitude stability constraints. This is because the reduction of prime power achieved with the maximum gain antenna results in a savings in excess of the cost to increase the antenna gain. Third, the wire-grid-tube construction method was selected for high gain antennas in the HF, VHF and UHF bands because it was representative of several advanced techniques that provide low weight, low volume packaging and low cost.

4.2.2 DESCRIPTION OF SELECTED ANTENNAS

In the following paragraphs, the antennas selected for each of the four configurations are described. Included in each description are the electrical design requirements, a physical description of the antenna, schematic drawings, and the resulting electrical and structural characteristics.

4.2.2.1 HF Antenna

4.2.2.1.1 Antenna Requirements

This antenna design was the most difficult in that a large bandwidth at a relatively high constant gain was required at a lower frequency. The final antenna requirements were as follows:

a.	Frequency	15.1 to 25.85 MHz
b.	Gain	14.4 db
c.	Beamwidth	20^{o}

d.	Scan	$\pm 15.75^{o}$
e.	RF Power	5.91 kw
f.	Polarization	Circular

Electrical requirements such as low gain dispersion, broad bandwidth, relatively high gain, and a large scan angle necessitated an array of cavity backed spiral elements. Based on minimum weight and packaging volume the wire grid tube technique was selected.

4.2.2.1.2 HF Antenna Description

Cavity-backed Spiral Element. The cavity of this element is 25 feet square and 15 feet deep. It is constructed of 2-in diameter wire grid tubes arranged as shown in Figure 4.2-1.

The cavity's sides and bottom are covered with a wire mesh screen. The spiral has a total length of 1 wavelength at the low frequency (15 MHz) and is constructed so that the effective conductor to air ratio is unity. The conductor, however, is itself not solid but is formed of four parallel 2-in diameter wire grid tubes. The spiral is held in place by nonconducting spokes.

Cavity-backed Spiral Array. Sixteen of the above elements are placed side by side to form a 4 by 4 element square array. Some additional truss work may be necessary to permit this structure to deploy in a 1 g field; however, none was considered in this preliminary design. Each element is fed by a separate transmitter via a light weight flexible coaxial cable and a specially designed balun.

This antenna is gas erected. Figure 4.2-2 shows this antenna in its deployed configuration.

4.2.2.1.3 HF Antenna Characteristics

Electrical. To obtain the required gain at the low end of the frequency band (15.1 MHz), the excitation of 16 elements is required. However, to provide the necessary coverage-sector of 20^{o} for 25.85 MHz, only 9 elements will be excited. Because the cavity-backed spiral is a relatively broad-beam element, the behavior of the cavity-backed spiral is similar to the dipole over a ground plane with a beamwidth variation of 60 to 80^{o}. To avoid the formation of secondary lobes, the interelement spacing must be restricted to 0.78 at the high end (25.85 MHz) of the frequency band. The corresponding spacing at 15.1 MHz will be 0.44. In order to scan the beam to an angle $\theta = \pm 16^{o}$ off broadside, it is necessary to provide a phase shift between adjacent elements. The maximum required phase shift is on the order of $\pm 44^{o}$ at 15.1 MHz and $\pm 77^{o}$ at 25.85 MHz.

The beamwidth of the 1/2 power points of the array for the two dimensional array is approximately 30 degrees at 15.1 MHz and 23^{o} at the higher end (25.85 MHz) of the frequency band. Assuming a 65% efficiency factor, the broadside gain of the array will be on the order of 14.4 db at 15.1 MHz and 17.1 db at 25.85 MHz respectively.

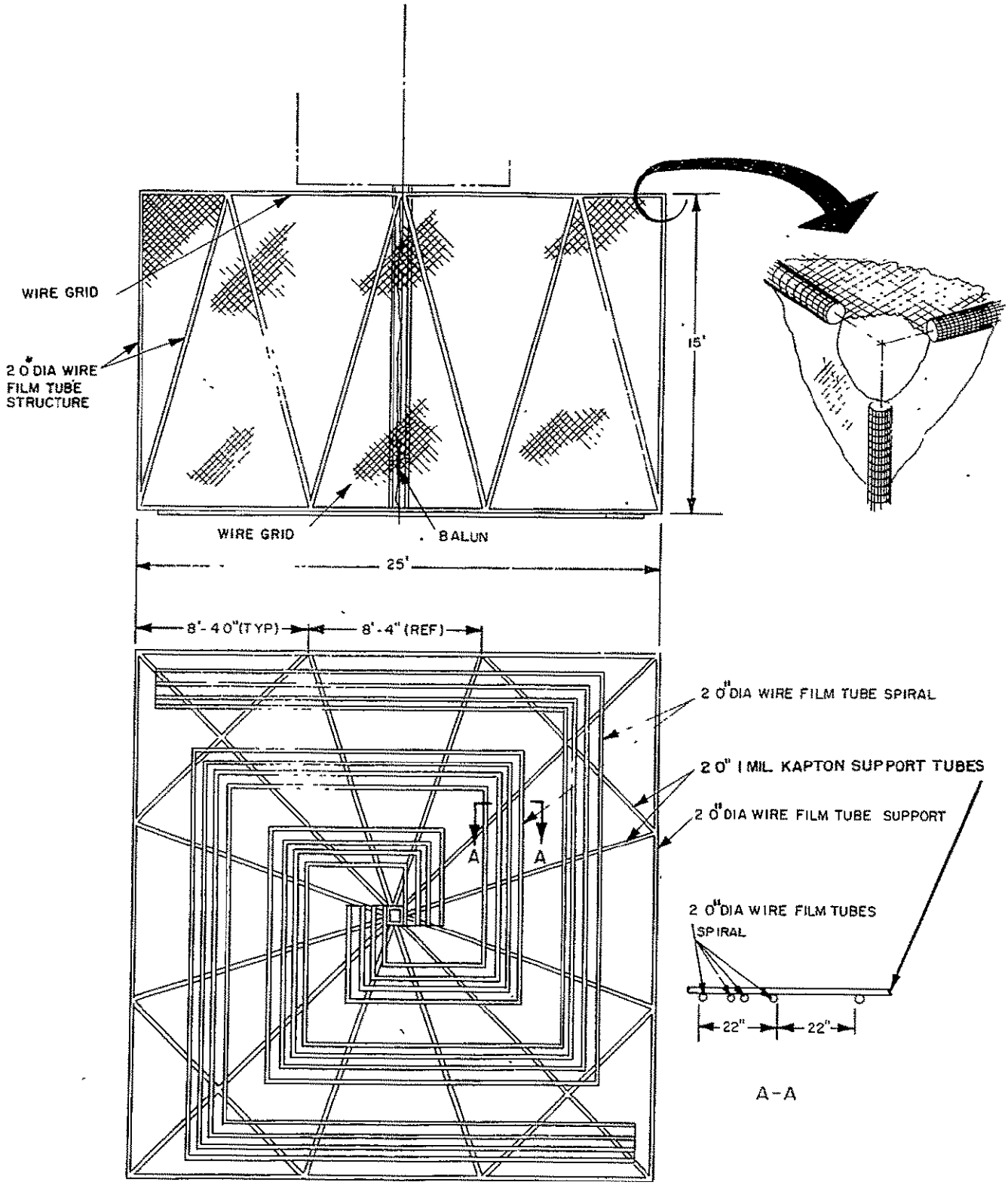

Figure 4.2-1. HF Antenna

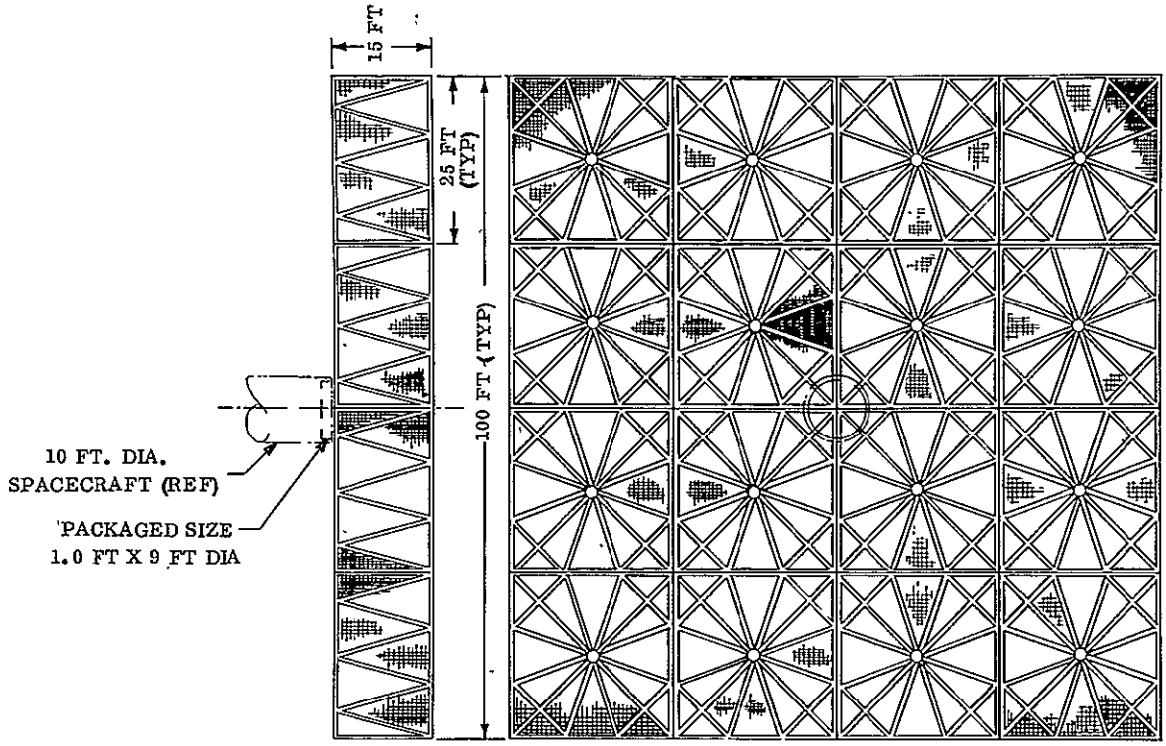

Figure 4.2-2. Spiral Array (16 Element)

Thus the 3db beam edge was used at the high end of the frequency band to establish pointing requirements, which resulted in a 2db beam pattern loss at the edge of the coverage area for the low end of the band.

Structural. The structural parameters are:

a.	Weight	620 lb	
b.	Volume (packaged)	60 ft^3	
c.	I_z	20,850 slug-ft^2	
d.	I_y	10,650 slug-ft^2	
e.	Effective Solar Area of Antenna	4,400 ft^2	(Solar area can be reduced by 2/3 by proper photolyzation of some of the film comprising the wire grid tubes.)
f.	Natural Frequency	0.96 Hz	
g.	Thermal Deflection	0.325 ft	

4.2.2.2 VHF No. 1 Antenna

4.2.2.2.1 VHF No. 1 Antenna Requirements

The following antenna characteristics must be achieved to satisfy the mission's requirements:

Frequency	100 to 108 MHz
Gain	26.9 db
Beamwidth	7.5 degrees
Scan	None
RF Power	7.07 kw
Polarization	Circular

Several elements and various arrays of these elements were considered. An array 51 by 51 feet of thirty-two helix elements was selected on the basis of electrical performance, structural rigidity, and minimum form factor in the deployed condition. Based on minimum weight and packaging volume the construction selected was wire grid tubes.

4.2.2.2.2 VHF No. 1 Antenna Description

Helix Element. The helix element has a 3.33 feet square cross section and is 12 feet long. It has a pitch angle of 14 degrees resulting in about 4 turns. Each side of the helix forms a Warren truss constructed of 2-inch wire grid tubes. For the desired electrical characteristics, the joints of the truss must be constructed of a nonconducting material. All support members of the truss must be electrically isolated from the RF conductor support members by at least 0.22λ to obtain the desired radiation patterns. Figure 4.2-3 is a sketch of one of these elements.

Helix Array. Thirty-two of the above elements spaced 8 feet apart are arrayed together to form a square 51 by 51 feet (includes ground plane) with an element missing from each corner. These elements are held together by a network of triangular trusses constructed of 2-inch wire grid tubes. The backup structure is covered with a wire screen or sucal cloth to serve as a ground plane for the helix elements. Each element is fed by a separate transmitter. The transmitters are electrically connected to the helix elements via a light weight flexible coaxial cable.

The antenna is sequentially gas inflated until all wire grid tubes are rigidized; then the gas is removed. The deployed antenna is shown in Figure 4.2-4.

4.2.2.2.3 VHF No. 1 Antenna Characteristics

Electrical. The total radiation pattern of an axial mode helix in an infinite array can be approximated by

$$E = \left(\sin \frac{90^{\circ}}{n}\right) \times \frac{\sin (n\psi/2)}{\sin (\psi/2)} \cos \phi$$

where

$\psi = 360^{\circ} \times S\,(1 - \cos \phi) + (1/2\ n)$

n = number of turns

ϕ = pitch angle

S = distance between turns (wavelengths)

Determining the array factor for a spacing of 8 feet, simple pattern multiplication techniques give the broadside radiation pattern of the array. From this pattern, one can determine the half-power beamwidth and, assuming some efficiency, deduce the power gain.

An efficiency of 65 percent was used here, resulting in a gain equation of

$G = \frac{27,500}{(\theta_{3\ db})^2}$ where θ_{3db} is the half power beamwidth. This equation includes a 0.21 db average loss for the cables feeding the array elements. The cable assumed was type H1 helix flexible cable.

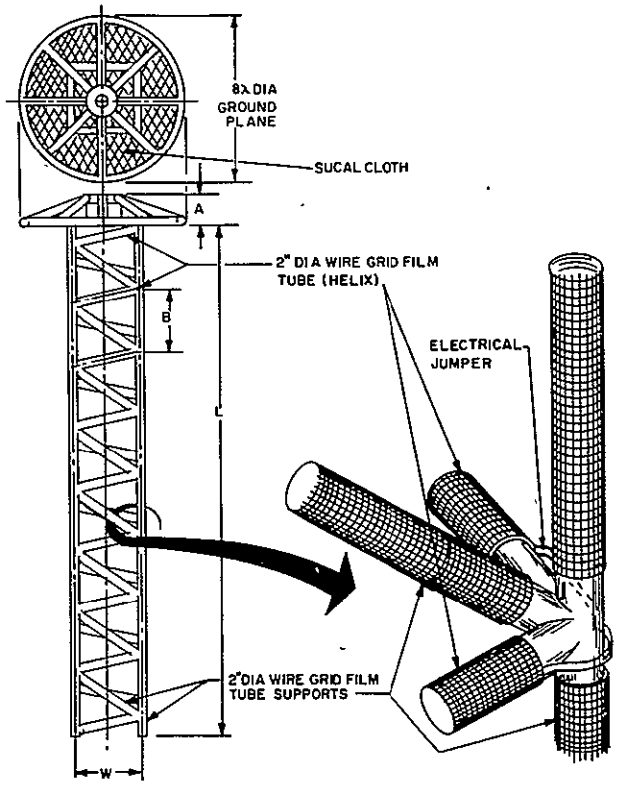

Figure 4.2-3. Helix Element

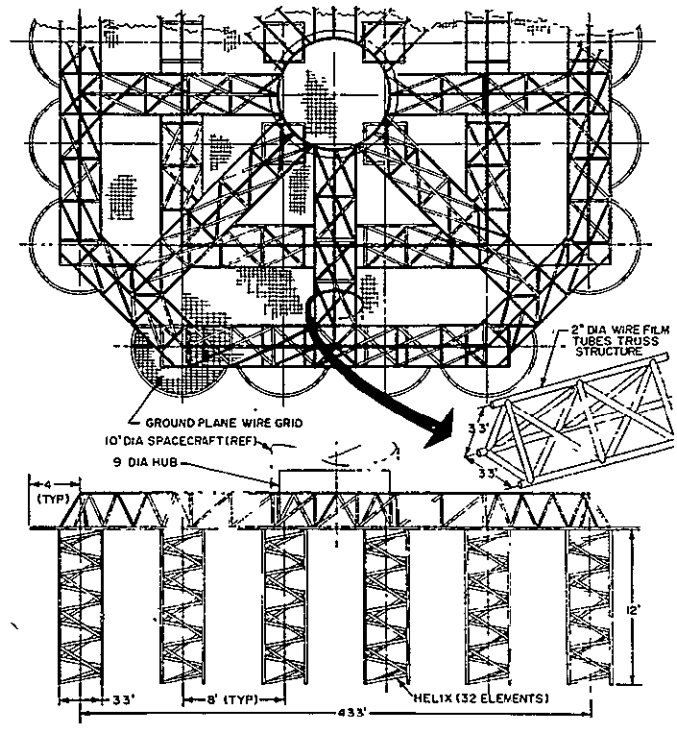

Figure 4.2-4. Helix Array

Structural. The structural characteristics of this antenna are:

Weight	360 lb
Volume	40 cu ft
I_z	2852 slug-ft^2
I_y	1822 slug-ft^2
Solar Area	2000 ft^2
Natural Frequency	0.4 Hz
Thermal Deflection	0.189 ft

4.2.2.3 VHF No. 2 Antenna

4.2.2.3.1 VHF No. 2 Antenna Requirements

Based on the final requirements for this mission, the antenna must meet the following specifications:

Frequency	100 to 108 MHz
Gain	19 db
Beamwidth	18.5 degrees
Scan	±12.5 degrees
RF power	820 watts
Polarization	Circular

A wire grid tube parabola with a diameter of 34.5 feet was selected as best meeting the requirements for this mission. An array of nine helixes was also considered. The fundamental parameters of the helix array and the parabola, both constructed of wire grid tubes, were nearly identical. The parabola was selected on the basis of requiring the least amount of new engineering and development. Other construction techniques were also considered but were discarded because of weight and/or package volume requirements.

4.2.2.3.2 VHF No. 2 Antenna Description

This antenna VHF No. 2 tolerance requirement necessitates 12 radial ribs with a rib depth of 2.07 feet (Figure 4.2-5).

Here the RF feed is somewhat more complicated since prime focus scanning is required. This is achieved as follows:

The feed is supported at 0.35 D by a telescoping column. The column is mounted at the periphery of a 6.5 solid hub. The hub is capable of rotating about the centerline (being motor driven). The extreme of the support column, closest to the feed, has a motor driven coaxial rotary joint. By a combination of these two rotations the feed, which is a 3-ft diameter cavity backed spiral, can be located over any point within a 6.5 ft circle thus providing the desired scan (See Figure 4.2-6)

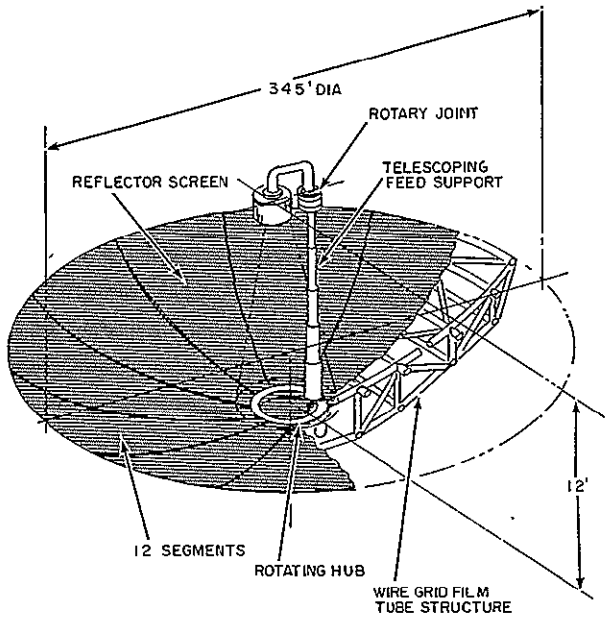

Figure 4.2.5. VHF No. 2 Antenna

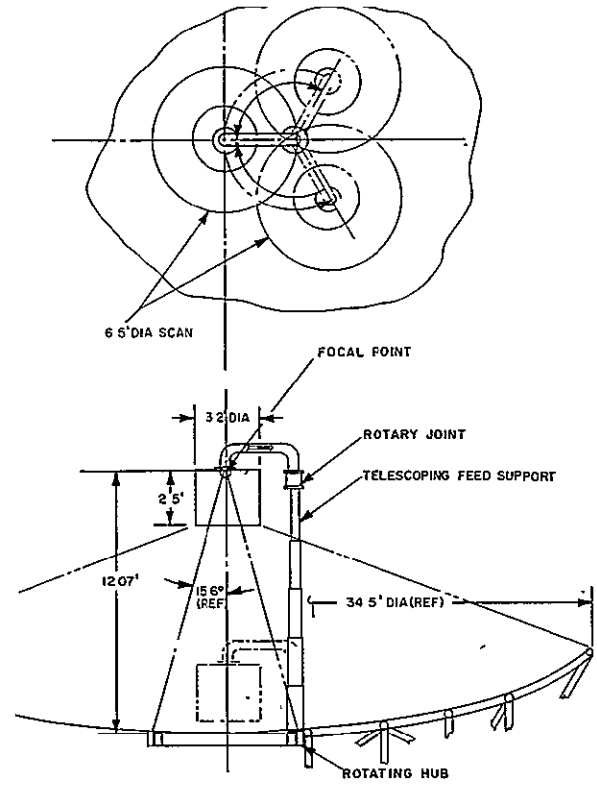

Figure 4.2-6. VHF No. 2 Antenna Feed System

4.2.2.3.3 VHF No. 2 Antenna Characteristics

Electrical.

a. Parabola - A half-power beamwidth of 18.5° for this mission requires a diameter of 34.5 for the parabola. Using an efficiency of 57 percent for this antenna, the following results are generated:

Frequency (MHz)	Beamwidth (deg)	Gain (db)
108	18.5	19.0
100	20.0	18.3

b. Feed - Scanning of this antenna of ± 12.5 degrees which is less than half-power beamwidth can be performed at the expense of less than 1 db of gain. Assuming a beam factor of 0.8, the feed is required to move in a cone of 15.6 degrees as measured from the vertex of the parabola.

Structural. The following data were arrived at for this antenna:

Weight	120 lb (28 lb Feed)
Volume	10 ft^3
I_z	106.9 $slug\text{-}ft^2$
I_y	103.7 $slug\text{-}ft^2$
Solar Area	400 sq ft
Natural Frequency	5.07 Hz
Thermal Deflection	0.14 ft

4.2.2.4 UHF Antenna

4.2.2.4.1 UHF Antenna Requirements

The final mission requirements for this antenna were as follows:

Frequency	850-890 MHz
Gain (at 890 MHz)	33.0 db
Beamwidth (at 850 MHz)	3.65 degrees
Scan	None
RF Power	1.15 kw
Polarization	Circular

A 22.5 foot parabola constructed of wire grid tubing was selected as the most promising antenna for these mission requirements. Several types of construction were considered for the parabola. However, the wire grid tube construction was found superior to the other concepts primarily on the basis of weight and volume.

4.2.2.4.2 UHF Antenna Description

The parabolic antenna is constructed of a wire grid tube truss network covered with a metallic wash sucal cloth RF reflector. The truss network is composed of radial ribs emanating from a central hub and tied together by a series of circumferential tubes. A conservative design tolerance of $\lambda/12$ peak deviations is satisfied for this antenna by 24 radial ribs, each with a depth of 1.38 feet. The reflector is a silver wash grid cloth material made by Suchy Division Inc., New York, N.Y. The antenna is gas inflated until all wire grid tubes have rigidized, the gas is then released through a diffusing orifice to minimize possible spacecraft disturbing torques.

The RF feed for this antenna is a cavity backed spiral located at 0.35 D by a telescoping support rod. This feed is broadband and produces the required polarization.

Figure 4.2-7 is a sketch of this antenna in its deployed condition.

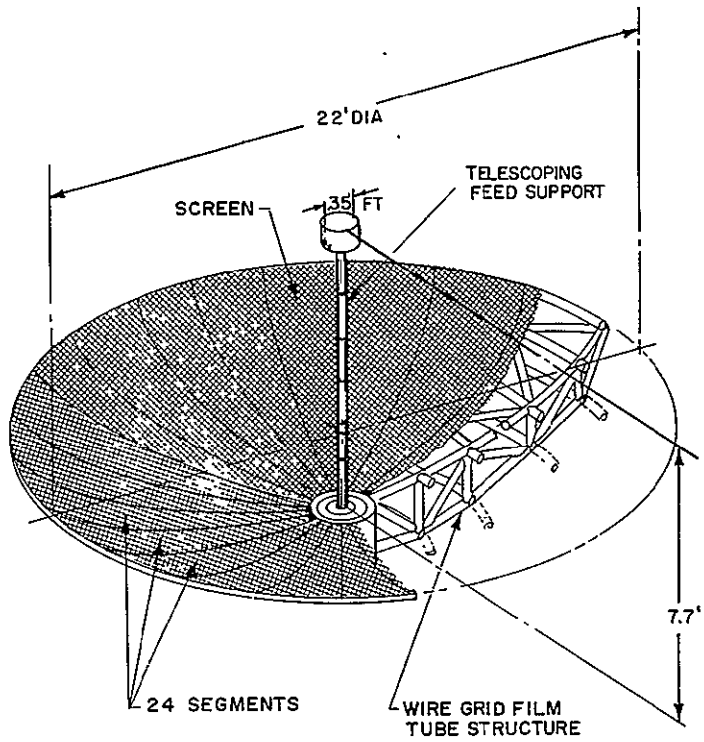

Figure 4.2-7. UHF Antenna, Deployed

4.2.2.4.3 UHF Antenna Characteristics

Electrical. A parabola was selected. A diameter of 22.5 ft, was necessary to provide the half-power beamwidth of 3.75°. Using an efficiency of 57%, the following characteristics were determined:

Frequency (MHz)	Beamwidth (degrees)	On-Axis Gain (db)
870	3.75	33

Structural. The structural analysis results of this analysis for this parabola are:

Weight	91 lb (18.0 lb feed)
Volume	9 ft^3
I_z	75 slug-ft^2
I_y	57 slug-ft^2
Solar Area	196 ft^2
Natural Frequency	8.92 Hz
Thermal Deflection	0.0855 ft

4.2.3 ANTENNA TECHNOLOGY EVALUATION

The purpose of the antenna technology evaluation was to survey and summarize the characteristics of feasible antenna configurations in order to determine which configurations showed promise for VBMS application and to eliminate those which were inherently unsuitable. This survey was carried far enough to select a list of candidate antennas which appeared to justify further study. This further study was iterative, with each candidate being re-examined in successively greater detail, as improved knowledge of mission requirements and constraints became available, until it was possible to select the most appropriate antenna for each VBMS system configuration. Supporting parametric studies were completed to provide a basis for conceptual design of the antennas selected.

4.2.3.1 Antennas Considered

The objective during the initial examination was to choose candidate antenna configurations based on an optimum combination of electrical performance, weight, size, and mechanical parameters. The antennas investigated were:

a. Paraboloid
b. Helix
c. Conical Horn
d. Yagi Uda Arrays
e. Quad Helix
f. Quad Yagi-Uda Arrays
g. Rhombic
h. Disc on Rod, Quad Disc on Rod
i. Vee Antenna
j. Log Periodic, Equiangular Spiral
k. Retro-Directive and Phased Array

A basic description and parametric curves for each of these antenna types were defined to compare types. These are given below along with the reasons for rejecting those found unsuitable.

Paraboloid. Figure 4.2-8 is a plot of gain vs half-power beam width (HPBW) and paraboloid diameter for HF frequencies (15 to 30 MHz), VHF frequency (100 MHz), and UHF frequency (470 MHz). The antenna gain is based on an assumed antenna efficiency of 50 percent and the half-power beamwidth on an assumed edge illumination of approximately 10 db. Assuming a 4 wavelengths limit, the minimum usable diameters are:

Frequency (MHz)	Diameter (ft) G = 19 db.
890	4.5
470	9
100	40
30	130
15	260

Based on diameter only, the paraboloid may be presumed feasible for the UHF and VHF bands of operation and a rather questionable choice for the HF band.

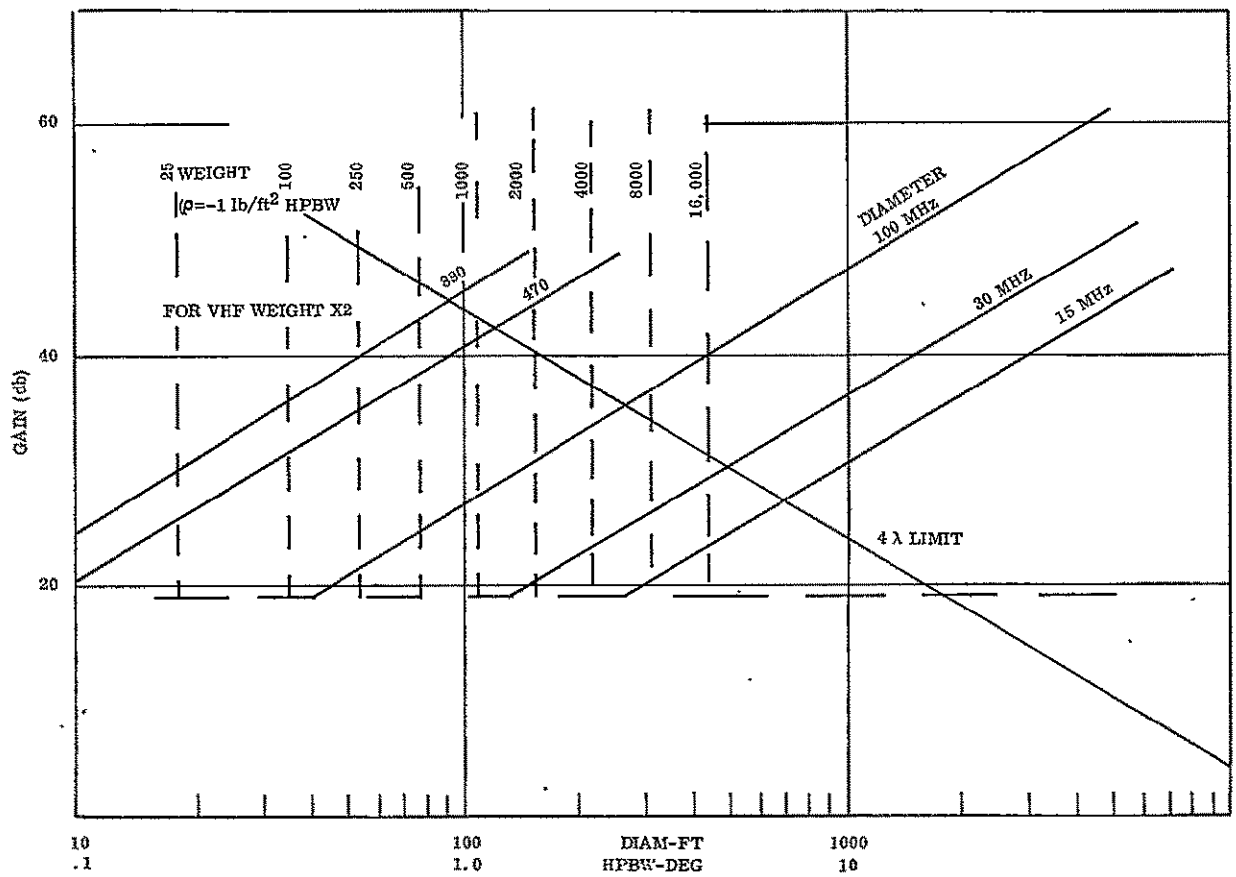

Figure 4.2-8. Paraboloid Gain and HPBW Diameter, Weight and Diameter

Helix. The gain vs half-power beamwidth and Helix length are shown in Figure 4.2-9 for f = 15, 30, 100, 470 and 890 MHz.

The gain and HPBW relation used in generating these curves were:

$$G = \frac{30,000}{\phi^2} \qquad \phi = \frac{60}{C_\lambda L\lambda} \quad \text{for } C_\lambda = 1.2$$

Assuming $S_\lambda = 0.264$ and $C_\lambda = 1.2$ means that the helix gain and HPBW are those existing at the high frequency and of an ≈ 1.5: 1 band (Peak Gain).

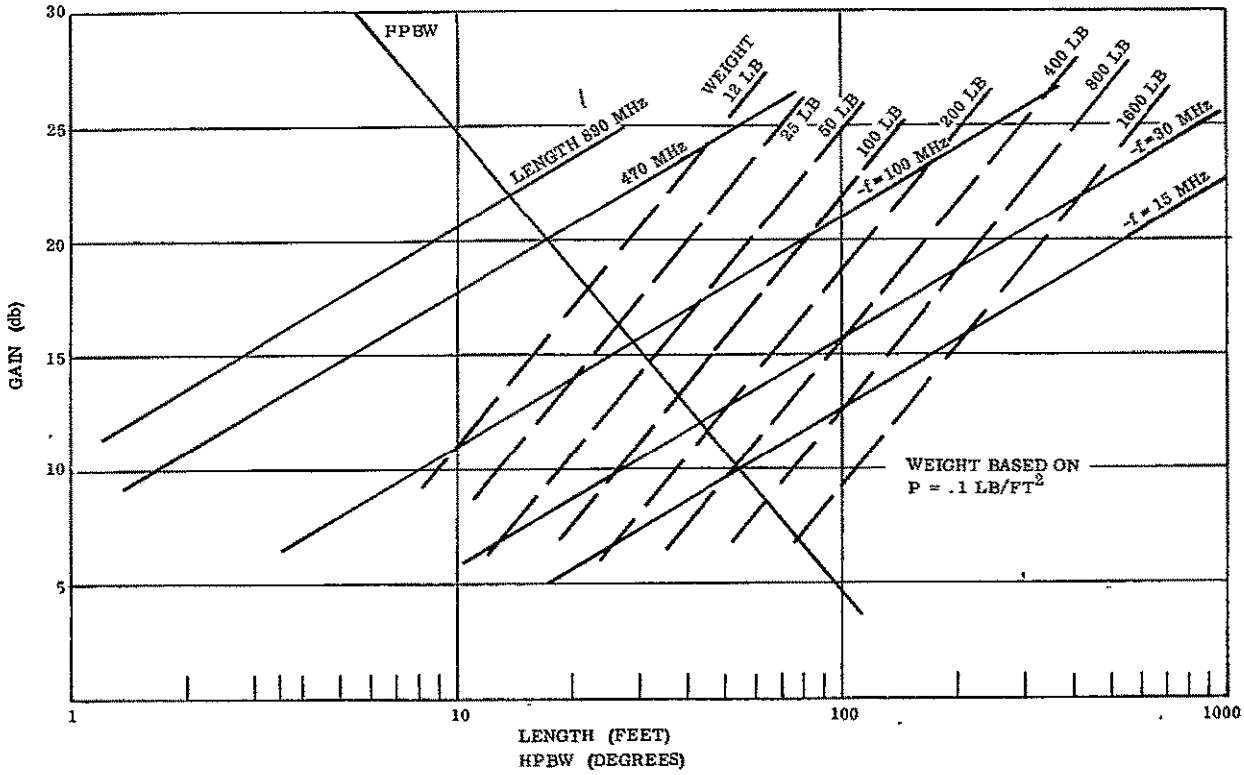

Figure 4.2-9. Single Helix Gain versus HPBW and Length, Weight versus Length

The maximum practical gain of a single helix has not as yet been established. It may be limited by dimensional tolerances. Assumptions of single helix gains greater than 20 db should be made rather guardedly.

Conical Horn. Figure 4.2-10 is a plot of gain vs half-power beamwidth and conical horn diameter. The following relationships were used in generating the curves:

$$G = \frac{A}{\lambda^2} \quad = \text{Gain of conical horn } (TE_{11} \text{ Mode}) \text{ with } 90^\circ \text{ phase error}$$

$$\text{HPBW} = \frac{75}{D_\lambda} = \frac{\theta_E + \theta_H}{2}, \text{ degree}$$

Assumed gain degradation due to phase error = 1.0 db

$$\phi = \frac{D^2}{4L}, \quad d = 0.75 \quad S = \frac{D - d}{2} D_\lambda$$

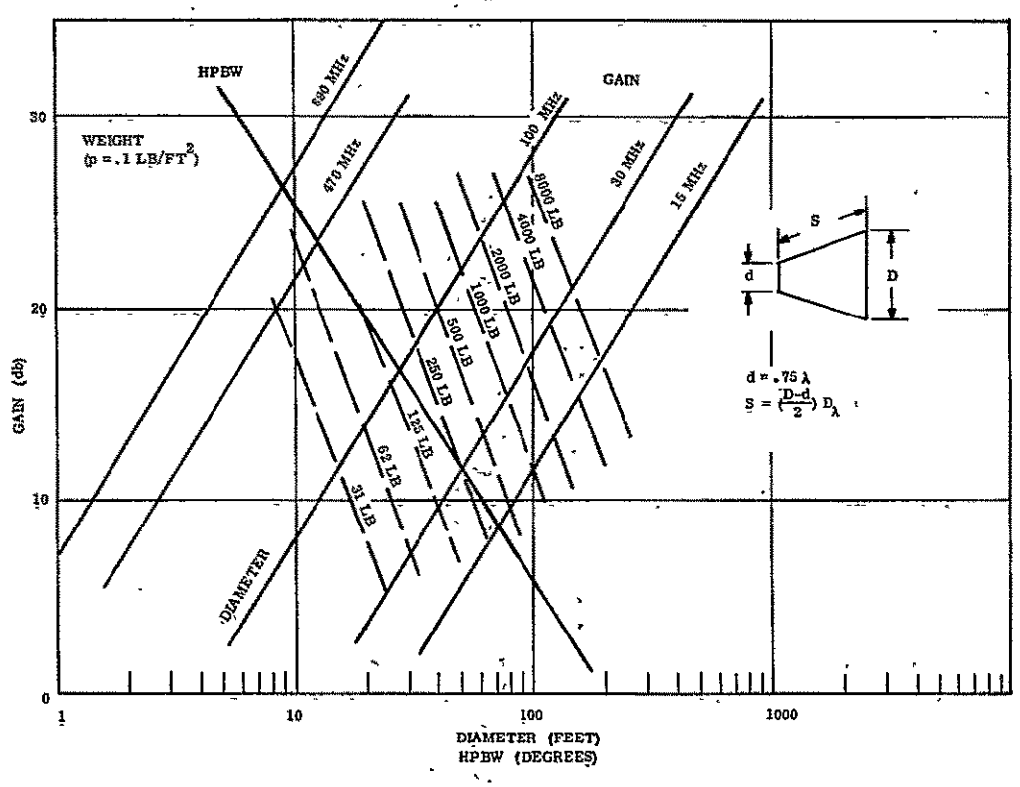

Figure 4.2-10. Conical Horn Gain versus HPBW and Diameter; Weight versus Diameter

Yagi-Uda Array. A limited amount of investigation was done on the Yagi antenna. The basic linearly polarized Yagi is an endfire antenna possessing a single drive element, a reflector element, and a number of parasitic or directive elements. Addition of an orthogonal set of elements and quadrature phasing leads to a circularly polarized design.

Many factors determine the suitability of a Yagi to a particular application. One of the great problem areas, from a basis of antenna design, is that Yagis possessing more than three elements must be empirically designed, since a closed form solution does not exist for the discrete element case. This fact circumvents the availability of the various electrical performance parameters (gain, element number, length, impedance, etc.) which are necessary for performance prediction in the general case. The most salient points of importance pertaining to the Yagi are:

a. Yagi's with gains less than 10 db are usually about 50 to 80 percent as long as a Helix with the same gain.

b. Above 10 db, the lengths required for a given gain of a Yagi or Helix approach each other.

c. Yagi's designed to produce maximum gain for a fixed number of elements are bandwidth limited. This bandwidth may range from 2 to 8 percent.

d. The driving point impedance of a Yagi is generally quite low and an impedance transforme or element modification is required.

As an example of (a) above, an 8 db Yagi can be designed with three elements with a length $\approx$ 0.28λ. An 8 db Helix requires ≈ 2 turns and will be $\approx 0.55\ \lambda$ long.

To illustrate (b) and (c) above, an 18 db gain Helix and Yagi antenna have virtually identical lengths. The expected bandwidth of the helix is 50 percent. The Yagi has less than 10 percent.

The utilization of a Yagi for the FM band is not recommended since gains greater than 20 db can be achieved with Paraboloids or Conical Horns with considerably higher confidence levels than Yagi designs. The AM bandwidth requirements of HF bands at 11 through 19 meters exclude the use of Yagi antennas.

Quad Helix. The Quad Helix is a natural outgrowth of the difficulty encountered in designing a very long endfire array. Theoretically, the gain of a quad array will be 6 db above that of the single elements. This means that a quad array of 4 helices, each of which have a gain of 14 db, will yield 20 db of gain.

For a given single element gain, there is a minimum separation required between the elements of a Quad Helix. This minimum separation calculated on the basis of effective area is plotted in Figure 4.2-11. The ground plane limit which occurs at 15 db, is the separation at which the individual Helix ground planes ($D = 0.8\lambda$) become tangent. In practical designs, the minimum separation would usually be increased by about 20 percent. However, since a particular design would reflect both coupling and array pattern considerations, the minimum separation based on effective area is chosen as applicable for discussion purposes. A table of physical parameters for 19 db Quad Helix antennas is listed below.

Frequency (MHz)	Sm (ft)	Ground Plane (ft)	Element Length L (ft)
890	1.5	2.6	1.8
470	3	5.2	3.5
100	14	24.0	16.0
30	45	79.0	53.0
15	90	142.0	110.0

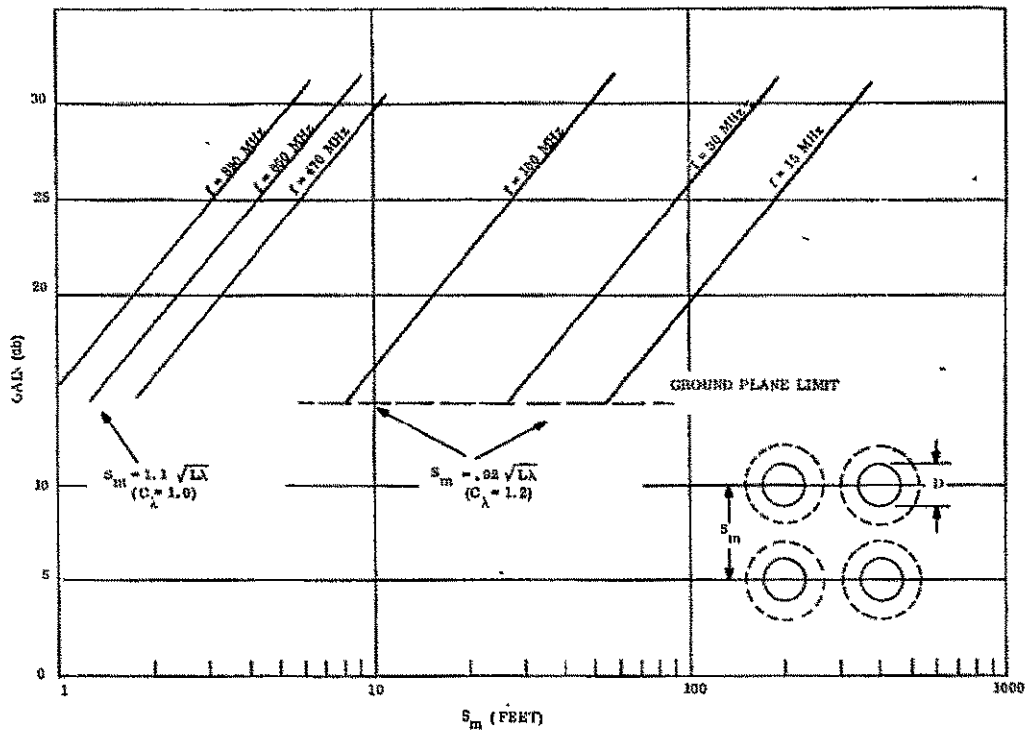

Figure 4.2-11. Quad Helix Gain and Minimum Separation for AM, FM, and UHF

Rhombic. The Rhombic antenna was considered as a transmit antenna contender because of its ease of construction (long wire antennas) and the large bandwidths (on the order of 1.8:1) which are available from the traveling wave versions.

Investigation revealed that the Rhombic is not acceptable due to the antenna efficiency and low gain/bandwidth product.

Disc-on-Rod, Quad-Disc-on-Rod. The Disc-on-Rod antenna is a surface wave antenna, the operation of which is analogous to the Yagi-Uda array. The advantages and disadvantages of the design of the Yagi-Uda array exist identically in the Disc-on-Rod antenna. This antenna is mentioned here because an inflatable version that utilizes Echo Balloon type material that rigidizes under pressure is being developed. Such an antenna promises light weight and efficient packaging and may in some respects be preferable to the Yagi array.

A single Disc-on-Rod antenna is not visualized as suitable for AM or FM applications because of the interference problems this essentially solid skin antenna would create with the up-link and the command and telemetry antennas.

Vee Antenna. On the basis of a GE investigation, the reflector rod Vee antenna configurations have limited performance capabilities, and a considerable amount of analytical and experimental effort would be required to optimize this particular arrangement.

The more favorable performance achieved with the reflector backed antenna is worthy of further investigation. A square horn structure with an extremely steep taper can be built around the Vee (double Vee for circular polarization) antenna. The Vee antenna appears capable of exciting this horn without incurring the large phase errors usually associated with a short, steeply flared horn.

Log Periodic, Equiangular Spiral Antennas. The maximum gains available from the Log Periodic and Equiangular Spiral antenna range from 10 to 20 db.

The primary advantage of this class of antenna is frequency independence. For the broad AM band, the periodic structures have merit.

Retro-Directive Arrays. Retro-Directive Antennas were considered but not pursued in depth due to the following difficulties:

a. Complexity in satellite installation
b. Requirement for ground stations in the broadcast zones
c. Possible two-way propagation constraints
d. State-of-the-art limitations

4.2.3.2 Antenna Selection Criteria

From the preceding types of antennas, the final selection was made based on the constraints listed below and on the basis of minimum weight and ease of packaging:

a. Mission Requirements - These included in particular those requirements that immediately limit the possible candidate antenna types. Beam pointing (not by spacecraft orientation), gain level, and frequency bandwidth were limiting criteria.

b. Dynamic Constraints - As the primary interface is structural, it therefore must meet the dynamic constraints of launch, orbit injection, and final operation modes. Special consideration was given to attitude control constraints in the final operation mode.

The relatively high gain requirements for all mission, the known technology bounds, and the dynamic constraints of the operational mode were used as criteria to discard single element endfire antennas and conical horn antennas for all configurations. In general, neither of the foregoing types are considered practical for the gain values required for these frequency bands.

Arrays of endfire antennas of disc-on-rod and crossed Yagi types were suitable for the planned missions; however, these were discarded due to the relatively complex feed systems and limited bandwidth capability.

For each configuration, a physical form factor plot was drawn comparing the size of arrays of helical elements and the equivalent gain parabola. The helix antenna was chosen as giving an extremely compact array due to the higher relative gain achievable by using the maximum permissible diameter for an axial mode system. The selection criteria between these two candidate antenna systems was resolved as a weight, size and cost tradeoff. Qualitative judgement was used to determine the deployment reliability as being the factor most influencing cost.

4.2.3.3 Structural Type Selection

Many structural methods were reviewed for the candidate antennas. The methods considered were the inflatable, telescoping mechanical elements and chemical rigidizing technologies. Deployment and packaging concepts were generated for each of these structures. The wire grid tube film was selected as the structural element for all candidate antennas to illustrate the capabilities of advanced structural and deployment techniques.

The wire grid type was selected from among the candidate structure types because more design data has been developed on this type, thus permitting the analysis given in this section. The major disadvantage of the wire grid tube techniques (as with other advanced techniques considered) is that more development and ground testing will be required to verify design values.

The primary structural element of the antennas is a 2-inch diameter wire grid tube. The elements of the cylindrical tube are wires that are oriented in the longitudinal and circumferential directions. This 1/8 inch by 1/4 inch 10-mil aluminum wire grid is bonded to 2 layers of 1/4-mil Mylar film to provide the pressure vessel required for deployment of the tube from its packaged condition.

The distance between circumferential wires is set equal to one-half of that between the longitudinal ones so that, under 2:1 stress ratio of the pressurized cylinder, each wire is subjected to the same stress level. When the pressure is increased to a point at which the stress in the wires exceeds the yield strength of the wire material, the wire-grid-tube is rigidized. This means that the tube will retain its deployed shape after the inflation pressure is removed. By employing wire-grid-tubes, large antennas and support structures can be relatively lightweight, compactly packaged, reliably deployed, and dimensionally accurate for these frequency ranges.

Wire grid tube structures can be easily deployed by compressed gas and do not require pressure after initial deployment. Testing in a 1g field can be achieved by maintaining pressure in the tubes to compensate for the effect of gravity. Due to the grid type wire spacing, relatively high RF power can be radiated by antennas built of these tubes. The tube construction in some cases allows relatively small solar area(which can be made even smaller by photolyzing film).

In summary, the characteristics of wire grid tube construction are:

a. Low weight
b. Small packaging volume
c. Low solar area
d. Ease of deployment
e. High RF power capability
f. High strength and stiffness to weight ratios

4.2.3.4 Wire Grid Tube Structural Analysis

Symbols		Units
I	Inertia	Slug-ft^2
f	Frequency (Mechanical)	Hz
F_{ty}	Yield Strength	psi
p	Inflation pressue	psi
d	Wire diameter	inch
R	Tube radius	inch
$S_{,}$	Longitudinal wire spacing	inch
w	Unit weight	lbs/inch
γ	Density	pci
t	Thickness	inch
A	Area	inch^2
E	Modulus of elasticity	psi
δ	Deflection	inch
P	Load in a truss member	lb
P_1	Load in a truss member due to the dummy unit loading	lb
W_1	Total structural weight per truss	lb
W	Feed weight	lb
α	Angular acceleration	d/sec^2
g	Acceleration due to gravity	ft/sec^2
ℓ	Beam length	ft
EI	Flexural stiffness	lb-ft^2
h	Beam depth	ft
k_s	Constant for shear effects upon deflection	
k_f	Constant for shear effects upon natural frequency	
α	Linear coefficient of thermal expansion	in./in./^{o}F
T	Temperature differential	

Subscripts

B	Beam	f	Film	t	Thermal
w	Wire	T	Truss		

Results

The analysis was carried out on the wire grid tube element described earlier in the report. Its properties are listed below along with the loading conditions that were considered for all of the antennas. The numerical results are listed in Section 4.2.2.

a. Tube - 2-inch diameter, 10-mil aluminum wire at 1/8 inch by 1/4 inch grid with 2 layers of film, each of 1/4-mil Mylar

Inflation pressure:

For soft aluminum $F_{ty} = 6000$ psi

$$\therefore \quad p = \frac{F_{ty} \pi d^2}{2 R S} = \frac{(6000)\ \pi\ (10)^{-4}}{(2)\ (1)\ (0.25)} + 3.78 \text{ psi}$$

Unit weights:

Inflation gas (air), $w_a = \frac{(3.78)}{14.7}\ (0.07635) - 0.0196$ pcf

Wire, $w_{ws} = 2\pi R\ \frac{3}{8}\ \frac{\pi d^2}{4}\ \gamma w$

$$= 2\pi(1)\ \frac{3}{0.25}\ \frac{\pi \times 10^{-4}}{4}\ (0.1) = 5.95 \times 10^{-4} \text{ lb/in}$$

Film, $w_f = 2\pi R\ t_f \gamma_f = 2\ \pi\ (1)\ (5 \times 10^{-4})\ (0.05) = 1.57 \times 10^{-4}$ lb/in

$$w_w + w_f = 7.52 \times 10^{-5} \text{ lb/in}$$

Tube Stiffness:

$$AE = E \frac{\pi d^2}{4S}\ (2\pi R) = (5 \times 10^{6*})\ \frac{\pi \times 10^{-4}}{1}\ (2\pi) = 9,860 \text{ lb}$$

b. Loading Conditions - Inertia loads due to an angular acceleration of 2×10^{-3} degrees per second square were considered. For the arrays and the paraboloid, the acceleration was applied at a point on the axis of the rotational symmetry located 5 feet behind the platform or the vertex of the dish.

$$\delta T = \frac{p_1^{\,p}}{AE} \qquad (1)$$

This was then compared to the bending deflection as given for a beam under the triangular distributed inertia loading, i. e.,

$$\delta B = \frac{11 W \alpha \ell^4}{120 gEI} \tag{2}$$

The difference of these deflections represents the shear deflection. Since the ratio of the truss to beam deflection depends upon the depth to span ratio, the above comparison was used to determine the constant, k, in the general expresssion,

$$\frac{\delta T}{\delta B} = 1 + k\frac{h^2}{\ell} \tag{3}$$

The deflections of the remaining antennas were determined by the applicable beam equations along with a factor as given by equation (3) to account for shear effects.

c. Natural Frequency - For a cantilevered beam of constant stiffness, the natural frequency is given by:

$$f_B = \frac{3.52}{2\pi\ell^2} \qquad \frac{EIg\ell}{W} \tag{4}$$

Again, to account for shear deflections, equation (3) was used. Since the natural frequency is proportional to the square root of deflection, the beam frequency was reduced by,

$$K_f = \frac{\delta B}{\delta T} \tag{5}$$

$$\text{Then } f_T = K_f f_B \tag{6}$$

d. Thermal Deflection - The thermal deflection equation for a constant depth component with one end held and the other free was applied, i. e.,

$$\delta_t = \frac{\alpha \Delta T \ell^2}{2h} \tag{7}$$

e. Solar Pressure - For each antenna, the view that presents the greatest projected area was determined by inspection. The total of the projected tube lengths was determined and multiplied by the tube diameter to yield the solar area.

f. Moments of Inertia - The moments of inertia equations for a square helix and a parabolic dish with an f/D = 0.4 are given below:

SQUARE HELIX

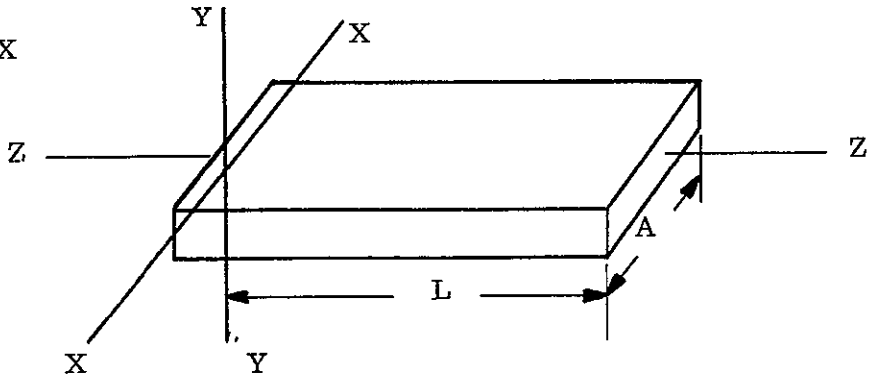

$$I_z = \frac{W_1 A^2}{96.51} \quad (\text{slug ft}^2)$$

$$I_y = I_x = \frac{W_1}{386.04} \quad (2A^2 + 4L^2) \quad (\text{slug ft}^2)$$

PARABOLIC DISH (WITH FEET)

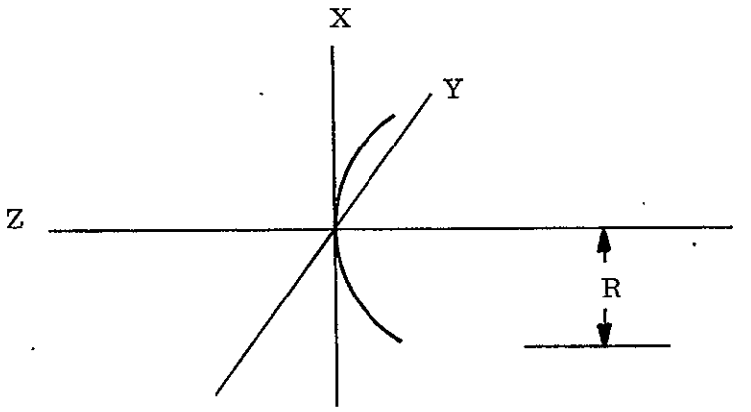

$$I_z = 0.0119\, R^2 W^*$$

$$I_x = I_y = 0.0067\, R^2\, W^* + \frac{W^t L^2}{96.6}$$

---

* Dish structural weight

t Feed weight

4.2.3.5 Packaging and Deployment

Antenna Packaging and Deployment

a. Packaging - The packaging arrangements will essentially be the same for any of the proposed antennas. The antenna is packaged in and around the hub, with the hub forming part of the canister.

   The air (gases) is removed from the antenna tubular members. With the tubes collapsed, the antenna trusses or elements are packaged using "accordion" folds. The folded members are placed in the canister so each section will deploy in proper sequency.

   The antenna packaging volumes will vary due to the number and type of tube joints or truss intersections.

b. Deployment - All of the proposed antennas have essentially the same deployment mechanism. The energy source for the required forces of deployment is proposed to be a gas stored at high pressure (3000 psi).

A schematic of a typical deployment system is shown in the following Figure 4.2-12. The system will provide a controlled inflation-deflation sequence for antenna deployment. After receipt of a command signal, the deployment sequences will initiate the squib actuated main control valve, thereby releasing the stored gas and simultaneously opening the solenoid shutoff valve. A pressure reducer and control orifices will control the gas flow so that the desired deployment rates are achieved. Controlled exhaust of the deployment gas will begin immediately after the design pressure is attained and the antenna is fully deployed. All gas will be expelled through a throttling and diffusing arrangement at the hub so that the net thrust of the exhausting gas produces no overturning moments.

4.2.3.6 Electrical Analysis

A special analysis of the electrical properties of the Warren Truss helix element was conducted. The helix element was considered to be superior to other endfire antennas on the basis of its large frequency bandwidth capability. The relatively high gain characteristics related to its size and weight made the helix element a prime candidate for phased array applications. The Warren Truss type method of the wire-grid tube construction however, posed a critical electrical/structural interface. Experimental work on a helix model was completed to determine the effect of the structural members on the basic helix characteristics and to confirm its frequency bandwidth capability.

Analytical

A literature survey was made to determine appropriate gain, beamwidths, and bandwidths for various helices. Krauss investigated thoroughly, both analytically and experimentally, helixes whose length is about one wavelength. For longer helixes, it is necessary to use the work of Maclean. Maclean investigated both gain and bandwidth of helixes up to 86 wavelengths long. His results are summarized below as they apply to this program. An empirical gain equation was found that satisfies not only Maclean's data for long helixes but also the data of Krauss.

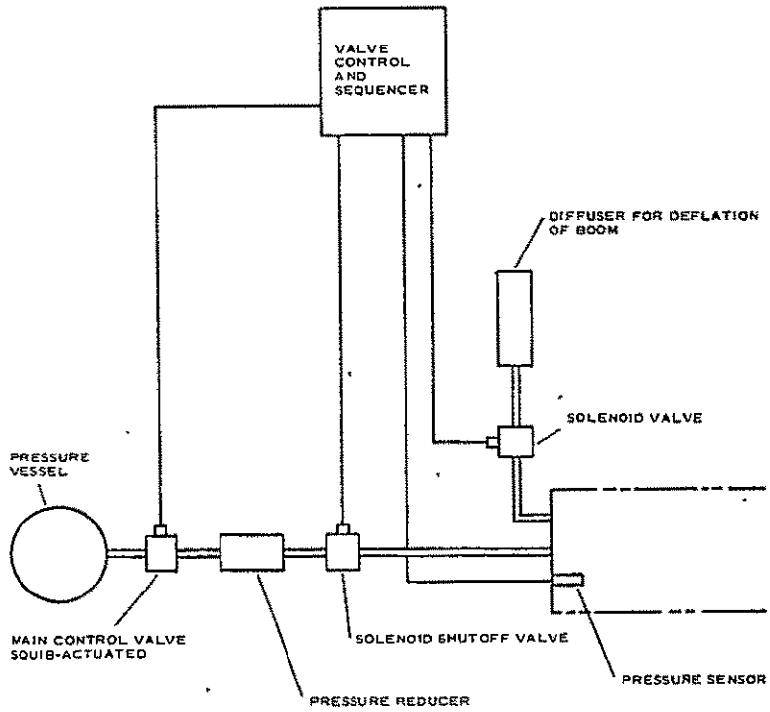

Figure 4.2-12. Proposed Deployment System

The bandwidth of helical antennas is dependent upon the pitch angle, ψ and the length per unit wavelength. The upper cutoff frequency of these antennas is defined as where the sidelobe level has increased to 45 percent of the main beam. The lower cutoff frequency is taken as that frequency at which the appropriate transmission mode fails to be launched.

The lower frequency cutoff at which the number of waves being propagated on the helix is reduced by one-half is a function of the pitch angle ψ. Figure 4.2-13 shows the dependence of the lower cutoff value $C\lambda$ on the pitch angle ψ.

The upper frequency limit is a function of the number of turns on a helix. The number of turns, in addition, is a function of the length, diameter, and pitch of the helix

$$N = \frac{L\lambda}{C_\lambda} \quad \text{ctn}\,\psi$$

Figure 4.2-14 shows this dependence.

It can be seen from the figures that for a given length the bandwidth is virtually constant.

Maclean has also investigated, (see Figure 4.2-15), the power gains of helix antennas up to 86 wavelengths long. His experimental gain was only given for C_λ's less than 0.9.

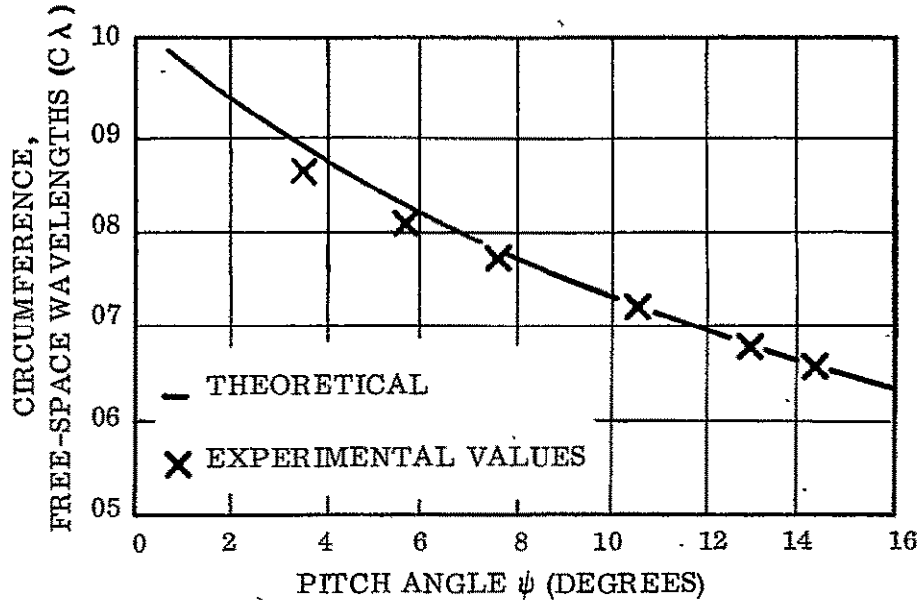

Figure 4.2-13. Dependence of Lower Cutoff Frequency on Pitch Angle

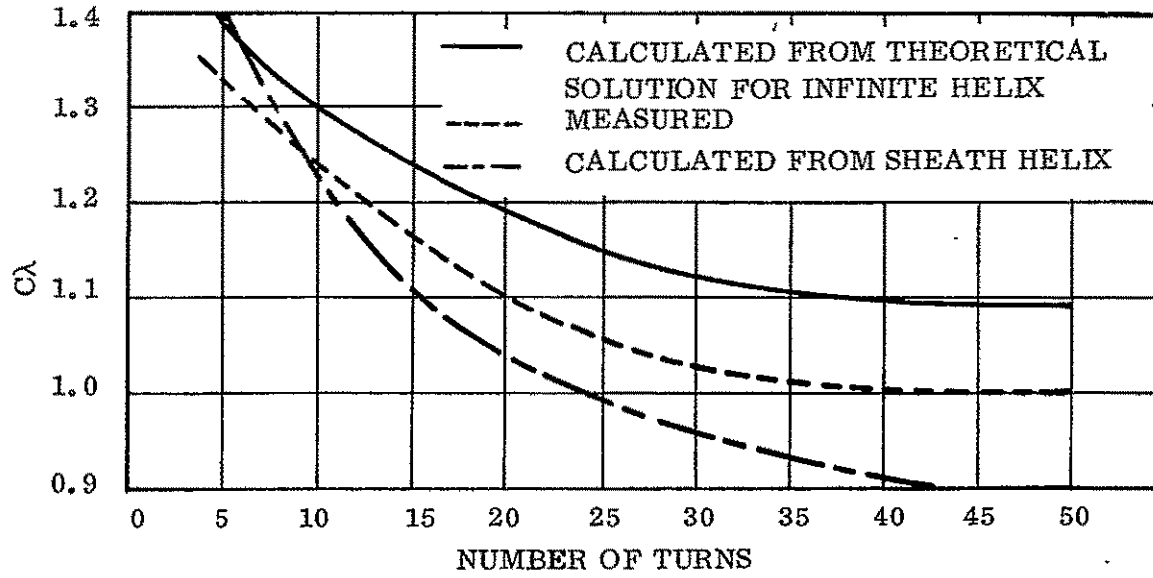

Figure 4.2-14. Upper Frequency Limit and Number of Turns for $\psi = 13^{\circ}$

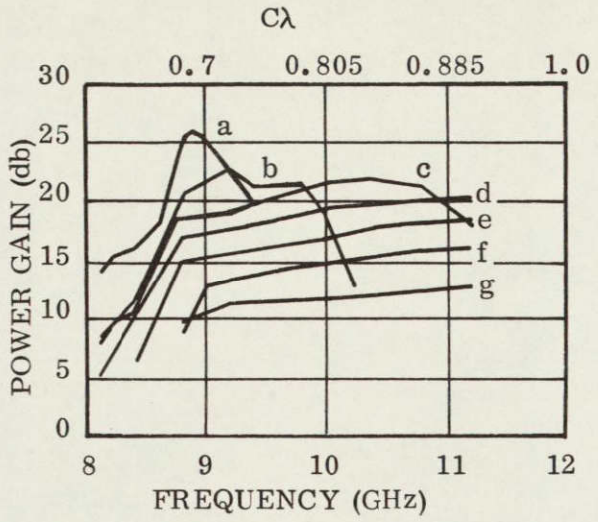

CURVE	LENGTH IN λ AT 8-7 Gc/s	TURNS ON HELIX
a	86	556
b	43	278
c	21.75	139
d	10.9	69
e	5.4	35
f	2.7	17
g	0.95	6

Figure 4.2-15. Power Gain of Helical Antenna

The following empirical equation was derived from this data. This equation agrees to within 1 db of the experimental data. It is also in reasonable agreement with Krauss' data for shorter helices. The equation is

$$G = 21^{*}\ C_{\lambda}^{\ 2}\ L_{\lambda}^{\ 2/3}$$

The preceding data indicates that for a given number of turns, when the passband exists between $0.76C_{\lambda}$ and $0.9C_{\lambda}$, the gain increases as (at least) C_{λ} to the third power, and in some cases to a power greater than 4. It is doubtful that these shorter helixes will continue to increase at this rate throughout the entire passband. This is shown to be a reasonable assumption in that the long helixes, whose passband is contained within the 0.76 to $0.9C_{\lambda}$, show a definite leveling off in gain at their upper frequencies.

*Constant was determined at 0.9C

Experimental

An experimental program was initiated to investigate the following helix characteristics:

a. Pattern degradation versus structural loading

b. Bandwidth versus helix length

c. Gain and beamwidth versus helix length

A first attempt (Figure 4.2-16) consisted of a 10λ square helix. The dimensions are as follows:

(1) Length 55.5 in.
(2) Side 1.48 in.
(3) Pitch 1.47 in.
(4) Ground plane 6 in.
(5) Wire diameter 0.12 in.
(6) Wire length 23 ft
(7) 37 Turns

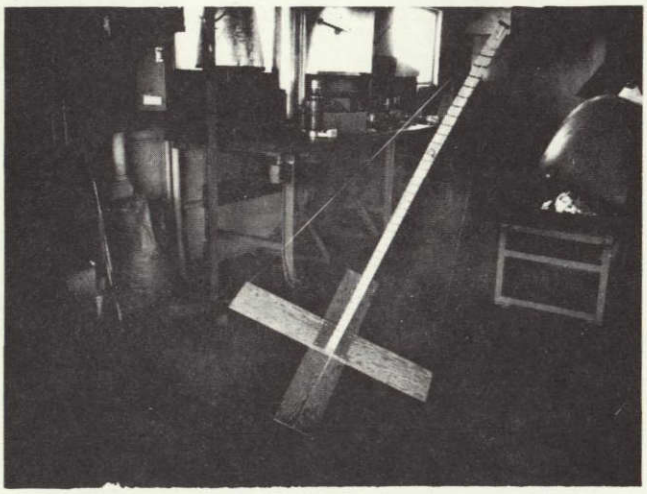

Figure 4.2-16. Scale Model 10λ Helix

The helix was designed to operate at 2.0 GHz. Figure 4.2-17 depicts the dimensions and major components. The helix winding used a solid balsa wood column for mechanical support. Nylon cord was used to guy the helix to the ground plane structure.

The prime purpose of these test was to determine the effects of certain structural members on the operating characteristics of a helical antenna. The helix operates in the endfire mode with a half-power beamwidth of approximately 17^{o}.

Pattern tests were performed on an antenna test range 100 feet in length and approximately 25 feet above ground.

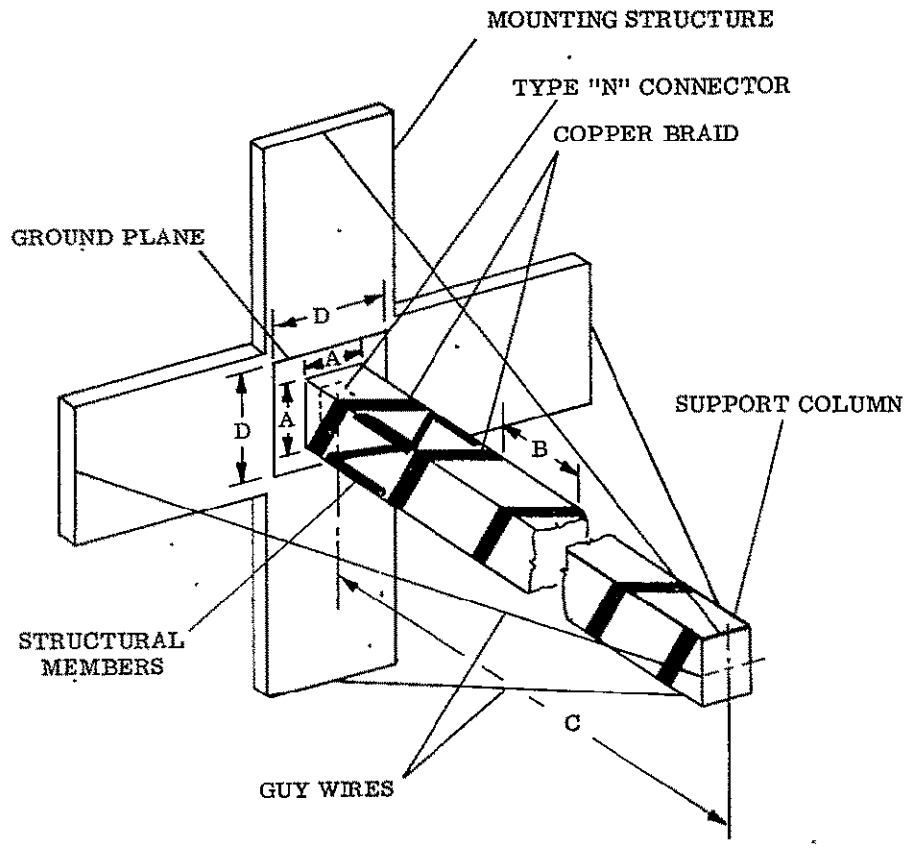

HELIX-MODEL GEOMETRY					
SUPPORT COLUMN	A	B	C	D	DESIGN FREQUENCY
BALSA WOOD	1.43	1.47	55.5	6.0	2.0 GH_z (37 TURNS REF)
URETHAME FOAM	1.9	1.9	17.1	11.4	1.5 GH_z (9 TURNS REF)

Figure 4.2-17. Scale Model 2λ Helix

The test procedure evolved as follows. At each frequency, the two orthogonal principal plane patterns were recorded. The helix was rotated about its long axis and received signal level monitored to determine circularity. In some cases, for gain measment, the antenna was matched by the use of double stub tuner and a slotted line.

Testing was performed in the following sequence:

a. Patterns were recorded and circularity checked on the helix at 2.4, 2.2, 2.1, 2.0, 1.8, and 1.6 GHz. Gain measurements were made at those frequencies where the helix was operating in the endfire mode.

b. The longitudinal structural members were put in place on the test model. Patterns were recorded and circularity checked at 1.8 GHz.

c. The diagonal structural members were set in place on the model. Patterns were recorded and circularity was checked at 1.2, 1.4, 1.6, 1.8, 2.1, and 2.2 GHz.

To gain further knowledge on these types of helixes, a shorter model was built. The prime purpose was, again, to measure pattern breakup as a result of the structural loading. Another important characteristic to be determined for this shorter helix was the usable bandwidth. Gain was again considered only secondarily.

The model was scaled from a designed helix based on Maclean's data operating in the AM band. This HF (25.85 MHz to 15.1 MHz) helix design was as follows:

Assume:

a. L/λ at 15.1 MHz = 1.7
b. C/λ at 15.1 MHz = 0.75

Results in: (for circular helix)

a. D = 15.6 ft
b. L = 111 ft
c. $\alpha = 14^{o}$
d. N = 9 turns

This model was then scaled 75:1 in frequency so that

15.1 MH became 1.125 GHz

The scaled dimensions for the circular helix are then:

a. D = 2.5 in.

b. L = 17.76 in.

c. $\alpha = 14^{o}$

d. N = 9 turns

Radiation patterns from the above tests are shown in Figures 4.2-18 and 19.

Conclusions

a. If the bandwidth is defined as that region where an endfire lobe is formed, then the results are in good agreement with Maclean's work.

b. The addition of structural members does reduce the bandwidth of the 2λ helix antenna from 1.85:1 to 1.4:1.

c. The gain of the test model is somewhat lower than that which would be expected from either Krauss' curves or the estimating formula.

$$G = \frac{27,000}{(\text{HPBW})^2}$$, or Maclean's results (for equal beamwidths in both planes)

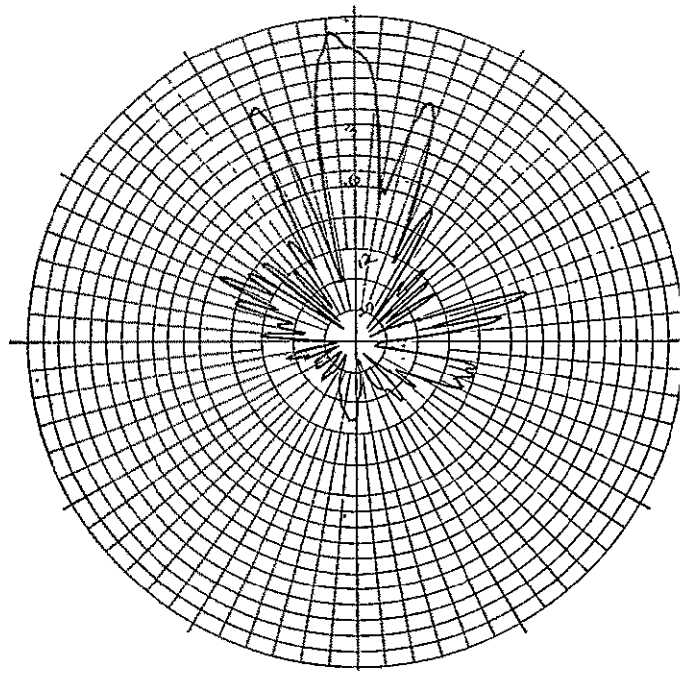

a. With Members

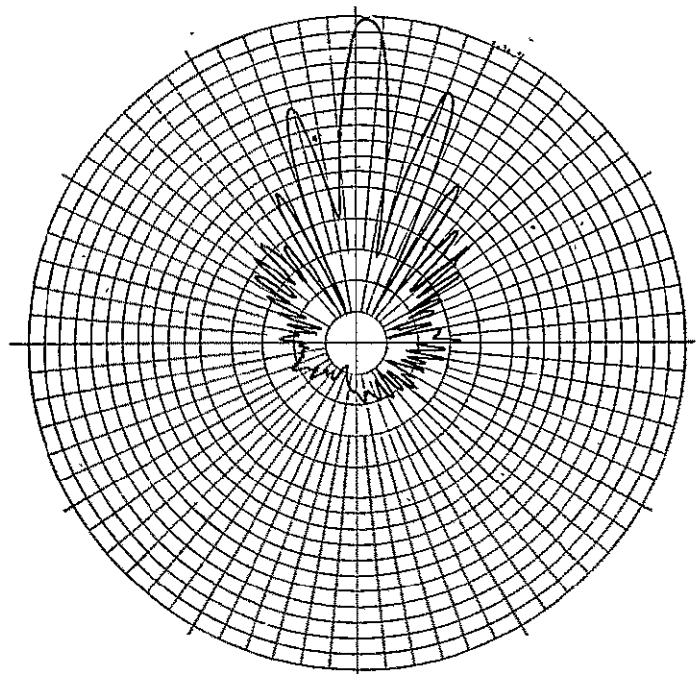

b. Without Members

Figure 4.2-18. Radiation Patterns for 10λ Helix With and Without Longitudinal and Diagonal Members.

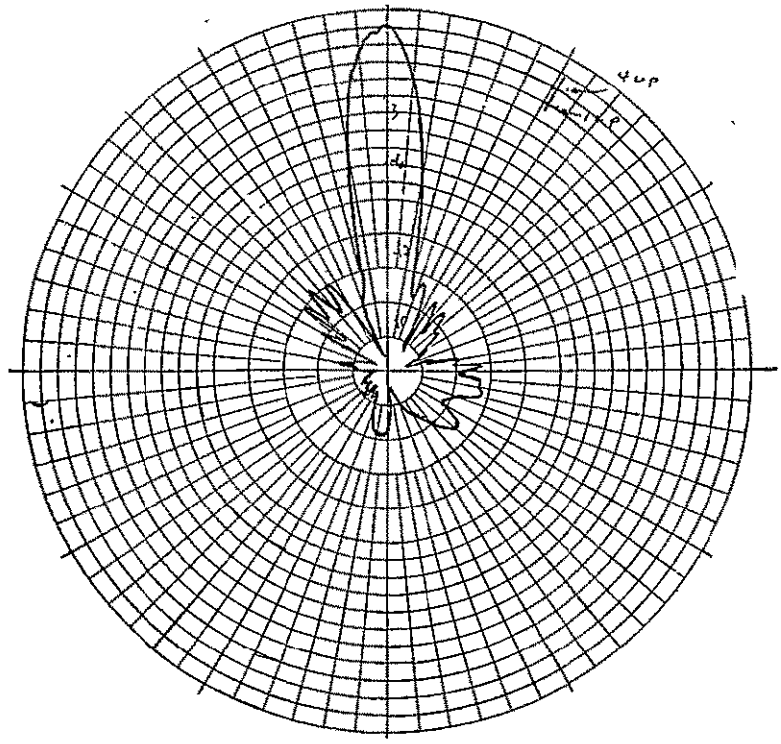

a. With Members

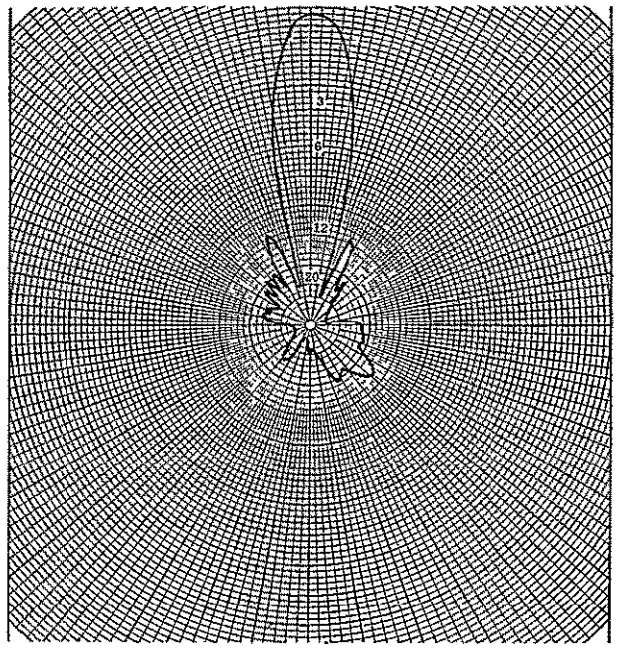

b. Without Members

Figure 4.2-19. Radiation Patterns for 2λ Helix With and Without Longitudinal and Diagonal Members.

4.2.3.7 Electronic Control of Phased Arrays

Phased array antennas were employed on the HF and VHF No. 1 configurations. A solid state transmitter fed each of the antenna elements of the array. An electronic control technique for the phased arrays was employed.

The north-south and east-west pointing of the beam can be controlled by separate 5-bit words sent by ground command as part of the uplink transmission. On typical missions the north-south angle will be fixed during an orbit for a particular earth coverage sector. The east-west angle would be stepped by approximately 2-percent increments at a maximum rate of one step every 3/4 of a second.

The north-south and east-west commands are translated into dc voltages by two 5-bit digital to analog converters. The output of each converter is fed to a resistive divider which divides the voltage into equal fractions.

These two sets of voltages from the N-S and E-W converters are combined in a matrix to produce a unique control voltage for each element. Each antenna element is driven by a separate transmitter which in turn is driven through a low level (1 milliwatt or less) varactor phase shifter from a common RF signal. Each phase shifter will be controlled by the sum of the N-W and E-W voltage derived from the digital to analog converters and dividers.

4.3 SATELLITE TRANSMITTER

4.3.1 INTRODUCTION

The satellite broadcast electronics is composed of the receiver, translator and transmitter. The transmitter consists of the amplifiers necessary to raise the power from the milliwatt level supplied by the translator to the required output power level. The HF transmitter also includes an audio modulator. This section of the report discusses primarily the high level power amplifiers and the necessary active devices. The translator is discussed as part of the satellite receiver in Section 4.4.

4.3.1.1 Summary

For all configurations, the crucial parameters of the satellite transmitter are centered around the power amplifiers. The areas where there are major problems:

a. RF Powers

b. Efficiency

c. High peak power demands

d. Thermal control requirements

e. Life and reliability

The VBMS system requirements which precipitated these problems:

a. High Power Levels - The anticipated requirement of some configurations for relatively high levels of radiated power made the question of efficiency and peak-power requirements critical because of the high costs of prime power capability in spacecraft. In addition, because even at high efficiencies a considerable power loss remains, the problem of rejecting the resulting heat would place a considerable burden upon the thermal control subsystem.

b. Long-Life Reliability - The requirement for a 2-year mission life with very high probability of successful completion posed problems because of the difficulty of developing active devices which would be reliable for 2 years operation. Attempts to this problem imposed solve difficulties of their own; e.g., efficiency for derated devices, and circuit complexity for redundant arrangements.

One of the major choices which had to be made was between vacuum tubes and transistors for the power amplifiers. Transistors tend to be more rugged, reliable, and at the lower frequencies more efficient than vacuum tubes; however, for the time scale of the VBMS, transistor power amplifier efficiencies decrease drastically at the high frequencies (UHF).

4.3.1.2 Conclusions

It was determined that between tubes and transistors, efficiency cross-over was likely to occur somewhere between 200 and 500 MHz. Below that range transistors would be quite efficient. On this basis and the basis of other considerations (ruggedness, reliability, etc.) transistors were selected for the HF and the two VHF configurations. Vacuum tubes were selected for the UHF configuration when transistor efficiencies are unacceptable. Special power combining circuits and, for the HF configuration, a special AM circuit, supported the effective use of transistors. The lower level circuits presented no serious problems. All lower level circuits and components are readily available. As a result, the study emphasized only the high level circuit and component problems.

The technical performance of all the required power amplifier devices can be achieved with state-of-the-art techniques. Specifically, only a minor modification of any one of several existing transistors is required to achieve the power levels and efficiencies used in the transmitter designs. The hybrid-combining techniques conceived in the design analysis of this study permitted the use of large numbers of low power devices to achieve the required high output powers. This approach achieved the maximum efficiency by requiring a simple modification to upgrade the efficiency of existing low power transistors by increasing their operating voltage levels.

The GE-7399 tetrode was selected for the UHF transmitter from among all the vacuum tube types considered because it is the only known tube operating at this power level that has both (1) a sufficient ruggedness to withstand the launch environment (due to its ceramic construction) and (2) a long-life capability established in operational service.

Even the selected tube is marginally adequate for a demonstration of 2 years of continuous operation. New approaches are necessary as operational life requirements are defined in excess of 2 years.

The major characteristic which determines tube life is the cathode depletion rate. Advances in the state-of-the-art are underway to develop cathodes with many tens of thousands of hours of life at high current densities (necessary for high power level). An example is the GE L-64 tube, now in pilot production, which uses a Phillips cathode. Phillips has predicted a cathode life of 8000 hours at 2 amps/cm^2 and 70,000 hours at 0.6 to 0.7 amps/cm^2. To utilize these advances in space applications, however, will require several years for the cycles of manufacturing design refinement and extensive testing necessary to flight qualify the life capability of production tubes.

4.3.2 TRANSMITTER SELECTION

4.3.2.1 HF Transmitter Selection

The HF transmitter was required to operate in the 15.1-25.85 MHz frequency range, providing approximately 5910 watts of radiated power into a 16-element array or approximately 369 watts per element.

A transistorized power amplifier was selected, using a high voltage version of the 2N3950 modified type transistor, which must be qualified. The selection was made on the basis of efficiency, ruggedness and reliability. The characteristics of the transmitter are discussed below. Figure 4.3-1 shows a single, eight-unit HF transmitter. (There are 16 units of this type in the transmitter).

The carrier power output is 5.91 kw; the transmitter efficiency, calculated as RF power to solar array power total is 59%. The bandwidth is 15.1-25.85 MHz, to allow any of the four carrier frequencies to be transmitted. The volume of the transmitter is 0.43 cubic feet and the weight is 22 pounds. The transmitter will have the form factor of a thin package. The power output will be supplied by 128 silicon transistors. The solar array output, at the correct transmitter voltage, will require no power converter. Modulation will be achieved by digital synthesis, as shown in Figure 4.3-2 and discussed below. The power output of the transistors will be combined by hybrids for each of the 16 individual transmitters.

There is one of these transmitters for each of 16 antenna elements. The input carrier level is 1.88 mw or one-sixteenth of the receiver carrier power output. This signal is amplified 39.9 db to 18.4 watts. This signal is divided between the eight output devices. Each device receives carrier power at 2.3 watts and amplifies 13 db to a power level of 46 watts. Each of the 16 transmitter units therefore supplies 369 watts for a total carrier power of 5.91 watts. Each of the 16 transmitter units therefore supplies 369 watts for a total carrier power of 5.91 kw. Because the carrier is 100% amplitude-modulated, peak power must be four times this carrier power. The carrier is modulated by turning each of the eight devices either off, one-quarter on, or completely on. The output power is combined in hybrids.

Digital Synthesis

AM Technique. The AM transmitter requires special explanation. Transistor power gains are optimized for a range of collector currents. As the current increases above this range, the gain drops rapidly. Therefore it is impossible to achieve a 4:1 ratio of peak to average power as required in 100% AM by collector modulation unless the stage is operated well into the Class A region at carrier level. This would result in low efficiency. In addition, because the gain decreases with increasing power output, it would be necessary to modulate the drive power. Operation as a linear amplifier is possible, but results in extremely low efficiency because of very limited peak to average power capability.

To produce 100% modulation with maximum efficiency, a digital technique is used. The AM wave form is synthesized out of 20-microsecond pulses generated by high efficiency Class C pulse amplifiers. The power is varied by turning on the proper number of amplifiers in the array. A 3 db loss in power would result if one amplifierwere operated into a hybrid with the other amplifier off. To reduce this loss, the amplifiers are operated at two power levels by switching their collector voltage from one-half voltage to full voltage. Therefore, each hybrid can be varied in 4 steps; i.e., 0%, 6%, 25%, 57% and 100% of full power. By turning on in this manner there is only a 0.43 db power combining loss at the 57% step, none at the 25% step, and 0.43 db at the 6% step. Because these losses occur at reduced power, they contribute less that the stated amount of loss to the total power output. With this technique, the transmitter can achieve 93% of the efficiency of cw transmitter.

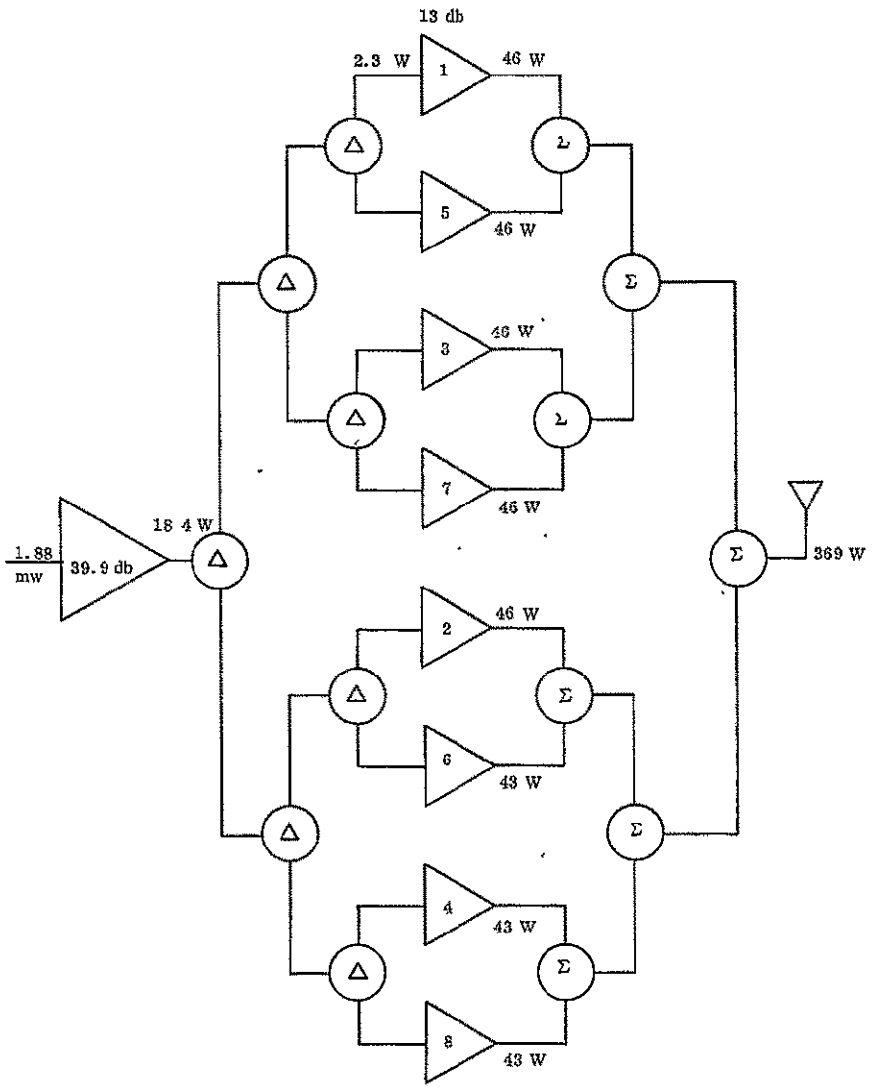

Figure 4.3-1. Single HF/AM Transmitter

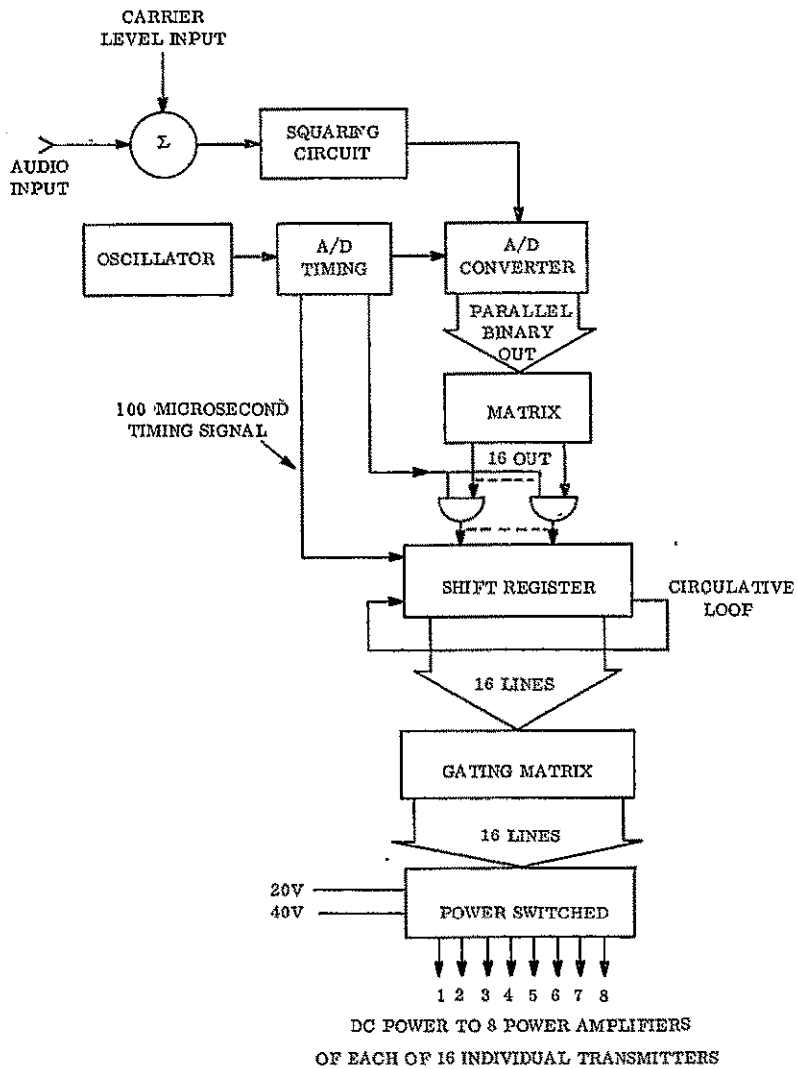

Figure 4.3-2. Digital Synthesis AM Modulator to to Modulate Each of 16 Individual HF Transmitters

In AM, the output power is proportional to the square of the algebraic sum of the carrier level and the modulating signal. A signal proportional to the output power required is created by summing and squaring the audio input and a carrier level signal. The analog to digital converter changes this information to digital form. The matrix changes the binary outputs to 16 parallel lines of on-off signals. An oscillator and an A/D timing generator provide the timing required. A shift register is interposed to force all the transistor output devices to share the peak power. The gating matrix interconnects the 16 lines to the 16 power switches which switch each of the eight sets of power amplifiers to 0, 20, or 40 volts. The modulating waveform is thus quantized into 32 levels. The distortions produced will be above ten kHz, and will not be passed by the audio portion of the receivers.

Triodes or tetrodes were not used as the output devices because they have lower overall efficiency, lower reliability, and would require a more expensive solar array. A power converter was not used because it is more efficient to design the solar array for the transmitter, which uses most of the power, and uses power converters for the other subsystems.

Several alternatives to the use of hybrids for power combining were considered. Direct paralleling was not used because it provides lower efficiency, lower gain, reduced bandwidth, and lower reliability. Impedance matching of directly paralleled stages is undesirable because of lower reliability and interaction of stages. Push-pull operation of the output devices also suffers from low reliability, low efficiency, and low gain.

An alternate to the digital synthesis modulation system described above is collector modulation of the output devices. This system was not used because it is less efficient and because it requires modulation of the drive signal, because transistor gain decreases with increasing power.

The required RF bandwidth (15.1 - 25.85) offers no serious difficulty. The digital synthesis subsystem advantages over the major alternate (provision of separate narrow bands) are simplicity and reliability. The instantaneous bandwidth for any given transmission is only 10 kHz.

Frequency and amplitude distortion must be controlled in the HF transmitter. Phase distortion has little effect on the quality of an AM signal and is not critical in the HF transmitter. Frequency distortion (variation of gain with frequency) can be held to the conventional standards of $\pm$ 2 db within the 100 to 5000 Hz audio region.

Amplitude or nonlinear distortion reduces audio fidelity by introducing harmonics and intermodulation frequencies within the audio bandpass. This effect is crucial in the HF transmitter before modulation; therefore, care in the design and development of low level circuits will be required. Subsequent to modulation, the effect will not be important because the frequencies produced will not be within the transmitter passbands. Little distortion will be introduced by the digital modulation because of the high sampling rate and number of levels.

The transistors which will be required for the HF configurations are only modifications of existing devices requiring about 1 year development time. The power combining hybrids are within state-of-the-art capability.

The hybrid configuration, which permits a slight diminution of power with failure of an individual transistor, together with the inherent reliability of transistors, provides an excellent long-life configuration. However, transistors are quite sensitive to overvoltages, overheating and hard radiations. Appropriate safeguards will be required.

Because of the amplitude modulation, it was necessary to demodulate the incoming signal to audio, then remodulate. Therefore it was necessary to depend upon a satellite-borne master oscillator for frequency stability. Long-term stability requirements will require a careful design, but can be met by a good crystal oscillator.

4.3.2.2 VHF No. 1 Transmitter

The VHF No. 1 configuration will operate in the 100 to 108 MHz region and will be a transistorized design, using ITT-3TE225 or some similar transistors.

The primary characteristics of the preferred design for the VHF No. 1 transmitter are as follows: The power output is 7.07 kw. The efficiency, given as RF power to solar array power output, is 65%. The volume is 0.375 cubic feet. The weight of this transmitter is 18.5 pounds. The transmitter will be built in the form of a thin package. Output devices of which 128 will be used will be silicon power transistors. No power converter will be used; the power combination technique will be hybrids.

Figure 4.3-3 is a block diagram of one of the 32 individual transmitters that will drive the elements of the phased array antenna. Input power of the proper phase to control the antenna beam is amplified from a one-mw level to 22 watts. It is then divided four ways by three in phase "Y" hybrids. The power is amplified by four separate power amplifiers. Each amplifier is isolated from the other by the hybrids and has a 10 db gain. The four outputs are combined by three hybrids, producing 220 watts. All elements have greater than the required 100 to 108 MHz bandwidth.

The alternate transmitter approaches are identical to those of the HF transmitter. The items considered were alternate output devices, the use of a power converter, and alternate power combining techniques.

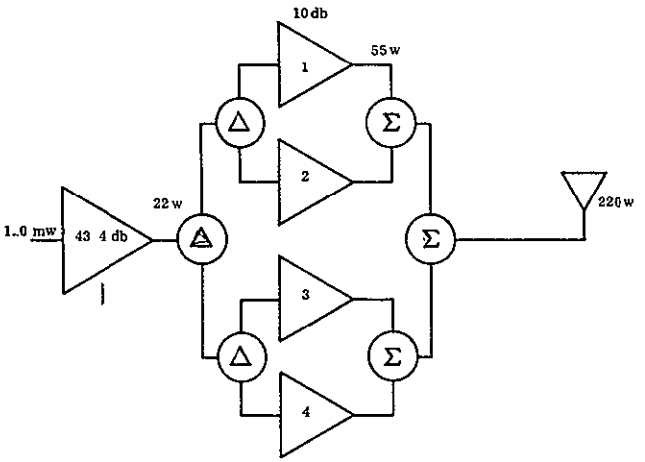

Figure 4.3-3. VHF No. 1 Power Amplifier (32 Required)

The VHF No. 1 transmitter, being FM and thus operating in Class C, does not require the relatively sophisticated digital synthesis modulation techniques required by the HF configuration. As a result, it is possible to obtain a high efficiency, and the constant power demand which is characteristic of FM.

The bandwidth required is manageable. The instantaneous bandwidth required for transmission is set by the standards of the receivers to be reached; i.e., of the order of 175 kHz.

Frequency distortion and amplitude distortion are not critical in either of the VHF configurations because they are FM systems. However, phase distortion could be significant because the characteristics of an FM signal are controlled by the relative phases of the sidebands. For minimum distortion, the transmitter is designed for maximally linear phase response.

Both the transistors required and power combining hybrids are state-of-the-art, but development will be required for power combining techniques for the higher powers. High power transistorized transmitters have not yet been space qualified.

As with the HF configuration, the VHF No. 1 transistor complex offers excellent long-life reliability, but is vulnerable to overvoltage, high temperatures, and hard radiations.

Because of the frequency translation technique used in the translator, frequency stability can be maintained by controlling the frequency of the uplink transmission.

4.3.2.3 VHF No. 2 Transmitter

The VHF No. 2 transmitter is to a considerable extent similar to VHF No. 1; i.e., it operates in the 100 to 108 MHz region, uses FM, and uses the same type of power-combining circuits.

The primary characteristics of the preferred design are: The power output is 820 watts. The transmitter efficiency, given as RF power to solar array output power, is 65%. The volume occupied is 0.15 cubic feet. The transmitter weighs 5 pounds; the transmitter will have the form factor of a thin package. The 16 output devices used will be a silicon power transistor. As in the HF transmitter, there will be no power converter. Hybrids will be used for power combining.

The alternative transmitter approaches are identical to those of the HF transmitter. The items considered were alternate output devices, the use of a power converter, and several alternate power-combining techniques.

Figure 4.3-4 is a block diagram of the complete VHF No. 2 transmitter. It consists of four individual transmitters. The 30 mw output of the receiver is divided between the four outputs of the individual transmitters. The signals are amplified to a 20.5 watt level and then supplied to the four output elements in the individual transmitter section. Each transistor has 10 db gain and a 51.4-watt output. The outputs of all the 16 output devices are combined to provide the 820 watts total transmitter power.

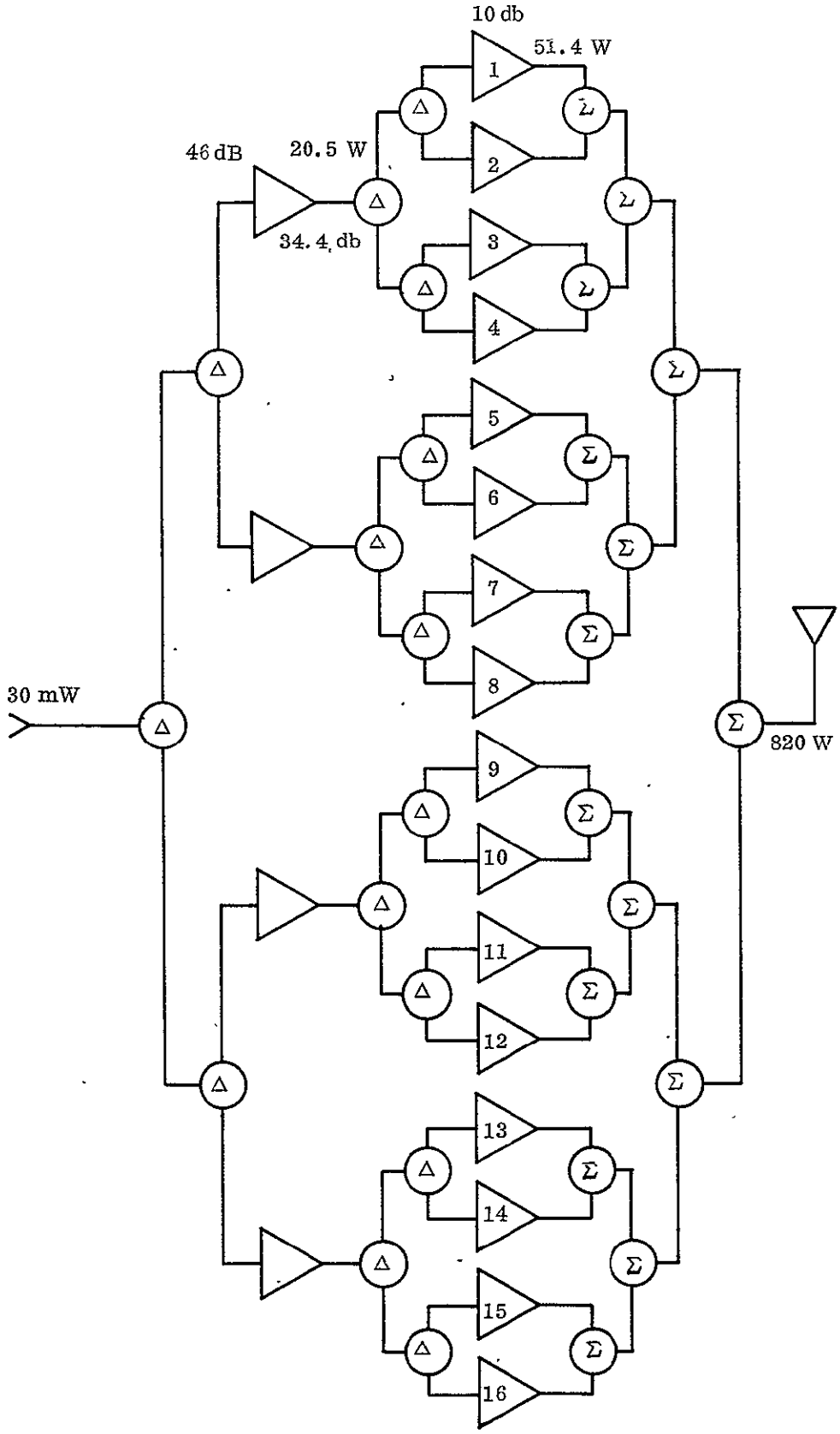

Figure 4.3-4. VHF No. 2 Transmitter

4.3.2.4 UHF Transmitter

The UHF transmitter will be required to operate at approximately 870 MHz, and a power level of approximately 575 watts for each carrier.

The UHF audio transmitter must provide two carriers. One carrier will be CW at the visual carrier frequency in the television channel selected. The other carrier will be frequency-modulated by the audio signal, and its frequency will be that of the aural carrier in the selected channel (4.5 MHz higher in frequency than the visual carrier). It has been determined that the two carriers should have equal power levels.

The two carriers will be amplified in separate channels and combined in a high level diplexer. All stages can be Class C in this implementation and much better efficiency will be obtained. All stages will use the grounded grid configuration.

The tube anode is external to a radial cavity and thus readily accessible for connection of the cooling system. The addition, the anode is RF grounded, having only the dc plate voltage on it so the presence of the capacity from the external anode to ground does not affect circuit operation. This makes possible a large area connection to the cooling system.

The overall power efficiency is 59%. The GE-7399 tube is used in the power amplifier stages, and the GE-Y1223 planar ceramic triode is used in the driver and low level stages. The stage lineup and stage gains are indicated on the block diagram (Figure 4.3-5).

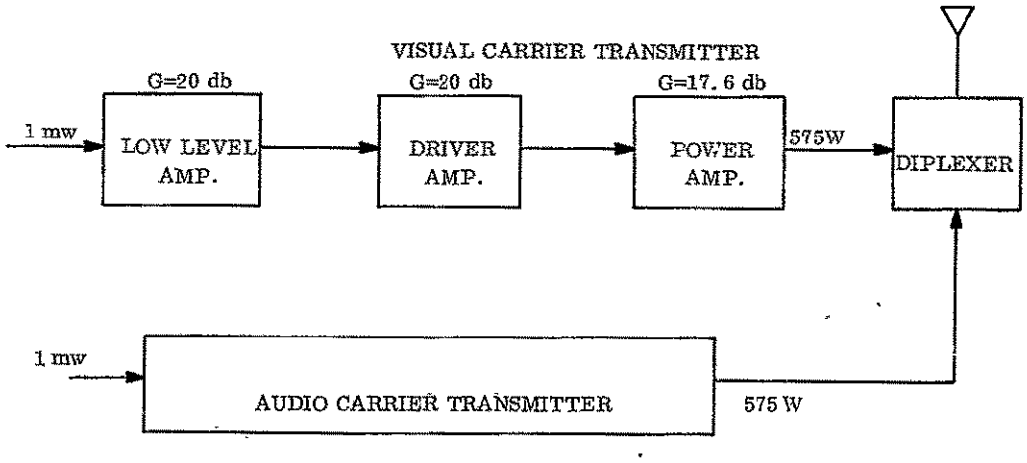

NOTES

A. AUDIO OPERATION (TWO CARRIERS)
   1. CIRCUIT TYPE: GROUNDED GRID CLASS C AMPLIFIER FOR EACH OF THE AURAL AND VISUAL CARRIERS; 59% OVERALL EFFICIENCY.
   2. ACTIVE ELEMENT: 7399 FOR POWER AMPLIFIER
      Y1223 FOR LOW-LEVEL AMPLIFIERS
   3. AMPLIFIER CAVITY TYPE: RADIAL

Figure 4.3-5. UHF Transmitter

4.3.3 TRANSMITTER TECHNOLOGY EVALUATION

4.3.3.1 Vacuum Tubes

4.3.3.1.1 Vacuum Tubes (Devices)

All vacuum tube types were considered, and all but gridded tubes were rejected for one or more of the following reasons:

a. Low efficiency

b. Short tube life

c. Lack of mechanical ruggedness.

The two most promising gridded tube types were the 7399 and a modified version of the L-64. These are discussed separately below. Other promising gridded tube candidates are listed in Table 4.3-1.

Table 4.3-1. Applicable Tubes and Their Significant Parameters

Tube Type	Vendor	Type of Cathode	Type of Envelope	Maximum Frequency MHz	CW Power Out
4Cx1000A	Eimac	Oxide-coated	Ceramic	VHF	1000 w
7650	RCA	Matrix-oxide	Ceramic	1000	300-500 w
7214	RCA	Matrix-oxide	Ceramic	1000	1000 w
6448	RCA	Thoriated-tungsten	Ceramic	1000	12 kw
6806	RCA	Thoriated-tungsten	Ceramic	1000	13 kw
Modified GL-6942 or ZP-1064	GE	Thoriated-tungsten	Ceramic	1000	2 kw

These power tubes were unsuitable for the VBMS application for one or more of the following reasons

a. Low maximum allowable seal temperature

b. Not rugged enough for space application

c. High heater power requirement

d. Insufficient cathode life.

Originally, the L-64 was considered a superior candidate because it incorporated the state-of-the-art for advances by as much as an order of magnitude improvement in the major performance characteristics such as power gain, current density, efficienty, operating temperature, and size. In addition, it has the promise of very long-life, the oxide cathode has been evaluated at a potential of 70,000 hours operation at a 0.7 a/cm^2 emission density (greater than 2 kw output). Reluctantly, however, this tube was rejected for the VBMS demonstration mission because the tube exists now only as a successful developmental model, and the program necessary to manufacturing and life-test a space qualified version would take from 3 to 5 years.

The GE-7399 was selected for the UHF transmitter for the following reasons:

a. Its performance characteristics, even though not as advanced as those of the L-64, are superior to the other candidates listed in Table 4.3-1.

b. Its tube life has been established by extensive operational use in ground installations.

The GE-7399 has an oxide cathode with a ceramic envelope. This cathode and the ceramic construction provide an inherent mechanical rigidity necessary for the launch environment. Its power capability of 1000 watts exceeds the UHF transmitter requirement of 575 watts. Operating at this lower level (575 watts) should extend the cathode life beyond that established in the ground operations.

The performance of the selected tube in the UHF transmitter is described in Section 4.3.2.4.

4.4.3.1.2 Gridded Vacuum Tube Circuits

Extensive analysis was completed on amplitude modulation circuits for the HF transmitter. These approaches were ultimately rejected because of the advantages of the solid-state designs. Vacuum tube circuits for FM signals did not require extensive analysis, because the well understood Class C amplifiers were the only choice for this service.

4.3.3.2 Transistorized Amplifiers

The technology evaluation of transistorized power amplifiers, in addition to considering present and future transistor availability, investigated to a considerable extent the circuit requirements. This was necessary because of the necessity to combine a large number of transistors to obtain the required output powers and the requirement (in the HF configuration) for amplitude modulation.

Solid-state techniques are feasible for transmitter powers well in excess of the VBMS demonstration requirements. At both 25 MHz and 100 MHz, transistors which are optimized for the given frequency give approximately the same performance. Their efficiency is limited primarily by saturation resistance and theoretical Class C amplifier losses. The 150-watt transistors can be manufactured for a particular frequency and 40-volt operation with present state-of-the-art techniques. These high power, high voltage types would give approximately 75% device efficiency. The development time necessary for these high

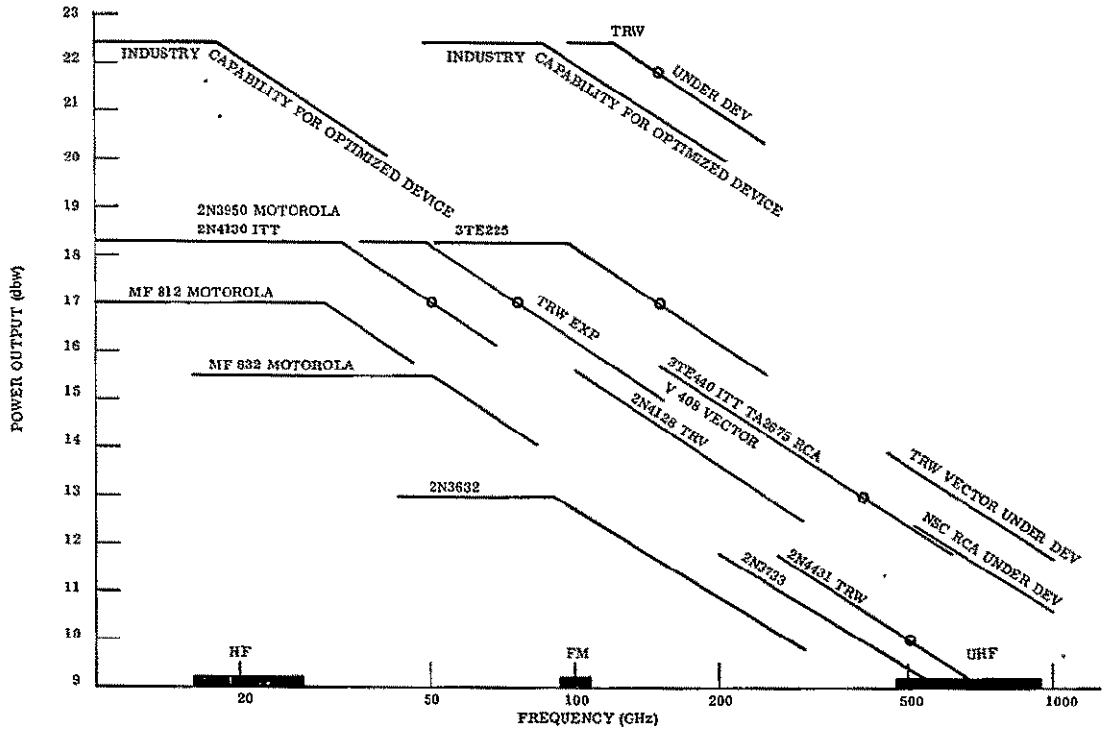

Figure 4.3-6. High Power Transistors

voltage transistors has been estimated by several vendors at 1 year.

Figure 4.3-6 shows the present capability of transistors between 10 and 1000 MHz.

Push-pull parallel circuit configurations can provide higher power outputs. The number of devices that can be connected with reasonable circuits are 8 for 25 MHz and 4 for 100 MHz. This would provide approximately 550 and 250 watts, respectively. In addition, these circuits can be further combined by hybrid matching networks. These networks will divide or combine without intrinsic loss provided the powers are equal and are in phase. If the powers are unequal, one-half the difference will be dissipated in the resistive leg of the hybrid. The hybrids isolate the circuits from each other, thereby allowing operation at partial power with one or more failures. The most convenient number of circuits would be 2, 4, or 8. For these numbers, Table 4.3-2 lists the maximum output power for each frequency and the effect of failure of 1 or 2 circuits.

Table 4.3-2. Maximum Output Power Per Number of Circuits

Number of Circuits	No. of Failures	25 MHz Power Output	100 MHz Power Output
1	0	550 w	250 w
1	1	0	0
2	0	1100 w	500 w
2	1	275 w	125 w
4	0	2200 w	1000 w
4	1	960 w	435 w
4	2	550 w	250 w
8	0	4400 w	2000 w
8	1	2530 w	1150 w
8	2	1910 w	1150 w

Two manufacturers have indicated the feasibility of 150 watt output per device for frequencies between 15 and 110 MHz. Further discussions with manufacturers on circuit techniques indicate that paralleling can be extended to 5 units, allowing 10 units in parallel push-up. It has been learned that one circuit manufacturer, on two occasions in actual flight space vehicles, provided all solid-state 100 MHz transmitters delivering from 500 and 1000 watts. These units, while not CW, did deliver long pulses.

The output power, as a function of the number of transistors for a solid-state transmitter by combining power transistors in the power amplifier, is illustrated in Figure 4.3-7.

The efficient operation of the power-combining scheme using hybrids depends upon close matching of both the phase and amplitude of the two inputs to a hybrid. The normal tolerances on transistor parameters may require an extensive selection process to obtain well-matched units. Differences in beta, V_{BE}, input and output impedances, and frequency response will affect circuit balance.

Typical life expectancy of two sample transistors is as follows:

UHF Transistor 11.6 watt: 11,000 hours in actual test

Silicon Power Transistor 20 watt: 100,000 hours (MTBF)

Figure 4.3-8 gives the predicted reliability of a typical VHF transmitter and the RF portion of a HF transmitter. The high probability of success is due to the many parallel redundant RF paths. The 0.68% per 1000 hour rate ascribed to the transistor is extremely conservative in view of the recommended 0.02% figure given in the TRA-873 Handbook. Because of the high rate used for the transistor, the passive components were neglected in the analysis.

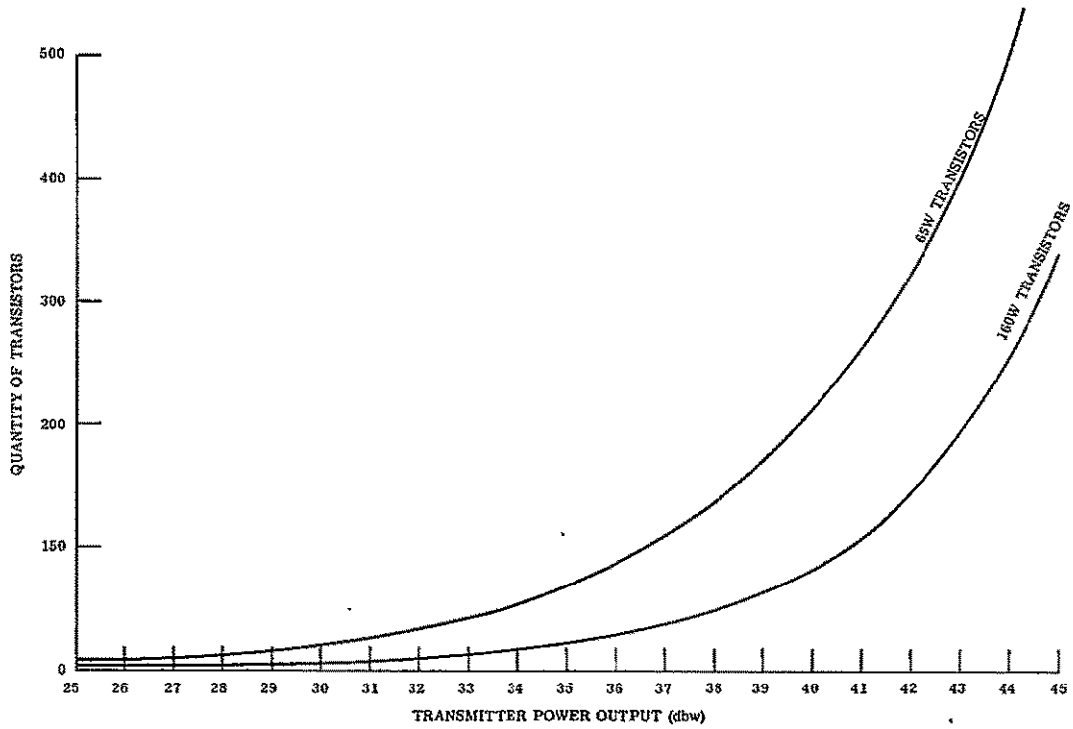

Figure 4.3-7. Outpower Expected from Solid-State Transmitter Combining Power Transistors in the Power Amplifier

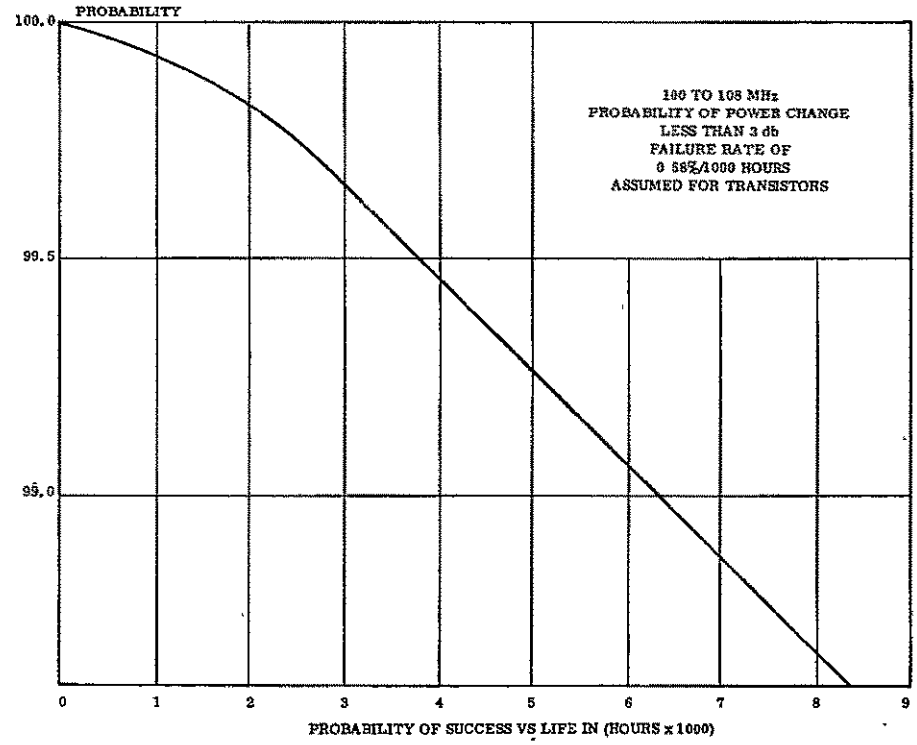

Figure 4.3-8. Probability of Power Change for Solid-State Transmitters

At both HF and VHF, the network shown to the right has been selected to both divide power for drive and to combine the output powers. The network will combine or divide power with less than 1.0 db loss over an octave bandwidth. Figure 4.3-9 gives the power loss due to unequal inputs and Figure 4.3-10 due to unequal phase. Note that the network is relatively insensitive because there is only a 1% loss for a 30% difference in power or a 10° phase difference.

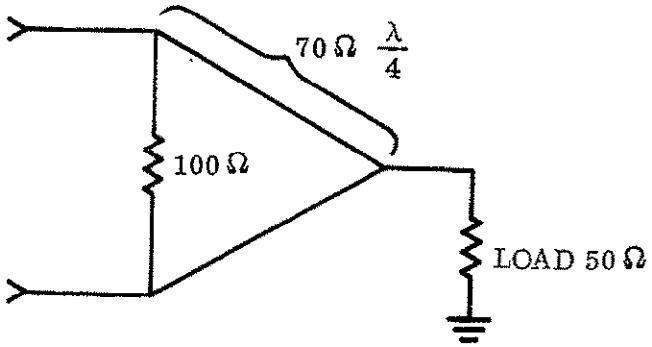

The power divider combiners are used as shown in Figure 4.3-11. They will be constructed from 70 ohm, semi-rigid coax at high powers for VHF. For HF, the high power hybrids will be lumped constant equivalent circuits in order to conserve volume.

The normalized half bandwidth at HF is 28.5%, and 3.85% at VHF.

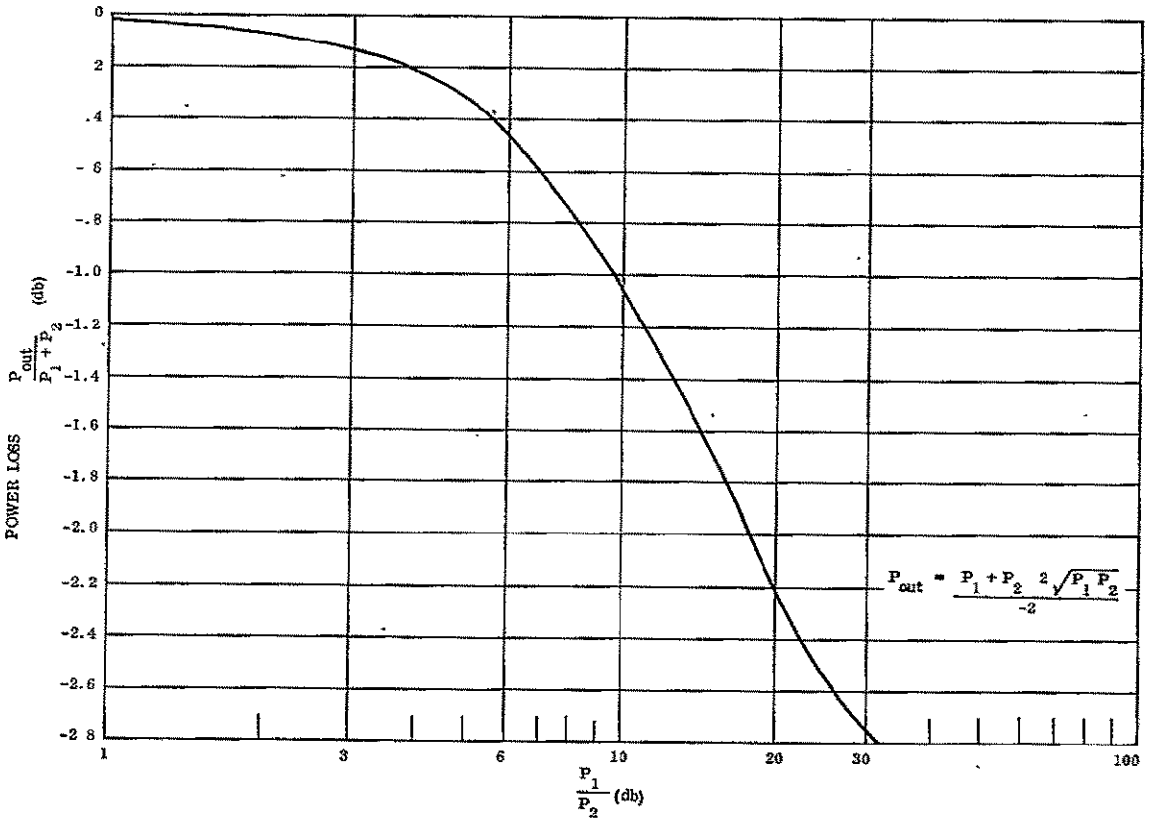

Figure 4.3-9. Network Power Loss Due to Unequal Inputs

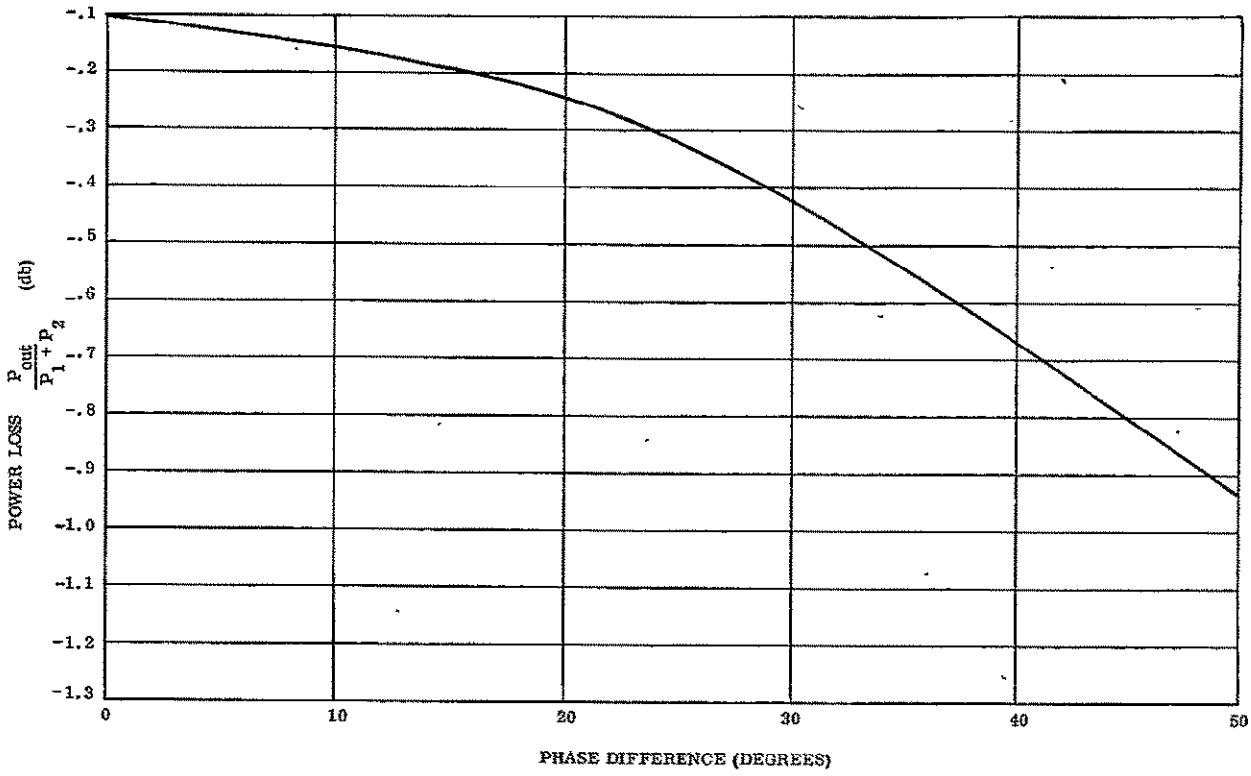

Figure 4.3-10. Network Power Loss Due to Unequal Phase

The power division deviation will be immeasurable for these ranges; and the isolation will be greater than 16 db across the HF band and greater than 30 db across the VHF band. This will ensure independent operation of the individual stages. If one stage fails, the other stage feeding the same hybrid will be protected by this isolation.

There are several other ways in which the power input of several transistors could be combined: (1) transistors could be directly paralleled but this has three main disadvantages: (a) the efficiency and gain of a pair are reduced compared with two single stages with hybrid combiners by the necessity to use emitter equalizing resistors to ensure equal sharing of drive power and current, (b) the bandwidth is reduced because of the reduced input impedance, (c) the reliability is reduced because the failure of one of a pair will detune the stage or the increased drive will fail the other transistor; (2) transistors could be operated in push-pull but this has the disadvantage of (1c) above and, in addition, the gain and efficiency are reduced because the input and output circuits are less efficient and can be optimized for only one of the pair; (3) parallel/push-pull transistors could be used, but this arrangement would have the combined disadvantages of (1) and (2) above; and (4) separate stages can be directly paralleled resulting in 25-ohm input and output impedances and then the pair transformed to 50 ohms at both terminals. The disadvantages of this method are the reduction in reliability because failure of one stage will detune the other due to the tight coupling between stages. This coupling will produce severe turning interactions under normal operating conditions. This method has promise, however, for the final power combiners in a large array

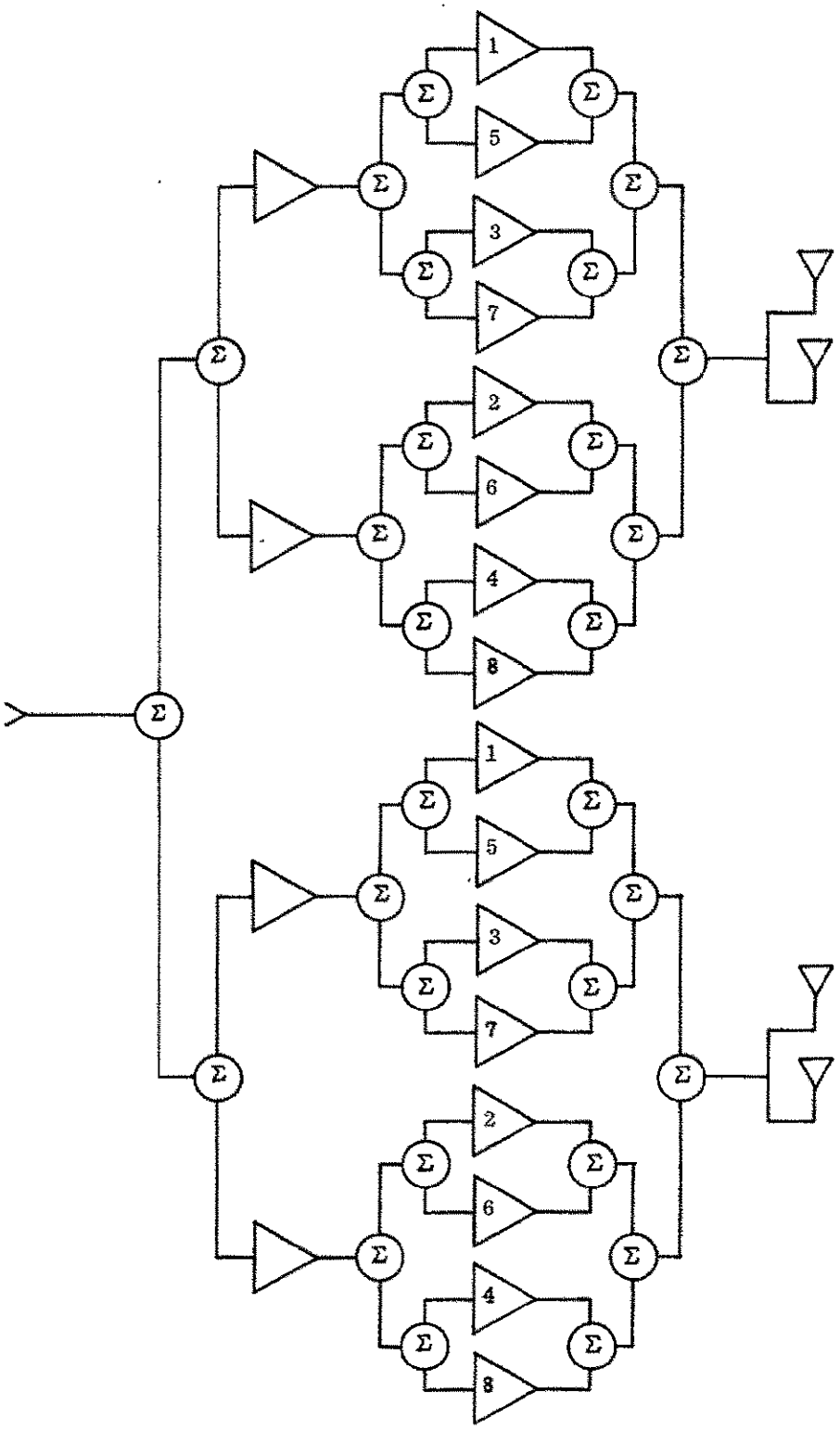

Figure 4.3-11. Typical Transmitter

of transistors if this type has been proceeded by one or two stages of hybrids.

The individual power amplifiers will be of the grounded emitter configuration with matching sections at both input and output. A grounded emitter is chosen because it gives higher gain than grounded base and is a stable configuration at these frequencies without neutralization. The network was chosen over transformer coupling because of its ease of adjustment and coupling efficiency. All stages will be fixed-turned for both the HF and VHF transmitters. If any tuning is required at HF to achieve higher efficiency at band edge, high voltage varactors will be used with preset voltages.

Transistors similar to the off-the-shelf ITT 3TE225 appear adequate for the VHF Nos. 1 and 2. The 3TE225 is now being manufactured in large volumes for high reliability military applications. The HF application will require a high voltage version of the 2N3950 or 2N4130 type transistor, even though the average power output will be well within the capability of off-the-shelf devices.

Figures 4.3-12 and 4.3-13 give the power input, efficiency, weight, and volume as a function of power output for the HF transmitters from 30 to 42 dbw outputs. The curves assume a 4-element array. Because the HF configuration resulted in a 16-element array, the transmitters are simplified by elimination of the higher power combiners. Figures 4.3-14 and -15 give the same information for the FM VHF transmitters.

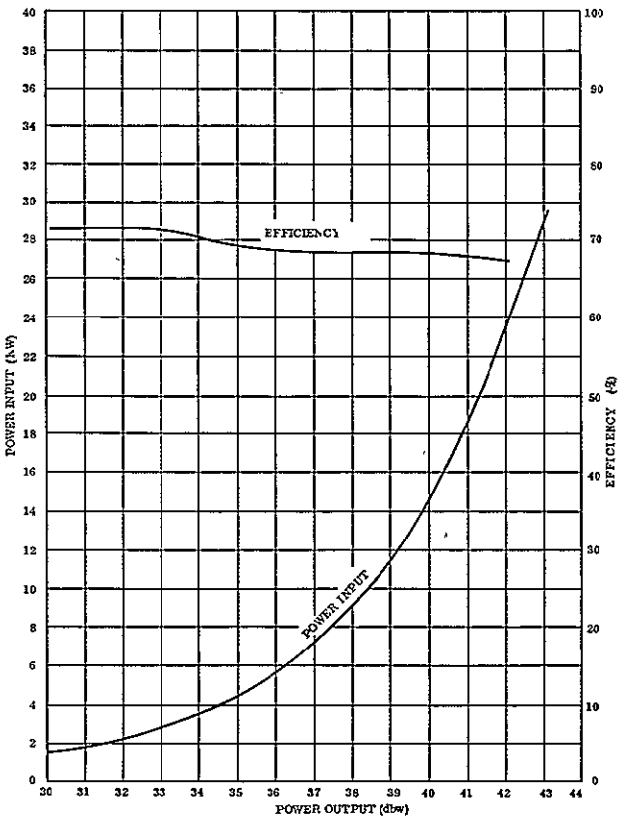

Figure 4.3-12. Power Input and Efficiency vs Power Output for HF Solid-State Transmitters.

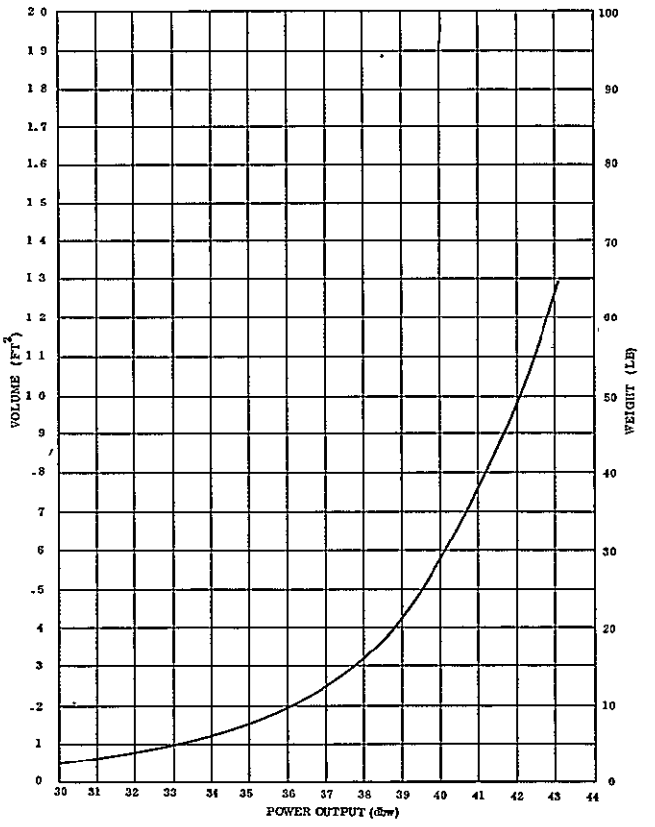

Figure 4.3-13. Weight and Volume vs Power Output for HF Solid-State Transmitters.

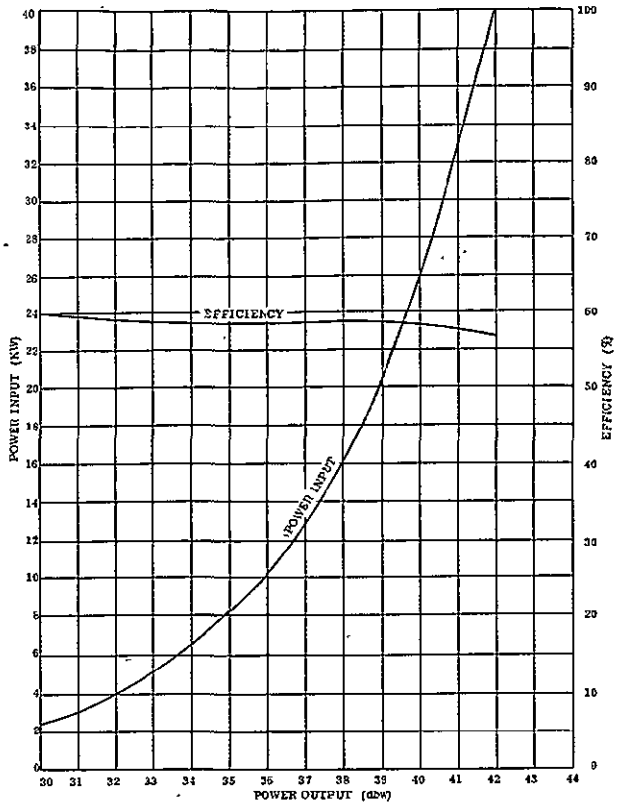

Figure 4.3-14. Power Input and Efficiency vs Power Output for VHF Solid-State Transmitters.

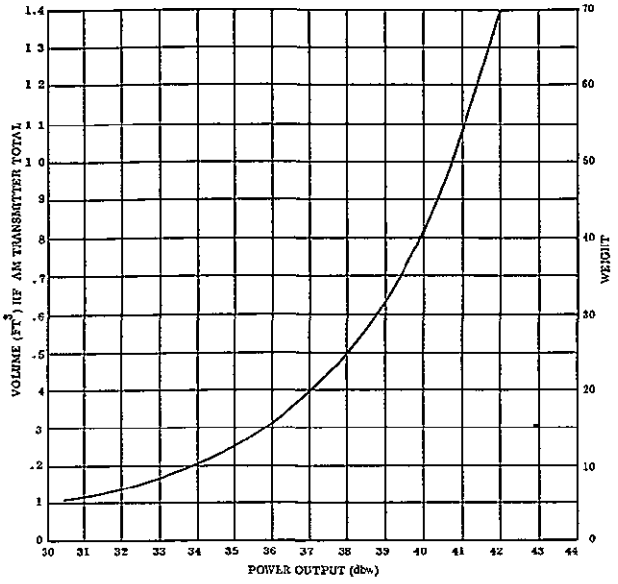

Figure 4.3-15. Weight and Volume vs Power Output for VHF Solid-State Transmitters.

4.4 GROUND TO SATELLITE UPLINK

4.4.1 INTRODUCTION

The uplink delivers the signal to the satellite transmitter without significant degradation of signal quality. Apparently the uplink would not be a critical subsystem, because similar links have been previously operated successfully. However, careful design and development will be required to insure economy, high standards of performance, and minimization of interference with other services.

The uplink consists of three major components: the ground station, the satellite receiver antenna, and the satellite receiver.

Because of the similarity of the program material, the ground-to-satellite geometry and the broadcast missions, the gross features of the uplink did not vary significantly from one configuration to another. The most appropriate frequency and modulation proved to be the same, as did the organization of the ground station and the general design of the satellite receiver. Important parameters which varied from one configuration to another included the gain of the satellite receiver antenna, the requirement for a ground tracking antenna in two of the configurations and the requirement for detection and conversion to AM in the HF configuration.

The major tradeoffs were frequency selection and transmitter/antenna ERP. The receiver antenna gains were fixed by the orbital altitudes and the necessity for providing coverage of the full visible earth. The performance requirements (signal-to-noise ratios, distortion, etc.) are fixed by considerations of subjective quality and broadcast standards. The supporting technological investigations were mainly concerned with the selection of the uplink frequency and the consideration of appropriate technical standards (i.e., baseboard bandwidth, percent modulation). The necessary equipment can be selected almost entirely from off-the-shelf and state-of-the-art items.

4.4.2 SUBSYSTEM DESCRIPTION

4.4.2.1 General

The gross technical parameters of the uplink subsystems are:

a. Frequency, 8.5 GH_2

b. Modulation, FM: Δf = 75 to 200 kH_z

c. Transmission Distance, 4000 to 20,000 nm

d. Transmitter Power, 10 kw

e. Transmitter antenna diameter, 6 to 30 ft (30-ft antenna is for UHF wideband)

f. Satellite Receiver antenna gain, 8 to 16 db

g. Transmitter antenna gain, 40 to 55 db

h. Satellite receiver noise threshold, -140 to -145 dbw

4.4.2.2 Ground Stations

The basic ground station will consist of an uplink transmitter with a power rating of from 1 to 10 kw. The 1-kw transmitter will consist of a klystron power amplifier cabinet containing the modulator exciter and local oscillator with harmonic generator.

The 10-kw transmitter will consist of a power amplifier cubicle, an exciter/modulator cabinet, including local oscillator and harmonic generator, klystron power supply cabinet, and heat exchanger.

Two different types of antenna systems will be used. For synchronous orbits, the antenna will incorporate a fixed parabolic reflector varying in size from 6 to 30 ft, with a prime focal feed system. The fixed antenna base will be manually adjustable. The elevation angle will be from 5° to 70° above horizon with a $\pm$ 50 vernier control. The azimuth adjustment will be $\pm$ 85° with a $\pm$ 5° vernier. The fixed mount will be a horizontal tilt type designed especially for this application.

For nonsynchronous orbits, a tracking parabolic reflector antenna system will be used. The tracking antenna system will consist of a 6- to 15-ft parabolic reflector with a plane-polarized focal feed system. The parabolic antenna will be mounted on an X-Y mount pedestal equipped with servodrive motors. The servosystem will consist of digital to analog converter for a remote TT&C location, servocontrol panel, and servoamplifiers to drive the X and Y axis drive motors in the pedestal mount. A remote readout and position monitor will feed back antenna position information to the servocontrol panel and amplifiers.

The station will be equipped with a control console with facilities for program transmitter, intercom, monitor and telecom control. Standard station monitors will be supplied to monitor the carrier frequency and deviation of the ground transmitter. An RF converter will be used to down-convert the uplink frequency to the downlink frequency. This enables the station to monitor the satellite downlink signal with the use of a tone radio frequency preamp driver.

Additional crystal-controlled monitor receivers will be provided to monitor the satellite broadcast signal on a full-time basis. In the case of the nonsynchronous orbit for the VHF system, one receiver will be used to monitor the downlink carrier frequency on a full-time basis and provide a doppler frequency correction signal. This signal will be processed by a doppler correction unit and applied to the local oscillator of the uplink ground transmitter for frequency correction.

The ground station will be equipped with a test and maintenance facility. This facility will be equipped to accomplish back-to-back testing of the ground transmitter equipment, operational and special testing of the ground and satellite system, and maintenance of the ground station.

Signal processing equipment for the audio signals will consist of an automatic gain control amplifier for increasing average program level and an audio peak limiter to prevent overmodulation of the ground transmitter.

For wideband signals, a stabilizing amplifier will be supplied to control signal level, regenerate synchronizing pulses, and remove hum from the signal before feeding the ground transmitter.

The block diagram of the HF, VHF No. 1 and VHF No. 2 configurations is shown in Figure 4.4-1.

The audio program source, either remote or local, will be fed into the control console where it will be selected, monitored, and adjusted.

The audio output from the control console will be applied to an automatic gain control amplifier which will control wide level changes and increase the average program level, before feeding the 75-microsecond preemphasis network.

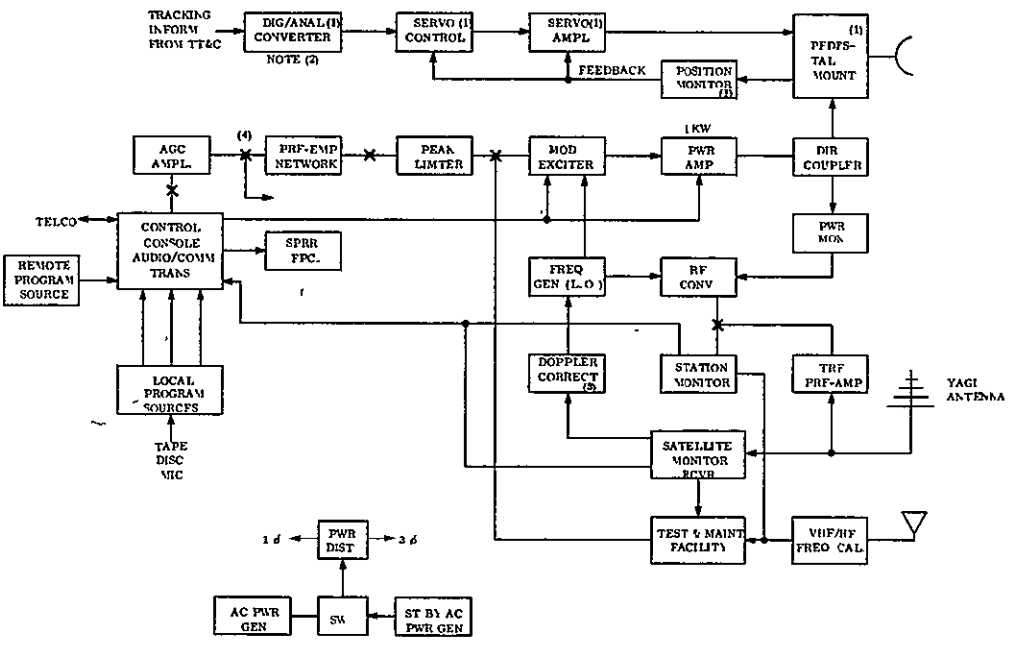

NOTES (1) HF & VHF 2 CONFIGURATIONS
(2) FOR REMOTE TT&C
(3) FOR VHF 2 DOPPLER FREQ CORRECTION
(4) X-DENOTES PATCH FACILITY

Figure 4.4-1. HF, VHF No. 1 and VHF No. 2 Station Block Diagram

The preemphasized audio signal will then be fed into a peak-limiting amplifier that will limit the program peaks to the 100% modulation point, thus preventing overmodulation of the transmitter. This signal will then be applied to the modulator/exciter of the transmitter where it will frequency-modulate a crystal oscillator. The basic modulated oscillator frequency will then be multiplied to a suitable frequency for mixing with the main local oscillator. The main local oscillator will be a highly stable crystal oscillator with a low FM jitter. The frequency of this crystal oscillator will then be multiplied up in frequency and fed into the modulator exciter. At this point, the FM carrier will be mixed with the main LO and up-converted to the final uplink frequency.

This modulated carrier will then be further amplified to a suitable level to drive the final 1-kw RF power amplifier. The output of the RF power amplifier will be passed through a directional coupler where the signal will be connected through a waveguide run to the tracking pedestal and the antenna feed system. For the synchronous orbit VHF No. 1 configuration, the waveguide will connect direct to the antenna feed system.

The attenuated carrier output of the directional coupler will be generated to a power monitor and an RF converter unit. A feed from the LO harmonic generator will be supplied to the RF converter where the modulated uplink carrier will be down-converted to the corresponding downlink frequency. This converted carrier will then be applied to the station monitor for further conversion and demodulation.

The station monitor is designed to meter the carrier frequency deviation and indicate the amount of frequency modulation present. These two signals, in addition to an audio feed, will be transmitted to the control console for monitoring purposes. An audio feed will also be fed into the test and maintenance facility for signal analysis.

A yagi antenna will be used to receive the downlink carrier. The output of the antenna system will be fed to a TRF preamp tuned to the downlink frequency and to the AM or FM monitor receivers. The output of the preamplifier will be used to drive the standard station monitor for checking the carrier frequency and the modulation level. The satellite monitor receiver will be designed to provide monitor signals for determining the received RF level and the downlink carrier frequency in conjunction with the test and maintenance facility.

For the VHF No. 2 configuration, the satellite monitor receiver will feed a correction signal to the doppler correction unit where this signal will be processed to control a motor-driven tuning circuit in the local oscillator unit of the transmitter exciter. This tuning system will change the local oscillator frequency of the uplink transmitter to correct for the doppler frequency shift. The motor-driven tuning approach is used to minimize any noise injection which might be contributed by use of an electronic circuit correction network.

The VHF No. 1 configuration will use a manually adjusted parabolic antenna system. For the nonsynchronous HF and VHF No. 2 approach, a tracking antenna system will be used which will be slaved to the TT&C tracking antenna system. Where the TT&C station is

remote to the ground uplink station, a digital-to-analog converter will be used to provide an analog signal feed to the servosystem. The analog output of the converter unit will feed a servocontrol panel. The servocontrol panel will be used to reposition the tracking antennas after each orbit and provide the corrected analog signal to the servodrive amplifiers. The servodrive amplifiers will provide the drive power to the X and Y axes drive motors in the pedestal.

The pedestal mount will contain a position readout device. This device will feed a signal to the position monitor in the control van. The output of the position monitor will be applied to the servocontrol panel and servoamplifier for a comparator check with the incoming TT&C control signal.

The functional description for the UHF configuration (Figure 4.4-2) is similar to the HF and VHF configurations. The tracking antenna system is not required as the UHF is a synchronous orbit configuration. This configuration requires an additional transmitter to generate an unmodulated visual RF carrier signal. The visual exciter will generate an unmodulated carrier which is 4.5 MHz below the FM aural carrier at the up-conversion point. This will allow the main LO to be used to up-convert both the aural and visual carriers to the final uplink carrier frequencies.

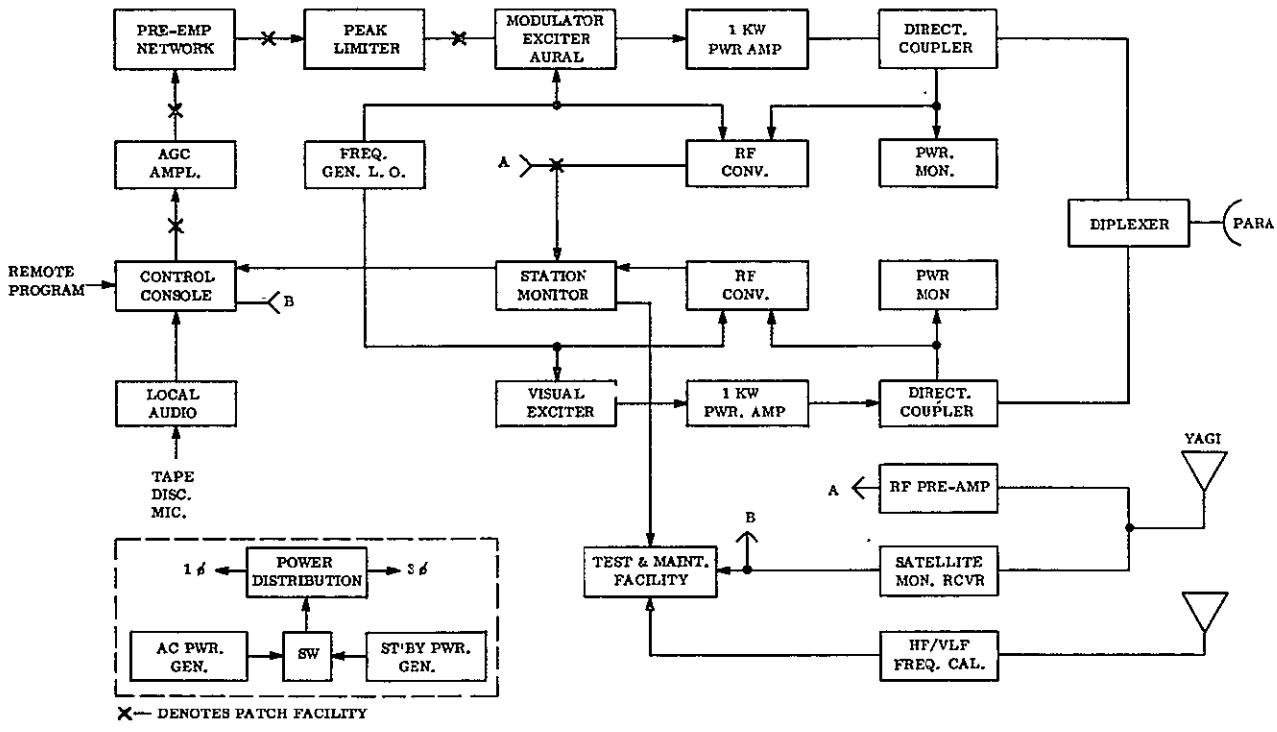

Figure 4.4-2. UHF-Aural Station Block Diagram

The up-converted visual carrier signal will be further amplified to a suitable level to drive the visual 1-kw RF power amplifier. The RF outputs of the visual and aural RF carriers will be diplexed together and fed into the fixed parabolic antenna feed system. The downlink visual and aural carrier frequencies will be monitored and the frequency drift of the downlink visual carrier will be corrected by adjusting the frequency of the uplink visual carrier. A parabolic antenna will be used to receive the downlink RF carrier signal to feed the satellite monitor receivers.

4.4.2.3 Satellite Receiver Antennas

The satellite receiver antenna gains were derived on the basis of full coverage of the visible earth. Antenna characteristics are given in Table 4.4-1.

TABLE 4.4-1

Configuration	Half Power Beamwidth (degrees)	Gain (db)
HF	53.0	11.5
VHF 1 and UHF	17.5	19.0
VHF 2	40.5	13.0

In the power budgets listed in Section 4.4.2.5, a 3 to 4 db allowance is factored in to account for the lower efficiency of the beam edge loss of the smaller antennas. Antenna design is shown in Figures 4.4-3, 4.4-4, and 4.4-5.

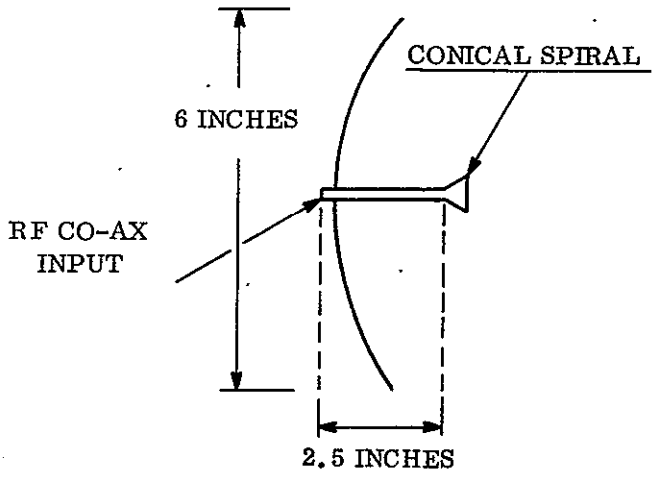

RF CHARACTERISTICS

- FREQUENCY 8.5 GHz
- GAIN = 19 db
- HPBW = 17.5°
- POLARIZATION - CIRCULAR

Figure 4.4-3. VHF No. 1 and UHF Uplink Antenna - Paraboloid

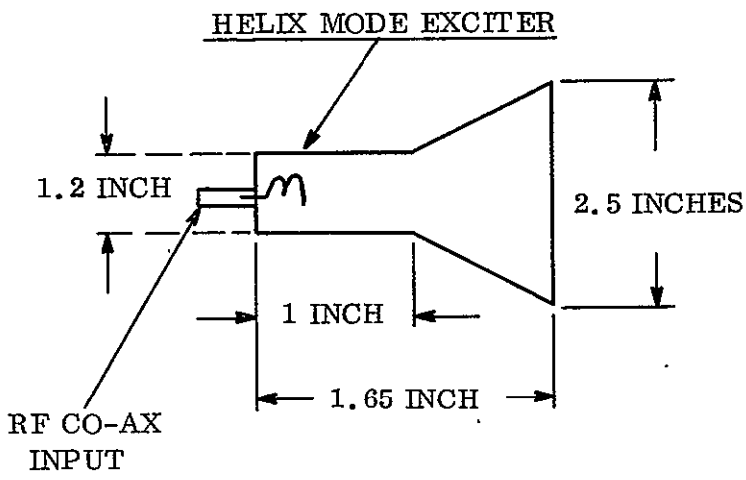

RF CHARACTERISTICS

- FREQUENCY 8.5 GHz
- GAIN = 13 db
- HPBW = 40.5°
- POLARIZATION - CIRCULAR

Figure 4.4-4. VHF No. 2 Uplink Antenna - Conical Horn

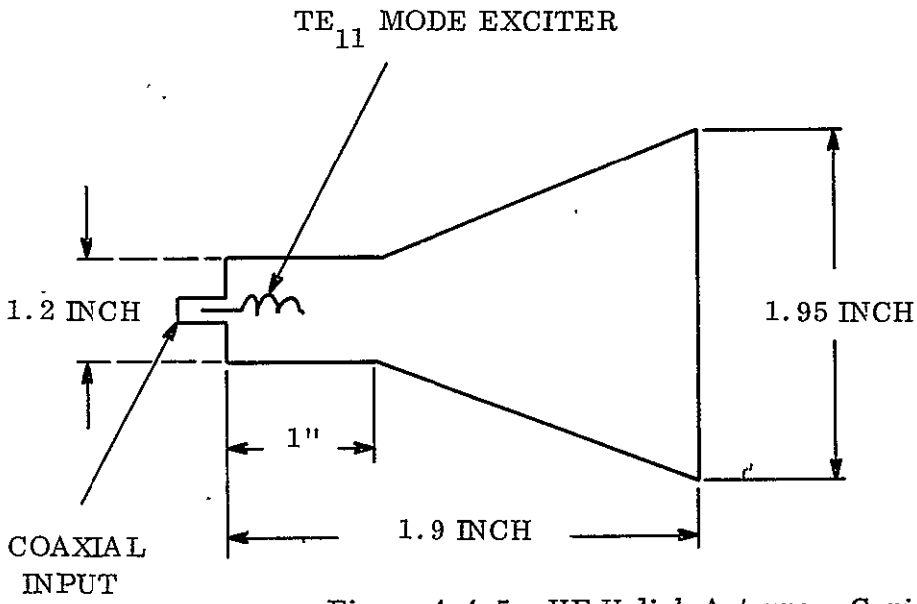

RF CHARACTERISTICS

- FREQUENCY 8.5 GHz
- GAIN = 11.5 db
- HPBW = 53°
- POLARIZATION-CIRCULAR

Figure 4.4-5. HF Uplink Antenna - Conical Horn

4.4.2.4 Satellite Receivers

The HF configuration is required to transmit a standard AM signal on any one of four ground selected HF carrier frequencies. The receiver section supplies the audio information signal and the correct carrier frequency to the transmitter/modulator. The uplink audio information signal is an X-band FM-modulated signal. The receiver is, therefore, required to receive an X-band FM signal, demodulate the FM audio information, amplify the resultant audio signal, and generate any one of four possible carrier frequencies.

The block diagram of Figure 4.4-6 illustrates the selected receiver configuration. The uplink signal is amplified, filtered and mixed down to an IF frequency. The IF signal is amplified, band-limited and demodulated. The audio output of the demodulator is amplified and delivered to the transmitter. Four oscillator-amplifiers supply the required carrier frequencies selected by a command link input.

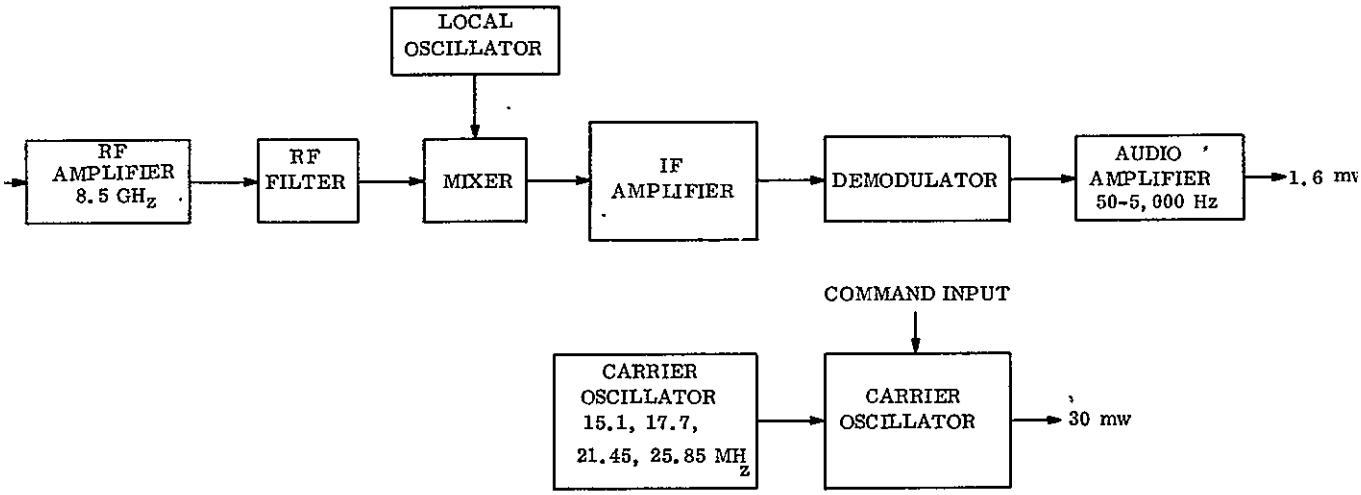

Figure 4.4-6. HF Receiver Block Diagram

The noise figure for the parallel redundant system is 7 db. The IF bandwidth is determined as 420 kHz information bandwidth plus 130 kHz doppler allowance. Bandwidth increase due to LO frequency shift is negligible for stabilities of the order of 10^{-6}. Long term LO drift can be compensated by ground station changes. The audio bandwidth will be 5 kHz to pass all uplink information.

The VHF configurations are required to transmit a standard FM signal at 100 to 108 MHz. The receiver section is required to supply this signal at a low level. The uplink signal is an X-band signal with standard FM modulation. The receiver is, therefore, required to receive this X-band signal and translate it to the 100 MHz band.

The block diagram of Figure 4.4-7 illustrates the selected receiver configuration. The uplink signal is amplified, filtered, and mixed down to an IF frequency. The IF signal is amplified, filtered, and up-converted to the transmitter frequency. Operation is similar to that of the HF configuration.

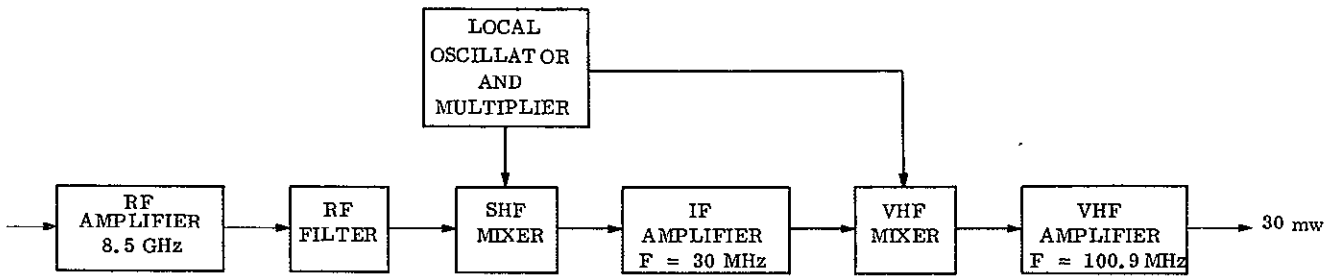

Figure 4.4-7. VHF Receiver Block Diagram

The noise figure for the parallel redundant system is 7.0 db as in the HF case. The IF information bandwidth is 240 kHz. Long-term LO stability must be 2.4×10^{-7} to meet the FCC carrier tolerance. Long-term frequency drift outside this limit could be compensated for by ground station frequency changes.

The receiver for both VHF configurations has been described above. VHF configuration No. 2 is a subsynchronous satellite and the uplink signal will experience a doppler shift. Because the downlink signal frequency is derived from the uplink frequency, the ground transmitter must change frequency to compensate for the doppler shift. The ground station will monitor the satellite broadcast to determine the required frequency shift.

The UHF satellite is required to transmit two types of broadcast. In the TV-aural mode, the transmitter broadcasts a UHF/TV picture carrier and sound signal. In the wideband mode, the transmitter broadcasts a wideband FM signal. The transmitter section will consist of three separate transmitters: one for the wideband transmission and one each for the picture carrier and sound signal. Each transmitter will require a separate input.

The receiver input will be an X-band signal. For the wideband mode, the uplink signal will have the required downlink modulation. In the TV-aural mode, the picture carrier and sound signal will have the required downlink modulation and frequency difference. The receiver is required to translate these inputs at the appropriate UHF frequencies.

The block diagram of Figure 4.4-8 illustrates the selected receiver configuration. The uplink signal is amplified, filtered and divided between two mixers. Through one mixer path, the wideband signal, if present, is down-converted, amplified, up-converted to the output frequency, and delivered to the wideband transmitter. Through the other mixer path, the TV-aural signal, if present, is mixed down, amplified, filtered to separate picture carrier and sound signal, up-converted to the correct output frequencies, and delivered to the appropriate transmitters.

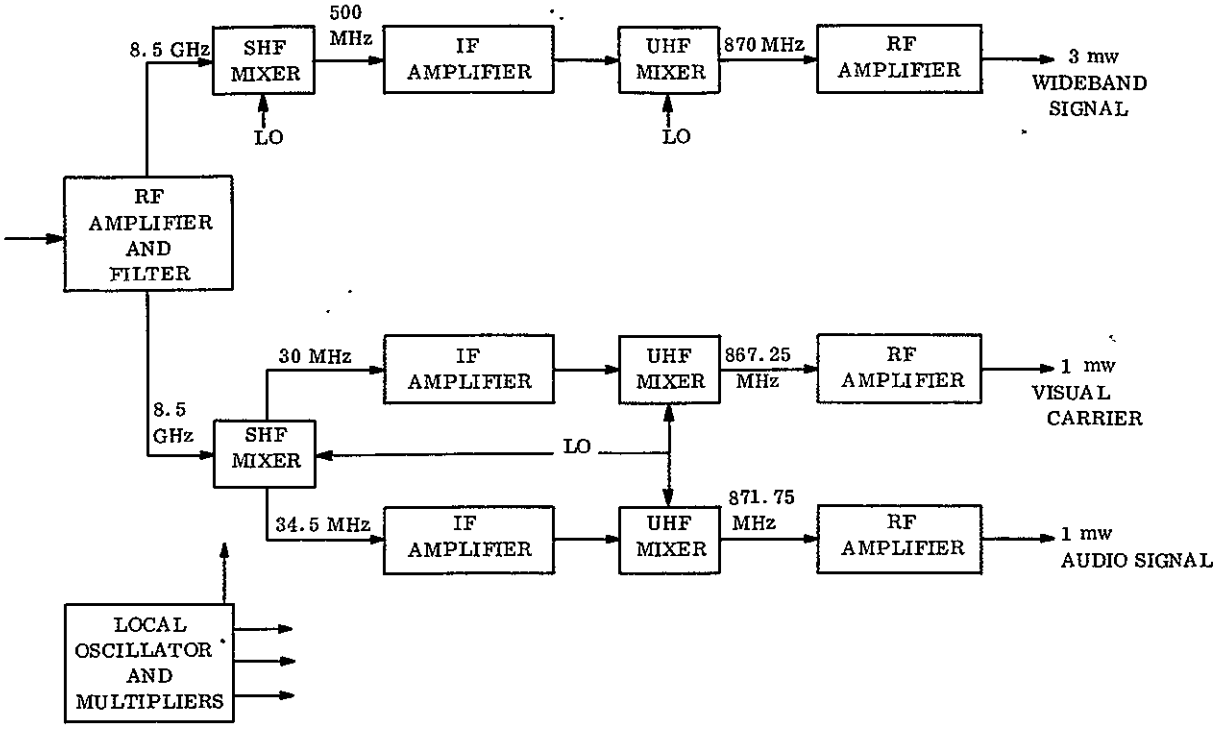

Figure 4.4-8. UHF Receiver Block Diagram

The noise figure for the parallel redundant system is 7.5 db. The IF bandwidth for the wideband system is 40 MHz. For the TV - aural picture carrier and sound signal it is 110 kHz. Long-term LO stability must be 1.2×10^{-7} to meet the FCC carrier requirements.

4.4.2.5 Power Budgets

Power budgets are shown for the following configurations:

a. HF, 4356 nm Orbit (Table 4.4-2)

b. VHF No. 1, Synchronous Orbit (Table 4.4-3)

c. VHF No. 2, 7556 nm Orbit (Table 4.4-4)

d. UHF, TV-aural, Synchronous Orbit (Table 4.4-5)

e. UHF/TV Wideband, Synchronous Orbit (Table 4.4-6)

Table 4.4-2. HF Power Budget

8.5 GHz Earth-to-Satellite
4356 nm Altitude Orbit

RF Gains

Satellite (Effective) Antennd Gain	8.0 db
Ground Antenna (6-foot)	41.7 db
Ground Transmitter (1 kw)	30.0 dbw
	79.7 dbw

RF Losses

Free Space Loss	193.5 db
Misc. Losses (Waveguide, feeder)	2.0 db
Fading Allowance	7.0 db
Total RF Losses	202.5

Received Signal = RF Gain - RF Loss = -122.8 dbw

Receiver Carrier To Noise (C/N)

C/N = (Received Signal) - (Receiver Noise)

C/N = -122.8 dbw - (-138.1 dbw) = 15.3 db

Signal Noise Ratio

$$S/N = C/N + 10 \log \frac{B_{if}}{2b} + 20 \log 3 \frac{\Delta F}{f_b} + Kp$$

Where

b = Audio Bandwidth in kHz
ΔF = Peak Deviation in kHz
Kp = Pre-emphasis improvement factor
B_{if} = IF Bandwidth
f_b = Highest Audio Frequency

$$S/N = 15.3 + 10 \log \frac{550}{10} + 20 \log 3 \frac{200}{5} + 7$$

S/N > 69 db (including effect of FM Residual Noise)

Table 4.4-3. VHF No. 1 Power Budget

8.5 GHz Earth-to-Satellite
Synchronous Orbit

RF Gain

Satellite Antenna (Effective) Gain	16.0 db
Ground Antenna (8-foot)	44.0 db
Ground Transmitter (1.0 kw)	30.0 db
	90.0 dbw

RF Losses

Free Space Loss	203.3 db
Miscellaneous (Waveguide, Feeder)	2.0 db
Fading Allowance	7.0 db
Total RF Losses	212.3 db

Received Signal = RF Gain - RF Losses = -122.3 dbw

Received Carrier-to-Noise (C/N)

C/N = (Received Signal) - (Receiver Noise)

C/N = -122.3 dbw - (-141.7 dbw) = 19.4 db

Signal To Noise Ratio (S/N)

$$S/N = C/N + 10 \log \frac{B_{if}}{2b} + 20 \log 3 \frac{\Delta F}{f_b} + Kp$$

Where:

b = Audio Bandwidth in kHz
ΔF = Peak Deviation in kHz
Kp = Pre-emphasis improvement factor
B_{if} = IF Bandwidth
f_b = Highest audio frequency

$$S/N = 19.4 + 10 \log \frac{240}{30} + 20 \log 3 \frac{75}{15} + 10$$

S/N = 57.0 db

Adding the effect of residual FM noise results in a system S/N = 50.8 db.

Table 4.4-4. VHF No. 2 Power Budget

8.5 GHz Earth-to-Satellite
7556 nm Altitude Orbit

RF Gains

Satellite (Effective) Antenna Gain	9.0 db
Ground Antenna (8-foot)	44.0 db
Ground Transmitter (1.0 kw)	30.0 dbw
	83.0 dbw

RF Losses

Free Space Loss	195.3 db
Miscellaneous Losses (Waveguide, Feeder)	2.0 db
Fading Allowance	7.0 db
Total RF Losses	-204.3 db

Received Signal = Gain - Loss = -121.3 dbw

Received Carrier-to-Noise (C/N)

C/N = (Received Signal) - (Receiver Noise)

C/N = -121.3 dbw - (-141.4 dbw) = 20.1 db

Signal-to-Noise Ratio (S/N)

$$S/N = C/N + 10 \log \frac{B_{if}}{2b} + 20 \log 3 \frac{\Delta F}{f_b} + Kp$$

Where:

b = Audio Bandwidth in kHz
ΔF = Peak Deviation in kHz
Kp = Pre-emphasis improvement factor
B_{if} = IF Bandwidth
f_b = Highest Audio Frequency

$$S/N = 20.15 + 10 \log \frac{260}{30} + 20 \log 3 \times \frac{75}{15} + 10$$

S/N = 58.3 db

Adding in the effects of residual FM noise reduces the S/N to 51.1 db

Table 4.4-5. VHF/TV Aural Power Budget

8.5 GHz Earth-To-Satellite
Synchronous Orbit

Total RF Gain

Satellite Antenna (EFF) Gain	16.0 db
Ground Antenna (15 foot)	49.5 db
Ground Transmitter (Aural) 1.0 kw	30.0 dbw
	95.5 dbw

RF Losses

Free Space Loss	203.1 dbw
Miscellaneous Losses (Waveguide, Feeder)	3.0 db
Fading Allowance	7.0 db
Total Losses	213.3 dbw

Received Signal = RF Gain-RF Losses = -117.8 dbw

Received Carrier-To-Noise (C/N)

C/N = (Received Signal) - (Receiver Noise)
= -117.8 dbw - (-145 dbw) = 27.2 db

Signal To Noise Ratio

$$S/N = C/N + 10 \log \frac{B_{if}}{2b} + 20 \log 3 \frac{\Delta F}{f_b} + K_p$$

Where:

b = Audio Bandwidth in kHz
F = Peak Deviation in kHz
Kp = Pre-emphasis improvement factor
f_b = Highest Audio Frequency
B_{if} = IF Bandwidth

$$S/N = 27.2 + 10 \log \frac{110 \times 10}{30 \times 10} + 20 \log 3 \frac{25}{15} + 10$$

S/N = 52 db

Adding in the effects of residual FM noise reduces the S/N to 49.5 db.

Table 4.4-6. UHF/TV Wideband Power Budget

8.5 GHz Earth-to-Satellite
Synchronous Orbit

RF Gains

Satellite Antenna (Effective) Gain	16 db
Ground Antenna (30 foot)	55 db
Ground Transmitter (10 kw)	40 dbw
	111 db

RF Losses

Free Space Loss	203.3 db
Fading Allowance	7.0 db
Misc. Losses (Waveguide, Feeder)	2.0 db
Total RF - Loss	212.3 db

Receiver Signal -101.3 dbw

Receiver Carrier to Noise (C/N)

C/N = (Received Signal) - (Receiver Noise)

C/N = -101.3 dbw - (-119.2) = 17.9 db

Signal to Noise Ratio (S/N)

$$S/N = C/N + 10 \log \frac{B_{if}}{2f_b} + 20 \log 3 \frac{\Delta Fp}{f_b} + Kpr + Kpp$$

Where:

S/N = Signal to Noise Ratio of the composite TV Signal expressed as peak-to-peak to rms noise

C/N = Unmodulated C/N Ratio
B_{if} = IF Bandwidth
Fp = Peak Deviation
f_b = Top Baseband Frequency
Kpr = Pre-emphasis and noise weighting improvement = 14.0 db factor for 525 line TV system (Monochrome or color system)
Kpp = Peak-to-peak to rms noise measurement = 9 db

$$S/N = 17.9 + 10 \log \frac{40}{10} + 20 \log 3 \frac{15}{5} + 14.0 + 9$$

S/N = 60 db (For Video Signal) where there is no multiplexed audio

The unweighted S/N = 49 db

Power Budget for a composite video signal with a multiplexed aural signal

Receiver Carrier to Noise (C/N) = 17.9 db

$$\text{Video } S/N = 17.9 + 10 \log \frac{40}{10} + 20 \log 3 \frac{13\text{MHz}}{4.3\text{MHz}} + 14 + 9$$

Video S/N = 61 db for color or monochrome (the unweighted video S/N = 50 db)

$$\text{Audio } S/N = C/N + 10 \log \frac{B_{ifs}}{B_{ifs}} + 10 \log \frac{B_{if}}{2b} + 20 \log \frac{\Delta Fs}{FMs} + 20 \log 3 \frac{\Delta F}{FM} + Kp$$

Where

$B_{if}r$ = IF Bandwidth of Radio
b = Audio Bandwidth
$B_{if}s$ = IF Bandwidth of Subcarrier
f_b = Highest Audio Frequency
ΔFS = Peak Deviation of Subcarrier on IF
ΔF = Peak Deviation of Audio on Subcarrier
KP = Pre-emphasis Factor
f_b = Audio Subcarrier Frequency

$$\text{Audio } S/N = 17.9 + 10 \log \frac{40\text{ MHz}}{300\text{ kMz}} + 10 \log \frac{300\text{ kHz}}{30\text{ kHz}} + 20 \log \frac{0.5\text{ MHz}}{4.9\text{ MHz}} + 20 \log 3 \frac{50\text{ kHz}}{15\text{ kHz}} + 10$$

Audio S/N = 54.0 db

Noise power is based upon the following receiver IF bandwidths: HF = 550 kHz; VHF No. 1 = kHz, VHF No. 2 = 260 kHz; UHF/TV Aural = 110 kHz; and UHF/Wideband = 40 MHz. A noise figure of 7.0 db has been used for the HF and UHF systems and 7.5 db has been used for the UHF configurations.

Standard peak frequency deviations are used for the VHF No. 1 and VHF No. 2 ($\pm$ 75 kHz) and UHF/TV Aural ($\pm$ 25 kHz). For the HF case, $\pm$ 200 kHz is used to make use of the FM improvement factor. This could be reduced if the need arises. For the UHF wideband configuration, $\pm$ 15 MHz is used for the video FM deviation.

Preemphasis is used for all four configurations. The theoretical noise gain improvement using a 75 microsecond preemphasis network for FM broadcast with an audio bandwidth of 15 kHz is 13.0 db. From a realistic standpoint, only 9 db is realizable because the audio modulation level to the transmitter has to be reduced to approximately 4 db to prevent overmodulation caused by the preemphasized high frequency component of the program intelligence. The above numbers have been verified in field tests by the National Broadcasting Company (NBC) and the British Broadcasting Company (BBC) by measurement and subjective listening tests.

The 7 db fading allowance included in the power budget is based on the following factors:

a. 2 to 5 db equipment attrition

b. Atmospheric fading including rainstorms

c. Radome losses including wet radome

d. Wind distortion and icing of the ground antenna (if radome is not used).

The required ERP for the power budgets has been determined on the basis of providing carrier power at a minimum of 20 db above the receiver noise or 10 db above the FM threshold. These factors include the fading allowance of 7 db.

The results are as follows:

Configuration	(C/N) Threshold	(C/N) With 7.0 db. Allowance
HF	12.2	22.3
VHF No. 1	9.5	26.4
VHF No. 2	9.7	27.1
UHF Aural	7.8	33.7
UHF Wideband	8.0	24.9

4.4.3 TECHNOLOGY EVALUATION

4.4.3.1 General

The major technological considerations for the uplink were selection of frequency and specification of technical standards.

Frequency selection depended upon technical considerations (i. e., selection of frequencies technically suitable) and spectral occupation (i. e., allocation by appropriate national or international bodies). Part of the problem of technical standards involved the question of the extent to which normal broadcast standards were applicable to the uplink; therefore, these standards were examined in some detail.

4.4.3.2 Frequency Selection

The major technical considerations in frequency selection are concerned with atmospheric transmission, background noise and antenna sizes.

The major atmospheric window for radio transmission is in the range between the ionospheric critical frequencies (above 10 MHz) and the beginning of serious absorption by rainfall and atmospheric gases (15 to 20 GHz). There are a number of windows in the range between 20 and 200 GHz, but reliable transmission through these windows becomes difficult in unfavorable weather.

Within this region: (1) the frequency range below 1 GHz requires large antenna sizes to maintain the narrow beamwidths desirable to minimize interference and (2) the frequency range above 12 GHz results in signal attenuation due to rainfall.

Variation of atmospheric attenuation with frequency is shown in Figure 4.4-9. Variation of rainfall attenuation with frequency is shown in Figure 4.4-10.

On the basis of these considerations, the preferred frequency range lies between 1 and 12 GHz. Operation above this range is feasible, but becomes increasingly affected by atmospheric and rainfall attenuation.

The other major frequency consideration, spectral allocation, is somewhat simplified by the fact that the uplink subsystem is a point-to-point link and so its interference can be minimized.

The bands suggested by the NASA Frequency Coordinator are, in order of priority:

1. 8.4 to 8.5 GHz Space Research, Government and non-Government
2. 8.025 to 8.4 GHz Communication-Satellite (Earth-to-Satellite)
3. 7.9 to 7.975 GHz Communication-Satellite (Earth-to-Satellite)

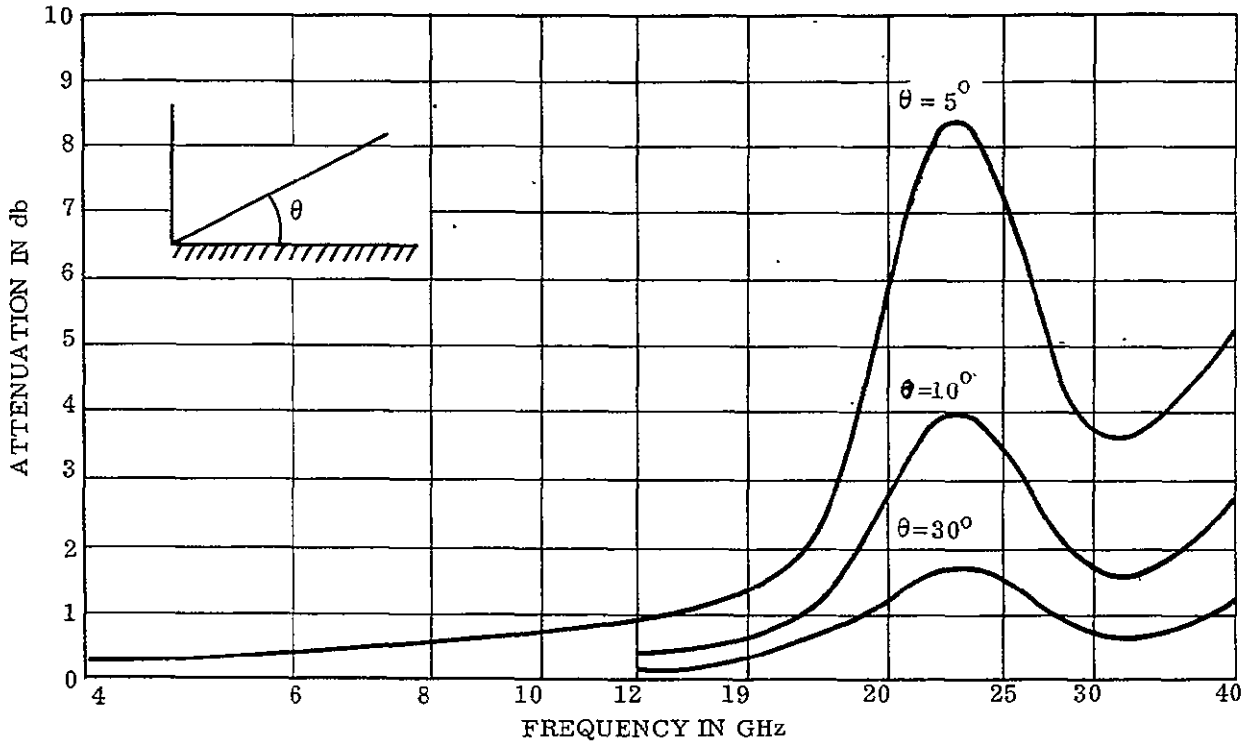

Figure 4.4-9. Atmospheric Attenuation Versus Frequency

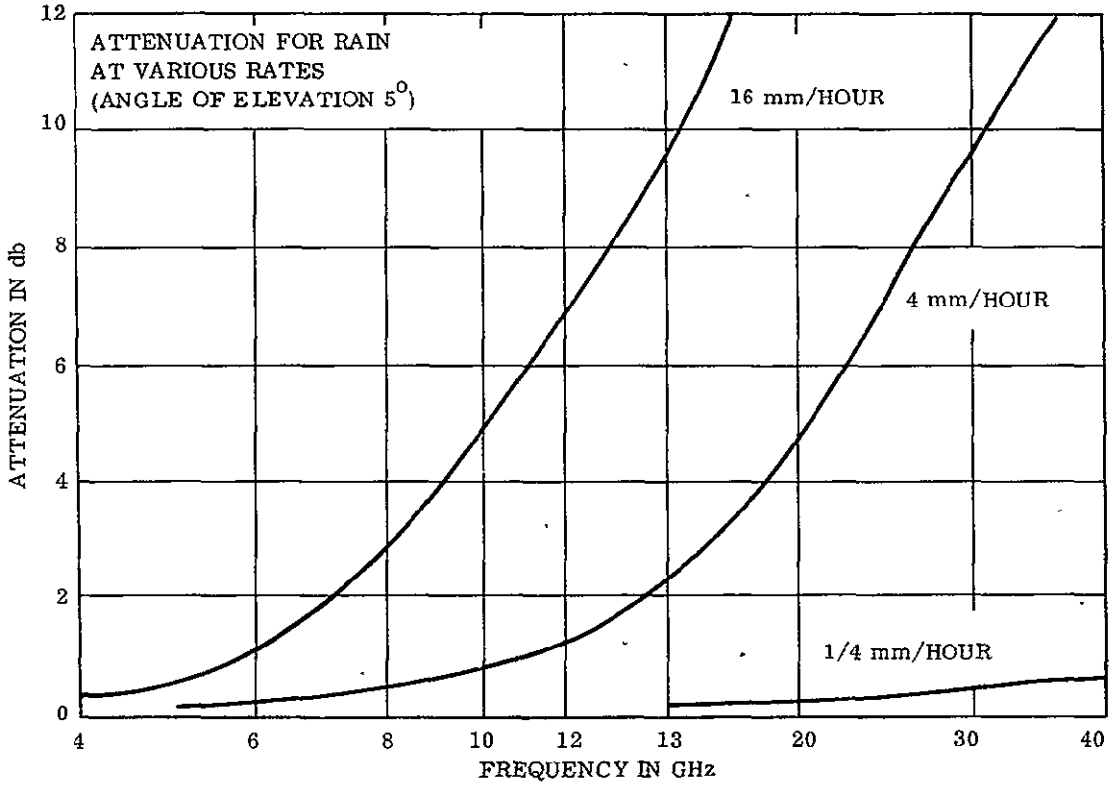

Figure 4.4-10. Rain Attenuation Versus Frequency

4. 5.925 to 6.425 GHz Communication-Satellite (Earth-to-Satellite)

5. 1.99 to 2.11 GHz Studio Transmitter Link

6. 6.875 to 7.125 GHz Studio Transmitter Link

The Frequency Coordinator saw no problem in obtaining a frequency in the 8.4 to 8.5 GHz Space Research band for the early phases of the VBMS program. When broadcast satellites become operational, frequencies in the adjacent band (8.025 to 8.4 GHz) could be obtained. This would permit early test data to be directly applicable to operation, and also it would avoid major hardware changes.

On the basis of the above considerations, a frequency of 8.5 GHz was chosen for all configurations.

4.4.3.3 Technical Standards

There are as yet no formal standards for direct space radio broadcasting to the public. However, it seems reasonable to assume that the present operating and performance standards as applied to the various terrestrial broadcast services will be adapted, or at least used as guides for satellite broadcasting to obtain the same quality service and interference control.

Table 4.4-7 summarizes the performance standards for a number of representative terrestrial services, and lists suggested standards for the uplink subsystem. Tentative overall standards for broadcast satellites are also suggested.

Table 4.4-7. System Performance Factors UHF Configuration

	Audio Facilities EIA RS-219	Aural Transmitter EIA RS-240	STL EIA RS-250	FCC Transmission Standards	Suggested Uplink Standard	Suggested Revised Overall Standard for Direct Broadcasting from Space	Remarks
Frequency Response	100-7500 Hz +0, -2db 50 Hz +0, -3 db 15,000 Hz +0, -3 db	50-15,000 Hz ± 1 db	100-7500 Hz ± 1.5 db 50 Hz +0, -2.0 db 15,000 Hz +0, -2.0 db	100-7500 Hz +0, -3 db 50 Hz +0, -4 db 15,000 Hz +0, -5 db	100-7500 Hz +0, -1.5 db 50 Hz +0, -2.0 db 15,000 Hz +0, -2.0 db	100-7500 Hz +0, -3 db 50 Hz +0, -4 db 15,000 Hz +0, -5 db	The EIA Standard RS-250 for STL performance is considered to be a logical standard for the equivalent uplink. The FCC transmission standards for TV/Aural are considered to be logical standards for the VBMS system.
Distortion, Total rms Harmonic	100-7500 Hz 1.0% 50-100 Hz 1.75% 7500-15,000 Hz 1.5%	50-100 Hz < 1.5% 100-7500 Hz < 1.0% 7500-15,000 Hz < 1.5%	50-100 Hz < 1.75% 100-7500 Hz < 1.25% 7500-15,000 Hz < 1.5%	50-100 Hz < 3.5% 100-7500 Hz < 2.5% 7500-15,000 Hz < 3.0%	50-100 Hz < 1.75% 100-7500 Hz < 1.25% 7500-15,000 Hz < 1.5%	50-100 Hz < 3.5% 100-7500 < 2.5% 7500-15,000 Hz < 3.0%	The EIA Standard RS-250 for STL performance is considered to be a logical standard for the equivalent uplink. The FCC transmission standards for TV/Aural are considered to be logical standards for the FBMS system.
FM Noise Reference 100% Modulated 400 Hz		> 58 db down	> 58 db down	> 55 db down	> 52 db down	> 49 db down	Reduction in overall standard suggested due to inherent limitation in down-link.
AM Noise Reference 100% Modulated 400 Hz		> 50 db down	> 58 db down	> 50 db down	> 50 db down	>50 db down	Reduction in overall standard suggested due to inherent limitation in down-link.
Modulation		± 50 kHz maximum	No Standard	± 25 kHz for 100% modulation	± 25 kHz for 100% modulation	± 25 kHz for 100% modulation	
RF Frequency Tolerance				± 1 kHz	± 100 Hz	± 1 kHz	Due to the fact that the ground station would be attended, practically all of the allowable frequency drift is allocated to the satellite transmitter.

4.5 ATTITUDE CONTROL

4.5.1 INTRODUCTION

4.5.1.1 Summary

This section presents the results of the analysis performed with respect to the selection of the attitude control and antenna pointing subsystems.

Section 4.5.2 describes the selected subsystems for the four VBMS configurationtions and a description of the closed-loop antenna pointing system.

Section 4.5.3 presents the technology evaluation of attitude control systems and components.

The attitude control system is one of the critical subsystems that affects spacecraft performance, cost, and reliability. The scope of this study was (1) to establish feasible conceptual designs for the attitude control system from the standpoint of stabilizing each spacecraft and (2) to decide the best method of pointing the broadcast antenna to the desired coverage area. This tradeoff study was dependent upon the ERP devision, which required a cost-weight interaction analysis of the attitude control, antenna, transmitter, and power subsystem. The selected subsystem then presented a basis for evaluation of the cost and technology development requirements.

4.5.1.2 Conclusion

The general conclusion reached for the attitude control subsystem was that the passive systems (gravity gradient or solar pressure stabilized) were not applicable to the VBMS systems. A hybrid passive system was selected for one configuration (VHF No. 2) and active attitude control systems were selected for the other three configurations.

The antenna pointing is adequately accomodated by open loop pointing from the stable platform for two of the configurations (HF and VHF No. 2) while the other two systems employ an interferometer signal from the coverage area to gain more accurate pointing.

4.5.2 SUBSYSTEM DESCRIPTION

The components needed for the attitude control subsystems selected are within the state of the art; however, design of attitude control subsystems for large flexible satellites require improved analytical techniques and test methods. Section 6.1.2 describes the recommended technology program necessary to overcome the development risk associated with designing attitude control subsystems for the HF, VHF No. 1 and UHF configurations.

4.5.2.1 HF Attitude Control Subsystem

The large size of HF antenna and power subsystems necessitate that they be erectable. The stabilization subsystem approach was to minimize articulation of parts and to minimize inertial rates of the satellite. Constrained controller dynamics produce the least structural compliance,

controller interaction by a minimized controller bandwidth. This configuration presents the greatest problems to be overcome in satisfying mission constraints. The orbit altitude (4356 nm) presents an environment in which the gravity gradient torque is large. Array and antenna dimensions are so large that significant moment arms for all solar pressure forces are provided. Configuration constraints in package and erection and the gross uncertainties in the evaluation of solar pressure torques for the large solar aspect changes due to orbital and seasonal motions preclude a passive system.

The satellite is required to broadcast 1 hour during each orbit at sunset. Five separate areas can be covered each day with the 4.8-hour period orbit. One area is covered during each orbit. After the fourth orbit, the pattern repeats itself. The array must be pointed to the sun for maximum efficiency, and the antenna must be pointed to the specified coverage area with an accuracy of ± 0.20 degrees per axis.

The antenna was rigidly mounted to the main body with the satellite pointed to the earth using an IR sensor for pitch and roll control and a Polaris tracker for yaw control. The body of the antenna points to the center of the earth. The antenna beam, then points electronically to the specified coverage area. Solar array articulation requires a two-axis mechanical gimbal because the vehicle frame has local vertical and equatorial north pole references. One gimbal rotation is a yaw rotation to allow for the motion of the sun as a function of time of year, and the other gimbal is a pitch rotation to allow for the motion of the sun as a function of position in orbit.

Because the antenna must point to the earth only during the transmission period (hour at sundown during each orbit) it was proposed that, at the end of its transmission period, control be switched from the IR sensor to a rate and position gyro package. This type package was developed for the Orbiting Astronomical Observatory program.

Figure 4.5-1 shows the sequence for switching from the IR sensor to the gyro package and back again. At Position 1 the IR sensor is locked on the earth and controlling the spacecraft in pitch and roll. The Polaris tracker which is pointing up out of the paper is locked onto the star Polaris and controlling the spacecraft in yaw. At Position 2, which is the end of transmission, control of the roll and pitch axes is switched from the IR sensor to the gyro package. By Position 3 attitude of the antenna and the main body is fixed inertially in order to mimimize the transient associated with reacquisition of the earth by the IR scanners and to avoid shielding of the solar array by the antenna. The attitude of the antenna and the main body (immediately after switching to the gyro package) will be slewed to and held at the attitude required a few minutes before the beginning of transmission. This attitude will be maintained until the spacecraft reaches Position 1 again. At this time, the IR sensor should measure a zero attitude error and the switch from the gyro package back to the IR scanner should be accompanied by only a minimum transient. A more descriptive illustration of the orbital motion is presented as Figure 4.5-2. Flywheels are used as actuators with mass expulsion for unloading.

The subsystem block diagram is shown in Figure 4.5-3. The coverage programmer requires updated information to reduce boresight and orbit uncertainties and adjustment of seasonal

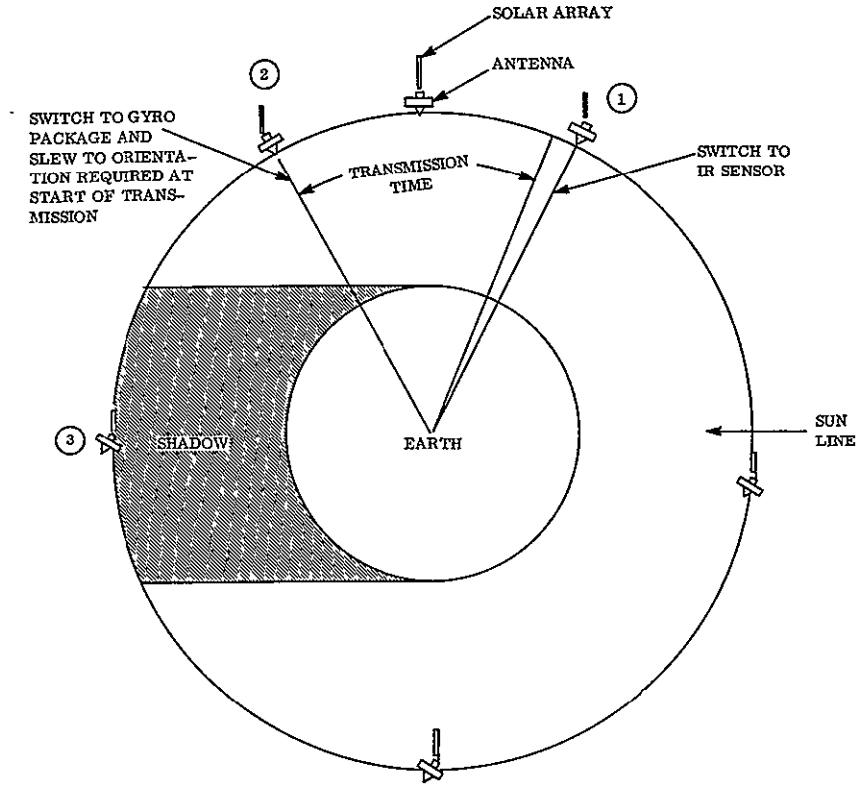

Figure 4.5-1. HF Orbital Motion

The attitude control subsystem components are listed in Table 4.5-1. This table includes the autopilot components as well because some components are used by both subsystems (attitude control and autopilot).

Table 4.5-1. HF Attitude Control Components

Component	Weight (lb)	Power (w)	Volume
Polaris Tracker*	6	5	4-1/2 x 5 x 11 in.
Sun Sensors	2		
Gyro Control Assembly*	18	20	7-1/2 x 7-1/2 x 7-1/2 in.
Signal Processor*	6	3	200 $in.^3$
Mass Expulsion System*	60	10	6 x 6 x 10 in.
Flywheels	20	2	16 in. dia., 5 in. high
Programmer	8.5	4.5	300 $in.^3$
AOGO IR Sensor	14	8.5	2 Scanner Boxes 6.5 x 7.5 x 3 in. 1 Electronics Box 5 x 7 x 3 in.
Solar Array Gimbal	100	20	

*Components used in both attitude control and autopilot functions.

The stabilization system performance goal is $\pm 0.20^{\circ}$ per axis for antenna pointing with a budget of $\pm 0.1^{\circ}$ for sensor errors, $\pm 0.05^{\circ}$ for the programmer resolution, and $\pm 0.05^{\circ}$ for beam pointing. Because the solar array is being driven by a gimbal, the natural frequency of the array must be at least a factor of ten greater than the crossover frequency of the gimbal control loop.

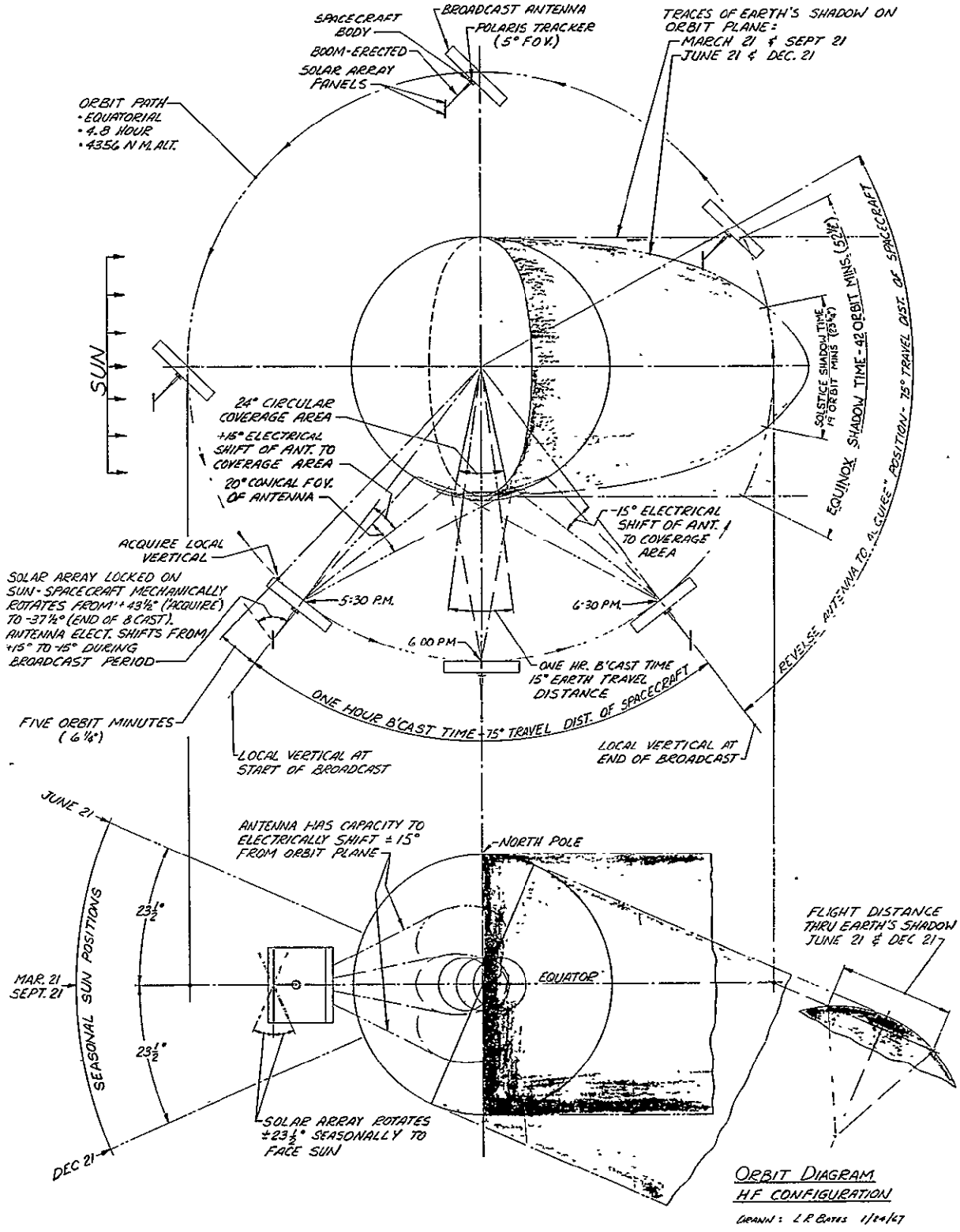

Figure 4.5-2. Detailed Orbit Diagram for the HF Configuration

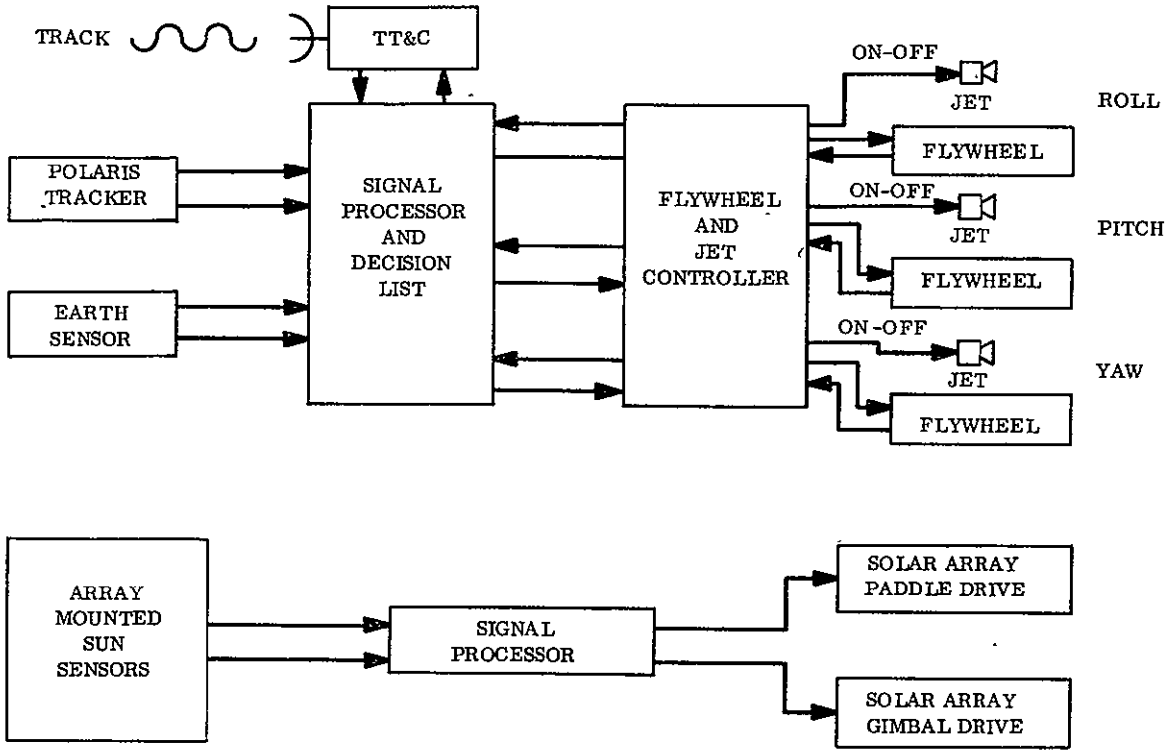

Figure 4.5-3. HF Attitude Control Subsystem Block Diagram

4.5.2.2 VHF No. 1 Attitude Control

This configuration demonstrates voice transmission in the FM band to conventional receivers for a nearly continuous duty cycle. A near-synchronous orbit is established initially and a programmed drift occurs until longitude for continental United States is achieved, at which time the satellite is stationed in the synchronous orbit for the rest of its mission life. Broadcasting will occur to variable locations during the drifting mode.

The primary design requirement to the attitude control subsystem is that the broadcasting is continuous (except during earth occultation), and therefore the antenna must point to the earth while the solar array tracks the sun. The pointing accuracy requirements for the antenna are 0.2^{o} per axis during the drift mode, and 0.1^{o} per axis during the final part of the mission.

The proposed subsystem is an active three-axis stabilization system with two axes stabilized to the local vertical and third axis control normal to the orbit plane. Sensors are earth scanners and a Polaris tracker. Actuators are momentum wheels on three axes with mass expulsion unloading. Solar array articulation is accomplished by means of two gimbals between the stabilization reference axes and the array. Gimbal drives are controlled by resolution of solar aspect angle signals produced by sun sensors located on the solar array face.

Antenna beam pointing, relative to the stabilization axes, is achieved electrically in the phased array. Beam pointing is accomplished by programmed ground command for the variable station mode. The pointing is open loop in this mode with reduced accuracy allowable by reduced area coverage requirements. The final operating mode is coverage of the continental United States requiring increased beam pointing accuracy. An interferometer located in the center of the coverage area will be used to increase the mode for this accuracy.

Sun tracking by the solar array does not have the pointing accuracy requirements of the antenna, a pointing accuracy of 5^{o} being adequate. Two gimbals are used to achieve this tracking. The first gimbal is a 360^{o} gimbal with an electrical slip-ring to allow the antenna to point to the earth. The second gimbal is a closed gimbal with flexible wire conductors and accounts for the $\pm 23.5^{o}$ engendered by the seasonal motion of the earth. The required rates of motion are so low that friction places the gimbal actuators automatically in a bang-bang mode for continuous control. A stepper system therefore seems to present a much more desirable mode than a continuous drive.

Sun sensors on the array face are used to generate the sun-tracker error signals. Signal processing and actuation is discontinuous. The entire system is array- and gimbal-mounted.

Figure 4.5-4 indicates the motion of the satellite about the orbit normal and the motion of the solar array with respect to the spacecraft frame.

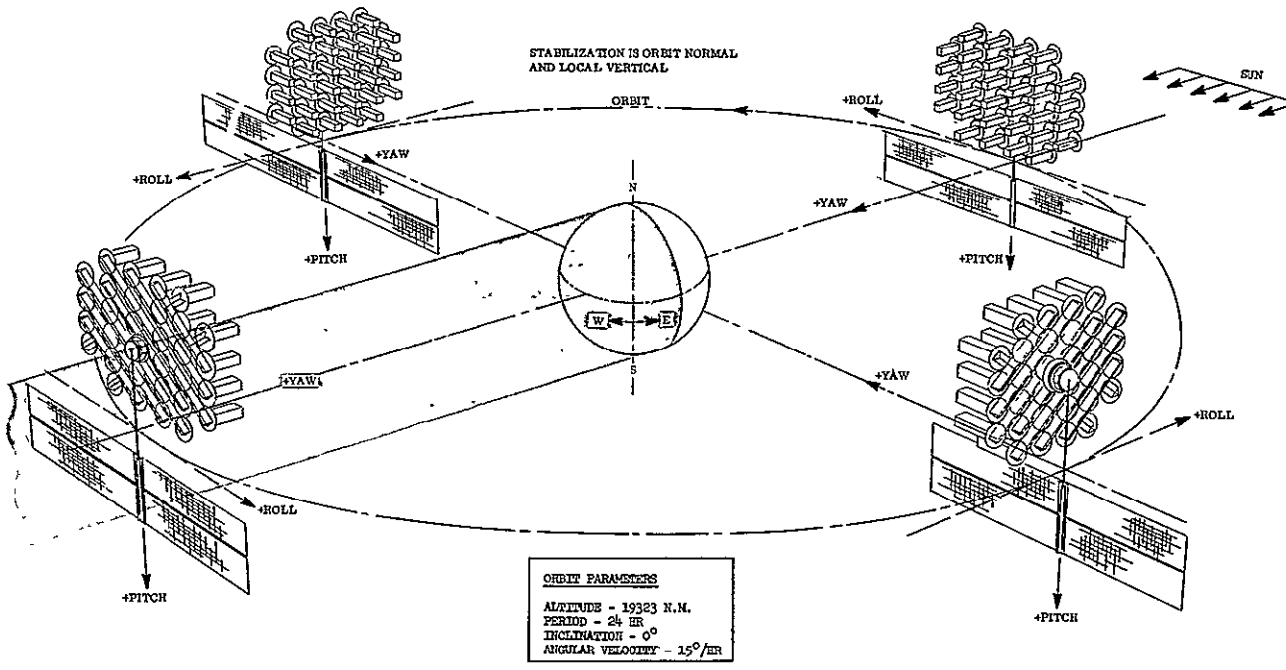

Figure 4.5-4. VHF No. 1 Configuration Orbital Motion

The subsystem block diagram is shown in Figure 4.5-5. The signal processor requires update information as the demonstration coverage requirements change with the programmed drift in satellite longitude during the first three months but will remain fixed during the balance of the mission (when in geocentric orbit).

The stabilization subsystem component descriptions are listed in Table 4.5-2. This table also includes the autopilot components because both subsystem functions use some of the same components. Common components are indicated by an asterisk.

Table 4.5-2. Stabilization Subsystem Components

Component	Weight (lb)	Power (Watts)	Volume ($in.^3$)
Rate Gyro Package (3)*	7.2	24	175
RAPS Gyro Package (3)*	18	20	350
Sun Sensors (6)	7.2	6.5	
Star Tracker (1)*	.12	8	247.5
Planet Scan (1)	8		
Accelerometer	2	5	15
Electronics	53	86	
Solar Array Drive (2)	37.2		
Flywheels (3)	40	30	1630
Mass Expulsion Hdw.*	104	13	
Gimbal Drive	19		

*Common attitude control and autopilot components.

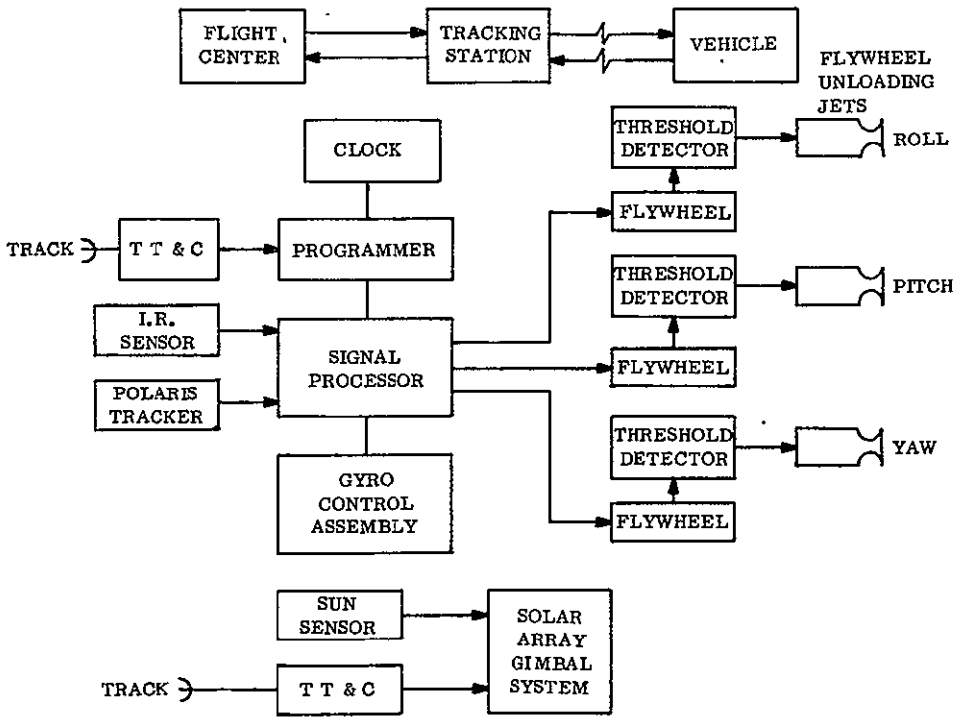

Figure 4.5-5. VHF No. 1 Attitude Control Subsystem Block Diagram

The attitude control subsystem performance goal is $\pm 0.2^{o}$ per axis for antenna pointing during world coverage and $\pm 0.1^{o}$ per axis during United States coverage. Error budgeting between sensors, programmer resolution and beam pointing are to be determined. Because the solar array is articulated, the array drive control bandwidth must not exceed the attitude controller bandwidth.

4.5.2.3 VHF No. 2 Attitude Control

The VHF antenna directivity required at the 7556 nm altitude allows a reasonable aperture size for these frequencies. Solar array size is manageable because the broadcast duty cycle allows energy collection for a time period greater than broadcast time. Batteries are used to store this energy for use during the broadcast time. The solar array is still required to be pointed to the sun for maximum energy collection.

The satellite for the VHF No. 2 mission will be launched into a circular, equatorial orbit with an altitude of 7556 nm and a period of 8 hours. It will be required to broadcast 1 hour during each orbit at sunset. During this time, the sun will be at an angle of $\pm 23.5^{o}$ with respect to the normal to the yaw or earth pointing axis. Therefore, the solar panel may be fixed to the body and extended along the yaw axis with only a small loss in power during the broadcast time. Control about the yaw axis will be required to maintain the plane of the solar panel nominally perpendicular to the sun line during the time of broadcast. Maximum allowable attitude control errors are $\pm 1^{o}$ in yaw and roll, and $\pm 2^{o}$ in pitch.

This configuration approximates a dumbbell which lends itself to gravity gradient control for the pitch and roll axes and flywheel for control about the yaw axes. It will have a single rod 150 feet long and a tip mass weight of 40 pounds. Two modulated flywheels are required for yaw control. By proper selection of flywheel speeds, the yaw axis can be controlled to any null. This will allow orientation of the solar panels so that they are nominally perpendicular to the sun line at the time of broadcast during the summer and winter, as well as during the spring and fall. The flywheels require an angular momentum storage capacity of 10 lb-ft/sec each. The damper is an inside-out ball damper. The rod deployment device and the damper will be placed in the tip mass to minimize weight. The rod deployment device will be controlled by a hard wire or remote control.

Because the vehicle could initially stabilize upside-down, an inversion scheme will be required the recommended scheme provides a torque about the pitch axis sufficient to rotate the vehicle about the pitch axis. When the vehicle has inverted, an equal and opposite torque will be applied. Because the orbit must be a recurring orbit, some form of period control will be required. This will be similar to the stationkeeping system used at synchronous altitude. To minimize the pitch error, the orbit must be nominally circular with an eccentricity of less than 0.015. This requires an orbit tolerance of less than ± 113 nm.

Antenna beam pointing will be performed by articulation of the parabolic antenna feed.

Figure 4.5-6 indicates the motion of the satellite about the orbit normal. The orbit geometry shown is at equinox. The antenna feed is at zero offset and coverage would be equatorial as shown. The time of transmission would correspond to a satellite position at the upper left of the figure. A more descriptive orbit diagram is presented as Figure 4.5-7.

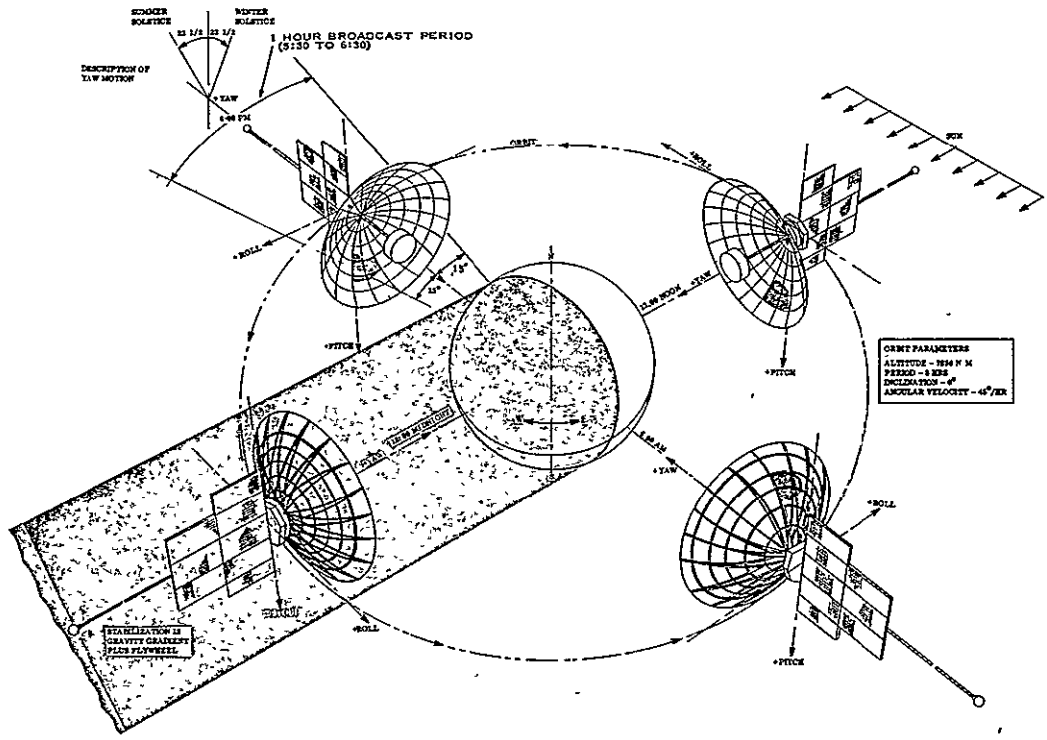

Figure 4.5-6. VHF No. 2 Orbital Motion

The subsystem block diagram is shown in Figure 4.5-8. The gyrocompass programmer requires update information to reduce offsets in stabilization and to compensate for the seasonal geometry changes.

The stabilization subsystem components are listed in Table 4.5-3.

Table 4.5-3. VHF No. 2 Stabilization Subsystem Components

Component	Weight (lb)	Power Average (Watts)	Size
Flywheels (2)	20	2	16 in. Dia. x 5 in. High
Rod			150 feet long
Rod Erection Device			
Damper	40		
Programmer	5	5	6 x 6 x 6 in.

4.5.2.4 UHF Attitude Control

This configuration demonstrates only voice transmission to conventional TV receivers for a nearly continuous duty cycle. To achieve a minimum power resulting in a small solar array and to reduce interference, an extremely accurate antenna pointing system is necessary. At synchronous altitude, solar pressure is the chief disturbance source.

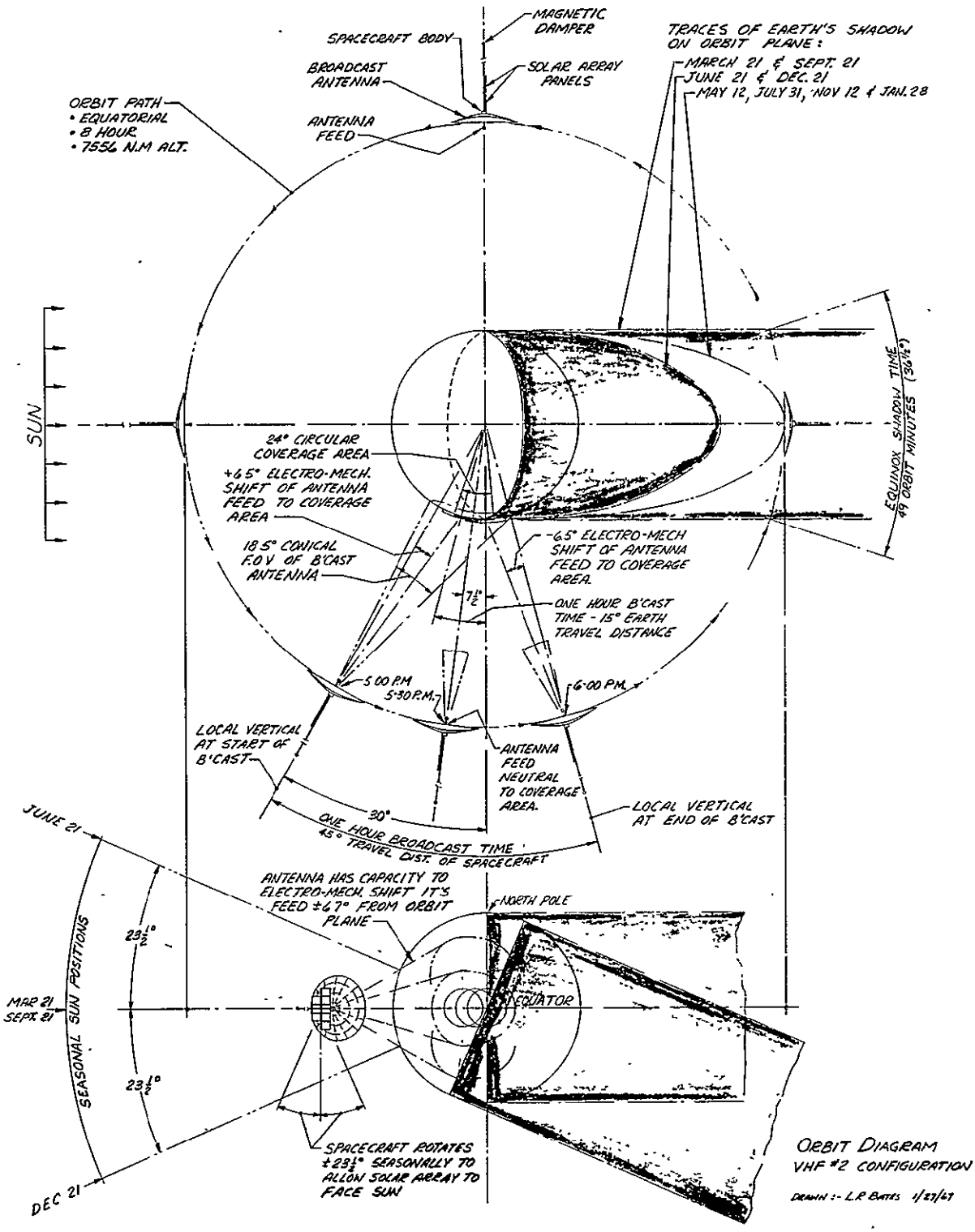

Figure 4.5-7. Detailed Orbit Diagram VHF No. 2 Configuration

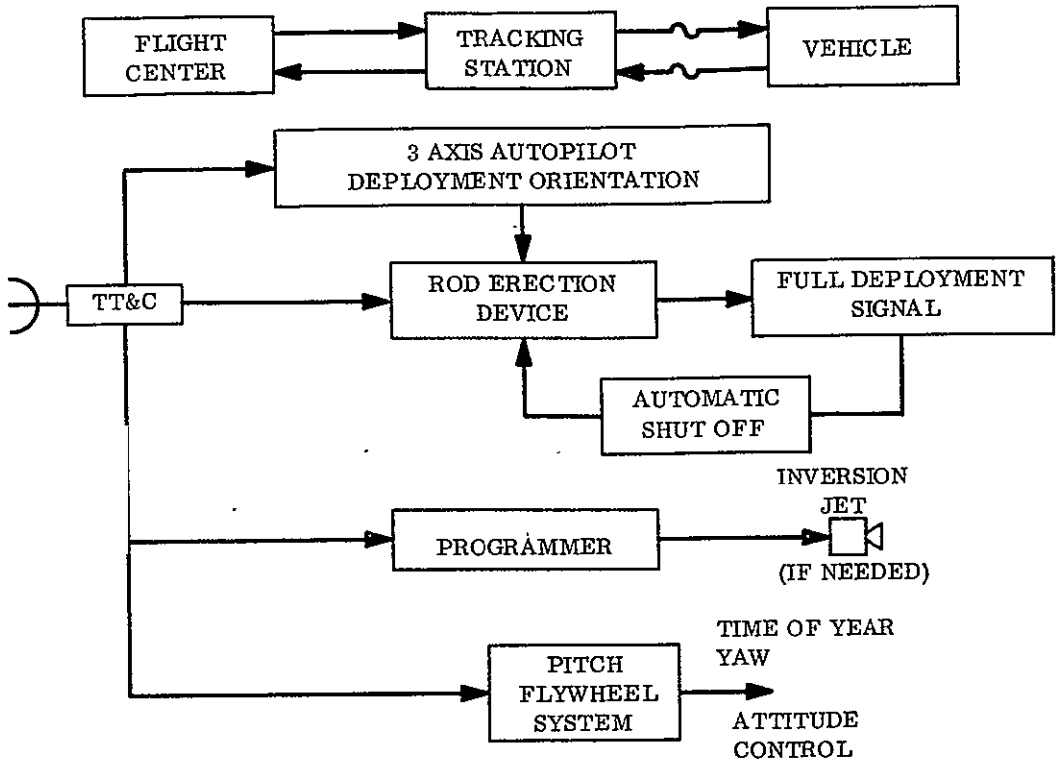

Figure 4.5-8. VHF No. 2 Stabilization Subsystem Block Diagram

The UHF antenna is small enough (22.5-ft diameter) that it possesses sufficiently high natural frequency to minimize coupling with the controller. The solar array dimensions are also small enough (438 ft^2) to controll natural frequency with minimum weight and cost penalty, and the membrane solar cell substrate itself can be tuned to avoid resonant coupling. Consequently, this configuration is considered to be compatible with a dynamically active controller.

Two axes (roll and pitch) are controlled to a time zone centered beacon with interferometer sensing on the spacecraft. The interferometer axes are coincident with the antenna axis and fixed to the vehicle. Articulation necessary for solar array and vehicle pointing is achieved by the paddle axis drive and the free space gimbal available about the spacecraft antenna axis.

Because the attitude reference system will be a central time zone beacon with interferometer sensing, the yaw position is a determinate time function and will be generated by a computer. Computations will resolve the sensor outputs into error signals with their null corresponding to the line to the center of the commanded coverage.

The actuation system selected consisted of flywheels with mass expulsion unloading. Lead network shaping will guarantee stability during the normal mode.

Orbital Motion Study. The vehicle rotates about its yaw axis as it moves in its orbit and a solar array drive on the pitch axis provides the second degree of articulation. Consider the spacecraft as shown in Figure 4.5-9. The positive roll axis is along the velocity vector with the positive yaw axis positioned to some point on the earth. The pitch axis forms the right-handed triad.

The physical constraints on the system are such that the yaw axis must point continually to a prescribed point on the earth while the solar array must remain normal to the sun. line. In this particular configuration, paddle stops are included thus allowing the solar array to move with respect to the body within limited motion (180°). The paddle stop location is usually determined by where in orbit a yaw maneuver is desired. A limited paddle drive may not be necessary. However, in this case, paddle stop placement has been set such that the solar array is initially in the roll-pitch plane at equinox noon, and θ is referenced from that point.

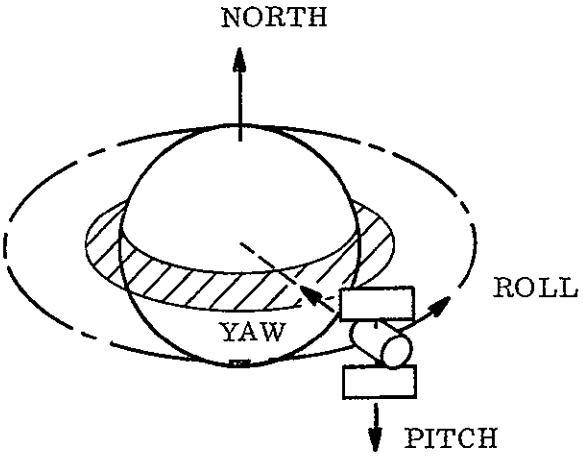

Figure 4.5-9. UHF Satellite Motion

Sun Motion

Let the inertial ecliptic reference system be given by E_1, E_2, E_3 as shown below.

Ecliptic:

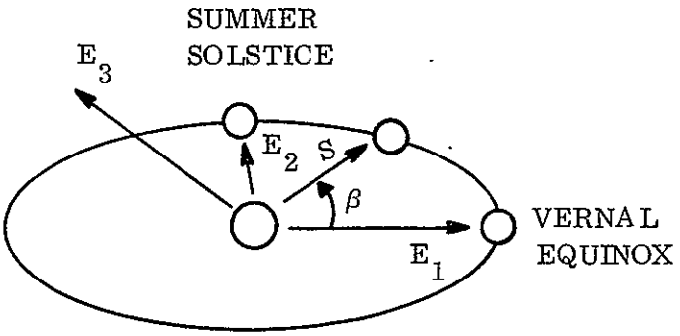

Let $\bar{S}$, be the unit vector of the direction to the sum or

$$\bar{S}_E = \begin{bmatrix} \cos\beta \\ \sin\beta \\ 0 \end{bmatrix}$$

Equatorial:

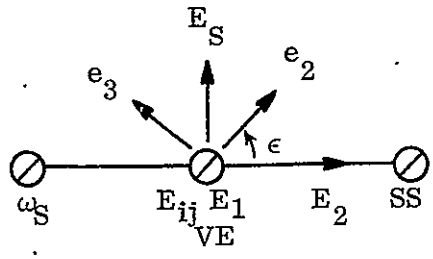

$$\begin{bmatrix} e_1 \\ e_2 \\ e_3 \end{bmatrix} = \begin{bmatrix} 1 & 0 & 0 \\ 0 & \cos\epsilon & \sin\epsilon \\ 0 & -\sin\epsilon & \cos\epsilon \end{bmatrix} \begin{bmatrix} E_1 \\ E_2 \\ E_3 \end{bmatrix}$$

$$\underline{e} = T_{E2e}\underline{E}$$

GEOGRAPHIC:

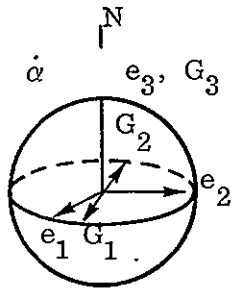

$$\begin{bmatrix} G_1 \\ G_2 \\ G_3 \end{bmatrix} = \begin{bmatrix} \cos\alpha & \sin\alpha & 0 \\ -\sin\alpha & \cos\alpha & 0 \\ 0 & 0 & 1 \end{bmatrix} \begin{bmatrix} e_1 \\ e_2 \\ e_3 \end{bmatrix}$$

$$\underline{G} = T_{e2G}\underline{e}$$

ORBITAL:

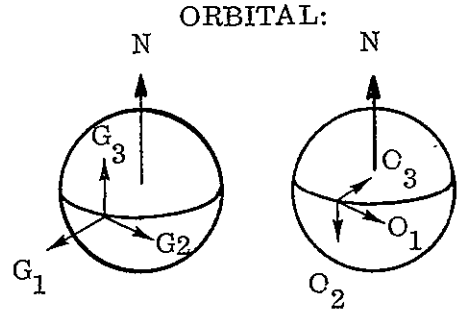

$$\begin{bmatrix} 0_1 \\ 0_2 \\ 0_3 \end{bmatrix} = \begin{bmatrix} 0 & 1 & 0 \\ 0 & 0 & -1 \\ -1 & 0 & 0 \end{bmatrix} \begin{bmatrix} G_1 \\ G_2 \\ G_3 \end{bmatrix}$$

$$\underline{0} = T_{G20}\underline{G}$$

LATITUDE:

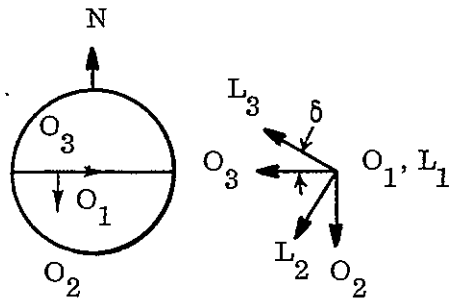

$$\begin{bmatrix} L_1 \\ L_2 \\ L_3 \end{bmatrix} = \begin{bmatrix} 1 & 0 & 0 \\ 0 & \cos\delta & \sin\delta \\ 0 & -\sin\delta & \cos\delta \end{bmatrix} \begin{bmatrix} 0_1 \\ 0_2 \\ 0_3 \end{bmatrix}$$

$$\underline{L} = T_{02L}\underline{0}$$

LONGITUDE:

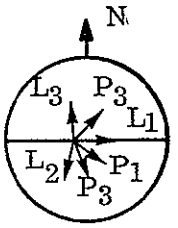

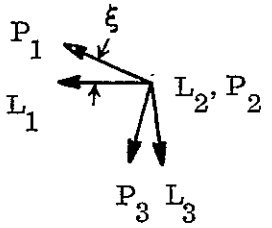

$$\begin{bmatrix} P_1 \\ P_2 \\ P_3 \end{bmatrix} = \begin{bmatrix} \cos\xi & 0 & \sin\xi \\ 0 & 1 & 0 \\ -\sin\xi & 0 & \cos\xi \end{bmatrix} \begin{bmatrix} L_1 \\ L_2 \\ L_3 \end{bmatrix}$$

$$\underline{P} = T_{L2P}\underline{L}$$

VEHICLE:

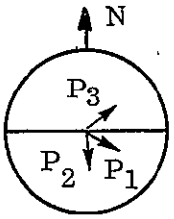

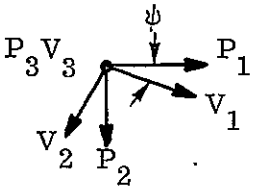

$$\begin{bmatrix} V_1 \\ V_2 \\ V_3 \end{bmatrix} = \begin{bmatrix} \cos\psi & \sin\psi & 0 \\ -\sin\psi & \cos\psi & 0 \\ 0 & 0 & 1 \end{bmatrix} \begin{bmatrix} P_1 \\ P_2 \\ P_3 \end{bmatrix}$$

$$\underline{V} = T_{P2V}\underline{P}$$

Thus the sun motion vehicle coordinates is:

$$\underline{S}_V = T_{P2V}\, T_{L2P}\, T_{02L}\, T_{G20}\, T_{e2G}\, T_{E2e}\, E$$

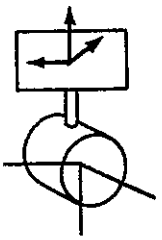

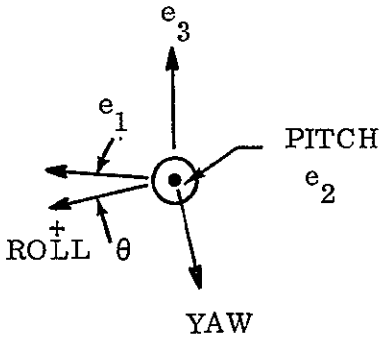

$$SA_V = \begin{bmatrix} \cos\theta & 0 & \sin\theta \\ 0 & 1 & 0 \\ -\sin\theta & 0 & \cos\theta \end{bmatrix} \begin{bmatrix} 0 \\ 0 \\ -1 \end{bmatrix}$$

$$\begin{bmatrix} SA_R \\ SA_P \\ SA_Y \end{bmatrix} = \begin{bmatrix} -\sin\theta \\ 0 \\ -\cos\theta \end{bmatrix}$$

It is now required that

$$\underline{SA}_V := \underline{S}_V$$

and

$$0 \le \theta \le 180^\circ .$$

thus

$$\underline{SA}_V = \underline{S}_V = T_{P2V}\ T_{L2P}\ T_{02L}\ T_{G20}\ T_{e2G}\ T_{E2e}\ E$$

$$\begin{bmatrix} -\sin\theta \\ 0 \\ -\cos\theta \end{bmatrix} = \begin{bmatrix} \cos\psi & \sin\psi & 0 \\ -\sin\psi & \cos\psi & 0 \\ 0 & 0 & 1 \end{bmatrix} \begin{bmatrix} \cos\xi & 0 & \sin\xi \\ 0 & 1 & 0 \\ -\sin\xi & 0 & \cos\xi \end{bmatrix} \begin{bmatrix} 1 & 0 & 0 \\ 0 & \cos\delta & \sin\delta \\ 0 & -\sin\delta & \cos\delta \end{bmatrix} \begin{bmatrix} 0 & 1 & 0 \\ 0 & 0 & -1 \\ -1 & 0 & 0 \end{bmatrix}$$

$$\begin{bmatrix} \cos\alpha & \sin\alpha & 0 \\ -\sin\alpha & \cos\alpha & 0 \\ 0 & 0 & 1 \end{bmatrix} \begin{bmatrix} 1 & 0 & 0 \\ 0 & \cos\epsilon & \sin\epsilon \\ 0 & -\sin\epsilon & \cos\epsilon \end{bmatrix} \begin{bmatrix} \cos\beta \\ \sin\beta \\ 0 \end{bmatrix}$$

which reduces to

$$= \begin{bmatrix} \cos\psi \left\{ (-\sin\xi \cos\delta \cos\alpha - \cos\xi \sin\alpha) \cos\beta + \left[(-\sin\xi \cos\delta \sin\alpha + \cos\xi \cos\alpha) \cos\epsilon - \sin\xi \sin\delta \sin\epsilon \right] \sin\beta \right\} - \sin\psi \left\{ \sin\delta \cos\alpha \cos\beta + (\sin\delta \sin\alpha \cos\epsilon - \cos\delta \sin\epsilon) \sin\beta \right\} \\ -\sin\psi \left\{ (-\sin\xi \cos\delta \cos\alpha - \cos\xi \sin\alpha) \cos\beta + \left[(-\sin\xi \cos\delta \sin\alpha + \cos\xi \cos\alpha) \cos\epsilon - \sin\xi \cos\delta \sin\epsilon \right] \sin\beta \right\} - \cos\psi \left\{ \sin\delta \cos\alpha \cos\beta + (\sin\delta \sin\alpha \cos\epsilon - \cos\delta \sin\epsilon) \sin\beta \right\} \\ (-\cos\xi \cos\delta \cos\alpha + \sin\xi \sin\alpha) \cos\beta + \left[(-\cos\xi \cos\delta \sin\alpha - \sin\xi \cos\alpha) \cos\epsilon - \cos\xi \sin\delta \sin\epsilon \right] \sin\beta \end{bmatrix}$$

The middle relation yields an equation in ψ which contains two unknowns. Thus, another expression must be generated. Its equivalent is a physical placement of ψ or its equivalent in the correct quadrant. Determination of θ is in closed form because two equations are available.

Solution of the above equations is shown in Figure 4.5-10. In this presentation $\beta = 0^{o}$ corresponds to the vernal equinox while α represents the daily motion. That is, for $\beta = 0^{o}$ $\alpha = 0^{o}$ occurs at the high noon position; $\alpha = 90^{o}$ corresponds to the 6:00 P.M. position; etc., when $\beta = 90^{o}$ (summer solstice) the high noon position now occurs at $\alpha = 90^{o}$ etc.

This approach was made highly desirable by the achievable antenna directivity with reasonable aperture size at this frequency and the pointing accuracy possible with an interferometer sensor. These two factors resulted in a manageable solar array area. Single articulation with respect to the body frame of the array represents an extension of the Nimbus design. The array size produces mass moments which will require gain scheduling in roll and yaw to compensate for the "changing" moments of inertia about these axes. This gain scheduling can be readily achieved by sensing only the single array drive position with respect to the body frame. Cross products of inertai produced by articulation will be minimized by judicious configuration design.

Figure 4.5-11 indicates the motion of the satellite about the yaw (antenna) axis and the motion of the solar array with respect to the spacecraft frame. The orbit geometry shown is at equinox and the antenna pointing is for north latitude, such as for the continental United States coverage.

The subsystem block diagram is shown in Figure 4.5-12. The diagram includes attitude update computers for roll and pitch offsets to be used along with the interferometer sensors to achieve time zone coverage for zones other than the Central Time Zone. Sun sensors or the orbit ephemeris are potential information information sources for the offset pointing function generation.

The stabilization subsystem components are described in Table 4.5-4. The mass expulsion hardware is that required for the unloading of the angular momentum management system used in the active stabilization for the two-year lifetime.

The stabilization subsystem performance goal is $\pm 0.1^{o}$ per axis for antenna pointing to the Central Time Zone and $\pm 0.2^{o}$ per axis for other time zones. The solar array pointing accuracy should be within 5^{o} of the sun line. Verification of the elimination of structural compliance controller interaction is required and will be an interface consideration in the configuration design.

4.5.2.5 Interferometer Attitude Control Sensing

Following is an interferometer design meeting all the requirements for the sensor for the VHF No. 1 and UHF configurations. The sensor requirements used in arriving at this design are:

Overall sensor accuracy (1σ)	0.05 degree
Unambiguous field of view	± 11 degrees
Output data rate	10 readings per second

NOTE

(1) IF ORBIT LOCATION IS 92° W LONG., THEN THE VEHICLE YAW AXIS POINTS TO THE EASTERN PART OF U.S.

(2) α = SOLAR ARRAY YAW ANGLE

(3) ϵ = 23.5° (ORBIT INCLINATION)

(4) δ = 6° (LATITUDE ROTATION)

(5) ξ = 5.6° (LONGITUDE ROTATION)

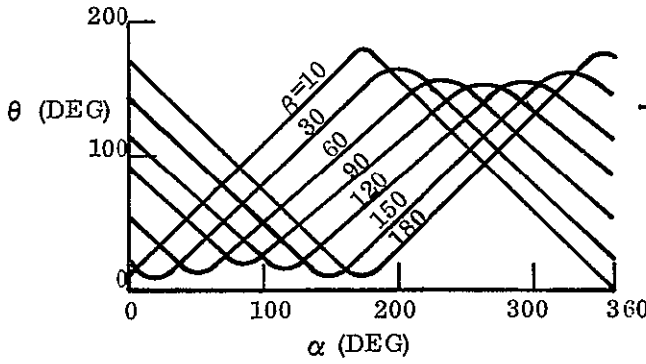

SOLAR ARRAY

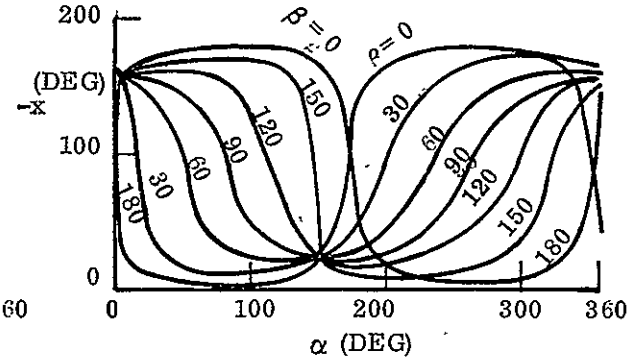

YAW ANGLE

MOTIONS FOR SPRING TO FALL

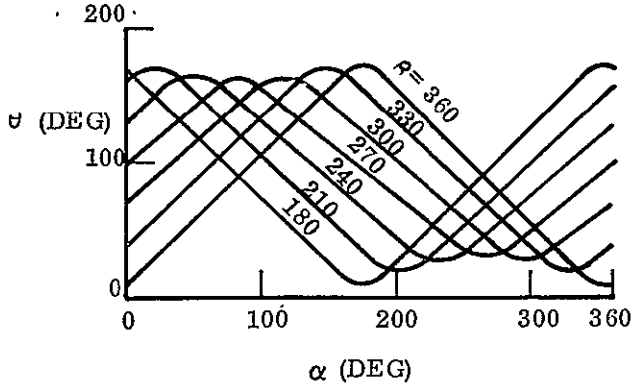

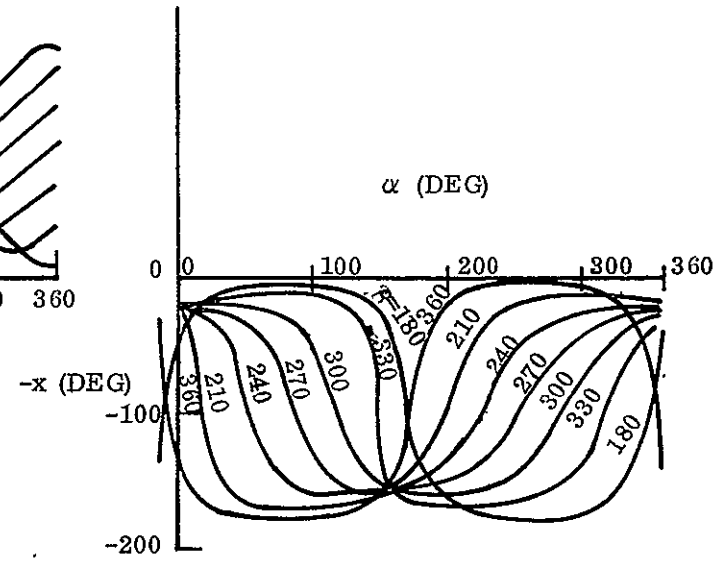

MOTIONS FOR FALL TO SPRING

Figure 4.5-10. Daily Yaw and Solar Array Motions for Season of Year (Pointing off Local Vertical)

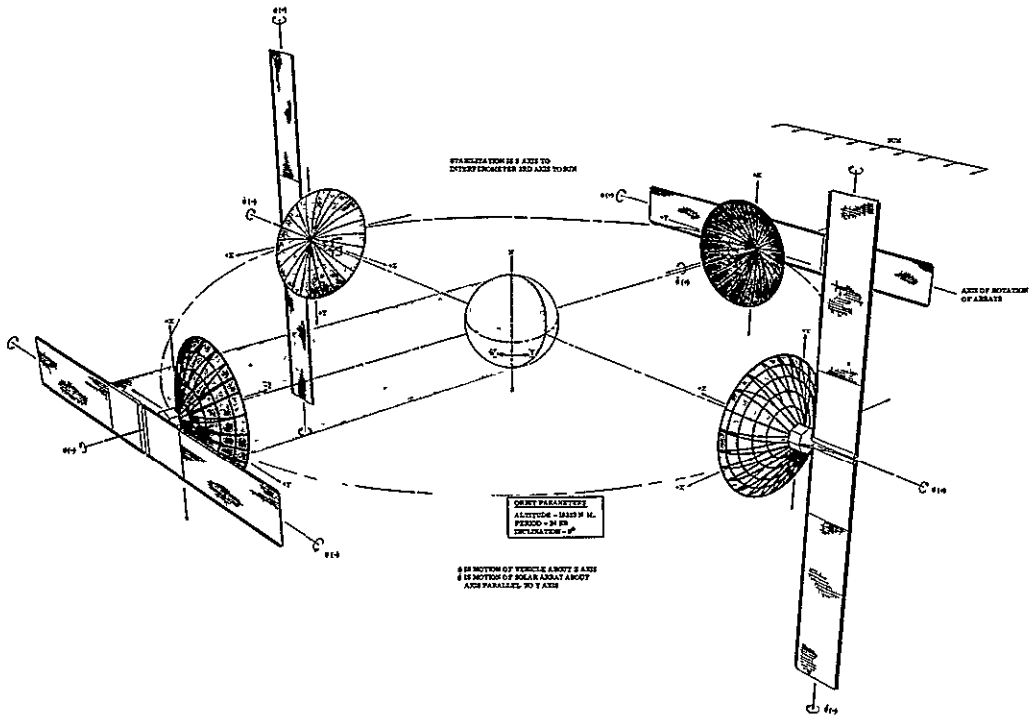

Figure 4.5-11. UHF Orbital Motion

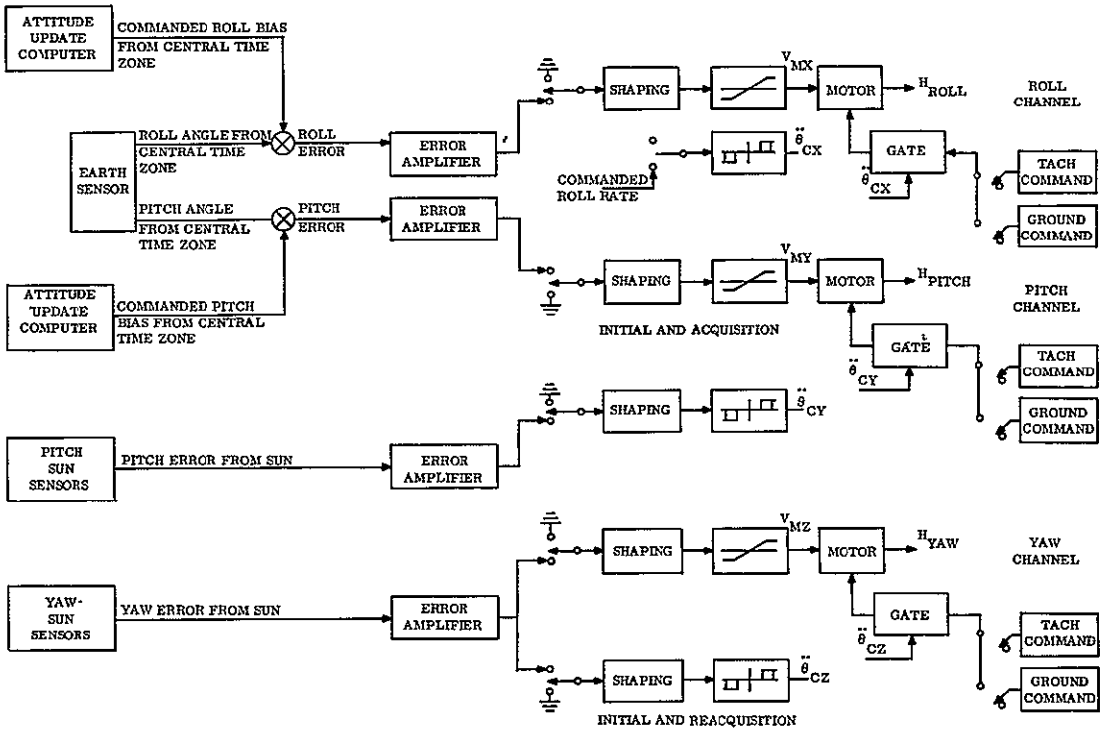

Figure 4.5-12. UHF Attitude Control Block Diagram

Table 4.5-4. UHF Subsystem Component Description

Component and Total Number	Weight (lb)	Power (watts)	Volume ($in.^3$)
Interferometer	29	20	268
Sun Sensors (14)	4	--	---
Rate Gyro Package (2)	9	20	550
Electronics (misc.)	30	75	---
Solar Array Drive (2)	37	--	---
Flywheels (6)	70	30	1200
Mass Expulsion Hardware (unloading) and Fuel	50	--	---
Function Generator Computer	7.3	4	240

The interferometer is to be fixed mounted on the satellite body (or UHF parabola or feed package) and used in the attitude control loop to provide a pointing reference for the entire satellite. The system described here is basically the same as the interferometer design used in the ATS-F & G study. The major difference is the use of a five-horn configuration rather than the eight-horn system used in ATS-F & G.

Figure 4.5-13 shows a simplified system block diagram, and Figure 4.5-14 shows the antenna mechanical mounting concept. The output error signals each consist of a parallel 8 bit (7 bits plus sign) binary number, updated at a 10 per second control system. Error signals versus signal boresight angle is shown in Figure 4.5-15.

A system error budget is presented in Table 4.5-5 and shows an overall 1 σ, two-axis accuracy of better than 0.05^{o}. Note that this error summary does not include boresight shifts in the antenna itself due to dynamics and thermal distortions. Boresight shifts in the antenna are believed to be a separate problem, but must be considered in the overall antenna pointing accuracy analysis. The error budget presented here is based on a fairly thorough analysis made on the ATS-4 study.

Preliminary size, weight, and power consumption for the interferometer package are summarized in Table 4.5-6.

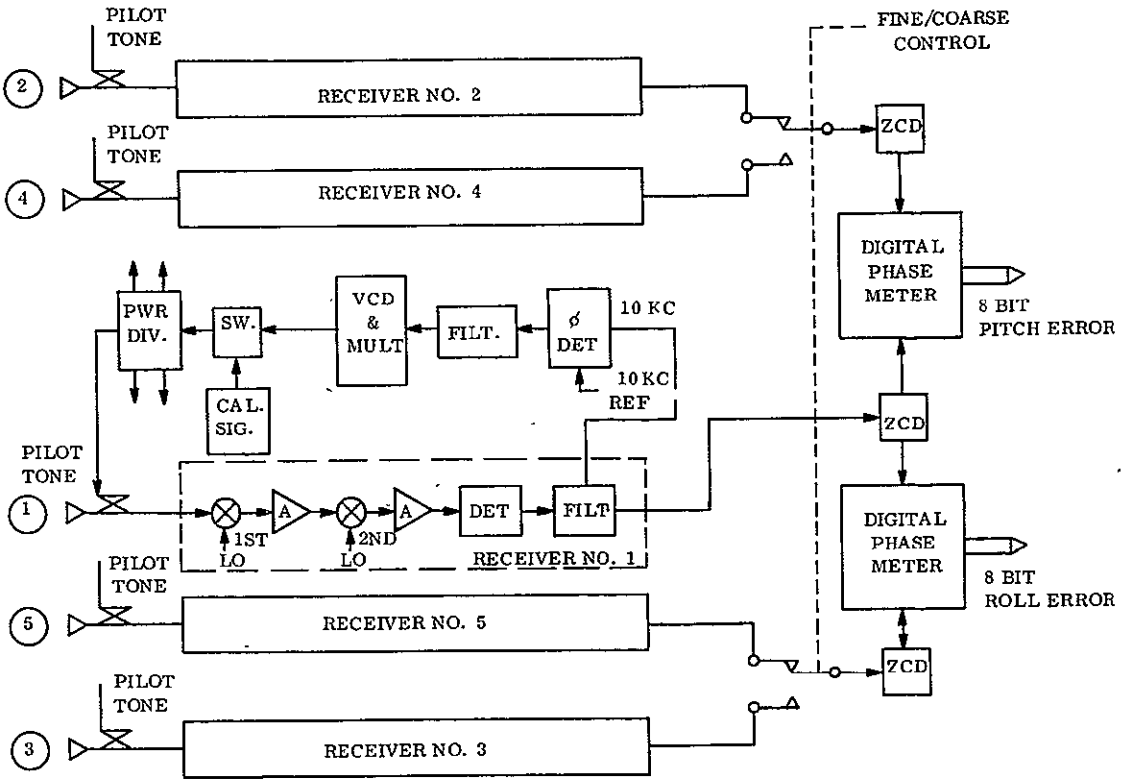

Figure 4.5-13. Interferometer Simplified System Block Diagram

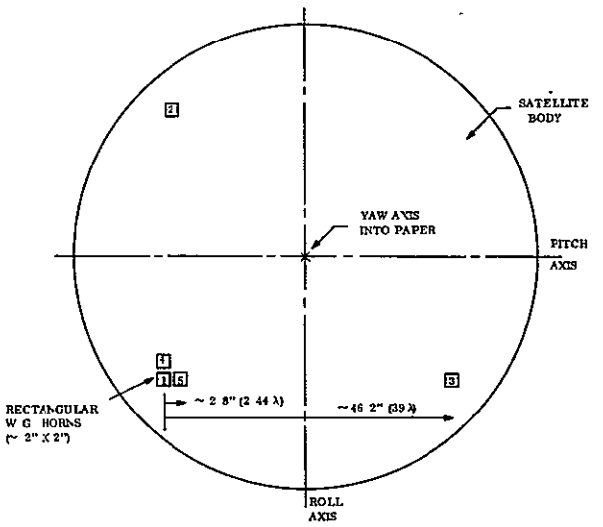

Figure 4.5-14. Interferometer Antenna Mounting Geometry

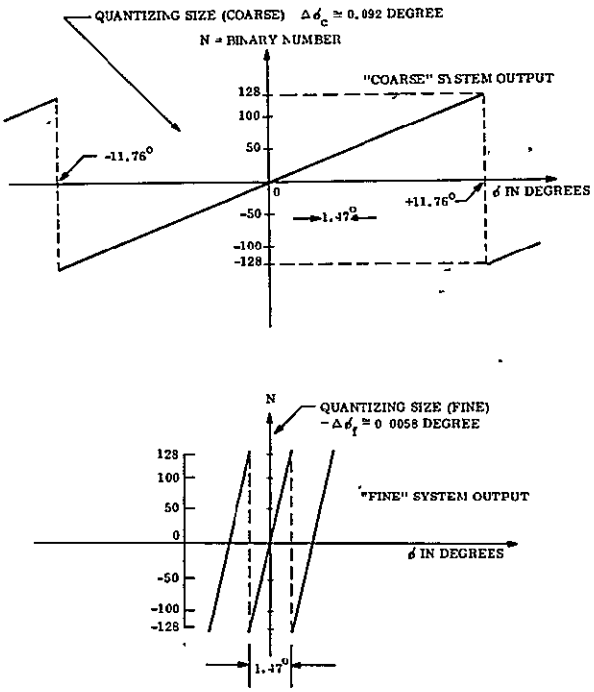

Figure 4.5-15. Interferometer Output Signal

Table 4.5-5. Interferometer Error Summary

Item		1σ Elect. Error	1σ Mech. Error
1. Propagation			
2. Equipment Electircal Errors			
a.	R. F. ϕ changes	2.000 degree	
b.	Quantizing Errors	0.088 degree	
c.	Receiver Noise	0.080 degree	
d.	Oscillator Noise	0.745 degree	
e.	ϕ Meter Jitter	0.250 degree	
f.	Phase Drifts (filters)	0.500 degree	
	RMS Total	2.20 degrees	0.009 degree
3. Mechanical Displacement Errors (assuming mechanical, thermal, and dynamic tolerance of 0.025 inch)			0.030 degree
	RMS Total		0.0314 degree
RMS Total, both axes = 2 (0.0134) = 0.045°			

Table 4.5-6. Size, Weight, and Power Estimates

Item	Size	Weight (lbs)	Power
Antennas (5 total)	2 in. x 2 in. x 2 in. (each)	1.1	0
Waveguide Sections	0.5 in. x 0.85 in. x 20 ft	6.0	0
Microwave Package	1 ft x 1 ft x 1 ft (144 in.^{3})	6.0	0
Electronic Package	12 in. x 8 in. x 1 in. (96 in.^{3})	11.7	16 Watts
Power, Conv., Package, Cabling	---	5.0	4 Watts
TOTAL		29.8 lb	20 Watts

4.5.3 TECHNOLOGY EVALUATION

4.5.3.1 General Survey

4.5.3.1.1 System Considerations

A survey of the different types of attitude control/stabilization concepts is presented herein listing general advantages, disadvantages, applicability and development status. The systems are classified as passive, hybrid, and active.

Passive systems are defined as those control systems in which the environmental torques produce a stable and desirable attitude and employ no moving parts (except for deployments necessary to establish the configuration). The theoretical lifetimes of such subsystems are infinite.

Hybrid systems are defined as those systems which supplement passive stabilization techniques with simple active components for increasing control system accuracy. In some cases, the passive torques are not sufficient and must be supplemented. In others, the environmental torques may be used to maintain the desired level of angular momentum and thus replace spacecraft mass expulsion systems.

Active systems are those control systems using moving parts, command links, and expendable control energy. Their main utility derives from the high loop gain response to unwanted environmental distrubance torques. However, the theoretical lifetimes of such subsystems are always finite, limited by the quantity of expendables on board or by the active element lifetime.

Examination of operational broadcast satellite cost effectiveness requirements would indicate that spacecraft lifetime would be a primary consideration and that passive attitude control systems would normally be preferred. However, the penalty for control error is very large in the case of the broadcast satellites due to the dominance of the power supply system with respect to cost and weight. Consequently, the passive systems, with their inherent inaccuracy, are less a contender than would be expected, and the two stabilization techniques which appear most applicable to voice broadcast missions are hybrid gravity gradient and active. These would be most appropriate for either low power systems or high power systems with a low duty cycle. Active attitude control subsystems would be most appropriate for either systems requiring an articulated solar array dictated by high power and continuous duty or high pointing accuracy systems dictated by operation at synchronous altitude. A flow chart showing the potential combinations of attitude control system types with types of other subsystems is presented as Figure 4.5-16.

4.5.3.1.2 Passive/Hybrid Stabilization Subsystems

Table 4.5-7 presents the results of the study analysis of passive, hybrid, and spin stabilization concepts in terms of hardware state of the art, and either applicability to the broadcast missions or stabilization accuracy capability.

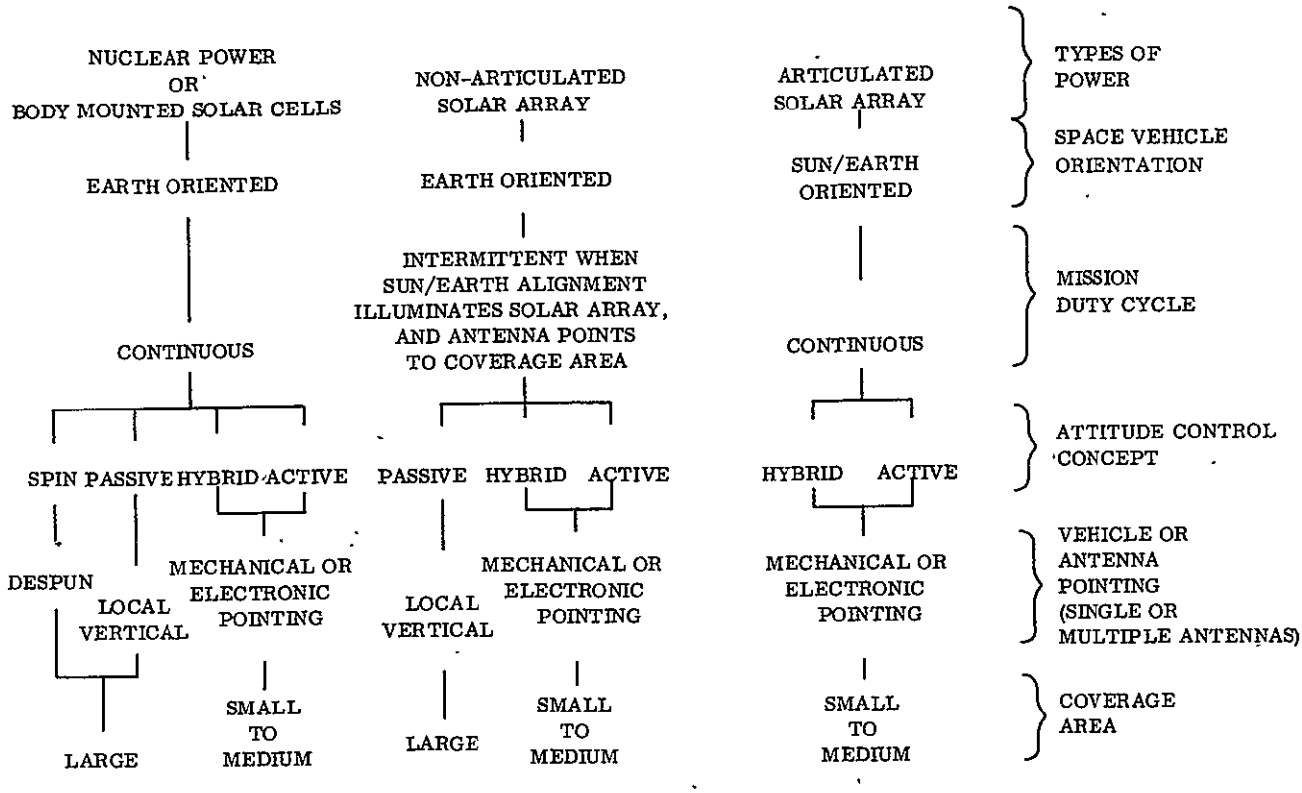

Figure 4.5-16. Interaction of Mission Requirements and Subsystem Types

Table 4.5-7. Applicability of Passive, Hybrid, and Spin Stabilization

Candidate Systems	State of the Art	Applicability
Pure Passive		
Magnetically anchored single rod	Flight-proven system	Pitch/roll $\pm 3^{\circ}$, no yaw control - for body-mounted solar cells or nuclear systems with a nonpointing antenna.
Magnetically or gravity anchored multiple rod	Flight-proven system	Pitch/roll $\pm 3^{\circ}$, yaw $\pm 6^{\circ}$ - for fixed arrays and low angle pointing antennas broadcasting a few hours per day
Hybrid		
Magnetically anchored dumbbell and flywheel	Flight-proven components, computer simulation of system	Pitch/roll/yaw $\pm 1^{\circ}$ to 2° - for fixed solar panels and pointing antenna broadcasting several hours per orbit.
Spin-Stabilized	Flight-proven system	1. With spin axis perpendicular to the orbit plan a low gain despun antenna must be used. 2. With spin axis and high gain antenna pointed to earth coverage area, the transmission will be limited to a short duty cycle per orbit.

4.5.3.1.2.1 Gravity Gradient Stabilization Concept. Gravity gradient stabilization techniques, although less accurate than active, are very attractive due to their inherent simplicity and reliability. To fully appreciate these techniques, one must understand the orientation and damping mechanisms.

Gravity Gradient Torque. The gravitational torque results from a displacement of the center of gravity from the center of mass in any direction which is not colinear with the gravity gradient. Because the force of gravity, ignoring oblateness, is inversely proportional to the square of distance from the gravitational center, a body with finite dimensions cannot have a coincident center of mass and center of gravity.

The displacement results from the fact that the points below the center of mass are closer to the center of attraction, and each element of mass at these points is subject to a greater force. The center of gravity is that point which can be said to move so as to follow Keplerian motion. The center of mass is a geometric average of mass displacements.

Gravity gradient torques operate on the pitch and roll axes, and gyroscopic torques operate on the yaw axis. Large differences in inertia between the axes generate the large torques for orientation of the body. Design goals maximize the inertia differences. Practical spacecraft system and payload considerations, however, force a compromise. Most stabilization configurations contain booms/rods (deployed after the spacecraft is in orbit) with tip weights or damping devices attached to the boom ends to obtain the preferred inertia. The number of rods is chosen to provide the system with a specific relationship among the moments of inertia. In general, the satellite moment of inertia offers a small contribution in achieving this relationship. The system moment of inertia will increase with satellite size due primarily to the need to "overshadow" the satellite moment of inertia, and to reduce the effects of the disturbance torques (most of which are dependent upon satellite size and weight). Properly designed, the spacecraft and integral boom system will stabilize as a result of the orienting torques that null in the preferred orientation.

Damping. Damping is necessary to provide the decay of initial errors and to prevent unstable buildup of oscillations due to distrubing torques. A gravity oriented vehicle will oscillate indefinitely if damping is not provided. A totally passive system is achieved when passive damping is used in conjunction with the orientation obtained by gravity gradient torques. A damper, to function properly, must contain an energy dissipation mechanism and a damper reference or anchor point. Any of four basic force fields can provide the anchor or referencing torque: magnetic, gravity, solar pressure, or atmospheric drag.

Disturbance Torques. To obtain good pointing accuracy, minimization of disturbance torques must be a major design approach. To achieve this, an understanding of the nature and importance of the individual distrubances is necessary.

For symmetrical vehicles, the nominal solar torque is zero. However, with asymmetries in the spacecraft structure, variations in the reflectivity and uncertainties in the center of mass position, it is not usually possible to locate exactly the center of solar pressure to induce no net moment about the system center of mass. The magnitude of the misalignment and the complexity of the analysis is a function of the satellite shape. Therefore to minimize

the analysis required and improve the confidence in the results, simplified body shapes are usually chosen. Then the resulting solar torques are usually evaluated on a digital computer.

An additional effect of the sun on the satellite is thermal bending of the gravity gradient rods. The side of the rod facing the sun is warmer than the side away from the sun, and differential thermal expansion causes the rod to bend. This thermal bending can change the location of the principal axes of inertia and also cause the center of mass to wander. The change in the location of the principal axes of inertia will cause the vehicle to attempt to realign itself with the orbital reference frame and have an effect similar to a distrubance torque. Wander of the center of mass produces misalignment between the thrust (for synchronous stationkeeping) and the center of mass causing a torque during the period of thrust.

Any magnetic dipole in the satellite will tend to align itself to the local magnetic direction. Thus, if there is misalignment between the dipole and the field, a torque will be produced on the satellite which will cause pointing errors. The design of the payload should be based upon the use of nonmagnetic materials whenever possible. Any significant residual permanent dipole should be balanced out to a level of less than four pole cm per pound of spacecraft weight.

Stationkeeping. To maintain a satellite on a specified station requires either periodic or continually applied microthrust. Any misalignment between the thruster and the system center of mass would cause a distrubance torque. Therefore, the magnitude of this stationkeeping thrust must be kept as small as possible. The continuous thrust level required to compensate for the effects of the elliptical equator for synchronous equatorial mission is about 10^{-6} pounds per hundred pounds of payload. To orient the thrust in the proper direction, yaw con control must be provided.

Semipassive Systems. Augmentation of a passive system is accomplished sometimes by adding active components to increase the accuracy of the system yet pressure its relative simplicity and reliability. One such component is a flywheel. The gravity gradient system will provide pitch and roll control the flywheel when its spin axis is along the pitch axis provides yaw control. This removes the necessity for continuous sensors, decision circuits, and actuators while providing a system that aligns itself in the orbit plane. This system provides an excellent means of achieving three-axis control with simplicity and reliability.

4.5.3.1.3 Active Attitude Control

Sun and earth-oriented, three-axis active attitude control systems were considered for concepts required to point simultaneously a solar array toward the sun and an antenna at the earth. Whether the vehicle was sun- or earth-oriented would depend upon the satellite orbital motion, solar array articulation, antenna articulation, and magnitude of the resulting distrubance torques.

Earth-oriented three-axis systems would be applicable for configurations having small solar arrays. A large fixed solar array could be used by limiting the broadcast time to a portion of the satellite orbit when the array would be in position to see the sun. The earth-oriented systems simplified the problem of pointing the antenna beam toward the earth.

Sun-oriented three-axis systems are advantageous for configurations with very large solar arrays that must always be pointed toward the sun for continuous broadcasting. The approach would permit solar trims to be employed so that the solar pressure could be used as a control force. However, this complicates the problem of pointing the antenna beam toward the earth.

A variety of sensors, actuators, and signal processors used in active attitude control systems are flight qualified. Satellites have been designed and orbited requiring pointing accuracies as low as seconds of arc (GE Orbiting Astronomical Observatory satellite attitude control subsystem) and requiring articulation of solar arrays toward the sun while antennas or sensors are articulated toward the earth (GE Nimbus and ATS-F&G satellites).

This section discusses some general control principles, summarizes the active systems that have been designed and delineates advancements which may be required in design techniques by broadcast satellites.

Active Stabilization Concept, The Control Law. Active stabilization of spacecraft is analogous to the regulator problem of classical control theory. A reference signal (input) is operated upon by the controller to reproduce the reference (output) with small error while the controlled element undergoes environmental disturbances. The disturbances are described mathematically as deterministic and stochastic. To implement an active stabilization subsystem, four distinct tasks are required to be performed.

a. A sensor must be specified and either selected from available hardware or developed from physical principles to a hardware item.

b. The appropriate description of distrubances must be determined either analytically from physical laws or empirically from test data.

c. Actuators must be selected which are adequate in both magnitude and bandwidth for the effective cancellation of the disturbances.

d. A control law must be derived to relate sensor errors to actuator commands. The signal processing required to implement the control law must be determined and designed. This signal processing has involved analog signal processing (continuous controller) and digital signal processing (discontinuous controller) and combinations of analog and digital.

Sensors. Spacecraft sensors are of two basic types, attitude sensors and force field sensors. Attitude sensors (exclusive of inertial platforms) are basically electromagnetic field sensors which detect the line of sight to electromagnetic energy sources such as the sun, stars, or the earth. Force field sensors include gravity gradient rods, gyroscopes, and mass balance accelerometers. Inertial platforms are open-loop sensors and would require electromagnetic sensors to update the platform due to inherent gyro drift of these open-loop techniques. This redundancy of sensing may be justified whenever the view requirements of electromagnetic field sensors are not compatible with orbital geometry or with the vehicle configuration design.

Electromagnetic field sensors were considered more applicable to the pointing accuracy requirements of the Voice Broadcast Mission Study and consequently were the only type considered for primary sensors. Force field sensors are required for secondary applications, such as in the nontransmission mode of the HF satellite.

Signal Processors. The systems which convey or operate upon sensor information to provide signals to, or make decisions for, the actuators are composed of electromagnetic components. The complexity of the processor is, of course, proportionate to the amount of signal processing to be performed. These functions are low power and mechanizable as solid state or minature. They include lead or lag networks, threshold detectors, derived rate networks, filters, logic circuits, amplifiers, A/D and D/A converters, etc.

Actuators. Actuators which have been employed to generate control torques include mass expulsion, electromagnetic, angular momentum storage, gravity gradient rods with tip masses and articulated parts.

a. Mass Expulsion - Actuators that have been used extensively are of the mass expulsion type. Particles present in the spacecraft are accelerated by various means and separated from the spacecraft. Some acceleration methods are:

   1. Potential Energy - Cold gas stored under pressure is released through an orifice (low fuel efficiency).

   2. Chemical Energy - Monopropellant or bipropellant is ignited in a chamber and escaping products are released through an orifice. Other ignition methods and fuel types are in development.

   3. Electric Energy - Ions are accelerated by a potential and released through an orifice.

b. Electromagnetic - A technique used to correct drift rate of spin-stabilized satellites is the electromagnet. The electromagnet is controlled to change the spacecraft magnetic dipole strength and sense. Interaction with the geomagnetic field results in a beneficial environmental torque; such systems are passive adaptable systems. Some effort has been expended in application of magnetic torquing to conservative systems. Drawbacks encountered are inability to torque about geomagnetic field vector and its time-varying characteristics.

c. Angular Momentum Storage - Angular momentum storage devices have been used to approach the long-life of systems while maintaining the accuracy of an active system. Environmental torques and slew commands are handled by rotating parts of the spacecraft. Slews are achieved by speed up and slow down of a wheel causing the spacecraft to slew. Disturbance torques on the vehicle are transferred by the controller to the wheels. With proper wheel sizing, the cyclic components of disturbance torques merely modulate wheel speeds. The cumulative components are stored and then unloaded by the creation of an external torque. Examples are Nimbus and OAO.

d. Gravity Gradient Rods - Although usually considered as a passive component, a gravity gradient rod could be used to reduce the gravity gradient induced distrubances by producing equal moments of inertia for all axes. A spherical mass distribution thus achieved would have no preferred orientation in an inverse square force field and the active controller would be free of any gravity gradient disturbances regardless of the commanded spacecraft orientation.

e. Articulated Parts - Articulation of parts of the vehicle relative to the controlled frame have been used (Mariner solar vanes). Solar vanes are articulated to adjust the center of solar pressure creating an external torque to control the vehicle attitude in a closed-loop fashion; these would be conservative systems. Two gimbal gravity gradient rods have been proposed to implement a passive system in which the gravity gradient, an external torque, is used to control the vehicle attitude in a closed-loop fashion. Inertia coupling (equal and opposite torques are applied internally during articulation) presents a response problem. Continuous articulation actuators present a power and reliability problem. Stepper actuators present a wide bandwidth problem. Even if the least bit step is small enough to avoid deleterious effects due to inertia coupling, a stability problem arises due to compliance modes excited by the step actuation. The controller mechanization complexity may be completely outweighed by the passive nature of these actuators particularly if the mission is long life.

Structures. Broadcast satellites have a predominant structural characteristic. By the nature of the missions, it is required that a large aperture antenna be stabilized in space. Launch constraints result in a minimum weight erectable structure. Such space structures display the following characteristics:

a. Difficult to model and analyze

b. Resonances are many and often low frequency

c. Ground testing of the complete satellite/controller will be impossible due to the ever present 1-g force field which becomes a significant force for large, light weight solar arrays and antennas.

The complications to the controller are of two types. The compliance of appendages may affect the controller resulting in an undersired limit cycle. The controller input to the structure, the actuator output, may excite a mode of vibration which has little or no damping.

A structure/controller limit cycle would produce excessive errors, large controller power expenditure, and component fatigue in the actuators or the structure. Excitation of a structural mode of vibration above the sensor bandwidth, such as might occur during a mass expulsion unloading of stored angular momentum, may produce large deformations. If the modal response is large, the antenna shape is deformed producing a degradation in the antenna performance. For the time period of this program, it is doubtful that appendage motion sensors or control actuators would be considered. The design approach then becomes one of bandwidth limiting of the controller in a deterministic sense and restrictions on actuator bandwidth in both a deterministic and stochastic sense.

Bandwidth-limiting designs would be acceptable with the constraints that command slews be performed slowly and that articulation drives do not create disturbances with deleterious spectral densities above the controller bandwidth.

4.6 AUTOPILOT

4.6.1 INTRODUCTION

The autopilot defined herein is the subsystem which controls the thrust vector of the engine used for final orbit trim. The subsystem may be self contained or may be integrated (share components or functions) with the attitude control or orbit maintenance systems. Two types of autopilots have been selected for the four configurations:(1) a three-axis sensing and thrust vector control system and (2) a spin thrust vector control system.

Two types of launch and injection systems were selected for the four configurations. The HF, VHF No. 1 and VHF No. 2 configurations employ direct injection wherein all thrusting is performed by the launch vehicle. A three-axis autopilot was selected for these configurations. The booster for the UHF configuration required an apogee kick motor to achieve the required orbit. A spin autopilot was selected for this configuration.

Section 4.6.2 describes the autopilot selected for each configuration and defines the degree of autopilot/stabilization integration. Section 4.6.3 presents subsystem selection data. The propulsion units employed with the autopilot and orbit maintenance systems, and the autopilot launch sequence functions are presented in Section 4.9.

4.6.2 AUTOPILOT SUBSYSTEM DESCRIPTION

4.6.2.1 HF, VHF No. 1, and VHF No. 2 Autopilots

The launch systems selected for HF, VHF No. 1, and VHF No. 2 satellites have upper stages (Titan 3F Transtage and Improved Agena D) which can place the satellites in the required orbits with small injection errors. The same basic autopilot system was selected for each. It is a modification of the Mariner midcourse correction system. Figure 4.6-1 shows the block diagram for this system.

Celestial references of the sun and Polaris are used to establish the body reference for a set of body-mounted gyros. Slews from this reference using the gyros as sensors are performed to align the engine axis with the commanded velocity direction. During thrust, a thrust vector control system using jet vanes performs the attitude control based on the gyro reference null. Ground commands select the attitude of firings and the velocity to be gained. Command slews are performed and the engine ignited upon slew completion. The engine is turned off when the velocimeter output equals the velocity to be gained.

The autopilot and attitude control systems are integrated for the HF and VHF No. 1 satellites. This resulted in weight and cost savings for the autopilot because active three-axis attitude control systems were required on these two satellites. The HF and VHF No. 1 autopilot component descriptions are colisted with the attitude control component descriptions in Section 4.5. The VHF No. 2 autopilot component descriptions are listed in Table 4.6-1.

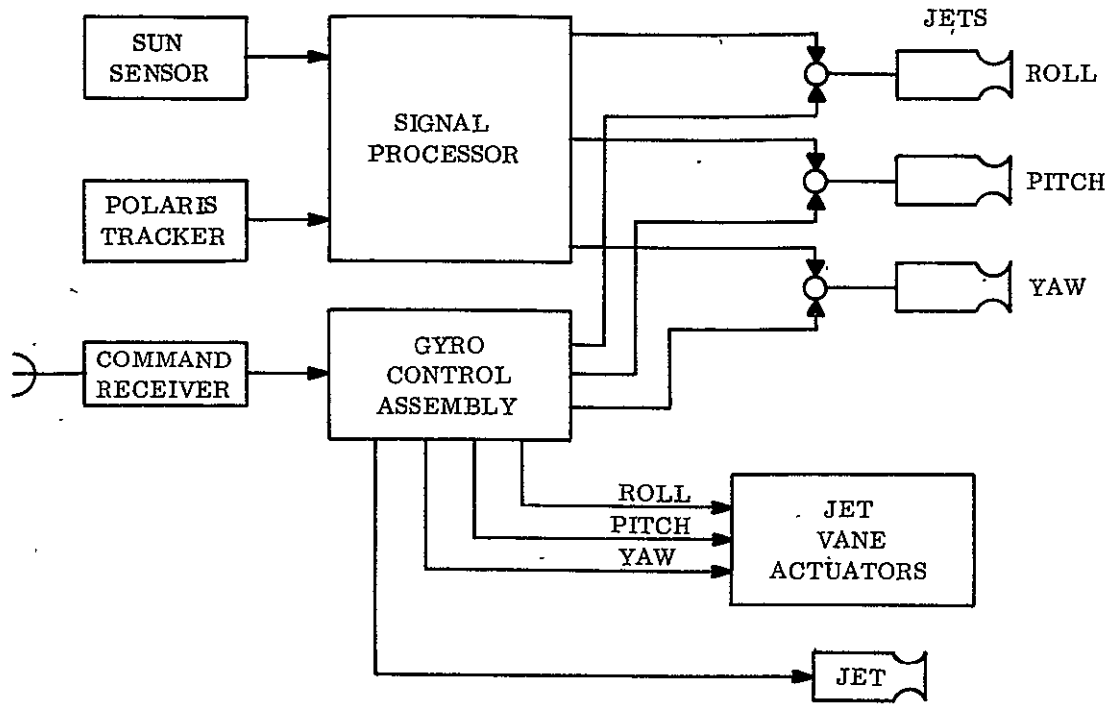

Figure 4.6-1. HF, VHF No. 1 and VHF No. 2 Autopilot Block Diagram

Table 4.6-1. VHF No. 2 Autopilot Component Descriptions

Component	Weight (lb)	Power	Size (in.)
Polaris Tracker	6	5 watts 3 watts Track	4-1/2 x 5 x 11
Sun Sensors	0.8	1.2 watts 0.2 watt cruise	
Gyro Control Assembly	11.2	14 watts 18 watts peak 400 cps	7-1/2 x 7-1/2 x 7-1/2
Signal Processor	5.2	10 watts 25 watts peak	4 x 4 x 9
Mass Expulsion System	60	10 watts	6 x 6 x 10

4.6.2.2 UHF Autopilot

The synchronous orbit can be obtained using the Atlas SLV-3A/Improved Agena D plus an apogee engine in the satellite. The Agena puts the satellite into an elliptic orbit with apogee at synchronous altitude at the desired satellite longitudinal location. Orbit injection correction ΔV is 6150 fps. Injection correction is to be done in a spinning mode with the spin axis normal to the orbit plan. Tangential and normal thrusting will be employed with tangential thrusting pulse synchronized to the spin rate. Orbit trim corrections are to be done in a nonspinning operational mode.

The total time of the spinning mode must be determined as a function of the allowable orbit errors at the end of this mode. This time is dependent upon the initial orbit errors associated with the application of the commanded velocity increments. That is, the time required in the spinning mode to reduce the initial orbit errors to allowable values is a function of initial errors, the final errors and the tracking errors, but independent of the errors of implementation of the guidance commands. Sensing of the spin axis direction is accomplished by sun sensors on the spacecraft and polarization angle measurements at ground tracking stations. All operations are identical to previously flown synchronous satellite systems except that unfavorable moments of inertia ratios will be encountered. An active nutation damping system will be required.

The subsystem block diagram is shown in Figure 4.6-2. Precission commands are required from the Flight Center to align and maintain the spin axis in the proper direction for the apogee kick. Station achievement and keeping autopilot functions are performed in the operational mode by the attitude control system.

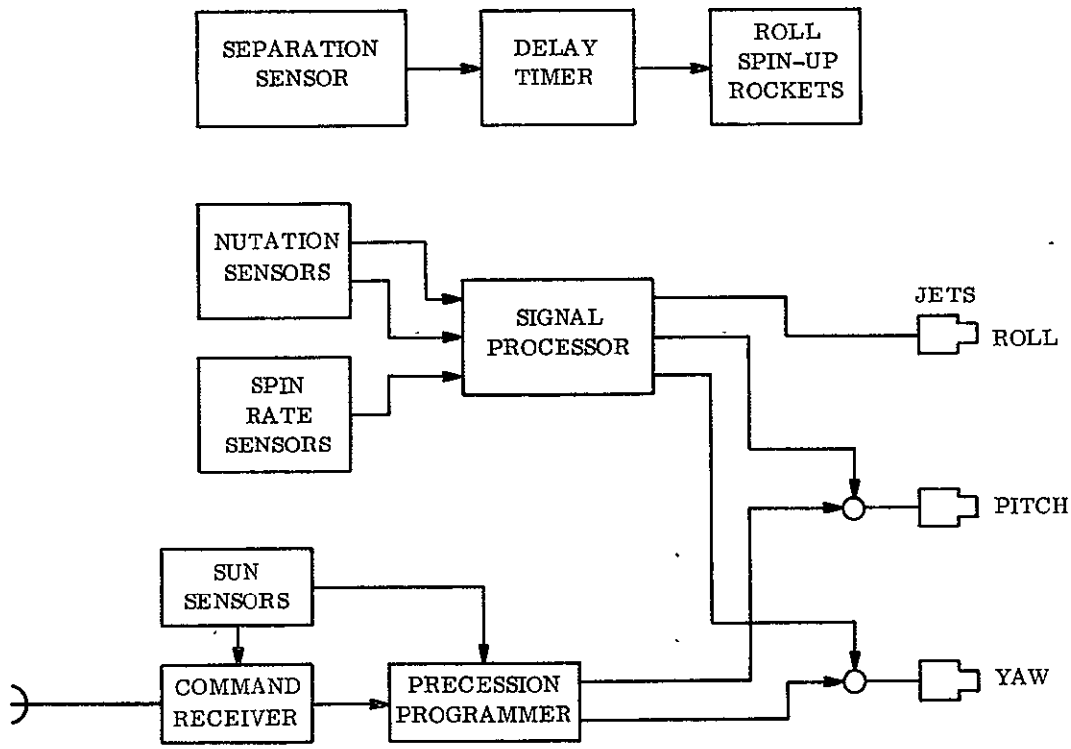

Figure 4.6-2. UHF Spin Autopilot Block Diagram

The autopilot component descriptions are listed in Table 4.6-2. The vernier system breakdown is given on the basis of the linear impulse estimates.

4.6.3 AUTOPILOT SUBSYSTEM SELECTION

A requirement of a broadcast satellite is that it maintain broadcast coverage of prescribed areas on the earth's surface at the same local time each day, everyday of the year. These requirements place very stringent requirements on the orbit period, inclination and eccentricity. The Titan 3-F Transtage and Atlas SLV-3A/Improved Agena launch systems selected for the four VBMS configurations do not possess the capability to inject the satellites into such precise orbits. Therefore, an autopilot is required for each system for final orbit trim and orbit maintenance.

When a satellite is to be placed into a high altitude orbit, several methods can be used. One method is direct injection by the booster which requires an autopilot controlled orbit trim system. This method requires a sophisticated and costly booster. With a second method, the booster is used only to place the satellite into a transfer orbit. This transfer orbit has an elliptical shape with a perigee at or near the injection point, and an apogee at the desired altitude. At apogee, a kick motor contained within the satellite is fired, circularizing the orbit at that altitude. For the thrust vector to be applied in the proper direction, the satellite must be properly aligned when fired. To accomplish this alignment, the satellite could: (1) contain a three-axis autopilot system or (2) be spin stabilized with the nominal spin axis through the center line of the rocket motor.

Table 4.6-2. Autopilot Component Summary

Component	Weight (lb)	Power (w)	Volume ($in.^3$)	Size	Vernier Breakdown
Spin-up rockets	2	100 (100 ms)		6-inch Diam.Sphere	1) Axial vel. correction (130 ft/sec) 2) Precession impulse (500 lb/sec) 3) Despin (1 lb thrust)
Apogee motor	1330	50 (50 ms)		37-inch Diam.Sphere and Nozzles	
Vernier system (blowdown)	71	10		13-inch Diam.Sphere and Nozzles	RCS Component Breakdown Weight (lb) Fill Valves (2) 2 Explosive vales (2) 0.6 Control valves (10) 10 Filter 0.5 Temperature Transducer 0.5 Pressure Transducer 5.5 Prop tank 5.1 Tubing 5.9 N_2 Pressurant 0.9 Hydrazine 25 Thrusters (10) 15
E-W Stationkeep	10	30		6-inch long x 5-inch Diam. Cylinder	
Spin sensors	5	10	350		
Sun sensors	0.8	--	--		
Precession controller	3	5	106		

Both direct and apogee kick injection systems employ tracking measurements to varying degrees. It is anticipated that existing tracking systems will be employed to determine the orbit parameters for VBMS missions.

4.6.3.1 Selection of the 3-Axis Autopilot (HF, VHF No. 1 and VHF No. 2)

For HF, VHF No. 1 and VHF No. 2, the autopilot function is the removal of orbit injection errors. These injection errors are uncertain in magnitude and direction; therefore, orbit trim corrections must be based upon incremental velocity as calculated from the ground using ground tracking data. The three-axis active autopilot is capable of accepting any attitude and magnitude as required by its guidance laws. To use a spin autopilot for these configurations would necessitate variable velocity increments and would require precession maneuvers, or would require the Syncom type two engine despin pulse system. The three-axis autopilot was selected because it is a less complex system and has minimum interface problems with the structure.

For HF and VHF No. 1 the autopilot is integrated with its attitude control subsystem including sensors and signal processing but exclusive of the actuators. This integrated design results in a reduced cost and weight autopilot for these two configurations.

4.6.3.2 Selection of the Spin Autopilot (UHF)

To put the UHF satellite into a geostationary orbit, a spin autopilot was selected. The Atlas SLV-3A/Improved Agena D is capable of establishing an elliptic transfer orbit only. Nominal operation results in synchronous altitude at apogee of the transfer orbit at the desired station longitude. A circularization thrust is required of the satellite system at apogee. The available engines to perform this apogee kick are restricted in that none have inherent thrust vector control. Rather than requiring engine modifications or a high level reaction control system for attitude control during burn, a spin stabilization approach was selected.

Another reason for selecting a spin autopilot is that it is a flight-proven technique for the class of solid propellant engines applicable to the apogee kick function. Sensing of the spin axis direction is accomplished by sun sensors on the spacecraft and polarization angle measurements at ground tracking stations. All operations are identical to previously flown synchronous satellite systems, except that unfavorable moments of inertia ratios will be encountered. An active nutation damping system will be required for pencil-shaped configurations engendered by the broadcast satellite as opposed to passive damping of can-shaped satellites such as Syncom.

4.7 POWER SUBSYSTEM EVALUATION

4.7.1 INTRODUCTION

Summary

Section 4.7.2 describes the power subsystems selected for the HF, VHF No. 1, VHF No. 2, and UHF configurations. The descriptions include block diagrams, weights, and array areas plus devices for energy storage, energy management and power conditioning.

Section 4.7.3 describes the technology evaluation performed to select the power subsystems for the four configurations. The types of power systems analyzed were:

a. Photovoltaic/Battery Subsystems

b. Solar concentrator subsystems, including Brayton Cycle, Rankine Cycle, Solar Thermionic and Solar Thermoelectric

c. Chemical subsystems, including batteries and fuel cells

d. Nuclear subsystems, including radioisotopes and reactors

Conclusions

An analysis of the above candidate power subsystems resulted in the selection of photovoltaic (solar cells) for all four configurations with the primary considerations being performance, cost and availability. The photovoltaics are state of the art, have short design cycles and can readily be scaled up or down in size; therefore, they provide both schedule confidence and performance flexibility.

4.7.2 DESCRIPTION OF SELECTED POWER SUBSYSTEMS

4.7.2.1 General

This section contains the results of studies performed to configure the solar array and size power supplies to meet the requirements of the four configurations. Table 4.7-1 contains a summary of the most pertinent mission requirements influencing the power subsystem.

The characteristics of the arrays selected for the four configurations are tabulated in Table 4.7-2.

Conventional foldup panels were chosen for the VHF No. 2 application because of the requirements to minimize development and provide the earliest possible launch date. This size array is state of the art and does not introduce development risk.

Table 4.7-1. Power Subsystem Requirements
(2 year life satellites launched from 1971 to 1972)

Configuration	Orbit	Power Level Required		Duty Cycle
HF	4.8 hr period 4356 nm alt.	Broadcast Transmitter Housekeeping	14,900 watts 500 watts	one hour per orbit continuous
VHF No. 1	Synchronous	Broadcast Transmitter Housekeeping	10,880 watts 50 watts	continuous* continuous
VHF No. 2	8 hr period 7556 nm alt.	Broadcast Transmitter Housekeeping	1,260 watts 100 watts	one hour per orbit continuous
UHF	Synchronous	Broadcast Transmitter Housekeeping	2,290 watts 250 watts	continuous* continuous

*continuous less shadow time

Table 4.7-2. Characteristics of Selected Solar Arrays

Configuration	Array Size (kw)	Array Type	Solar Cell Area (ft^2)	Array Weight (lb)
HF	* 7.0	Oriented Rollup	1788	730
VHF No. 1	11.38	Oriented Rollup	1968	836
VHF No. 2	1.36	Fixed Folding Panel	326	158
UHF	2.54	Oriented Rollup	438	197

*Batteries store 8.4 kw for total of 15.4 kw required

Rollup solar arrays were selected for the HF, VHF No. 1, and UHF configurations. The principal reasons were:

a. Small stowage volume available in booster shroud

b. Potential weight advantage

4.7.2.2 HF Power Subsystem

The HF power subsystem consists of four oriented roll-up solar arrays (each 12 by 37-1/2 ft), nickel-cadmium batteries, and power conditioning equipment. Figure 4.7-1 is a block diagram of the subsystem; Table 4.7-3 is a summary of the component weights. The subsystem is sized for operation in a 4.8 hour orbit with a continuous 500 watt housekeeping and stabilization load and a one-hour broadcast period per orbit during satellite day at a transmitter input power of 14.9 kw. Because of the high peak-to-average power ratio, the battery is sized to supplement the array during broadcast periods as shown in the power duty cycle plot (Figure 4.7-2).

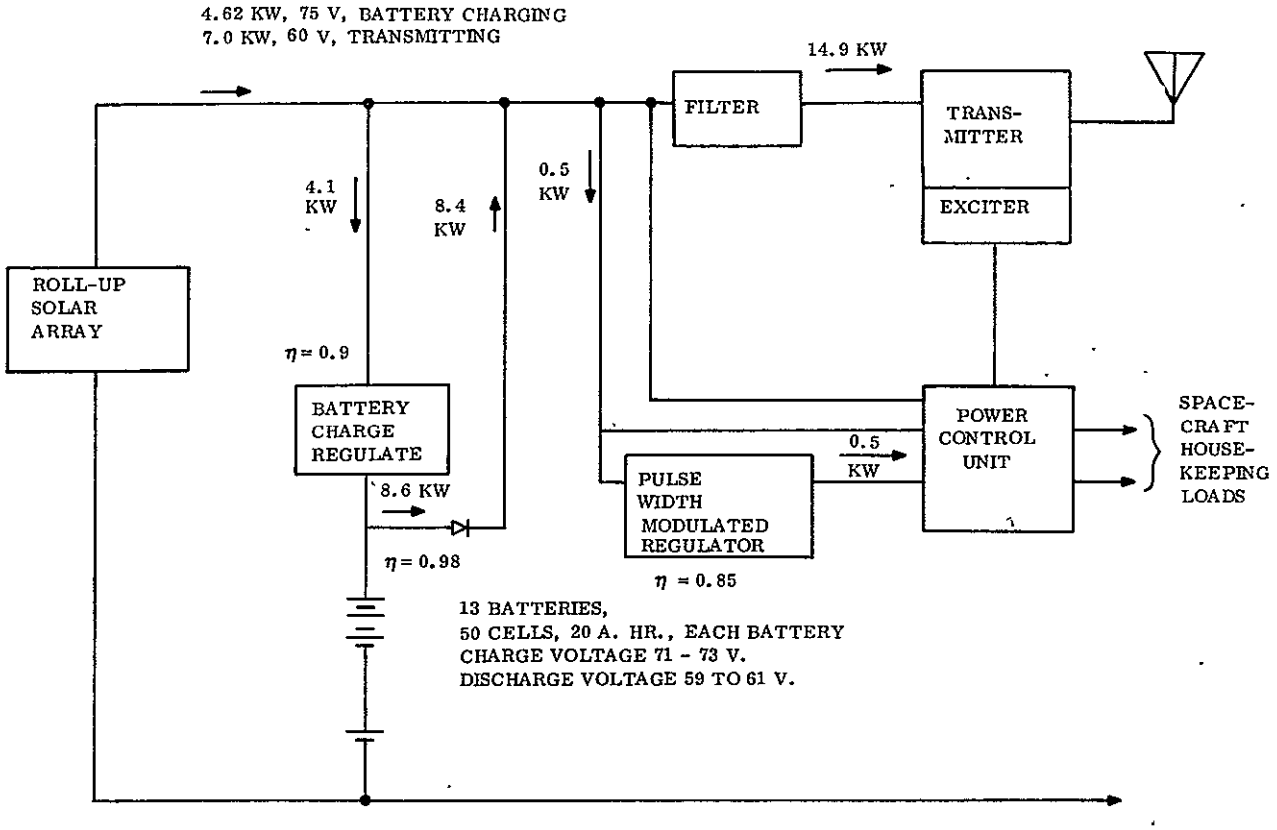

Figure 4.7-1. HF Power Subsystem Block Diagram

The HF transmitter uses AM modulation and therefore, the instantaneous power demand varies as the modulating frequency. To effectively match the transmitter to the power supply, a capacitor-inductor filter is used as an energy storage device to average the input power.

Table 4.7-3. HF Power Subsystem Component Weights (pounds)

Solar Array Rollout Panels	730
Batteries	1625
Battery Charge Regulators	50
PWM Regulator	20
Power Control Unit	5
Array Pointing	100
Total	2530

The power conditioning equipment consists of battery charge regulators (one for each battery) to provide constant current charging with a voltage limit, a pulse width modulated regulator to provide a regulated housekeeping bus, and a power control unit to provide for interface requirements.

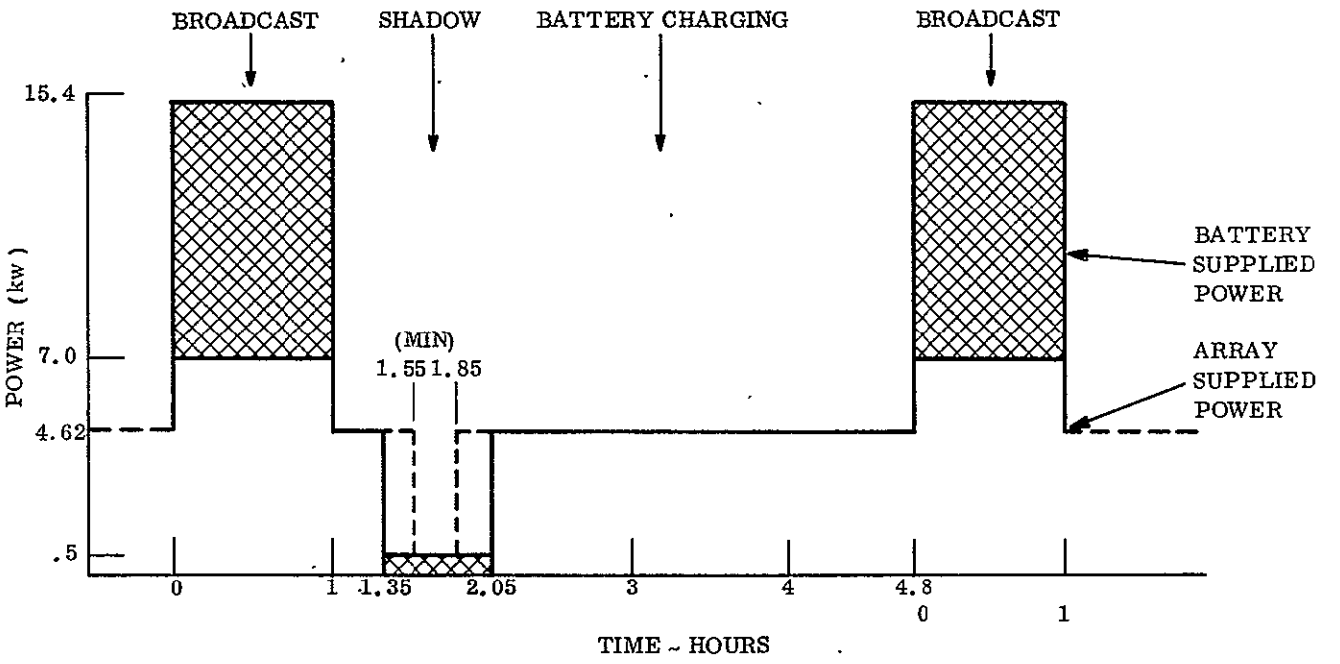

Figure 4.7-2. Power Profile HF Configuration

The HF/AM transmitters have a varying input impedance characteristic and hence, a varying input power requirement. The solar array operates most efficiently at a constant output. There is a potential power saving in the AM case by using energy storage between the array and the transmitter. Two methods of energy storage were evaluated: (a) filters, consisting of capacitors and inductors and (b) batteries.

a. Capacitor-Inductor Filter Energy Storage

The estimated sizes and weights of the filters, which would be required with each of the modulation methods for transmitter power outputs from 1 kw to 50 kw and with a range of 50 Hz to 300 Hz for the lowest modulating frequency, are tabulated in Table 4.7-4. The estimates of part sizes and weights are based on curves derived from standard catalog values and vendor information. A program directed at developing capacitors and inductors for the specific application could probably produce part designs with less volume and weight, but the ratios between the requirements for the different modulation techniques will probably hold.

Figure 4.7-3 shows the weight dependency on the lowest frequency of modulation.

Table 4.7-4. Requirements of Final Amplifier Input Filter

Type of Transmitter	RF Power Output (kw)	Lowest Modulating Frequency – 50 Hz					Lowest Modulating Frequency 100 Hz		Lowest Modulating Frequency 300 Hz	
		C	Parts Weight (lb)		Filter	Filter	Filter	Filter	Filter	Filter
		μf	L	C	Wt Lb	Size Ft^3	Wt Lb	Size Ft^3	Wt Lb	Size Ft^3
Vacuum Tube -	1	95	15.5	57	77	1.75	39	0.9	13	0.3
A.M	5	475	68	285	353	5.15	177	2.6	59	0.9
Doherty	15	1325	110	780	890	15.95	445	8	149	3
	50	4750	344	2850	3194	51.5	1597	26	533	9
Vacuum Tube -	1	11	15.5	22	37.5	0.97	19	0.5	9	0.2
A.M.	5	55	57	33	85	2.12	43	1.2	15	0 4
Plate Modulation	15	165	70	93	163	5.8	82	2.9	28	1 0
	50	550	256	330	586	21	298	11	98	4
Vacuum Tube -	1	135	13.5	81	94.5	1.36	48	0.7	16	0.25
A.M.	5	675	42	405	447	5.65	230	2.9	78	1.0
Linear Modulator	15	2025	76	1230	1306	15.7	653	8	218	2.8
	50	6750	168	4050	4218	50.7	2109	26	703	9
		(farads)								
Transistor	1	0.06	39	38	77	1.9	39	0.9	13	0.3
	5	0.28	78	178	256	6.7	128	3.4	43	1.2
Amplitude	15	0.85	234	540	774	20.5	387	11	183	4
Modulated	50	2.8	780	1780	2560	69	1280	35	427	12

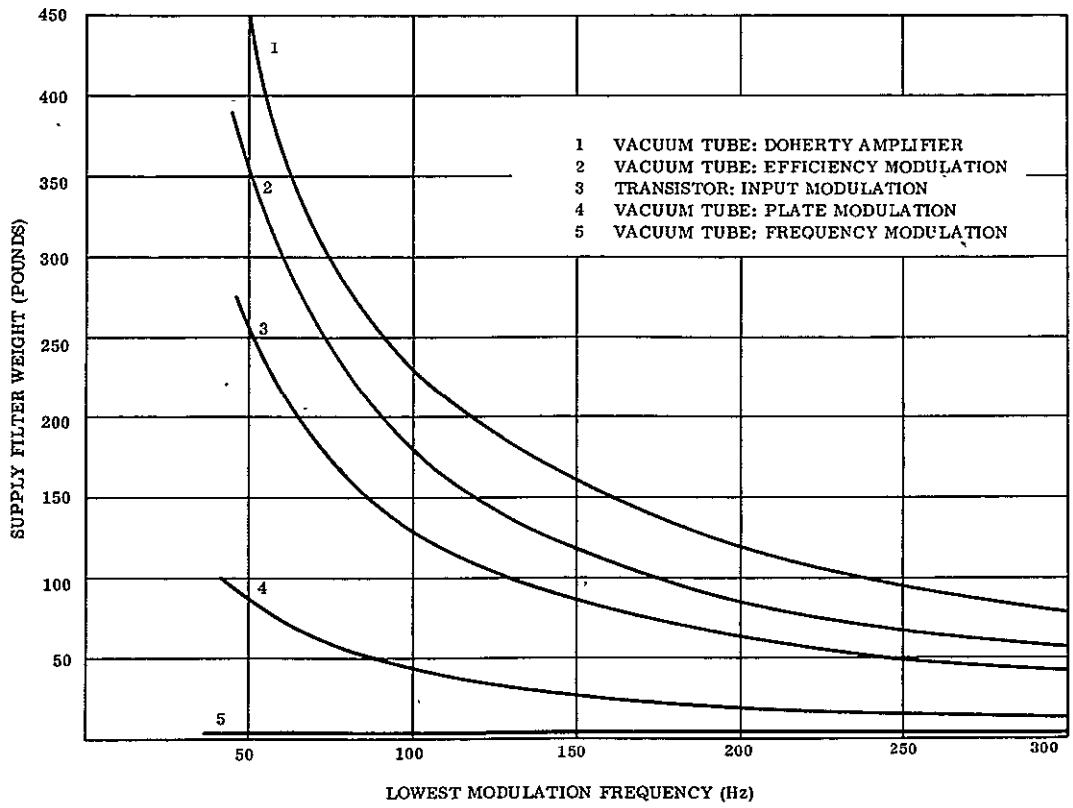

Figure 4.7-3. Filter Weight Vs Frequency of Modulation

b. Battery Energy Storage

The battery considered was a new type of nickel-cadmium battery (employing bipolar electrodes, and capable of high-rate operation) recently developed by Gulton Industries. Bipolar electrode batteries used a common electrode base plate, with a positive electrode on one side, and a negative electrode on the other facing an electrode of the opposite polarity. The base serves to separate cells, and consequently the cells in the battery are in series.

These batteries are sealed and possess the inherent long-life capability of the nickel-cadmium cell. Moreover, they are constructed in such a fashion that the internal resistance is considerably lower than for conventional Ni-Cad cells, and therefore, they are capable of much higher rate operation.

It was estimated by Gulton Industries that 250 pounds of these batteries, occupying about 6000 $in.^3$, could provide 50 kw peak power at 56 volts and 50 Hz.

This would be accomplished by the use of four bipolar electrode batteries operating in parallel. Each battery would be composed of 75 cells of 100 $in.^2$ electrode area connected in series. Two batteries could actually carry the load without undue strain, thereby allowing two redundant units. Of course, at lower power levels, less battery weight is required.

c. Selection

For the required AM modulation in this HF concept, the solid-state transmitter was selected for use. Comparison of the filter system (380 pounds) and the battery (270 pounds) by themselves shows a potential battery rate advantage. The battery may alternate at a lower frequency than the filter, but this would be adequate for voice transmission. However, the L-C filter is a very high efficiency device while the battery can not be expected to exceed around 70%. The battery charging power results in a larger solar array. The array is sufficiently larger such that it makes the battery alternative unattractive on a weight basis without even considering solar array cost. Therefore, on L-C filter was selected.

4.7.2.3 VHF No. 1 Power Subsystem

The VHF No. 1 power subsystem is required to supply 500 watts for housekeeping, plus 10.88 kilowatts to the transmitter continuously except during eclipse periods. Batteries supply housekeeping power during eclipse periods. An oriented solar array of four rollup panels (each 12 by 41 ft), nickel-cadmium batteries and power conditioning equipment make up the subsystem as shown in Figure 4.7-4 with the component efficiencies indicated. A list of the component weights is given in Table 4.7-5.

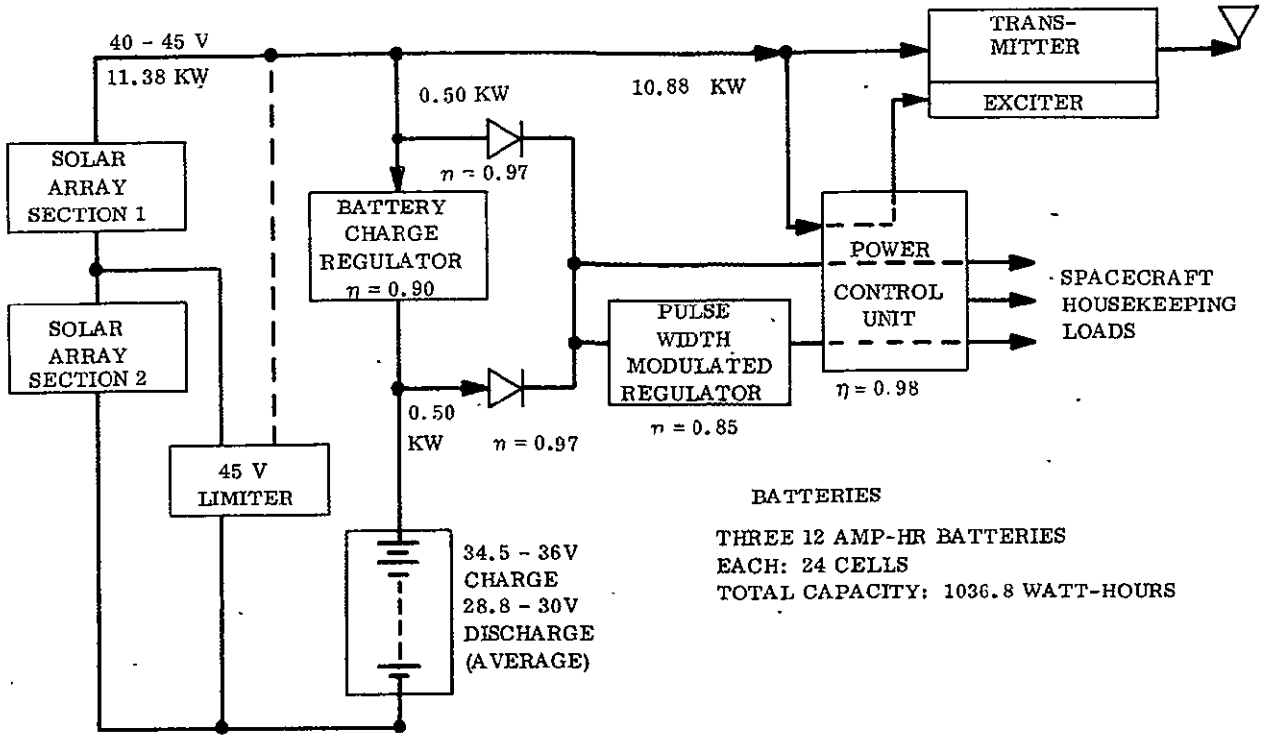

Figure 4.7-4. VHF No. 1 Power Subsystem Block Diagram

Table 4.7-5. VHF No. 1 Power Subsystem Component Weights (pounds)

Solar Array Rollout Panels	836
Batteries	114
Battery Charge Regulators	4
Voltage Limiter	22
PWM Regulator	20
Power Control Unit	3
Total	999

The power conditioning equipment consists of a partial shunt voltage limiter, a battery charge regulator for each battery, a pulse width modulated regulator and power control unit. The voltage limiter protects the other components from excessively high voltages by shunting current and limiting array voltage. This is particularly necessary when the array is new and following periods of eclipse when the array is cold and capable of producing a high voltage. The battery charge regulators limit the battery charging current to a C/18 rate which is a safe overcharge rate. The pulse width modulated regulator provides a regulated bus for the housekeeping and stabilization loads.

4.7.2.4 VHF No. 2 Power Subsystem

The VHF No. 2 configuration is sized for an 8-hour orbit with a 1.26 kw transmitter load for one hour during satellite day each orbit. The housekeeping and stabilization load is 100 watts, continuous. Prime power is supplied by a fixed solar array containing 8 foldout panels (each 4 x 9 ft) which is positioned to pass through its peak operating position (normal to the sunline) 40 minutes into the broadcast hour. At the start of the broadcast period, the array is misoriented 15 degrees (4% power loss). The shadow battery is used to supply some of the broadcast peak power as the satellite approaches the end of its two year life. For over 50% of the orbit the main array is not illuminated, therefore solar cells for housekeeping power are mounted on part of the panel reverse side rather than to increase the main array size and battery weights. The subsystem is shown in Figure 4.7-5. The component weight list is shown in Table 4.7-6.

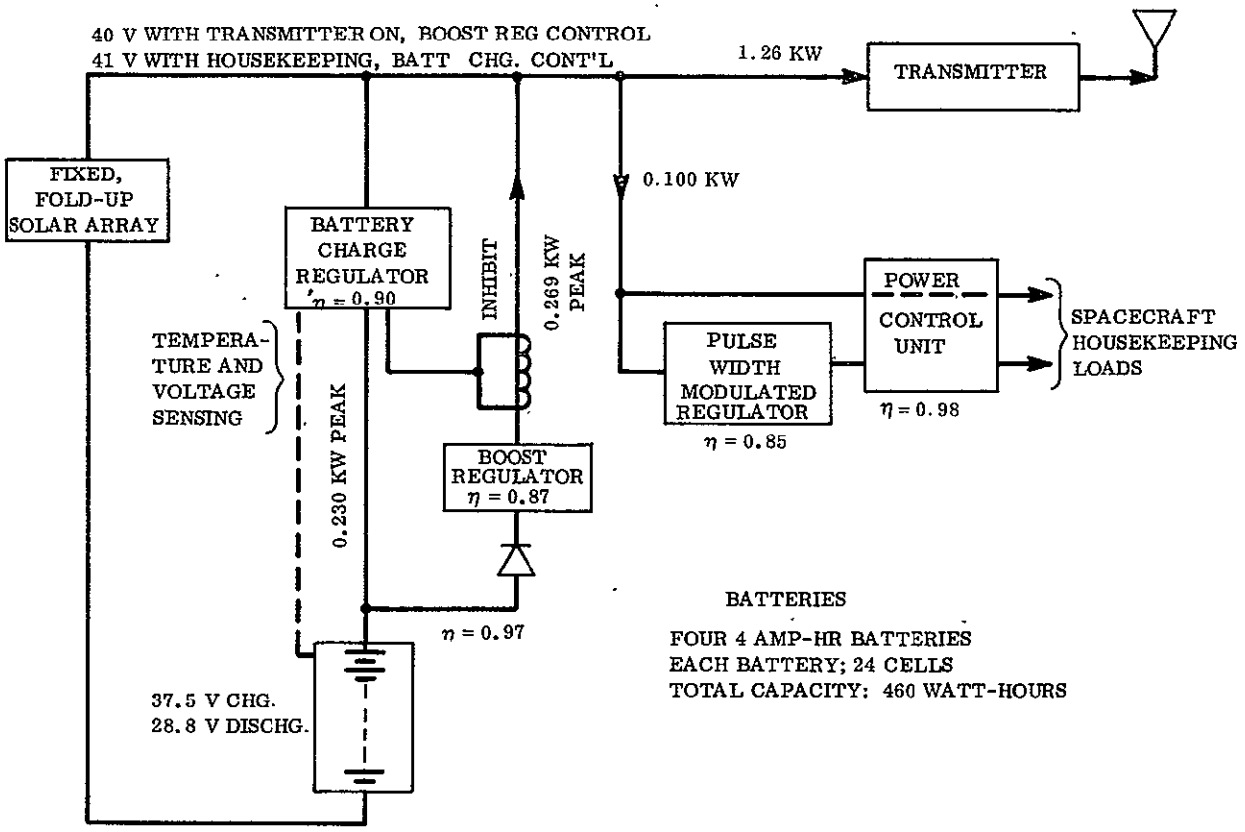

Figure 4.7-5. VHF No. 2 Power Subsystem Block Diagram

Table 4.7-6. VHF No. 2 Power Subsystem Component Weights (pounds)

Cells & Substrate	96
Structure	62
Batteries	52
Battery charge regulator	6
Boost regulator	8
PWM regulator	8
Power control unit	3
Total	235

The battery charge regulator consists of four separate current regulators, one for each battery, sharing a common package. The battery charge regulator includes battery voltage sensing circuits and charge cutoff circuits. These are made necessary by the need to use the high charging rates for the short periods when the solar arrays have surplus power capability. Voltage limit circuitry for the solar array for the periods of overcharge is also included in the battery charge regulator. Conversion of the battery power from the 28.8-volt level to the 40-volt bus level is accomplished by use of a boost regulator. A circuit to inhibit current flow in the battery charge regulator, when the battery is discharging, is also included.

4.7.2.5 UHF Power Subsystem

The UHF power subsystem is required to supply 250 watts for housekeeping plus 2.29 kilowatts to the transmitter continuously (except during eclipse periods), 180w regulated continuous load. This mode of operation is the same as the VHF No. 1 configuration and the same basic power subsystem configuration is used for both with the exception that a high voltage converter/regulator is required in the UHF case to supply high voltage to the tube-type transmitter. See Figure 4.7-6 for the system block diagram and efficiencies, and Table 4.7-7 for component weights.

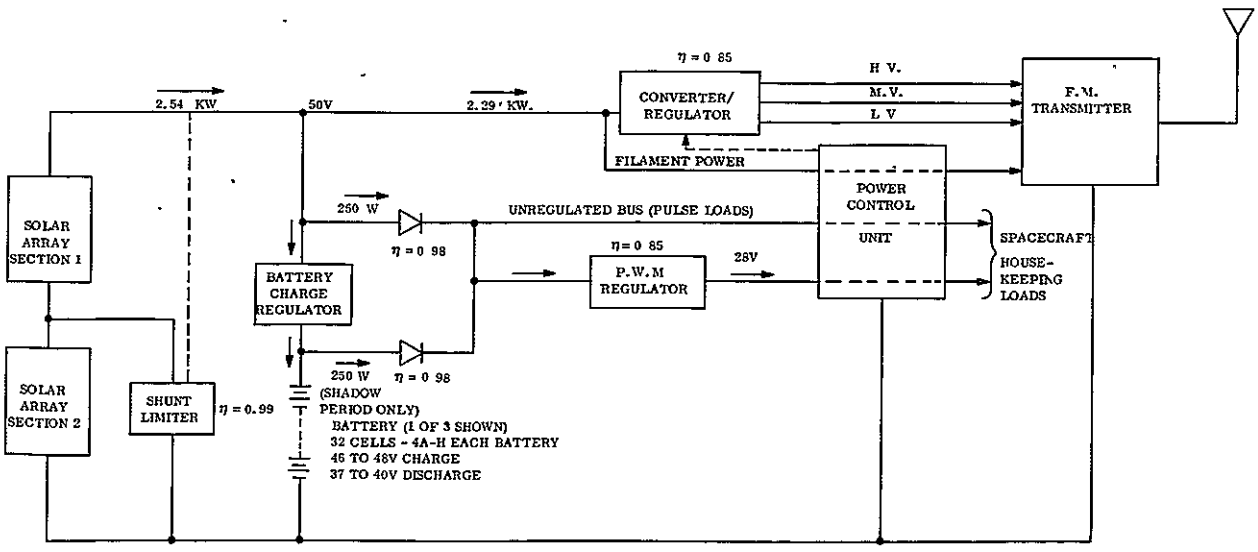

Figure 4.7-6. UHF Power Subsystem Block Diagram

Table 4.7-7. UHF Power Subsystem Component Weights (pounds)

Solar Array Rollout Panels	197
Batteries	54
Battery Charge Regulation	2
Converter/Regulator	50
PWM Regulator	10
Shunt Regulator	22
Power Control Unit	3
Total	338

An oriented solar array containing two rollout panels (each 7-2/3 x 28-1/2 ft) with a partial shunt voltage limiter supplies the main bus. The batteries are charged at a constant current rate. Diode isolation is incorporated to insure that the transmitter is not powered during eclipse periods. The PWM regulator supplies regulated voltage to the housekeeping and stabilization bus.

4.7.2.6 Solar Array Panel Areas

The solar array total cell panel area for each configuration to supply the required power after two years in orbit is as follows:

	Configuration			
Parameter	HF	VHF No. 1	VHF No. 2	UHF
Required Array Power (watts)	7,000*	11,380	1,510	2,540
Specific Power Output (watts/ft^2)	3.92	5.78	4.64	5.78
Solar Array Panel Area (ft^2)	1,788	1,968	326	438

*8,400 watts supplied by battery for total power required of 15,400 watts.

The required power for the broadcast transmitter and for housekeeping was given in previous paragraphs of this section. The specific power output per square foot was calculated for each configuration using the following expression:

$$P = S \times F_1 \times F_2 \times F_3 \times F_4 \times F_5 \times F_6 \times F_7 \times F_8 \times F_9 \times F_{10} \times F_{11}$$

where

P = Specific Power Output per square foot after two years in orbit
S = Solar constant at 1 A.U., 130 watts/ft^2

F_1 = Packaging density of active area of solar cells = 0.85

F_2 = Air mass zero efficiency of solar cells @ 82°F = 0.105 (For the HF case, an effective efficiency of 0.100 was used to account for mismatch conditions resulting from the unregulated battery)

F_3 = Temperature effect on efficiency = 2.417 - 0.0026 T (T in °R) = 0.909 at 120°F

F_4 = Loss due to addition of cover glass filter = 0.92

F_5 = Manufacturing degradation allowance = 0.96 (The packaging density, temperature, cover glass, and manufacturing losses are firm factors based on analysis and experience.)

F_6 = Ultraviolet degradation factor = 0.95 (The UV degradation is an estimate, based on experience, of the decrease in transmissibility of the cover glass/cell adhesive after UV exposure.)

F_7 = Micrometeoroid degradation factor = 0.95 (The micrometeoroid degradation is an estimate of the long-term effects of bombardment. It is known that a 5% degradation occurs when the front surface of a cell is sand blasted. One would expect that this would not be the case for the two-year space environment. However, some allowance must be made for cell elimination through large particle impingement.)

F_8 = Variation of the solar constant with time of year = 0.9668 to 1.0337 (assumed to be a function of the square of the earth to sun distance.)

F_9 = Orientation tolerance = 0.98

F_{10} = Loss factor for diodes and harness = 0.957 (Diode and harness losses are based on experience and estimates.)

F_{11} = Radiation degradation factor after 2 years of operations are based upon Figure 4.7-1. They are:

HF Configuration	0.54
VHF No. 2 Configuration	0.61
VHF No. 1 and UHF Configuration	0.76

4.7.2.7 Batteries

Sealed nickel-cadmium batteries are used in all four configurations. Other types of batteries (silver-cadmium and silver-zinc) do not have the required life capability and reliability. The depth of discharge proposed on the configurations (approximately 50%) is significantly higher than the design for most flown vehicles. However, ground test data and flight data, where the required performance has exceeded design, is available to support the selection of the higher final depth of discharge.

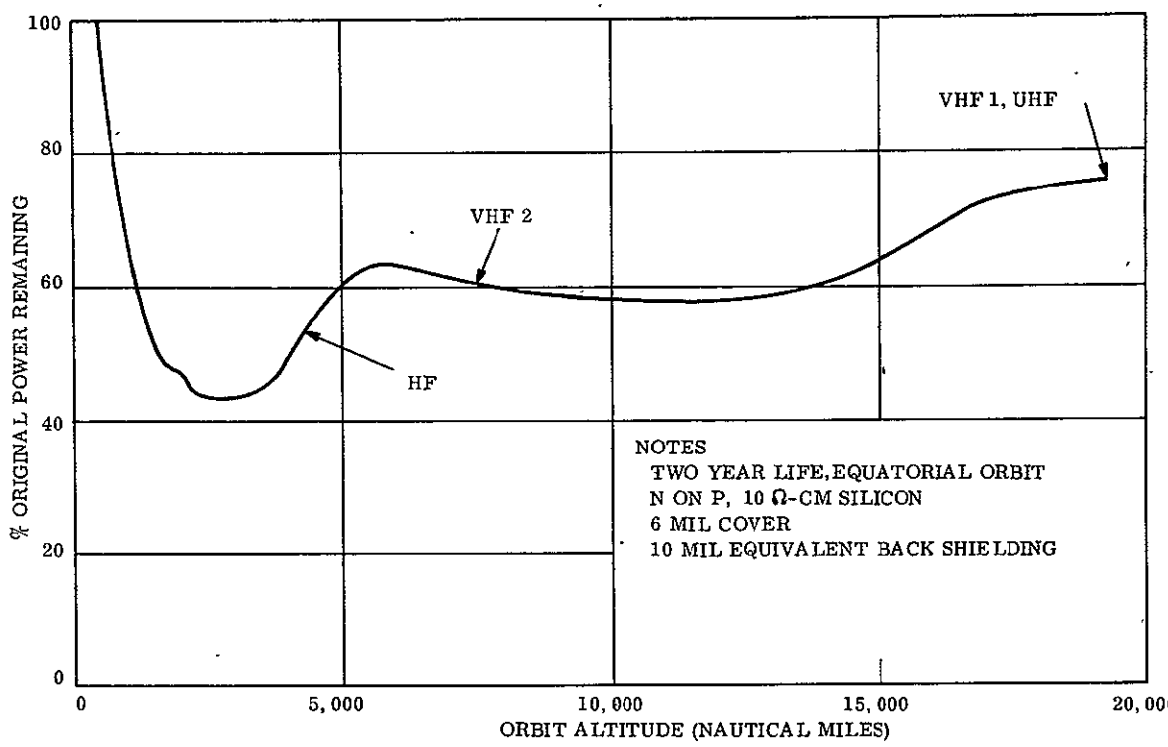

Figure 4.7-7. Radiation Degradation After Two Years as a Function of Orbit Altitude

4.7.3 POWER SUBSYSTEM TECHNOLOGY EVALUATION

4.7.3.1 Power Subsystem Selection

The following types of power subsystems were analyzed for their applicability for use on direct broadcast satellite to be launched in the early 1970's:

a. Photovaltaic/Battery Subsystems

b. Solar concentrator subsystems, including Brayton Cycle, Rankine Cycle, Solar Thermionic and Solar Thermoelectric.

c. Chemical subsystems, including batteries and fuel cells.

d. Nuclear subsystems, including radioisotopes and reactors.

Selection of power subsystems were based upon the following criteria:

a. Lowest cost (development, design, manufacture, and test)

b. Satellite weight dictated by power subsystem types and resulting system interfaces (shielding, cooling, attitude control accuracy, etc). These weights are related to costs by virtue of booster costs.

c. State of the art in terms of flight qualified hardware being available for demonstration flights in the early 1970's. The costs associated with state of the art assessment are included in (a) above.

d. Satellite complexity (and therefore reliability) dictated by both the power subsystem type and the resulting system interfaces (attitude control accuracy, cooling subsystem complexity, etc).

Figure 4.7-8 shows a plot of power systems versus weight for the different types of power subsystems studied. The plot shows a significant weight advantage for the oriented solar array over all systems except the solar thermionic (which was rejected because of high emitter temperatures and the resulting material problems, complex fluid heat transfer loops, and lack of current hardware development).

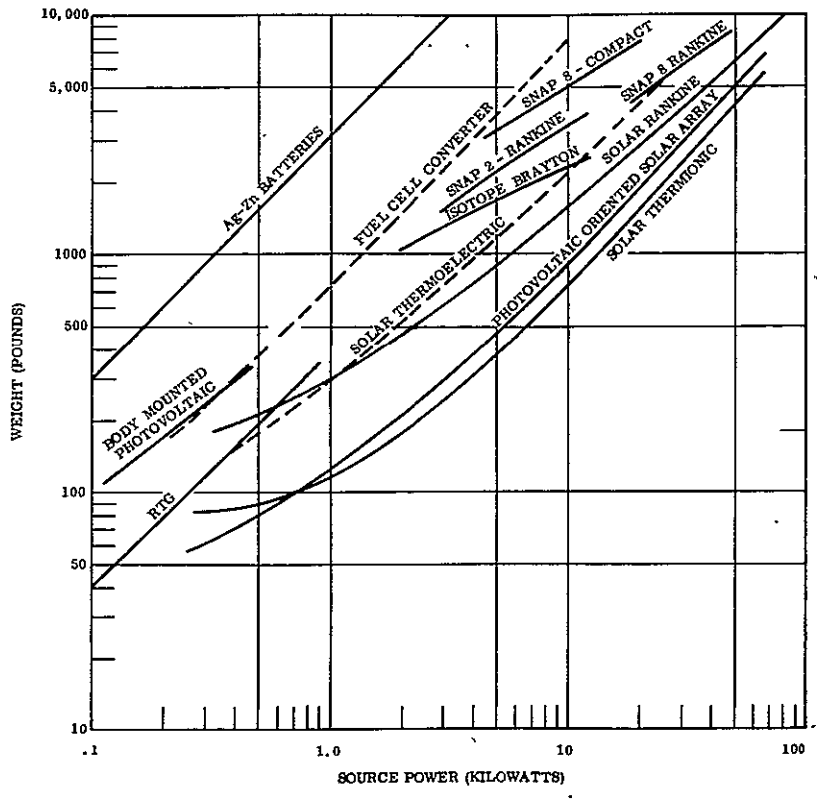

Figure 4.7-8. Estimated Weight Versus Raw Power for Power Subsystems

Table 4.7-8 shows the relative cost comparison of the power subsystem types considered. The launch costs were obtained from the weights given in Figure 4.7-8 and an average Titan launch cost of $5,000 per pound in orbit. No data was obtained for development costs of the nuclear systems since their heavy weight and resulting high launch costs made them non-competitive. Table 4.7-8 also shows, on a total cost basis, that the solar photovoltaic and solar thermionic are the least expensive choices. For higher cost per pound boosters (SLV3A/AGENA) the advantages for solar photovoltaic and thermionic are more pronounced.

Table 4.7-8. Power Subsystem Relative Costs

Power Subsystem	Relative Cost Per kw, Raw Power (Approximate For 1 to 10 kw Subsystems)			
	Develop	Design, Manufacture And Test	Launch	Total
Solar:				
Photovoltaic - Oriented Panels	0	0.5	0.6	1.1
Photovoltaic - Body Mounted Cells	0	2.5	2.6	5.1
Brayton Cycle	2.0	0.1	2.0	4.1
Rankine Cycle	2.0	0.1	1.5	3.6
Thermionic	0.6	0.1	0.5	1.2
Thermoelectric	0.6	0.2	1.5	2.3
Chemical:				
Ag-Zm Primary Battery	0	0.1	15.0	15.1
Fuel Cell	0	0.4	4.0	4.4
Nuclear:				
RTG (50 to 1000 watts)	*	5.0	3.0	8.0
Isotope Brayton (2 to 15 kw)	*	1.1	3.0	4.1
Isotope Rankine (2 to 15 kw)	*	2.2	4.5	6.7
Isotope Thermoelectric (1 to 5 kw)	*	3.9	5.0	8.9
SNAP-8/Compact Converter (5 to 20 kw)	*	0.5	2.5	3.0
SNAP-8 Rankine (20 to 50 kw)	*	0.2	1.8	2.0
SNAP-2 Rankine (3 to 11 kw)	*	0.2	1.9	2.1

*No data obtained on development cost

Table 4.7-9 shows the relative complexity of, the development required for, and the reasons for selection or rejection of the power subsystems analyzed. The oriented photovoltaic array was chosen as the best choice for direct broadcast satellites to be launched in the early 1970's. Since they are state of the art, they minimize risk. Since they have short design cycles and can be readily scaled up or down in size, they provide schedule confidence and performance flexibility.

Table 4.7-9. Power Subsystem

Candidate Systems	Satellite Complexity	Development Required	Reason Accepted or Rejected
Solar			
Photovoltaic - Oriented Panels	Moderate	Low	Yes - Light weight, lowest cost, loose ($\pm 15^{\circ}$) attitude control needed, flight proven
Photovoltaic - Body Mounted	Low	None	No - High cost
Brayton Cycle	High	High	No - 0.1° attitude control needed, complex, development needed, high cost
Rankine Cycle	High	High	No - 0.2° attitude control needed complex, development needed, high cost
Thermionic	Moderate	Moderate	No - 0.1° attitude control needed, material development needed, complex cooling
Thermoelectric	Moderate	High	No - 0.5° attitude control of large collector needed, high cost.
Nuclear			
RTG (0-1000 watts)	Low	Low	No - High cost, small power
LHS/Brayton (2-15 kw)	High	High	No - High cost, complex, development needed
LHS/Hg - Rankine (2-15 kw)	High	High	No - High cost, complex, development needed
LHS/Thermoelectric (1-5 kw)	Moderate	High	No - High cost, development needed
SNAP-8/Compact Converter (5-20 kw)	Moderate	Moderate	No - High cost
SNAP-8 (20-50 kw)	Very High	High	No - High cost, complex, development needed
SNAP-2 (3-11 kw)	Very High	Moderate	No - High cost, complex
Chemical			
(6 Month Mission, One Hr/Day			
Ag-Zn Primary Battery	Low	None	No - Weight, high cost
Fuel Cell	Moderate	Low	No - Weight, high cost

4.7.3.2 Power Technology Evaluation

This section presents summaries of electrical power systems examined, their characteristics and their relative states of development. Three energy source areas were considered: chemical, nuclear, and solar. The following guidelines were used in examining the power subsystem tapes:

a. Power requirements from 0.1 to 40 kw_e

b. Concepts considered to be 1968-69 state of the art for demonstration flights in the early 1970's.

c. Design life to be 2 years

d. Orbit altitude between 4000 nm and geostationary (19,300 nm).

e. Broadcast duration from one hour per day to continuous

4.7.3.2.1 Photovoltaic/Battery Power Subsystems

Photovoltaic/battery power equipment converts solar energy to electrical energy, stores electrical energy, and contains equipment to regulate and/or convert the electrical power to meet the user requirements. The corresponding hardware to accomplish this includes a solar cell array, batteries, energy storage equipment, and power conditioning equipment. The following sections discuss the considerations relevant to design of these items.

4.7.3.2.1.1 Solar Arrays. A primary consideration is the type of solar cell. Once a type (and efficiency) is chosen, the array power per unit area may be determined as a function of the environment and time. This sizes the array, and additional considerations can be made as to the mechanical method of support and deployment. The solar cell is currently used to supply electric power for virtually all long life (more than 1 month) satellites with the largest fabricated array being several kilowatts in magnitude (Reference 8). Many studies of larger arrays which will meet the power requirements of the Saturn class space vehicles have been completed or are in progress. The present state of the art weight is about one lb/sq of cell area. The goals of the VBMS Program are 1/2 lb/sq ft or less for either lightweight folding or rollup arrays.

Depending on vehicle orientation and control requirements, several types of cell groupings were analyzed. The problem of a braodcast satellite is complicated by the fact that the RF antenna must be earth oriented. Three methods were considered as typical of the range from no attitude control to full vehicle attitude and array control:

a. Flat Panel: Requires two-axis control (preferably $\pm 15^{\circ}$)

b. Gravity Anchored Solar Panel (GASP) Concept: Two-sided Prism (requires one-axis control)

c. Body Mounted Cell: Cells on all surfaces (requires no orientation)

These configurations were analyzed and the following relative area factors for the same minimum power output were determined:

Flat Panel:	1.00
Prism:	2.49
Cylinder:	6.59 (L/D = 0.84)

Conceptual sketches of these arrays are shown in Figure 4.7-9.

There are several development efforts underway with the goal of improving the performance of large solar arrays particularly with respect to weight. Several of these programs are summarized in Table 4.7-10.

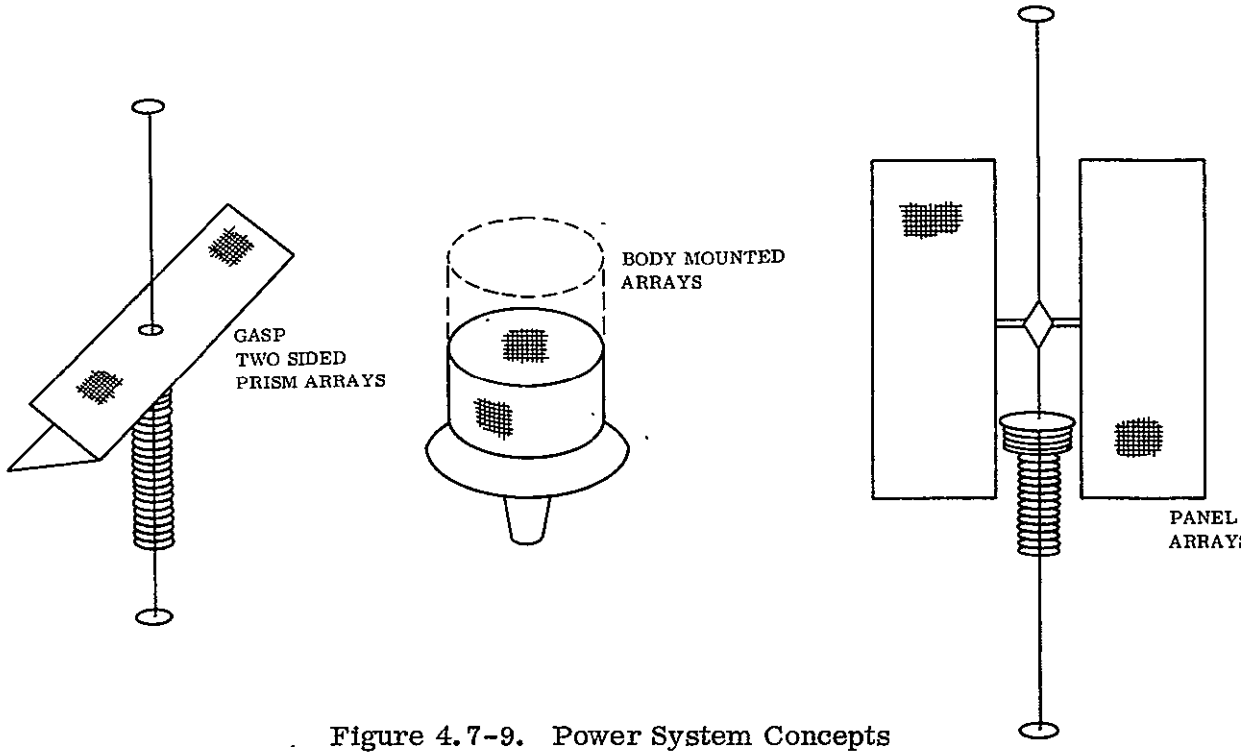

Figure 4.7-9. Power System Concepts

Table 4.7-10. Development Programs

Program	Contractor	Sponsor	Size	Performance Goals
Development of Lightweight Rigid Solar Panel	Electro-Optical Sys.	NASA-OART	10 kw	36.5 watts/lb
Flexible Intergrated Solar Cell Array (Rollup)	Hughes Aircraft	AF-RTD	20 kw	26.2 watts/lb
Large Area Solar Array Design (Folding Panel)	Boeing Aircraft	NASA-JPL	50 kw	20 watts/lb
Deployable Solar Array Structure (Rollup)	Ryan Aircraft	NASA-JPL	200 ft^2	0.6 lb/ft^2
Rollup Solar Array Technology	GE	NASA-JPL	10 kw	0.5 lb/ft^2

Two types of folding panel arrays are being investigated, with one being an improvement of the state of the art. One of the programs* is investigating electroformed structure and another** is developing the use of flexible substrate stretched in a rigid frame. Another approach is to mount the solar cells on a flexible substrate which is rolled on a drum in the stowed configuration. The array is deployed with an extendible boom structure by unrolling the array from the drum.

The differences in performance between the advanced folding panel design goals and the rollup concept are small and somewhat uncertain at this time. Recent successes (in the GE rollup solar array technology development program) in acoustic and vibration tests provide confidence that a rollup array development program could be carried out within the broadcast satellite schedule. The acoustic environment was 147 db for 5 minutes (Agena simulation) and 15 db for 2 minutes (Titan 3 environment simulation). The vibration environment was 5 g's up to 400 Hz sinusoid, 7.5 g's to 2000 Hz sinusoid, and 15.3g rms random (Agena simulation). The engineering model and vibration test units are shown in Figures 4.7-10 and 4.7-11.

4.7.3.2.1.2 Solar Cell Performance. Present state-of-the-art solar cell characteristics are as follows:

Material:	Silicon (10 ohm-cm)
Type:	N/P
Size:	2.0 cm x 2.0 cm
Thickness:	13 mils
Contacts:	Soldered
Weight:	0.42 grams
Efficiency:	10.5 percent (present) (12 percent in the 1970's)

N on P silicon cells (best present choice on a performance basis) were estimated to have, at best, a 12 percent conversion efficiency in direct solar flux and a power output of 130 watts/ft^2 at 85°F. Certain additional factors were considered:

Cover Glass Filter Attenuation Factor:	0.92
Meteor Particle Impact Damage Factor:	0.95
Manufacturing Processes:	0.96
Temperature Degradation:	(1.0 to 0.0026) per$^\circ$F above 85°F
Radiation Degradation:	Depends on orbit and cover glass

*Hanson, K. L., "Thermal Integration of Electrical Power and Life Support Systems for Manned Space Stations," General Electric Co., Missile and Space Division, NASA Report CR-216, November 1965.

**Woods, R.W. and Erlanson, E. P., "Study of Thermal Integration of Electric Power and Life Support Systems for Manned Space Stations," General Electric Co., Document No. 66SD4231, January 1966, Contract NAS 3-6478.

Figure 4.7-10. Engineering Model of Rollup Solar Array

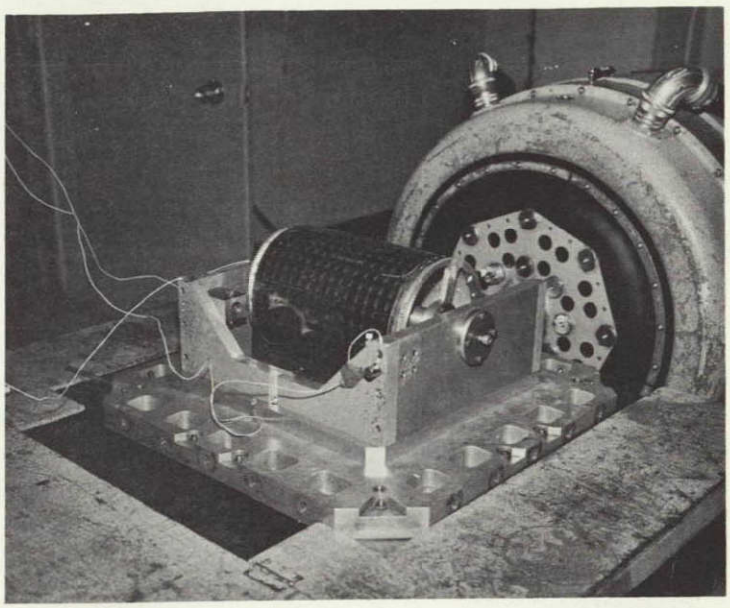

Figure 4.7-11. Vibration Test of Segment of Rollup Solar Array

Several approaches are being made to increase the performance of solar cells. These include techniques to increase the efficiency, decrease the weight, and increase the tolerance to radiation. Experience has shown that solar cells require extensive flight evaluation after even small modifications. At the present time, several cell improvements look feasible but are uncertain. Therefore, the VBMS design is based on the present state-of-the-art cells with the characteristics listed above. This is a worst case design. Should improved cells become available, they can be incorporated into the program.

Cadmium sulfide, cadmium telluride and gallium arsenide have shown the most promise as thin film solar cell materials. Cadmium sulfide has received the most attention and pilot production runs are capable of producing 5 percent efficient, air mass 1, 50 cm^2 cells. These cells can be made lightweight when deposited on a thin plastic substrate, and with advanced manufacturing techniques there is a potential array cost improvement of an order of magnitude over single-crystal cell arrays. Stability is a major problem with thin film cells as they are affected by storage, humidity, thermal cycling and ultraviolet. In view of this instability and lack of significant flight experience, thin film cells cannot be considered with any confidence for the present VBMS schedule. But for flights with design stages occurring in the 1972-1975 time period, thin film cells will probably look quite attractive.

The lithium doped P/N cell is an example of expected improvement. Tests have shown that this cell provides increased resistance to atomic particle damage. Cells were subjected

to fluxes of $10^{16}/cm^2$ 1-Mev electrons; and in a separate run, 10^{11} to $10^{12}/cm^2$ 17-Mev protons. The results showed a temporary loss in performance, with a return to the original output in a matter of hours as a result of the lithium diffusing to the radiation created vacancies. At space intensity, no degradation should occur since the lower bombardment rate will allow time for lithium diffusion. The useful life of this cell type is still uncertain; but it is believed that complete annealing can be expected, at least up to the presently tested total fluxes. The lithium doped cell apparently exhibits the slight initial efficiency advantage characteristically enjoyed by P/N cells over N/P cells. Recently, three cell vendors have initiated the manufacturing of lithium doped cells. Their availability should lead to greater testing throughout the industry with consequent detailed properties in the near future.

4.7.3.2.2 Solar Concentrator Subsystems

All of the following solar systems require a collector (or concentrator) and absorber located at the collector focus to use the solar energy at high temperature for the heating of working fluids. The size required for each type power system is dependent on the power output desired and conversion equipment thermal efficiency. These collectors require orientation with respect to the sun vector of 0.1° to 0.5°, depending on absorber temperature desired. The collector may be oriented separately from the satellite, depending on the relative ease of collector and antenna orientation. Collectors and absorbers are under active development, but the assumed efficiencies and weights for this study are goals rather than present state-of-the-art.

4.7.3.2.2.1 Solar Brayton Cycle. The Brayton cycle converts collected and absorbed solar energy into electric power by compressing argon, heating it, and then allowing it to expand through a turbine which drives an alternator. Addition of a recuperator increases efficiency, and a space radiator is included to provide closed cycle operation. The primary attraction of the Brayton cycle is its relatively high thermal efficiency and small collector area for even the relatively low power level systems being considered. This thermal efficiency is at the expense, however, of precision collector pointing (0.1°) to attain high absorber temperature ($\sim 1700^{\circ}F$).

Critical component development has been going on at NASA-Lewis for this system. In addition, both Pratt & Whitney (isotope Brayton) and AiResearch (solar Brayton) have received contracts for fabrication of Brayton systems in the 5 to 10 kw range. The goals of these programs are 10,000 hr continuous operation. These systems are not tied to a specific mission, but it is anticipated they will fulfill the power needs for manned space stations with 4 to 6 men in the 1970-72 period. In order to achieve a high degree of confidence in obtaining a VBMS Brayton power system, the VBMS peculiar requirements must be identified immediately and factored into the current development programs.

4.7.3.2.2.2 Rankine Cycle. This method of energy conversion depends on two-phase liquid (such as mercury) for operation. The liquid is compressed and vaporized in a boiler. The resulting vapor expands through a turbine which drives an alternator. A condensing

radiator is used to return the wet vapor to the liquid state. The ideal Rankine cycle approaches Carnot cycle efficiency. Thus, this method of conversion could attain efficiencies competitive with and surpassing the Brayton cycle for given temperature levels.

To date, the space application Brayton cycle has generally been operated between wider temperature extremes, yielding higher thermal efficiencies than the Rankine system. Some reasons are the relative corrosiveness and handling ease of the Argon and mercury working fluids, and the necessity of a two-phase fluid in the Rankine cycle. The present space application characteristics are modest upper temperatures (1250°F), high rejection temperatures (600°F) for small radiators, slightly wider attitude tolerance and lighter weight than for the Brayton cycle. In the 3 to 6 kw range, extensive component development has been done on the "Sunflower" program at TRW. The work showed several thousand hours of operation of space-weight components. However, this work is apparently not continuing due to the lack of mission requirements and more interest in the Brayton cycle at these power levels. Larger (35 kw_e) turbine systems work is going on for the SNAP-8 nuclear program. Another program using the Rankine cycle is the SNAP-2. In the hundred kilowatt class, GE-Space Power in Evendale, Ohio, has been life-testing potassium and sodium conversion system components under contract with NASA-Lewis. These systems are operating at higher temperatures; boilers up to 2000°F and turbines to 2000°R. Again, as for the Brayton cycle, the VBMS peculiar requirements for a Rankine cycle need to be identified right now to obtain high confidence in a flight date for the early 1970's.

4.7.3.2.2.3 Solar Thermionic Generator. In the thermionic system, electron flow through a cesium vapor gap is stimulated by a high temperature emitter. At the same time, heat is transferred from the emitter to collector and then must be rejected to space. The usual method uses external fins. Operating temperatures of the emitter normally exceed 3000°F creating severe material problems for an efficient long-life system. The high operating temperatures permit efficient heat rejection through relatively small radiating surfaces. For large systems such as those conceived for VBMS, it is probable that a secondary fluid loop between the absorber and power generating elements is required. If heat pipe concepts prove feasible, then the increase in complexity is slight. However, for an actively pumped fluid, this system becomes complex. The relative weight is light based on the collector/absorber assumptions used. Work to date has been twofold: (1) to increase thermal efficiencies, and (2) to develop long-life high temperature materials. Results indicate progress in both areas. The approach for the VBMS study was to identify probable temperature/efficiency ranges to meet the early 1970's with a two-year life. This results in a thermal efficiency of around 12 percent with some optimism in extension of current component life data. Again, availability of this system depends on immediate identification of VBMS needs and initiation of a development program.

4.7.3.2.2.4 Solar Thermoelectric Generator (STG). A thermoelectric generator contains thermoelectric elements that convert a portion of heat energy passing through them into electrical energy (known as the Seebeck effect). The generator is composed of many of these elements to obtain the desired voltage/current output. Since there are large numbers of static elements, the system can be constructed to provide high reliability of operation. The

limiting items for the present technology are conversion efficiency and material temperature resistance. As in the case of the thermionic system, a separate fluid loop is probably required for the desired VBMS output ranges. Based on the element materials currently under development, the expected overall thermal efficiency is in the order of 6 percent. This results in a large collector size for a given power output. The low absorber temperature does allow a greater attitude tolerance than the other collector systems. The combination of large collector and the many thermoelectric elements places this system among the heavier ones under consideration. The STG development would be based on the collector development and RTG development currently underway. However, if this method of power conversion were selected, VBMS needs should be identified immediately, and a developed program initiated.

4.7.3.2.3 Chemical Energy Conversion

4.7.3.2.3.1 Silver-Zinc Primary Battery. Primary batteries are currently extensively used for short-life (less than 2 weeks) space vehicles. The disadvantage to longer life use is the weight increase as a function of time. The cost is less than other power source competitors for low output/short life. The area and launch volumes are also comparatively small. The basic shortcoming is the total energy required in orbit.

4.7.3.2.3.2 Fuel Cell. The hydrogen-oxygen fuel cell fulfills power system requirements for time periods from 2 weeks to 2 or 3 months. Again, the system is energy-sized, and a fuel penalty occurs for each kilowatt hour generated.

4.7.3.2.4 Nuclear Energy Conversion

4.7.3.2.4.1 Radioisotope Power Generating Systems. The conversion systems discussed in the preceding section could also be combined with a radioisotope heat source in place of a solar collector. The resulting system provides a reduction in deployed area and eliminates any orientation requirements. However, the isotope-conversion equipment combination would be heavier in each case because of shielding and re-entry requirements. Cost and availability of the iosotope fuel is of great concern. Development of these systems is less likely than the chances for the solar concentrating systems for the early 1970's with the exception of radioisotope thermoelectric generators (RTG). Small sizes, up to 50 watts, have already demonstrated operation. The static heat transfer technology is applicable up to about 1 kw electrical power levels. For higher power systems, active fluid loops are required, with consequent reduction in performance (watts/lb) and reliability.

If the time period is extended to the mid-1970's, then isotope thermionic systems become attractive candidates. The higher operating temperatures and higher thermal efficiencies will yield improved performance and smaller size. However, this technology capability is beyond the present study time period.

The dynamic conversion of isotope heat energy to electrical power has been under investigation in particular using a Brayton cycle. The relatively high thermal efficiency already achieved by this cycle would indicate it as a sound choice over the Rankine system. The performance

advantage is due to the use of inert working fluid with consequent higher practical operating temperatures. The technology is currently under development by NASA-Lewis, but direct application to a VBMS launch is improbable. Fuel availability and cost is generally recognized as a real barrier to this system as well as all multikilowatt electrical output isotopic power systems.

4.7.3.2.4.2 Reactor Source Energy Conversion. An alternate nuclear power area is to use a reactor as a heat source, as is being done with ground based electrical service around the world. The problem is to apply existing technology for large, heavy designs to an extremely small output, lightweight requirement. There has been considerable effort in the development of such a reactor in the SNAP-2, 8 and 10A programs. The SNAP-2 and 10A are similar designs with 40 to 200 kw thermal outputs. The SNAP-8 design supplies from 600 to 800 kw thermal outputs. Emphasis on long life and space weight materials selection has resulted in very modest operating temperatures and efficiencies for these units.

The conversion methods that have been applied are thermoelectric and Rankine. The technology can be considered "semideveloped." The major remaining problem is generation of data demonstrating a reliable life in the order of 20,000 hours. Effort is continuing only for the SNAP-8 reactor, with emphasis on the Mercury Rankine conversion system. However, it is questionable whether a direct broadcast satellite launch in the early 1970's could have a reactor power system designed for a 2-year life. In thermoelectric conversion were used, this would increase converter reliability but decrease performance. The potential costs of developed reactor source power systems are quite modest, especially compared with isotopic source systems. There is a continuing weight problem, which is not helped by the reactor high radiation levels.

4.7.3.2.4.3 Nuclear Power System Cost Comparisons. Cost comparisons were made to determine if nuclear systems offered significant advantages. A typical evaluation for a 2.5 kw system is shown in Table 4.7-11. It is assumed that the nuclear powered configuration is passively stabilized to eliminate the cost of an active attitude control subsystem. The nuclear power subsystem is a SNAP-2 type which is feasible for this application.

Table 4.7-11.. Photovoltaic vs. Nuclear Tradeoff

Item	Photovoltaic	Static Nuclear
Cost (Development and Manufacturing	4.0×10^6	$> \$ 20 \times 10^6$
Development Time	20 months	45 months
Weight	320 pounds	2000 pounds
Station Weight	1200 pounds	3200 pounds
Booster	Atlas-Imp. Agena plus Kick Motor	Titan 3 + 7 Seq.
Booster Coast	$\$ 8.5 \times 10^6$	$\$ 25.0 \times 10^6$
Attitude Control Subsystem Cost	$\$ 6.0 \times 10^6$	$\$ 0.5 \times 10^6$
Total Incremental Cost	$18.5 Million	$45.5 Million

In the first three items, the development costs were included because development of the nuclear system within this time frame would be charged to the broadcast satellite. In addition to this comparison, a separate cost comparison was made to determine the relative position for active and gravity gradient attitude control coupled with differing booster requirements (last item). This comparison shows that the nuclear system is more expensive than the photovoltaic.

4.8 TELEMETRY, TRACKING, AND COMMAND (TT&C)

4.8.1 GENERAL

The TT&C requirements and equipment will be almost identical in all four VBMS configurations. Variations which may have some effect on the equipment include different ground-to-satellite transmission distances and periodic loss of contact with the ground stations (in the HF and VHF No. 2 configuration).

The functions of the TT&C subsystem in the VBMS are conventional: to support operation, evaluation, diagnosis and correction of malfunctions, and tracking of the satellite. Because the initial VBMS will be experimental, the evaluation requirement is quite important. This results in a somewhat heavy telemetry data load.

The TT&C subsystem will be compatible with the NASA Space Tracking and Data Acquisition System. Design of the subsystem is straightforward; essentially all equipment and components are off-the-shelf or state-of-the-art. The total subsystem weight is estimated at approximately 60 pounds and the power requirement up to 100 watts.

4.8.2 REQUIREMENTS

4.8.2.1 Telemetry

The estimated telemetry data load is shown in Table 4.8-1.

Table 4.8-1. Telemetry Data Requirements

Number of Data Channels	Sampling Rates or Frequency Response	Data Accuracy	Data Rate or Bandwidth
200 analog	1/10, 1/1, 5/1, 10/1 samples per second	±1% to ±10%	5.1 kbps
20 digital 15 analog	10/1 30-2000 Hz	"1", "0" ±5%	5.1 kbps 100 kHz

The telemetry format will include satellite identification, word and frame synchronization and 8-bit NRZ-C data words. Subcommutation will be used for low data rate channels and supercommutation (cross-strapping) for high data rate channels. Modulation will be PCM-PSK-PM and FM/FM for digital and analog data, respectively. The PCM data rate will be 5.12 kbps.

Selected portions of the telemetry data may be stored on magnetic tape for later playback at an accelerated rate. Speedup ratios of 20:1 to 25:1 are well within the state-of-the-art. At such a rate, 4 hours recorded data could be played back in from 10 to 12 minutes.

4.8.2.2 Command

The estimated command data load is shown in Table 4.8-2.

Table 4.8-2. Command Data Requirements

Number of Commands	Type of Command	No. of Bits Per Word or ON/OFF	Max. Comm. Rate
30	discrete	ON or OFF	1 bps
20	selection	5-16 bits per word	1 bps

The command data format will include vehicle identification, address code, data bits, and parity bit. It will also include bit, word, and frame synchronization. The data will be PCM-NRZ-C. Command words will be frequency shift-keyed onto subcarriers in the 7 to 9 kHz band. The subcarriers will amplitude modulate the S-band (2200 to 2300 MHz carrier.

Commands will be verified both on-board and on the ground (via telemetry). Command storage will be required, for use when the satellite is out of communication with the ground stations and for storage of commanded programs for later execution. A stored command is time tagged, and executed when the time tag matches the spacecraft clock.

The spacecraft clock will be required to provide timing signals and frequency sources for the satellite equipment. It will include a function generator and counting mechanism. For the PCM telemetry the time will be encoded into data words. For FM/FM telemetry one subcarrier will be used to transmit spacecraft clock time. During real-time transmission, ground based timing signals will be recorded simultaneously with the spacecraft clock signals.

4.8.2.3 Tracking

Spacecraft tracking will be performed by the NASA Space Tracking and Data Acquisition System. For this purpose, a CW beacon compatible with the Minitrack system and a transponder compatible with the NASA Range and Range Rate System will be required.

4.8.3 TT&C SUBSYSTEM

4.8.3.1 Subsystem Design

A summary of the major parameters of the TT&C subsystem is shown in Table 4.8-3. The subsystem is shown in block diagram form in Figure 4.8-1.

Table 4.8-3. TT&C Major Parameters

TRACKING		TELEMETRY	
• Equipment	Range and Range Rate Transponder and Tracking Beacon	• Frequency	2.2 GHz
• Frequencies	Ground-to-Satellite, 2270 MHz Satellite-to-Ground, 1705 MHz (Transponder) 135 MHz (Beacon)	• Modulation	FM/FM; PCM-RSK-PM
		• Data Rate	5.1 kbps 100 kHz (WB Analog)
BASIS FOR PARAMETER SELECTIONS		COMMAND	
• Frequencies	Compatibility with Projected NASA Installations	• Frequency	2.2 GHz
• Modulation	Compatibility and Efficiency	• Modulation	AM-FSK
• Data Rates	Dictated by Data Loads	• Information Rate	128 bps to 1000 bps

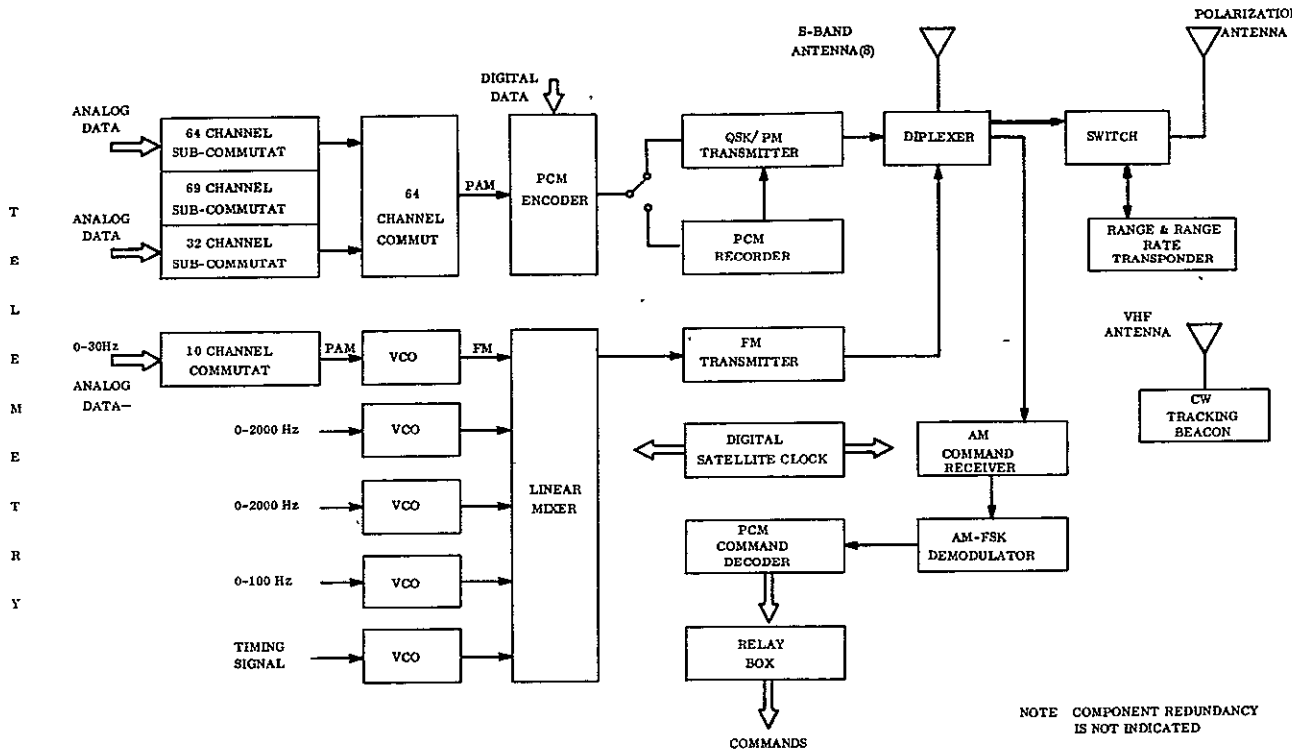

Figure 4.8-1. VBMS Telemetry Tracking and Command Subsystem

The telemetry subsystem consists of a PCM/PSK/PM and an FM/FM data processing modulation group. In each group, commutators or VCO's may be changed as required to suit each of the four satellite configurations. Both the PCM and FM transmitter signals are diplexed to a common antenna(s). The command decoder also contains a command storage. The satellite clock serves as time reference and frequency generator for the entire TT&C subsystem and possibly to support other subsystems. A CW beacon is shown which will provide a tracking reference for the Minitrack system as part of the STADAN network. The range and range rate transponder assist in determining the yaw axis position during powered flight by transmitting a signal via the polarization antenna to ground where the polarization angle (POLANG) is measured. In the stabilized mode the transponder will

be used to determine range, range rate and angle. Circuit and component redundancy may be applied to critical components to increase life and reliability. For simplification, component redundancy is not shown on the block diagram.

4.8.3.2 TT&C Components

The type and number of components, their weight, size, and power consumption are shown in Table 4.8-4. Type of circuitry and special functions are also indicated. Components which may require some development are specifically the PCM commutators, encoders, command decoder, command storage, AM/FSK demodulator, relay box, linear mixer and satellite clock. Other components will be available or will need only slight modification.

Table 4.8-4. Illustrative TT&C Component Summary

Component	Amount	Weight (lb)	Size (in.)	Power (w)	Type of Circuit	Special Functions
64 Channel Subcommutator	2	0.5 ea.	3 x 2 x 2	1 ea.	Microcircuit	
32 Channel Subcommutator	1	0.5 ea.	3 x 2 x 1	1 ea.	Microcircuit	
64 Channel Commutator	1	0.5 ea.	3 x 2 x 2	1	Microcircuit	
PCM Encoder	1	1	4 x 3 x 2	2	Microcircuit	
PCM Transmitter	1	2.5	8 x 4 x 2	50	Solid State RF	5w RF Power
PCM Recorder	1	10	10 x 10 x 4.3	<12	Electro-Mechanical	2 Track Digital Data - 4 hrs. Recording
10 Channel Commutator	1	0.5	2 x 2 x 1	0.5	Microcircuit	
VCO's	5	0.05 ea.	1 x 1 x 0.5	0.35 ea.	Microcircuit	
Mixer Amplifier	1	0.2	1.5 x 1.5 x 1.5	0.6	Microcircuit	
FM Transmitter	1	2.5	8 x 4 x 2	50	Solid State RF	Dual Receiver
Command Receiver	2	4.0 ea.	6.5 x 4.5 x 2.5	2.5 ea.	Solid State RF	
Command Decoder	2	2 ea.	5 x 3.5 x 2.5	2	Microcircuit	Dual Decoder (Includes Command Storage)
Relay Box	1	2	8 x 4 x 0.5	(0.1 stby.)	Electro-Mechanical	
Range & Range Rate Transponder	1	9	14 x 7 x 4	25	Solid State RF	
CW Beacon	2	0.5 ea.	4 x 2 x 1	2	Solid State RF	136 - 137 MH.
Satellite Clock	1	2.2	5 x 4 x 2	2	Microcircuit	
S-BD Diplexer	1	0.5	4 x 3 x 0.5	--	Microwave	Strip Line Techn.
S-BD Switch	1	0.2	2 x 2 x 0.8	3	Diode or Ferrite	Solid State SPDT

4.9 PROPULSION

4.9.1 INTRODUCTION

a. Summary

This section presents the study effort related to selection of the launch vehicle and other propulsion subsystems for the four VBMS satellite configurations. The selected launch vehicles were Titan III series vehicles for the two large satellites and Atlas-Agena systems for the other two. Selected vernier attitude control mass expulsion systems were all hot gas monopropellant systems, and station-keeping systems were chosen to be cesium ion engines. The design requirements, selection rationale, and descriptions of the systems and their operation are presented in Section 4.9.2.

A survey of candidate boosters is presented in Section 4.9.3. A state-of-the-art survey of engines applicable to the vernier trim, attitude control mass expulsion, and station-keeping functions was performed, with the results presented in Section 4.9.3.2. An analysis showing East-West (E-W) station-keeping change in velocity (ΔV) requirements for satellites stationed in a geostationary orbit was performed. The maximum ΔV required for E-W station-keeping was found to be about 7 fps/year.

b. Conclusions

The launch vehicles selected for the VBMS mission were chosen on the basis of availability of required payload capability and minimization of cost. The particular selections made could vary with changes in our national booster inventory such as decisions to go ahead on the development of particular stage combinations not yet funded, or development of new higher energy stages, etc. For purposes of sizing the VBMS spacecraft configurations and estimating their costs, the data presented is satisfactory, and no gross design changes are anticipated. The one system with marginal payload capability (VHF No. 2) would have to rely on launch vehicle performance improvement or establishment of more rigid weight allocations to subsystems.

The vernier trim/attitude control mass expulsion systems were chosen to be combined into one system (a liquid monopropellant system using hydrazine) with commonality of all primary components, including thrust nozzles where possible. This approach resulted in a reasonably optimistic estimation of subsystem design weight, cost, and feasibility.

The selection of ion engines was made for the station-keeping or ephemeris control, primarily on the basis of minimizing weight. The design of the specific orbit maintenance system is highly configuration dependent (e.g., possible orientation of thrust vector strongly influences thrust level and subsequent disturbance torque), and the particular systems thus selected can be considered representative only for this preliminary design phase.

The UHF apogee kick motor was considered to be a "rubber" engine; i.e., nominal values of specific impulse (Isp) and mass fraction (M. F.) were used for size estimation. In actuality there are existing motors of the Surveyor series which could likely be modified to satisfy the specific mission requirements, and although the performance would likely suffer with the usge of components originally designed for other applications, the cost reduction associated with using off-the-shelf hardware will likely justify this approach.

4.9.2 DESCRIPTION OF SELECTED SUBSYSTEMS

The design requirements for the VBMS propulsion subsystems are presented in Table 4.9-1.

Table 4.9-1. Propulsion Subsystem Design Requirements

Design Specification	HF	VHF No. 1	VHF No. 2	UHF
Orbital Altitude (nm) (Note 1)	4356	19323	7556	19323
Spacecraft Injected Weight (lb) (Note 5)	4870	2649	835	2641(Note 2)
Orbit Trim ΔV (fps)	18	39	75	130
Impulse for Attitude Control (lb-sec)	1000	1000	1000	1000
Station-keeping ΔV (fps)	NA	12	NA	10
Station Change ΔV (fps)	-	106(Note 3)	-	-
Apogee Kick ΔV (fps)	-	-	-	6150
Spin-Despin (rpm)	-	-	-	120(Note 4)

Notes

1. Circular, equatorial.
2. Into elliptical transfer orbit with synchronous orbit altitude.
3. 60 fps (99^{o}E, 135^{o}E); 46 fps (135^{o}E, 97^{o}W).
4. Spinup to 60 rpm and despin.
5. Includes booster adapter weight.

4.9.2.1 HF Propulsion

4.9.2.1.1 Launch Vehicle/Launch Sequence

a. Booster

The booster selected is the Titan IIIF/Stretched Transtage system which consists of the Titan III currently being developed for the MOL program (seven-segment 120 in. solid motors, stretched Stage I tankage, and expansion ratio change on the Stage I engines) plus a transtage with tankage volume modified to permit a 35,000 lb propellant loading. The increase in Transtage propellant load is required to permit full utilization of the lower stage performance potential. The payload capability into the selected orbit is in excess of 5000 lb compared to the actual weight of 4870 pounds.

b. Launch Sequence

The mission profile involves launch into a 100 nm parking orbit, Hohmann transfer to the desired 4356 nm altitude from the first equatorial crossing, followed by turn and injection into the desired circular equatorial orbit at apogee of the transfer orbit. The launch sequence of events is tabulated and shown schematically in Figure 4.9-1.

The ground trace of the ascent trajectory for establishing the HF (4.8 hr period) orbit is shown in Figure 4.9-2. A launch azimuth of 90 degrees is chosen. Since this orbit is not 24-hr synchronous, the longitude of injection is not particularly important, but rather the time of day is. In actual practice, the launch azimuth may be made to vary as a function of time into the launch window in order to obtain injection at the required local time of day. Thus, only the 90 degree launch azimuth ascent trajectory is shown. For launch azimuths less than 90 degrees, injection occurs a little farther to the east than shown in the figures; for launch azimuths greater than 90 degrees, to the west.

4.9.2.1.2 Vernier/Attitude Control Propulsion

A hydrazine engine with jet vanes will work in conjunction with a Mariner type autopilot. The system will be constant pressure-constant thrust and will have twelve 0.05 lb engines used for slow control and unloading manifolded to the same propellant tank. The schematic is shown in Figure 4.9-3, and weight is shown in Table 4.9-2. Orbit trim will initially be accomplished with the hydrazine engine. The final trim and orbit maintenance will be accomplished with a 400 micro-lb thrust cesium ion engine that weighs 15 lb and uses a maximum of 100 watts of power while operating.

4.9.2.2 VHF No. 1 Propulsion

4.9.2.2.1 Launch Vehicle/Launch Sequence

a. Booster

The selected booster is the Titan IIIF/Transtage as described for the HF configuration, but with the existing transtage in place of the "stretched" stage. The payload capability is 3200 lb compared to the 2649 lb design weight.

b. Launch Sequence

In order to achieve a synchronous orbit at 135°E longitude, five phases of the launch injection sequence of events were analyzed:

1. Boost
2. Parking Orbit
3. Transfer Orbit
4. Synchronous Orbit
5. Positioning

FOLDOUT FRAME 1

FOLDOUT FRAME 2

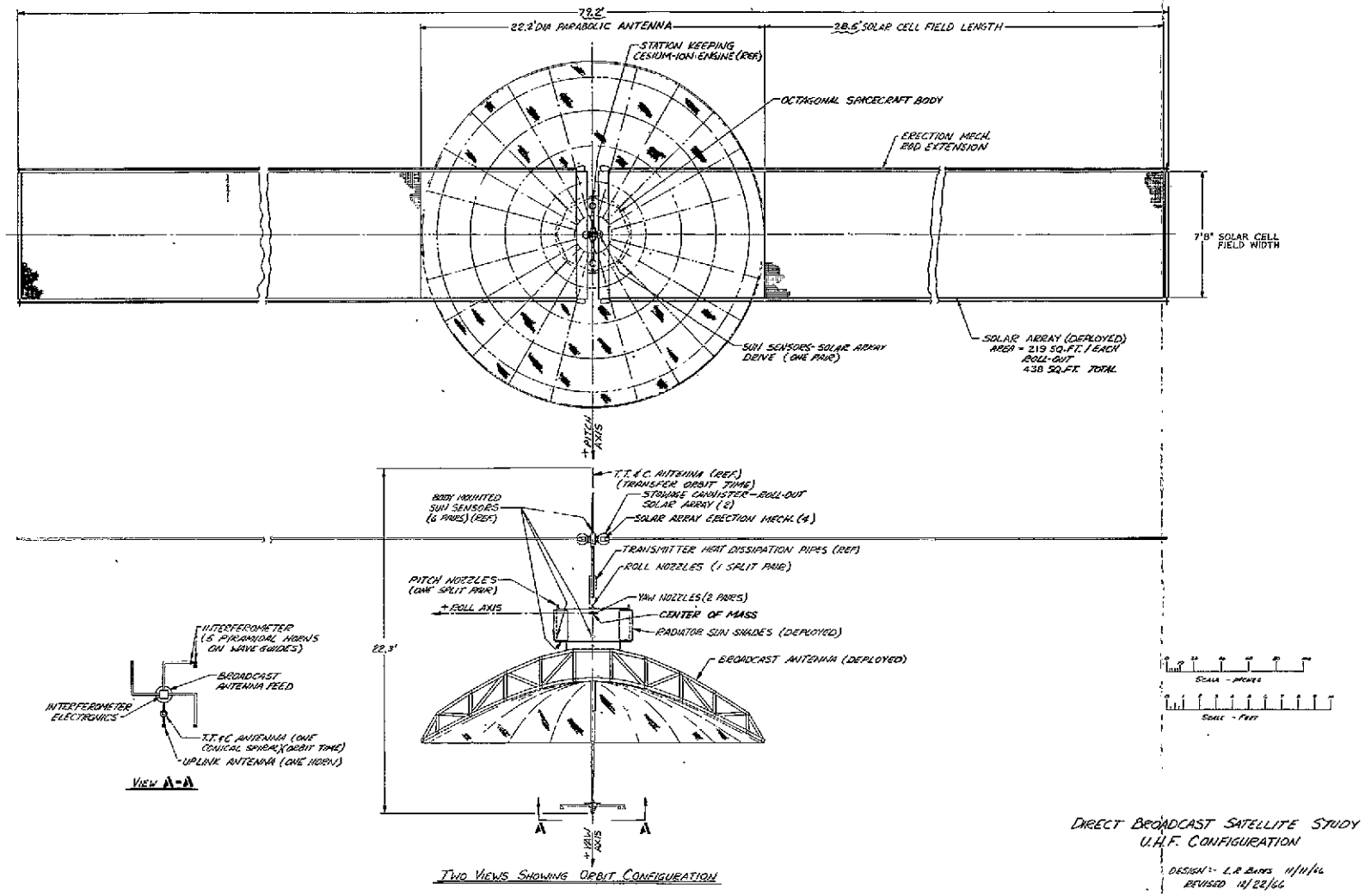

Two Views Showing Orbit Configuration

DIRECT BROADCAST SATELLITE STUDY
U.H.F. CONFIGURATION

DESIGN:- L.R. Bates 11/11/66
REVISED 12/22/66

Figure 5-13. UHF Orbital Configuration

FOLDOUT FRAME 1

FOLDOUT FRAME 2

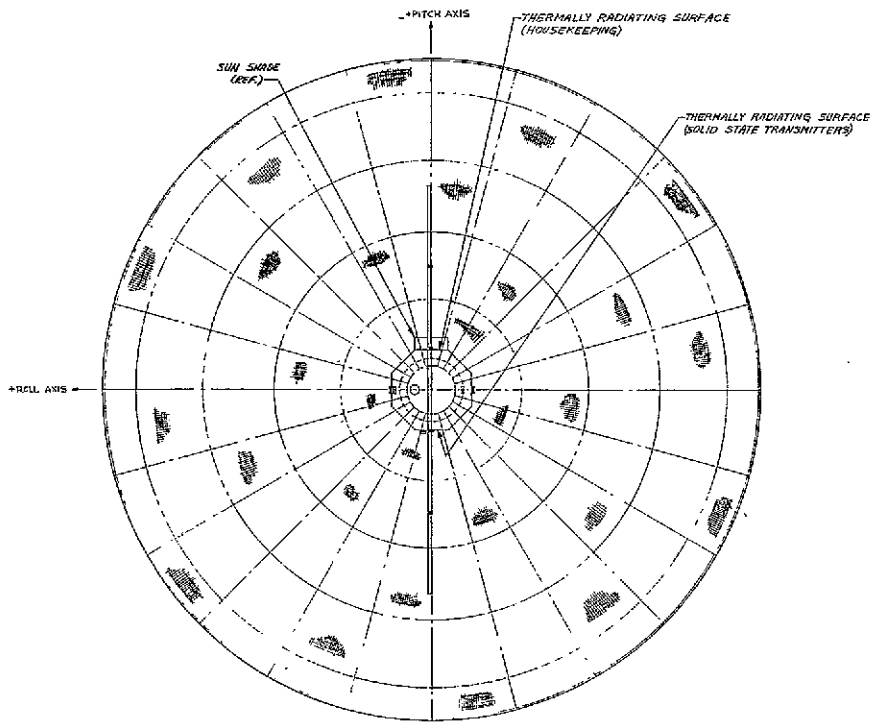

TWO VIEW ORBIT CONFIGURATION

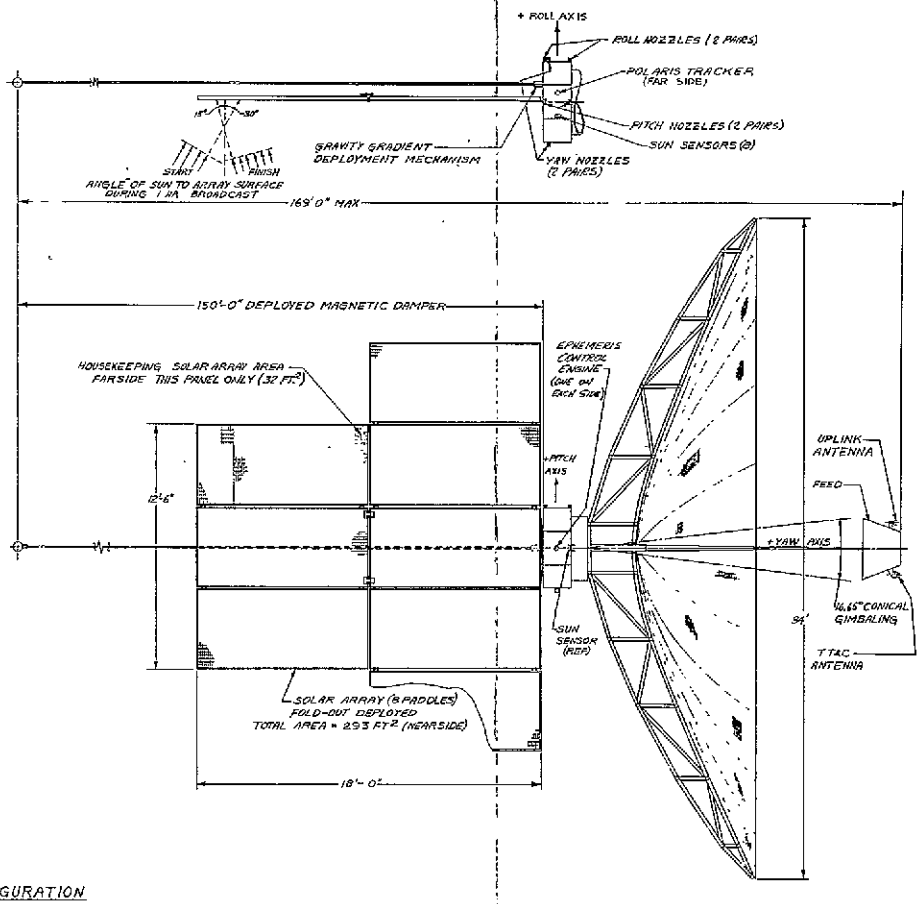

VHF #2 CONFIGURATION

DIRECT BROADCAST SATELLITE STUDY

SCALE: 1/20

Figure 5-10. VHF No. 2 Orbital Configuration

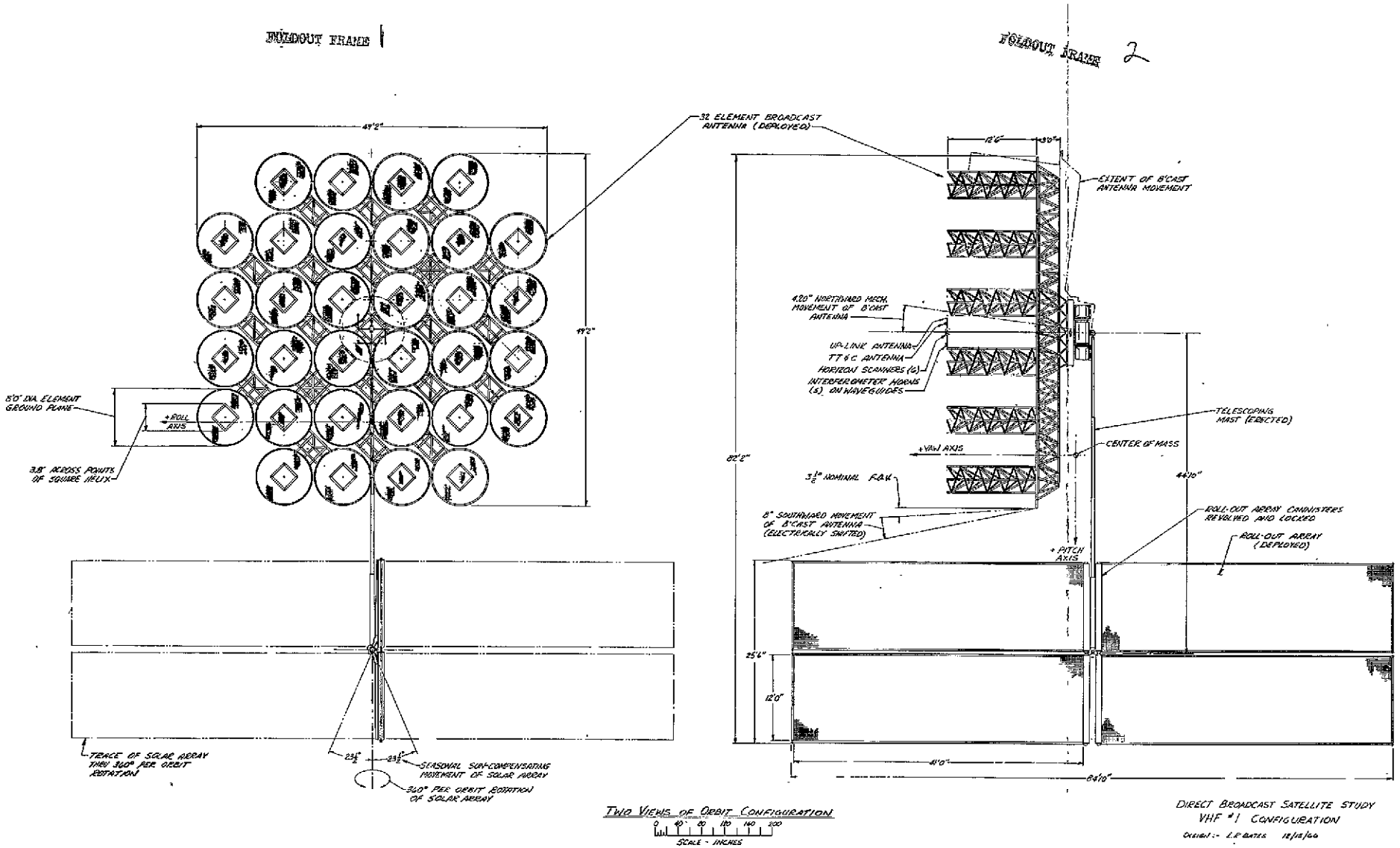

Figure 5-7. VHF No. 1 Orbital Configuration (Two-View)

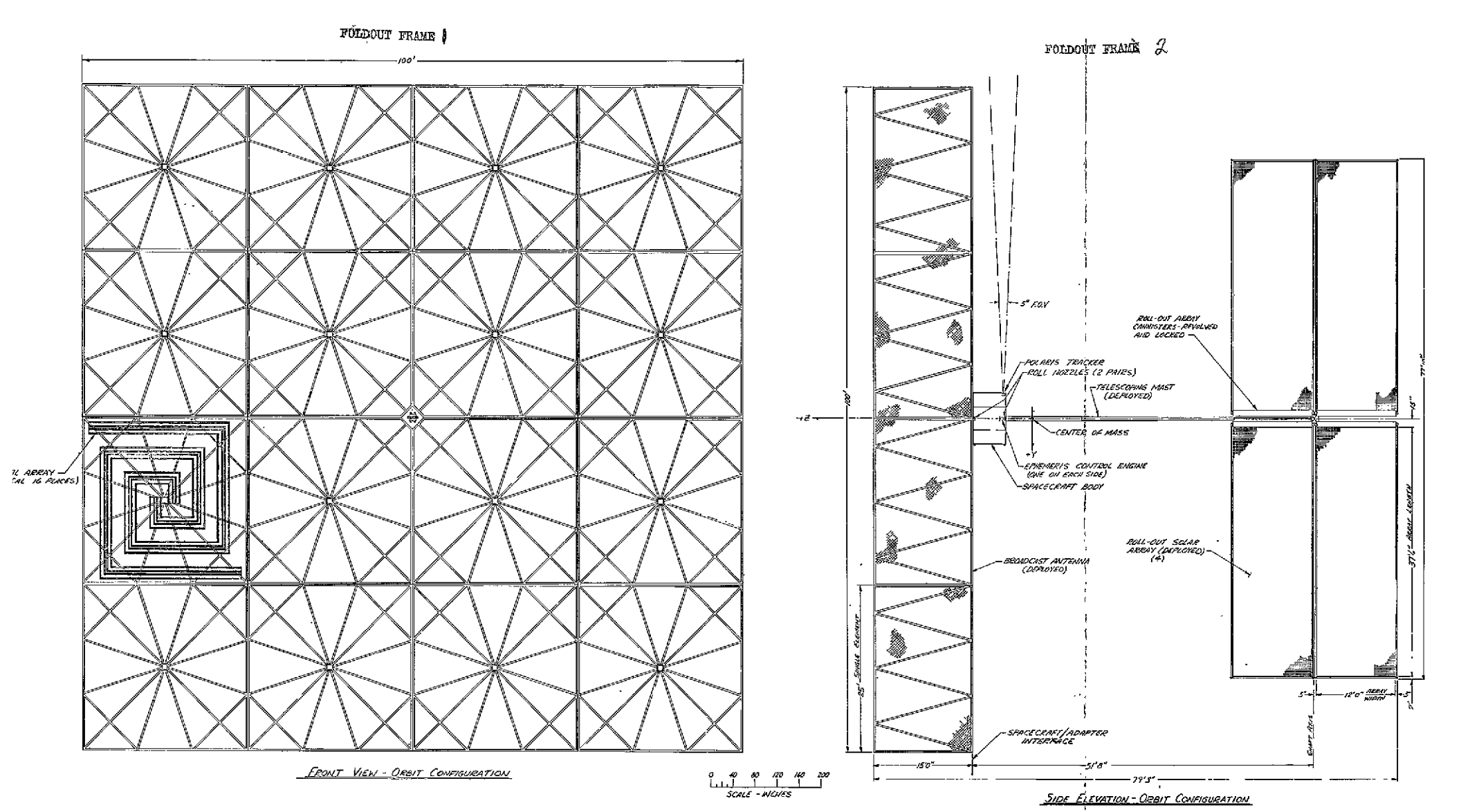

Figure 5-3. HF Orbital Configuration (Two-View)

FOLDOUT FRAME 1

FOLDOUT FRAME 2

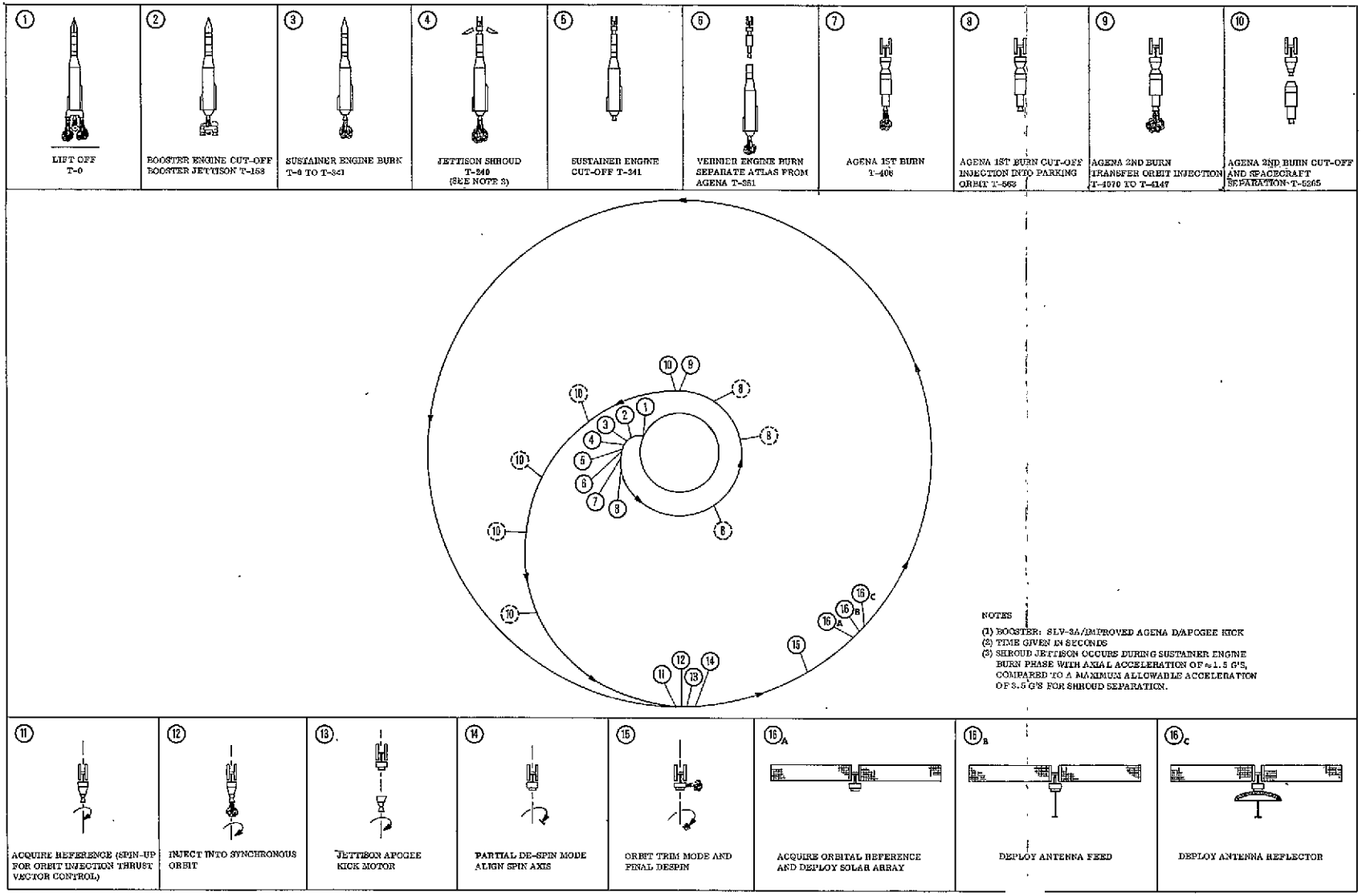

Figure 4.9-8. UHF Sequence of Flight Events

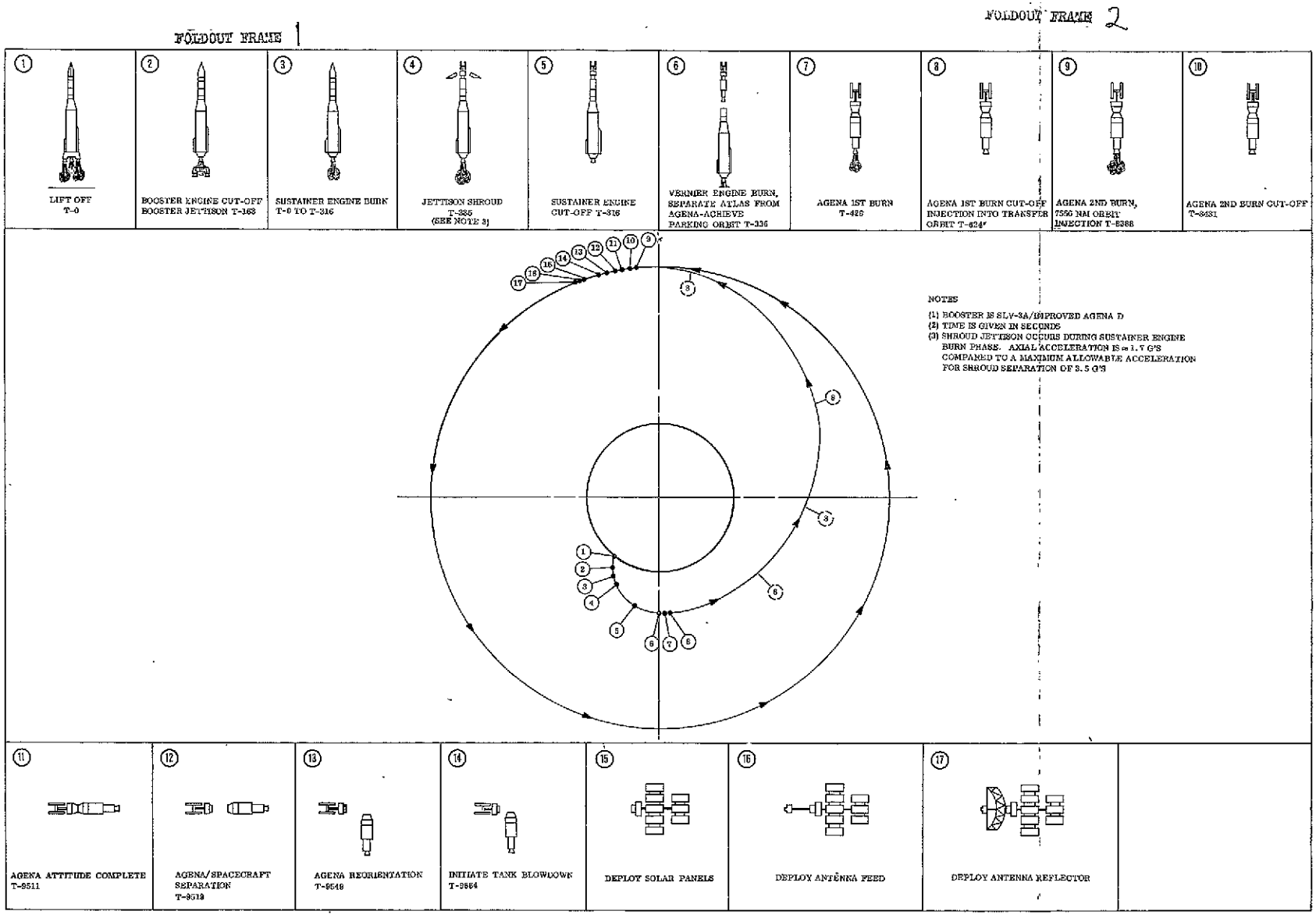

Figure 4.9-6. Sequence of Flight Events for VHF No. 2

FOLDOUT FRAME 1

FOLDOUT FRAME 2

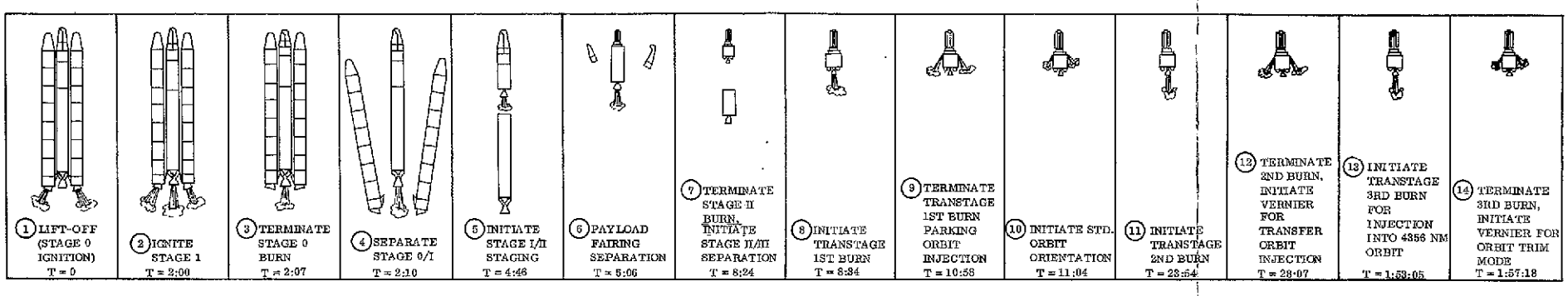

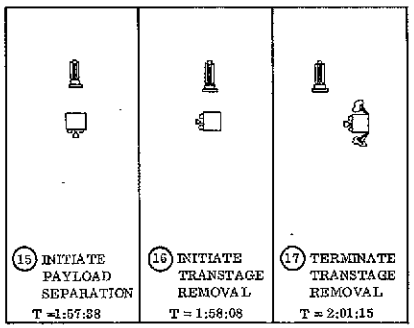

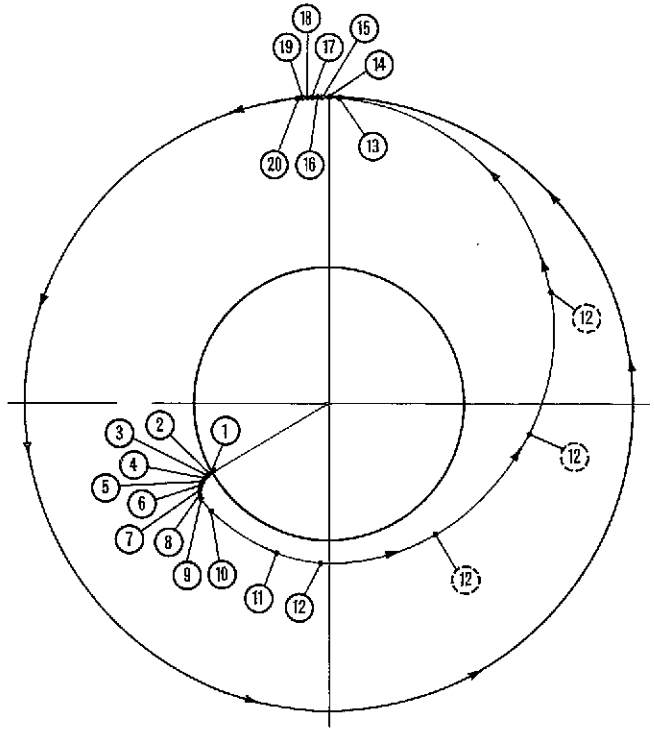

NOTES:

(1) BOOSTER IS TITAN IIIF/TRANSTAGE
(2) TIME GIVEN IN HR:MIN:SEC

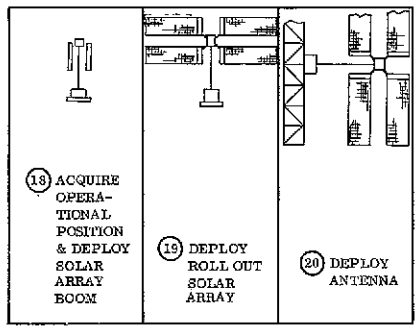

Figure 4.9-1. HF Sequence of Flight Events

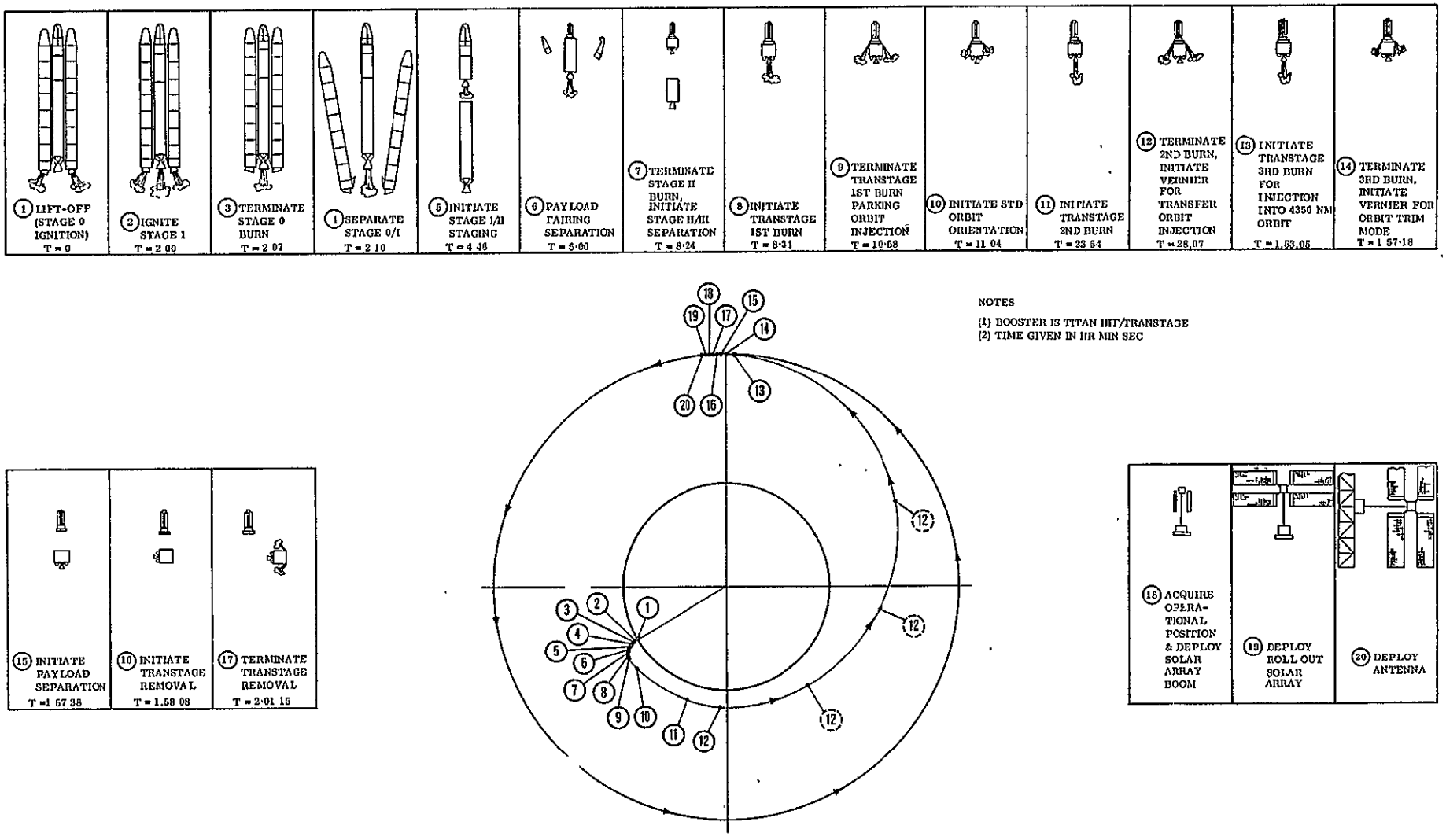

NOTES

(1) BOOSTER IS TITAN IIIC/TRANSTAGE
(2) TIME GIVEN IN HR MIN SEC

Figure 4.9-1. HF Sequence of Flight Events

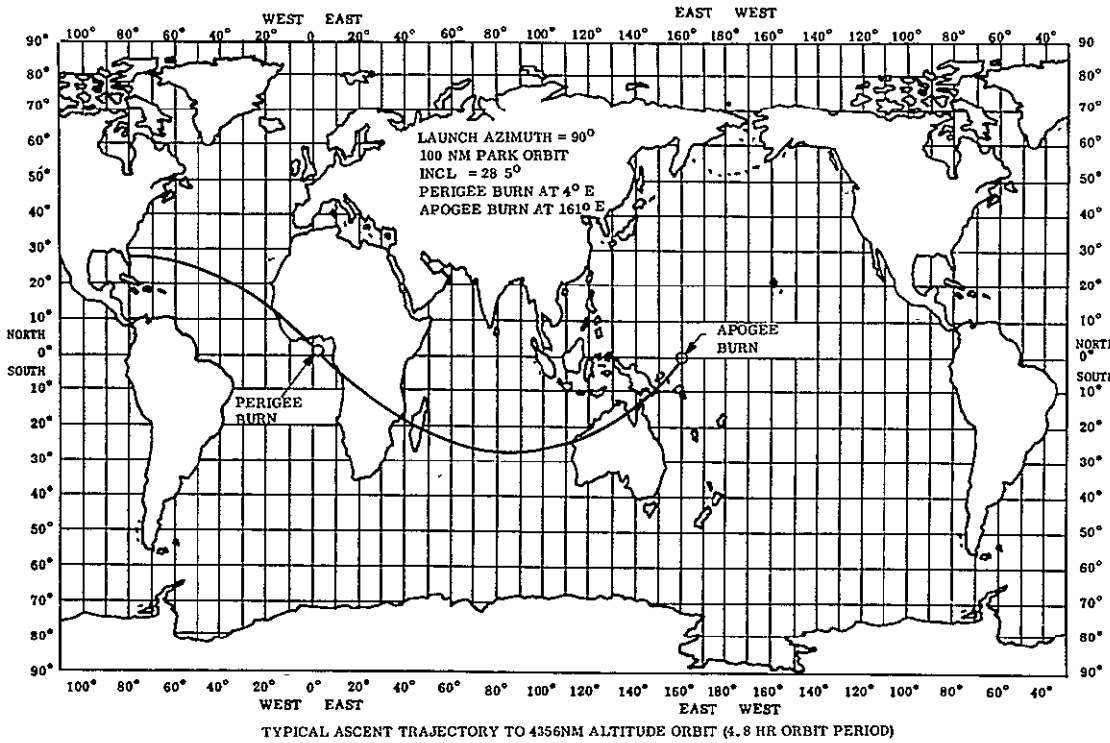

Figure 4.9-2. HF Trajectory Ground Trace

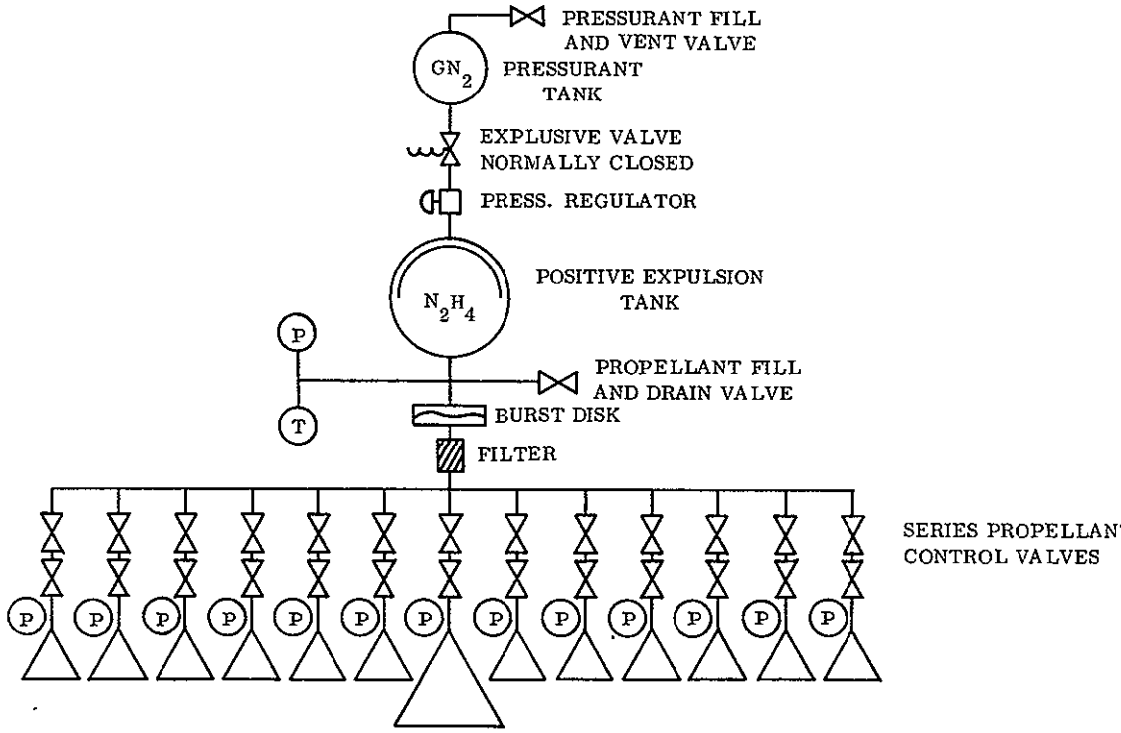

Figure 4.9-3. N_2H_4 Vernier and Attitude Control for HF

Table 4.9-2. HF Hydrazine Engine Weight Breakdown

Fill Valves 2 @ 0.22 lb	0.44 lb
Temp. Transducer 1 @ 0.4 lb	0.40
Press. Transducers 14 @ 0.38 lb	5.32
Exp. Value 1 @ 0.55 lb	0.55
Regulator 1 @ 1.2 lb	1.20
Burst Disk & Filter 1 @ 0.5 lb	0.50
0.05 lbf Reactor w/valve 12 @ 1.25 lb	15.00
0.50 lbf Reactor w/valve	2.50
Jet Vane Actuators	2.50
Pressurant Tank	1.60
Propellant Tank	6.50
	36.51
Tubing & Brackets (15%)	5.48
N_2 Pressurant	0.75
Hydrazine	16.00
Total	58.74 lb

The Titan IIIF booster is launched at a flight path azimuth of 90 degrees and injected into a 90 nm parking orbit at longitude 64.1°W and latitude 27.1°N. The spacecraft coasts in the parking orbit until the first southerly crossing of the equator of 9°W, at which time the transtage first burn occurs injecting the system into the elliptical transfer orbit. The apogee of the transfer orbit, at synchronous altitude of 19,323 nm, is reached at longitude 103°E, at which time the second Transtage burn is effected to circularize the orbit and remove the inclination. The sequential launch events are shown in Figure 4.9-4 and the ground trace is shown in Figure 4.9-5.

It is now necessary to position the spacecraft at 135°E longitude; i.e., the spacecraft must be moved from 103°E to 135°E, an angular deplacement of 32 degrees. Depending on the time required to move the spacecraft, the ΔV requirements will vary. For each degree/day that the spacecraft is to drift, a ΔV of 10 ft/sec is needed to initiate the drift, and a ΔV of 10 ft/sec is needed to stop the drift. Consequently, the approximate time required for positioning the spacecraft with the alloted $\Delta V = 60$ fps (which is a drift rate of 3 degrees/day) is 11 days.

4.9.2.2.2 Vernier/Attitude Control/Station-keeping Propulsion

A system identical to that for HF will be used (Figure 4.9-3). Tank size and total weight of hydrazine are different. The system weight breakdown is given in Table 4.9-3. The station-keeping will be performed with a 400 micro-lb thrust cesium ion engine system weighing 15 lb and using 100 watts while operating.

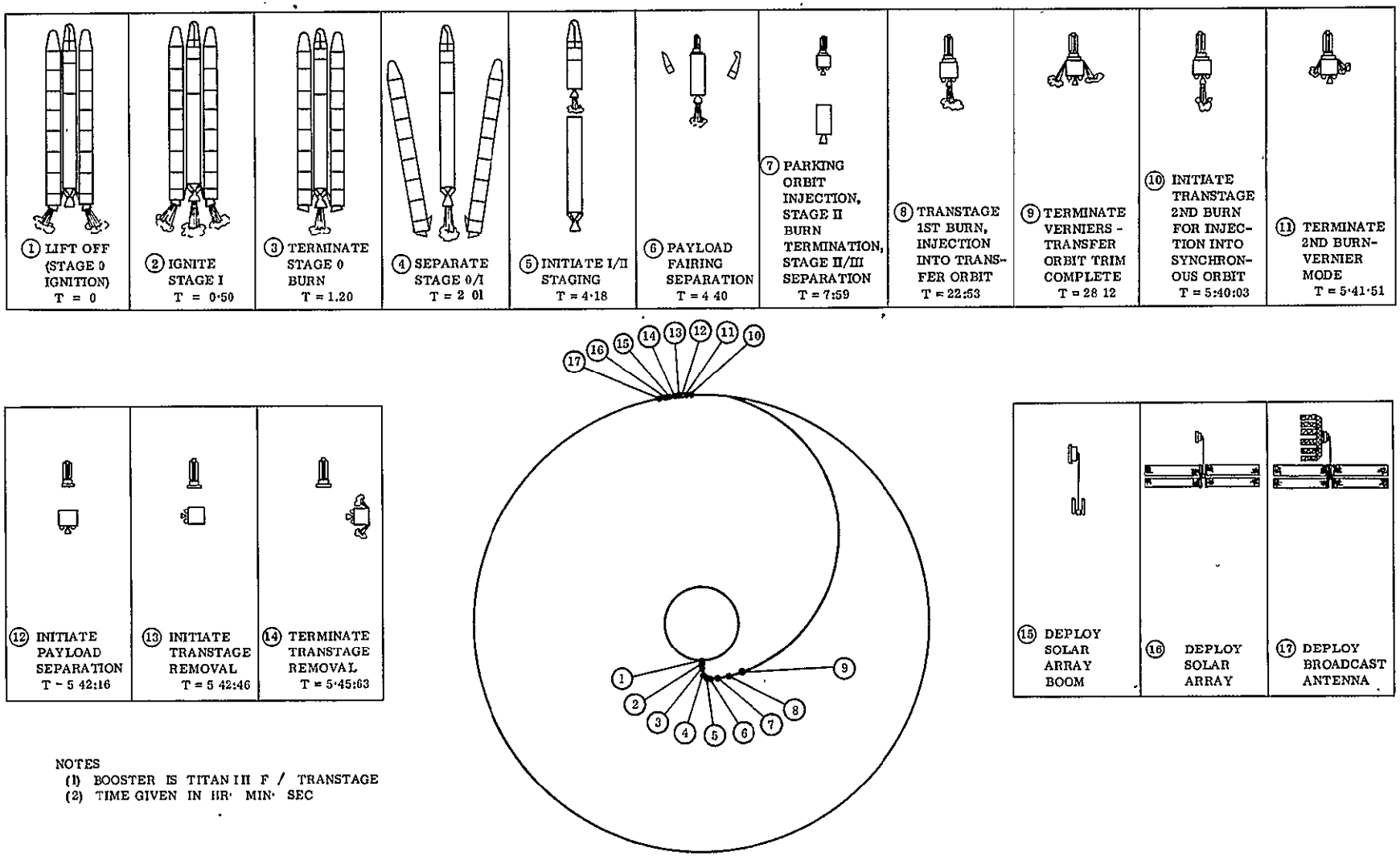

Figure 4.9-4. Sequence of Flight Events Liftoff to Orbit (VHF No. 1)

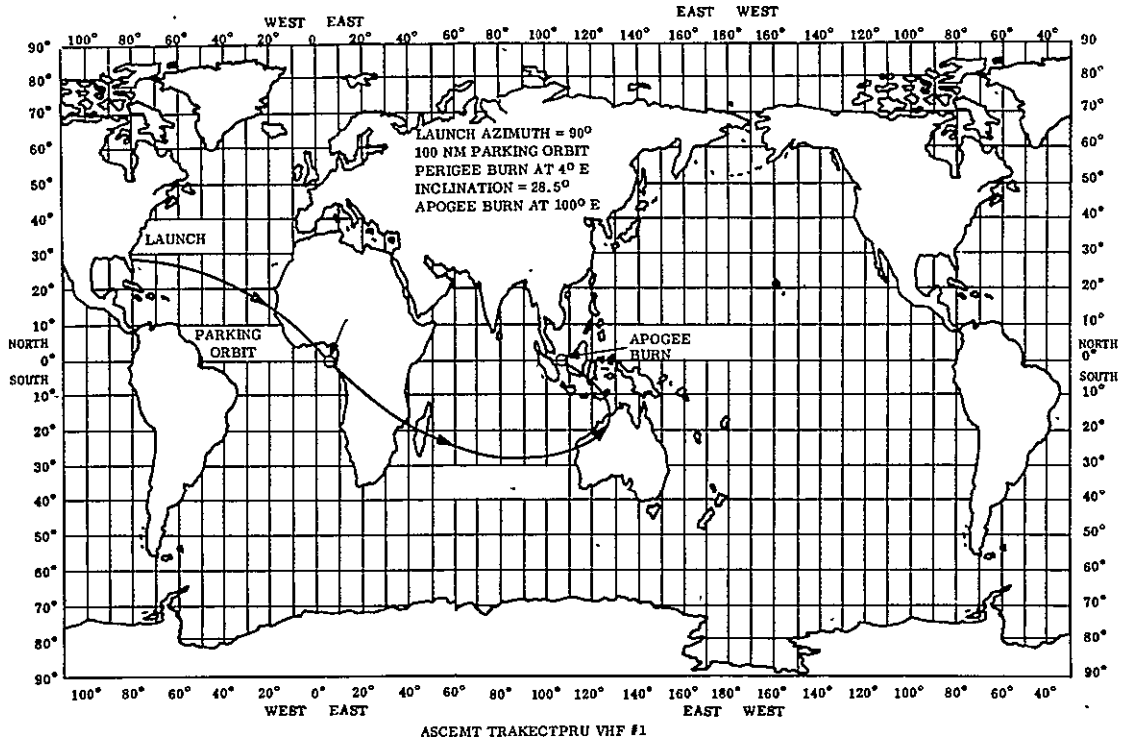

Figure 4.9-5. VHF No. 1 Trajectory Ground Trace

Table 4.9-3. VHF No. 1 Hydrazine Engine Weight Breakdown

Fill valves 2 @ 0.22 lb	0.44 lb
Temp. Transducers 1 @ 0.4 lb	0.40
Press. Transducers 14 @ 0.38 lb	5.32
Exp. Valve 1 @ 0.55 lb	0.55
Regulator 1 @ 1.2 lb	1.20
Burst Disk & Filter 1 @ 0.5 lb	0.50
0.5 lbf Reactor w/valves 12 @ 1.25 lb	15.00
50 lbf Reactor w/valve	2.50
Jet Vane Actuator	2.50
Pressurant Tank	1.60
Propellant Tank	13.00
	43.01
Tubing and Brackets (15%)	6.45
N_2 Pressurant	1.50
Hydrazine	45.00
Total	95.96

4.9.2.3 VHF No. 2 Propulsion

4.9.2.3.1 Launch Vehicle/Launch Injection

a. Booster

The booster selected for the VHF No. 2 configuration is the SLV-3A/Improved Agena D, which has an estimated payload capability of 800 lb as compared to a payload requirement of 835 lb. This payload deficiency may require the addition of an apogee kick motor which would increase the cost somewhat and create potential shroud volume problems. The decision was made to assume booster performance improvement or spacecraft weight reduction, rather than select an apogee kick motor at this time.

b. Launch Sequence

The launch sequence of events is shown in Figure 4.9-6. The comments made about the HF trajectory longitude and time of day of launch are also applicable to the VHF No. 2 since it is also a subsynchronous orbit (8-hr period). The ground trace of the trajectory is shown in Figure 4.9-7.

4.9.2.3.2 VHF No. 2 Vernier/Attitude Control/Orbit Maintenance Propulsion

A propulsion system for the Vernier/Attitude Control function similar to that of the HF Satellite was selected (Figure 4.9-3). The only change is tank size and propellant weight. System weights are presented in Table 4.9-4. Orbit maintenance will be performed with a 40 micro-lb cesium ion engine weighing 14 lb and using 30 watts when operating.

4.9.2.4 UHF Propulsion

4.9.2.4.1 Launch Vehicle/Launch Injection

a. Booster

The booster selected for the UHF configuration was an SLV-3A/Improved Agena D, which has a payload capability of 2850 lb into an elliptical transfer orbit with synchronous altitude apogee as compared to the satellite launch weight of 2641 pounds. Of the 2641 lb, 1515 lb are allocated to an apogee kick motor and adapters, resulting in a net satellite orbital weight of 1126 pounds. If the full capability of the booster were used, the net satellite orbital weight could increase to 1235 lb for a margin of 109 pounds.

b. Launch Sequence

The launch sequence of events is shown in Figure 4.9-8, and the ascent trajectory ground trace is shown in Figure 4.9-9.

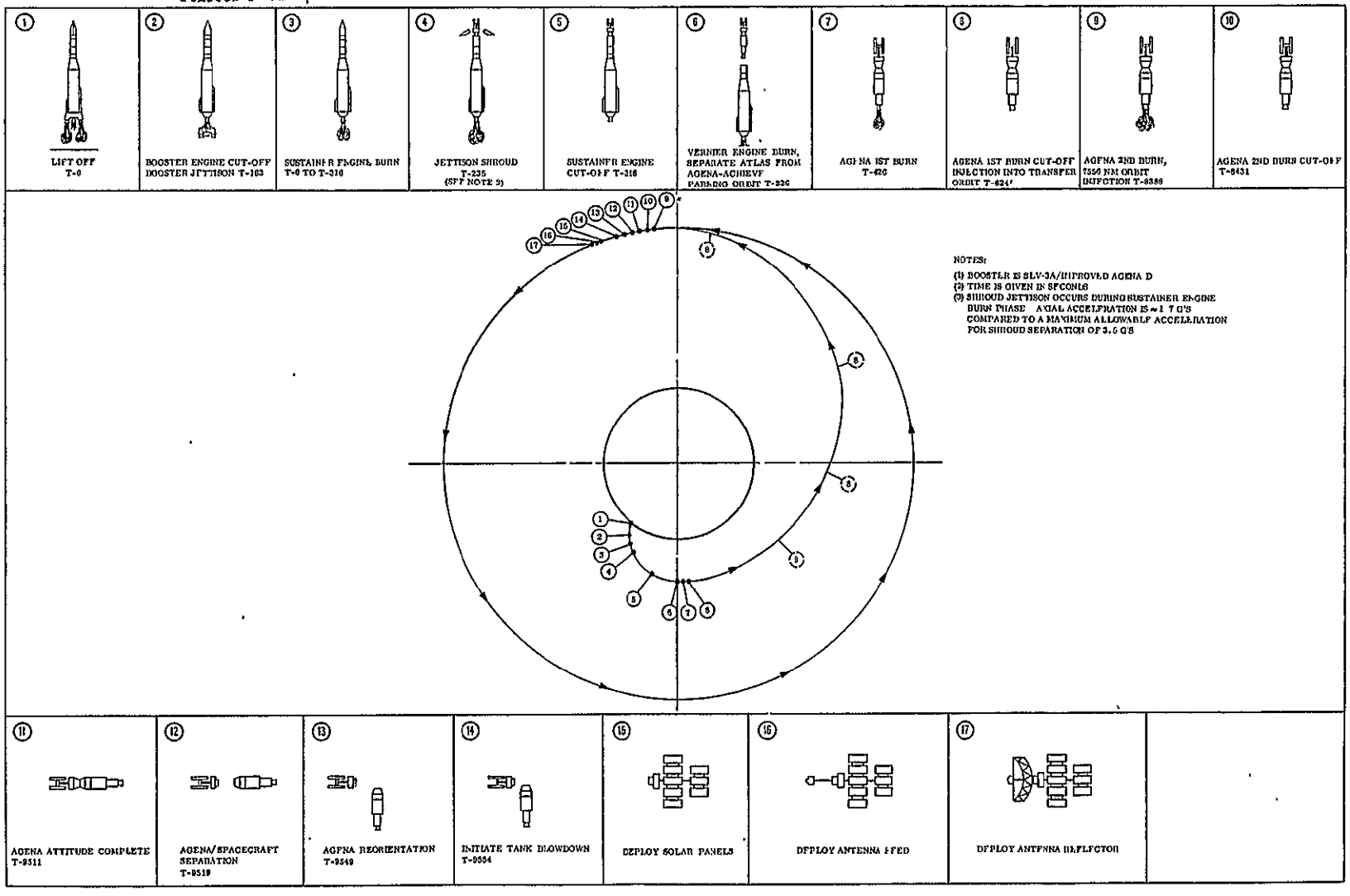

Figure 4.9-6. Sequence of Flight Events for VIIF No. 2

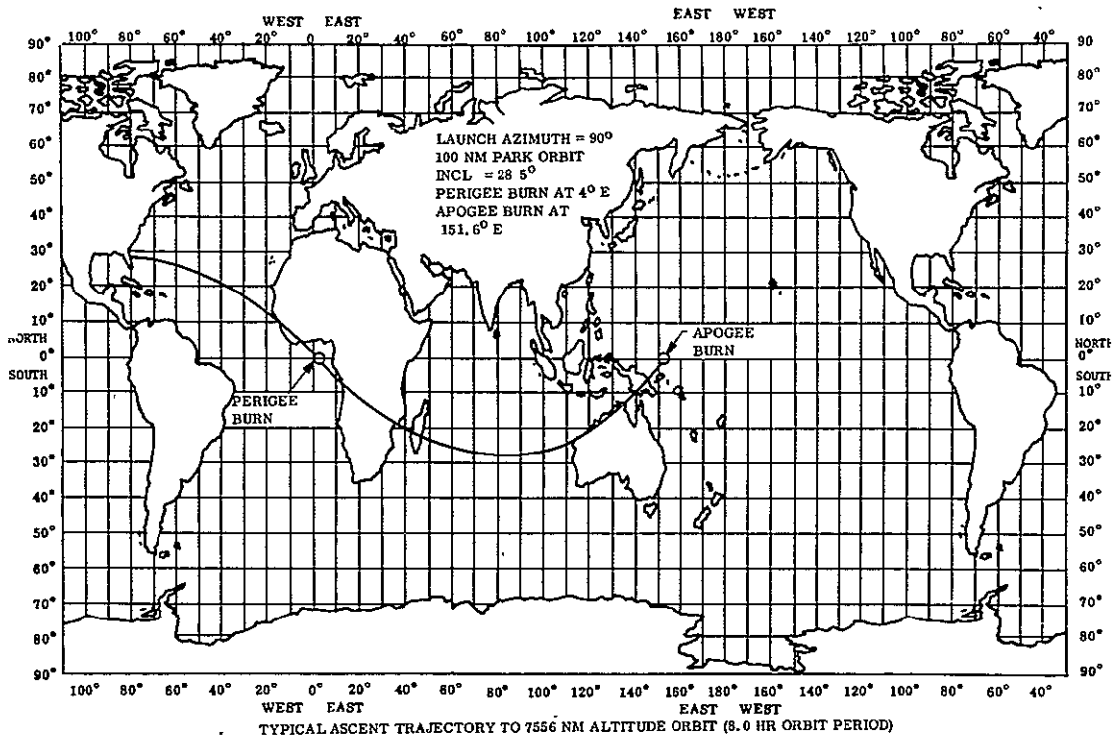

Figure 4.9-7. VHF No. 2 Trajectory Ground Trace

Table 4.9-4. VHF No. 2 Hydrazine Engine Weight Breakdown

Fill Valve 2 @ 0.22 lb	0.44 lb
Temp. Transducer 1 @ 0.4 lb	0.40
Press. Transducers 14 @ 0.38 lb	5.32
Exp. Valve 1 @ 0.55 lb	0.55
Regulator 1 @ 1.2 lb	1.20
Burst Disk & Filter 1 @ 0.5 lb	0.50
0.05 lbf Reactor w/valve 12 @ 1.25 lb	15.00
50 lbf Reactor w/valve	2.50
Jet Vane Actuators	2.50
Pressurant Tank	1.60
Propellant Tank	6.50
	36.51
Tubing & Brackets (15%)	5.48
N_2 Pressurant	0.75
Hydrazine	15.50
Total	58.24 lb

FOLDOUT FRAME 1

FOLDOUT FRAME 2

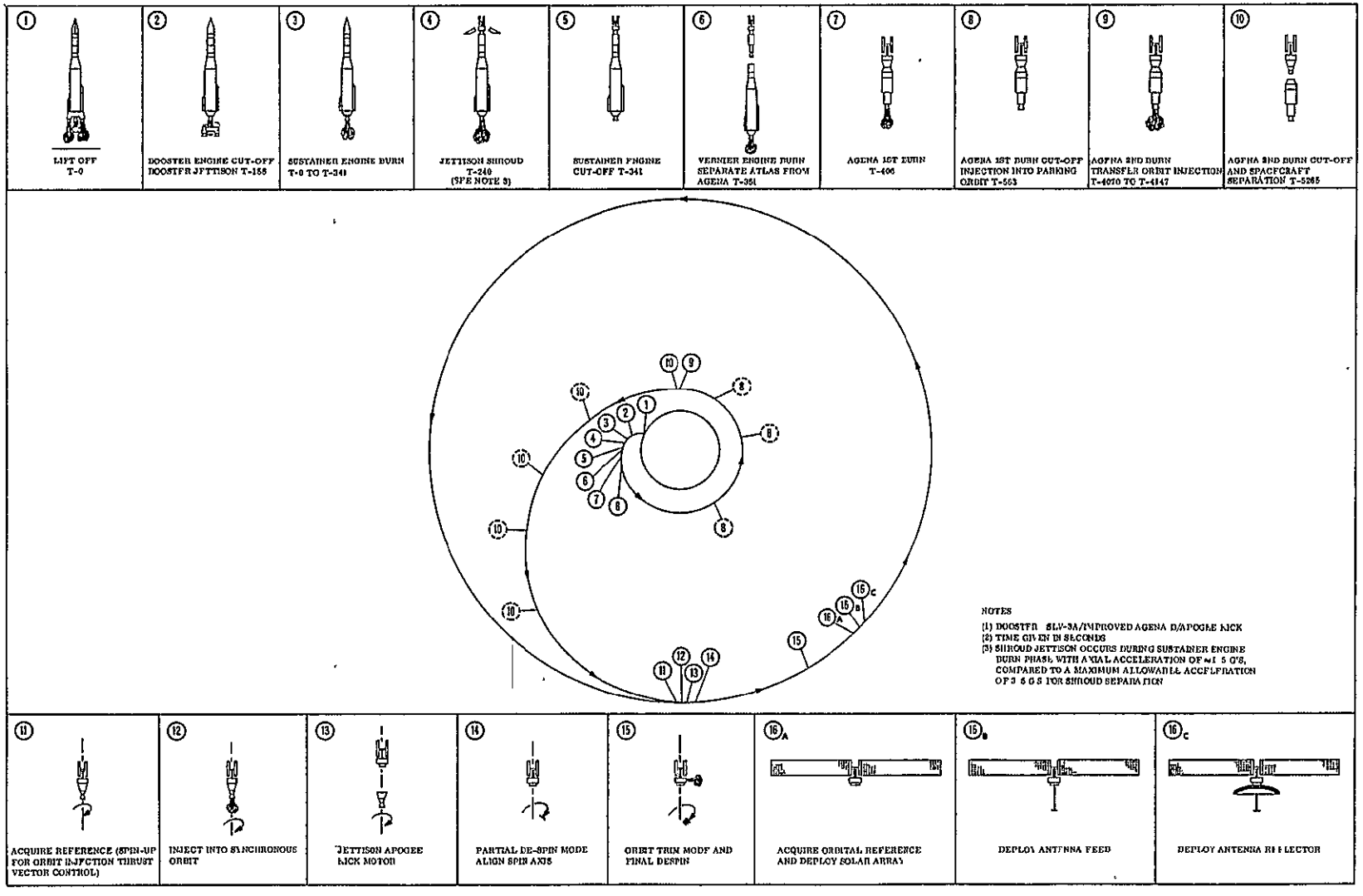

Figure 4.9-8. UHF Sequence of Flight Events

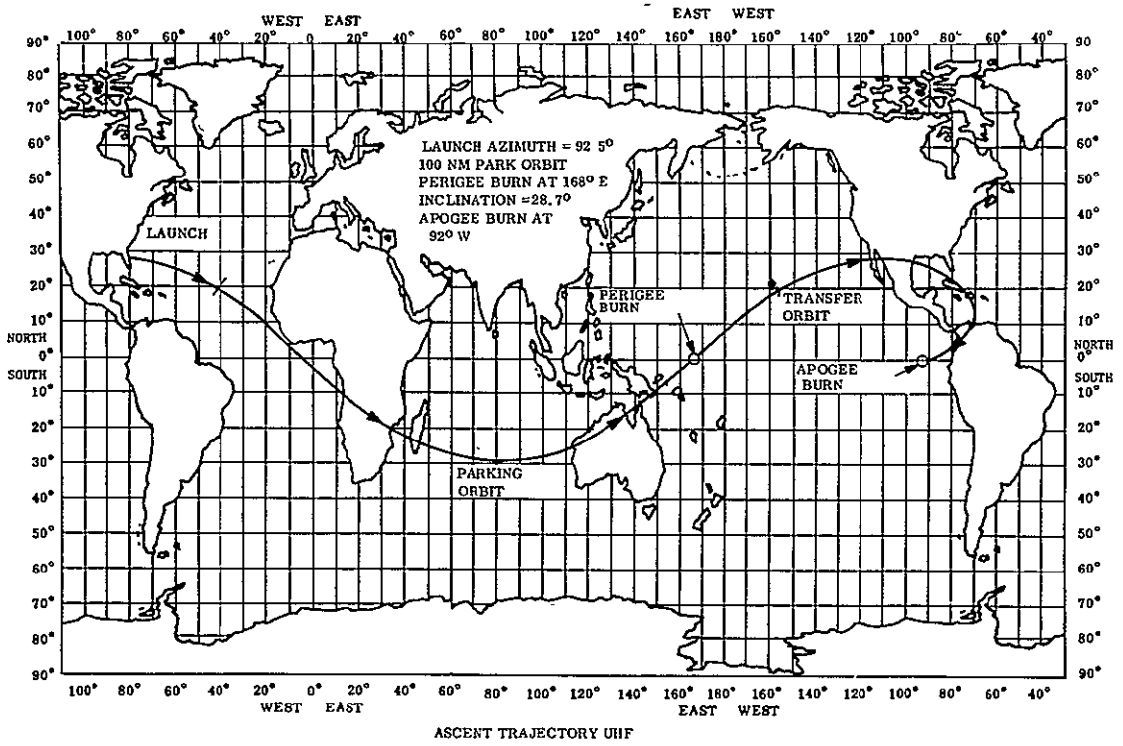

Figure 4.9-9. UHF Ascent Trajectory

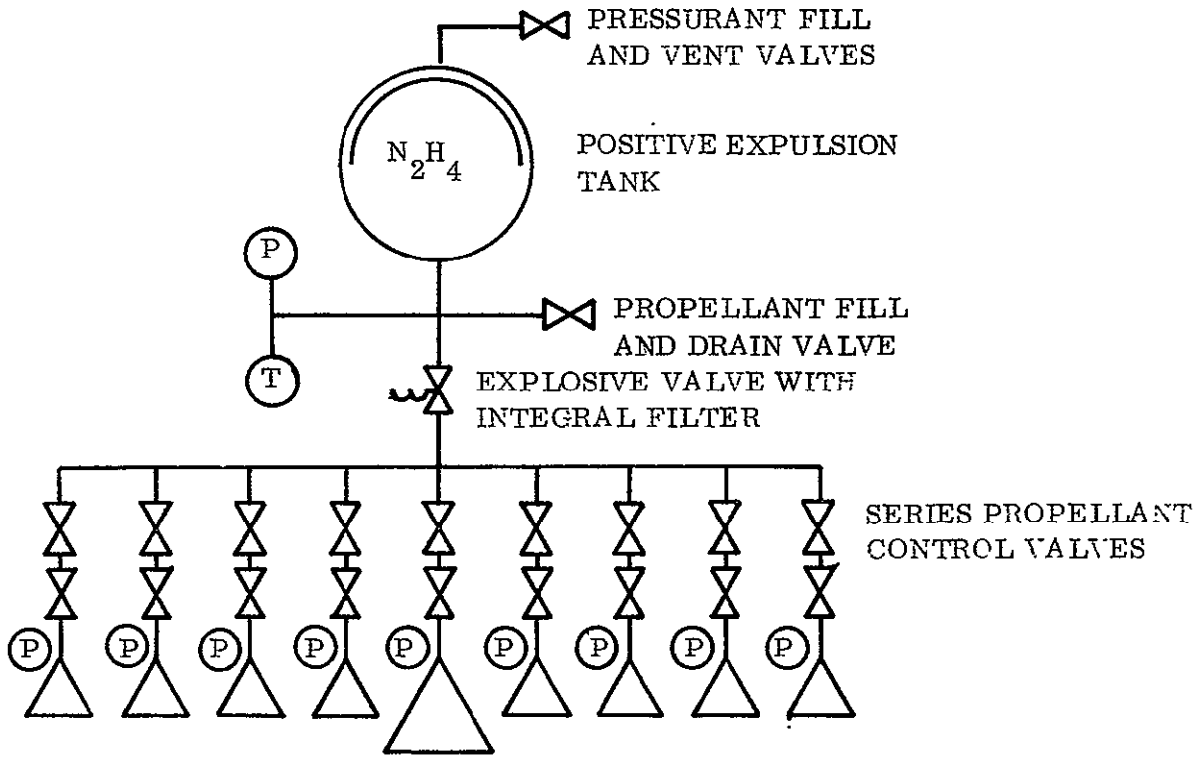

Figure 4.9-10. N_2H_4 Vernier and Attitude Control for UHF

4.9.2.4.2 Vernier/Attitude Control/Stationkeeping Propulsion

A 5 lb thrust hydrazine engine is used for vernier correction and an assemblage of eight one pound engines are used for despin, precession control and wheel unloading. For added reliability the system operates in a blowdown mode, reducing the number of components needed for the system. The schematic is shown in Figure 4.9-10 and the weight of components is given in Table 4.9-5. A 50 micro-lb cesium ion engine weighing 11 lb and using 30 watts power will accomplish station-keeping.

Table 4.9-5. UHF Hydrazine Engine Weight Breakdown

Fill Valves 2 @ 0.22 lb	0.44 lb
Temp. Transducers 1 @ 0.4 lb	0.40
Press. Transducers 10 @ 0.38 lb	3.80
Exp. Valve w/filter 1 @ 0.55 lb	0.55
1 lbf Reactor w/control valves 8 @ 2.0 lb	16.00
5 lbf Reactor w/control valves 1 @ 3.5 lb	3.50
Propellant Tank	7.00
	31.69
Tubing and Brackets (15%)	4.76
N_2 Pressurant	1.00
Hydrazine	31.50
Total	68.95 lb

4.9.3 PROPULSION TECHNOLOGY

4.9.3.1 Candidate Boosters

4.9.3.1.1 Boosters and Apogee Motors

Payload capability data for the Atlas/Agena, Atlas/Centaur, Titan and Saturn family of boosters is presented in Table 4.9-6 for those orbits that were of interest for the Voice Broadcast Mission Study (VBMS). The data in the upper half of the table gives payload capabilities for direct injection from ETR to the specified circular orbit altitude. In the lower half of the table, the use of apogee kick motors is investigated. (The number above the slash is the transfer orbit payload of the launch vehicle, while the number under the slash is the useful circular orbit payload which does not include rocket motor inert weight or propellant.)

a. Titan Family

Payload weights were supplied by the Martin Company specifically for the VBMS. Values are $\pm$ 5 percent accurate. All members of the Titan family listed will be operational by 1969.

Atlas Family

Data was provided by GD/A for the VBMS. Atlas SLV-3X boosters are at about 50 percent probability of funding to fly by 1969. Other family members are already funded. The Agena launch vehicles all assume a 5-ft diameter shroud. Use of the OAO shroud will result in lower payload numbers by a few hundred pounds in the transfer orbit. Payload weights are 3 σ numbers for direct injection and elliptical orbit capabilities. Apogee kick payload capabilities have been calculated using the following calculations:

W_1 = elliptical orbit payload supplies by GD/A (-3σ)

W_2 = weight of S/C after apogee burn

$W_1 - W_2$ = propellant expended

$$W_m = \frac{W_1 - W_2}{MF} = \text{weight of motor}$$

where MF = propellant mass fraction (ratio of usable propellant to total motor weight)

$W_1 - W_m$ = useful payload

$$\Delta V = g\, I_{sp} \ln \frac{W_1}{W_2} .$$

The ΔV is the velocity increment required to circularize a 28.5 degree inclined orbit or to circularize and dogleg the orbit into the equatorial plane (0 degree inclination). Apogee motor characteristics assume state-of-the-art performance (I_{sp} = 290 sec, MF = 0.90), ΔV data is included in Table 4.9-7.

c. Saturn Family

Data from the Saturn handbooks published by Douglas Aircraft was used. Note that the S-I is severely limited in circular orbit capability for these orbits because it has no long burn, multiple restart upper stage. Addition of the Centaur results in significant payload capability for each orbit.

d. Apogee Motors

It is unlikely that an existing apogee motor will be optimum for the orbit and launch vehicle selected in the VBMS. It is impossible to study each of the more than 100 apogee kick possibilities still in the program at this time. Therefore, the use of a set of motor characteristics (I_{sp} = 290; MF = 0.90) will provide payload capability consistent with state-of-the-art, but cost of the motor cannot be evaluated

Foldout FRAME 1

ORBIT ALT. (nm) ↑ / BOOSTER / ORBIT INCLINATION (°) →	TITAN FAMILY (± 5% Numbers)										
	T3A			T3C			SLV-3/Agena			SLV-3/	
	0	30	90	0	30	90	0	30	90	0	3
200/7000	—	1580		—	14060		—	2940	(5)	—	345
200/14900	—	350		—	8500		—	2110	(5)	—	251
4700				3250	7600		640	1870	1250(2)	80	225
5600				3050	6620		590	1620	1010(2)	840	197
6600			(5)	2880	5780	(5)	540	1400	(5)	780	173
7500	(4)	(4)		2720	5740		500	1250	(5)	740	157
10200				2390	4190		420	960	(5)	640	122
10900				2300	3880		400	900	470(2)	620	118
19300				1850	2750		290	580	—	490	800
4700							/1820	3590/2398	—	/1425	418
5600							/1195	3340/2061	—	/1390	389
6600							/1152	3110/1860	—	/1235	363
7500							/1125	2930/1718	—	/1327	348
10200							/1085	2620/1979	—	/1272	308
10900							/1057	2500/1401	—	/1235	294
19300							/931	1980/1091	—	/1118	238

Notes:

(1) Table can be read as follows:

(a) Direct Injection - payload into specified orbit resulting from direct injection launch from ETR.

(b) Indirect Injection - the number to the left of slash is the payload injected from a 100 n.m. parking orbit into an elliptical transfer orbit of inclination = 28.5° with apogee at the circular orbit altitude. The number to the right of the slash is the net payload after circularization and inclination change by an apogee kick motor which has an Isp = 290 seconds and a propellant mass fraction of 0.90.

(2) 160° Launch Azimuth, Atlas Dogleg, Violates R. Range Safety.

(3) Centaur Two Burn Limit

(4) Less than 200 lb

(5) Range safety restriction

(6) Centaur two burn limit restrict

(7) Payload capability zero at 500 l

(8) Status in 1969-72 uncertain

Fallout FRAME 2

ATLAS FAMILY (3 σ Numbers)

Agena	SLV-3X/Agena (8)			SLV-3C/Cent. (3)			SLV-3X/Cent.		
90	0	30	90	0	30	90	0	30	90
(5)	—	4350	(5)	—	5550	(5)	—	6960/5	(5)
(5)	—	3200	(5)	—	4280	(5)	—	5470/5	(5)
1540(2)	1240	2380	2100(2)	—	—	—	—	—	—
1320(2)	1200	2540	1810(2)	—	—	—	—	—	—
(5)	1130	2240	(5)	—	—	—	—	—	—
					Note(6)			Note(6)	
(5)	1080	2050	(5)	—	—	—	—	—	—
(5)	960	1680	(5)	—	—	—	—	—	—
690(2)	940	1600	1040(2)	—	—	—	—	—	—
(5)	800	1170	(5)	—	—	—	—	—	—
662 —	/1760	5190/3300	—	/2370	6950/4430	5600(2)/3568	/2930	8620/5485	7270(2)/4635
395 —	/1745	4890/3015	—	/2350	6560/4045	5210(2)/3215	/2925	8170/5040	6320(2)/4200
172 —	/1685	4560/2725	—	/2300	6210/3710	—	/2880	7780/4640	—
027 —	/1670	4350/2545	—	/2260	5950/3600	—	/2860	7450/4360	—
740 —	/1615	3890/2202	—	/2225	5370/3030	—	/2815	6770/3825	—
547 —	/1567	3920/2087	—	/2205	5250/2940	4150(2)/2320	/2780	6600/3910	5500(2)/3095
312 —	/1437	3060/1686	—	/2175	4410/2420	—	/2650	5640/3100	—

apability of this system

altitude

Foldout Frame 3

Table 4.9-6. Summary of Candidate Booster Payload Capabilities

SATURN FAMILY									
SIB			SIB/Centaur(3), (8)			SATURN V			
0	30	90	0	30	90	0	30	90	
	9000		—	20000	—	—	155000	—	
	2500		—	15000	—	—	130000	—	
—	—	—	—	16000	—	—	122000	—	
—	—	—	—	15000	—	—	110000	—	
—	—	—	—	14000	—	—	100000	—	
	Note(7)								
—	—	—	—	13500	—	—	95000	—	
—	—	—	—	11500	—	—	88000	—	
—	—	—	—	11000	—	—	85000	—	DIRECT INJECTION
—	—	—	—	9000	—	62000	72000	—	
/5450	16000/10180	—	/8170	24000/15270	—	/63100	185000/117600	—	
/5010	14000/8630	—	/8250	23000/14160	—	/63200	176000/108400	—	INDIRECT INJECTION
/4620	13000/7780	—	/8170	22000/13160	—	/62200	168000/96000	—	
/4500	11700/6860	—	/8250	21500/12600	—	/62900	164000/96000	—	
/3120	9000/5080	—	/8100	19500/11000	—	/63000	152000/85900	—	
/3570	8500/4760	—	/8000	19000/10580	—	/61500	146000/81800	—	
/1173	2500/1375	—	/7050	15000/8250	—	/62000	132000/72500	—	

at the present time. If the size of a given motor is of interest, the total impulse may be calculated by

I_{tot} = 261 (Elliptical P/L - Useful P/L),

d a search made for existing or anticipated motors of this size.

Table 4.9-7. Apogee Velocity Requirements

Final Altitude	Inclination (Notes 1&2) (deg)	ΔV_2 (fps)	W_1/W_2 (Note 3)
4700	28.5	3700	1.487
	0	8400	2.46
5600	28.5	3950	1.527
	0	8050	2.37
6600	28.5	4200	1.568
	0	7800	2.305
7500	28.5	4350	1.594
	0	7550	2.245
10200	28.5	4650	1.645
	0	7000	2.115
10900	28.5	4710	1.655
	0	6880	2.090
19300	28.5	4850	1.680
	0	6050	1.912

Notes
1. 0 degree inclination represents 28.5° dogleg
2. 28.5 degree inclination represents 0 dogleg
3. Apogee Motor I_{sp} = 290; mass fraction = 0.90

4.9.3.1.2 Alternate Boosters for HF Configuration

Additional consideration of the booster for the HF configuration was undertaken when it became evident that the status of the initially recommended launch vehicle (Titan 3F/Stretched Transtage) was uncertain for the 1972 time period. The possible forcing programs for the development of the enlarged Transtage were considered, as were various other candidate launch vehicles. Payload into synchronous equatorial orbit was used as a comparison basis since data for this orbit is readily available. The Hohmann transfer ΔV requirements from 100 nm circular orbits to the synchronous equatorial are compared with ΔV requirements for 4356 nm in Table 4.9-8.

Table 4.9-8. Hohmann Transfer ΔV Requirements

Velocity Increment (fps)	Altitude	
	Synchronous	4356 nm
Injection into transfer	8070	4450
Final circularization and inclination change	6050	8350
Total ΔV	14120	12800

Previous data has shown that a payload advantage of 20 to 40 percent of the higher payload weight will be realized when using the lower altitude orbit instead of the synchronous orbit, and that the ratio of synchronous equatorial orbit payload weight to 4356 nm orbit payload weight is about 60 percent for Titan IIIC, and about 80 percent for the seven-segment Titan III.

Alternate booster candidates for the payload range in question include those listed in Table 4.9-9. Note that no known firm implementation funding or planning exists for any of them.

Table 4.9-9. Alternate Booster Candidates

Launch Vehicle	Synchronous Payload (lb)
Titan 3C (5 Segments)/Centaur	6500
Titan 3 (7 Segments)/Centaur	7400
Saturn 1B/Centaur	7000 to 9900
Titan 3C/Agena-D (Replacing Transtage)	3300
Titan 3C/Improved Agena (Replacing Transtage)	3950
Titan 3F (7 Segments)/Transtage	3200
Titan 3F (7 Segments)/Restart Second Stage)/ Transtage	4000 to 4500
Titan 3F (7 Segments)/Transtage with 12000 lb Additional Propellant	4000 to 4500
Titan 3C/Transtage (Fluorine)	3900
Titan 3C/Transtage (Stretched with Fluorine)	6000

4.9.3.2 Orbit Maintenance and Vernier Propulsion Engines

4.9.3.2.1 Milli and Micro Pound Thrustors

Table 4.9-10 summarizes the present state of development for resistance jets, subliming solid thrustors, ion engines, SPET (Solid Propellant Electrolysis Rocket), Cap Pistol, and ELM (Electrical Liquid Metal) thrustors. These thrustors range from 3×10^{-6} lb to 10^{-3} lb in thrust, except for the electrolysis rocket which is 10^{-2} to 1 pound. A subliming solid is scheduled to fly within a year on an ATS vehicle, and a resistance jet (Spring 1967) on an NRL vehicle.

Depending upon the size of the spacecraft, the power available and the purpose (which defines total energy requirements), each thrust approach has a potential application. Development time and cost can vary from 6 to 18 months and from $100,000 to $1,000,000, depending upon the complexity of the system requirements.

SPET, Cap Pistol, and ELM are impulse kick thrustors with delivery time of impulse bit of 10 to 100 μseconds. Resistance and resisto jets can be pulsed or operated steady-state. The valved subliming solid potentially can be pulsed 50 to 100 μseconds or operated for short durations steady-state. Ion engines are preferably operated on the order of seconds rather than in a pulse mode. They can be built to offer thrust vector control in one or two planes to at least $\pm$ 10 degrees. ELM is in an early state of development.

4.9.3.2.2 Liquid Monopropellant Thrustors

Liquid monopropellant engines have been built in thrust ranges of 0.05 to 500 pounds. Past flight experience is largely with hydrogen peroxide but virtually all new system designs are shifting to hydrazine. The I_{sp} of hydrogen peroxide is about 150 to 160 sec while that for hydrazine is 215 to 240 seconds.

Silver screen catalyst beds provided spontaneous starts for hydrogen peroxide but early catalysts for hydrazine required auxiliary heat or hypergolic slug propellant starts. Hence, all early systems, requiring multiple firings, used the lower performing hydrogen peroxide. Within the past 3 years a spontaneous catalyst has been developed for hydrazine, hence, the shift for new systems to this propellant. Hydrogen peroxide slowly decomposes to oxygen and water. Oxygen is only slightly soluble in hydrogen peroxide and, unless the spacecraft is spin stabilized, the oxygen cannot be separated or vented off from the liquid. Consequently, a three-axis stabilized craft for long-life of 6 months to 1 year and longer, cannot use hydrogen peroxide. Fortunately, hydrazine has a higher performance and is not beset with a stability problem. The new global ComSat satellite, although spin stabilized, will still use hydrazine. The engine may be pulsed 10 mseconds and up or operated in steady-state.

Procurement time would be 10 to 18 months and cost of development and qualification would range from several hundred thousand to one to two million dollars depending upon size and number of engines and overall complexity of the system being acquired.

Table 4.9-10. Milli- and Micropound Thrustors

Thrustor	Company	Thrust		I_{sp}		Power		Propellant	Life and Test History	Hardware status	Limiting Problems and Comments
		range	demo	des.	demo.	des.	demo.				
Resistance Jet	GE	3×10^{-6} 5×10^{-2}	3×10^{-6} 22×10^{-6} 485×10^{-6}	50 80 100- 220	50 80 106- 220		3w 3.5w 4.5w	ammonia ammonia ammonia	30 day vacuum test 100 hr vacuum test	10 22 & 485 μlb units del	10 μlb unit del. to NRL will give ca. 80 for Isp. 24 & 485 μlb feasibility units to NASA-Goddard for evaluation
Resistojet	Avco	3×10^{-6} 5×10^{-2}	20×10^{-6} 450×10^{-6}	75- 200	110- 120		3 5w	ammonia ammonia	50 hr vacuum test	20 & 450 μlb units del.	20 & 400 μlb units built for feasibility for NASA-Lewis.
Subliming Solid	Lockheed	10^{-6} 10^{-3}	10^{-5} 10^{-4}	50- 100	52- 55		3w	solid	14 hr vacuum test		Valveless nozzles, also built valved version. ATS flight April 1967.
Subliming Solid	Rocket Research Corp.	10^{-6} 10^{-3}	10^{-5} 10^{-3}	50- 100	55		1 5- 8w	solid	6 hr vacuum test	quality flight system del.	Delivered flight qualified system to General Dynamics. 10 μlb unit scheduled NRL flight early 1967
Ion Engine	Hughes	10^{-6} 10^{-2}	10^{-5} 500×10^{-6}	2000- 10000	5400 5000	15w	15w 75w	cesium	50 hr vacuum test 1800 hr vacuum test	prototype units	Can TVC in 2 planes $\pm 10^{0}$. 10 μlb unit all flight size but power conditioning
Ion Engine	E.O.S. Inc.	10^{-5} 10^{-3}	10^{-5}	5000 6000	4500?	10w	20w	cesium	limited testing	prototype	Still in lab development for low thrust low power units. thrust (10^{-2} - 10^{-5}) use much more power.
SPET	GE	10^{-6} 10^{-4}	10^{-6} 10^{-5}		2000		0.5w 5.0w	special	4000000 cycles	prototype	Fuel problem solved, trigger tube life solved, power conditioning needs repackaging
Electrolysis Rocket	Hughes	10^{-2} 1 0	10^{-2}	380	300- 350		7 w hr per lb sec	water to $0_2 + H_2$	prototype tests	prototype	Gas-liquid separation OK for spinning vehicle, not solved for 3 axis stabilized vehicle.
CAP PISTOL	Curtis Wright	.008 lb sec per pulse			220		29w per pulse	solid propellant		flight models built	Stepper motor life a potential problem as is energy management thru: needed in only one direction Are developing larger bit units.
ELM	GE	10^{-6} 10^{-3}		2000			?	mercury	laboratory testing		First phase of laboratory testing. Flight units several years away

4.9.3.2.3 Liquid Bipropellant Engines

Engines ranging in thrust from 0.2 to 15000 lb are in development and/or qualified. Generally these use dinitrogen tetroxide N_2O_4 (NTO) and hydrazine compounds as fuels. Two fuels in particular are monomethyl-hydrazine (MMH) and 50% hydrazine - 50% unsymmetrical dimethylhydrazine (UDMH) (50-50 or aerozine 50). The delivered Isp varies from 270 to 310 sec for steady-state performance and is largely related to thrust level of the engine. The smaller engines (0.2 to 100 lb) can be used in pulse mode as short as 10 to 20 msec and up to steady-state. Chamber life at the 100 lb thrust level as great as 30,000 sec has been demonstrated. The development and qualification of a bipropellant engine system will take 18 to 24 months and cost three million dollars and up depending upon the complexity of the system.

4.9.3.2.4 Propellant Feed Systems

For the monopropellant hydrazine and the storable bipropellant engine system, positive expulsion for long-lived systems is a potential problem. Butyl or ethylene-propylene rubber (EPR) or teflon can be used for positive expulsion bladders to store hydrazine up to 1 to 2 years. Only teflon is compatible with both N_2O_4 and hydrazine for the bipropellant system. The best butyl and EPR currently available may not have adequate compatibility with hydrazine beyond 2 years. Teflon is subject to radiation damage so its orbit life is perhaps only 1 to 2 years. Several different approaches utilizing surface tension-surface force interaction are under development to allow a minimum quantity of propellant at the exit port of the tank at the time of an engine firing. The firing of the engine will provide sufficient acceleration so that adequate propellant will be settled at the exit port, free of pressurizing gas bubbles, to sustain any duration of steady-state firing required. At least one or more surface force approaches are certain to be qualified and flight tested by the 1970-1971 period.

4.9.3.2.5 Performance Regimes

Figure 4.9-11 shows an approximate relationship between thrust level and total impulse required for systems usage and the major areas of application for cold gas, subliming solids, resistance jets, ion and plasma engines and liquid monopropellant and bipropellant thrustors.

Figure 4.9-12 shows the relationship between system weight and total impulse for a number of potential propulsion systems.

At 10000 lb/sec, total impulse there is small difference in weight between a liquid monopropellant and bipropellant system. At 1000 lb/sec, cold gas (N_2) is somewhat heavier than the liquid system. However, there is a system requiring about 8000 lb-sec which uses cold gas rather than the liquid system because of simplicity and reliability. For small satellites (200 to 1000 lb) the station-keeping and attitude control functions can be accomplished by subliming solids, resistance jets, SPET, and/or ion engines.

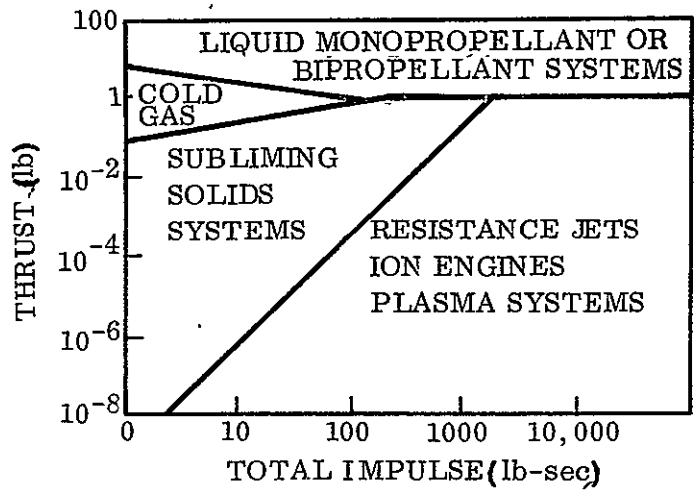

Figure 4.9-11. Reaction Control System Operational Regimes

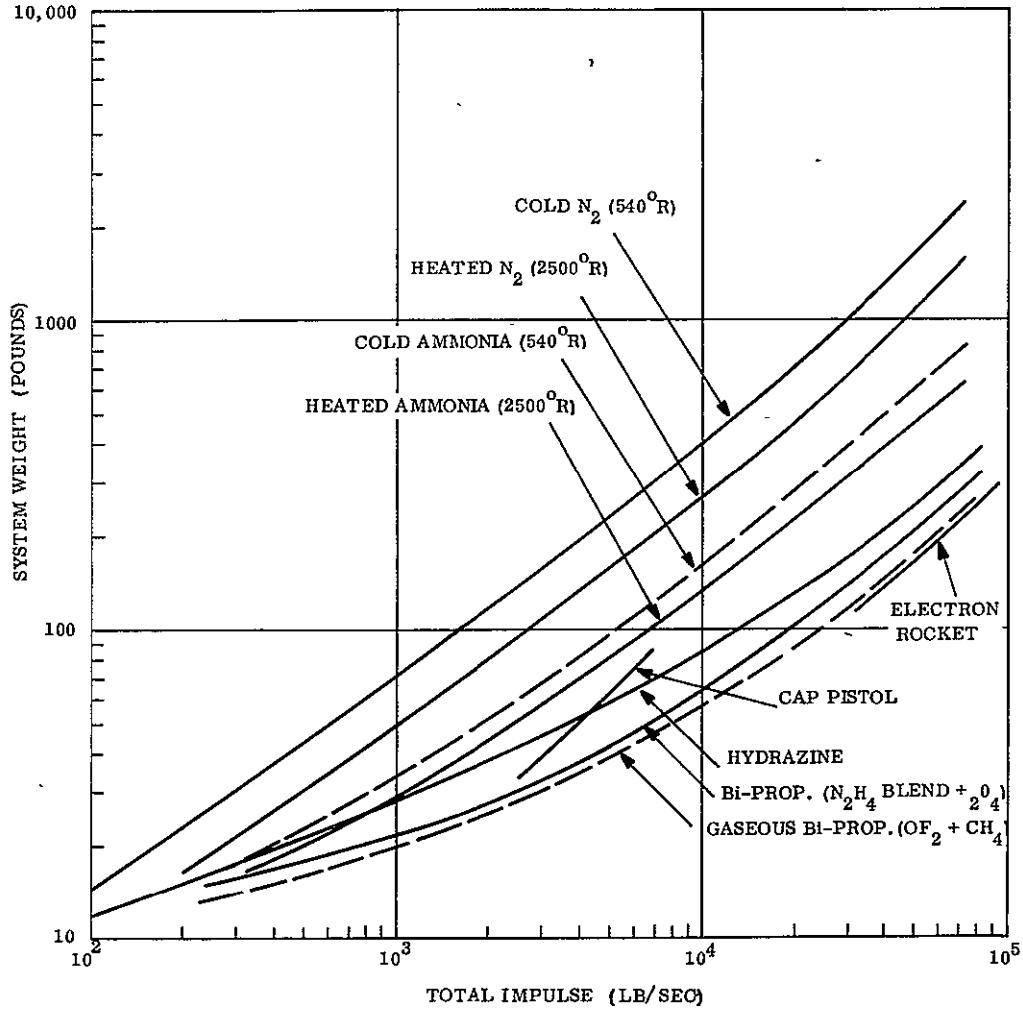

Figure 4.9-12. Propulsion Weight Comparison

4.9.3.3 Station-Keeping

A spacecraft in a synchronous orbit (i.e., altitude = 19,323 nm, velocity = 10,087 ft/sec, inclination = 0 degree, eccentricity = 0) is perturbed by several forces. These forces are due to:

a. The triaxiality of the earth.
b. The sun and the moon.

By triaxiality of the earth is meant the equatorial bulge, as well as the ellipticity of the earth's equatorial section. If a synchronous satellite is placed above the extension of the minor axis of the earth's equatorial section, the spacecraft will remain at the location indefinitely (i.e., a position of stable equilibrium). If the spacecraft is placed at any other location, the spacecraft will oscillate about the minor axis with an amplitude equal to the original angular displacement from the minor axis and a period dependent on the amplitude of vibration. If the spacecraft is placed over the extension of the major axis, it will be in a position of unstable equilibrium. That is, the slightest perturbing force will tend to cause an oscillation of ± 90 degrees about the minor axis towards which the spacecraft was originally displaced.

Figure 4.9-13 shows the on-board yearly ΔV requirements necessary to maintain the spacecraft at the various synchronous locations shown.

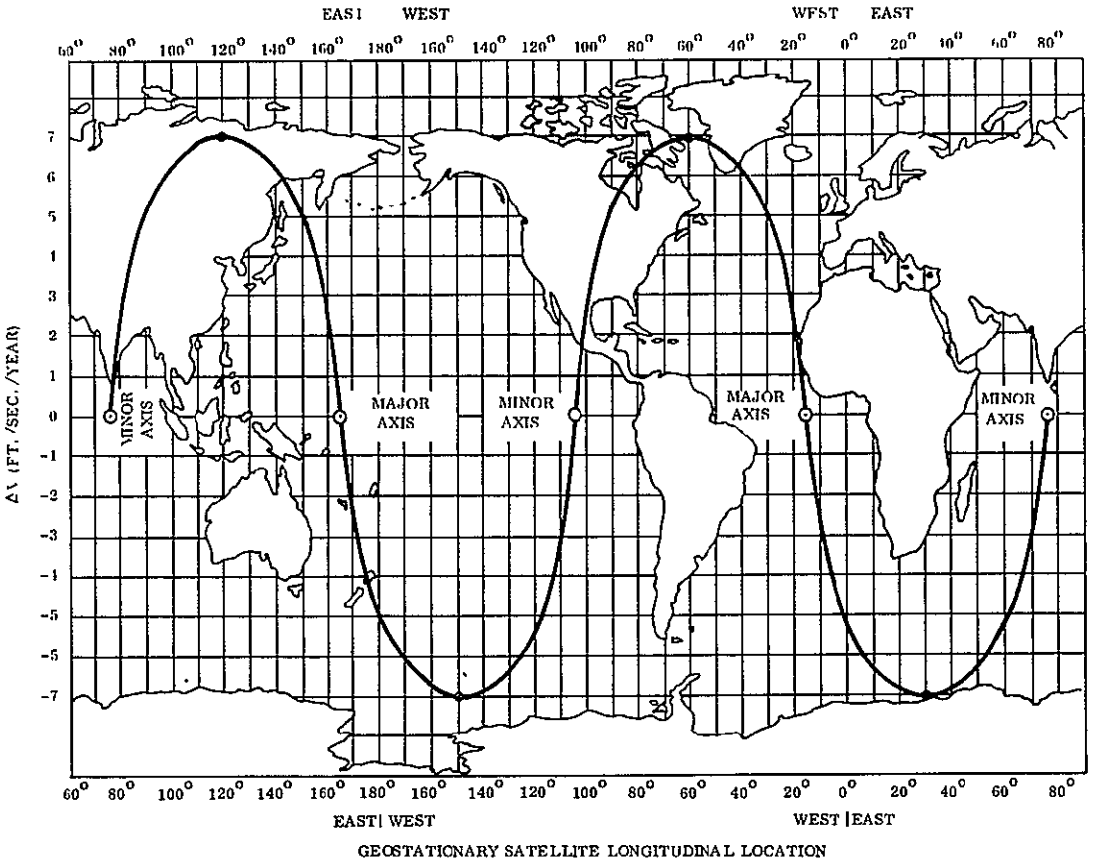

Figure 4.9-13. ΔV Requirement as a Function of Synchronous Locations

The major effect of the sun and moon is to produce an increase in the inclination of the orbital plane at the rate of 0.86 degree per year. This would require an on-board capability of 150 ft/sec to remove each degree of inclination. If no ΔV capability exists, the ground trace of the spacecraft will be equal to the inclination, and the maximum east/west longitudinal displacement will be given by $\Delta L_{Max} = ki^2$ ($0^o \leq i \leq 10^o$), where i = inclination in degrees and $k = 4.4 \times 10^{-3}$ deg^{-1}.

4.10 THERMAL CONTROL ANALYSIS

4.10.1 INTRODUCTION AND CONCLUSIONS

This section presents the results of the thermal control analysis performed during the VBMS.

Section 4.10.2 presents the descriptions of the selected subsystems for the four configurations.

Section 4.10.3 presents the technology considerations and the tradeoff studies made with respect to the four configurations.

The VBMS satellite broadcast equipment performance requirements and variable duty cycle impose severe design constraints on the thermal control system. The high heat dissipation requirements at relatively low heat rejection temperatures (for those configurations using solid-state transmitters) couple with the effects of the limited duty cycle and earth occultation to require state-of-the-art advances in thermal control technology. The primary problem is that the peak dissipation load during broadcast operation is much larger than during the nonbroadcast periods and thus requires either (1) a large surface area and corresponding devices to vary surface emissivity over a wide range, or (2) a heat sink to absorb the peaks of the thermal cycle.

The significant relation of thermal control technology to broadcast satellites is that the thermal control system becomes much more influential to establishment of the spacecraft design than for current satellite programs. Although the specific performance of the thermal control systems (measured by ratio of thermal control weight to heat dissipated) is somewhat higher than current satellites, the absolute magnitude of the thermal control system becomes very large in relation to other subsystems because of the total heat load. The specific performance improves because the major heat dissipator is the broadcast transmitter, which operates at relatively high temperature compared to normal spacecraft equipment.

Heat rejection surface area requirements sized the spacecraft body for all of the satellites except UHF, which utilized a heat pipe system to accommodate the concentrated high thermal load of the vacuum tube power amplifier.

4.10.2 DESCRIPTION OF SELECTED SUBSYSTEMS

4.10.2.1 HF Configuration

The HF configuration has an octagonal body 60 inches high. A circular, equatorial orbit at an altitude of 4356 nm is specified for this particular mission. The orbit period is 4.8 hours.

A transmitter duty cycle of one hour per orbit results in the dissipation of up to 8.8 kilowatts of power. Housekeeping electronics dissipate 500 watts continuously. In order to reduce the array area, batteries supply the primary power during transmission. The batteries are charged during the remaining 3.1 hours allowing 0.7 hours maximum occultation.

The spacecraft rotates $\pm 23.5^{\circ}$ on the roll axis to maintain the sun normal to the solar array which is contained in the roll-pitch plane. Therefore, only three panels of the body are illuminated by the sun. The five remaining panels are available for temperature control.

Transmitter

The solid-state transmitter consisting of 128 output transistors dissipate up to 8.8 kw every hour of transmission. A passive radiator to dissipate this quantity of heat would require over 150 ft^2 of area and would be subject to wide temperature variations. A semi-passive technique utilizing change of phase material (COPM) reduced the area to 23 ft^2 reducing support structure, improving thermal efficiency, and improving transmitter packaging. The weight of COPM required is 225 pounds.

The COPM will absorb about 80% of the heat dissipated during transmission by undergoing a phase change (melting) at constant temperature (176°F). In the 3.8 hours remaining, the COPM will release the stored energy by reversing the direction of phase change (solidifying) again at constant temperature. At the time of the next sequential transmission all the COPM will have solidified. The degree to which the product of the weight of COPM and the latent heat of fusion matches the heat dissipation of the transmitter will control the variation in temperature of the transmitter radiator panel. Nominally this variation should not exceed 35°F.

The transmitter panel will be located on the north panel of the octagonal body.

Housekeeping

The 0.5 kw load of the housekeeping subsystems, since it is a continuously operating system, can be adequately controlled by passive means. For nominal temperatures of $70^{\circ}\text{F} \pm 30^{\circ}$, an area of 29 ft^2 is adequate. The south panel and part of the adjacent panel have been selected as the location of the housekeeping subsystem electronics (see Figure 4.10-1).

The coating characteristics of the panels are emissivity (ϵ) = 0.9 and absorptivity (α_s) = 0.25.

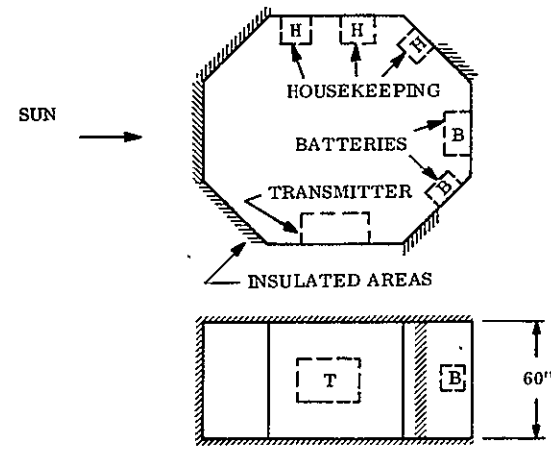

Figure 4.10.1. HF Thermal Control

Battery Pack

The use of batteries to supply primary power has reduced the array size and deployment complexity. However, a total of 1625 lb of batteries are required. The per battery heat dissipation will vary widely during the charge/discharge cycle.

The large mass of batteries and the reasonable battery temperature limits of $32^{\circ}F$ to $90^{\circ}F$ allow a passive temperature control system to be used. An area of 24 ft^2 and an ϵ of 0.9 on the panel opposite the sun plus part of the adjacent panel is adequate to maintain the batteries in a range of temperatures of about $60^{\circ}F \pm 15^{\circ}$.

General

Insulation will be required on the top and bottom panels, the three sun facing panels, and a portion of the two angular facing panels near the battery panel. Coating characteristics are not critical since the solar influence on panel temperatures is not significant.

4.10.2.2 VHF No. 1 Configuration

The VHF No. 1 satellite possesses a 30-inch high octagonal body, similar to that of the HF satellite. The two flat ends are oriented so that a normal axis through their centroid would be coincident (or parallel) to the antenna beam axis. This axis then makes one revolution per day with respect to the sun, with the two long sides (of the eight body sides) parallel to the orbit plane. Heat flux from the earth and albedo sources on the spacecraft are negligible due to the orbit being at synchronous altitude.

Transmitter

The temperature control of the spacecraft in the VHF No. 1 configuration is complex and difficult. A basic requirement to locate the transmitter near the antenna, in conjunction with the restriction that slip rings cannot be used for RF power, imposed a severe external environment on the thermal control subsystem. Heat flux from the sun would impinge on all surfaces to a varying degree as a function of orbit time and time of year. The antenna interface with the bottom of the spacecraft body also eliminated that surface from thermal consideration.

The total area available for heat rejection is 117 sq ft, of which a 47 sq ft area is on the top. The 41.5-inch end panels would be illuminated by the sun during a part of each orbit, as would the top surface. As a function of the time of year, the surfaces parallel to the orbit plane would be illuminated by the sun at an incidence angle of $23\text{-}1/2^{\circ}$.

The operating temperature of the transmitter transistors and the housekeeping electronics are different, up to $200^{\circ}F$ for the transistors and to $100^{\circ}F$ for the housekeeping equipment. In order to compensate for the sun heat load, the operating temperature level would have to be decreased. Under steady-state conditions, (worst case) one square foot of radiator at $100^{\circ}F$ can reject 44 watts. Of this, 20 watts will be solar heat. Therefore, the design rating of the radiator cannot exceed 24 watts/sq ft, which would result in a minimum

temperature of 10°F with no solar illumination. This is too low a temperature and too wide a variation in temperature, since $70^{\circ}F \pm 30^{\circ}$ is the normally desired range.

The selected thermal design of the transmitter would accommodate the previously discussed problem. The transmitter transistors were located on the top surface of the two, 60-inch panels. A power density of 61 watts/sq ft would be applied to the side panels and 48.5 watts/sq ft on the top. The maximum and minimum operating temperatures would be 80°C and 64°C for the side panels, and 78°C and 45°C for the top. Change-of-phase material would be incorporated into the passive radiators to minimize the temperature change during periods of occultation.

Housekeeping

The heat dissipation in these subsystems would be 500 watts on a continuous basis, with temperatures controlled to $70^{\circ}F \pm 30^{\circ}$. Since the top and long sides of the octagon were utilized for the transmitter, only the end panels remained for the housekeeping equipment. At the nominal design temperature of 70°F and with no solar input, a passive heat transfer area of 14 square feet would be adequate. However, the areas available would be illuminated either by the full solar constant of 78% of the solar constant. Therefore, the surfaces were derated. In addition, the normal multishutter arrangement cannot be used since the effective solar absorptivity of this arrangement is about 1.5 times the unshuttered surface value. Therefore, the design of the shutters for this configuration would be either a single blade covering the whole surface or two blades, each covering half the surface. These shutters were hinged from the top and bottom and would open at opposing angles. The angular movement of these shutters must be 135 degrees to prevent reflection of solar heat onto the panels.

Figure 4.10-2 illustrates the thermal design of the VHF No. 1 spacecraft body.

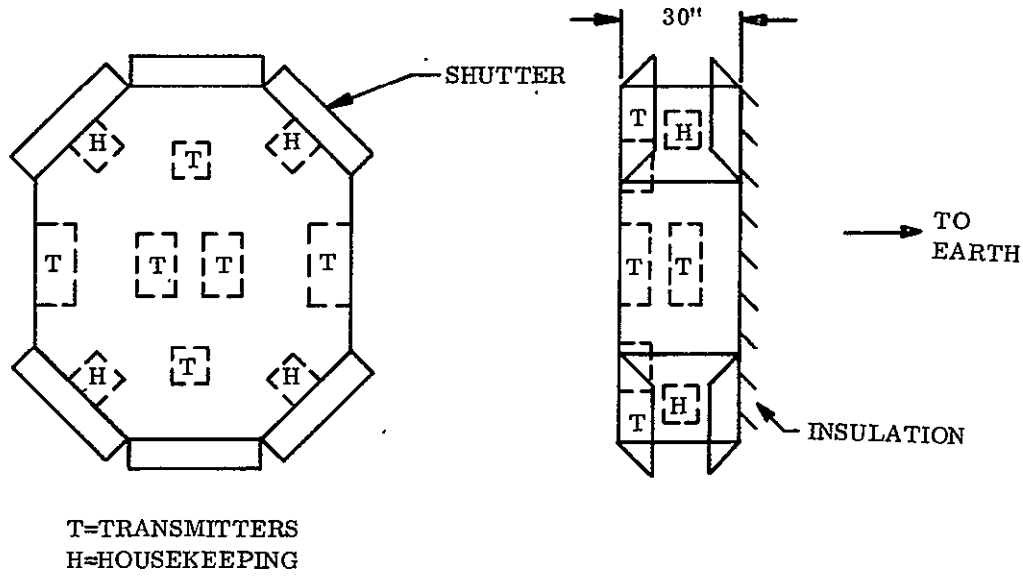

Figure 4.10-2. VHF No. 1 Thermal Control

The thermomechanical interface with the antenna has not been defined but for purposes of this study was assumed adiabatic. No actuation devices have been selected for the shutters; any one of several devices would suffice in terms of weight, cost, and reliability.

4.10.2.3 VHF No. 2 Configuration

The VHF No. 2 spacecraft body is a regular octagon 18 inches high and 55 inches across the flats. The heat loads to be controlled are 440 watts for one hour per orbit on the transmitter, and 100 watts continuously in the housekeeping electronics.

Transmitter

The short duty cycle of the transmitter in this configuration, with a completely passive design, or modified by heat pipes, would expose the elements of the transmitter (the transistors) to a widely fluctuating temperature.

By combining the semipassive heat pipe technique for improving thermal radiator efficiency with a change-of-phase material, it is possible to reduce the area required and greatly improve the system time constant. In this manner, the temperature variation and level can be substantially reduced. By storing most of the heat dissipated during the one hour transmission, and rejecting it in the remaining 7 hours, approximately one square foot of the radiator is required, operating at a temperature of 148°F. The weight of COPM required at 100 Btu/lb is 14 pounds. Arbitrarily selecting the north-facing panel, one of the panels which is parallel with the orbit plane, the influence of the sun during summer solstice will be minimized. Using a coating with an α of 0.25 and an ϵ of 0.90, the temperature rise will be less than 14°F when solar heating does occur.

Housekeeping

The 100 watts of heat dissipated continuously in the housekeeping equipment can be adequately controlled by passive techniques. The south-facing panel opposite the transmitter panel will be used to minimize the influence of solar heating. (Albedo and earth radiation can be ignored at this altitude.) A 10-inch sun shield to shade the radiator at winter solstice will be required. Using the sun shield allows only one panel to be required. Without the sun shield, the solar influence would require more area than is available on the south panel.

General

All the surface areas of the vehicle, other than the areas described above, require super-insulation. This area is about 50 ft^2. No internal insulation behind the transmitter will be required, since heat leakage back into the interior of the vehicle will help keep temperatures more evenly distributed. The temperature control schematic is shown in Figure 4.10-3.

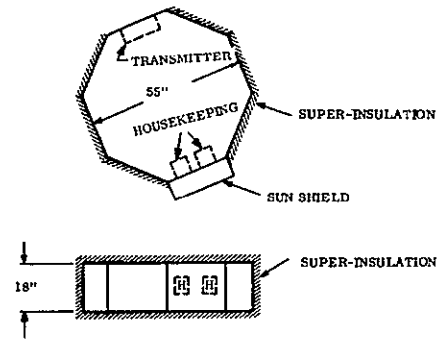

Figure 4.10-3. VHF No. 2 Thermal Control

4.10.2.4 UHF Configuration

The UHF configuration presents a relatively simple problem in temperature control selection. There are two basic sources of heat: (1) the transmitter output tube, and (2) the housekeeping electronics. Both of these systems operate continuously (except during shadow), minimizing the transient effects of duty cycle.

Housekeeping

The spacecraft employs an earth-pointing antenna and a fully-oriented solar array, with the articulation being implemented by a single degree-of-freedom rotation of the solar array and a spacecraft yaw maneuver. This motion thus provides two opposing spacecraft sides which always have their surface parallel to the sun's rays. Therefore, the housekeeping electronics were located on these panels. Sun shields were used to reduce the solar influence on the other panels used for thermal control. Passive temperature control was used for the housekeeping equipment, requiring a total radiating area of 16.5 ft^2, with a thermal coating having values for $\alpha \leq 0.25$ and $\epsilon \geq 0.88$. The heat load to be dissipated is 590 watts. The sun shields will be thermostatically operated to close during occultation in order to minimize temperature variation, although this is not mandatory.

Transmitter

The transmitter output tube, with a total heat dissipation of 800 watts, presents an altogether different problem since this heat source will be concentrated in a very small area. A passive radiator was considered, but eliminated, because of the excess weight it presented and the long time constants involved with variations in tube power as a function of modulation. A semipassive technique, the heat pipe, was selected on the basis of weight, reliability, ease of assembly, and installation.

The heat pipe configuration, two parallel 0.75-inch O.D. tubes, approximately 36 inches long with 2.6 square feet of radiator fin welded to the 18 inches of heat pipe exposed to space, is shown in Figure 4.10-4.

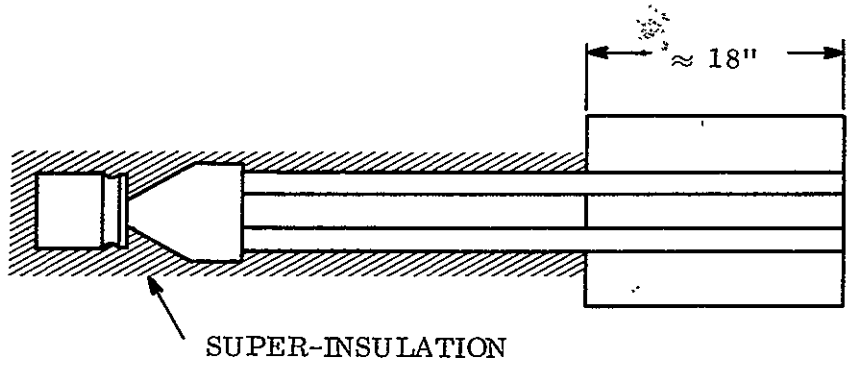

Figure 4.10-4. Heat Pipe Configuration

The interface of the heat pipe with the transmitter tube will be through a copper mounting block. The heat pipes will be welded into the copper block, and the block attached to the molybdenum anode at a BeO interface to electrically isolate the tube from the heat pipe. A small heater (< 50 watts) will be required to maintain the tube above the minimum temperature during the longest occultation periods.

General insulation would be required on all nonheat transfer surfaces of the spacecraft. This super-insulation would be the multibarrier type, made up of 30 layers of embossed, aluminized mylar. External protection of the insulation can be provided by any of several means. Amfab (teflon impregnated fiberglass cloth) is suggested, but a coated layer of 1-mil mylar would suffice.

The transmitter tube will also have to be isolated from the spacecraft due to its higher temperature. The thermal control schematic is shown in Figure 4.10-5.

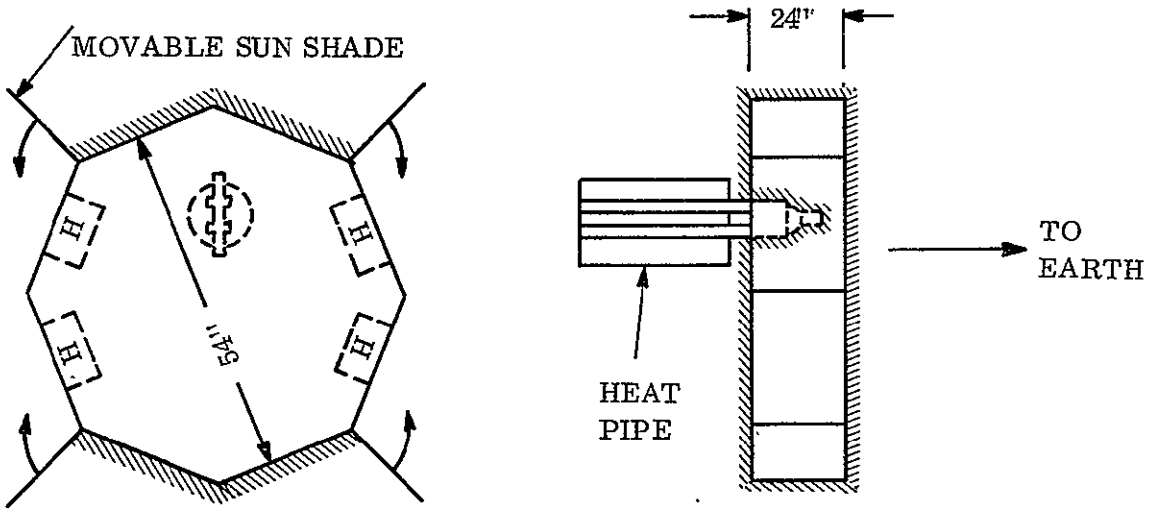

Figure 4.10-5. UHF Thermal Control

4.10.3 THERMAL CONTROL TECHNOLOGY

4.10.3.1 General Description

The temperature control concepts considered for the VBMS series of spacecraft are listed below with definitions for each:

a. Passive - restricted to thermal coatings and insulation

b. Semipassive - heaters, variable emissivity devices (shutters), heat pipes and change of phase material

c. Semiactive - liquid loops using pumps, valves, and radiators (rejection of heat at or below source temperature)

d. Active - liquid/vapor loops using compressors, valves, radiators (rejection of heat at a higher temperature than the source).

For the great majority of spacecraft, the thermal designs incorporate combinations of items a and b in varying degrees. All spacecraft have coatings and insulation.

The thermal design of any spacecraft must consider the interrelation of many restricting, and sometimes contradictory, influences. In the approach taken for the VBMS vehicles, since the life requirements are quite significant, no consideration was given to active or semiactive systems since the life expectancy of those systems, even extrapolated to 1971, is inadequate. Therefore, only passive and semipassive techniques have been considered. In the following paragraphs, the performance and criteria used in selecting a system will be discussed.

4.10.3.2 Passive Temperature Control

Passive temperature control is achieved by the use of thermal coatings with specific solar absorptivity (α) and emissivity (ϵ) values, and insulation or combinations of the two. Whether insulation or coatings are required is a function of local conditions at a surface, and the external environment. Insulation may be used to minimize the heat leak, either into or out of the surface.

The treatment of a surface to maintain an acceptable thermal balance is a function of:

a. The external environment in terms of incident heat fluxes from solar, reflected solar, reflected and the earth

b. The surface area with its absorptivity (α) and emissivity (ϵ) characteristics

c. The heat dissipation and time dependence of equipment

d. The required temperature control limits.

For instance, if a surface of a space vehicle is located such that there is no external heat flux, the surface area is two ft^2, and the heat dissipation is a constant 10 watts; then passive control is very simple. A heat balance is established as follows:

$$SA\,\alpha + SaA\,\alpha + EA\,\epsilon + Q = \epsilon A\,\sigma\,T^4 \qquad (1)$$

where:

S = solar constant

A = area

α = absorptivity

S_a = albedo flux

E = earth flux

Q = heat flow rate

ϵ = emissivity

σ = Boltzmann Constant

T = radiating temperature

Since the external heat fluxes are 0 by definition, then the heat balance is reduced to:

$$Q = \epsilon A \sigma T^4 \tag{1a}$$

If a temperature of $70^{\circ}F$ is desired, then the ϵ required is determined by rearranging Equation 1a to

$$\epsilon = \frac{Q}{A\sigma T^4} \tag{1b}$$

$$\epsilon = \frac{10 \times 3.41}{2 \times 137} = 0.125$$

This is a very small and difficult to obtain (and retain) value of "ϵ". If the heat dissipation can be confined to only one square foot, then the insulation can be applied to one square foot and a coating with an ϵ of 0.26 applied to the radiating surface. This process can be continued until the ϵ required approaches 0.9 as a practical limit.

However, if the duty cycle of the equipment is less than 100%, then the heat capacitance of the component and structure must be considered, and the dynamic temperature range becomes significant. A transient thermal analysis of an iterative nature is required. As the ratio of on to off time becomes small, then the steady-state design point is strongly influenced by heat capacitance, such that for large values of Wc_p, the radiation term can be reduced. This means that the heat dissipation will be absorbed by the thermal mass primarily and rejected by radiation secondarily. In the off mode, heat will continue to be radiated and the temperature will decrease. A compromise is necessary at this time to assure that the combination of heat dissipation, duty cycle, and heat capacitance result in a temperature range and levels which are acceptable. In actual practice, such a condition may be achieved very simply. The contribution of heat by conduction from other areas of the spacecraft may be ample. Under other circumstances, a completely passive design may not be practical; in which case, heaters may be needed, the temperature range must be expanded, or the spacecraft may be repackaged.

The influence of the sun impingement angle is very significant. In the following tabulation, the heat rejection per square foot for a surface with an α of 0.25 and an ϵ = 0.85 at various sun angles with a fixed temperature of $100^{\circ}F$:

Sun Angle	Q/A (watts/ft^2)
0	42.0
30	25.9
60	13.2
90	9.8

Secondary considerations are the heat leaks through insulation and from exposed structure. Insulation heat leaks become significant as the ratio of insulated area to total heat dissipation becomes less than 1/3. When this condition exists, the influence of the essentially unknown heat leaks is greater than that of the primary radiation surfaces, and is therefore to be avoided.

Exposed structure cannot always be avoided for obvious reasons, nor is it always possible (or desirable) to thermally isolate these elements. When it is possible and allowable to isolate external, exposed structure, it is preferable to do so since this will minimize the heat leak and improve the reliability of the passive temperature control system.

Passive temperature control, considering all of the normally expected variables, cannot control temperature much closer than $\pm 30^{\circ}$F about a nominal design value. Local circumstances may allow an improvement but could also result in an expanded range. The maximum total heat rejection of which a passive design is capable is about 36 watts/ft^2 for a temperature of 75°F. This value can be decreased by lowering the value of ϵ or the radiation area. However, in order to increase the heat rejection, the temperature must be increased.

The passive design is inherently reliable since there are no moving parts. However, care must be taken to assure good adherence of the coating to the radiating surfaces.

4.10.3.3 Semipassive Temperature Control

The use of semipassive temperature control techniques can take one of several forms: (1) electric heaters, (2) shutters, (3) change of phase materials, (4) heat pipes, and (5) combinations thereof.

a. Electric heaters are used with thermostats or by command to maintain minimum temperatures for a thermal design (radiation area, insulation area, and emissivity) which has been optimized to control the high temperature. This concept is basically a natural extension of the passive design concept.

b. Shutters are sophisticated in concept and more complex in application. These devices function by changing the heat rejection term "ϵA" of Equation 1 by changing the effective ϵ. This is normally accomplished by moving insulated surfaces (shutters which expose more or less of the primary radiating surface behind the shutters). The normally expected range of effective emissivity of a shutter system

is from 0.15 to 0.65. This range can be expanded by close control of design, manufacture, and surface properties of the shutter blades

Based on the Nimbus design, the total heat rejection characteristics of a shutter system are shown on Figure 4.10-6. (The actuation range of the actuator is 66°F to 81°F, but this can be arbitrarily defined.)

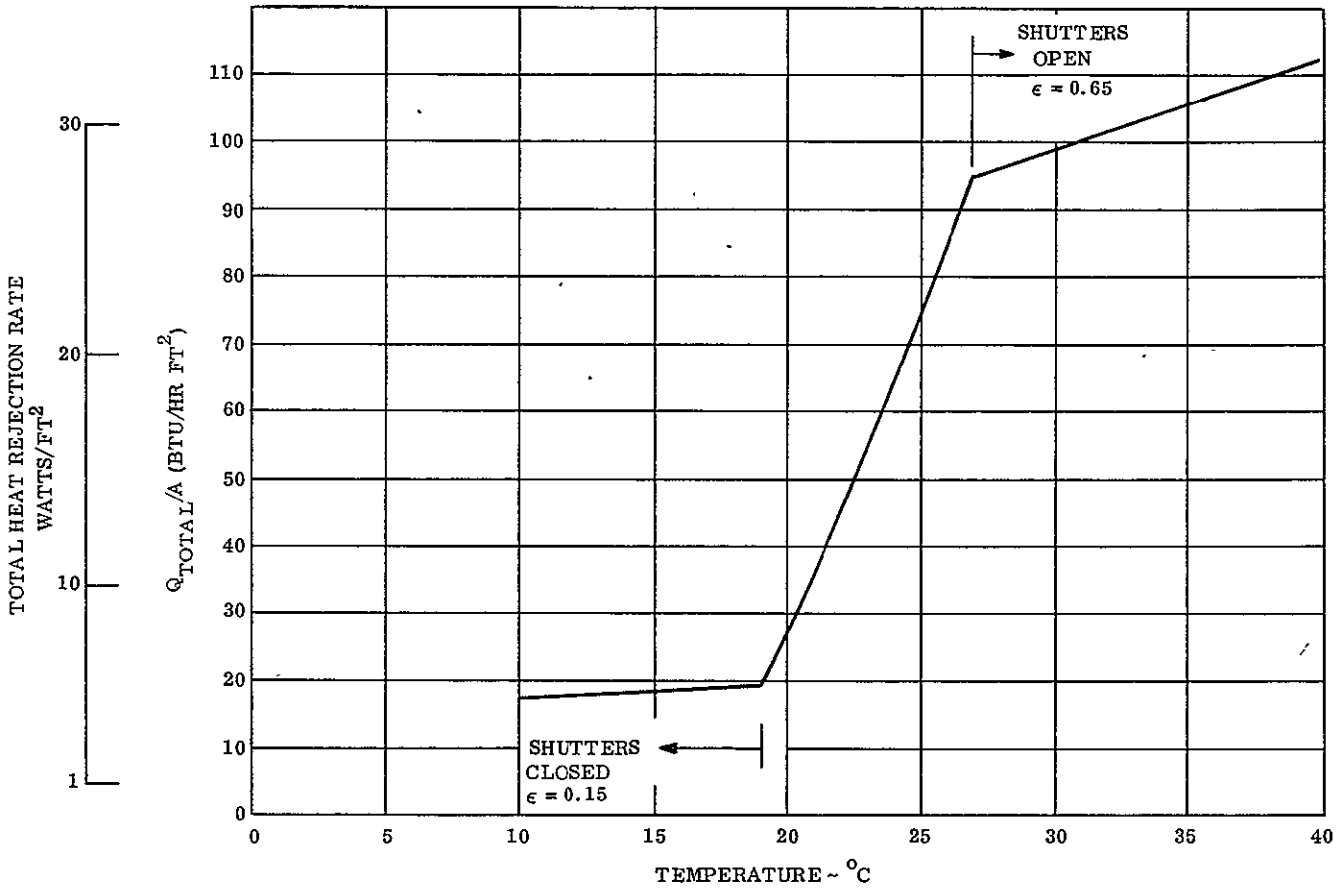

NOTE: (1) EMISSIVITY (ε) IS A FUNCTION OF SHUTTER POSITION
(2) $Q_{TOTAL} = \epsilon A \sigma T^4 = SA\alpha + S_a\alpha + EA\alpha$

Figure 4.10-6. Typical Shutter System Characteristics

If the sun impinges directly on the shutter surface continuously, then the equilibrium temperature (with no heat dissipation) is 150°F, with the open shutter values of $\alpha = 0.35$ and $\epsilon = 0.65$. The result of any heat dissipation will cause the temperature to increase at a rate of roughly 3°F/watt.

With this obvious difference in performance, it is possible to draw the conclusion that shuttered surfaces should not be used on sun-facing surfaces unless the time constant of the local surface is long compared with the duration of solar impingement, and the solar illumination time is short with respect to one orbit. Nimbus takes advantage of this condition, but only by limiting the heat dissipation of the equipment in the affected compartments to orbit average values within the local capability.

Actuation of the shutters can be achieved by any of several methods: (1) change of phase fluid in a bellows; (2) bimetallic springs; (3) expansion of solids; (4) electric motor drive; or (5) solenoids. Sensing of temperature to activate the actuator will (or can) vary as much as the choice of actuators -- conductive or radiation coupling, thermistor output into an electronic circuit, or full actuation by electrical impulse, simultaneously with equipment operation. There are advantages and disadvantages to each of several combinations of actuator and sensor mechanisms. These tradeoffs must be made at the preliminary design stage when the various system parameters and constraints are established.

c. Change of phase solids have been considered analytically and tested in models for the last several years. This concept is particularly applicable to systems (or components) having large heat dissipations and short duty cycles. In practice, the concept is implemented as follows:

The orbit average heat dissipation rate is calculated (including environmental heat input), and the area and emissivity requirements are determined on this basis, similar to the passive design. However, at this point an additional mass of substance is interposed between the heat source and the radiator. This substance would be a material having a melting point near to required operating temperature. The heat source would be thermally connected to change-of-phase material (COPM) which would absorb heat isothermally by melting, taking advantage of the latent heat of fusion. The mass of COPM required is a function of the total heat to be absorbed and the latent heat of fusion of this material. Optimally, this design could furnish an isothermal heat sink for a heat source, with the maximum temperature excursion being the ΔT required to conduct the heat from the source to the COPM. Curve "a" of Figure 4.10-7 illustrates how the design might perform on an optimum basis, while curve "b" shows how a more practical design might operate. The deviation from constant temperature is caused by (1) complete melting of all the material with heat input and a temperature rise due to the thermal mass (W_{c_p}) with continued heat input, and (2) by complete fusion during the off cycle followed by a decrease in temperature with continued heat loss. This design is considered more practical since the weight penalty of an optimum system design could be quite high depending on the heat dissipation rate and duty cycle of the source.

The implementation of this scheme is not so simple, however. In order to work properly, the heat must be uniformly conducted to the COPM which requires a good packaging design. A poor packaging design will result in thermal gradients

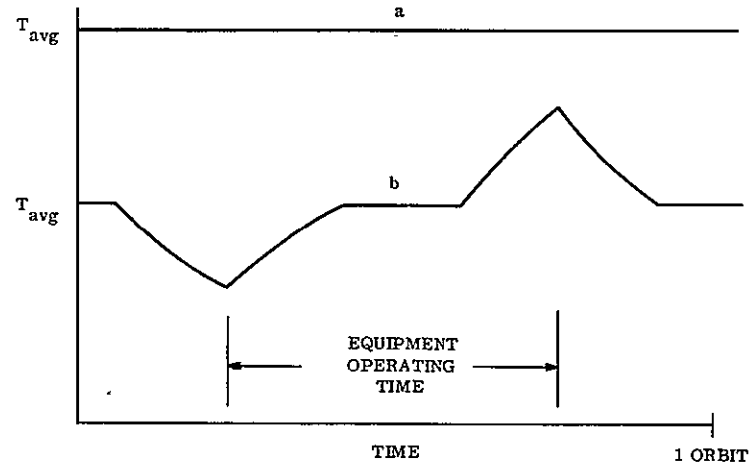

Figure 4.10-7. Illustrative Performance of Change-of-Phase Material Design

in the COPM, minimizing its usefulness. Actually, some gradient is unavoidable but should be minimized for maximum efficiency.

Some of the problems associated with this concept are: (1) fully filling the container of the COPM; (2) sealing the container; (3) accommodating pressure rises due to overheating; and (4) providing adequate thermal paths to minimize gradients and assure complete melting of material.

d. Heat pipes are simple devices that can be used directly for heat rejection purposes or to convey heat from one point to another with small temperature differences. Figure 4.10-8 illustrates the principle of operation.

Heat pipes can take many forms, depending on the application, from low power and temperature, to high power and temperature. Data exists for heat pipe operations in the cryogenic range, as well as above 1800°C.

Anticipated uses of these devices for the VBMS series range from specific cooling devices for high power transmitter tubes, to improving the efficiency of solid state transmitter panels, as well as to provide a basically isothermal vehicle structure.

e. There are several applications for combined systems that are immediately apparent.

1. Heat pipes and passive radiators
2. Heat pipes, COPM, and passive radiators
3. Heat pipes, COPM, and shuttered radiators

The selection of a combination will be based on many variables. Some of the more apparent variables are external environment variation, component heat dissipation, size, duty cycle and operating temperature limits.

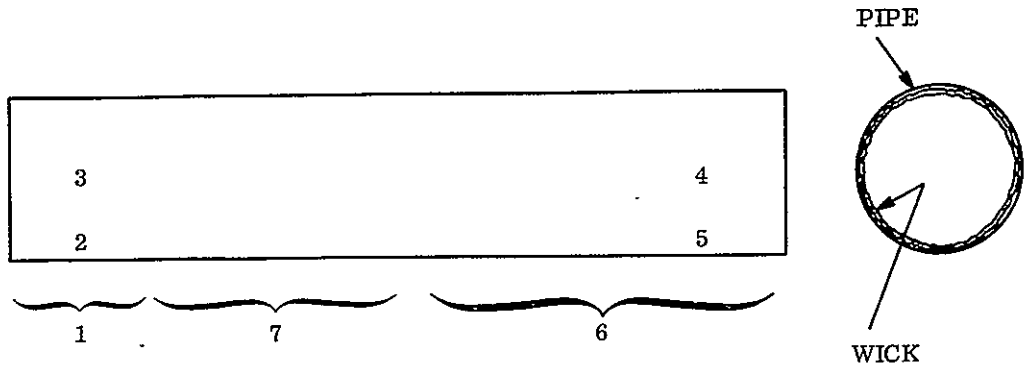

1 – Heat input section (circumferential and through end plate)

2 – Liquid evaporation at inner surface of pipe

3 – Vapor flows from pt 3 to pt 4 due to variation in local vapor pressure

4 – Vapor condenses onto surface at pt 5

5 – Heat flows from pipe at pt 6 due to conduction radiation or convection to an appropriate heat sink

6 – Liquid flows from pt 5 to pt 2 due to capillary action created by wicking material at the inner surface of the pipe

7 – Section 7 is an arbitrary length of insulated pipe

Figure 4.10-8. Heat Pipe Principles of Operation

SECTION 5

SATELLITE DESIGN

5.1 INTRODUCTION AND SUMMARY

During the course of the study, conceptual satellite systems for four broadcast missions were designed. The scope of the study did not permit sufficient design iterations or analytical depth to arrive at "optimum" combinations of subsystems. The main intent was to generate designs that could be considered feasible and that would permit system cost and schedule evaluation to the accuracy desired.

Mission requirements most pertinent to conceiving the representative satellite configurations are given in Table 5-1. The subsystem design values and characteristics for each configuration are summarized in Table 5-2. The weight summary for each satellite is presented in Table 5-3.

5.2 CONFIGURATION DESCRIPTION

5.2.1 HF SATELLITE

An artist's representation of the HF Satellite is presented in view (a) of Figure 5-1, showing the satellite at approximate time of broadcast (6:00 PM). An isometric view of the satellite with pertinent characteristics is presented in view (b) of the same figure.

5.2.1.1 Launch Configuration

The satellite is shown in the launch configuration in Figure 5-2. The booster interface is that of the Titan III Transtage and the 8 corner points of the spacecraft adapter and body are spaced so as to mate with the Transtage 8 point interface, thus minimizing load redistribution structure requirements in this region.

Table 5-1. Mission Design Requirements

Parameter \ Configuration	HF	VHF 1	VHF 2	UHF
ERP, dbw	52.1	65.4	48.1	63.6
Coverage	24° ECA; 45°N - 45°S Lat.	U.S.	24° ECA; 60°N - 60°S Lat.	U.S. by Time Zone
Duty Cycle	1 Hr/Orbit	Continuous Except Shadow	1 - 1-1/3 Hours/Orbit	Continuous, Except Shadow
Frequency, MHz	15.1, 17.7, 21.45, and 25.85	100-108	100-108	870
Altitude, N.M.	4356	19323	7556	19323
Period, Hours	4.8	24	8.0	24
Min. FOV	18.5°	7.0°	10.8°	3.4°

Table 5-2. Subsystem Design Values

CONFIGURATION / SUBSYSTEM	HF	VHF NO. 1	VHF NO. 2	UHF
ANTENNA				
Type	Phased Array with 16 Cavity-backed Spiral Elements	Phased Array with 32 Helix. Elements	Parabola	Parabola
Size	100' x 100' x 15'	51' x 51' x 15'	34.5' diam.	22 5' diam.
HPBW, Degrees	20 0	7.5	18.5	3.75
Gain, db	14 4	26.9	19.0	33.0
TRANSMITTER				
Type	Solid State	Solid State	Solid State	Vacuum Tube
RF Power Out, kw	8.8 (at 100% Mod.)	7.07	0.82	1.15
Efficient, %	0.59	0.65	0.65	0.59
Power In, kw	14.9	10.88	1.26	1.95
POWER				
Prime Power for Xmtr, kw	14.9	10.88	1.26	2 29
Prime Power for S/C, kw	0 5	0.50	0 10	0 25
Tot. Prime Power, kw	15.4	11.38	1.36	2 54
Type of System	Oriented Solar Array plus Batteries	Oriented Solar Array	Non-oriented Primary and Secondary Array and Battery	Oriented Solar Array
Array Area, ft^2	1788	1968	326 (Both Arrays)	438
THERMAL CONTROL				
Radiator Area, ft^2:				
Transmitter	26	72	1	2.6
Housekeeping	29	44	2.9	16 5
ATTITUDE CONTROL				
Type Antenna/Body Module	Local Vertical Orbit Normal for Antenna Body Module during broadcast-gyro package reference during remainder of orbit	1st Mode (walking from Australia to US) Orbit normal/local vertical for antenna/body module. 2nd Mode (stationed over US): Earth signal to interferometer/orbit normal	Hybrid (dumbell) Gravity Gradient and constant speed flywheel	Stabilized to Interferometer ground station/sun
Solar Array Module	Sun Sensor +2 DOF Gimbal to fully orient the array to sun	Sun Sensor +2 DOF Gimbal to fully orient the array to sun	Fixed to antenna/body module	Oriented to sun by 1 DOF gimbal + vehicle yaw
Accuracy, Degrees per axis	± 0.2	1st Mode ± 0.2 2nd Mode ± 0.1	± 1.0 yaw and roll ± 2.0 pitch	± 0.1
ANTENNA POINTING	Open Loop Electrical scanning from main body platform + antenna pointing to local vertical during broadcast	1st Mode Electrical scanning from antenna axis pointed to sub-satellite point, from stable platform. 2nd Mode: Electrical axis of antenna aligned to closed loop interferometer axis (determination of electrical axis requires calibration mode and alignment maintenance is accomplished by elect. scan)	Open loop scanning from vehicle platform with movable feed	Electrical axis is determined by ground test and mechanically aligned to interferometer axis which is maintained by closed loop control

Table 5-3. Weight/Payload Summary

VBMS Configuration Item	HF	VHF No. 1	VHF No. 2	UHF
Satellite Subsystems				
Transmitter/Receiver System	(311)	(27)	(14)	(97)
Transmitters	22	18	5	86
Receivers	9	9	9	11
Filter	280	-	-	-
Broadcast Antenna System	(620)	(360)	(120)	(91)
Power System	(2530)	(1019)	(235)	(338)
Power generation	730	836	158	197
Batteries	1625	114	52	54
Conditioning	75	49	25	87
Array Pointing	100	20	-	-
Attitude Control, Stabilization, & Orbit Correction System	(188)	(344)	(181)	(277)
Autopilot	included in stabilization	included in stabilization	23	9
Mass Expulsion	59	96	58	71
Stabilization	129	235	85	186
Stationkeeping	15	13	15	11
Telemetry, Tracking, & Command	(60)	(60)	(60)	(60)
Structure	(480)	(250)	(80)	(120)
Thermal Controls	(352)	(400)	(31)	(63)
Electrical Distribution	(200)	(100)	(50)	(80)
Spacecraft Wt. (in orbit)	4741	2560	771	1126
Spacecraft Adapter	-	-	-	78
Apogee Motor	-	-	-	1330
Spacecraft at Booster Separation	4741	2560	771	2534
Booster Adapter	129	89	64	107
Launch Weight	4870	2649	835	2641
Booster	Titan 3F/ Stretched Transt.	Titan 3F/ Transtage	SLV-3A/ Improved Agena D	SLV-3A/Imp. Agena D & Apogee Kick
Payload Capability	5000	3200	800	2750

Numbers within parentheses indicate total subsystem weight

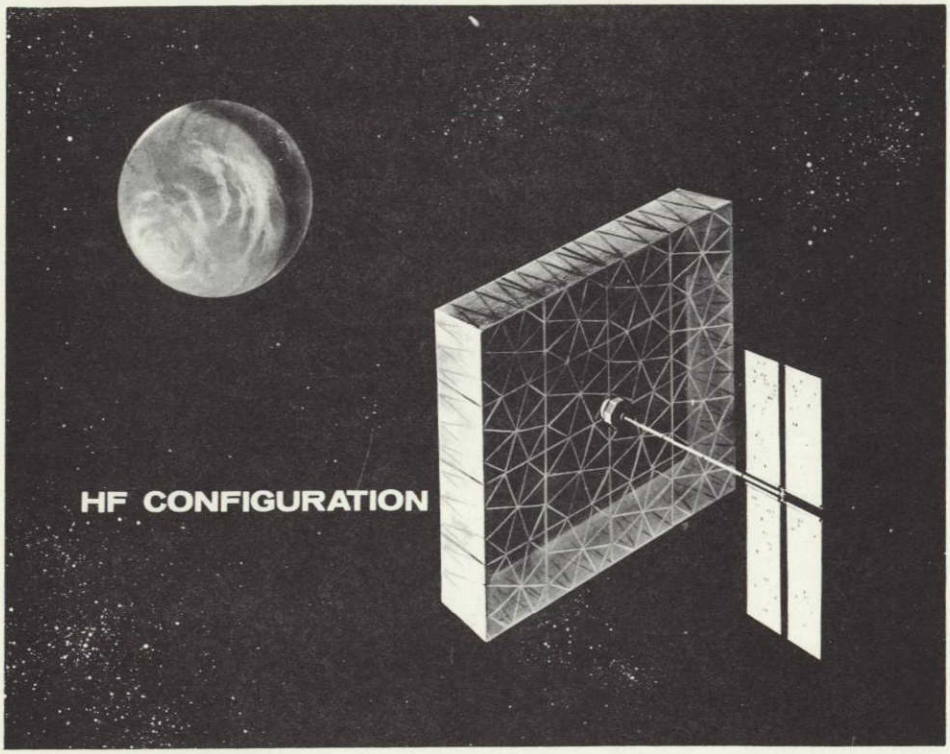

a. Artist's Representation

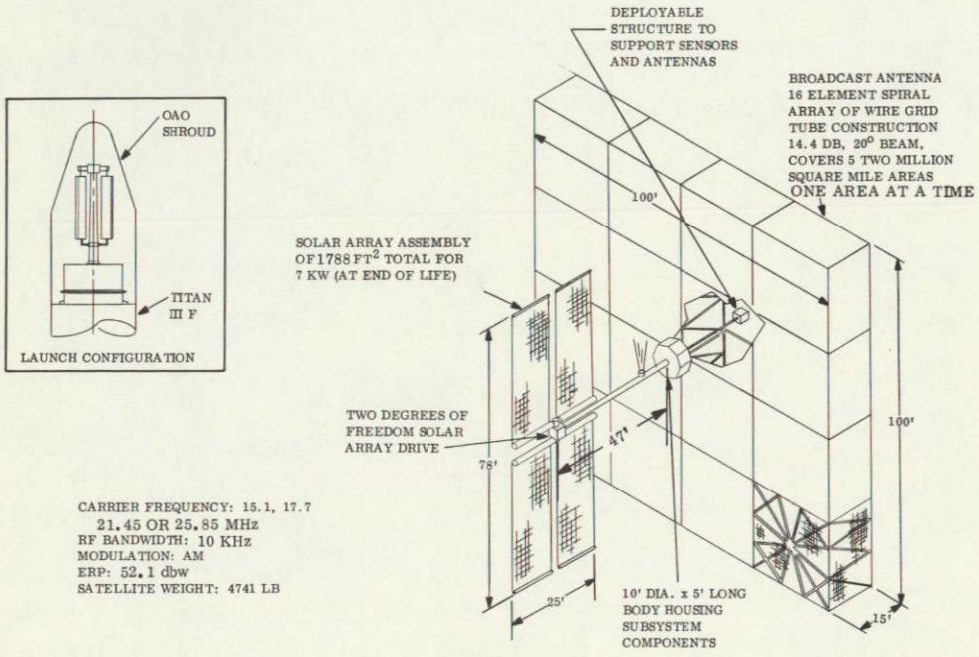

b. Isometric

Figure 5-1. HF Configuration

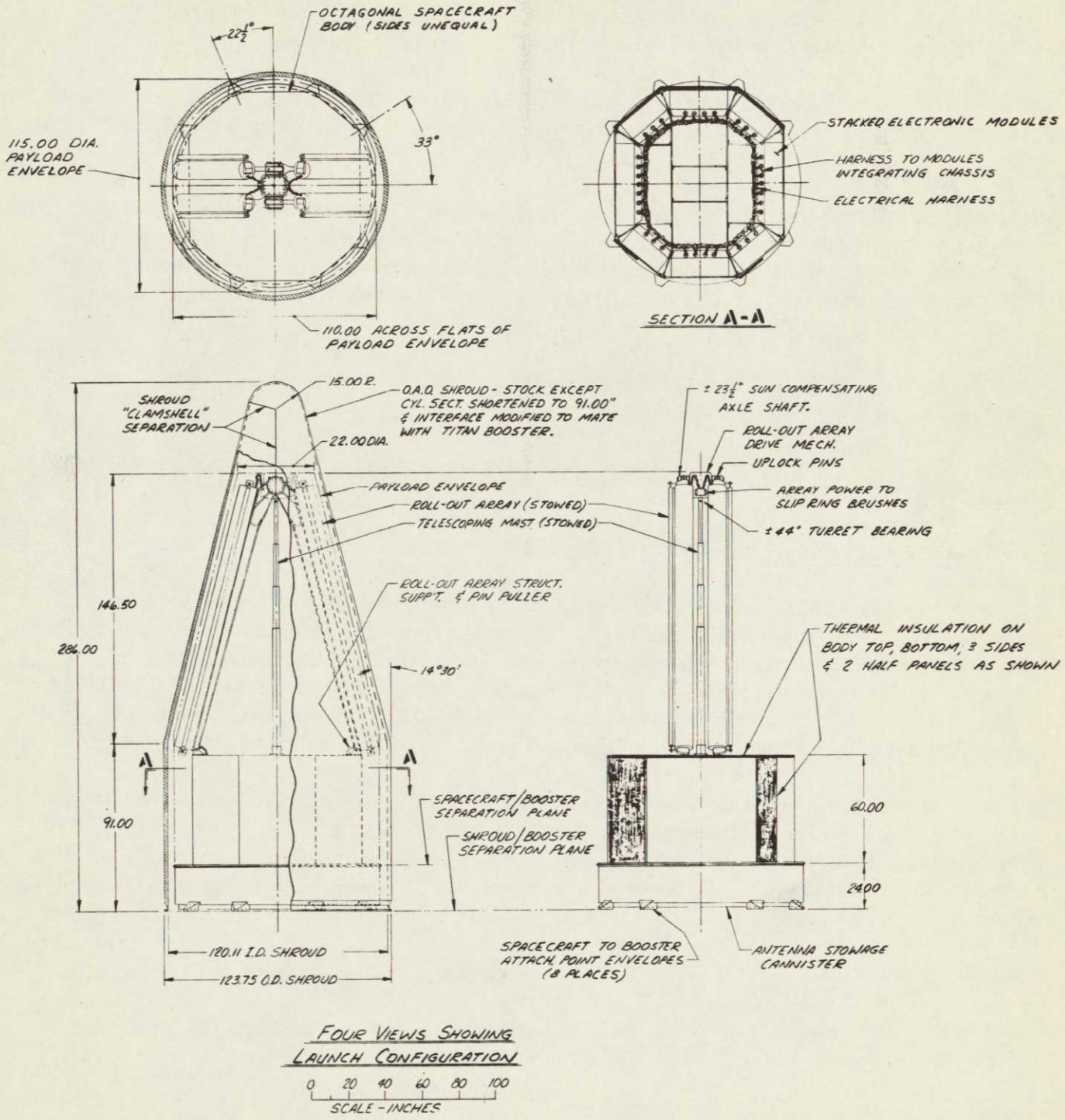

Figure 5-2. HF Launch Configuration

The shroud selected is a modified OAO shroud, with the cylindrical section shortened 61 inches; this selection was made on the basis of availability and relative ease of modification and adaptation to the Titan III. An additional consideration was the lower shock pulse associated with the OAO separation technique employing explosive nuts, as compared to the shaped charge separation systems employed by other candidate shrouds.

The four roll-out arrays are stowed so that they become an integral unit for accommodation of the launch loads, by utilization of fittings tieing down each stowage drum to the spacecraft body.

Electronic components are assigned to a toroidal section around the periphery of the body so as to accommodate heat dissipation requirements. Flat sides were chosen for the body to permit usage of modularized electronic packaging techniques similar to those employed on Mariner and Ranger. Harnessing is shown as a ring harness around the inside of the equipment section.

The antenna stowage canister is housed within the booster adapter and is exposed upon spacecraft separation from the adapter.

Standard electro-explosive devices are assumed for the initiation and/or actuation of the required separations and deployments.

5.2.1.2 Orbital Configuration

A general arrangement two-view of the HF orbital configuration is presented in Figure 5-3, and a plan view is presented in Figure 5-4. The positions of the articulating components are related to the subsatellite point being at a 4:00 PM earth time at either vernal or autumnal equinox, which is approximately 6 minutes after start of broadcast (thus the area being broadcast to on the earth is approximately at 5:36 PM). The +Z axis then points to earth along the local vertical, with the axes determined by the standard right-hand rule.

The most significant geometrical aspect of the satellite is the size of the broadcast antenna and solar array, and the necessary separation to avoid shadowing of the solar array by the antenna during the latter period of broadcast. This effect along with the considerations with respect to broadcast time noted above, can be more easily seen by referring to the orbital motion diagrams of Section 4.5.

5.2.2 VHF NO. 1 SATELLITE

An artist's representation of the VHF No. 1 configuration is shown as view (b), of Figure 5-5. as view (b), of Figure 5-5.

5.2.2.1 Launch Configuration

The satellite is shown in the launch configuration in Figure 5-6, in a very similar arrangement to that of the HF configuration. The booster interface is the Titan transtage with the same general comments applicable. The OAO shroud was selected for the same reasons as in the HF system, and the solar array stowage is similar.

FOLDOUT FRAME 1

FOLDOUT FRAME 2

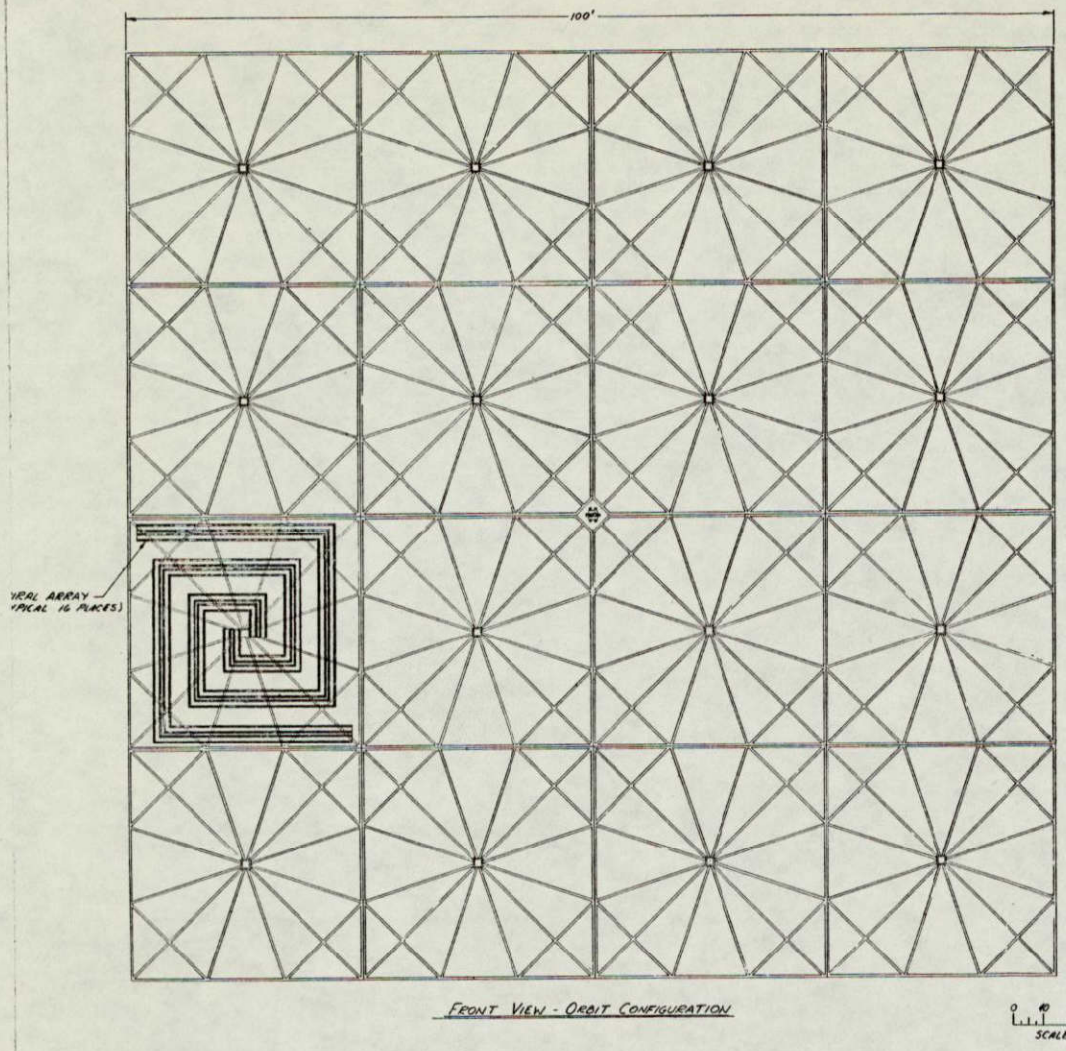

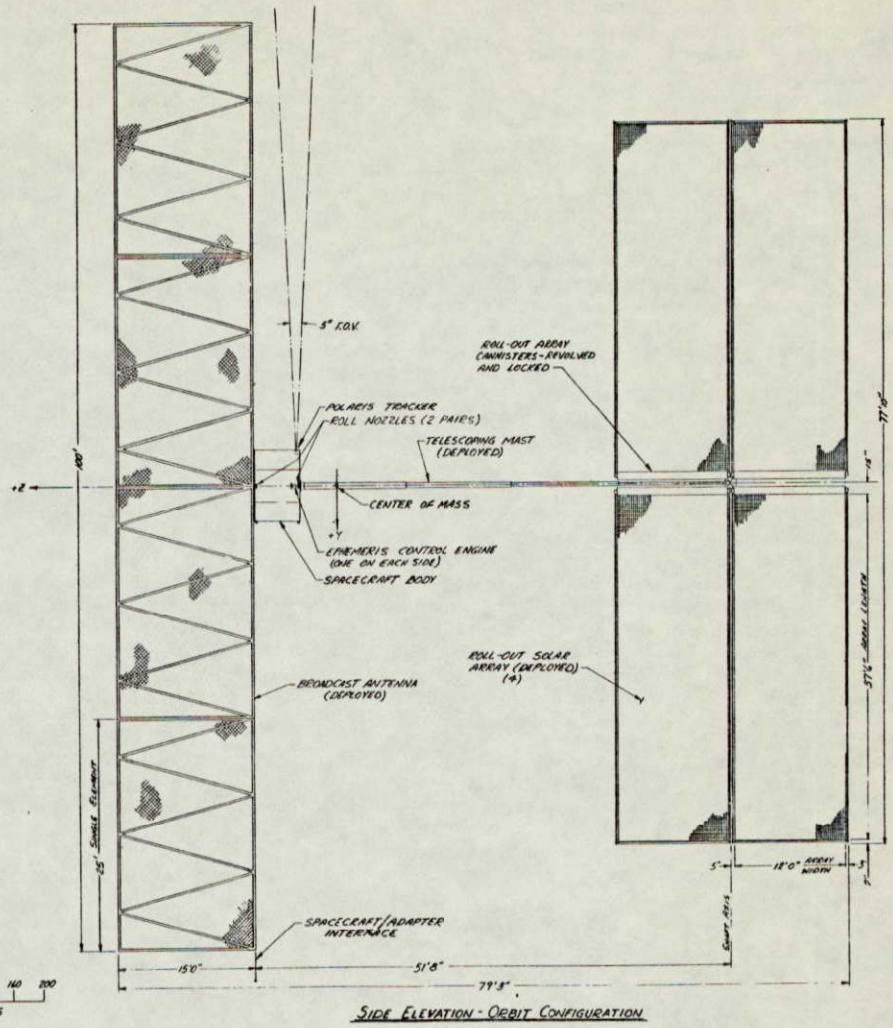

Figure 5-3. HF Orbital Configuration (Two-View)

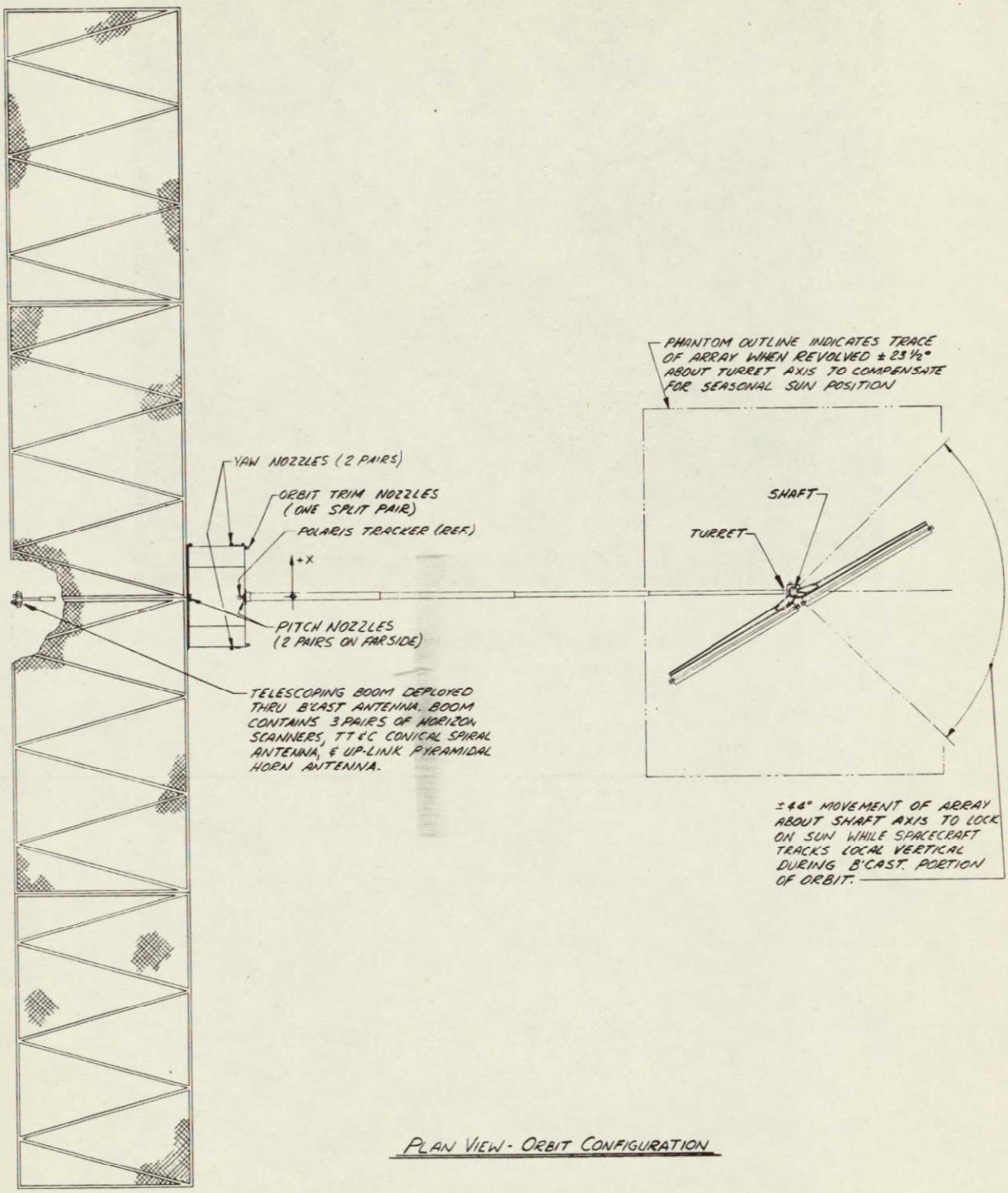

Figure 5-4. HF Orbital Configuration (Plan View)

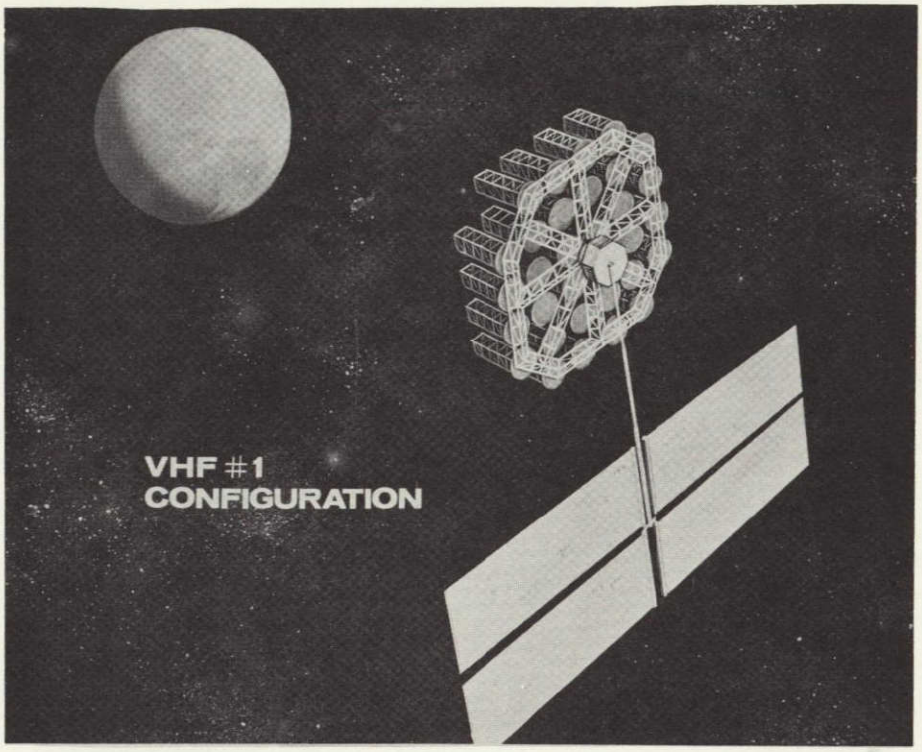

a. Artist's Representation

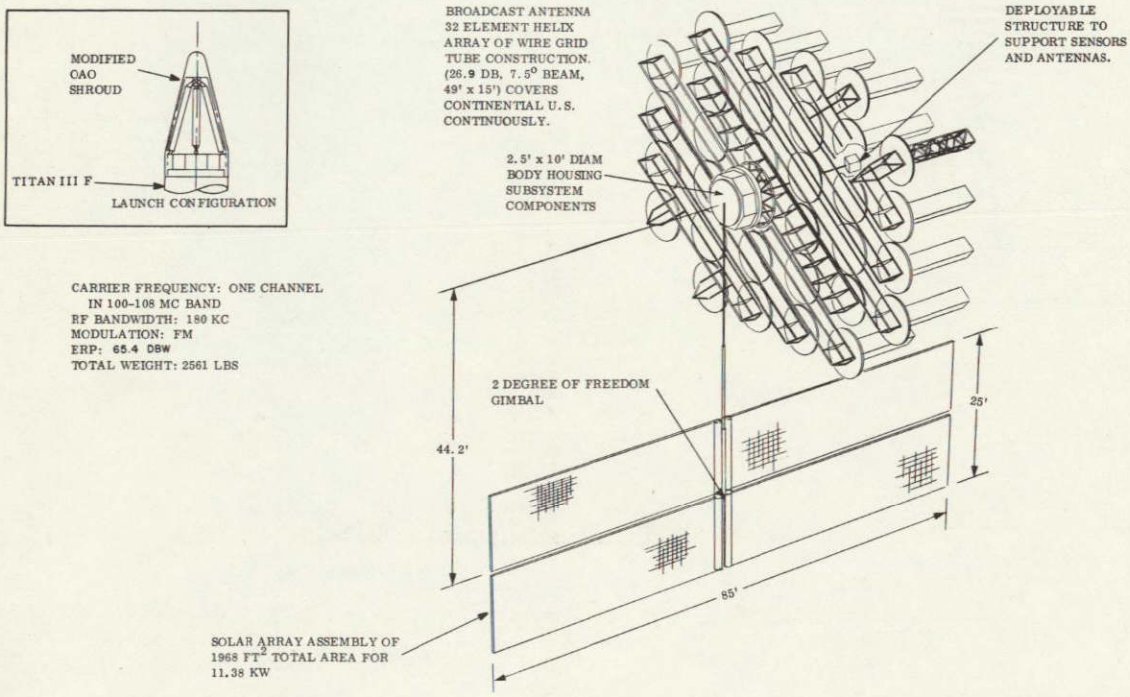

b. Isometric

Figure 5-5. VHF No. 1 Configuration

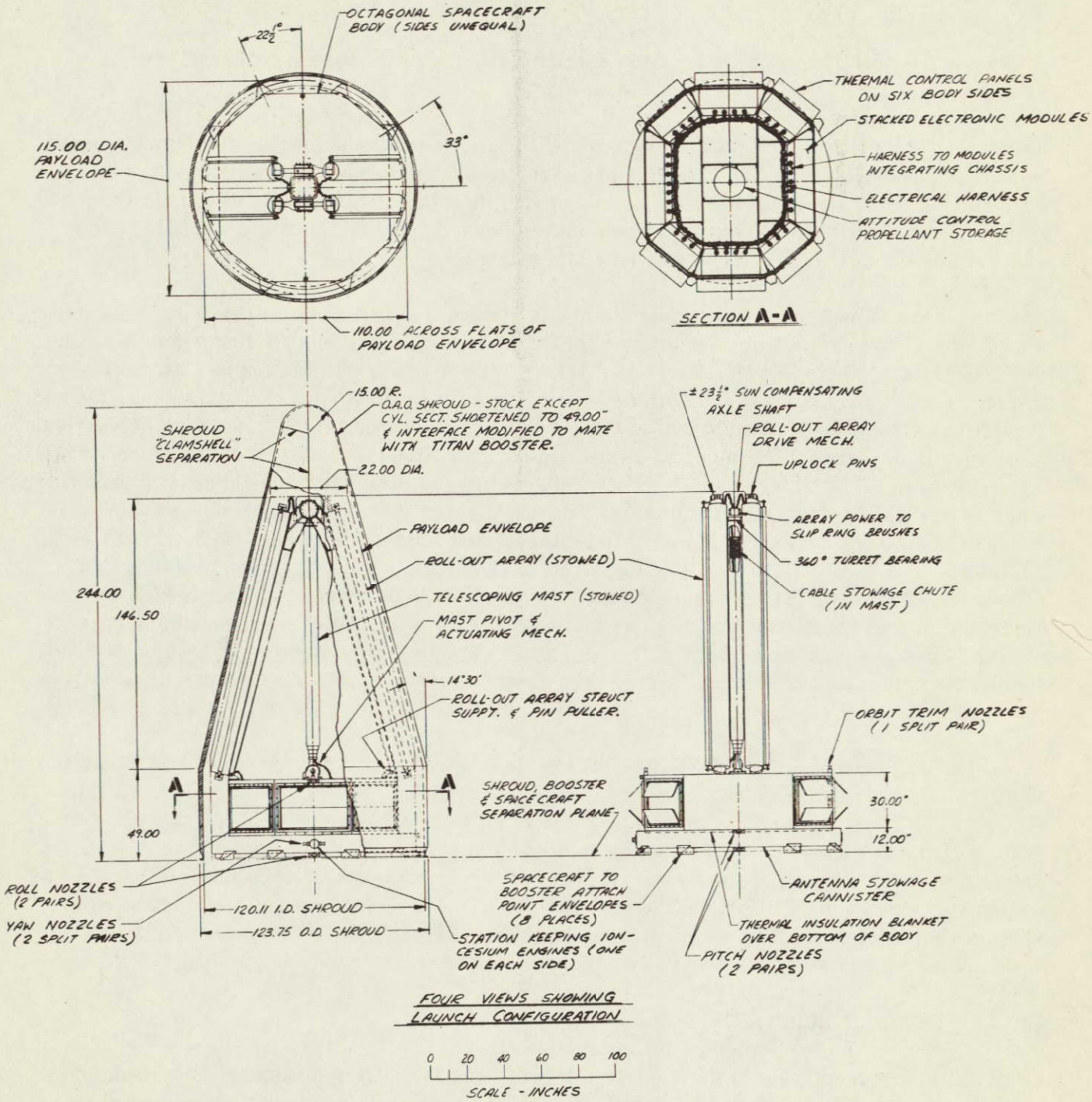

Figure 5-6. VHF No. 1 Launch Configuration

The only significant difference is the location of electronic equipment on the top surfaces as well as around the eight sides.

5.2.2.2 Orbital Configuration

A general arrangement two-view of the satellite in the orbital configuration is presented in Figure 5-7.

The satellite as shown would be at the 6:00 PM position at equinox, when the antenna axis is parallel to the local vertical. The axis of the telescoping mast is maintained normal to the orbit plane by means of a Polaris tracker and the mast/antenna/body assembly then makes one revolution per day around this axis. Seasonal variation of the sun line is then removed by another single degree of freedom gimbal.

The articulation described above takes place at the gimbal at the hub of the deployed solar array, the first being accomplished by a 360^{o} bearing - electrical slip ring assembly, and the second by a single degree of freedom joint ($\pm$ 23 1/2^{o}) and flexible cable. The decision to place the spacecraft body (containing the transmitter components) on the antenna side of the articulations was primarily due to the tradeoff between rotating RF joints and electrical slip rings being strongly in favor of using slip-rings. An additional trade considered was selection of the type of body-mounted station keeping engines, which would be different if the body were rotating with the antenna or fixed with the array. A rotating body has the capability of utilizing a continuously operating microthrust engine, whereas the fixed body is restricted to a higher thrust short pulse system at certain points in orbit. Another consideration was the displacement of the thrust vector from the center of mass which is considerable in this configuration; the lowest thrust system was desirable from the standpoint of being able to accommodate the disturbance forces with the momentum wheels on a continuing operation basis, since this E-W thrust vector creates a cyclic torque with a daily period.

A significant disturbance torque on the vehicle is caused by solar pressure. Positioning of the various items has been made to minimize this torque.

Four roll-out solar arrays were chosen to provide a practicable unit size and to enable location of the gimbal near the center of mass of the array system, thus minimizing the variance of moments of inertia with respect to time. The deployment mast must be provided with sufficient rigidity to accommodate the flexible structure/attitude control interaction, and may be the object of a development program.

5.2.3 VHF NO. 2 SATELLITE

An artist's representation of the VHF No. 2 configuration during broadcast is presented as view (a) of Figure 5-8. View (b) shows the satellite isometric view, with pertinent physical characteristics.

FOLDOUT FRAME 1

FOLDOUT FRAME 2

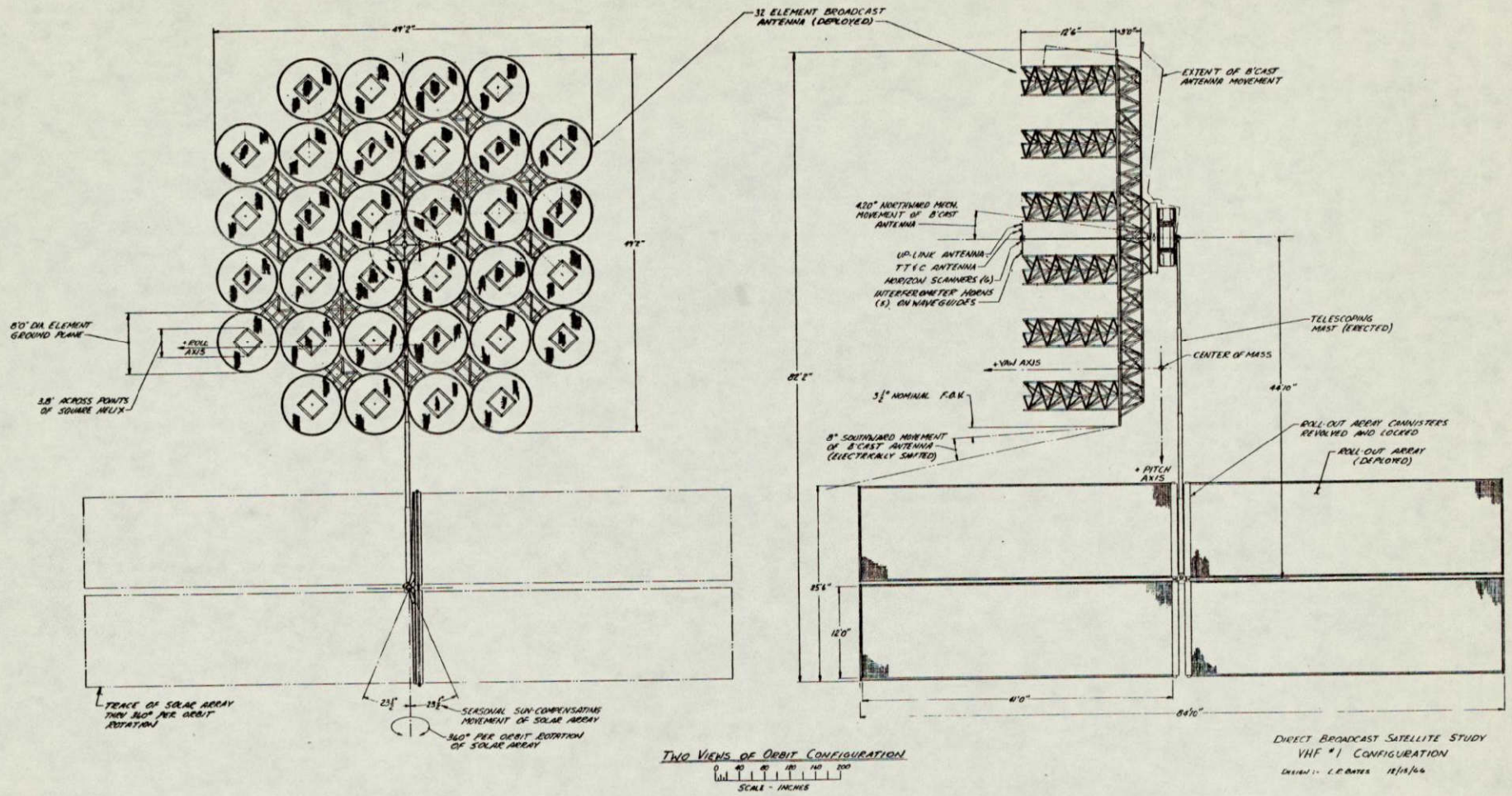

Figure 5-7. VHF No. 1 Orbital Configuration (Two-View)

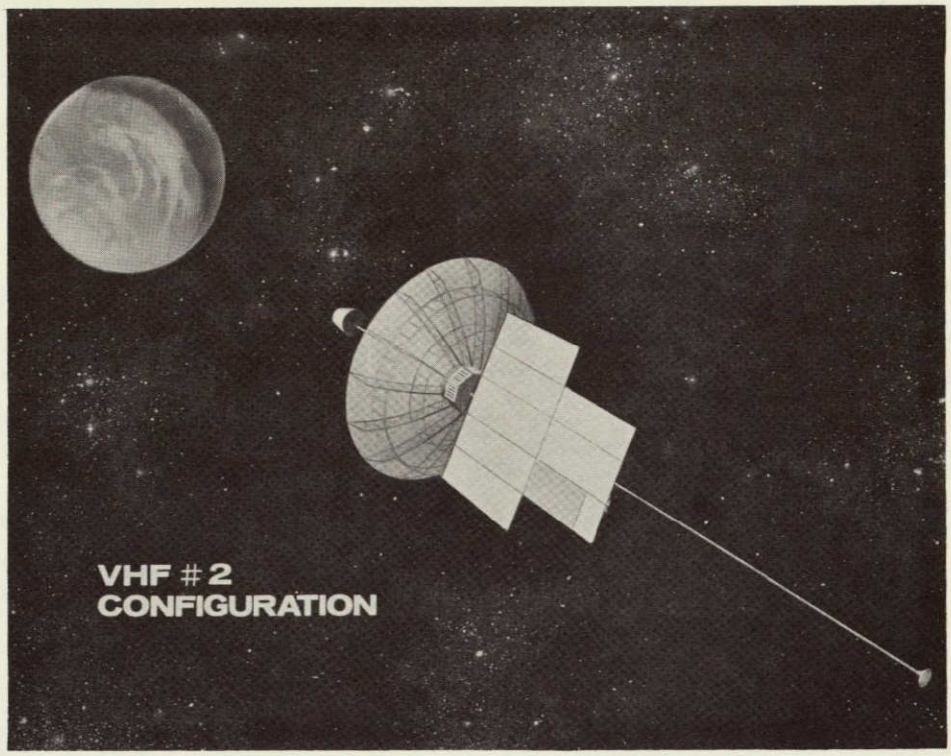

a. Artist's Representation

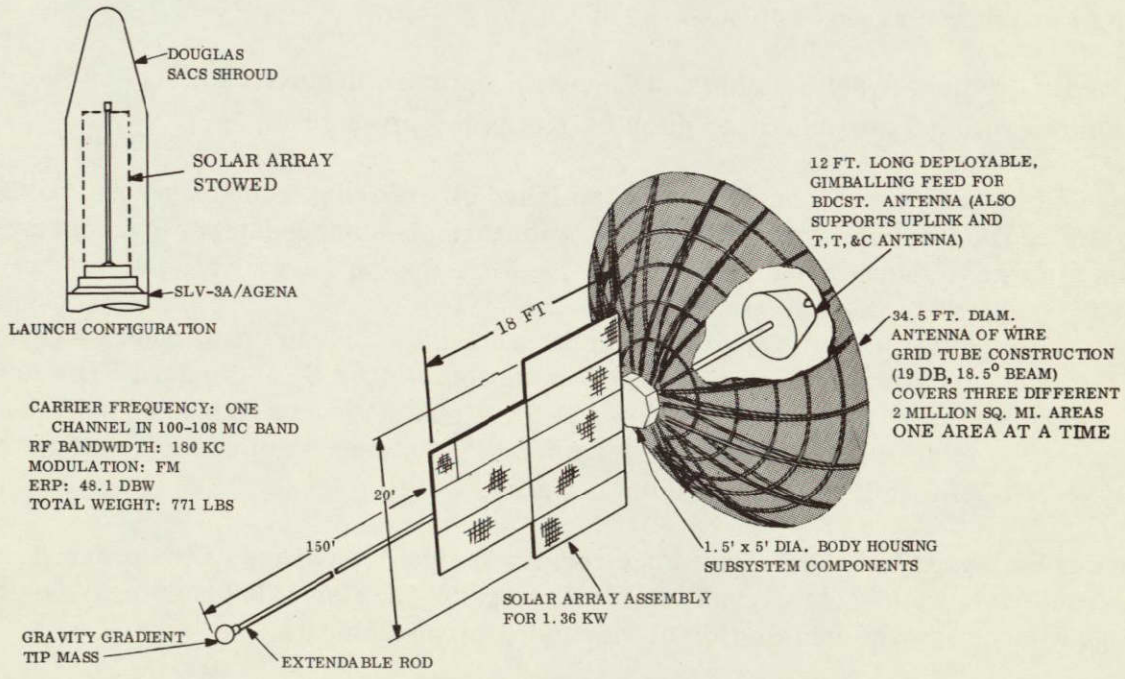

b. Isometric

Figure 5-8. VHF No. 2 Satellite

5.2.3.1 Launch Configuration

The satellite is shown stowed for launch in Figure 5-9. The booster selected was the SLV-3A/Improved Agena D.

Choice of shrouds was limited to the 5-foot diameter Douglas SACS shroud or to the 10-foot diameter class, such as the OAO or Surveyor shrouds.

The selection of the SACS shroud was made possible by the selection of the wire grid tube antenna and its small package volume before deployment, and it was therefore selected on the basis of available payload, shroud availability, flight qualifications, and cost.

5.2.3.2 Orbital Configuration

The spacecraft is shown in the orbital configuration in Figure 5-10. One significant design consideration is the antenna control which is accomplished by antenna feed pointing plus a flywheel-stiffened gravity gradient earth-oriented system. This permits proper angle of incidence of the sum with the plane of solar cells during broadcast, and the thermal control and power requirements during the rest of the orbit.

The drawing shows the satellite in the nominal broadcast position at 6:00 PM with the + yaw axis pointing to the earth along the local vertical vector. The (+) pitch axis then nominally points to celestial south (Canopus) at the solstices and the (-) pitch axis to Polaris at time of the equinox, with variation in between to nominally keep the solar array surface normal to the sun line. The variation of solar flux incidence during broadcast is shown in the top view, showing a maximum angle of 30^{o}.

The gravity gradient system employs a 15-pound tip mass deployed 150 feet as shown to maintain the ratio of yaw inertia to pitch inertia in the proper balance ($I_{yaw}/I_{pitch} = 0.10$).

Deployment of solar array panels is accomplished by uncaging launch tie-down points and automatic sequential unfolding of the panels with torsion-spring-damper-overcenter latch devices similar to those being developed on the JPL-Boeing Large Area Solar Array program.

The two degree-of-freedom gimballing mechanism for the antenna feed must be caged to withstand the launch environment. Release will be accomplished by a standard EED device, such as a pin-puller. The uplink antenna and the TT&C antenna are housed with the main antenna feed to minimize interface problems with the antenna and to accommodate the scan requirement for the uplink along with the downlink.

The octagonal shape body with eight longerons is desirable because of the proxmity of the body structure to the 8-point Agena interface. Again, the flat-sided body provides easy component mounting and installation of thermal control elements.

Another feature to be noted is the 32 square feet of auxiliary solar cells to be used to supply the housekeeping power for the orbit phase from early morning to noon. At this time, the main solar cell surface of 294 square feet is pointed away from the sun.

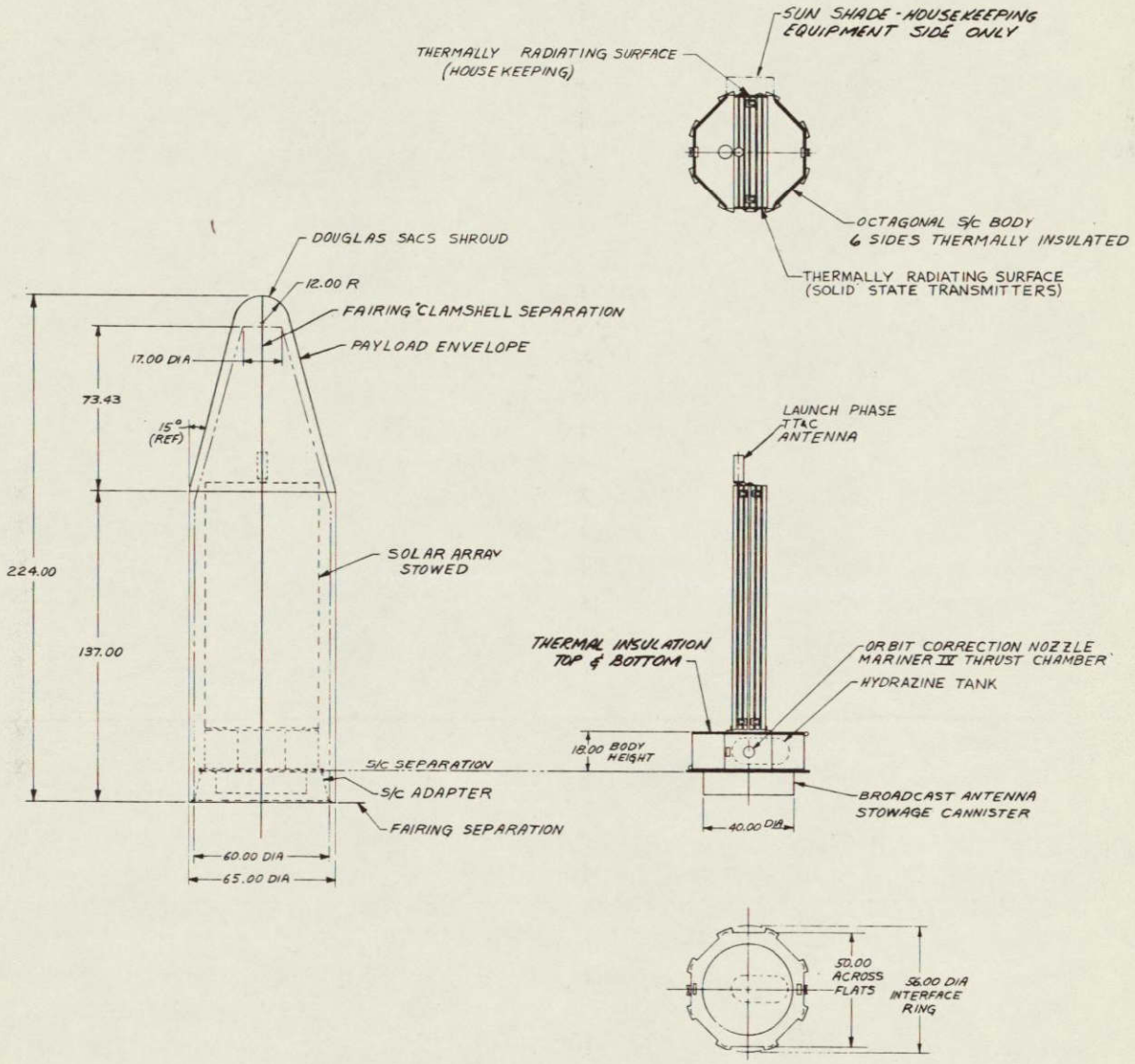

LAUNCH CONFIGURATION & S/C BODY DETAILS

Figure 5-9. VHF No. 2 Launch Configuration

FOLDOUT FRAME 1

FOLDOUT FRAME 2

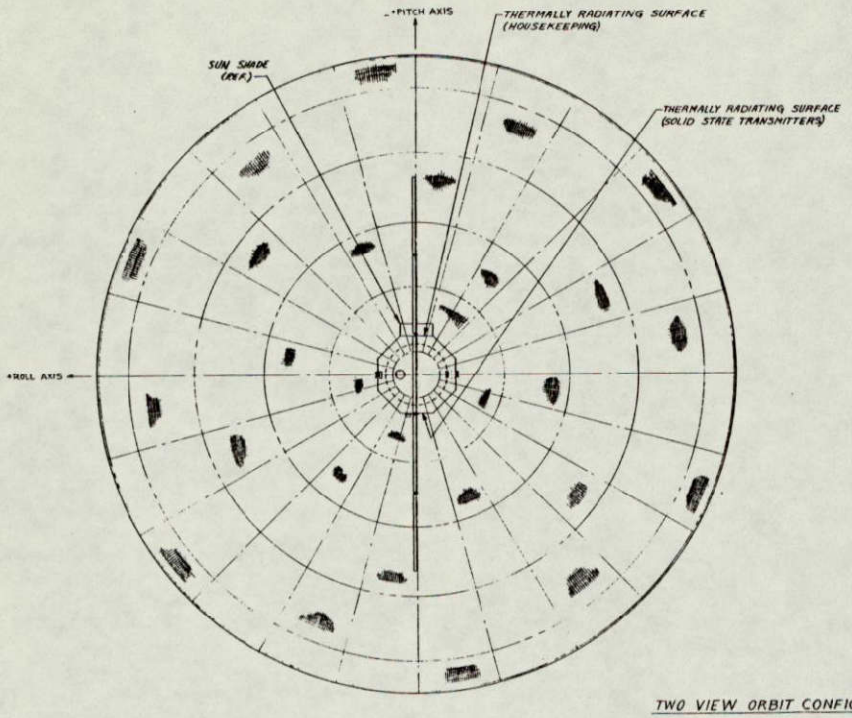

TWO VIEW ORBIT CONFIGURATION

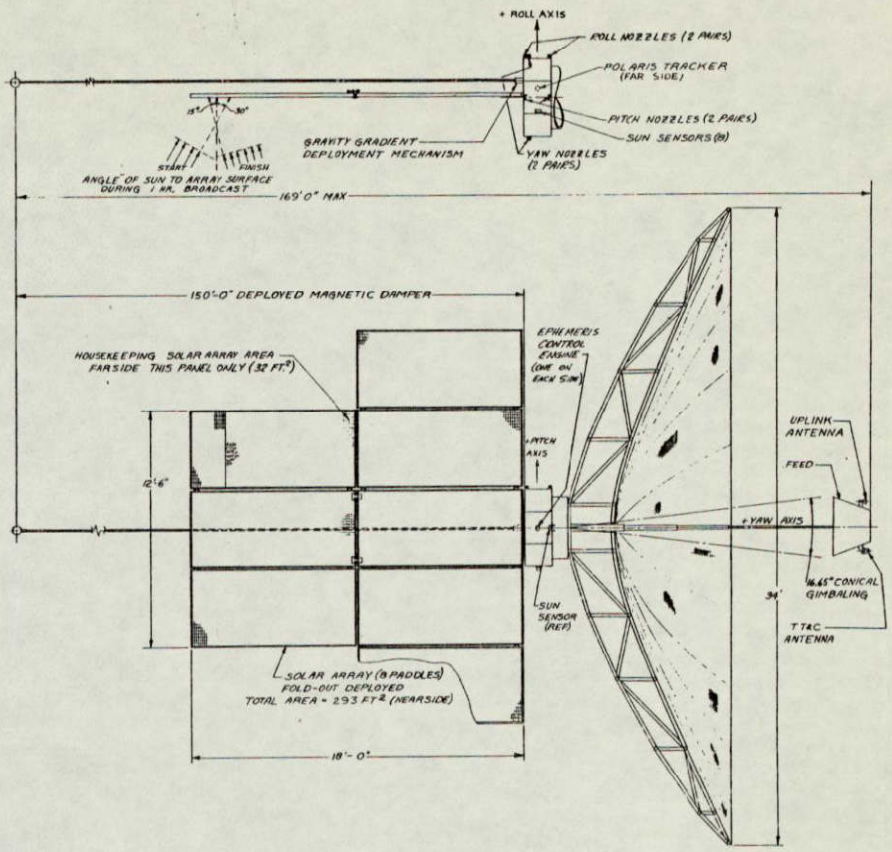

VHF #2 CONFIGURATION

DIRECT BROADCAST SATELLITE STUDY

SCALE: 1/20

Figure 5-10. VHF No. 2 Orbital Configuration

The antenna feed system was envisioned as a telescoping system to be deployed pneumatically or with a motor-driven sliding rail system. The deployed feed has requirements for structural stiffness and damping characteristics which impose design/development problems, and is subject to further study.

5.2.4 UHF SATELLITE

An artist's pictorial representation, showing the UHF satellite at 6:00 PM, is shown as view (a) of Figure 5-11. The satellite isometric with pertinent characteristics is shown in view (b) of the figure.

5.2.4.1 Launch Configuration

The UHF launch configuration is presented in Figure 5-12. Selected booster was the SLV-3A/Improved Agena D/Surveyor series apogee kick motor. The booster adapter has a booster interface very similar to that of the Nimbus spacecraft, but the interface to the apogee motor is expected to be an 8-point V-clamp/cable system similar to the Mariner system. The spacecraft adapter accommodates the 3-point adapter of the Surveyor motor and the 8-point interface with the vehicle body. Separation after apogee motor burn is effected by a V-clamp joint.

Rocket nozzles placement minimizes plume impingement on any surface during the spin axis precession, orbit injection, and orbit trim modes. Resultant thrust vectors during any mode must be directed through the center of mass.

5.2.4.2 Orbital Configuration

The spacecraft is shown in Figure 5-13 as having deployed to the orbital configuration by uncaging and erection of the roll-out solar panels and the antenna. Initiation of all uncaging, separating, and deploying devices would be effected by standard squib-actuated devices such as explosive nuts, pin-pullers, or gas thrusters, since the design requirements do not appear to require any unique features.

The roll-out solar array panels would be deployed by extendable rod devices along the principles of Hunter spirator, the deHaviland STEM, or possibly the Ryan foldable beam concept, depending upon the natural frequency requirements of the system.

Utilization of a membrane substrate on the solar cells will permit relatively easy detuning of the array frequency from the expected vibration environment. The solar array panels were symmetrically arranged in two panels to minimize solar pressure pitch torques in the noon and midnight positions. The particular stowage and deployment arrangement permits utilization of a central drive motor system to rotate the arrays.

The antenna structure is deployed by means of a pneumatic system to pressurize the wire grid tube members. The antenna feed is a fairly rigid telescoping-type structure to support the necessary additional equipment and maintain a desired natural frequency.

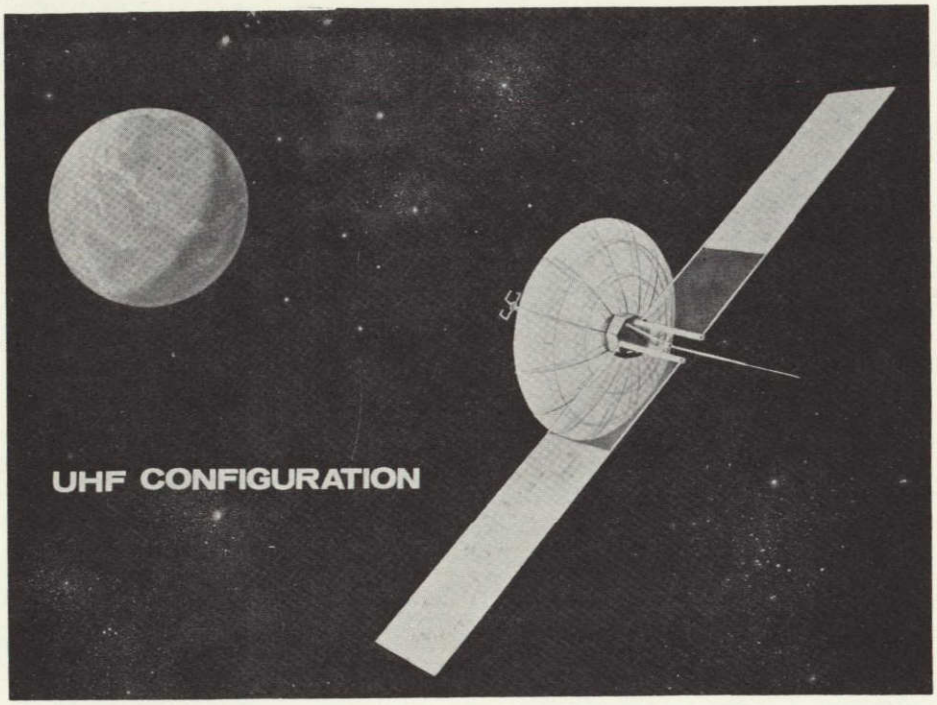

a. Artist's Representation

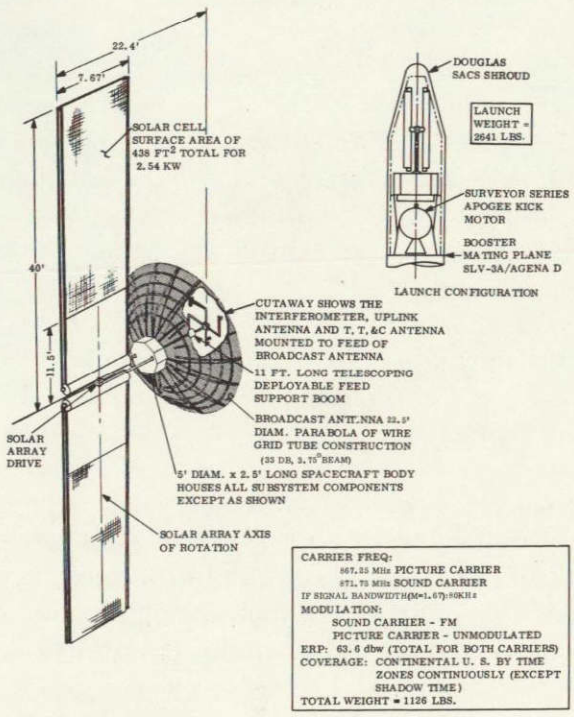

b. Isometric

Figure 5-11. UHF Satellite

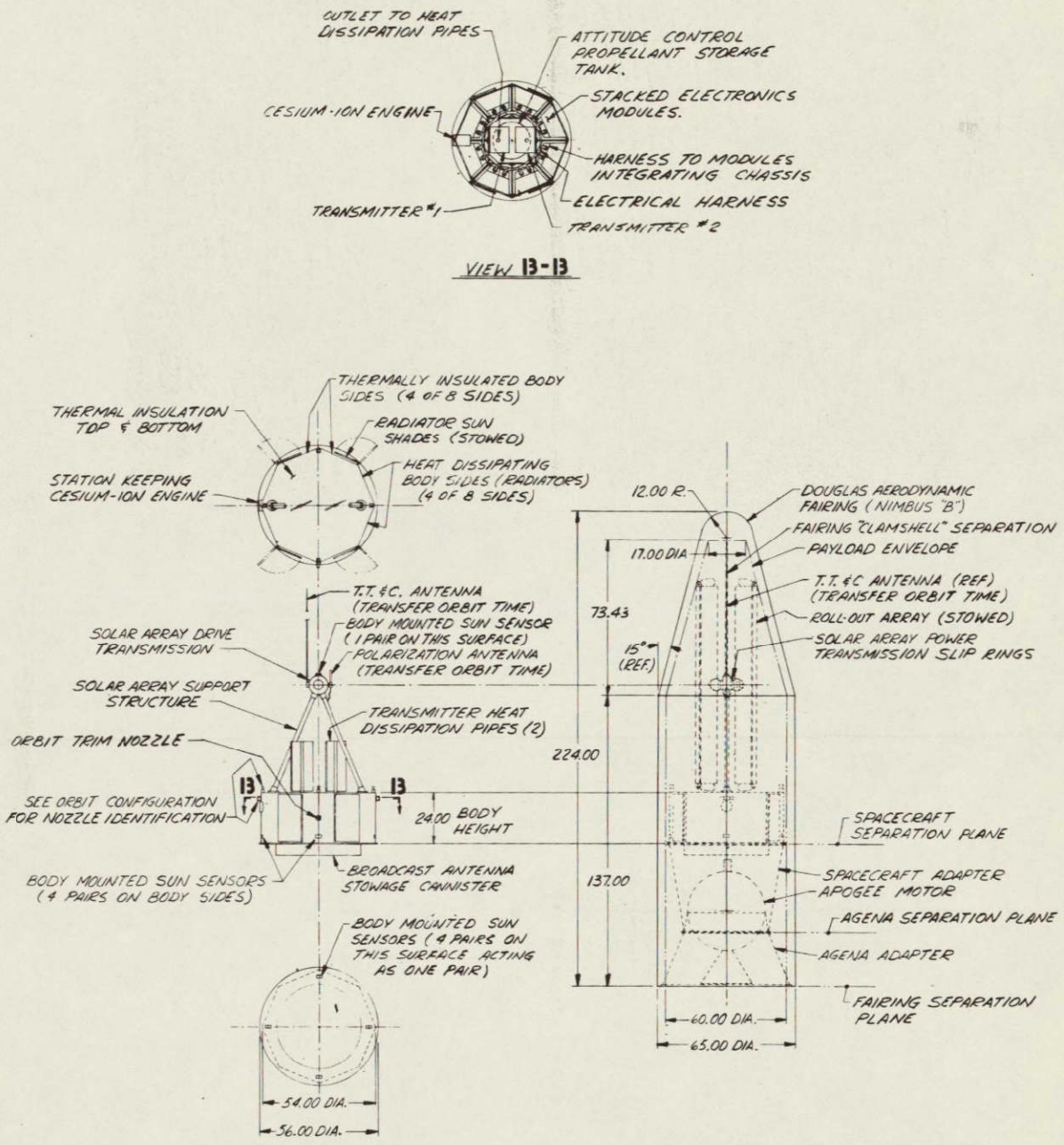

Figure 5-12. UHF Launch Configuration

FOLDOUT FRAME 1

FOLDOUT FRAME 2

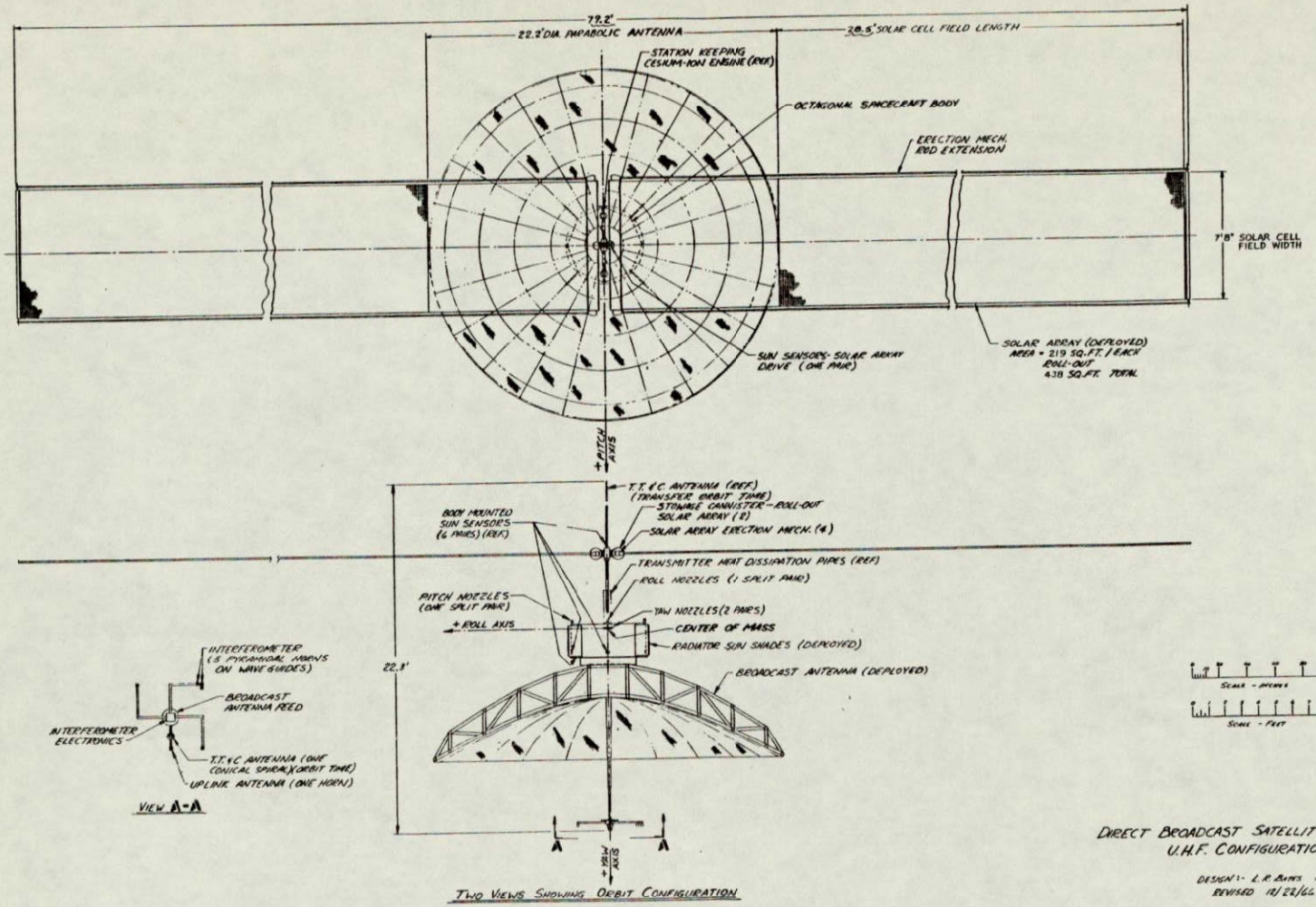

Two Views Showing Orbit Configuration

Direct Broadcast Satellite Study
U.H.F. Configuration

Design :- L.R. Bates 11/11/66
Revised 12/22/66

Figure 5-13. UHF Orbital Configuration

The selection of an 8-sided structure rather than 4 or 16 sides was made based upon an 8-point back-up structure in the booster. The other considerations made were packaging volume related to package size and surface area and orientation requirements for thermal control. Flat sides rather than circular were selected to facilitate standardized component packaging techniques (such as used on Mariner, Ranger and Nimbus) that are compatible with thermal control requirements.

The heat pipes for transmitter temperature control were mounted on the end of the spacecraft nearest the solar array. The vacuum tube operates at a high temperature enabling a compact design of this system. Two pipes are shown for redundancy.

The housekeeping system utilized four radiating surfaces and four automatically operated sun shades to prevent sun impingement on the surfaces and to act as insulation during the occultation periods.

SECTION 6

SYSTEM AND SUBSYSTEM EVALUATION

6.1 TECHNOLOGY EVALUATION

Each of the subsystem technologies applicable to voice broadcast satellites was evaluated to determine whether the current and projected state-of-the-art will permit the performance required of the subsystems by the early 1970's. The discussions in this section are limited to those technologies which present difficulties or significantly affect the overall system performance, costs, or development schedules. More specifically, technologies have been identified as critical on the basis of:

a. Long lead time required for design and test.

b. Technology state-of-the-art must be extended.

c. High cost of obtaining flight qualified hardware.

Each of the subsystems considered as critical, falls into one or more of the above categories. Subsystems not considered critical (TT & C for example), were not investigated in detail during the study.

6.1.1 CRITICAL TECHNOLOGIES

The subsystems most critical to configuration designs are the power, attitude control, antenna and transmitter. The power and attitude control subsystems both require more time and money to obtain flight qualified hardware than the other subsystems. The antenna and transmitter both require an extension in the technology state-of-the-art which is not now being funded adequately. The reasons for each subsystem being listed as critical are not, of course, completely exclusive. The evaluation of approaches to representitive configurations included examination of a large range of types and of components for each of these critical subsystems. This range is summarized in Table 6.1-1 to establish the context in which the final technology evaluation was conducted. Selections for the four baseline configurations are identified by parenthesis in Table 6.1-1.

Table 6.1-1. Ranges of Critical Technologies

Transmitter	Output Device:	Vacuum Tubes (UHF) Transistors (HF, VHF 1, 2)
	Circuits:	Final Stage Modulation: Class C Amplifier (UHF, VHF 1, 2) Digital Synthesis (HF)
Antenna	Types:	Aperture (UHF, VHF 2) Endfire (HF, VHF 1)
	Construction:	Rigid Folding Inflatable (All)
Power	Energy Source:	Solar (All) Nuclear Chemical
	Conversion:	Photovoltaic (All) Thermionic Thermoelectric
	Pointing:	Fully Oriented (UHF, HF, VHF 1) Fixed Panels (VHF 2) Body Mounted
Attitude Control	Passive:	Gravity Gradient Solar Pressure
	Spin:	
	Hybrid:	(VHF 2)
	Active:	Earth Pointing (VHF 1, HF, UHF) Sun Pointing

Each of the technology areas considered critical to the design of a voice broadcast satellite was found to be within the state-of-the-art for early 1970 systems. However, extensive design is required for any particular satellite configuration. The following is a summary of the evaluation of the critical technologies as they affect a voice broadcast satellite.

Critical Area	EVALUATION
Solar Array	No extension of state-of-the-art needed Large size & deployment techniques require design effort
Attitude Control	Sensor & control components are state-of-art Stabilization of flexible vehicles Stabilization of flexible vehicles are design problems
Antenna	Materials & elements are state-of-art Deployment is a design problem
Transmitter	Devices within state-of-art
Long Life	To achieve long life requires design effort in every subsystem area

Each of these areas is described in the following paragraphs as they pertain to representitive configurations.

6.1.2 EVALUATIONS AND RECOMMENDATIONS

6.1.2.1 Power

The feasible level of solar array output powers as a function of time has been estimated through 1975. This was based on past performance and the probably future capability, as determined by the existing development contracts. The estimated limit of feasibility is shown by the line in Figure 6.1-1. Also shown in the figure for comparison are the estimated power levels and launch times of the four representitive configurations. While, the power requirements of each of the configurations is within the estimated feasibility limit, significant design and test efforts will be required for implementation.

Another measure of the power subsystem performance feasiblity is the power-weight density. As in the power level, an estimate of the feasibility limit was made based on past and projected capabilities. This is illustrated in Figure 6.1-2 by the dashed line. The representative configurations

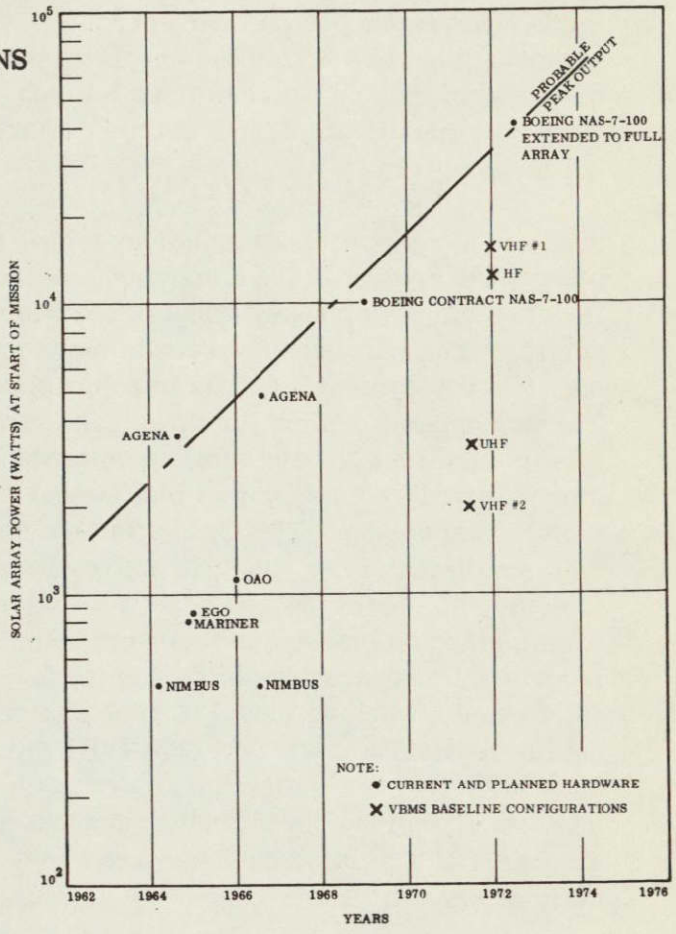

Figure 6.1-1. Solar Array Power versus Time

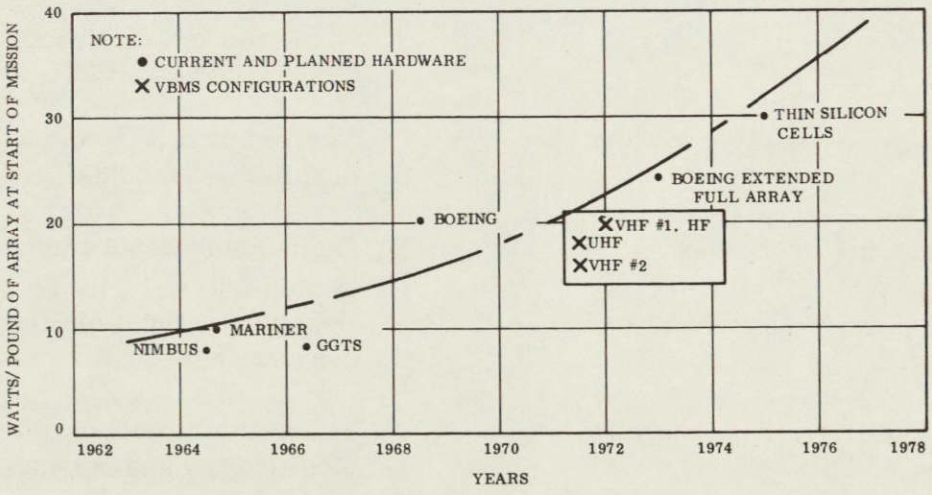

Figure 6.1-2. Solar Array Watts/Pound versus Time

are also shown for comparison. Each of them requires a capability improvement (higher watts per pound) over current technology but are within the expected state-of-the-art for the estimated launch times. However, significant design and test efforts will be required.

Still another significant technology factor for power subsystems is the deployment method. Because the power subsystems of the representative configurations were all solar arrays, only two deployment methods were considered. The deployment method for three configurations was to unroll the array from the powered flight storage drum by extension of bias wound metallic tape rods. The tape is in turn stored on a smaller storage spool; it is prestressed to deploy and form the rod so as on release. This method has been demonstrated with models and appears feasible. Figure 6.1-3 illustrates a working model of such an array deployment. The fourth concept (VHF No. 2) uses rigid frames. The frames are deployed by spring-forced rotation about hinge points on release. This method is an extension of similar techniques used on past space vehicles and can be considered present state of the art.

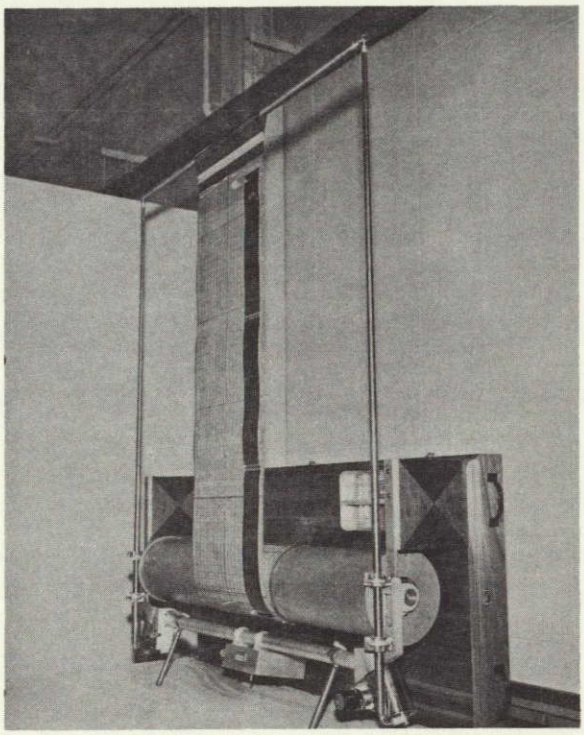

Figure 6.1-3. Rollout Array Model

In summary, each of the four satellite power subsystems is technically feasible for flights in the early 1970's. However, the specific designs are not without problems. These problem areas and the recommended approach to solving them during the design phases are listed below.

Problem Areas	Solution Approaches
Deployment - errection system	Environment & performance testing of full scale models.
Manufacturing Processes	Semi-automated technique required
450° temperature excursions of array	Design of compatible flexible electrical connections
High reliability voltage converter (UHF)	Exhaustive breadboard testing, analysis, Modification and retest.

6.1.2.2 Attitude Control

The evaluation of attitude control technologies differed from the other subsystems in that the performance requirements for the representative configurations are an order of magnitude less stringent than the current state-of-the-art would permit. Satellites have been developed with pointing and stability requirements as low as 0.01 degree. However, these were significantly different in structural characteristics and did not have flexible appendages such as the VBMS inflatible antennas and roll-out solar arrays. The detailed analyses and tests required to verify that the state-of-the-art techniques are sufficient for the VBMS type satellites were beyond the scope of the study but related analyses conducted on other programs indicate that the control subsystems are technically feasible.

The design efforts required to implement any of the "flexible" satellite configurations includes development of mathematical models of the structural interactions and the environmental disturubances, development of control synthesis techniques, and design and development of unique sensors, signal processors, and actuators. Each of these problem areas are discussed below.

6.1.2.2.1 Mathematical Model Development

The first area requiring development is the mathematical model of the spacecraft structure. The broadcast and solar energy collection functions result in several new modeling considerations. The articulation of parts to effect sun and earth pointing concurrently requires that a two-body coupled kinematrix be modeled. The necessity for erection of large structures in orbit requires careful representation of the vehicle transfer functions. The interaction which results from controller/compliance effects may have such deleterious effects upon performance that this phenomenon may be the constraint which determines the weight for the structure.

6.1.2.2.2 Environmental Forcing Functions Model Development

The second area requiring development is the mathematical model of the environmental disturbances which act upon the orbital configuration. Past modeling has been for structures and surface areas which were simply configured and rigid. It will be required to investigate: (1) solar pressure forces acting on flexible solar arrays and on open truss structured antennas, (2) magnetic effects due to large current loops for high power transmitters and large ferromagnetic components, and (3) gravity gradient torques due to mass distributions with large moments, time varying geometry and time varying orientation with respect to the gravity force field direction.

6.1.2.2.3 Development of Synthesis Techniques for the Control Functions

Given the appropriate mathematical model, the environmental disturbance model, and the desired motion of the vehicle and its parts, it is required to develop synthesis techniques for the control forcing function. The techniques developed could be extensions of present synthesis techniques with simulation of the total spacecraft/controller as a verification of

the extensions. The simulation must include any compromises of the desired control forcing functions due to implementation constraints of sensors and actuators.

6.1.2.2.4 Development of Sensors, Signal Processors, and Actuators

The sensor development is important, particularly in the area of RF interferometers to be used to sense the line of sight from the spacecraft to a beacon located in a coverage area. This may be the only sensing method practical for extreme accuracy of beam pointing. Other sensing techniques do not result in sufficient accuracy, except for celestial references which are not readily employed in an earth-pointing mode.

No development requirement is foreseen for other sensors employed, although verification of their static and dynamic accuracy is required along with all interface requirements.

Design of signal processors with high power gain is required. Compensation for low bandwidth controllers as envisioned for large flexible structures will require that low-frequency systems be developed.

Actuators must be designed which are bandwidth limited to very low frequencies. As configured both flywheels and mass expulsion actuators are required. The running noise of the flywheels cannot be allowed to have spectral densities at structural frequencies. Either extremely good bearings must be developed or a mechanical filter must be developed to "float" the flywheel with respect to the spacecraft frame.

6.1.2.3 Antenna

The technology evaluation for satellite antennas has determined that each of the major characteristics of the four VBMS representitive configuration antennas can be independently achieved. However, the combination of these electrical and mechanical characteristics in a space qualified antenna has yet to be done. The gains required at the three frequency bands are not excessive compared to that achieved in ground antennas. Similarly, the surface tolerance requirements are not difficult to achieve.

The phasing of the array antenna elements is similar to techniques currently employed on ground antennas. Even the structural method selected (wire grid tubes) has been demonstrated on smaller antennas and has been flight tested on space structures such as the Echo balloons. The problem for the VBMS antennas is verifying that combining these cahracteristics is indeed feasible. All of the structural and electrical analyses indicate feasibility but extensive testing of the actual antennas or suitable models is required. The major risk area that necessitates the testing is the deployment of the inflatable structure. The testing may be quite difficult because of the requirement to simulate weightlessness (e.g., floating the test item on water or filling it with lighter-than-air gases to overcome gravity) or to reinforce the test structure for testing in a 1-g environment and extrapolating the results to estimate the performance in space.

6.1.2.4 Transmitter

The evaluation of transmitters was conducted in three parts, circuits, vacuum tubes and transistors. In each of these, it was determined the VBMS performance requirements can be met with the current technology capability. However, there are design problems and there are several areas where technology advancement would improve system performance.

The design problems and suggested design approaches to solution for the gridded vacuum tube transmitters are:

Problem Areas	Solution Approaches
Tube Life	Tube parameter derating, high reliability modifications, accelerated life testing
Launch environment	Mechanical isolation, testing

For the solid state transmitters, the design problems and suggested approached to solution are:

Problem Areas	Solution Approaches
Digital modulation technique	Breadboard testing
Multi-Element circuits-combining	Breadboard testing

Two developments that would enhance performance were identified. The first of these relates to vacuum tube life. The vacuum tube is the life limiting component because of cathode wearout. The most promising method of extending the life consistent with maximum device efficiency, would be to use bonded oxide cathodes. These show promise of many tens of thousands of hours of continuous operation. While this development may take too long to permit inclusion of bonded oxide cathode tubes in demonstration flights in the early 1970's, development efforts should begin now so that the resulting long life tubes will be available for later operational missions.

The second area is in solid state device technology. Development is required to increase the voltage rating of existing high power, high frequency transistors, in order to significantly improve their efficiency.

6.1.2.5 Long Life

Historically, the majority of U.S. missile and space programs have involved systems with relatively short operating life requirements, ranging from minutes to months. As a result, reliability effort has not been directed towards the problem of lifetime. Virtually no effort has been given to the problem of zero failure rate for a specified time period, although

work on these factors has increased as a result of the increasing demand of longer duration space operations.

In a broadcast satellite system lifetime and failure-free operation become dominant design factors. The first reason for this is the relatively great cost of the satellite. This means that the satellite equipment must be considered as a long-term investment item, rather than as a short-term expense item. The characteristics of the satellite must be such that there is a reasonable expectancy of attaining the desired life so that charges for "insurance" against its failure are reasonable. In addition, in many broadcast services, the penalties for outage in transmission time are severe. Thus, maintenance of scheduled operation is an important requirement of the system.

In other fields lifetime has always been important. The basic principles and practices of long-life design used in these field are well documented in the literature. One of the earlier and important contributions to this literature is the "Symposium on the Trans-Atlantic Submarine Telephone Cable" published in the Transactions American Institute of Electrical Engineers, 76, Part I (1957). This described the special approaches in research, development, design, fabrication, and test which are necessary if a low-risk, long-life system is to be obtained. Many of these operating principles have been applied in recent programs, i.e., in the Telstar satellites and in the Mariner Mars-Probe vehicles. Theoretical analysis of these techniques is given in the book "Engineering Reliability and Long-Life Design," D. Van Nostrand, publishers.

The principles described in the above programs and references can only be applied when the design phase of a program is instituted. They were not possible to apply in the study since control of lifetime is basically accomplished at the material and component level. As a result, for this study it has been necessary to use evaluations and estimates of what could be accomplished in a realistic long-life program.

It has been noted that normal reliability analysis of the type used in the missile program is not very accurate when applied to a new field (as measured in terms of the absolute accuracy of prediction). However, the relative accuracy of prediction of the comparative characteristics of several designs is quite good. This observation has been used to give a relative measure of the difficulty, and hence the relative cost and duration of the design and fabrication programs for the various satellites considered. The absolute measures of the program schedules and costs given in Sections 6.2 and 6.3 have been derived by review of programs of equal complexity and difficulty. In addition, each major subsystem has been investigated for critical problem areas. Where these have been found, approaches to solutions to the problems have been indicated and the risk areas for these approaches tabulated.

Table 6.1-1. Summarizes the long-life risk areas in terms of hardware complexity and development status for the major subsystems employed in one or more of the four configurations conceived during the study.

Table 6.1-2: Technology and Hardware Status

State-of-the-art / Complexity of Subsystem	Requires Research and Development	Requires Design and Qualification Test	Available Flight Qualified Equipments
Simple, electronic, or passive		• Fixed Solar Array	• Low Power Transmitters • Small Antennas • Power Conditioning
Moderately complex, electro-mechanical, or hybrid	• High-Power Rotary Joints, • Interferometer	• Hybrid Stabilization, • Medium Articulated Solar Arrays, • Semi-Passive Cooling, • Phased Array Antennas, • Flywheels for Large Spacecraft • High Power Transmitter	• Kick Motors • Receivers • TT&C • Station Keeping • Earth Sensors
Very complex, deployed, or active	• Active Flexible Stabilization • Large-Deployed Solar Arrays, • Large-Deployed Antennas • Articulated Large Appendages	• Active Cooling,	• Active Rigid Stabilization • Boosters • Star Sensors • Injection Autopilot

6.2 PROGRAM PLANS

6.2.1 INTRODUCTION

In order to display the several parallel and interrelated events on a time scale of the program, a summary schedule and a project schedule are presented for each configuration (Figures 6.2-1 through 6.2-8).

The NASA Phased Project Planning approach was used as a basis for these schedules. The objective was to attain an optimal balance between time, money, and risk.

6.2.2 PHASE PROJECT PLANNING

The major task areas for phases B, C and D are listed below:

a. Phase B - Project Definition Phase

1. System and design analysis
2. Selection of preferred system
3. Initiation of critical item development
4. Development of preliminary system specification
5. Development of preliminary subsystems specifications
6. Development of initial work breakdown structures
7. Preparation of phase C program development plan and schedule in detail
8. Preparation of preliminary phase D program development plan and schedule
9. Development of project management plans to include engineering, integrated test, quality control, reliability, manufacturing, procurement, safety, configuration management, project control and data management plans
10. Preparation and submission of phase B final report

b. Phase C - Design Development

1. Development of preliminary design to the component level
2. Completion of system analysis
3. Finalization of system and subsystem specifications

4. Preparation of component and interface specifications

5. Design and fabrication of test support equipment

6. Design, fabrication and test of subsystems for various system units

7. Design, fabrication and test of structural dynamics model

8. Design, fabrication and test of Engineering Development model

9. Start assembly of Prototype Spacecraft

10. Finalization of all phase D technical and management plans

11. Start of design and fabrication of launch support and checkout equipment

12. Start of modification effort on ground stations

c. Phase D - Operational Hardware Phase

1. Completion of design and fabrication of launch support and checkout equipment

2. Completion of ground station modifications

3. Complete fabrication and testing of prototype spacecraft

4. Fabrication and full flight acceptance testing of two flight spacecraft

5. Delivery of flight vehicle to launch site and provision for launch support

6. On-orbit operation support of the satellite

It should be noted that the development effort on critical items must be scheduled in advance of phase C in order to perform within the schedule depicted. These are necessarily the pacing items and the duration of the entire program is a function of when their development begins.

6.2.3 SCHEDULE

The objective in developing the schedules was to blend risk, time and money into a logical and yet practical plan from conceptual studies to launch.

Total system interaction will be verified with the assembly and testing of the Engineering development spacecraft. This model is used not only to prove design under earth ambient conditions, but also to gain confidence that the system will survive the operational environment.

Rather than use the serial approach to phase project planning and have phase D begin upon the completion of the procurement cycle for prototype and flight spacecraft, an overlapping of phase C and D activities was used in the overall schedule. This was done to:

a. Eliminate restart time needed in serial approach

b. Maintain continuity of personnel

c. Shorten procurement time

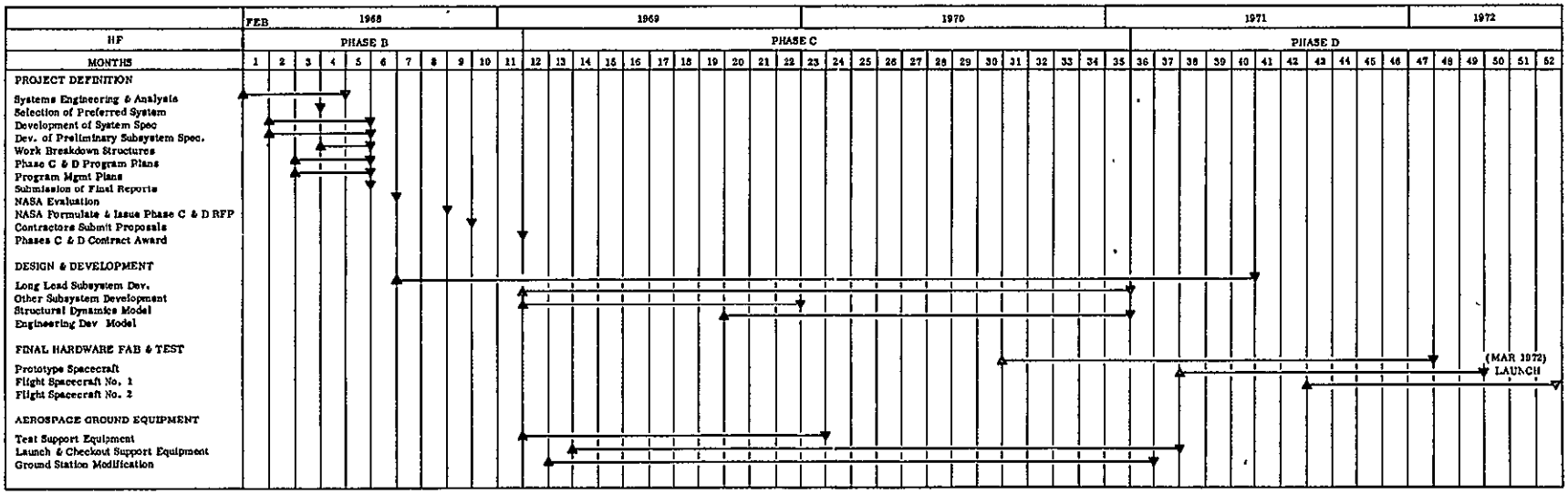

Figure 6.2-1. HF Summary Schedule

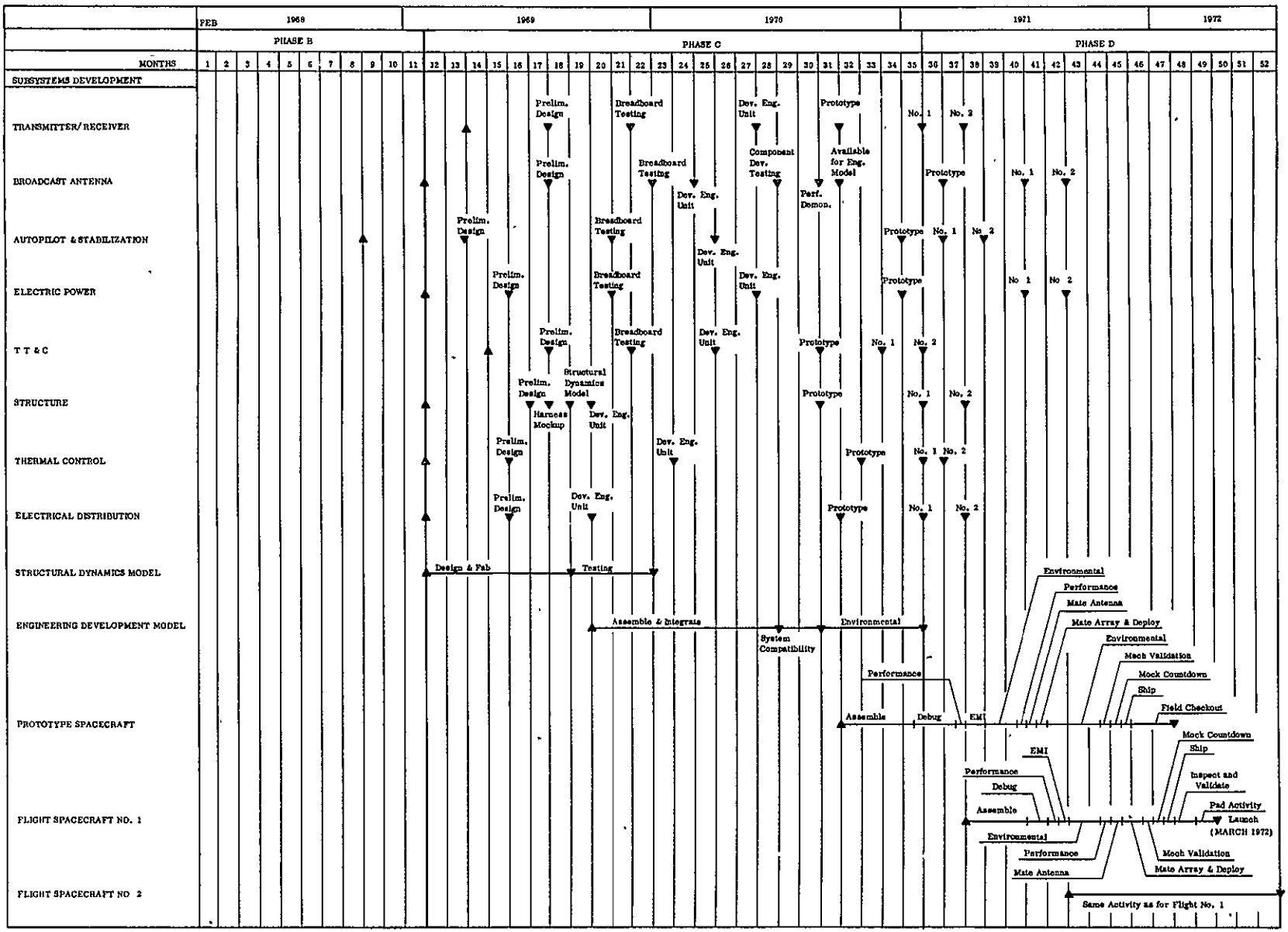

Figure 6.2-2. HF Project Schedule

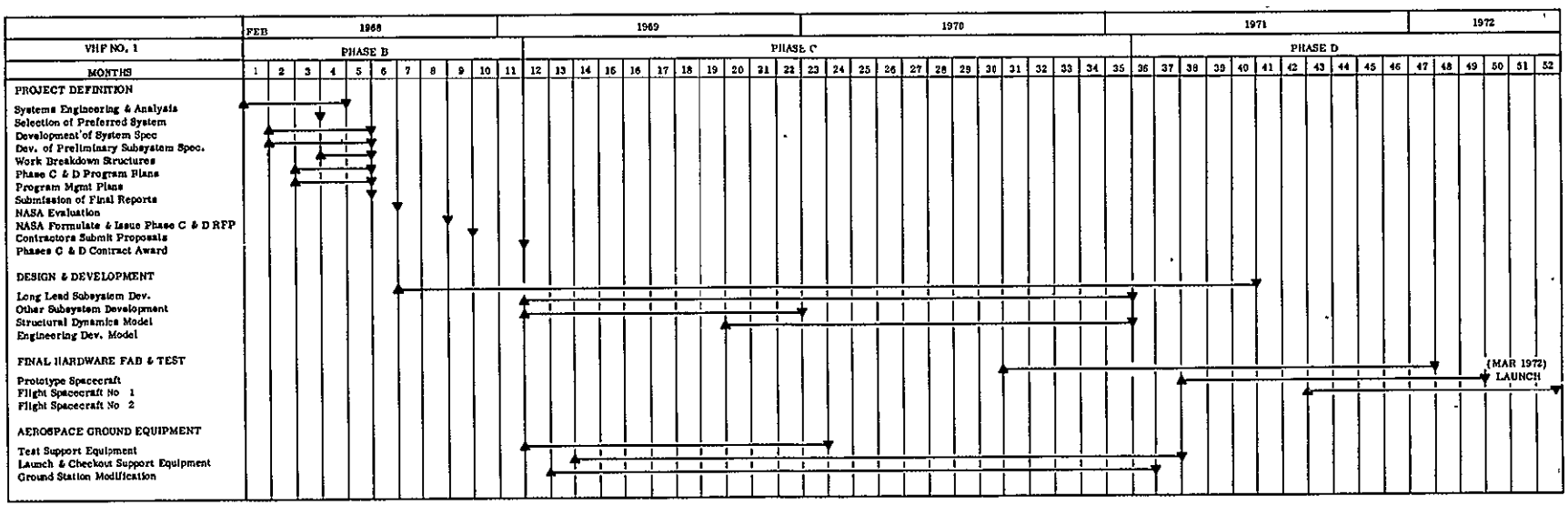

Figure 6.2-3. VHF No. 1 Summary Schedule

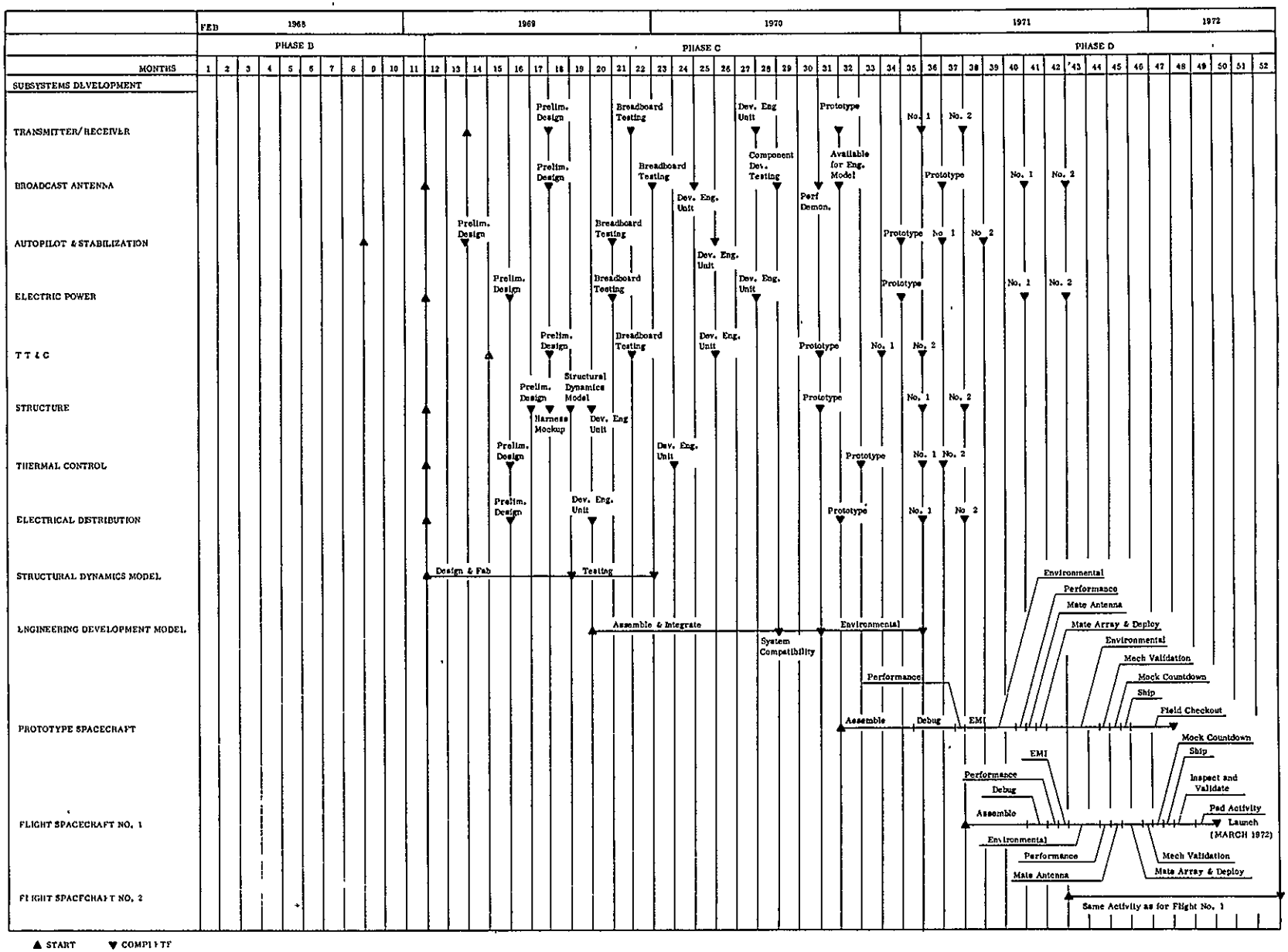

Figure 6.2-4. VHF No. 1 Project Schedule

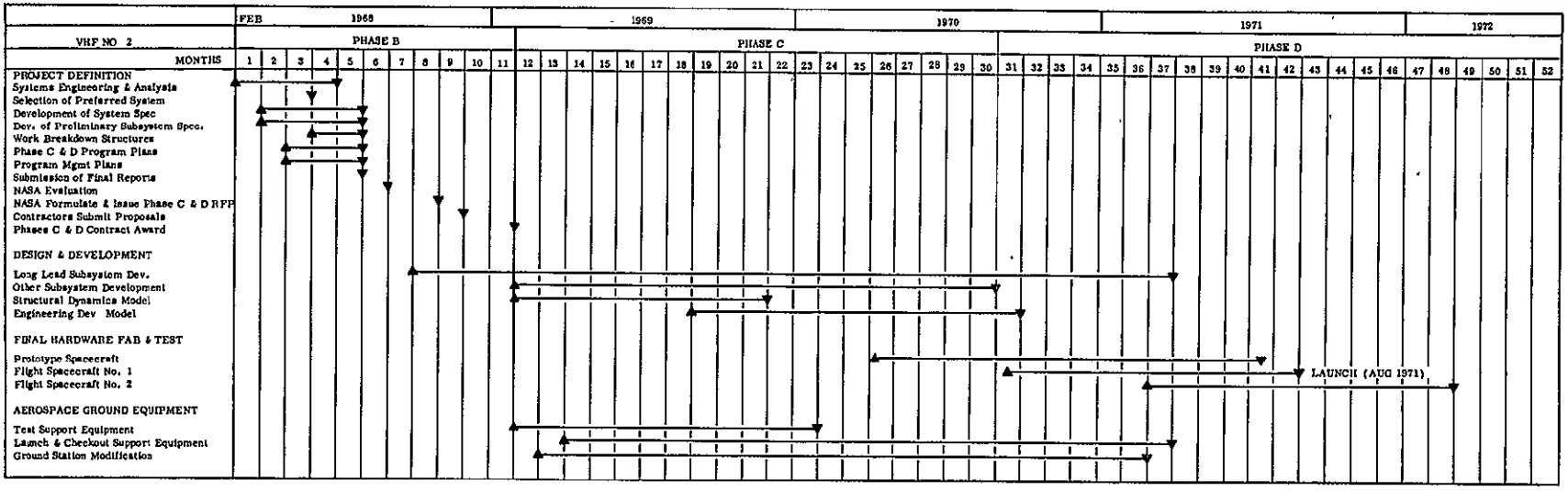

Figure 6.2-5. VHF No. 2 Summary Schedule

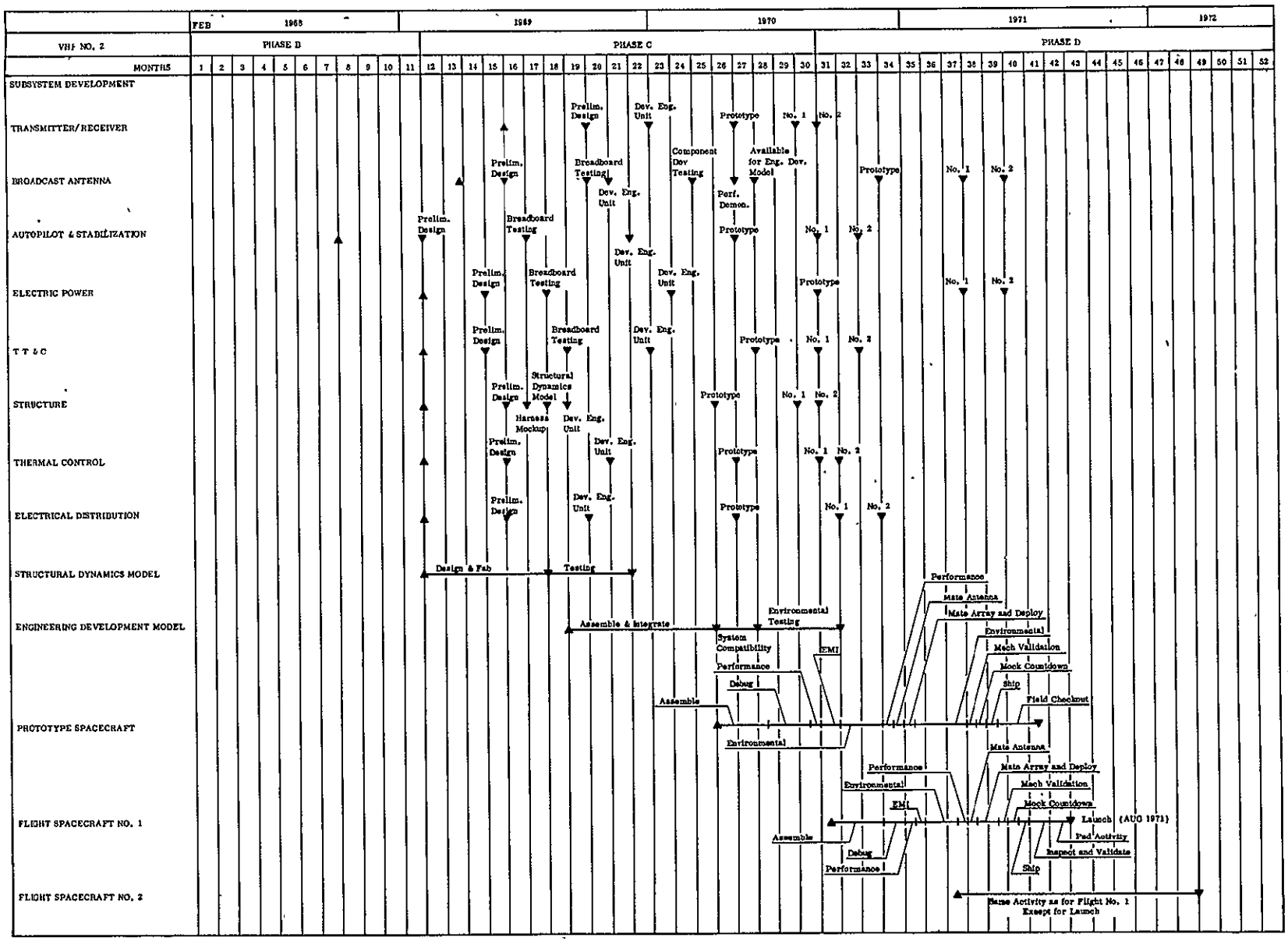

Figure 6.2-6. VHF No. 2 Project Schedule

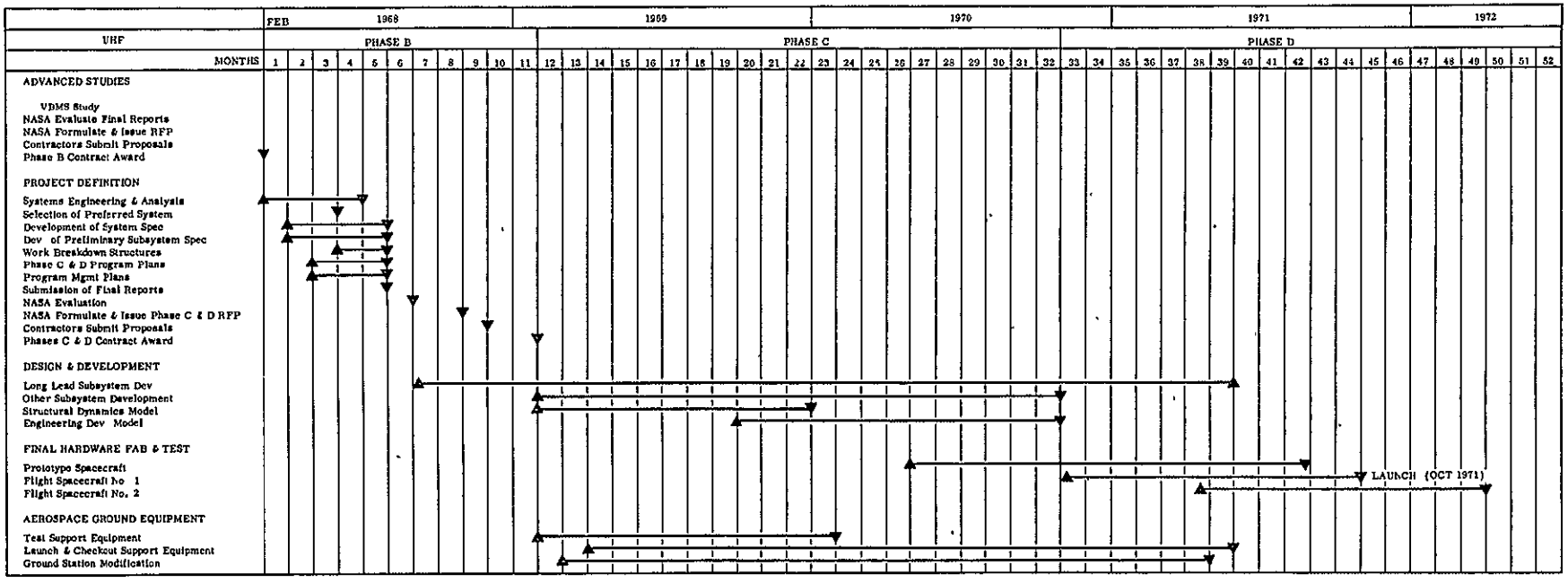

Figure 6.2-7. UHF Summary Schedule

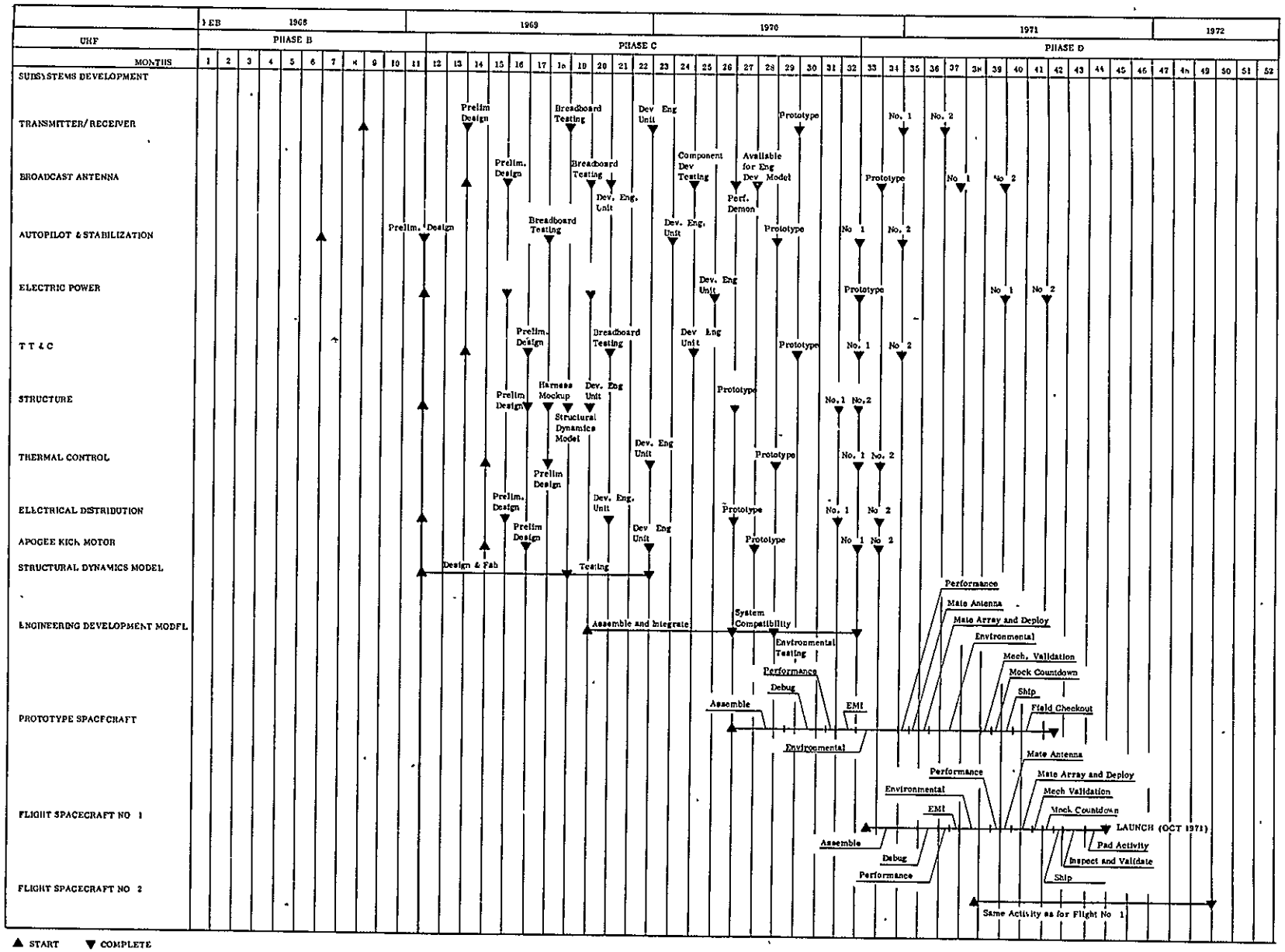

Figure 6.2-8. UHF Project Schedule

6.3 PROGRAM COST DETERMINATION

6.3.1 INTRODUCTION

The approach taken in making cost estimates for the satellite systems was to utilize available subsystem design and fabrication cost data, and to extend estimates in new design areas with detailed examination of required development and testing time and costs. Components (or subsystems) were then combined and multiplying factors used to account for items such as systems integration and testing, program management, and contingency provisions for production revisions.

Other program costs not directly related to the satellite, such as for AGE, boosters, launch facilities, etc., were estimated by using historical data supplemented by current costs from the Air Force and NASA.

The cost data for the two groups above (satellite system and supporting systems) were then divided into three categories convenient to system analysis: (1) Development, (2) Operational, and (3) Investment.

The resulting costs for the four VBMS satellite concepts are summarized in Table 6.3-1. Data presented there includes launching of two satellites, and the associated operational costs over an intervening two-year time period.

Table 6.3-1. Broadcast Programs Costs (Millions of Dollars)

Configuration	Development Cost	Operational Cost	Investment Cost	Total Cost
HF	30.1	58.9	12.5	101.5
VHF No.-1	28.6	58.9	11.6	99.1
VHF No. 2	18.3	24.9	5.0	48.2
UHF	23.1	26.3	6.1	55.5

6.3.2 CALCULATION METHOD

In determining the subsystem costs, the preference for sources was as follows:

a. Historical information from completed contracts

b. Present contracted costs

c. Estimated costs for hardware bids or completed study contracts

6.3.2.1 Development Costs

The satellite system development cost category includes design engineering and development hardware requirements per subsystem. The total of the subsystem development costs are then multiplied by a factor of 1.42 to account for inclusion of systems integration and testing, and this total in turn is then multiplied by a 1.18 factor to include program management.

The development costs for the supporting systems are limited to estimates for the design and fabrication of the AGE, and for development of tracking and communication facilities.

6.3.2.2 Operational Costs

The operational costs for the satellite subsystems are derived from estimates of the subsystem direct manufacturing costs which are then modified. The total subsystem manufacturing costs are multiplied by a factor of 1.2 to provide a contingency for production revisions anticipated due to the limited number of spacecraft being produced. This total is then multiplied by the previously mentioned factors of 1.42 and 1.18 for systems integration and test and program management, respectively, to provide total replacement cost for the satellite system.

Operational costs of the supporting systems are limited to (1) launch vehicle cost, (2) launch facility refurbishment and operation during launch, (3) tracking and communication facility operation, and (4) miscellaneous ground maintenance personnel.

6.3.2.3 Investment Costs

Investment costs are confined to the supporting systems for such items that are unique to the program or that the program must use exclusively, and subsequently cannot be charged as GFE. These are reflected in the following items for the VBMS programs: (1) launch facility modifications, (2) AGE, and (3) tracking and communications facilities.

6.3.3 RESULTS

The results of the costing exercises performed on the VBMS systems are presented in Tables 6.3-2 through 6.3-5.

It should be noted that the solar array development costs are minimized by assuming that array electrical performance can be proven with a very few sections of the basic solar cell arrangement. Functional deployment and structural qualifications tests for the total array can be conducted with simulated solar cells made of low cost materials.

Table 6.3-2. HF Configuration Itemized Cost

Item / Categorized Data	COST IN $ MILLIONS		
	Development Costs	Operational Costs (Two Units)	Investment Costs
Satellite System			
Subsystems			
Transmitter/Receiver	0.49	0.17	
Broadcast Antenna	2.36	0.50	
Power System	3.55	7.37	
Attitude Control	3.79	1.02	
Telemetry, Tracking & Command	1.79	0.85	
Structure	0.77	0.24	
Thermal Controls	0.66	0.45	
Electrical Distribution	0.31	0.08	
Injection Engine	---	---	
Subtotal	13.72	10.68	
Production Revisions	---	2.14	
Systems Integration & Testing	5.78	5.39	
Program Management	3.50	3.29	
Subtotal	23.00	21.50	
Supporting Systems			
AGE	7.00	---	3.00
Launch Facilities	---	6.00	8.21
Booster	---	30.00	---
Tracking/Communications	0.05	1.02	1.33
Facilities Maintenance	---	0.43	---
Subtotal	7.05	37.45	12.54
Totals	30.1	58.9	12.5

Table 6.3-3. VHF No. 1 Configuration Itemized Cost

Item / Categorized Data	COST IN $ MILLIONS		
	Development Costs	Operational Costs (Two Units)	Investment Costs
Satellite System			
Subsystems			
Transmitter/Receiver	0.34	0.17	
Broadcast Antenna	1.86	0.27	
Power System	3.06	8.50	
Attitude Control	5.15	1.46	
Telemetry, Tracking & Command	1.82	0.86	
Structure	0.70	0.16	
Thermal Controls	0.48	0.41	
Electrical Distribution	0.31	0.08	
Injection Engine	---	---	
Subtotal	13.72	11.91	
Production Revisions	---	2.40	
Systems Integration & Testing	5.78	6.04	
Program Management	3.50	3.66	
Subtotal	23.00	24.01	
Supporting Systems			
AGE	5.50	---	3.00
Launch Facilities	---	6.00	8.07
Booster	---	28.00	---
Tracking/Communications	0.06	0.54	0.50
Facilities Maintenance	---	0.35	---
Subtotal	5.56	34.89	11.57
Totals	28.6	58.9	11.6

Table 6.3-4. VHF No. 2 Configuration Itemized Cost

Item / Categorized Data	COST IN $ MILLIONS		
	Development Costs	Operational Costs (Two Units)	Investment Costs
Satellite System			
Subsystems			
Transmitter/Receiver	0.39	0.09	
Broadcast Antenna	1.03	0.14	
Power System	1.94	1.43	
Attitude Control	2.99	0.76	
Telemetry, Tracking & Command	1.81	0.86	
Structure	0.39	0.06	
Thermal Controls	0.40	0.07	
Electrical Distribution	0.21	0.05	
Injection Engine	---	---	---
Subtotal	9.16	3.46	
Production Revisions	---	0.69	
Systems Integration & Testing	3.86	1.75	
Program Management	2.36	1.06	---
Subtotal	15.38	6.96	
Supporting Systems			
AGE	2.80	---	1.40
Launch Facilities	---	5.00	2.21
Booster	---	11.60	---
Tracking/Communications	0.08	1.02	1.38
Facilities Maintenance	---	0.28	---
Subtotal	2.88	17.90	4.99
Totals	18.3	24.9	5.0

Table 6.3-5. UHF Configuration Itemized Cost

Item \ Categorized Data	COST IN $ MILLIONS		
	Development Costs	Operational Costs (Two Units)	Investment Costs
Satellite System			
Subsystems			
Transmitter/Receiver	0.86	0.17	
Broadcast Antenna	0.76	0.08	
Power System	2.31	2.01	
Attitude Control	3.68	0.90	
Telemetry, Tracking & Command	1.81	0.86	
Structure	0.57	0.07	
Thermal Controls	0.55	0.10	
Electrical Distribution	0.25	0.06	
Injection Engine	0.83	0.18	
Subtotal	11.62	4.43	
Production Revisions	---	0.89	
Systems Integration & Testing	4.90	2.24	
Program Management	2.98	1.38	
Subtotal	19.50	8.94	
Supporting Systems			
AGE	3.5	---	2.00
Launch Facilities	---	5.00	2.47
Booster	---	11.60	1.00
Tracking/Communications	0.05	0.30	0.65
Facilities Maintenance	---	0.50	---
Subtotal	3.55	17.40	6.12
Totals	23.1	26.3	6.1

6.4 BROADCAST SYSTEM PERFORMANCE EVALUATION

The ultimate worth of a broadcast service is dependent upon the audience reached for a given cost. The satellite concepts presented were evaluated for cost effectiveness in terms of the ground signal strength, potential audience size in the area of coverage, and satellite operation (including replacement) cost and was measured in cost per receiver-hour. Present commercial operations were evaluated on the same basis, and the ground/satellite alternatives compared for relative worth.

Ranges of satellite ERP's were considered to determine the potential audience variation and specific costs as a function of ground signal strength. This introduced the effects of the different receiver antenna gains and the noise levels encountered. These resulting data illustrate the best economic operating point and the influence on cost of reaching varying percentages of the potential audience.

The field strength and its distribution within the coverage area were computed to determine maximum level, level at edge of coverage area, and variation as function of environment. The signal strength over the area was averaged to indicate the number of receivers reachable.

6.4.1 SIGNAL QUALITY AND COVERAGE EVALUATION

6.4.1.1 Signal Quality Evaluation

The minimum and maximum signal-to-noise ratios obtained for each of the configurations was calculated using the range of signal strengths (from antenna beam center to edge) achieved by each of the configurations in the selected example coverage areas (see Section 6.4.2 for the signal strength determinations). The parameters used in the calculations are:

E = Field strength, $\mu v/m$

ϕ = Power density, w/m^2

H = Satellite altitude, nautical miles

R = Maximum Range, nautical miles

$\Delta Long$ = Difference in longitude between satellite and ground point, degrees

ΔLat = Difference in latitude between satellite and ground point, degrees

λ = Wavelength, meters

T_{mm} = Man-made noise temperature, ^oK

T_g = Galactic noise temperature, ^oK

T_{atm} = Atmospheric noise temperature, ^{o}K

T_a = $T_{mm} + T_g + T_{atm}$

F = Receiver noise figure, numerical

L = Line loss, numerical

G_r = Effective receiving antenna gain, numerical; single asterisk means 3 db polarization loss was taken into account; double asterisk means 3 db polarization loss plus 3 db pointing loss were taken into account.

Δf = Frequency deviation in FM, kHz

m = Modulation index in AM

B = Audio bandwidth, kHz

B_{if} = IF = RF bandwidth, kHz

ERP = Effective radiated power, watts

N = Equivalent noise power at receiver input, watts

C = Carrier power at receiver input, watts

G_d = Pre-emphasis improvement factor, db

$\frac{S}{N}$ = Audio signal-to-noise ratio

The calculations for each of the configurations are shown below:

(1) HF - 15 MHz

Given: E=158 (Min) to 433 (Max);

$T_{mm} = 2.9 \times 10^4$ (rural); $T_g = 8.5 \times 10^4$; $T_{atm} = 9.1 \times 10^6$; $\lambda = 20$

F = 10; $G_r = 1.585$**(Yagi); m = 0.3; B = 5; $B_{if} = 10$; L = 1.59

$$N = kB_{if} \left\{ T_a + T_o \left[(L-1) + L(F-1) \right] \right\}$$

$$= (1.38 \times 10^{-23})(10^4) \left\{ 219 \times 10^4 + 8.5 \times 10^4 + 9.1 \times 10^6 + 290. \left[0.59 + (1.59)(9) \right] \right\} = 1.27 \times 10^{-12} \text{ W}$$

$$P_{Min} = \frac{E_{Min}^2 \, G_r \, \lambda^2}{480\pi^2} = \frac{(1.58 \times 10^{-4})^2 \, (1.585) \, (20)^2}{480\pi^2} = 3.3 \times 10^{-9} \text{ W}$$

$$P_{Max} = \frac{(4.33 \times 10^{-4})^2 \, (1.585) \, (20)^2}{480\pi^2} = 2.5 \times 10^{-8} \text{ W}$$

$$\frac{P_{Min}}{N} = \frac{3.3 \times 10^{-9}}{1.27 \times 10^{-12}} = 2.6 \times 10^{3}$$

$$\frac{P_{Max}}{N} = \frac{2.58 \times 10^{-8}}{1.27 \times 10^{-12}} = 2.03 \times 10^{4}$$

$$\frac{S}{N} = \left(\frac{m^2}{1 + \frac{m^2}{2}} \right) \left(\frac{P}{N} \right)$$

At m = 0.8:

$$\left. \frac{S}{N} \right|_{Min} = 1260 = 31 \text{ db}$$

$$\left. \frac{S}{N} \right|_{Max} = 9850 = 39.9 \text{ db}$$

(2) VHF No. 1 - 100 MHz

Given : E = 204 (Min) to 273 (Max);

T_{mm} = 9.15×10^5 (urban); T_g = 3000; F = 10; G_r = 0.815*(dipole);

Δf = 75; B = 15; B_{if} = 175; L = 1/2 db; λ = 3

$$N = kB_{if} \left\{ T_m + T_g + T_o \left[(L-1) + L(F-1) \right] \right\}$$

$$= (1.38 \times 10^{-23}) (1.75 \times 10^5) \left\{ \frac{9.15 \times 10^5}{1} + 3000 + 290 \quad (1.1-1) + 1.1 \, (10-1) \right.$$

$$= -116.5 \text{ dbw}$$

$$C_{Min} = \frac{E_{Min}^2 \, G_r \, \lambda^2}{480\pi^2} = \frac{(2.04 \times 10^{-4})^2 \, (0.825) \, (3)^2}{480\pi^2} = 6.5 \times 10^{-11} \text{ W}$$

$$C_{Max} = \frac{\left(2.73 \times 10^{-4}\right)^2 (0.825)\ (3)^2}{480\pi^2} = 1.16 \times 10^{-10}\ W$$

$$\left.\frac{C}{N}\right|_{Min} = \frac{6.5 \times 10^{-11}}{2.22 \times 10^{-12}} = 29.5 = 14.7\ db$$

$$\left.\frac{C}{N}\right|_{Max} = \frac{1.16 \times 10^{-10}}{2.22 \times 10^{-12}} = 52.2 = 17.2$$

$$\left.\frac{S}{N}\right|_{Min} = 10 \log 3 + 20 \log \frac{\Delta f}{B} + 10 \log \frac{B_{if}}{2B} + 10 \log \frac{C}{N}_{Min} + G_d$$

$$= 4.77 + 13.9 + 7.66 + 14.7 + 9 = 50.1\ db$$

$$\left.\frac{S}{N}\right|_{Max} = 4.77 + 13.9 + 7.66 + 17.2 + 9 = 52.6\ db$$

At 100% Modulation

(3) VHF No. 2 - 100 MHz

Given: $E = 77$ (Min) to 99 (Max); $T_{mm} = 9.15 \times 10^3$ (suburban); $\lambda = 3$;

$T_g = 3000$; $F = 10$; $G_r = 0.825$* (dipole); $\Delta f = 75$; $B = 15$; $B_{if} = 175$; $L = 1$

$$N = kB_{if}\left\{T_a + T_o\left[(L-1) + L(F-1)\right]\right\}$$

$$= (1.38 \times 10^{-23})\ (1.75 \times 10^5)\left\{9.15 \times 10^3 + 3000 + 290\ (10)\right\} = -134.4\ dbw$$

$$C_{Min} = \frac{E^2_{Min}\ G_r\ \lambda^2}{480\pi^2} = \frac{(7.7 \times 10^{-5})^2\ (0.825)\ (3)^2}{480\pi^2} = 9.22 \times 10^{-12}\ W$$

$$C_{Max} = \frac{(9.9 \times 10^{-5})^2\ (0.825)\ (3)^2}{480\pi^2} = 1.53 \times 10^{-11}\ W$$

$$\left.\frac{C}{N}\right|_{Min} = \frac{9.22 \times 10^{-12}}{3.64 \times 10^{-14}} = 253 = 24\ db$$

$$\left.\frac{C}{N}\right|_{Max} = \frac{1.53 \times 10^{-11}}{3.64 \times 10^{-14}} = 422 = 26.3 \text{ db}$$

$$\left.\frac{S}{N}\right|_{Min} = 10 \log 3 + 20 \log \left(\frac{\Delta f}{B}\right) + 10 \log \left(\frac{B_{if}}{2B}\right) + 10 \log \left.\frac{C}{N}\right|_{Min} + G_d$$

$$= 4.77 + 13.9 + 7.66 + 24 + 9 = 59.4 \text{ db}$$

$$\left.\frac{S}{N}\right|_{Max} = 4.77 + 13.9 + 7.66 + 26.3 + 9 = 61.7 \text{ db}$$

} At 100% Modulation

(4) UHF - 870 MHz

Given: $E = 99$ (Min) $= 144$ (Max);

$T_{mm} = 3780$ (urban); $T_g = 300$; $F = 10$, $G_r = 0.89$* (rabbit ears);

$\Delta F = 25$; $B = 15$; $B_{if} = 120$; $L = 3$db; $\lambda = 3/8.7$

$$N = kB_{if}\left\{T_a + T_o\left[(L-1) + L(F-1)\right]\right\} = kB_{if}\left\{T_{mm} + T_g + T_o\left[(L-1)+L(F-1)\right]\right\}$$

$$= (1.38 \times 10^{-23})(1.2 \times 10^{5})\left\{3780 + 300 + 290\,(19)\right\} = 1.59 \times 10^{-14}\text{W} = -138 \text{ dbw}$$

$$C_{Min} = \frac{E^2_{Min}\, G_r\, \lambda^2}{480\pi^2} = \frac{(9.9 \times 10^{-5})^2\,(0.89)\left(\frac{3}{8.7}\right)^2}{480\pi^2} = 2.21 \times 10^{-13} \text{ W}$$

$$C_{Max} = \frac{(1.44 \times 10^{-4})^2\,(0.89)\left(\frac{3}{8.7}\right)^2}{480\pi^2} = 4.6 \times 10^{-13}$$

$$\left.\frac{C}{N}\right|_{Min \text{ (at discriminator)}} = 10 \log \left(\frac{2.21 \times 10^{-13}}{1.59 \times 10^{-14}}\right) - 4.2 = 7.4 \text{ db}$$

$$\left.\frac{C}{N}\right|_{Max \text{ (at discriminator)}} = 10 \log \left(\frac{4.6 \times 10^{-13}}{1.59 \times 10^{-14}}\right) - 4.2 = 10.4 \text{ db}$$

} The $\frac{C}{N}$ is reduced from the single channel case by 4.2 db because of the 3 db noise contribution of the picture carrier and the degradation in the video detector.

$$\left.\frac{S}{N}\right|_{Min} = 10 \log 3 + 20 \log \left(\frac{\Delta f}{B}\right) + 10 \log \left(\frac{B_{if}}{2B}\right) + 10 \log \left.\frac{C}{N}\right|_{Min} + G_d$$

$$\left.\begin{aligned} &= 4.8 + 4.4 + 6 + 7.2 + 9 = 31.6 \text{ db} \\ \left.\frac{S}{N}\right|_{Max} &= 4.8 + 4.4 + 6 + 10.4 + 9 = 34.6 \text{ db} \end{aligned}\right\} \text{ at 100\% Modulation}$$

6.4.1.2 Coverage

A computer program was developed for the Voice Broadcast Mission Study that permits rapid calculation of constant ground field strength contours for a given satellite position and ERP. Propagation loss was included, based on ionospheric layer height, transmitting frequency, latitude, and time of day. The program is capable of computing ground signal strengths at a given point that are exceeded 50, 90, or 99 percent of the time, based upon propagation conditions. The geometry of the situation is sketched in Figure 6.4-1.

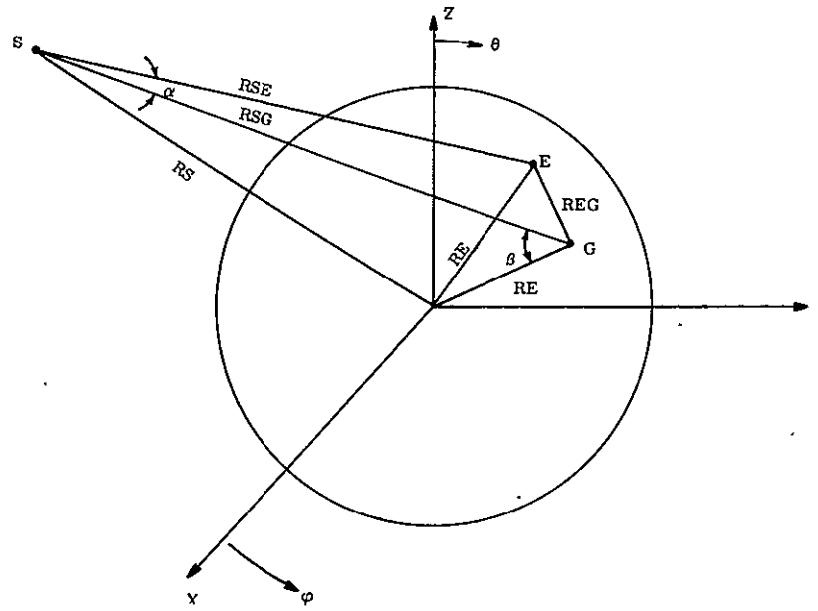

Figure 6.4-1. Coverage Geometry

A description of the program's calculations follows:

From the law of cosines,

$$\alpha = \cos^{-1} (RSE^2 + RSG^2 - REG^2)/2RSE(REG)$$

and represents the angle between the antenna axis and the line of sight to the desired point. The antenna gain $G_t(\alpha) = G_{max}\, G_{(\alpha)}$, $G_{(\alpha)} \leq$, is assumed cylindrically symmetrical.

The field strength, E_f, in rms volts/meter at a ground point G is then given by

$$\frac{E_f^2}{120\pi} = \frac{P_t G_{max} G(\alpha)}{4\pi RSG^2}$$

Define $P_t G_{max} \equiv$ ERP; then

$$E_f = \frac{1}{RSG} \quad 30 \text{ ERP } (G\alpha) \quad \text{v/m (free-space)}$$

From the sketch,

$$\beta = \cos^{-1} \quad (RE^2 + RSG^2 - RS^2)/2RE(RG)$$

Hence, elevation angle, $\eta = \beta - 90^o$

incidence angle, $\chi = 180^o - \beta$

Let ρ be the propagation loss factor. That is, the received field strength $E = \rho E_f$, hence,

$$E \text{ (uv/m)} = \frac{10^6}{RSG} \cdot \rho \quad 30 \text{ ERP } (G\alpha)$$

(Note that for this program, the form $G(\alpha) = -(\alpha^2)$ (db) has been assumed. Any other "one-dimensional" functional form can be used.)

The factor ρ is a function of many variables and has been obtained empirically. It has the general functional form $\rho = \rho\ (F, t_m)$

where

$$F = (F_{\infty, 100})\ (1\text{-Hi/H})\ \sec^{3/2} \chi\ (100/f)^2$$

where

$F_{\infty, 100}$ = (empirical) factor

H_i = Ionospheric layer height

f = frequency, MHz

t_m = time margin (confidence level); e.g., if $t_m = 1\%$, $\rho \geq (F, 1)$ for 99% of the time.

The quantity $F_{\infty, 100}$ depends on latitude and time of day and has been stored in tabular form. Curve fitting expressions were obtained for ρ.

Taking all the above into account, values for E, given all other necessary variables, can be obtained at any point on the ground. These values of E can then be plotted on a map and constant field strength contours drawn.

The above equations have been programmed in FORTRAN II for use on the Desk Side Computer System (DSCS). The entire program exists as one main program - Contor and four sub-routines in the authors catalog.

A more detailed explanation of the program follows:

A spherical coordinate system is used, with origin at the earth's center. Point S is the satellite position; line SE is the satellite antenna beam axis; point G is some arbitrary point on the ground.

The Greenwich meridian is assumed at $\varphi = 0^{o}$, and from the sketch, latitude = $90^{o} - \theta$, where North latitude is positive and South latitude is negative.

Let LATX represent the latitude of point X;

LONGX represent the longitude of point X;

Then, $RSE^2 = RE \cos(\pi/2 - LATE) - RS \cos(\frac{\pi}{2} - LATS)^2 + RE \sin(\frac{\pi}{2} -$

LONGE - RS $\sin(\frac{\pi}{2} - LATS)$ in LONGS ^{2} +

RE $\sin(\frac{\pi}{2} - LATS)$ cos LONGS

Where

RE = earth's radius

RS = RE + H

H = S

Similar equations exist for RSG and REG.

Table 6.4-1 shows the necessary input data. The first input line titles the case of interest, and the next input line is the necessary data. The symbols shown are those used in the FORTRAN programming.

The first three quantities relate information about the transmitter and antenna. FREQ is the transmitting frequency in MHz. ERP (effective radiated power) is the total radiated power in watts multiplied by the maximum gain of the antenna. THE represents the 3db beamwidth of the antenna in degrees.

Table 6.4-1. Inputs for CONTOR

(Title not to exceed 40 characters)																
=																
	FREQ	ERP	THE	ZLATS	ZLONGS	H	ZLATE	ZLONGE	ITIME	M	ZLAT	FLAT	DLAT	ZLONG	FLONG	DLONG
=	,	,	,	,	,	,	,	,	,	,	,	,	,	,	,	,
	MHZ	WATTS	DEG	DEG	DEG	NM	DEG	DEG	HRS		DEG	DEG	DEG	DEG	DEG	DEG

The next three input quantitites relate information about the transmitting position (satellite position for this instance). ZLATS and ZLONGS stand for the known latitude and longitude of the satellite, and H represents the altitude of the satellite in nautical miles.

The next three input quantities provide information concerning the point on the ground at which the antenna axis is pointing. ZLATE and ZLONGE represent latitude and longitude and ITIME (a fixed point quantity) gives the "local-time" at this point. ITIME can only be inputed as an hour of the day (a number from 1 to 24), with 1 representing 1:00 a.m. and 24 representing 12 Midnight.

M is the propagation time margin option taking on a fixed-point number from 1 to 3. M = 1 would be input if the desired time margin were 1%, i.e., the signal calculated is met or exceeded 99% of the time or gails to meet 1% of the time. M = 2 represents a 10% time margin, and M = 3 represents a 50% time margin.

The program calculates signal strength at the ground, in microvolts/meter, at each point in the "grid" input as the next six quantitites. The "grid" is expressed as latitude by longitude. First the program iterates latitude by traversing the first inputed longitude line from south to north. It then moves westward to the next line of longitude and again iterates latitude. Latitude in this program is inputed as positive for north latitude (0^o represents the Equator and $+90^o$ represents the North Pole), and negative for south latitude (-90^o representing the South Pole). Longitude, on the other hand, is inputed as a positive quantity from 0^o to 360^o where 0^o represents the meridian passing through Greenwich, England. Lines of longitude are then traversed westward from 0^o.

ZLAT and ZLONG represent the coordinates of the lower right-hand corner of the grid. The iterations will begin at these coordinates. FLAT and FLONG represent the coordinates of the last point calculated in the grid (upper left-hand corner). DLAT and DLONG then represent the constant increments to be iterated in between.

The print-out gives signal strength at the ground as a function of latitude and longitude within the grid. Also printed out is (1) the elevation angle of the satellite seen by an observer on the ground, (2) the angle between the antenna axis and this observer, and (3) the ionospheric attenuation of the signal in db.

The output of this program permits a thorough analysis of possible coverage areas throughout the world. The results of this program were used to determine effective coverage areas for each of the configurations.

Figures 6.4-2 through 6.4-5 illustrate the coverage results for the four baseline configurations. The signal is indicated here in terms of the actual microvolts per meter reaching the ground.

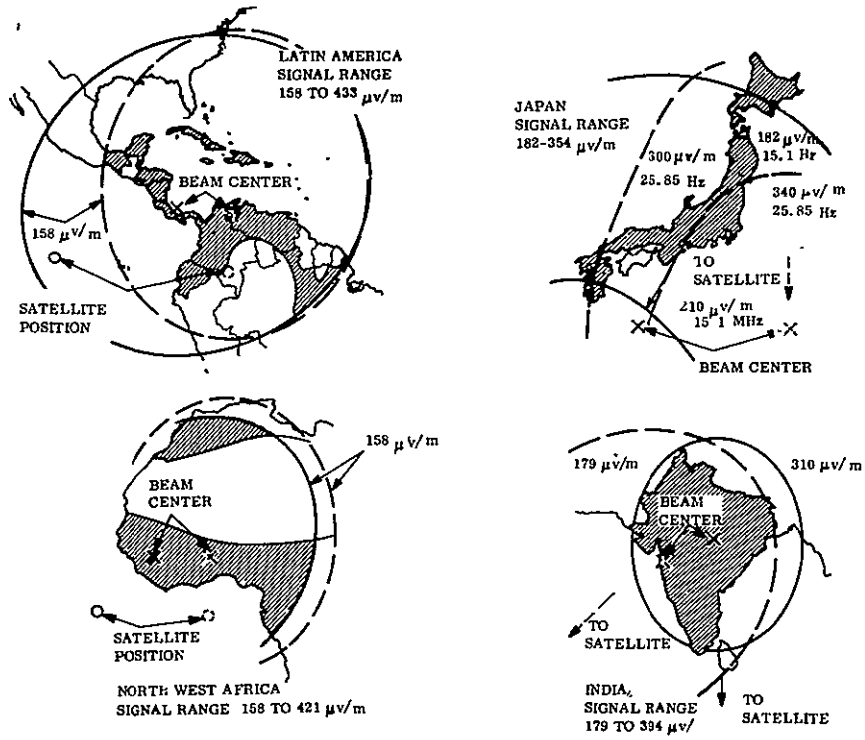

Figure 6.4-2. HF Signal Contours

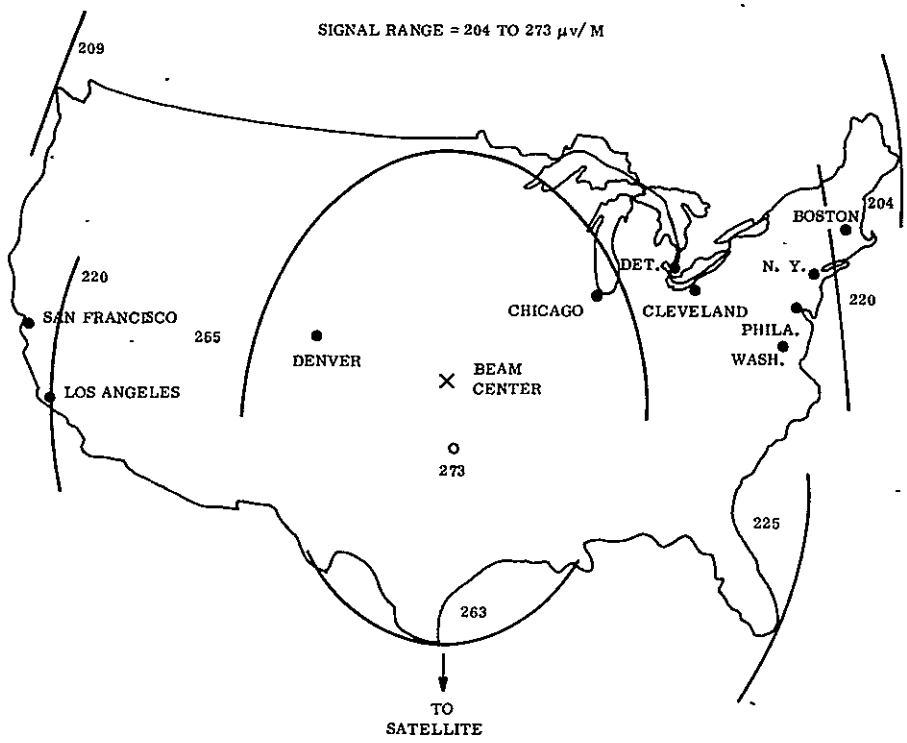

Figure 6.4-3. VHF No. 1 Signal Contours

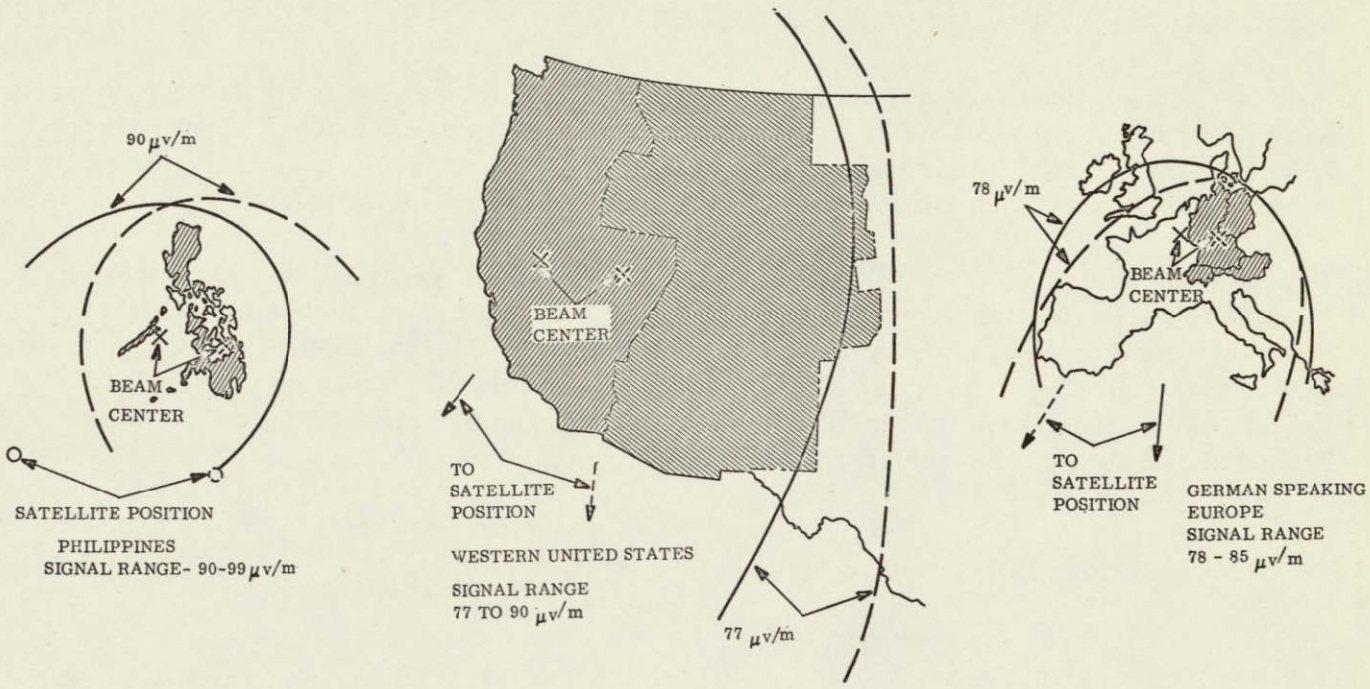

Figure 6.4-4. VHF No. 2 Signal Contours

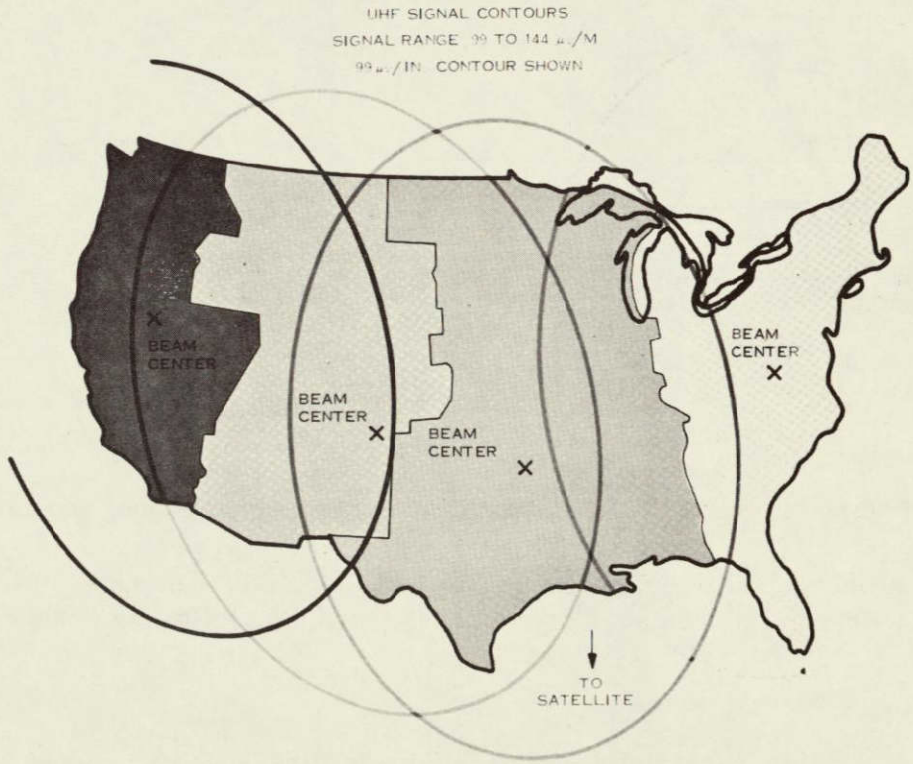

Figure 6.4-5. UHF Signal Contours

6.4.2 ANALYSIS OF AUDIENCE REACHABLE

In the previous section, the ground signal levels produced by the four satellite configurations were described for the example coverage areas. These signals were used, along with the 1970 projected receiver distributions in the example coverage areas, to evaluate the quantity of receivers reachable as a function of the environment and receiving antenna type.

The potential audience for the HF-AM configuration is shown (Figure 6.4-6) for the example geographic areas selected to evaluate coverage performance. The number of receivers reachable, as a function of the ground signal strength in each area, is shown on the plot. The dashed vertical arrows show the range of ground signal strength generated in each area by the HF-AM configuration (the number of receivers reachable corresponding to the mean ground signal strength in each area is also shown on the plot).

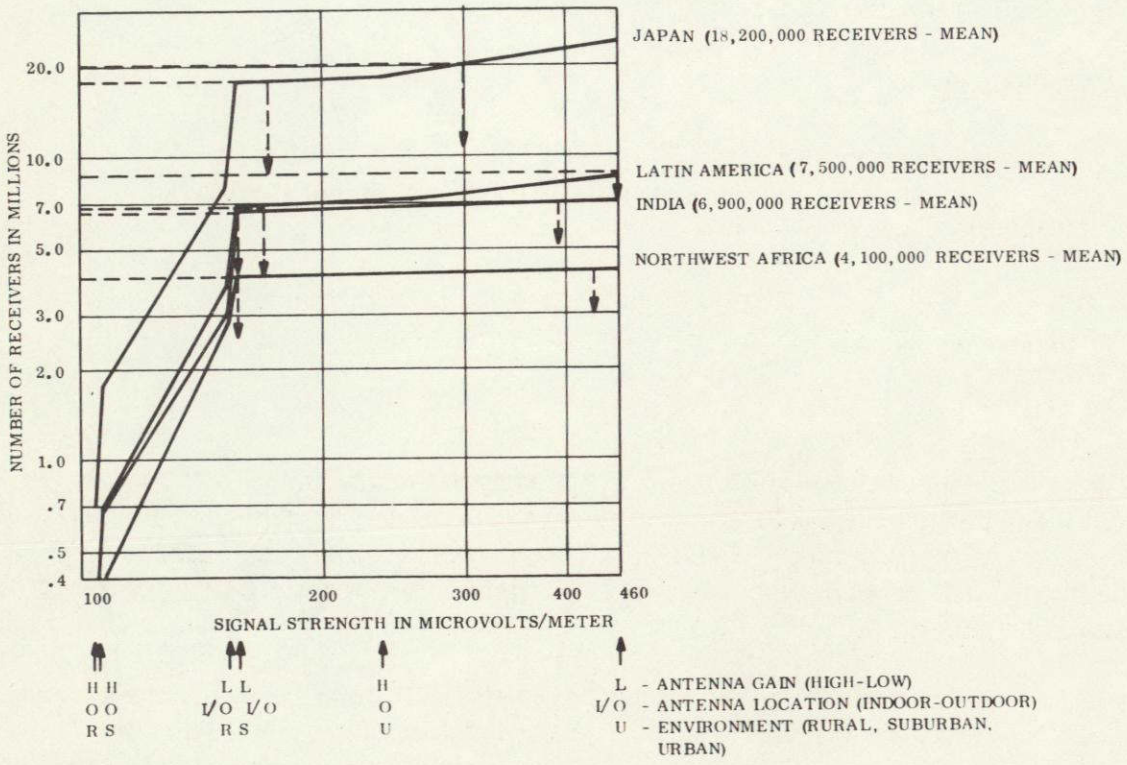

Figure 6.4-6. HF-AM Potential Audience Versus Signal Strength

The example coverage areas selected were 1) Japan, 2) Latin America, 3) India, 4) Northwest Africa, and 5) French Polynesia. For the areas noted, the following comments apply:

Japan

Japan's highly industrialized economy made it reasonable to assume that its receiver distribution most nearly resembled other highly industrialized areas, i.e., the United States and Western Europe. Japan's growth rate was based upon the rate predicted for the Far East.

Latin America

The countries in Latin America reached by the HF-AM configuration are:

Mexico (part of)	Panama
Guatemala	Colombia
Honduras	Venezuela
El Salvador	Ecuador
Nicaragua	Cuba
Costa Rica	Trinidad

French Polynesia

The curve of audience reachable is not shown in Figure 6.4-6 because the number of receivers available is less than 100,000. However, the percentage reached ($\approx$ 75%) is similar to the other areas shown.

Northwest Africa

The countries in Africa reached by the HF-AM configuration are:

Mauritania	Guiana	Dahomey	Algeria (partial)
Mali	Sierra Leone	Nigeria	
Niger	Cape Verde Islands	Cameron	Ivory Coast
Senegal	Liberia	Morocco	
Gambia	Upper Volta	Gabon	
		Chad	

The potential audience for the VHF No. 1 Configuration is shown in Figure 6.4-7. The selected coverage area is the continental United States. The dashed lines show the range of signal strength provided. This signal range reaches in excess of 95% of the receivers in the area. All types of installations are reached, including low gain antennas in the indoor urban environment.

Figure 6.4-8 shows the potential audience for the VHF No. 2 Configuration. The areas selected to evaluate coverage are: (1) western United States (Mountain and Pacific Time Zones); (2) the Philippine Islands; and (3) German-speaking countries of Europe (Germany, Austria and Switzerland). The number of receivers estimated for Switzerland has been reduced to one-half to allow for the German-speaking segment.

Figure 6.4-9 shows the potential UHF audience in the United States by time zones. The receivers were apportioned among the time zones according to the population distribution given in the 1960 census.

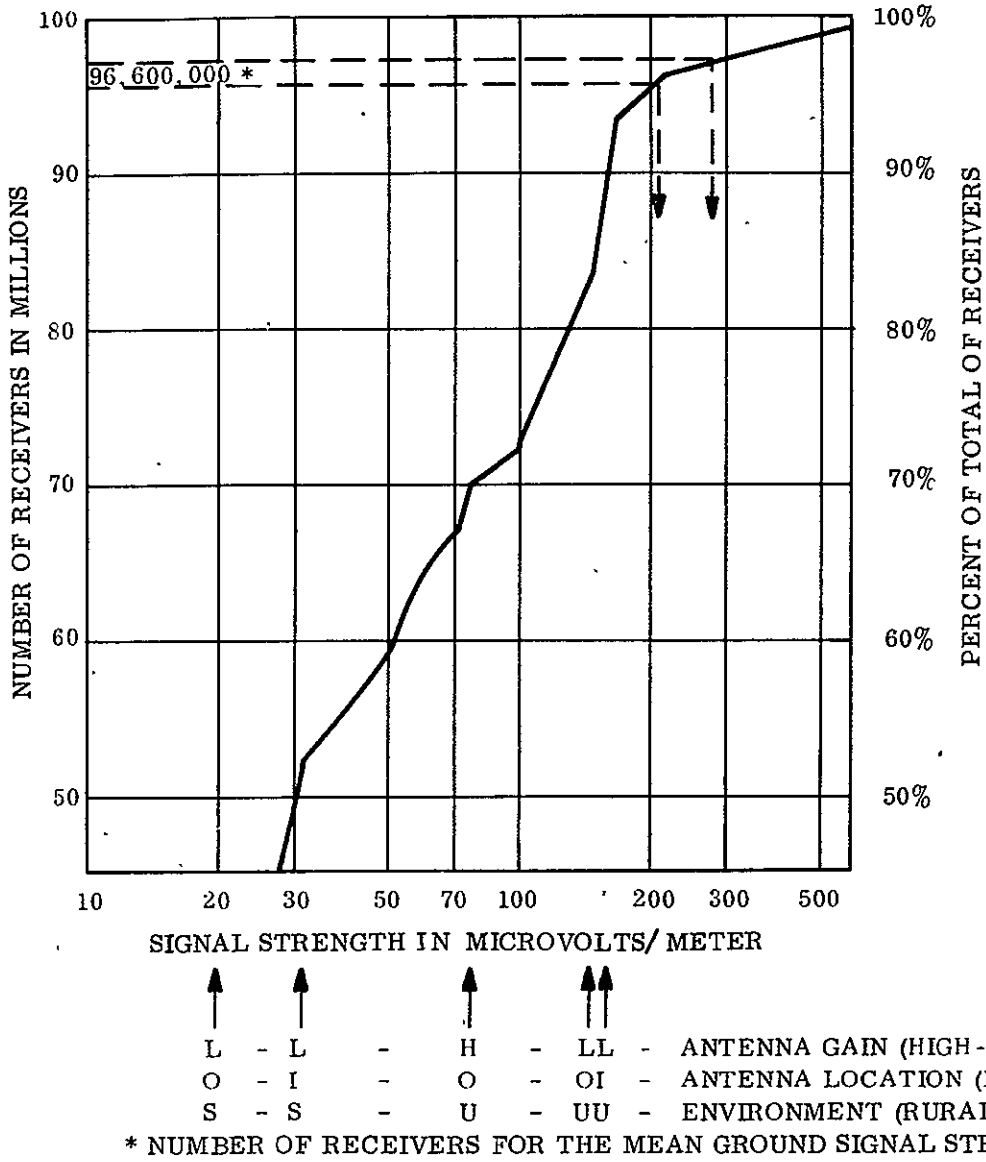

Figure 6.4-7. VHF No. 1 Potential Audience Versus Signal Strength

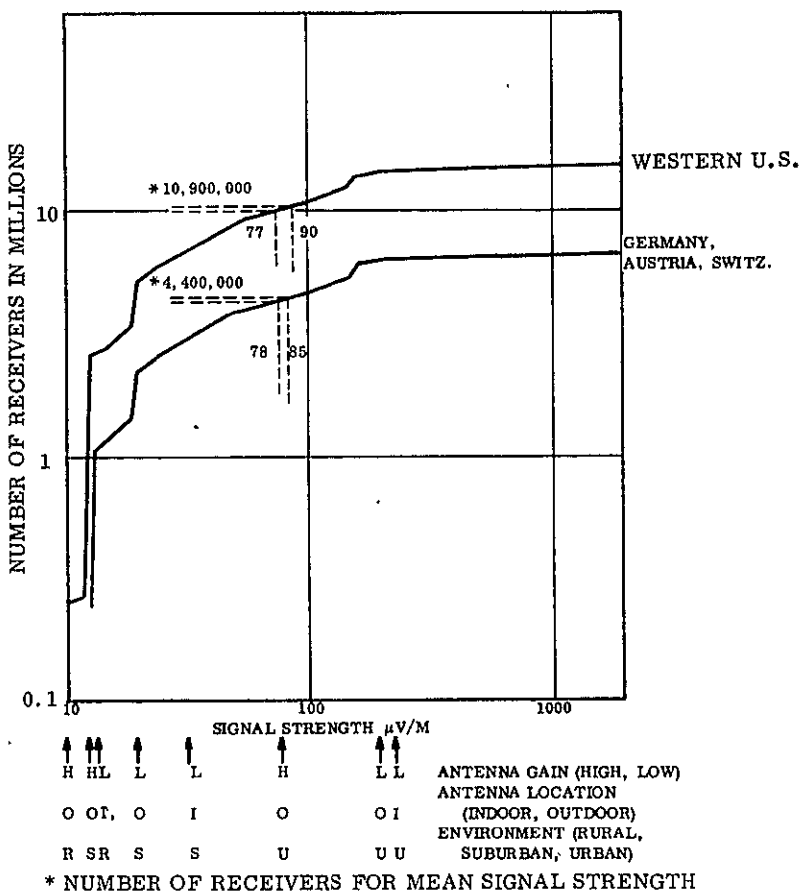

Figure 6.4-8. VHF No. 2. Potential Audience Versus Signal Strength

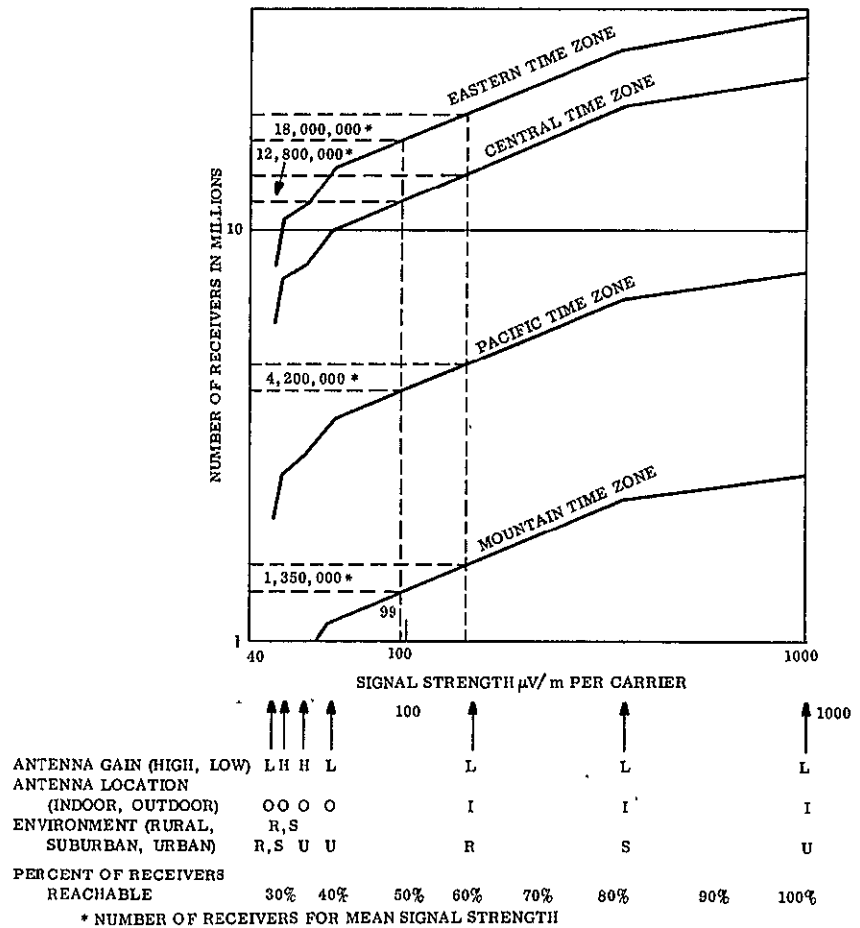

Figure 6.4-9. UHF-United States. Potential Audience Versus Signal Strength by Time Zones

6.4.3 COST EFFECTIVENESS ANALYSIS

6.4.3.1 Introduction

Section 6.3 presented costs for the four baseline configurations (HF, VHF No. 1, VHF No. 2 and UHF) conceived and analyzed during this study. Each of these configurations was sized to broadcast to a specific audience; i.e., a percentage of the total audience which (1) was located in a certain combination of rural, suburban or urban environments; (2) employed a receiver of specified sensitivity; and (3) used either a high or low gain antenna in either an indoor or outdoor location. Therefore, these costs are applicable to only the combination of audience and equipment parameters selected for each configuration.

This section presents a series of cost tradeoff curves extrapolated from each of the four baseline configurations. These curves permit costs to be estimated for missions other than the four for which the baseline configurations were sized. Total program (2 satellites) and yearly operating (one satellite with an assumed 2-year life) costs are plotted versus ground signal strength. These costs are defined in Section 6.3. The cost effectiveness parameter of cents per receiver hour is also plotted versus ground signal strength.

Table 6.4-2 shows the range of costs and cost effectiveness for each type satellite within the ground signal strength bounds considered. The VHF No. 1 type is more cost effective (by a factor of three) than average current terrestrial VHF/FM broadcast service costs of 0.0043 cent per receiver hour. The UHF type is more cost effective (by a factor of four) than average current terrestrial UHF/TV broadcast service costs of 0.066 cent per receiver hour; however, it is less cost effective (by a factor of four) than the service costs for the VHF/FM mentioned above. The other configurations are not cost effective due to their short duty cycles and the low receiver density in the coverage example areas.

Table 6.4-2. Costs versus Ground Signal Strength

Parameter Variation	Configuration Type			
	HF	VHF No. 1	VHF No. 2	UHF
Ground Signal Strength (μv/m)	30 to 450	40 to 400	30 to 450	20 to 350
Total Program Costs ($ Millions)	75 to 135	63 to 125	45 to 91	53 to 97
Yearly Operating Costs ($ Millions)	9.5 to 25.5	7.0 to 21.5	5.5 to 19.0	6.0 to 17.5
Cost Effectiveness (¢ per receiver hour)	0.18 to 0.31	0.0014 to 0.0048	0.11 to 0.25	0.016 to 0.028

6.4.3.2 Total Program Costs

The system cost was determined as the signal level at the ground was varied for each configuration. It was assumed that the signal level variation was generated by changing the magnitude of the broadcast transmitter output. Basically, this meant a variation in the cost and weight of the prime power supply. Other factors, such as antenna gain, coverage area, and orbit, remained constant. As the satellite weight changed, so did the booster and its associated cost. The parameters used for booster selection are listed in Table 6.4-3.

Table 6.4-3. Booster Data

		Capability-lb (for circular orbits of 0° including in.)		
Booster	Cost/Launch (millions of dollars)	Synchronous	7500 nm	4360 nm
SLV 3A/Improved Agena	7.5	490	800	890
SLV 3A/Improved Agena/Kick	8.5	1300	1450	1475
SLV 3C/Centaur/Kick	13.5	2180	2280	2370
Titan 3 + 5 segments	15.5	2150	3050	3600
Titan 3 + 7 segments	17 + 8 investment	≈4250	≈4900	≈5300
Titan 3 + 156 segments	21 + 8 investment	>6000	>6500	>7000
Uprated Saturn I/Centaur	30	9000	13,500	16,000

Total program cost then consisted of baseline cost plus variable satellite cost plus booster cost difference for two launches.

The variation in signal strength from the baseline case was assumed to be in the ratio of the square root of the power ratio.

The results of varying the satellite size in terms of total program cost is shown in Figure 6.4-10 through 6.4-13. Discrete steps are shown in each case as booster changes (due to increasing weight) are made. Note that a triangle symbol in the figures indicates the final calculated performance/cost of the four baseline configurations.

6.4.3.3 Yearly Operation Costs

The total program costs contain three components: development, investment, and operation. The yearly costs are concerned with the operation only, composed of flight vehicle cost, booster cost, launch cost, and ground station operation. The yearly cost was assumed to include 50% of a single booster, launch, and flight vehicle price, plus ground station operation and investment maintenance for a year. As such, it is approximately one-fourth of the total operation cost of the program. The 50% factor is based on 2-year satellite design life. The result of varying the satellite size in terms of yearly operation costs is shown in Figures 6.4-14 through 6.4-17. Extending the design life of the satellite will reduce the operating cost. However, the specific effects of a varaible life were not evaluated during the study.

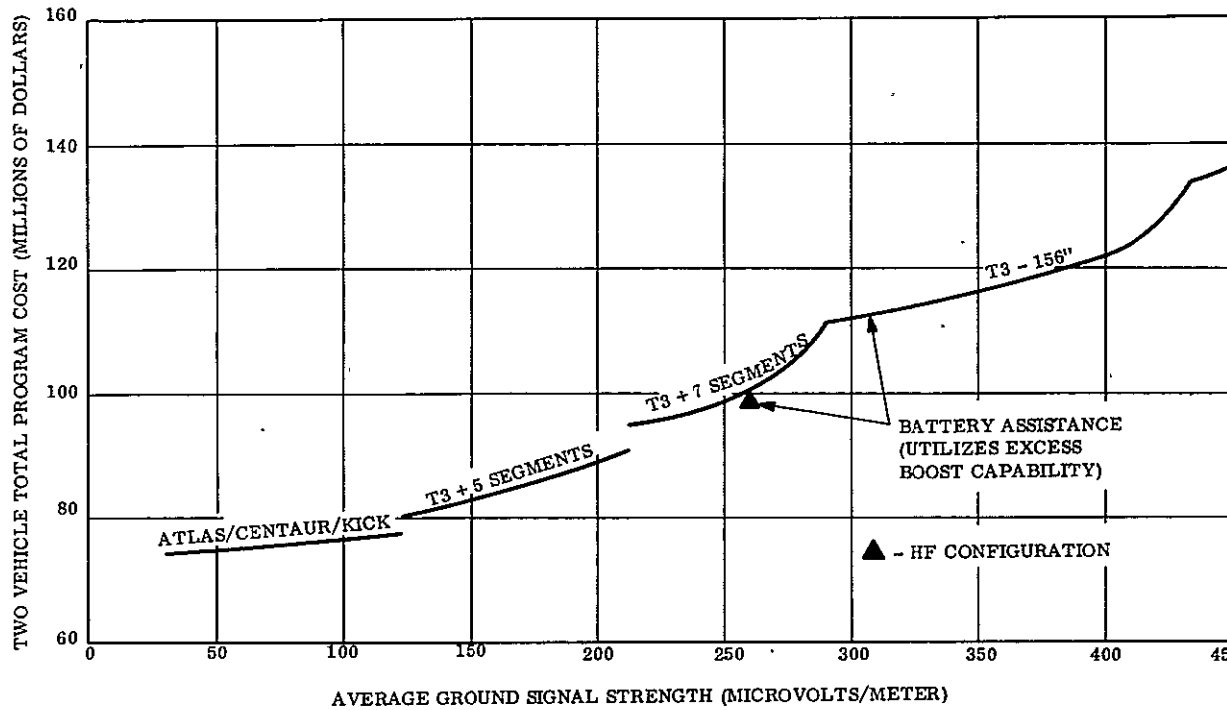

Figure 6.4-10. HF Type Configuration Total Program Cost Variation with Ground Signal Strength

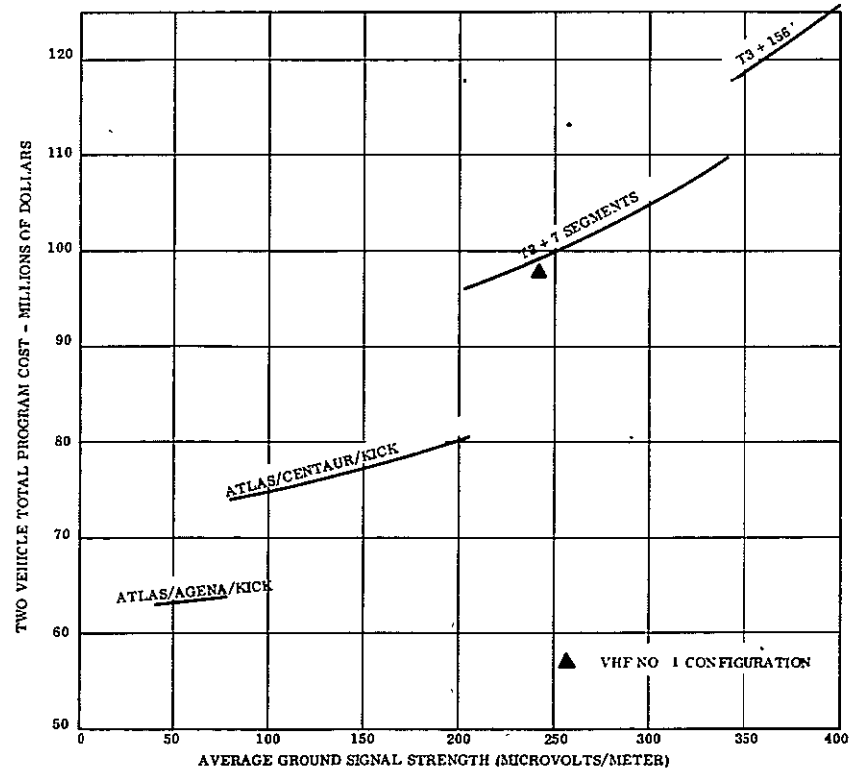

Figure 6.4-11. VHF No.1 Type Configuration Total Program Cost Variation with Ground Signal Strength

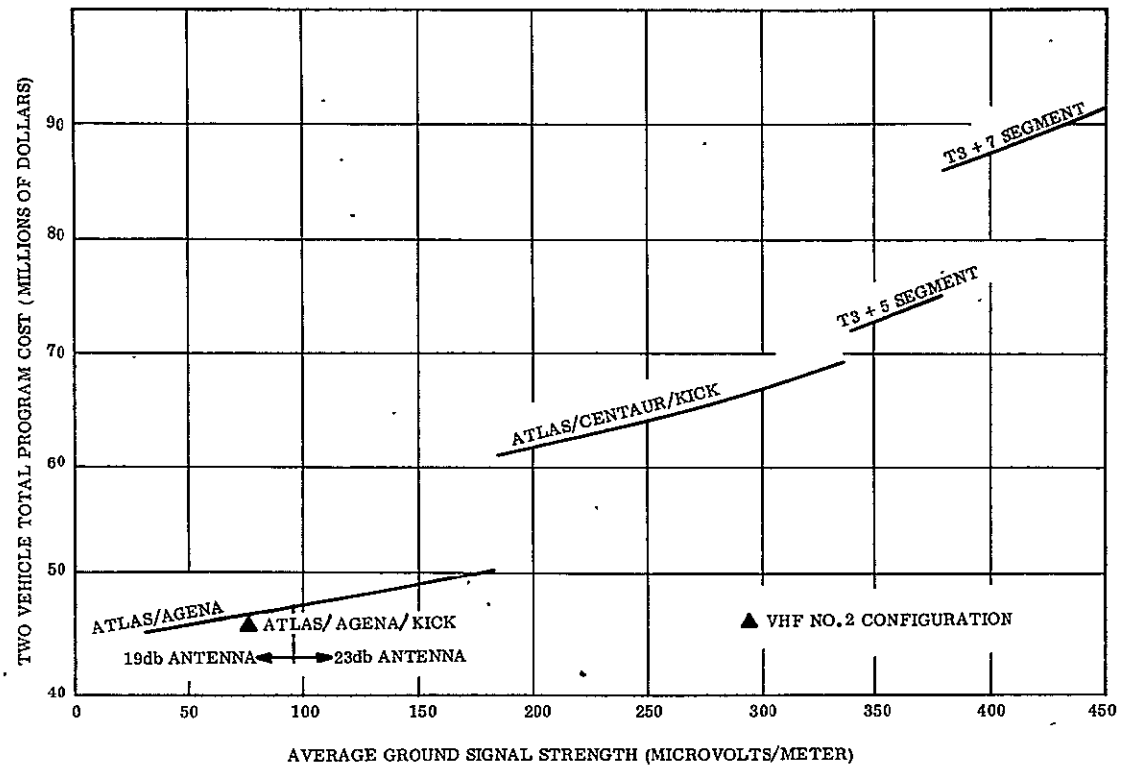

Figure 6.4-12. VHF No. 2 Type Configuration Total Program Cost Variation with Ground Signal Strength

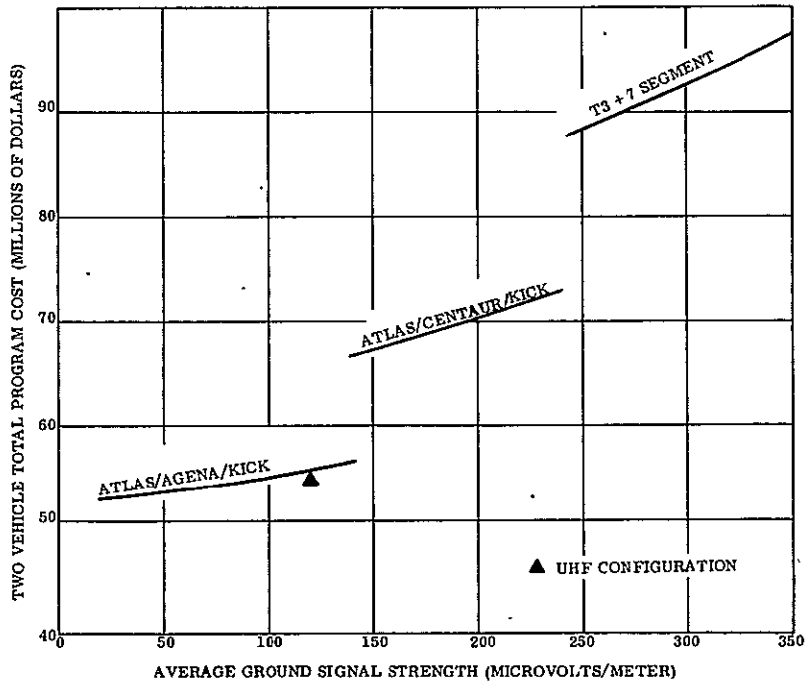

Figure 6.4-13. UHF Type Configuration Total Program Cost Variation with Ground Signal Strength

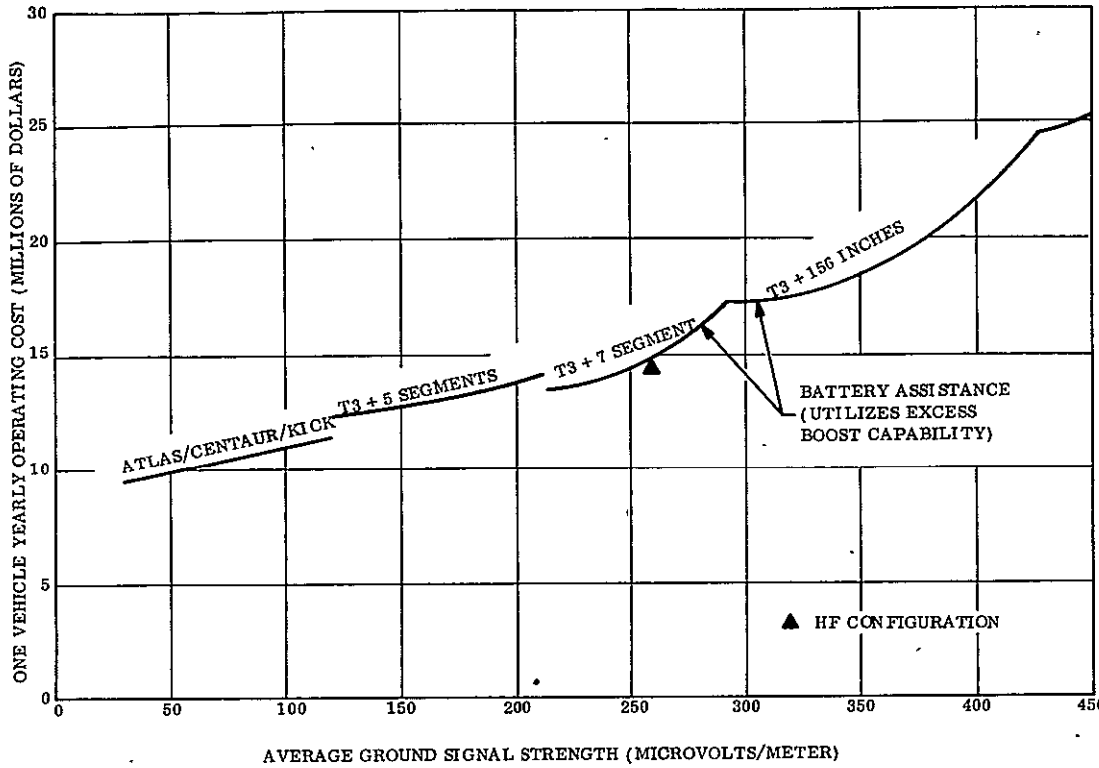

Figure 6.4-14. HF Type Configuration Yearly Operation Cost Variation with Ground Signal Strength

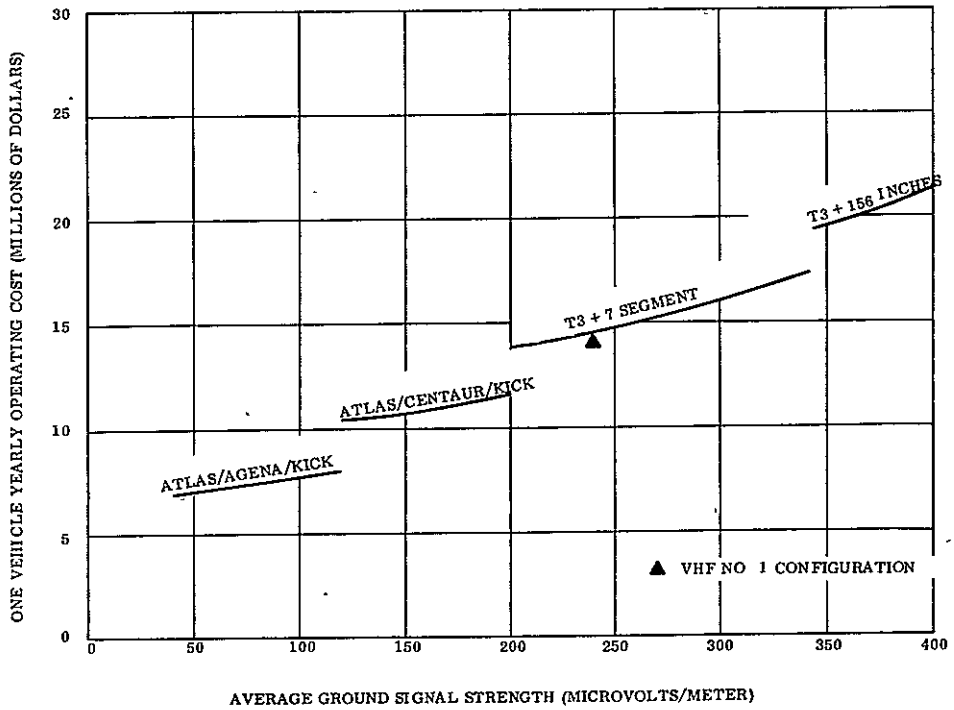

Figure 6.4-15. VHF No. 1 Type Configuration Yearly Operation Cost Variation with Ground Signal Strength

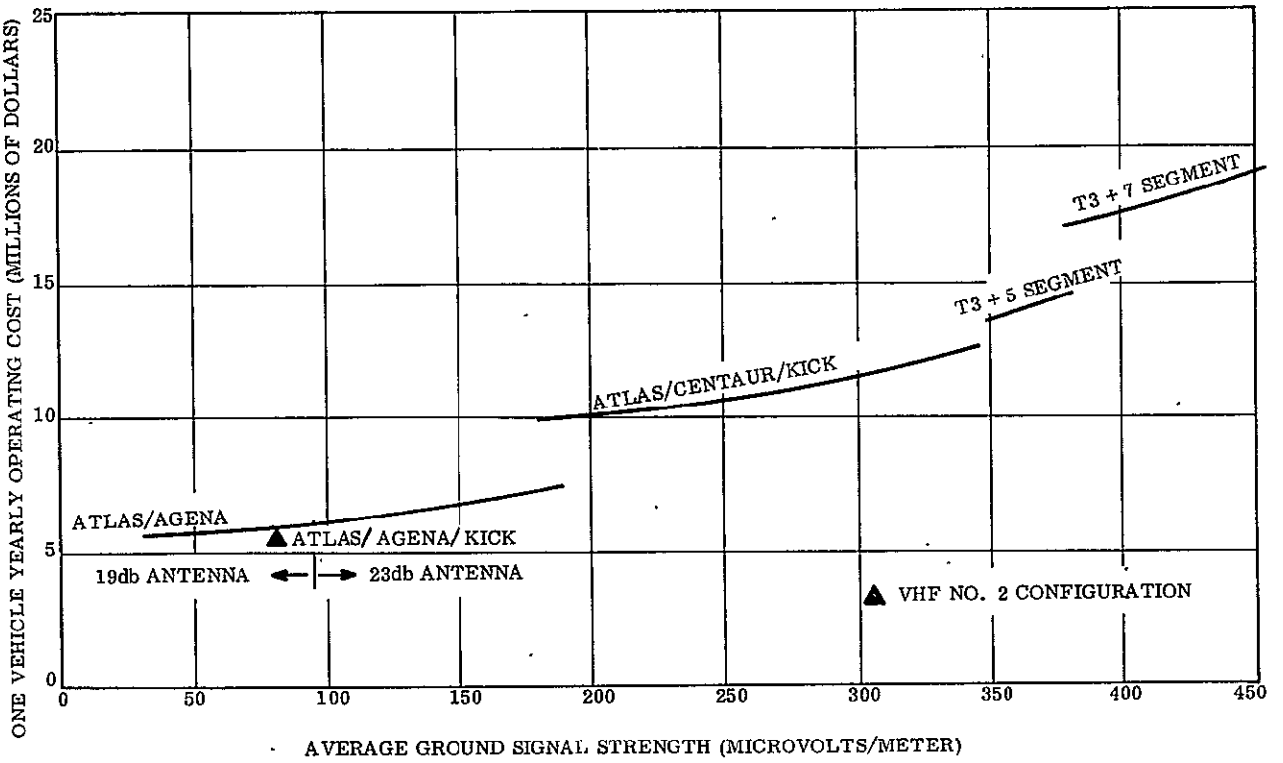

Figure 6.4-16. VHF No. 2 Type Configuration Yearly Operation Cost Variation with Ground Signal Strength

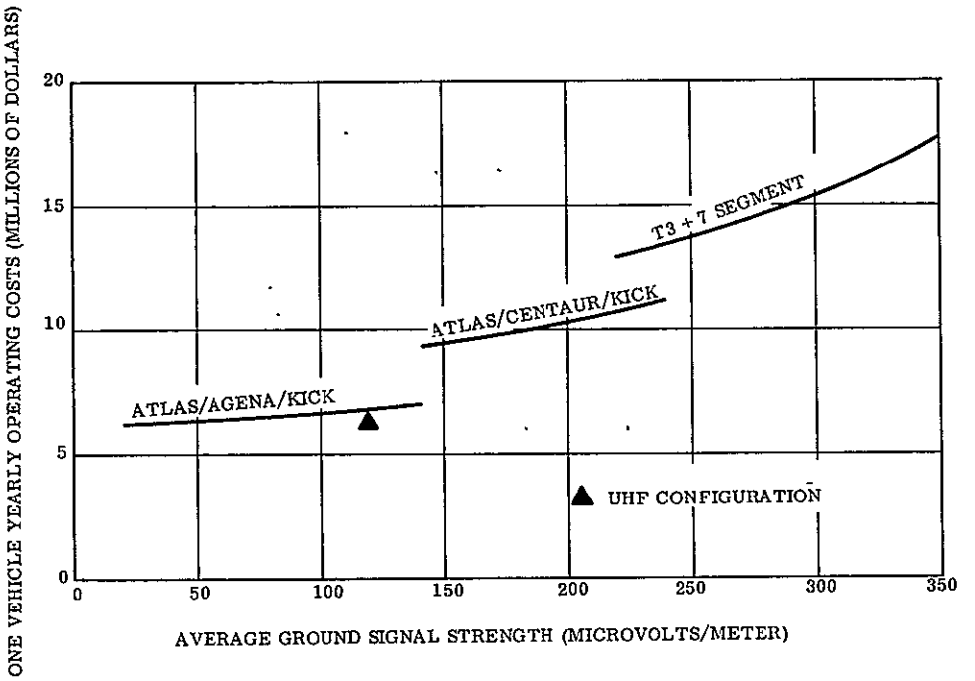

Figure 6.4-17. UHF Type Configuration Yearly Operation Cost Variation with Ground Signal Strength

6.4.3.4 Cost Effectiveness

The potential audience, defined in number of receivers reachable, was determined as a function of the delivered signal strength, using data presented in Section 2.6. Combining these audience values with the yearly operation costs derived for those ranges of signal strengths allowed a calculation to be made of cost per receiver reached versus signal level. This was refined by estimating the number hours of operation per year and the relative rating of the specific broadcast time of day (See Table 6.4-4). The result was defined as the cost effectiveness of the configuration and was measured in cents per receiver-hour.

Table 6.4-4. Coverage Time vs Configuration

Configuration	Time	Relative Rating
UHF	6 to 7 AM	0.5
	10 to 11 AM	0.33
All four time ones in seq.	2 to 3 PM	0.33
	6 to 7 PM	1.0
	10 to 11 PM	1.0
VHF No. 1	20 hrs/day weighted to 12.64 hrs/day	
	0700 to 2300	1
	0100 to 0700 (17 hrs/day)	1/6
VHF No. 2	1 hr/day	*
HF	1 hr/day	*

*Equal ratings for all areas because they receive broadcasts at the same local time each day.

The cost effectiveness values were extrapolated from the values for the baseline configurations for a range of ground signal strengths. The resulting curves are shown in Figure 6.4-18 for each of the four types of configurations. Also shown in this figure are comparative operating costs for commercial FM and for commercial UHF/TV broadcast stations. These curves show that the only configurations which are cost effective, as compared with a nearly identical terrestrial service, are VHF No.1 and UHF. The reasons for this are high duty cycles and large number of receivers in the selected coverage area (USA). The other configurations might have significantly improved values of cost effectiveness if the missions were reoriented to include higher duty cycles and coverage areas with more receivers. On the figure, the solid triangles denote the cost-effectiveness for the baseline configurations. The steps are again a result of the steps in booster costs from type to type. The sharp slope of the HF plot is due to the influence of the noise environment below the 150 μv/m signal level.

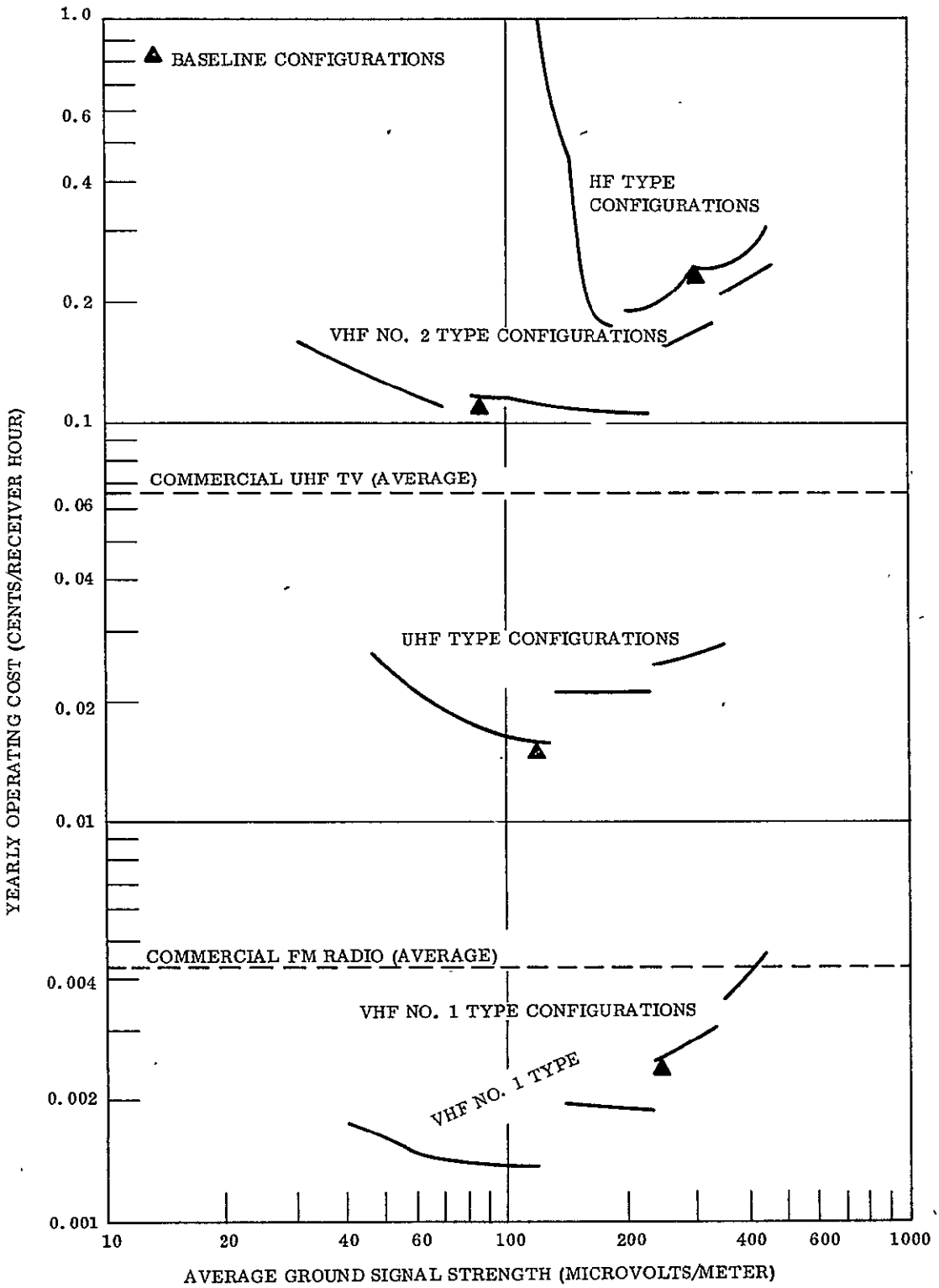

Figure 6.4-18. Specific Operating Cost as a Function of Ground Signal Strength

GENERAL
ELECTRIC

MISSILE AND SPACE DIVISION
Valley Forge Space Technology Center
P.O. Box 8555 • Phila. Penna., 19101